Identification of biomarkers of colitis to monitor effects of dietary omega-3 polyunsaturated fatty acids in the interleukin-10 gene-deficient mouse model of inflammatory bowel diseases

A thesis presented in partial fulfilment of the requirements for the

degree of

Doctor of Philosophy

in

Nutritional Science

at Massey University, Manawatū,

New Zealand.

Nadja Berger

2016

ABSTRACT

Inflammatory bowel diseases (IBD) are characterised by chronic inflammation of the gastrointestinal tract including the colon (colitis). Increased dietary intake of salmon, which is rich in eicosapentaenoic acid (EPA), was well tolerated by IBD patients, leading to a perceived decrease in symptoms. However, better knowledge of the mechanisms by which EPA-rich diets affect IBD severity, and appropriate biomarkers for assessing these effects, are needed for potential targeted nutritional interventions.

This dissertation aimed to determine the temporal effects (early (9 weeks of age) vs. established (12 weeks)) of a diet containing 3.7% EPA, and the dose-dependent effects (15% to 45%) of a salmon diet at 12 weeks of age, on the severity of colitis. Molecular responses in colon and/or liver of the interleukin-10 gene-deficient (*Il10*$^{-/-}$) mouse model of IBD and healthy mice were assessed. Caecum digesta, urine and blood were mined to identify biomarkers (microbiota, metabolites and genes) of these responses.

The EPA diet reduced the severity of colitis only in 12-week-old *Il10*$^{-/-}$ mice. This response was associated with changes in gene expression associated with lymphocyte function, eicosanoid signalling and peroxisome proliferator-activated receptor gamma signalling. The blood immune cell gene expression profile did not correlate with reduced colitis in these mice, but the urine metabolite profile was related to changes in colonic tryptophan metabolism.

The effects of the salmon diets on colitis were dose-dependent in 12-week-old *Il10*$^{-/-}$ mice. The intermediate amount of salmon (30%) reduced the severity of colitis and lymphocyte-related gene expression, while enhancing genes in metabolic pathways. Tryptophan metabolism was not affected in these mice, but the urinary metabolite profile correlated with effects on hepatic tocopherol metabolism, as shown by reduced abundance of gamma-carboxyethylhydroxychroman glucoside. The abundances of *V. akkermansia*, *Eubacterium* spp., and an unclassified *Rikenellaceae* were further affected in these mice.

This is the first report describing molecular responses in the colon and liver of *Il10*$^{-/-}$ mice fed a salmon diet associated with reduced colitis. Ultimately these responses could be validated for use in humans, and potentially enable management of IBD with diet.

ACKNOWLEDGEMENTS

I would like to express my sincerest gratitude to my supervisors Assoc Prof Nicole Roy, Dr Emma Bermingham, Prof Warren McNabb (all AgResearch Grasslands, Palmerston North, NZ) and Dr Janine Cooney (Plant & Food Research Ruakura, Hamilton, NZ) for your guidance and support throughout this project. Thank you for your encouragement, wisdom and finally your patience. I could not possibly have reached this point without you. I also acknowledge AgResearch for funding this project within the Nutrigenomics New Zealand partnership.

I would like to thank Dr Matthew Barnett (AgResearch Grasslands) for letting me be part of the "EPA time-course experiment" after one of my own mouse experiments had failed. Your enthusiasm and positivity was much appreciated when I did not know how to continue.

I am grateful to Dr Wayne Young (AgResearch Grasslands), an expert in 'Omics' and microbiota analyses, for providing various codes in R and helping with all enquiries. Also, thank you for proof-reading parts of this dissertation and providing valuable feedback.

Proteomics work was performed at Plant & Food Research in Auckland under the guidance of Ms Di Brewster. Thank you Di for taking the time to teach the art of 2D-DIGE and your ongoing technical advice. Also, thanks to all members from this laboratory for your welcoming attitudes which made an otherwise difficult process great. I am also grateful to Dr Janine Cooney for conducting MS identification.

A number of people behind this project deserve to be both acknowledged and thanked here: Mr Shuotun Zhu (University of Auckland, Auckland, NZ) for histological analysis. Ms Kelly Armstrong for the training in histology, RNA extraction and microarray analysis. Dr John Koolaard (AgResearch Grasslands) for statistical advice. Mr Paul Maclean (AgResearch Ruakura) for assistance with microarray data processing. Mr Jason Peters and Ms Leigh Ryan for help with animal work (AgResearch Grasslands). Mr Bruce Sinclair (AgResearch Grasslands) for reading various drafts of this dissertation and lending a helping hand during experiments. Dr Mark McCann (AgResearch Grasslands) for assistance with qPCR validation. Metabolomics experts Dr Karl Fraser and Dr Jan Huege (who sadly passed away during the course of this project) for their

valuable advice and sharing their expertise (AgResearch Grasslands). Thank you all for your help and contribution!

I am grateful to Prof Chris Evelo for giving me the opportunity to conduct parts of my last research chapter in the BigCaT Bioinformatics Group at the University of Maastricht in the Netherlands and would like to thank all the members from this group for making my stay in Maastricht a great one. Special thanks to Dr Lars Eijssen for assistance with data analysis, sharing his knowledge in R and the good times biking through the streets of Maastricht on the search for a beer (or two).

I have been very lucky to go through this process with a group of people that provided moral support and most importantly their friendship. Thank you to Ms Denise Martin (AgResearch Grasslands) for your encouraging words when I had already given up. You are an incredible person and have become a true friend. A huge thanks to my fellow postgraduate students for the chats around the lunch table and the many laughs we shared during road trips to Auckland or a girls-night-out. You truly made the day more enjoyable.

Finally I would like to thank my family with all my heart. My parents Nora and Wolfgang for your ongoing love and support. My brother Gerold for watching over me since 1987. My granny Waldtraud and aunt Traudi for your generosity. To my partner Paul thank you for being absolutely amazing throughout the last few years.

TABLE OF CONTENTS

LIST OF FIGURES

LIST OF TABLES

LIST OF APPENDICES

LIST OF ABBREVIATIONS

AA	Arachidonic acid
ALA	Alpha-linolenic acid
AMP	Antimicrobial protein
ANOVA	Analysis of variance
CAM	Cell adhesion molecule
CD	Crohn's disease
CEBPB, CEBPD, CEBPE	CCAAT/enhancer binding protein (alpha, beta, delta)
CEHC	Carboxyethylhydroxychroman
CFU	Colony-forming units
CIF	Complex intestinal microbiota
DHA	Docosahexaenoic acid
DIGE	Difference gel electrophoresis
DPA	Docosapentaenoic acid
DSS	Dextran Sodium Sulfate
EF	*Enterococcus faecalis* and *E. faecium*
EF×CIF	Solution for bacterial inoculation
EPA	Eicosapentaenoic acid
ESI	Electrospray ionisation
FC	Fold-change
FDR	False discovery rate
GIT	Gastrointestinal tract
GLA	Gamma-linolenic acid
GSEA	Gene Set Enrichment Analysis
GWAS	Genome-Wide Association Study
HE	Haematoxylin and eosin
HIS	Histological injury score
HMDB	Human Metabolome Database
IBD	Inflammatory bowel diseases
IEF	Isoelectric focussing
IL[number]	Interleukin [number]
Il10$^{-/-}$	Interleukin-10 gene-deficient
IPA	Ingenuity Pathway Analysis
KEGG	Kyoto Encyclopedia of Genes and Genomes
LA	Linoleic acid
LC	Long-chain
LPS	Lipopolysaccharide
LysoPC	Lysophosphatidylcholine

LysoPE	Lysophosphatidylethanolamine
m/z	Mass-per-charge ratio
MANOVA	Multivariate ANOVA
MDT	Marine-derived tocopherol
MS	Mass spectrometry
n-3 PUFA	Omega-3 polyunsaturated fatty acid
n-6 PUFA	Omega-6 polyunsaturated fatty acid
NCBI	National Center for Biotechnology Information
NKT cell	Natural killer T cell
NMR	Nuclear magnetic resonance
OA	Oleic acid
OTU	Operational taxonomic unit
PAMP	Pathogen-associated molecular pattern
PBMC	Peripheral blood mononuclear cell
PBS	Phosphate-buffered saline
PC	Principal coordinate
PCA	Principal Component Analysis
PCoA	Principal Coordinate Analysis
pI	Isoelectric point
PLS-DA	Partial Least Squares-Discriminant Analysis
PPAR	Peroxisome proliferator-activated receptor
PRR	Pattern recognition receptor
QIIME	Quantitative Insights Into Microbial Ecology
qRT-PCR	Real-time reverse transcription polymerase chain reaction
REML	Restricted maximum likelihood
REST	Relative Expression Software Tool
RIN	RNA integrity number
ROS	Reactive Oxygen Species
RT	Retention time
SCFA	Short-chain fatty acid
SDS	Sodium dodecyl sulphate
SDS-PAGE	Sodium dodecyl sulphate polyacrylamide gel electrophoresis
SNP	Single nucleotide polymorphisms
TG	Triacylglycerol
Th cell	T helper cell
TMAO	Trimethylamine N-oxide
TNBS	Trinitrobenzenesulfonic acid
Treg	Regulatory T helper cell
UC	Ulcerative colitis

INTRODUCTION

Inflammatory bowel diseases (IBD) are a group of disorders characterised by chronic inflammation of the gastrointestinal tract (GIT) with as yet no known cause. It is postulated that a complex interplay between genetic factors, the commensal microbiota and the environment drive an excessive immune response that leads to chronic inflammation in the GIT. IBD was recently identified as an emerging disease globally with incidence rates rising in many regions [1]. Symptoms can be severe, and often affect a patient's quality of life. To date there is no long-term cure. Many patients require medication, often these are anti-inflammatory agents that inhibit inflammatory pathways to achieve a quiescent phase of IBD, known as remission. However, these immune suppressants cannot be considered long-term due to their significant negative side effects [2]. An alternative treatment option is desirable to improve their quality of life.

Nutrients are considered signalling molecules that can target the cellular sensor system and subsequently influence cellular processes and molecular mechanisms. These molecular changes can be beneficial or adverse, and in the case of IBD, are related to observed phenotypical changes, *i.e.* alleviated or exacerbated symptoms. Previous research has shown the ability of dietary lipids, especially omega-3 polyunsaturated fatty acids (n-3 PUFA), to modulate colitis [3-7]. Salmon is one of the richest natural sources of n-3 PUFA and may be a nutritional option to reduce the risk of IBD. The use of diet as an alternative treatment is well known for coeliac disease, where a gluten-free diet reduces disease risk [8].

For IBD, a food frequency questionnaire has shown that a limited number of foods (including white fish, salmon and tuna, gluten-free products, oatmeal, bananas, boiled potatoes, sweet potatoes (kumara), pumpkin, soya milk, goat's milk and yoghurt) were perceived to reduce symptoms of IBD [9]. The effectiveness of these foods varied with individuals, and while one food alleviated symptoms for some, it may have been detrimental for others. To use diet as a complementary solution to conventional treatments, any effects of diet need to be monitored using markers that predict metabolic or physiological changes associated with increased or decreased risk of IBD.

Biomarkers are indicators of a particular disease, risk of disease, or other physiological state and can include specific cells, molecules, genes, enzymes or any

measurable indicators [10]. For IBD, biomarkers are measures of intestinal inflammation that need to correlate with disease activity, and ideally, should be detectable in the early stages of disease. To date there are limited biomarkers of IBD and none exist that predict the effects of dietary intervention with foods such as salmon on IBD, more specifically on colitis.

Chapter 1

Review of literature

Part of this chapter was published as a mini-review in:

Roy, N. C., Berger, N., Bermingham, E. N., McNabb, W. C., & Cooney, J. M. (2011). The effects of n-3 polyunsaturated fatty acid-rich salmon on Inflammatory Bowel Diseases. In: Inflammatory Diseases - A Modern Perspective. Dr. Amit Nagal (Ed.). Rijeka, Croatia: InTech. ISBN 978-953-307-444-3.

1.1 Inflammatory bowel diseases

In 2012, Molodecky *et al.* [1] reviewed the global incidence and prevalence of IBD, a disorder of the GIT characterised by chronic inflammation. Although concrete data was lacking for developing countries, IBD was identified as an emerging disease globally, with incidence rates in many regions rising. Countries with a westernised lifestyle showed the highest rates of both incidence and prevalence, and among these, IBD was most prevalent in Canada and Europe. In New Zealand approximately 15,000 people are affected by IBD [11].

Ulcerative colitis (UC) and Crohn's disease (CD) are the two most common forms of IBD and although the two forms have distinctive characteristics, they share many common symptoms and can be difficult to distinguish clinically [12]. CD can affect any section of the GIT and usually manifests the entire depth of the intestinal wall. UC is most commonly restricted to inflammation of the colon but a few individuals also develop ileal inflammation. In contrast to CD, UC generally only affects the intestinal mucosa [2]. Individuals that suffer from IBD have an increased risk of developing colorectal cancer [13]. The symptoms of the disorder range from diarrhoea, abdominal pain, rectal bleeding, vomiting, to fatigue and fever. IBD is a relapsing condition, with times when the disease is active and symptoms are observed (flares) and times when the disease is in an inactive state and there are few or no symptoms (remission).

IBD is often accompanied by malnutrition, caused in part by poor dietary intake or impaired nutrient digestion and absorption, that can further contribute to weight loss, poor growth in children, or even delays in recovery from illness or surgery [14]. The exact aetiology of IBD is still unknown, but several factors have been suggested to contribute to the pathogenesis of the disease (Table 1.1). It is generally accepted that within a genetically susceptible host, the normal tolerance of the mucosal immune system towards the commensal microbiota is disrupted and dysregulation of the immune system occurs [15]. Additionally, environmental factors such as diet, antibiotic use and stress play a contributing role. As a multifactorial disorder, the development and progression of IBD can be attributed to not only one factor, but the interaction between factors.

Table 1.1 Overview of factors that contribute to the pathogenesis of inflammatory bowel diseases (IBD) and the disease phenotypes ulcerative colitis (UC) and Crohn's disease (CD).

Factor	*Contribution*	*Details*
Genetics	Single nucleotide polymorphisms (SNPs) are variations in the DNA sequence that contribute susceptibility.	163 SNP known to date. Loci/genes commonly associated with the intestinal immune response, intestinal epithelial barrier function (common to UC) and microbial recognition and autophagy (common to CD).
Mucosal immune-regulation	Loss of barrier function of the intestinal epithelium that forms a physical barrier between intestinal lumen and host tissue.	Increased permeability ("leaky gut") allows more pathogens to penetrate host tissue and trigger an inflammatory response.
	Dysregulation of the intestinal immune system mostly associated with T cells.	CD: atypical responses of Th1 and Th17 cells. UC: atypical responses of Th2, Th17 and specialised NKT cells.
	Community profile of the intestinal microbiota is altered ("dysbiosis").	Decreased bacterial species diversity. Increased taxa of *Enterobacteriaceae*, *Escherichia coli*, *Ruminococcus gnavus*, *Clostridium difficile*, and *Bacteroides* (but decreased species diversity within the genus). Decreased taxa of *Faecalibacterium prausnitzii*, *Lachnospiraceae* and *Akkermansia*. No established differentiation between UC and CD.
Environment	Often associated with a "Western" lifestyle.	Diet: unbalanced lipid profiles promote pro-inflammatory phenotype. Stress: increases intestinal permeability. Antibiotic use: Disruption of community structure of the commensal microbiota. Others such as smoking, exercise and sleep.

NKT cell: Natural killer T cell; Th cells: Effector T cell.

See text for references.

1.1.1 Genetic susceptibility

Family studies have shown that susceptibility to IBD (in particular CD) is inherited [16-18]. For example, the risk of a child developing IBD is greater than 30% if both parents are affected by IBD [19], and identical twins are more likely to be concordant for IBD than non-identical twins [17, 18]. The genetics of IBD is complex and it is suggested that genetic variation in key genes play a role. Single nucleotide polymorphisms (SNPs) are variations in the DNA sequence, where only one nucleotide is changed. Approximately seven million common SNPs have been found across the human population [20]. While only a few of these SNPs may have a functional effect [21], some variations can affect health or even cause disease [22]. Genome-wide association studies (GWAS) examine associations between common SNPs and diseases such as IBD. One of the first susceptibility loci for IBD was found to be a SNP of the gene caspase recruitment domain family member 15 (*CARD15*), which encodes the protein nucleotide-binding oligomerisation domain 2 (NOD2) [23, 24]. Since then, GWAS have identified 163 loci/genes that contribute susceptibility to IBD [25]. Of these 163 loci, 110 were associated with both disease phenotypes, while 30 were specific to CD, and 23 to UC (Figure 1.1).

Linking the susceptibility loci/genes to their known biological functions provided insights into the contribution of genetics to the disease mechanisms [26]. For example, UC-specific loci/genes were commonly associated with the intestinal epithelial barrier function (*e.g.* the locus hepatocyte nuclear factor 4 alpha), while CD-specific loci/genes pointed to a dysregulated microbial recognition and autophagy (*e.g.* NOD2) [26]. Genes associated with intestinal immune response (*e.g.* interleukins 12B and 23 (*IL12B* and *IL23*), IL23 receptor (*IL23R*), and Janus kinase 2 (*JAK2*)) were common to both disease phenotypes, suggesting a critical role for mucosal immune-regulation in the disease pathogenesis [26].

1.1.2 Mucosal immune-regulation

The intestinal surface is the largest interface between a mammalian host and its external environment, and is constantly exposed to pathogens and potentially harmful antigens. The intestine acts as a barrier to prevent pathogens from entering, while allowing the entry

of nutrients and water. In a mammalian host, the intestinal barrier comprises four elements, (i) the mucus as chemical barrier, (ii) the commensal microbiota, (iii) the epithelial layer for physical separation, and (iv) immune cells forming the immunological defence (Figure 1.2) [27].

1.1.2.1 Intestinal epithelium

The intestinal epithelium is the physical barrier that separates the lumen from the underlying lamina propria (Figure 1.2). The integrity of the epithelial barrier is an important feature in the pathophysiology of IBD [28]. The majority of cells lining the epithelium are absorptive enterocytes, which make up more than 80% of the epithelial cells and are specialised in providing digestive and metabolic functions to the host. The remainder of the epithelium comprise of goblet cells, enteroendocrine cells, and Paneth cells. The single-layered epithelium is arranged into invasions that extend down to the muscularis mucosa (crypts of Lieberkühn), and finger-like projections called villi [29]. The main site for digestion/absorption of nutrients is the small intestine, where the villi allow a more efficient absorption of nutrients.

Goblet cells produce mucin glycoproteins which form a gel-like mucus layer, allowing the colonisation by commensal microbiota. Only the outer, loosely adherent mucus layer is the site for microbial colonisation, whereas the inner layer, firmly adherent to epithelial cells, is depleted of microbiota [30]. The importance of the mucus layer in intestinal inflammation was shown in mice, where a deficiency in secretory mucin MUC2 leads to spontaneous colitis development [31]. To limit bacterial growth and penetration, mucus contains antimicrobial proteins (AMP) and secretory immunoglobulin A (sIgA) (Figure 1.2). AMPs include a variety of protein families (*e.g.* the C-type lectin Regenerating islet-derived 3 gamma (REG3G)) and are secreted by Paneth cells situated at the base of the crypts [32-34]. As the colon contains only a limited number of Paneth cells, AMPs are also produced by enterocytes. REG3G is important for the spatial separation of the intestinal microbiota and the epithelium as shown in REG3G knock-out mice [35]. In these mice, increased epithelial contact with microbiota was observed which resulted in low-grade inflammation [35]. sIgA is produced by plasma cells (differentiated from B cells) of the lamina propria [36] and transported across epithelial cells in a receptor-mediated process known as transcytosis [as reviewed in 37]. In the mucus layer,

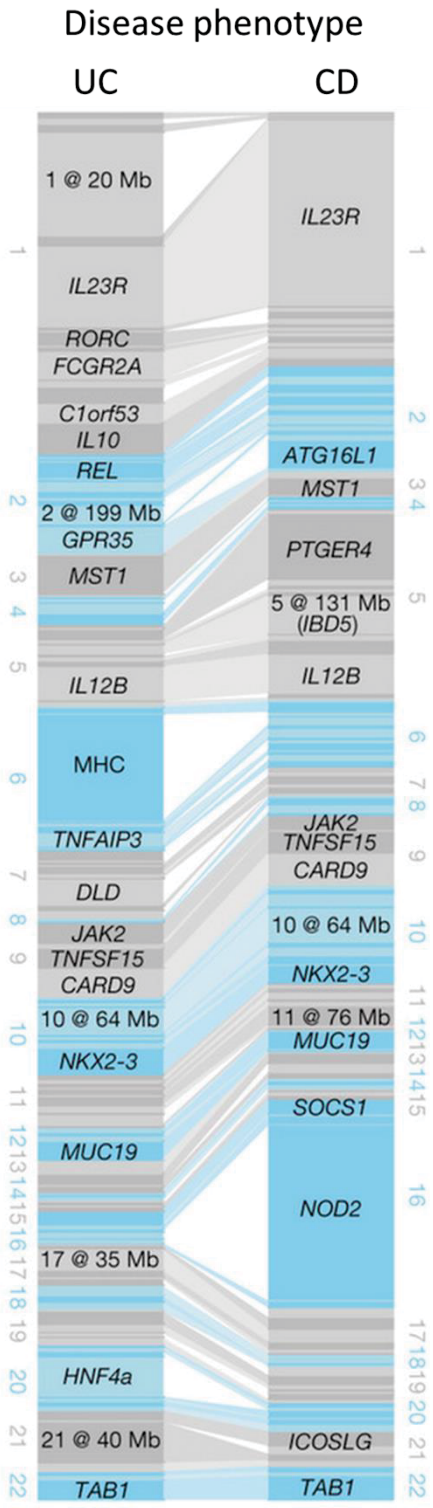

Figure 1.1 Susceptibility loci for the disease phenotypes Crohn's disease (CD) or ulcerative colitis (UC) as identified by genome-wide association studies (GWAS). Each bar represents an independent locus mapped to the genomic location. Loci that are labelled with an identifier (either candidate gene or chromosome and position of the locus) contribute more than 1% of the total variance explained by all loci within the disease phenotype. The width of bar reflects the variance explained by that locus in either CD or UC. Two bars that are connected between the phenotypes contribute susceptibility to both disease phenotypes. Reprinted by permission from Macmillan Publishers Ltd: Nature, Jostins *et al.* [25]. See Reference [25] for abbreviations of genes.

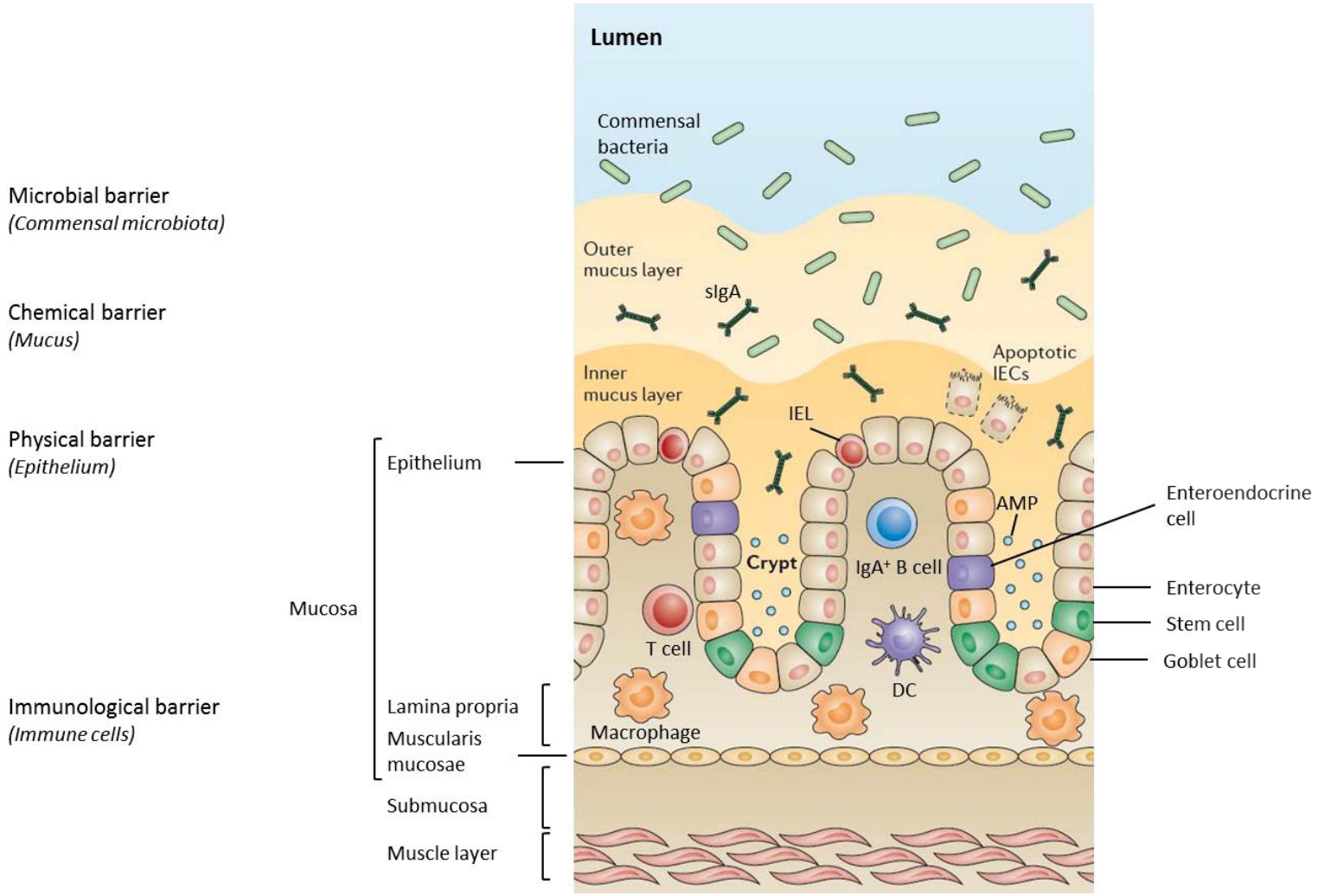

Figure 1.2 Structure of the colonic mucosa (adapted from Mowat *et al.* [38])
IEL: Intraepithelial lymphocyte; DC: Dendritic cell; sIgA: Secretory Immunoglobulin A; IECs: Intestinal epithelial cells; AMP: Antimicrobial protein

sIgA reduces microbial densities [36] and restricts microbial penetration across the intestinal epithelium [39].

Tight junctions form intercellular barriers between the intestinal epithelial cells and regulate the transport of large molecules [40], allowing nutrient influx into host tissue but preventing microorganisms from entering. In a functional intestinal barrier, luminal microorganisms and antigens are unlikely to breach the epithelium, but increased paracellular permeability has been implicated in diseases such as IBD ("leaky gut") (Figure 1.3). This was reported in relatives of IBD patients [28], and in patients with inactive CD where increased intestinal permeability was indicative of a flare [41]. Molecular changes underlying the perturbed epithelial permeability in inflamed tissues can be attributed to the apical junctional complex itself (*i.e.* tight junctions and adherens junctions), or to the remodelling of the actin cytoskeleton (a mechanism that mediates junctional disassembly (Figure 1.3)) [42-44]. Zeissig *et al.* [45] reported that the expression of several tight junction proteins (*e.g.* claudins 5 and 8) were decreased in colon lesion biopsies of CD patients with mild to moderately active disease. The actin cytoskeleton is connected to the tight junctions and adherens junctions, while providing support and structure to the cell membrane [as reviewed in 46, 47]. Increased permeability may further allow bacteria to infiltrate the epithelium and trigger an inflammatory cascade [48]. The lamina propria underlying the epithelial cell layer further harbours several distinct immune cell types (Figure 1.2) that limit bacterial penetration across the epithelial barrier, and if the barrier is breached, regulate immunological responses.

1.1.2.2 Intestinal inflammation

The inflammatory response is the beginning of an immunological process and is necessary to protect the body against invading pathogens. When pathogens cross the intestinal epithelial barrier, a non-specific inflammatory response is mediated by the innate immune system and driven by leukocytes (white blood cells: dendritic cells, natural killer cells, monocytes, macrophages, and neutrophils). The innate immune cells have pattern recognition receptors (PRR) on their surface (*e.g.* toll-like receptors (TLR) and NOD-like receptors) that recognise a broad spectrum of infiltrating bacteria/pathogens by pathogen-associated molecular patterns (PAMPs), such as the bacteria-derived endotoxin lipopolysaccharide (LPS). The resulting inflammation is characterised by increased blood flow into the affected tissue, and the release of eicosanoids (*e.g.* prostaglandins) and

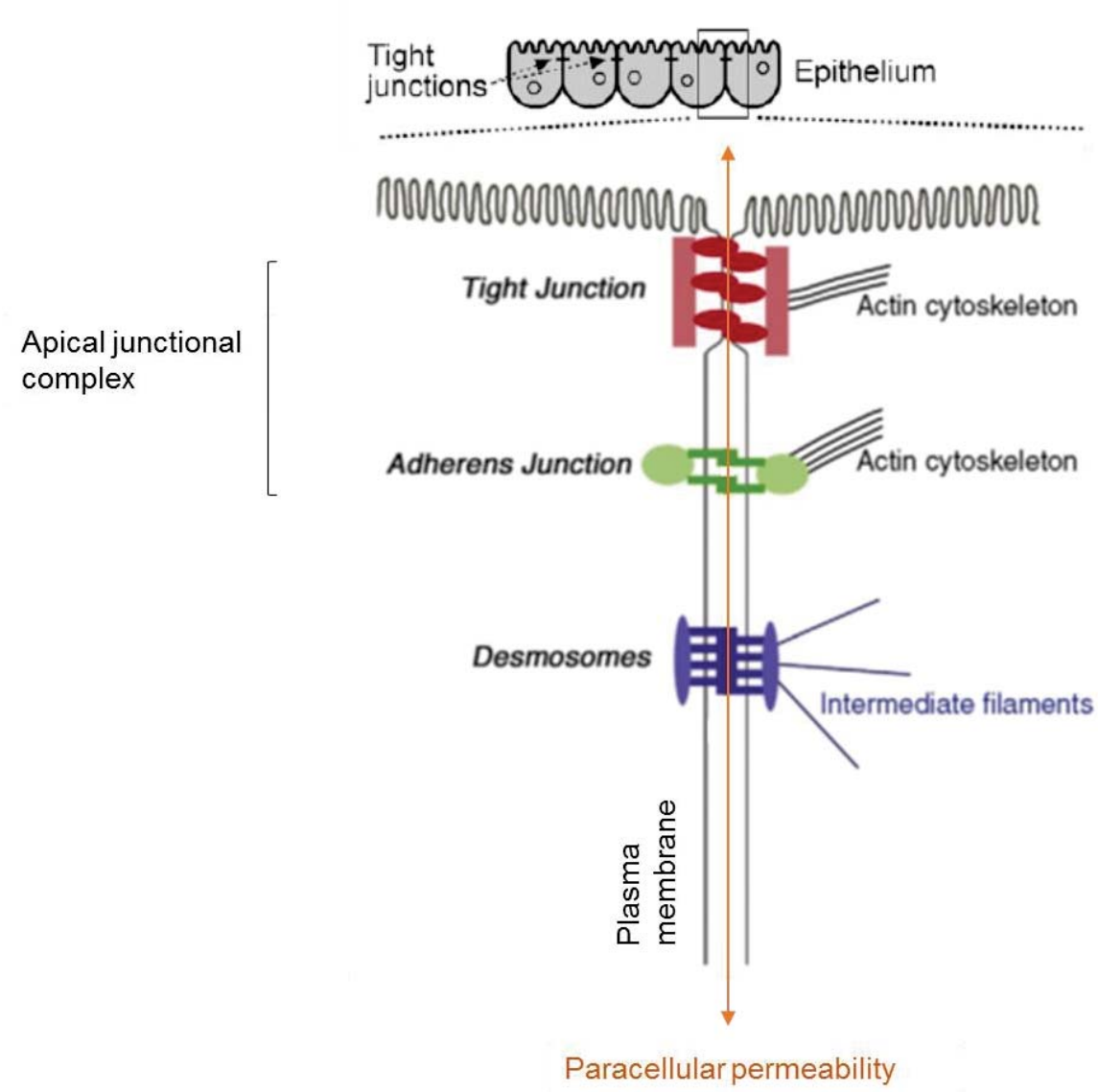

Figure 1.3 Structure of tight junctions and adherens junctions (together known as apical junctional complex) between epithelial cells of the intestine and actin cytoskeleton (adapted from Steed *et al.* [47] and Ulluwishewa *et al.* [49]).

cytokines (*e.g.* interleukins, chemokines and interferons), recruiting more immune cells to the site of inflammation.

The activation of the adaptive immune system is mediated by T lymphocytes and B cells (Figure 1.4), but IBD is mostly attributed to a dysregulation of T cell-mediated immunity [50-55]. T cells recognise antigens that are bound to specific receptors, the major histocompatibility complexes (MHC) class I and class II. MHC class I molecules are expressed and presented by all nucleated cells, while MHC class II molecules are primarily expressed by specialised antigen-presenting cells, including dendritic cells, macrophages and B cells [as reviewed in 56]. Cytotoxic T cells (also known as $CD8^+$ T cell) actively kill other cells by inducing apoptosis, while T helper (Th) cells (also known as $CD4^+$ T cell) regulate the innate and adaptive immune response by recruiting other immune cells to the site and assisting in maturation of other white blood cells (*e.g.* B cells into plasma cells and memory B cells, and activation of cytotoxic T cells and macrophages). Upon encountering antigens, naïve $CD4^+$ T cells and naïve $CD8^+$ T cells become activated and differentiate into a variety of T cell subsets. Naïve $CD4^+$ T cells differentiate into one of several subtypes, including effector T cells (Th1, Th2, Th3, Th9, Th17, or follicular Th cells), memory Th cells, regulatory Th cells (Treg), or natural killer T (NKT) cells. This differentiation depends on the antigen presented to the naïve $CD4^+$ T cells, and is coupled to the release of various cytokines that affect cells in the local environment, resulting in recruitment of different types of immune cells that ultimately drive the immune response. As illustrated in Figure 1.4, the cytokine pattern and immune cell responses are characteristic to the disease phenotypes. CD is linked to an excessive activation of Th1 and Th17 cells [53, 55, 57], while UC is suggested to be connected to Th2, Th17 and specialised NKT cells [50, 55]. The activation/production of these molecules must be ordered and controlled to avoid excessive damage to host tissue and chronic inflammatory disorders. A defect in resolving the inflammation and returning the target tissue to homeostasis is a hallmark of IBD.

1.1.2.3 The commensal microbiota

The human GIT harbours a vast, diverse, and dynamic microbial community which is suggested to play a role in the excessive immune response that drives intestinal inflammation in IBD. Up to 10^{14} microorganisms reside in the human GIT [58], with the colon presenting one of the most dense microenvironments on earth [59]. Approximately

99% of microorganisms in the intestine are of bacterial origin, with the remainder being archaic, and to a lesser extent eukaryotic and viral [60]. The intestinal microbiota can be viewed as its own organ, "composed of different cell lineages with a capacity to communicate with one another and the host; it consumes, stores, and redistributes energy; it mediates physiologically important chemical transformations; and it can maintain and repair itself through self-replication" [61]. It is therefore not surprising that the microbiota has a profound impact on the host metabolism. Complex interactions between the host's innate and adaptive immune systems protects against microbial invasion, while maintaining tolerance towards the commensal microbiota. In a chronic inflammatory state, such as IBD, the protection of the host's immunity to the commensal microbiota is defective [15], and when coupled with a loss of mucosal tolerance, it leads to an uncontrolled mucosal immune response and ultimately, a severe disruption of intestinal tissue [62].

Considering the size of the microbial pool, the bacterial diversity in the adult GIT is fairly low, with the phyla *Bacteroidetes* and *Firmicutes* dominating the large intestine [60]. In IBD, the community profile of the microbiota is altered (Table 1.2), commonly referred to as "dysbiosis". Despite large interpersonal variation, common themes of dysbiosis have been observed in IBD [as reviewed in 63]: (i) decreased bacterial species diversity, (ii) increased taxa of *Enterobacteriaceae*, *Escherichia coli*, *Ruminococcus gnavus*, *Clostridium difficile*, and *Bacteroides* (but decreased species diversity within the genus), and (iii) decreased taxa of *Faecalibacterium prausnitzii*, *Lachnospiraceae* and *Akkermansia*. It is yet to be confirmed whether the changes in the microbial community profile are causative to the inflammatory process (due to a disturbed balance of detrimental/beneficial bacterial species), or are a consequence of the inflammatory process. Frank *et al.* [64] reported that shifts in the intestinal community profile correlated with susceptibility loci/genes of CD patients (*e.g.* NOD2), postulating that bacterial dysbiosis cannot be a consequence of inflammatory processes alone. Others suggest that the alterations in the community profile may be explained by the inflammatory state in the GIT that is characteristic of IBD [65, 66]. For example, increasing bile acid influx might disturb the fragile environment [65], or the introduction of oxygen into the intestine that favours the growth of facultative anaerobe bacterial strains (*e.g. Enterobacteriaceae* including *E. coli*), while depleting obligate anaerobes, which are abundant in a healthy host (*e.g.* oxygen-sensitive *F. prausnitzii*). This "oxygen

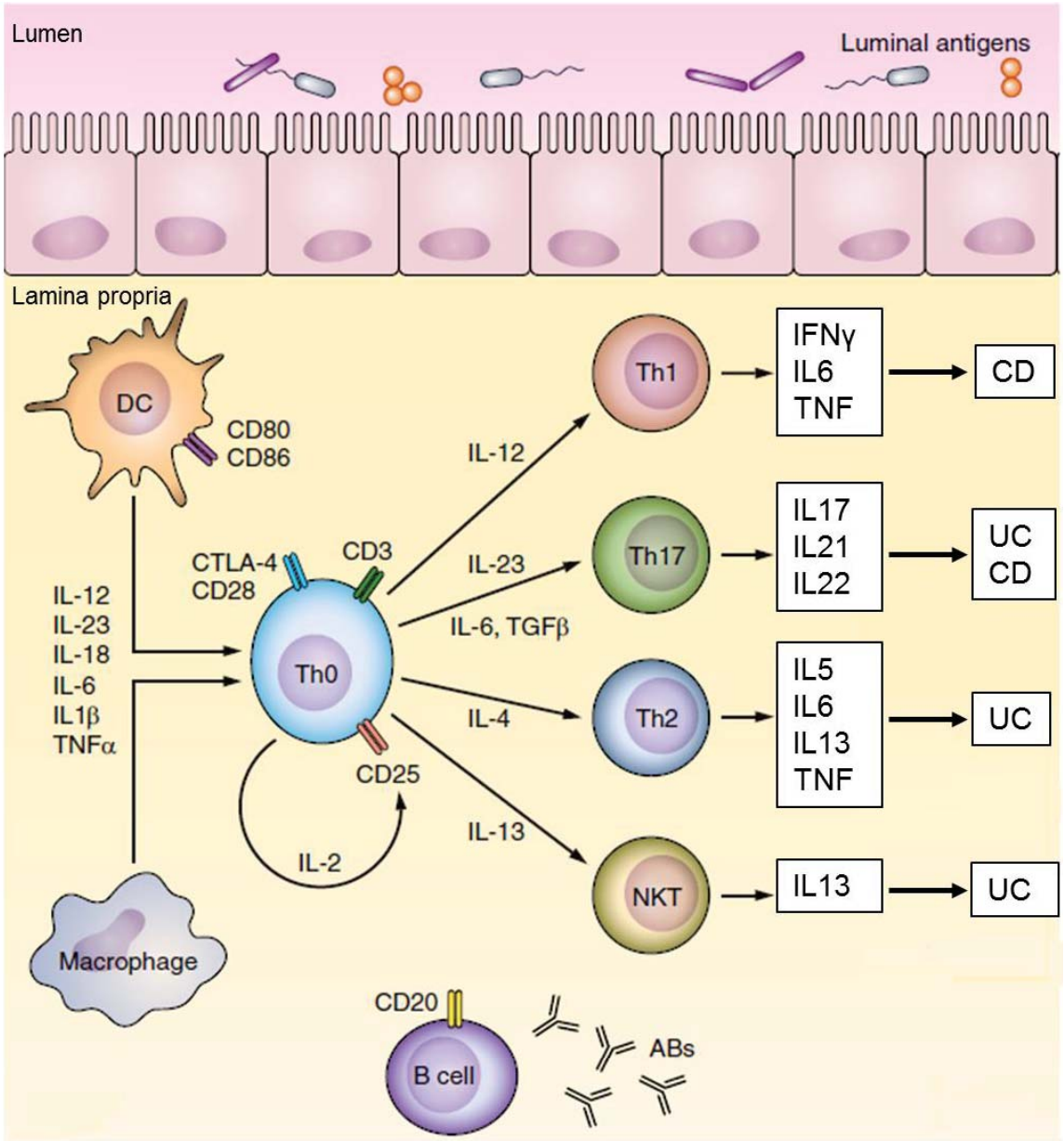

Figure 1.4 Overview of regulatory pathways involved in the cell-mediated immune response and the characteristic defects in the disease phenotypes Crohn's disease (CD) and ulcerative colitis (UC). Upon encounter with antigens presented by dendritic cells and macrophages, naïve T cells (Th0) differentiate into Th1, Th2, Th17 or natural killer T cells that further produce cytokines (interleukins, interferon γ, tumor necrosis factor) and drive the immune response. Atypical responses of Th1 and Th17 cells are linked to CD, while atypical responses of Th2, Th17, and natural killer T cells are linked to UC. Adapted from Valatas *et al.* [67], and Neurath [68].

ABs: Antibodies; CD[number]: Cluster of differentiation [number]; DC: Dendritic cell; IFNγ: Interferon gamma; IL[number]: Interleukin [number]; NKT cells: Natural killer T cells; Th[number]: T helper cell [number]; TNF: Tumor necrosis factor.

Table 1.2 Characteristic changes in microbial community composition in inflammatory bowel diseases (IBD) compared to healthy individuals, obtained from human intestinal biopsies ("B") and/or faecal samples ("F") and identified by 16S rRNA gene sequencing. Reprinted from Berry *et al.* [63] with permission from Elsevier.

Observation	*Sample origin*
Increased taxa	
Enterobacteriaceae	B, F
Escherichia coli	B, F
Adherent-invasive *E. coli*	B
Mycobacterium avium subspecies *paratuberculosis*	B
Bacteroides (decreased species richness within the genus)	B, F
Desulfovibrio spp.	B, F
Members of the *Epsilonproteobacteria* (*Campylobacter* and *Helicobacter*)	B
Ruminococcus gnavus	B, F
Clostridium difficile	F
Decreased taxa	
Faecalibacterium prausnitzii	B, F
Lachnospiraceae	B, F
Akkermansia	B, F

hypothesis" is suggested to be linked to blood entering the GIT during chronic inflammation and the release of haemoglobin carrying oxygen into the mucosa [66].

1.1.3 The role of the environment

IBD has previously not been associated with developing nations but the adaptation of a "Western" lifestyle may have increased the risk of developing chronic disease, such as IBD [69, 70]. This "Westernisation" is associated with dietary changes, smoking, antibiotic use and stress. A recent meta-analysis highlighted that the risk of developing CD was higher in individuals that were exposed to antibiotics [71] and generally "subjects diagnosed with IBD were more likely to have been prescribed antibiotics 2 to 5 years before their diagnosis" [72]. Exposure to antibiotics leaves an imprint in the microbial community structure that can remain for up to four years post treatment [73]. In children, antibiotic treatment during infancy greatly increases the risk of paediatric IBD [74]. As discussed earlier, the integrity of the intestinal epithelial barrier is an important feature in the pathophysiology of IBD [28], with increased permeability reported in IBD patients ("leaky gut"). It has further been found that stress can exacerbate IBD by increasing small intestinal permeability in humans [75].

"Western" diets contain high levels of trans-fatty acids, saturated fats, omega-6 polyunsaturated fatty acids (n-6 PUFA), but are relatively deficient in n-3 PUFA [76]. This may result in an n-6/n-3 ratio of approximately 15-20:1 in the diet [77], whereas humans evolved at a ratio of approximately 1:1 [78]. The high levels of n-6 PUFA in "Western" diets may lead to an unbalanced plasma n-6/n-3 PUFA ratio, which may promote the pathogenesis of many diseases, including IBD [77]. High cellular concentrations of n-6 PUFA can serve as substrates for pro-inflammatory lipid mediators [as reviewed in 79]. It has been suggested that lowering the n-6/n-3 ratio in the diet should be achieved by increasing the amount of n-3 PUFA rather than by simply reducing n-6 PUFA [80], and a higher level of n-3 PUFA in the diet may help to reduce the risk of developing IBD [7]. Food frequency questionnaires among IBD patients have shown the possibility of alleviating IBD symptoms by dietary choices, with the aim of inducing and maintaining remission. Salmon, a rich source of n-3 PUFA, was perceived as one of the most beneficial foods to alleviate symptoms of IBD [9]. In this study, 446 CD patients rated food items and their perceived effects on disease symptoms. No single food item was considered beneficial in all cases, however, a limited number of foods were

frequently perceived to be beneficial: white fish, salmon and tuna, gluten-free products, oatmeal, bananas, potatoes, sweet potatoes (kumara), pumpkin, soya milk, goat's milk and yoghurt. The exact mechanisms of action by which foods (*e.g.* n-3 PUFA-rich salmon) influence molecular pathways in intestinal inflammation remain to be determined. Due to practical limitations of human clinical studies, models that mimic aspects of human IBD are necessary to elucidate these molecular responses to n-3 PUFA.

1.1.4 Animal models of IBD

Human clinical studies have shown the potential of nutritional intervention to mitigate IBD, but the usefulness of these studies are limited by factors such as access to target tissues, control of environmental factors, duration of the study, and number of participants. People also may not follow the recommended dietary guidelines and study outcomes may be affected by recall bias which are often observed in food frequency questionnaires [81]. As *in vitro* models cannot mimic the complexity of an entire organism, animal models are essential in understanding the role of diet in intestinal inflammation. Disease pathogenesis differs across animal models, making it difficult to compare results between models [82] (Table 1.3). For an animal model to be representative for human IBD, the model ideally replicates the factors that contribute to the disease pathogenesis [83]: a loss of tolerance against the commensal microbiota that leads to an unrestrained and exaggerated immune response within a genetically susceptible host. Ideally, all of these factors are prominent in a model with chronic inflammation ("endogenously triggered inflammation").

It has recently been shown that some models of acute inflammation (chemically induced injury models such as 2,4,6-trinitrobenzene sulfonic acid (TNBS) and Dextran Sodium Sulfate (DSS)) do not correlate with human IBD [84]. Chemically induced models are self-limiting (*i.e.* intestinal inflammation does not develop without external manipulation), do not spontaneously relapse (characteristic for human IBD), and repair of injured tissue is generally observed when the chemical is withdrawn. Interleukin-10 (IL10; an important regulator of the immune response [as reviewed in 85]) is suggested as a key mediator for the maintenance of intestinal homeostasis [86], and has been linked to genetic susceptibility in IBD [25]. The general importance of IL10 in intestinal homeostasis and the immune system as a pluripotent cytokine supports the use of interleukin-10 gene-deficient (*Il10*$^{-/-}$) mice as a model of human IBD.

Table 1.3 Most commonly used mouse models of inflammatory bowel diseases (IBD) [collated from information in 67, 83, 87, 88-101]. The "Induction model" is based on the method of establishment of intestinal inflammation, with a background and short description. "Model type" indicates resemblance to the human disease phenotypes ulcerative colitis (UC) and Crohn's disease (CD), and "molecular changes" briefly explain the T cell-mediated immune responses.

Induction model	*Background*	*Short description*	*Model type*	*Molecular changes*	*Advantage*	*Drawback*
Chemical induction						
	Increased intestinal permeability				* Dose alters severity * Duration of administration can be adjusted, thus acute and chronic inflammatory responses can be studied * Synchronised onset and severity * Inexpensive	* Requires an external source for disease manifestation, therefore not ideal model for human IBD ("self-limiting") * No spontaneous relapse or tissue repair after withdrawal of dose * High mortality at high doses
DSS	Colitis induced by chemical agent DSS	DSS increases apoptosis while decreasing proliferation in the epithelium, followed by disruption of the barrier integrity	UC	* Acute phase: Th1-mediated immune response (increased TNF, IFNG, IL1B, IL6, (unclear IL17), and IL12) * Chronic phase: Th2-mediated (increased IL4, IL6, IL10, and IFNG)		* Unclear role of Th17 cells * Luminal bacteria has limited role to no role
TNBS	Colitis induced by chemical agent TNBS	TNBS is a hapten that binds to high molecular weight protein, similar to an antigen	Both forms (primarily CD)	* Acute phase: Th1-mediated immune response (increased IL12, IL17, and IFNG) * Chronic phase: Th1/Th17-mediated (IFNG, IL1B, IL12 and IL17)	* Relevant for development of mucosal inflammation	* Ethanol (as carrier) causes inflammation, so colitis not only attributed to TNBS

Adoptive transfer models						
	Chronic colitis is T cell-mediated					
T cell transfer	Disruption of T cell homeostasis	Adaptive transfer of $CD4^{+}CD45RB^{high}$ T cells (naïve T cells) from wild-type mice into syngeneic recipients that lack T and B cells	UC and CD	Th1/Th17-mediated immune response (increased TNF, IL1B, IL6, and IFNG)	* Synchronised onset and severity * Possibility to follow immunological events from induction of colitis to perpetuation of disease	* Expensive * Mice are hard to breed, making it difficult to obtain the correct numbers for an experiment (Source: The Jackson Laboratory)
Genetic models						
	Knock-out of susceptibility loci/genes for human IBD					
Mdr1a$^{-/-}$	Targeted deletion of multi-drug resistance gene 1A (*MDR1A*)	MDR1a is a protein involved in xenobiotic clearance	UC (Banner *et al.* [93] suggested resemblance to CD)	Th1-mediated immune response (increased IFNG and IL8)	* Compromised intestinal permeability is similar to human IBD	* Colitis caused by dysfunctional epithelial barrier rather than lymphocyte function
Il10$^{-/-}$	Targeted deletion of interleukin-10 (*IL10*)	The cytokine IL10 is produced by immune cells and suppressor of immune response	CD	Th1/Th17-mediated immune response (increased TNF, IL1A, IL6, IL12, IL23, and IFNG)	* Chronic colitis is similar to human IBD * Severity of intestinal inflammation can be adjusted by choice of background model (*e.g.* C57BL/6, BALB/c or 129/SvEv)	* Onset and severity are variable * Continuous inbreeding lowers the penetrance and severity of colitis

DSS: Dextran Sodium Sulfate; IFNG: Interferon gamma; IL[number]: Interleukin [number]; Th[number]: T helper cell [number]; TNBS: 2,4,6-trinitrobenzene sulfonic acid; TNF: Tumor necrosis factor.

1.1.4.1 The interleukin-10 gene-deficient mouse model

The *Il10*$^{-/-}$ mouse, first described in 1993 [95], is one of the most commonly used models for IBD [83, 102]. The model was generated by targeted mutation of IL10, a cytokine-coding gene initially thought to be only expressed in Th2 cells upon activation [95]. Advances in technology have shown that IL10 is produced by most cells of the innate (macrophages, monocytes, neutrophils, eosinophils, dendritic cells, mast cells and natural killer cells) and adaptive (T killer cells, effector T cells and B cells) immune system [as reviewed in 103, 104]. In unstimulated tissues, IL10 expression levels are generally low, and immune cells require a stimulus to induce IL10 production [105]. Different types of immune cells respond to specific stimuli to induce IL10 production, but there are common mechanisms. Cells of the innate immune system largely depend on the stimulation of PRR (especially TLR) by pathogen-derived products to induce IL10 production [85]. Naïve T cells cannot produce IL10 and need to differentiate into effector T cell subsets before IL10 production can be initiated [85]. The cytokine signalling that directs the differentiation of each Th cell subset is also required for the induction of IL10 production, showing a feedback loop that prevents excessive inflammatory processes. IL10 further induces the differentiation of IL10-secreting Treg cells to resolve inflammation [106].

The immune-suppressive properties of IL10 are especially important in the resolution phase of inflammation by inhibiting pro-inflammatory responses from innate and adaptive immune cells [104]. Different levels of IL10 can be released from the same cell type depending on the type and/or strength of stimuli [85]. The effects mediated by IL10 generally depend on releasing cell type, stage of the immune response, and anatomical location of release [86]. The IL10 signalling cascade is mediated *via* its receptor complex (comprising of IL10RA and IL10RB), located on the immune cell membrane. By acting on antigen-presenting cells, IL10 indirectly inhibits cytokine secretion by these cells and suppresses further T cell activation [107].

Il10$^{-/-}$ mice develop chronic colitis (characterised by infiltration of lymphocytes, plasma cells, macrophages and neutrophils, showing similarities to human CD [108]) within 4 to 8 weeks under conventional housing conditions [95]. It was reported that in the colon of *Il10*$^{-/-}$ mice, the IL17A cytokine initiates the inflammatory cascade even before histological signs of colitis [99]. The immune response is further driven by overexpression of interferon gamma (IFNG), coupled to a reduced frequency of Treg cells

that would otherwise dampen the inflammatory cascade [99]. The severity of chronic colitis depends on the mouse background strain, with those on a C57BL/6 background developing the least severe colitis when compared to other strains, such as BALB/c or 129/SvEv [109]. The importance of GIT microbiota in the development of IBD has been confirmed in humans, and appears to be similar in mice, as virtually no model develops IBD when raised under germ-free conditions [110-114]. *Enterococcus faecalis*, a bacterium commonly found in the GIT of humans and animals, was demonstrated to induce IBD, dysplasia, and carcinoma in germ-free *Il10*$^{-/-}$ mice [115]. *E. faecalis* and *E. faecium* (a second *Enterococci* commonly found in humans) were shown to increase colitis in *Il10*$^{-/-}$ mice at 12 weeks of age [116].

1.2 The concept of systems biology

Systems biology aims to provide a holistic view of how signalling networks lead to "emergent properties of the system as a whole" [117]. The phenotype of a living cell is defined by its intracellular processes: genetic information, in the form of DNA, is transcribed to mRNA, mRNA is translated to proteins, and the activity of proteins generates various molecules and metabolites (Figure 1.5) [118]. The increase or decrease in expression levels of a gene that codes for a certain protein does not necessarily result in changed protein abundance or activity [119]. Several influences, including the degradation of mRNA, post-translational modifications, and protein degradation can affect protein abundance and activity. Gene and protein expression changes only indicate cellular changes [120], whereas metabolites are definite products of metabolism [121]. Recent research has identified the GIT microbiota as a fourth level, which has been shown to be shaped by the genetic makeup of the host [122], dietary preferences [123, 124], and disease [125]. Systems biology aims to explore the interactions within and between each process using 'Omics'-technologies [117, 126-131]:

- Transcriptomics measures the complete collection of gene transcripts
- Proteomics measures the set of proteins encoded by the genome, as well as their isoforms and modifications
- Metabolomics measures the metabolite profile (*i.e.* metabolome); represents a vast number of components belonging to a wide range of compound classes
- Microbiomics classifies the microbial community structure

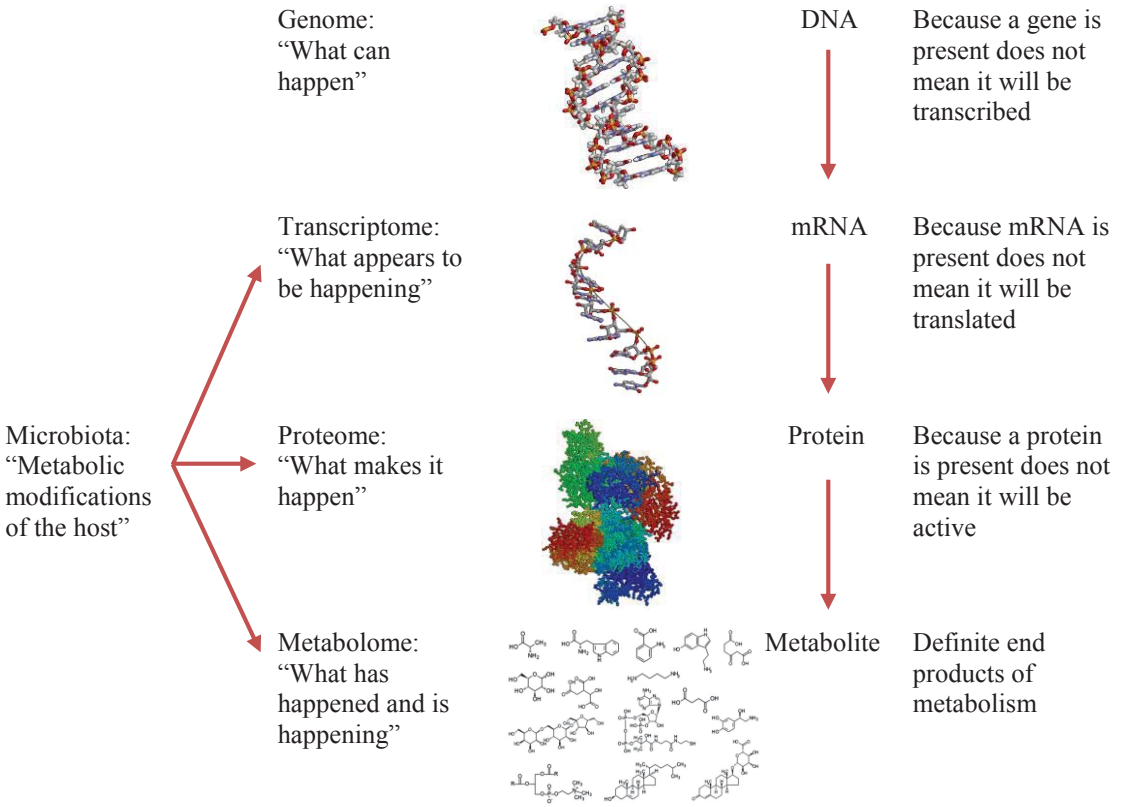

Figure 1.5 From genes to metabolites in biological systems and the influence of microbial metabolism (adapted from Dettmer *et al.* [132] and Roux *et al.* [133]).

The systems biology approach stands in opposition to the reductionist approach that focusses on one or two factors [134]. However, no single 'Omics' platform can fully explain the observed phenotype, and systems biology enables the assessment of an individual's response to, for example, nutritional intervention, by capturing multiple levels, for example genes, proteins, metabolites and microbiota, and may reveal how these processes interact to define the observed phenotype (*e.g.* colitis).

1.2.1 Nutrigenomics

From its research concept to practical application, nutrigenomics is a domain of systems biology [117]. The aim of nutrigenomics is to elucidate the molecular mechanisms underlying the interaction of the environment (nutrients) with a biological system (an individual's genome). In nutrigenomics research, nutrients are considered signalling molecules that can target the cellular sensor system, thus influence either the gene sequence itself, the transcription into RNA, the modification of proteins, or the presence of metabolites. These dietary signals can cause changes in the organism, tissues, or single cells, and can influence homeostasis [135-137]. An improved understanding of the interactions between diet and a biological system may be the key to a personalised strategy for health maintenance and/or reducing disease risk [138].

1.2.2 Exploration of biomarkers of intestinal inflammation

Biomarkers are defined as any factor that can be used as an indicator of a particular disease, risk of disease, or other physiological state, and can include molecules, genes, hormones, or even complex organ functions. In the case of IBD, biomarkers are objective indicators of colitis, and changes in these biomarkers can provide evidence of the efficacy of, for example, nutritional intervention. Exogenous metabolites may arise from the absorption, digestion and metabolism of food components (*i.e.* biomarkers of intake or exposure [139]) or represent diet-induced changes in endogenous metabolism and therefore offer access to unexplored metabolic pathways that are affected by diet (*i.e.* biomarkers of effect [140, 141]).

To investigate the efficacy of foods such as n-3 PUFA rich salmon as nutritional treatment in IBD, the use of appropriate biomarkers is crucial to monitor the effects that correlate with disease activity, ensuring improvement of conditions [10, 142]. A good

biomarker reflects metabolic or physiological changes associated with increased or decreased risk of chronic disease, and is detectable in the early stages of a disease to allow time for intervention as part of a preventative approach. In intervention studies with IBD patients, the general inaccessibility of the affected intestinal tissues requires a surrogate to reflect the metabolic or physiological changes induced by n-3 PUFA-rich diets in the inflamed tissue, and ideally, it can be collected with minimally invasive methods.

A pioneer study (EMBARK – EMerging BiomARKers in IBD) to discover biomarkers of CD and UC in easily accessible tissues was recently conducted [143], which suggested that faecal biomarkers may be a preferred surrogate "tissue" for IBD due to the ease of sample collection and specificity to the GIT [143-145]. It was reported that faecal calprotectin (also called S100A8/A9) and serum matrix metallopeptidase 9 (MMP9) correlated with disease activities in UC and CD, but lacked the ability to distinguish between the disease phenotypes. UC and CD differentiation was achieved by the addition of serum IL22, and showed good correlation with disease activity in CD. However, Pot *et al.* [146] showed that concentrations of faecal calprotectin were unaffected by the increased consumption of salmon for six months in patients with increased risk of colorectal cancer.

Peripheral blood mononuclear cells (PBMCs) infiltrate various tissues *via* the blood circulation and might contain information of metabolic or physiological changes that occur in other tissues [147]. PBMCs are round-nucleus blood cells (mainly comprise of lymphocytes, while monocytes, and dendritic cells are minor cell types [148-150]), and are critical components of the immune system. PBMCs have recently been used to study the effects of dietary intervention in healthy subjects [151] and in patients with chronic diseases [152-155]. In healthy elderly subjects, dietary fish oil reduced the expression of nuclear factor kappa B (NFKB) target genes, pro-inflammatory cytokines, and genes involved in eicosanoid synthesis in PBMCs [151], indicating the potential to use PBMCs in dietary intervention studies among IBD patients.

The minimally invasive nature of sample collection makes urine a convenient source for biomarkers of colitis [156-158]. Untargeted metabolic fingerprinting of human urine after the consumption of smoked salmon detected several metabolites, including trimethylamine N-oxide (TMAO), anserine and 1-methylhistidine. TMAO arose from the metabolism of trimethylamine, itself a degradation product formed from carnitine in fish.

The presence of anserine and 1-methylhistidine were connected to the metabolism of ingested histidine and histidine-derived dipeptides, which are abundant in the muscle of salmon. These metabolites were specific to those on the salmon diet, and absent in those not consuming salmon [139]. No study has yet investigated the effects of dietary salmon on urinary metabolites in connection with colitis in animal models or humans.

1.3 Dietary salmon and intestinal inflammation

Early evidence of the potential health benefits of fish was found among Greenlandic Inuit, where a correlation between dietary fish intake and a lower risk of coronary atherosclerotic diseases was established [159]. The food consumed by Inuit is mostly of marine origin and provides high amounts of long-chain (LC) n-3 PUFA (including eicosapentaenoic acid (EPA) and docosahexaenoic acid (DHA)). Compared to other foods, marine fish (especially salmon) are naturally rich in n-3 PUFA [160].

Recent studies have demonstrated the benefits of dietary fish intake in IBD [9, 146, 161]. In a study of 446 New Zealand CD patients who rated food items and their effects on disease symptoms, a positive association of salmon with IBD was reported [9]. No single food item was considered beneficial in all cases, but there were a limited number of foods frequently perceived as beneficial, including white fish, salmon and tuna. Results in this study were, however, based on the patients' perceptions, and these can be biased [81]. To confirm this association between perception and actual benefits of salmon intake, a metabolic or physiological measure of disease state (biomarker) would be required [135]. Other intervention studies involving patients with active CD have also shown favourable effects of dietary salmon on IBD. After eight weeks on a diet including 600 g Atlantic salmon per week, the clinical colitis activity index was improved and the plasma n-3/n-6 ratio increased [161]. Pot *et al.* [146] reported that the weekly consumption of two 150 g portions fatty (farmed salmon) or lean fish (Icelandic cod) lowered the levels of the systemic inflammation marker C-reactive protein (CRP) in the serum after six months, suggesting that lean fish has beneficial effects as well as oily fish in patients with previous colorectal adenomas or inactive UC. Nevertheless, concentrations of faecal calprotectin were unchanged by the fish intake in these patients [146].

1.4 Anti-inflammatory effects of specific salmon components

1.4.1 Micronutrients

Salmon contains micronutrients which could compensate for the nutritional deficiencies that are commonly observed in IBD subjects from poor dietary intake [162] or impaired nutrient absorption [163]. Of particular clinical relevance are deficiencies in calcium, vitamins D, B6, B12, and E [164, 165], all of which are present in salmon (Table 1.4). Several of these micronutrients have shown to suppress inflammation in rodents with experimental colitis. For example, supplementing diets with vitamin D and calcium showed protective effects in *Il10*$^{-/-}$ mice (associated with tumor necrosis factor (TNF) pathway) [166] and selenium protected rats with experimental colitis [167].

Vitamin E is naturally present in salmon (mostly as α-tocopherol [168]) and as an antioxidant protects against lipid peroxidation in the muscle of the fish [169]. This antioxidant property of vitamin E could be useful in intestinal inflammation. n-3 PUFA are prone to peroxidation, and oxidised PUFA can activate transcription factors such as NFKB and subsequently trigger pro-inflammatory gene expression. A study has shown that diets supplemented with α-tocopherol protected rats from the oxidative stress associated with colitis [170]. Nevertheless, conflicting results regarding the anti-inflammatory and cancer-preventative features of tocopherols have been reported. The Selenium and Vitamin E Cancer Prevention Trial (SELECT) demonstrated that supplementation with α-tocopherol increased the risk of prostate cancer in healthy men [171, 172]. The authors further observed a 50% decrease of γ-tocopherol in plasma, concluding that the α-tocopherol supplementation may have reduced the beneficial effects of γ-tocopherol (potentially linked to bioavailability). While the tocopherol levels in plasma of the study participants were sufficient before supplementation, it was suggested that vitamin E supplementation may only benefit patients with a vitamin E deficiency [173], including those with IBD [164]. A unique form of vitamin E was identified in marine animals and termed “marine-derived tocopherol” (MDT) [174]. Further research discovered that MDT is specific to fish from cold-water environments and protects against lipid peroxidation at lower temperatures [175, 176]. While its structure is similar to α-tocopherol, it is biologically more active than other forms of tocopherol [177], and may further explain the health benefits of dietary fish.

Table 1.4 Nutritional profile of farmed New Zealand Chinook salmon fillets (*Oncorhynchus tshawytscha*).

Component	*Amount*
Energy	1334 kJ
Protein	18.0 g
Carbohydrate	<1.0 g
Fat	23.1 g
Saturated	4.9 g
Trans	0.05 g
Monounsaturated	7.7 g
Polyunsaturated	5.2 g
Omega-3	3.1 g
Eicosapentaenoic acid (EPA)	1.0 g
Docosahexaenoic acid (DHA)	1.3 g
Docosapentaenoic acid (DPA)	0.5 g
Alpha linolenic acid (ALA)	0.2 g
Omega-6	2.1 g
Linoleic acid (LA)	1.7 g
Arachidonic acid (AA)	<0.1 g
Elements	
Sodium	28 mg
Potassium	374 mg
Phosphorus	235 mg
Magnesium	26 mg
Calcium	9.2 mg
Iron	0.2 mg
Selenium	0.02 mg
Iodine	0.005 mg
Vitamins	
Vitamin A	0.06 mg
Vitamin B1 (Thiamine)	0.15 mg
Vitamin B2 (Riboflavin)	0.10 mg
Vitamin B3 (Niacin)	6.79 mg
Vitamin B6	0.47 mg
Vitamin C	3.00 mg
Vitamin D	0.02 mg
Vitamin E	5.31 mg
Vitamin B12	<0.01 mg

Table adapted from The King Salmon Company webpage [178], accessed 29th September 2011. Values presented per 100 g fresh fillet without skin.

1.4.2 Peptides

After digestion, peptides are either absorbed through the intestinal wall and/or affect the intestine locally [as reviewed in 179]. The antioxidant activity of fish protein hydrolysates (breakdown products of enzymatic conversion of fish proteins into smaller peptides [180]) has previously been shown [181-183] and potentially induce synergistic effects in combination with other nutrients [184, 185]. For example, Grimstad *et al.* [185] demonstrated that the expression of selected genes and pro-inflammatory cytokines (*e.g.* TNF or IL1B) were largely unaffected by dietary supplementation with hydrolysed salmon peptides or a fish oil diet in rats with DSS-induced colitis, but the combined supplementation of these fish products revealed synergistic effects on eicosanoid synthesis. While the fish oil diet increased the levels of EPA-derived eicosanoid prostaglandin E3 in the colon, the combined supplementation of fish oil and peptides further increased its levels. The authors linked this increase to elevated enzymatic activity of prostaglandin-endoperoxide synthase 2 (PTGS2, also called COX2), the enzyme that metabolises EPA to prostaglandin E3 [185].

1.4.3 Lipids

New Zealand Chinook salmon (*Oncorhynchus tshawytscha*) has a higher natural oil content than other salmon species [186, 187]. Fatty acids, comprising a hydrocarbon chain with a carboxyl moiety at one end and a methyl group at the other, are the major building block for complex lipids and can be saturated (no double bond between the carbon atoms), monounsaturated (one double bond (MUFA)), or polyunsaturated (two or more double bonds (PUFA)). The classification into n-3 and n-6 PUFA is based on the position of the first double bond starting from the methyl end of the hydrocarbon chain. Short-chain fatty acids (SCFA) refer to 19 or fewer carbon atoms, and long-chain to 20-24 carbon atoms. Lipids play critical roles in the body, from structural (as membrane phospholipids), to sources of energy, and cell signalling.

In particular the LC n-3 PUFA DHA and EPA (and to a yet unknown extent docosapentaenoic acid (DPA)) are thought to be important for maintaining health. EPA and DHA are supplied to tissues from dietary sources, either directly or *via* the precursor n-3 PUFA α-linolenic acid (ALA). ALA cannot be synthesised in the human body and must be derived from the diet. The conversion of ALA to longer-chain n-3 PUFA occurs

via several elongation and desaturation steps that mainly take place in the liver (Figure 1.6). The conversion of ALA to EPA is, however, limited and further conversion from EPA to DHA is even lower [188, 189]. The limiting steps in these conversions are the competition for the same enzymes in the n-6 pathway (metabolising the precursor n-6 PUFA linoleic acid (LA) to arachidonic acid (AA) (Figure 1.6)). Additionally, the activities of the enzymes depend on diet [80], hormones [190], and feedback inhibition by end products [191, 192]. Hence, direct DHA and EPA supplementation is more effective than *de novo* synthesis in increasing circulating LC n-3 PUFA concentrations.

Several studies have tested the anti-inflammatory potential of pure n-3 PUFA or fish oil (as a source of PUFA), however the results of these studies are inconsistent. Some studies reported detrimental effects of fish oil diets on colitis in *Il10*$^{-/-}$ mice [193] or in infectious colitis mouse models [194]. Others have reported reduced colitis in response to fish oil diets in TNBS-dosed rats [195] and in *Il10*$^{-/-}$ mice [196], in DSS-dosed rats fed a soybean/fish oil mixture [5] and in DSS-dosed rats fed an olive oil/fish oil mixture [7]. These studies were conducted with a mixture of DHA and EPA and observed effects cannot be specifically attributed to DHA or EPA. Some studies have reported potential anti-inflammatory effects of pure EPA in *Il10*$^{-/-}$ mice [6] and DSS-dosed mice [197]. The inconsistent results between these studies using n-3 PUFA diets may arise from differences in IBD induction models, intervention times (prevention vs. treatment), the dose of PUFA, lipid profiles of diets, or changes in bioavailability. Furthermore, Trebble *et al.* [198] demonstrated that the production of the pro-inflammatory cytokines TNF and IL6 by PBMCs appeared to show a "U-shaped" dose-response after n-3 PUFA supplementation. In this study, the supplementation of dietary fish oil in healthy humans resulted in decreased TNF and IL6 production by LPS-stimulated PBMCs at the lowest level (0.3 g/d n-3 PUFA). Maximum inhibition was observed at intermediate levels (1.0 g/d n-3 PUFA), and the least inhibition was seen at the highest supplementation levels (2.0 g/d n-3 PUFA). It was hypothesised that molecular mechanisms by which n-3 PUFA affects cytokine production could have maximum effects at different intake levels of n-3 PUFA, resulting in the observed "U-shaped" dose-response curve [198]. The timing of PUFA supplementation may also be an important factor [199]; feeding diets before colitis induction could have different effects (preventive) when compared with a therapeutic approach (where diets are fed when colitis is already present [199]).

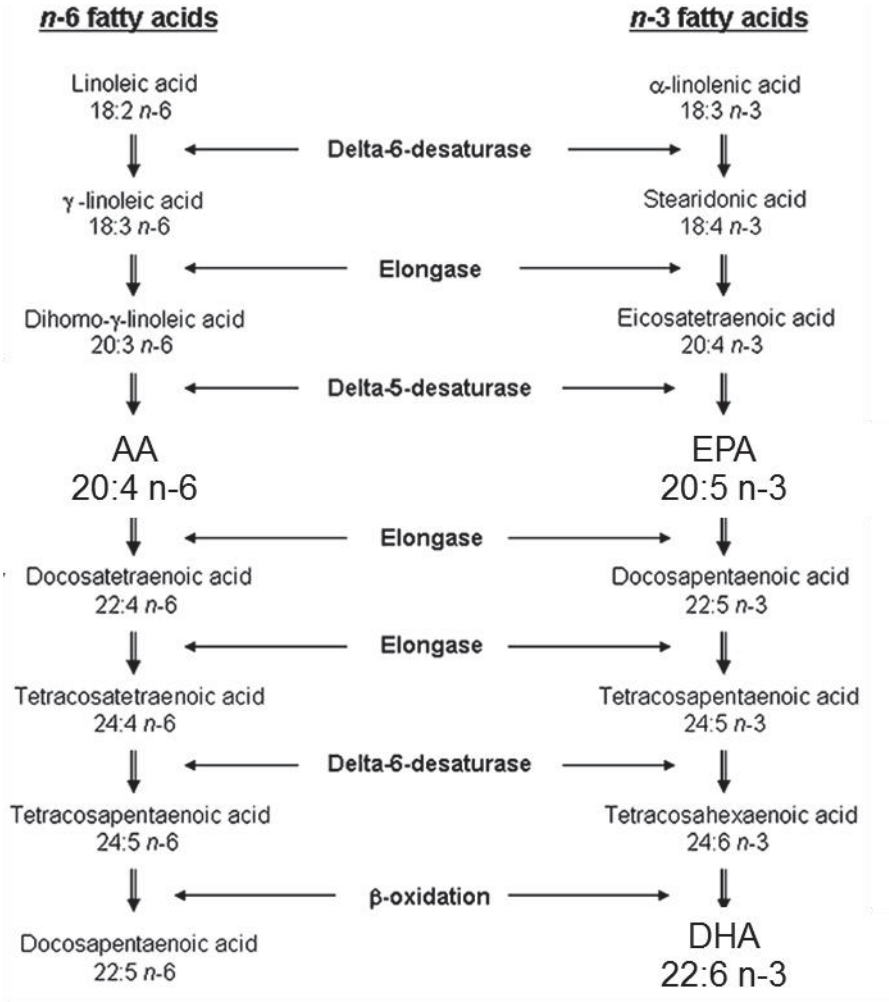

Figure 1.6 Metabolism of omega-6 and omega-3 polyunsaturated fatty acids (n-6 and n-3 PUFA) from precursor fatty acids with focus on arachidonic acid (AA) in the n-6 pathway and eicosapentaenoic acid (EPA) and docosahexaenoic acid (DHA) in the n-3 pathway [adapted from 200].

The anti-inflammatory effects of n-3 PUFA may be different when in a food due to changes in bioavailability of n-3 PUFA [201]. Bioavailability is defined as "the proportion of a drug or nutrient which enters the circulation when introduced into the body and so is able to have an active effect" [202]. Fish intake may increase the bioavailability of n-3 PUFA because (i) the ingestion of whole foods is followed by a more effective activation of digestion/absorption in the intestine compared to capsules [203-205]; (ii) lipids in salmon are mostly in the form of triacylglycerol (TG), with n-3 PUFA mostly in central position of the TG molecule (which facilitates absorption [206, 207]); and (iii) the bioavailability of EPA is improved when ingested with a high-fat meal [208]. Human studies have reported that eating salmon was more efficient in increasing n-3 PUFA levels in serum and plasma than taking fish oil capsules [204, 205]. However, this contrasts to results from Arterburn *et al.* [209], who reported that algal oil capsules and cooked salmon were comparable in terms of bioavailability of DHA to plasma phospholipids and erythrocytes. The results of these studies [204, 205, 209] may depend on several factors [210], including genetic differences of the individual subjects, the oxidation rate of n-3 PUFA in capsules, and differences in encapsulation (*e.g.* hard vs. soft gelatine capsules).

The duodenum and jejunum are the main sites for lipid digestion [211, 212], where digestive enzymes hydrolyse TG (the main form of dietary lipids) to monoacylglycerols and fatty acids and further form mixed micelles (Figure 1.7). Micelles diffuse to the brush border of the enterocytes, where the lipid substances are absorbed by epithelial cells. Absorption is facilitated by transport proteins, namely plasma membrane-associated fatty acid binding protein (FABPpm) [213], CD36 [214] and fatty acid transport protein 4 (FATP4) [215]. Whether passive diffusion or transporter-facilitated absorption dominates is unclear, and while this may depend on fatty acid concentration, Schwenk *et al.* [216] suggested transporter-mediated absorption dominates. In the enterocytes, fatty acids and 2-monoacylglycerols are transported to the endoplasmic reticulum in association with a family of proteins known as cytoplasmic fatty acid binding proteins (FABPc) [as reviewed in 217] where they are re-esterified, forming first diacylglycerols, then TG (Figure 1.7). Newly synthesised TG are transported out of the enterocyte in the form of chylomicrons and enter the lymphatic capillaries in the intestinal villi. Chylomicrons are supplied to peripheral tissues *via* the bloodstream, while only approximately 2% of dietary lipids enter the colon *via* the intestinal lumen [218].

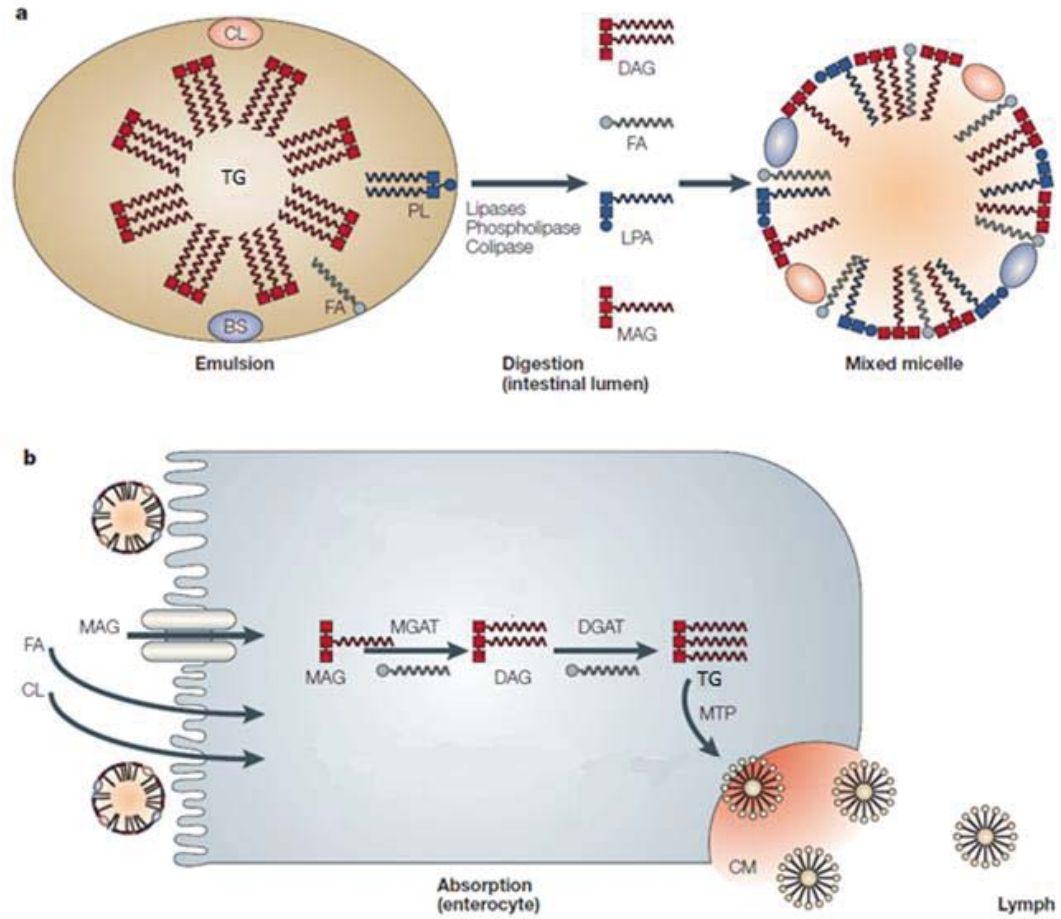

Figure 1.7 Intestinal digestion and absorption of dietary lipids. (A) The main site for lipid absorption is the small intestine, where large fat droplets are emulsified with bile salts from the liver. Pancreatic juices hydrolyse TG to monoacylglycerol, diacylglycerol, and fatty acids, and phospholipids to lysophosphatidic acid. Micelles are formed from digestive products and mixed with bile salts and cholesterol. (B) Mixed micelles diffuse to the brush-border of the enterocytes, where micelles are broken down and digestive products enter the enterocytes by passive diffusion and facilitated by transporters. Intracellular enzymes re-esterify free fatty acids and monoacylglycerols sequentially to diacylglycerols and TG. TG enter the lymphatic capillaries in form of chylomicrons. Adapted from Shi *et al.* [219] with permission from Macmillan Publishers Ltd: Nature Reviews.

BS: Bile salts; CL: Cholesterol; CM: Chylomicrons; DAG: Diacylglycerol; DGAT: Diacylglycerol acyltransferase; FA: Free fatty acids; LPA: Lysophosphatidic acid; MAG: Monoacylglycerol; MGAT: Monoacylglycerol acyltransferase; MTP: Microsomal triglyceride transfer protein; PL: Phospholipids; TG: Triacylglycerol.

1.4.4 Putative mechanisms of action of lipids

After hydrolysis of TG to free fatty acids and glycerol, fatty acids pass through the capillary walls to be utilised as major substrates for energy production, storage, and induction of signalling and metabolic processes in cells. The overall physiological outcome in cells depends on several factors, for example, cell-specific fatty acid metabolism (oxidative pathways, kinetics, and competing reactions), cellular abundance and type of membrane receptors and transcription factors, and quantity and type of the fat ingested [as reviewed in 220]. It is suggested that an increased intake of n-3 PUFA results in a partial membrane replacement of n-6 PUFA in virtually all cell types, including PBMCs [155, 221], neutrophils [222, 223], red blood cells [224], lamina propria lymphocytes [225], and colonocytes [226]. Putative mechanisms of action of n-3 PUFA on immune cell function are illustrated in Figure 1.8 and include alterations in (i) cell membrane composition, (ii) lipid mediator synthesis, (iii) gene expression, and (iv) protein expression. Furthermore, the increased intake of n-3 PUFA potentially affects the membrane fatty acid composition of bacterial adhesion sites on intestinal epithelial cells [227] and the adhesion of bacterial strains to the mucosal surface in the intestine [228], hence impacting on the microbial community structure and its function.

1.4.4.1 Modulation of cell membrane lipid rafts

Lipid rafts are micro-domains in the cell membrane enriched with sterol- and sphingolipids that, upon activation, compartmentalise the activated receptor complexes and associated signal-transducing molecules [229]. It is suggested that lipid rafts serve as signalling platforms and are involved in T cell activation [230], transcriptional activation [231], and cytokine secretion [232, 233], potentially playing a role in chronic inflammation. The dietary intake of foods rich in EPA and DHA results in a partial membrane replacement of n-6 PUFA [234] that modulates the lipid composition of the cell membrane and affects signalling pathways [221, 235-237]. It is suggested that this replacement occurs in most cells, but especially in platelets, erythrocytes, neutrophils, monocytes, and liver cells [as reviewed in 238]. It remains unknown whether DHA and EPA exert similar effects on rafts, but it is suggested that EPA is less efficient in modulating lipid rafts compared to DHA [239].

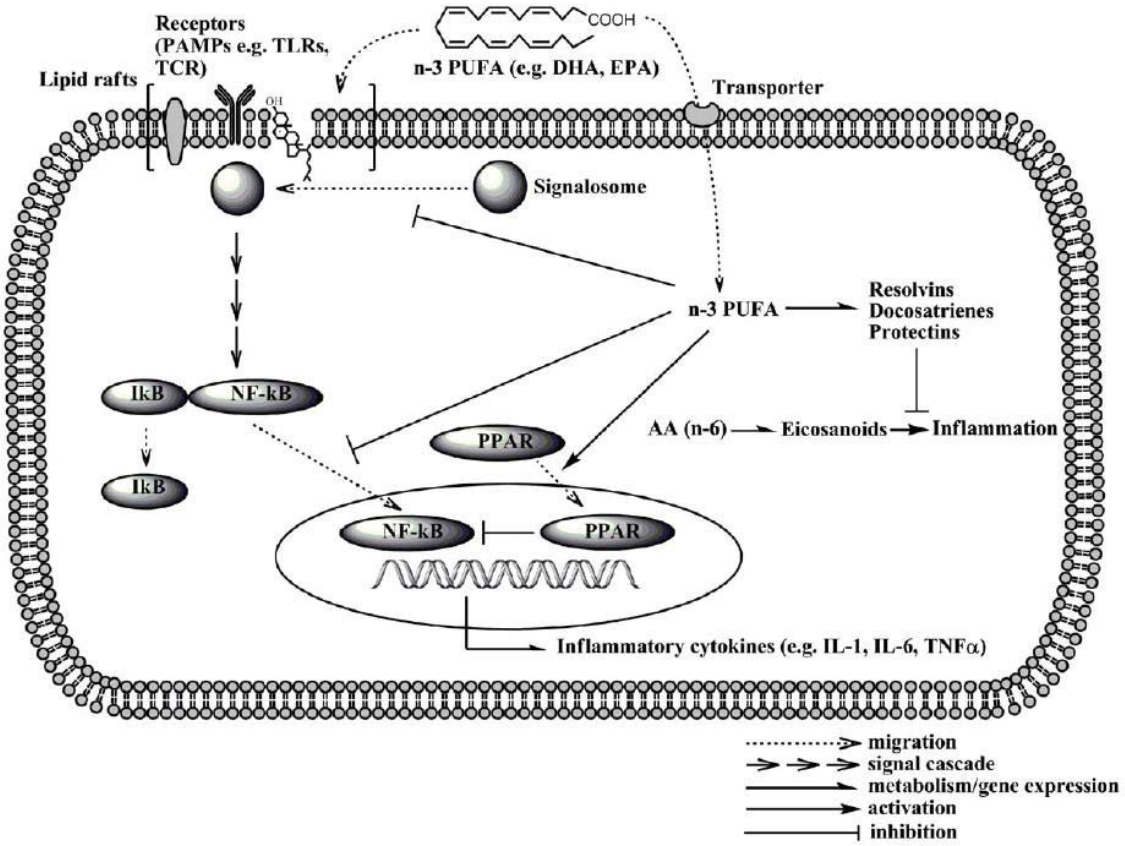

Figure 1.8 Putative mechanism of action of omega-3 polyunsaturated fatty acids (n-3 PUFA) on immune cell functions. These include alterations in lipid mediator synthesis, gene/protein expression, lipid composition of cell membrane and signal transduction. Reprinted from Chapkin *et al.* [240] with permission from Elsevier.

AA: Arachidonic acid; DHA: Docosahexaenoic acid; EPA: Eicosapentaenoic acid; IκB: Nuclear factor of kappa light polypeptide gene enhancer in B-cells inhibitor; IL: Interleukins; NF-κB: Nuclear factor kappa B; PAMPs: Pathogen-associated molecular patterns; PPAR: Peroxisome proliferator-activated receptor; TCR: T cell receptor; TLR: Toll-like receptor; TNFα: Tumor necrosis factor.

1.4.4.2 Formation of lipid mediators

Lipid mediators, including eicosanoids, resolvins and protectins, are regulators of inflammation and are generated from intracellular PUFA (Figure 1.8), with its biological activity and potency dependent on the type of PUFA. The majority of eicosanoids derived from AA are pro-inflammatory, however prostaglandin E_2 and lipoxin have been shown to exert anti-inflammatory effects [241]. During the inflammatory response, AA-derived lipid mediators (pro-inflammatory prostaglandins and leukotrienes) are produced and secreted within seconds to minutes recruiting neutrophils to the site of inflammation. Over the next hours to days, leukocytes, monocytes and macrophages appear that further increase lipid mediator concentration [as reviewed in 242]. The pro-resolution phase that follows is characterised by increased secretion of pro-resolving mediators from LC n-3 PUFA. EPA gives rise to the anti-inflammatory eicosanoids and resolvins (*e.g.* series-3 prostaglandins and thromboxanes, series-5 leukotrienes, and E-series resolvins) and hydroperoxy- and hydroxy-eicosapentaenoic derivatives [243, 244]. DHA gives rise to both anti-inflammatory and pro-resolution mediators (*e.g.* resolvins and neuroprotectin) [245, 246]. The enzymes which catalyse these conversions include cyclooxygenases (COX), lipoxygenases (LOX), and cytochrome P450s (CYP) [as reviewed in 247]. Thus, by increasing dietary n-3 PUFA, lipid mediator production could be altered to decrease (mainly) pro-inflammatory lipid mediators from n-6 PUFA, while increasing anti-inflammatory resolvins from n-3 PUFA EPA and DHA [243].

1.4.4.3 Modulation of gene expression

Apart from altering lipid mediator synthesis and lipid raft composition, fatty acids can affect gene expression [220]. The mechanisms for these influences may be *via* intermediates (*e.g.* transcription factors, nuclear hormone receptors and lipid secondary messengers) that subsequently alter gene expression, or by direct interaction with target genes [248]. The expression of genes encoding several key proteins involved in inflammation, metabolism and energy utilisation have been reported to be modulated by n-3 PUFA.

PUFA-enriched diets were able to alter the expression of several genes associated with inflammation by modulating the transcription factors *NFKB* and peroxisome proliferator-activated receptor (*PPAR*) in inflamed tissues [3, 4, 249-252]. The three isotypes *PPARA*, *PPARB/D* and *PPARG* are encoded by different genes and

exhibit broad, isotype-specific tissue expression patterns [253, 254]. When activated by ligand binding, PPARs can form heterodimers with the retinoid X receptor (RXR) and the dimer subsequently binds to specific response elements (PPREs) within promoter regions of target genes, modulating gene transcription [as reviewed in 255]. *PPARA* was shown to be an important transcriptional regulator in the small intestine [256], and *PPARA* deficiency was also connected to impaired hepatic lipid oxidation capability [257]. As natural receptors of fatty acids, the expression of *PPARA* was increased by EPA-enriched diets in the colon of *Il10*$^{-/-}$ mice [6]. This activation of *PPARA* was associated with reduced *NFKB* gene expression, a regulator of the inflammatory response and oxidative stress [4], and may partly explain the reduced severity of colitis in those mice [6]. In a pig model of IBD, dietary n-3 PUFA activated *PPARD* gene expression and accelerated colonic regeneration and clinical remission [3]. Supplementation of EPA and DHA in the form of fish oil also increased the *PPARG* isoform in myocardial tissue of cardiac surgery patients [251].

Studies in mice support the reduced expression of several pro-inflammatory cytokines (*e.g. IL1B* and *TNF*) or chemokine receptors (*e.g. CCR5*) after PUFA supplementation. AA-enriched diets decreased levels of *IL1B* transcripts in the inflamed colon of *Il10*$^{-/-}$ mice [258], but *IL1B* was not differentially expressed after EPA supplementation compared to a control diet [6, 259]. The evidence for DHA was inconclusive; Cho *et al.* [260] reported reduced levels of colon *IL1B* in a DSS mouse model, but Turk *et al.* [259] did not detect changes in a similar model. However, Turk *et al.* [259] further showed that the continued supplementation of DHA to mice with colitis decreased *IL1B* gene expression levels in the colon compared to wild-type mice shortly after DSS treatment was stopped. The effects of EPA on *TNF* gene expression in mouse models of IBD were inconclusive. In *Il10*$^{-/-}$ mice, EPA-enriched diets did not affect colon mRNA transcript levels of *TNF* [6], but decreased *TNF* levels were observed in the DSS-dosed mice after EPA supplementation [259]. DHA supplementation did not change *TNF* expression in the inflamed colon of mice compared to those fed a control diet [259, 260]. A meta-analysis in humans with chronic diseases reported that fasting blood levels of TNF and IL6 were decreased, with intakes of oils containing mixtures of n-3 PUFA. When evaluating the effects of fish intake in chronic diseases, the study noted a lowering effect on blood IL6 levels, but no influence on TNF levels [261].

Furthermore, EPA- and AA-enriched diets induced the expression of genes associated with metabolism of xenobiotics (*i.e.* foreign compounds) in the colon of *Il10*$^{-/-}$ mice compared to those fed a control diet (*e.g.* CYP, glutathione S-transferases, and membrane-bound ATP-binding cassette transporter proteins). These proteins interact to transform and eliminate xenobiotics that could damage the intestinal epithelial surface [as reviewed in 262, 263]. In IBD, the elimination of xenobiotics is perturbed and could contribute to the pathophysiology of the disease by damaging the epithelium [264]. The increase in expression of xenobiotic metabolism genes during EPA and AA supplementation may have supported xenobiotic elimination from the colonic epithelial cells, and reduced toxin damage in the colon of *Il10*$^{-/-}$ mice.

1.4.4.4 Modulation of protein expression

Gene expression analysis explains only part of the observed phenotype, as the increase or decrease of expression levels of a gene that code for a certain protein does not necessarily result in changed protein abundance [130]. A number of other factors can also affect protein abundance, including mRNA degradation, post-translational modifications (affecting the activity of the protein produced), and protein degradation.

The reduced functionality of biochemical pathways in mice with experimental colitis may result in inadequate energy resources for epithelial cells during the inflammatory response [265, 266]. The depleted energy levels may further affect important processes, for example selective permeability or epithelial nutrient transport, which may exacerbate colitis. Similar observations were made in IBD patients, where decreased expression of several genes involved in the metabolism of fatty acids was detected in mucosal biopsies (*e.g.* fatty acid transport proteins and fatty acid binding proteins [267]). In *Il10*$^{-/-}$ mice, AA-enriched diets may have enhanced pathways related to energy homeostasis [268], potentially contributing to improved colon tissue morphology compared to those fed control diets [258]. Increased expression of proteins in metabolic pathways were observed in glycolysis (aldehyde dehydrogenase (ALDH1B1) and pyruvate kinase (PKM2)), citrate cycle (aconitase 2 (ACO2)), fatty acid metabolism (FABP 4 and 6 and ALDH1B1) and oxidative phosphorylation (ATP synthase (ATP) 5A1 and 5B). This may have provided the mucosal cells with more energy for a more robust response to inflammation, and the ability to support other energy-demanding processes [268]. When *Il10*$^{-/-}$ mice were fed an EPA-enriched diet, these

metabolic modifications were not observed in the colon [268]. Nevertheless, in healthy C57BL/6 mice, fish oil supplementation modified hepatic protein expression of several metabolic pathways, for example, lipid metabolism, carbohydrate metabolism, and citric acid cycle [269], further supporting the findings that n-3 PUFA may beneficially influence metabolic pathways but these effects may be dependent on tissue.

The improvement in colon tissue morphology in response to EPA supplementation may have also been due to changes in the expression levels of proteins in signalling processes. Transcriptomic analysis showed EPA-enriched diets activated *PPARA* gene expression in the inflamed colon of *Il10*$^{-/-}$ mice, which may have inhibited the NFKB signalling cascade and contributed to reduced severity of colitis in those mice compared to when they were fed a control diet [6]. Proteomic analysis supported these results, showing that EPA may have influenced PPARA signalling by reducing expression of a heat shock protein (HSP) in *Il10*$^{-/-}$ mice [268]. HSP90 has been shown to inhibit PPARA activity *in vitro* [270], thus reduced expression of HSP90AB1 in *Il10*$^{-/-}$ mice in response to EPA supplementation may have resulted in increased activity of the nuclear receptor and subsequently modified expression of its target genes [268].

1.4.4.5 Modulation of the intestinal microbiota

The intestinal microbiota can influence host gene expression [271, 272], post-translational protein modification [273], induce Th17 cell differentiation [274], and alter intestinal barrier function [275]. Diet can affect the intestinal microbial composition [123, 124] and its function [276]. Previous studies suggested that dietary PUFA may be able to modify the membrane fatty acid composition of bacterial adhesion sites on intestinal epithelial cells [227, 277]. This could affect the adhesion of bacterial strains to the mucosal surface in the intestine [228] and promote or prevent the growth of certain types of bacteria. For example, when *Il10*$^{-/-}$ mice were fed an EPA-rich diet, an increase in *E. coli* numbers was detected, combined with a reduction in colitis [6, 277]. The authors concluded that by modulating the fatty acid composition of bacterial adhesion sites, non-virulent strains of *E. coli* colonisation may have been favoured in the caecum [277]. Subsequently, *E. coli* may have formed a biofilm, thereby protecting the epithelium by limiting attachment of other bacteria [278].

In an infectious murine model of colitis the colon microbial community was different between mice fed a corn oil-rich diet and those fed a fish oil-rich diet [279].

While mice fed the corn oil diet showed increased numbers of *Enterobacteriaceae*, segmented filamentous bacteria and *Clostridia* spp., those fed the fish oil diet showed reduced growth of these bacteria, and further favoured the growth of *Bifidobacteria* spp. and *Lactobacillus* spp. The authors concluded that n-3 PUFA-rich fish oil limited detrimental bacteria while promoting the growth of beneficial bacteria, such as *Lactobacillus* spp. and *Bifidobacteria* spp. [279]. *Lactobacillus* spp. and *Bifidobacteria* spp. are probiotic strains that may have promoted epithelial barrier integrity thus contributing to the reduced colitis in the fish oil-fed mice [279].

1.5 Conclusion and outlook

IBD is a group of disorders of the GIT with yet unknown causes. It is postulated that a complex interplay between genetic factors, the commensal microbiota, and the environment drives an excessive immune response that leads to chronic inflammation in the GIT. Research into the effects of dietary n-3 PUFA using pure EPA reported reduced colitis in mouse models of IBD. This mitigation of colitis was attributed to the effects of n-3 PUFA on molecular processes in the colon, specifically the expressions of genes and proteins in inflammatory processes and metabolic and signalling pathways, and the alteration of the microbial composition in the large intestine. Not all studies using fish oil or other PUFA mixtures reviewed here reported beneficial effects in colitis, and it has been suggested that a dose-response may explain the inconsistent evidence.

It remains to be determined whether LC n-3 PUFA modulate similar gene and protein regulatory mechanisms in colitis when consumed as a food such as salmon. Using food frequency questionnaires among IBD patients showed the potential to alleviate symptoms of IBD with dietary salmon, but the general inaccessibility of the human colon and other tissues makes these molecular and physiological responses (beneficial or adverse) difficult to obtain. An increasing body of research has used accessible “tissues” such as PBMCs, urine and faeces as surrogates for these responses. While there is some research into the effects of dietary n-3 PUFA in these “tissues”, the value of PBMCs, urine or faeces for biomarkers of colitis that are responsive to dietary salmon has not been determined. Ultimately, the utilisation of valid, specific and sensitive biomarkers may allow early detection of metabolic or physiological changes (translating to beneficial or adverse effects of diet) in IBD after dietary intervention with salmon and better predict the effect of diet (*i.e.* enriched in salmon) to reduce the risk of IBD. To date there are no

biomarkers of colitis that predict responses to dietary intervention with n-3 PUFA-rich salmon.

1.6 Hypothesis and aims of the dissertation

The aims of this dissertation were to determine the molecular, morphological and/or metabolic changes induced by n-3 PUFA-enriched diets on colitis, demonstrate that these effects are also observed for food rich in n-3 PUFA, and further mine these responses to n-3 PUFA for identifying candidate biomarkers of colitis in surrogate "tissues". Using a systems biology approach, the changes after supplementation with dietary salmon were determined on multiple processes, *i.e.* gene and/or protein expression in colon/liver/PBMCs, the community profile of the caecal microbiota and urinary metabolite abundance. This novel systems approach is different to the usual reductionist approach, which investigates only one process at a time, and may omit important information of the effects of n-3 PUFA in colitis. Beyond this dissertation, these effects of n-3 PUFA could support the validation of candidate biomarkers for use in human dietary intervention studies. This will allow early detection of the responses to intervention with n-3 PUFA-rich foods such as salmon, and potentially enable a complementary solution to conventional treatments in IBD.

The main hypotheses were that diets enriched with (i) purified EPA and (ii) EPA-containing salmon reduce the risk of developing colitis in the *Il10*$^{-/-}$ mouse model of IBD by altering the expression of genes and proteins in the colon and/or liver and affect the microbial community profile, (iii) surrogate "tissues" (blood and urine) contain information of the changes in colitis in response to EPA/salmon-enriched diets, and (iv) these surrogates are useful sources of candidate biomarkers of the impact of n-3 PUFA on colitis.

1.7 Approach and structure of the dissertation

A flowchart of the dissertation structure is shown in Figure 1.9. To achieve the aims of this dissertation, two dietary interventions using n-3 PUFA-enriched diets were carried out in *Il10*$^{-/-}$ mice ("EPA time-course experiment" and "salmon diet experiment"). In both experiments, the effects of n-3 PUFA-enriched diets on colitis were measured using high-throughput 'Omics'-technologies, *i.e.* transcriptomics (gene expression), proteomics

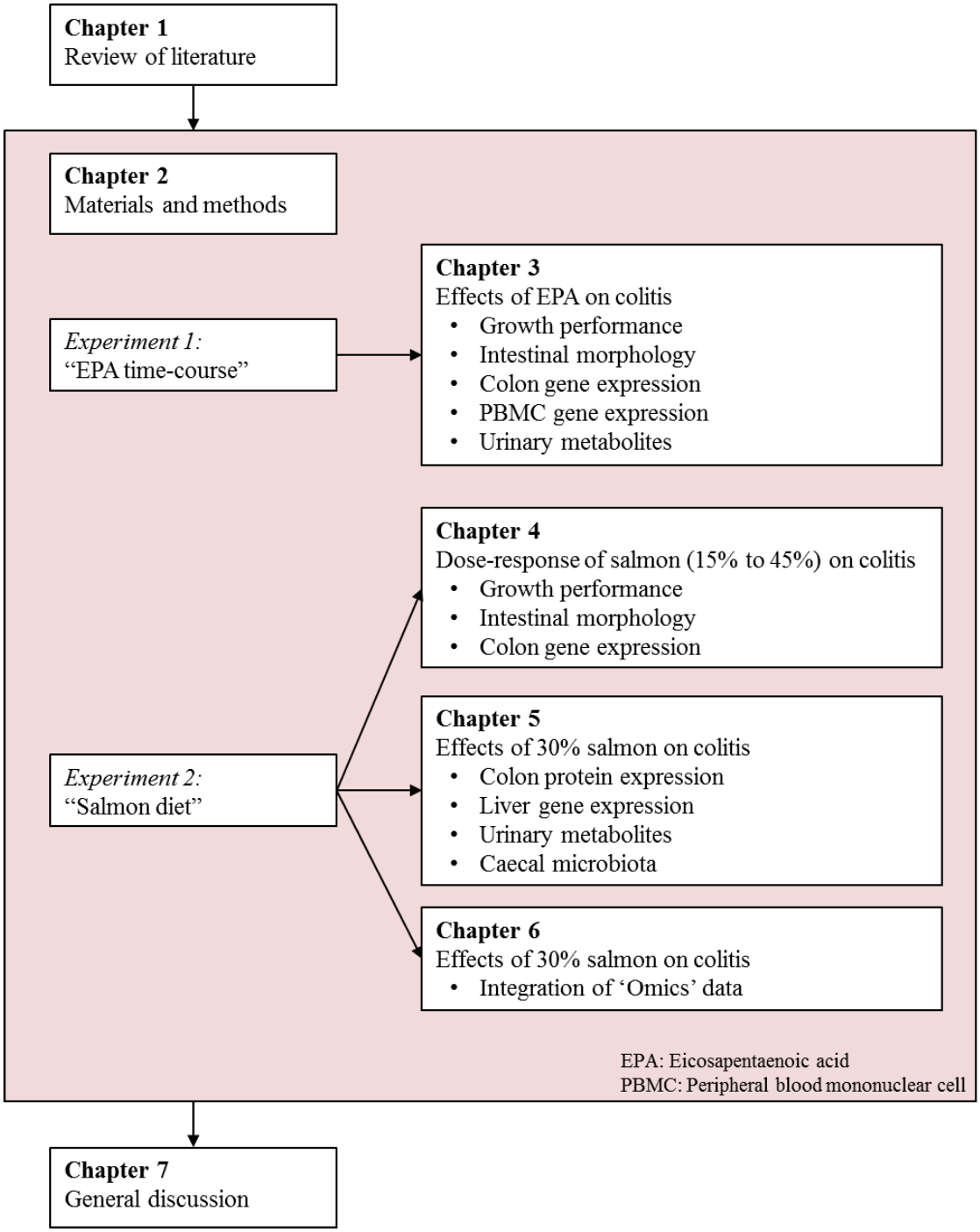

Figure 1.9 Overview of chapters in this dissertation.

(protein expression), metabolomics (metabolite abundance) and/or microbiomics (microbial community profile). Chapter 2 describes these 'Omics'-technologies in detail.

The "EPA time-course experiment" was performed to determine the value of blood and urine as surrogate "tissues" to monitor the effects of EPA-enriched diets during the development of colitis and when colitis was established (Chapter 3). *Il10*$^{-/-}$ and C57BL/6J mice were fed a diet supplemented with 3.7% EPA and severity of colitis, colon and PBMC gene expression profiles, and urinary metabolite profile were assessed at early stages of colitis (9 weeks of age) and/or when established (12 weeks of age).

The "salmon diet experiment" was performed to determine whether an EPA-rich food such as salmon reduces the severity of colitis. *Il10*$^{-/-}$ and C57BL/6J mice were fed one of three diets supplemented with controlled amounts of lyophilised salmon fillets (15%, 30% or 45%) and severity of colitis and colon gene expression profiles were assessed when colitis was established (Chapter 4).

Colon protein expression was performed to determine whether it provides novel insights into regulatory mechanisms by which a diet containing 30% salmon improved the colon inflammatory phenotype in *Il10*$^{-/-}$ mice. PBMCs were not a suitable predictor of the molecular responses to the EPA diet, therefore liver gene expression was analysed to provide additional knowledge to colon molecular responses, supporting the identification of candidate biomarkers of colitis. The intestinal microbiota was analysed to determine signature shifts in the community profile in response to the 30% salmon diet that could be mined for biomarkers of colitis in accessible "tissues" such as human faeces. The value of urinary metabolites as candidate biomarkers to monitor the effects of dietary salmon on colitis were further assessed (Chapter 5).

To identify candidate biomarkers of colitis in *Il10*$^{-/-}$ mice fed a 30% salmon diet, data from individual 'Omics' platforms were integrated to show biological interactions (Chapter 6).

Chapter 7 comprises the general discussion and summarises how these 'Omics' platforms contribute to the identification of candidate biomarkers for future animal and human nutritional intervention studies to assess the effect of n-3 PUFA-rich diets on colitis.

Chapter 2

Materials and Methods

2.1 Introduction

To achieve the aims of this dissertation outlined in Chapter 1, two dietary interventions in the *Il10*$^{-/-}$ mouse model of IBD were carried out ("EPA time-course experiment" and "salmon diet experiment"):

- The "EPA time-course experiment" was carried out to determine colitis phenotype and colon gene expression in *Il10*$^{-/-}$ mice at early stages of colitis and when established, the effects of an EPA-enriched diet on those, and the value of accessible "tissues" such as blood and urine as surrogates for these responses.
- The "salmon diet experiment" was carried out to determine whether an EPA-rich food such as salmon could modify the severity of colitis in *Il10*$^{-/-}$ mice, and if so, to determine the changes in colon gene and protein expression, liver gene expression and caecal microbiota. A systems biology approach was used to explore the interactions within and between biological processes, with the aim to identify candidate biomarkers of these responses in surrogate "tissues" such as urine.

This chapter describes the experimental designs, preparation of diets, animal husbandry and sampling procedures for each experiment. Molecular characterisation of responses to n-3 PUFA-enriched diets was performed using 'Omics'-technologies that capture diet-induced changes in a high-throughput manner. Transcriptomics and proteomics enabled the identification of metabolic pathways and key gene/protein regulatory "hubs" in the colon, liver and/or blood. A metabolomic approach allowed the detection of metabolites in mouse urine. These metabolites may arise from the absorption, digestion and metabolism of n-3 PUFA-enriched diets, or represent diet-induced changes in endogenous metabolism and therefore offer access to unexplored metabolic pathways that are affected by diet. The caecal microbiota was classified to measure its diversity and changes in the community structure that may influence host metabolism (microbiomics). The integration of 'Omics' data may identify new metabolic pathways or signalling processes that could ultimately be mined for biomarkers of colitis that are responsive to n-3 PUFA-rich diets.

2.2 EPA time-course experiment

2.2.1 Experimental design

The experiment was conducted according to a factorial design, with mouse genotype, diet and sampling time as factors (Figure 2.1). The experimental diets were based on the AIN-76A diet formulation and either (1) supplemented with purified EPA, (2) supplemented with purified oleic acid (OA), or (3) unmodified to act as a reference enabling comparison between studies. The two mouse genotypes were (1) C57BL/6J control mice and (2) *Il10*$^{-/-}$ mice. Mice were sampled at two time-points, (1) at 9 weeks of age to determine effects of the EPA-enriched diet in early stages of colitis, and (2) at 12 weeks of age when colitis was established. These time-points were selected based on previous studies reporting gene and protein expression data in *Il10*$^{-/-}$ mice at 12 week of age [116, 280] and metabolite concentration data at times corresponding to early and established colitis [281].

2.2.2 Mouse model and induction of colitis

The experimental procedures were approved by the AgResearch Grasslands Animal Ethics Committee (AEC 12536) and conducted according to the New Zealand Animal Welfare Act 1999.

50 male *Il10*$^{-/-}$ mice (C57BL/6J background; formal designation B6.129P2-Il10^{tm1Cgn}/J) and 46 male C57BL/6J control mice were sourced from Jackson Laboratory (Maine, USA). At time of arrival, C57BL/6J mice were 5.2 weeks of age and *Il10*$^{-/-}$ mice were 4.2 weeks of age (n = 25) and 5.2 weeks of age (n = 25) due to limitations in availability of age-matched mice from the supplier (all ages ± 3 days). For convenience, age of all mice was considered 5.2 weeks at time of arrival at the facility. Mice were individually housed in standard-sized cages (332 × 150 × 130 mm) containing ALPHA-dri bedding and plastic tubes and metal rings for environmental enrichment. The room was maintained under conventional conditions at approximately 22°C, 50% relative humidity and under a 12-hour light-dark cycle. Water was provided *ad libitum* and refreshed once a week. Bodyweight and food intake were measured three times weekly.

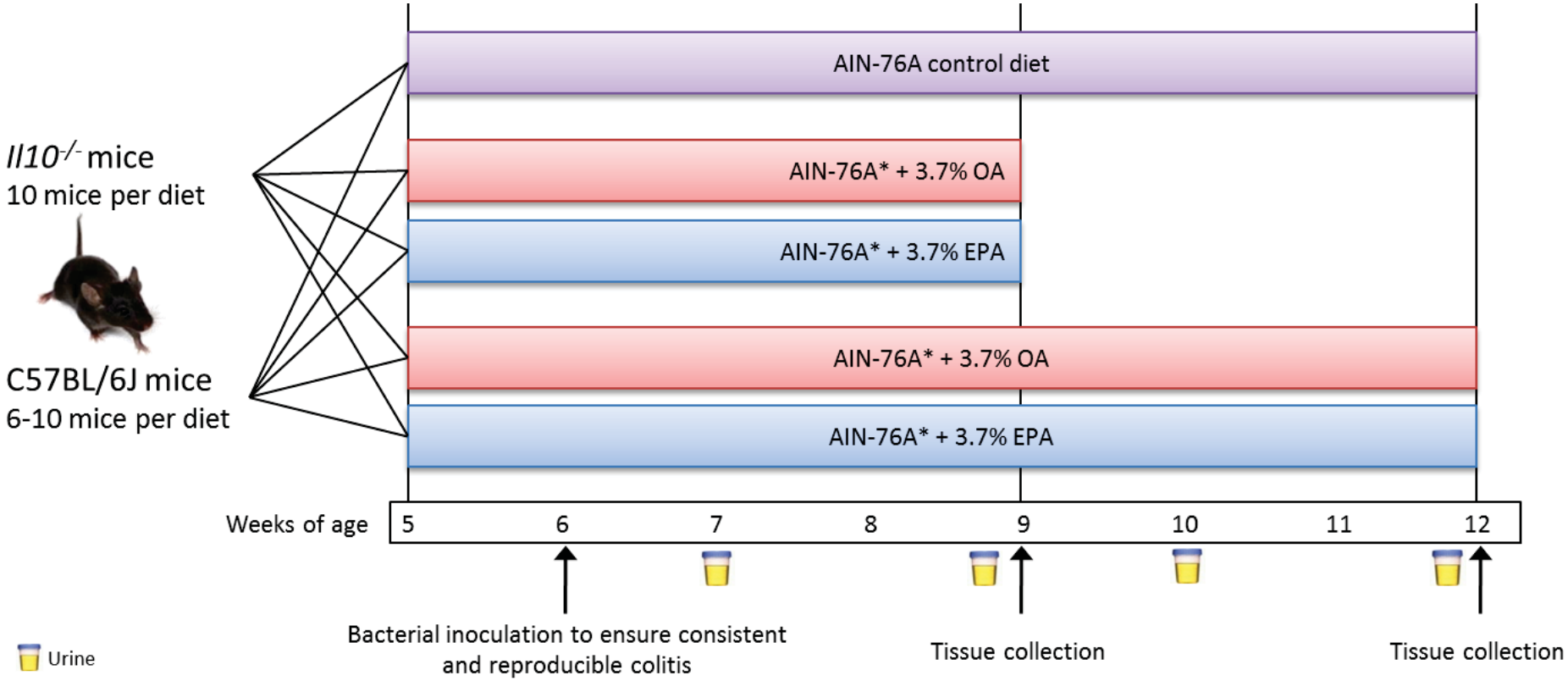

Figure 2.1 Design for the "EPA time-course experiment". 4-5-week-old *Il10*$^{-/-}$ mice (n=50) and C57BL/6J mice (n=46) were assigned to AIN-76A diets, either unmodified, or enriched with oleic acid (OA) or eicosapentaenoic acid (EPA). A time-series of urine was collected during the experiment. Mice received a bacterial inoculation at the start of the experiment and were sacrificed at 9 weeks (early colitis) or 12 weeks (established colitis) [116, 281]. (*) fat-free AIN-76A premix

Eleven days after arrival, mice received an oral inoculation of pure cultures of *Enterococcus faecalis* and *E. faecium* (EF), mixed with complex intestinal microbiota (CIF) derived from age-matched C57BL/6 mice to produce a more consistent and increased colitis in *Il10*$^{-/-}$ mice [116]. *E. faecialis* and *E. faecium* are two bacterial strains common to the human intestine [282, 283], but have shown to induce IBD-like symptoms in germ-free *Il10*$^{-/-}$ mice, potentially linked to an ability to acquire virulence factors [115, 284]. The preparation of EF was conducted using six pure *E. faecalis* and six pure *E. faecium* strains which were isolated from the faeces of calf and poultry. The strains were sub-cultured onto fresh Slanetz & Bartley medium (Oxoid Ltd., Hampshire, UK) for 48 h at 42°C. A single colony from each strain was transferred to Todd-Hewitt broth (Oxoid Ltd., Hampshire, UK) and incubated at 37°C for 24 h. Thereafter, the bacteria were separated by a 10-min centrifugation at 3,000 × g at 4°C (Sorvall RC-5 centrifuge with SM24 rotor, Thermo Fisher Scientific, Massachusetts, USA). The supernatant was removed and the pellet resuspended in 10 ml sterile 1x phosphate-buffered saline (PBS; GIBCO by Thermo Fisher Scientific, Massachusetts, USA). All cultures were pooled and brought to a final volume of 60 ml with sterile 1x PBS. Colony-forming units (CFU) were established on Slanetz & Bartley medium (Oxoid Ltd., Hampshire, UK), incubated at 37°C and counted after 24 h. On average, the EF solution provided 8.9 x 10^7 CFU per 100 µl inoculum.

CIF was derived from the digesta of the GIT from three age-matched C57BL/6 mice (Small Animal Facility, AgResearch Ruakura, New Zealand). Briefly, mice were euthanised *via* CO_2 asphyxiation, followed by cervical dislocation and removal of the GIT. Digesta from stomach to the caecum were transferred onto a Petri dish using sterile 1x PBS and brought to a final volume of 30 ml with sterile 1x PBS. The final EF×CIF inoculation solution was obtained by mixing equal volumes of EF and CIF. All mice were inoculated with 200 µl of the final EF×CIF solution.

2.2.3 Experimental diets

All diets were prepared by Research Diets Inc. (New Jersey, USA) and based on the AIN-76A diet formulation [285], containing 5% fat and only differing in their fatty acid profile (Table 2.1). The quantities of EPA in the diet were based on the findings of Knoch *et al.* [6] who demonstrated an anti-inflammatory effect of a diet containing 3.7% pure EPA. The OA diet was chosen as an appropriate control diet due to the lipid profile similarity

to the EPA diet relative to the AIN-76A diet [286] and was reported to have no effect on tissue lipid composition and eicosanoid production [287]. The OA and EPA diets were supplemented with 1% corn oil, 0.06% ALA and 0.2% LA for nutritional adequacy [288]. Ethyl ester of EPA (> 97% purity) was sourced from Photonz (Auckland, New Zealand) and produced by fermentation from a microalgal source. Ethyl esters of OA, ALA and LA (> 99% purity) were sourced from Nu-Check prep (Minnesota, USA). Diets were stored at -20°C and fresh food was thawed three times weekly. 0.001% tertiary butylhydroquinone was added as antioxidant to the EPA and OA diets.

2.2.4 Sampling procedure and tissue collection

Urine samples were collected from each mouse at a mean age of 7.1, 9, 10.1 and 12 weeks and stored at -80°C until analysis. The effects of EPA on early stages of colitis were established at 9 weeks of age, when urinary metabolites associated with early colitis peaked in *Il10*$^{-/-}$ mice [281]. The effects of EPA were also determined at 12 weeks of age, when colitis in *Il10*$^{-/-}$ mice was established [116]. Before tissue collection, mice were subjected to a standardised feeding regime to minimise the effect of the last food intake on gene expression [289]. Briefly, mice were fasted overnight (14 h), re-fed for 2 h and fasted for 2 h prior to sampling. Mice were euthanised *via* CO_2 asphyxiation followed by cervical dislocation.

Blood for isolation of PBMCs was collected post-mortem *via* cardiac puncture using syringe and needle coated with the anti-coagulant ethylenediaminetetraacetic acid (EDTA; 0.5 mole/L and pH 8.0; GIBCO by Thermo Fisher Scientific, Massachusetts, USA). The GIT was flushed with ice-cold 0.9% NaCl to remove digesta and sectioned into duodenum, jejunum, ileum, caecum and colon. All intestinal sections were fixed in 10% phosphate-buffered formalin for histological evaluation. A piece of colon tissue was additionally stored in RNAlater overnight at 4°C and thereafter at -20°C (Ambion; Life Technologies, California, USA) to preserve RNA for subsequent extraction.

Table 2.1 Formulation of the unmodified AIN-76A diet and AIN-76A-based eicosapentaenoic acid (EPA) and oleic acid (OA) diets for the "EPA time-course experiment"

	AIN-76A diet		*OA diet*		*EPA diet*	
Component (%)	g	kcal	g	kcal	g	kcal
Protein	20	21	20	21	20	21
Carbohydrate	65	65	65	65	65	65
Fat	5	12	5	12	5	12
Total		100		100		100
Energy (kcal/g)	3.9		3.9		3.9	
Ingredient (%)						
Casein	20	80	20	80	20	80
DL-Methionine	0.3	1.2	0.3	1.2	0.3	1.2
Sucrose	50	200	50	200	50	200
Dextrin	15	60	15	60	15	60
Alphacel, Non-Nutritive Bulk	5	0	5	0	5	0
Corn oil	5	45	1	9	1	9
Linoleic acid, 99%+	0	0	0.2	2	0.2	2
α-linolenic acid, 99%+	0	0	0.06	0.5	0.06	0.5
Oleic acid, 99%+	0	0	3.7	34	0	0
Eicosapentaenoic acid, 97%+	0	0	0	0	3.7	34
AIN-76A Mineral mix	3.5	0	3.5	0	3.5	0
AIN-76A Vitamin mix	1	4	1	4	1	4
Choline Bitartrate	0.2	0	0.2	0	0.2	0
Ethoxyquin	0.01	0	0	0	0	0
Tertiary butylhydroquinone	0	0	0.001	0	0.001	0
Total	100	390	100	390	100	390

Ethyl esters of eicosapentaenoic acid (EPA; 97%+ purity from Photonz (Auckland, New Zealand)) and oleic acid (OA; 99%+ purity from Nu-Check prep (Minnesota, USA)) were incorporated at 3.7% *(w/w)* into a basal AIN-76A diet. Ethyl esters of linoleic acid and α-linolenic acid (Nu-Check prep (Minnesota, USA)) were added for nutritional adequacy. Other ingredients were sourced and diets formulated by Research Diets Inc. (New Jersey, USA).

2.2.5 Statistical evaluation of growth performance

Body weight and food intake data were evaluated using the Predictmeans package written in R 3.1.0. For the body weight data, the model fitted initial weight, day centred and day centred quadratic term (to reflect the growth over time) as covariates, with genotype and treatment (sampling time and diet) as factors. The individual mice were considered as random effects. A similar repeated measurements model was used for the analysis of food intake, with incorporation of initial weight and day centred as covariates, genotype and treatment (sampling time and diet) as factors and mouse as random effects. The models were visually checked for goodness of fit against individual mouse data. Predicted means of body weight and food intake were estimated from the model and significance evaluated using an analysis of variance (ANOVA) followed by an LSD post-hoc test. P-values less than 0.05 were considered significant and p-values between 0.05 and 0.1 were considered a trend. Mice that were sampled prior to their scheduled sampling time were included in the analysis of growth performance.

2.3 Salmon diet experiment

2.3.1 Experimental design

The experiment was conducted according to a factorial design, with mouse genotype and diet as factors (Figure 2.2). The experimental diets were based on the AIN-76A diet formulation and either (1) supplemented with increasing amounts of salmon (15%, 30% and 45%), (2) modified to match the salmon diets in macronutrient composition, or (3) unmodified to act as a reference enabling comparison between studies. The two mouse genotypes were (1) C57BL/6J control mice and (2) *Il10*$^{-/-}$ mice.

2.3.2 Mouse model and induction of colitis

The experimental procedures were approved by the AgResearch Grasslands Animal Committee (AEC 12085) and conducted according to the New Zealand Animal Welfare Act 1999.

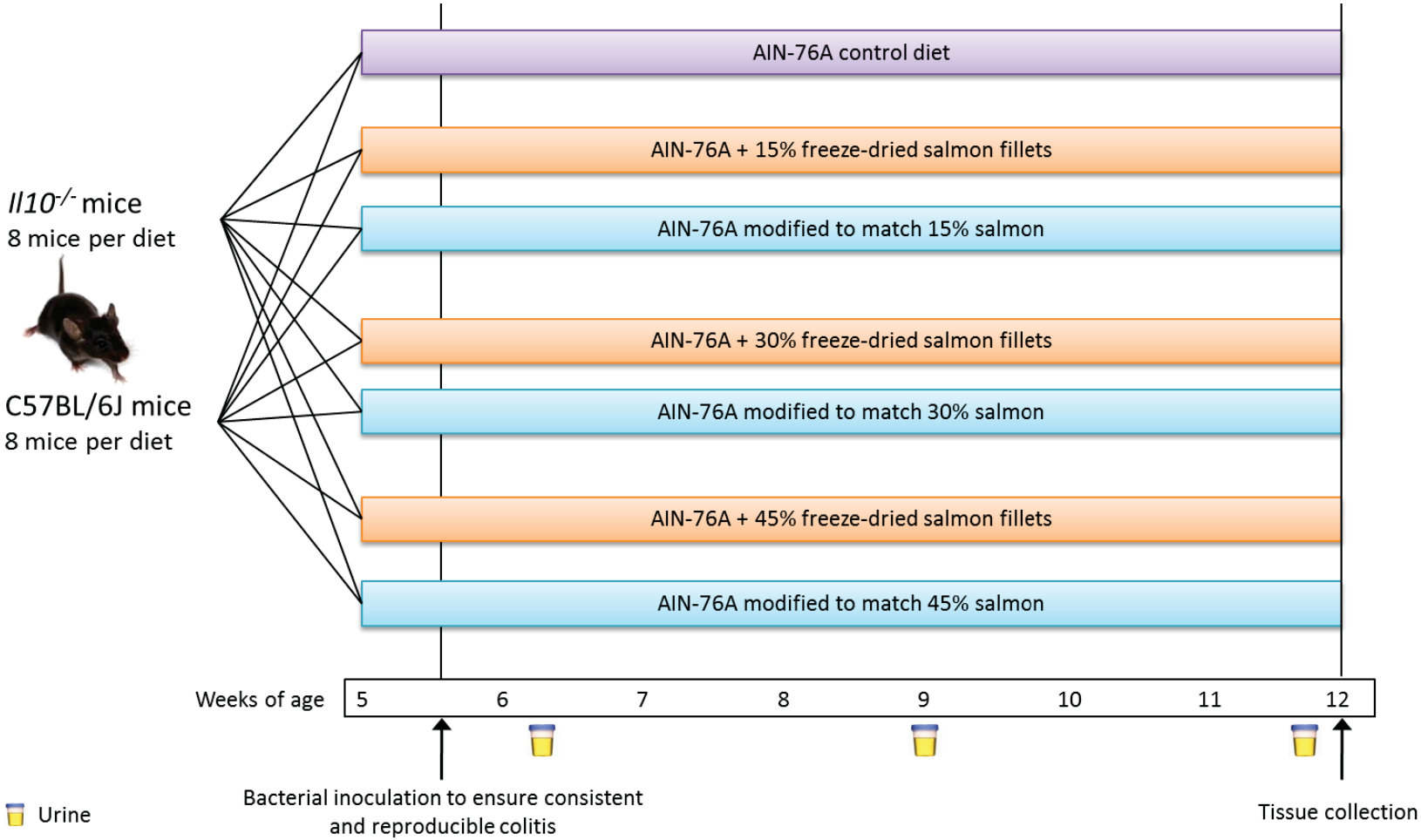

Figure 2.2 Design for the "salmon diet experiment". 4-5-week-old *Il10*$^{-/-}$ mice (n=56) and C57BL/6J mice (n=56) were assigned to either a control diet or a salmon diet. Lyophilised salmon fillets were incorporated at 15%, 30% and 45% by dry weight. The control diets were based on the AIN-76A formulation and modified to match the respective salmon diet in macronutrient composition. A time-series of urine was collected during the experiment. Mice received a bacterial inoculation at the start of the experiment and were sacrificed at 12 weeks of age [116, 290].

A total of 56 male *Il10*$^{-/-}$ mice and 56 male C57BL/6J control mice were sourced from Jackson Laboratory (Maine, USA) at 4 to 5 weeks of age, housed according to Section 2.2.2 with the modification that fresh diets were provided daily to prevent spoilage of the salmon diets, and mice received the bacterial inoculation five days after arrival (mean age 5.5 weeks of age). On average, the EF solution provided 6.7 x 10^7 CFU per 100 µl inoculum.

2.3.3 Experimental diets

The incorporation of salmon fillets into a pelleted mouse diet was achieved by lyophilisation and fortification of a basal AIN-76A standard diet with the salmon powder. Alternative approaches included feeding salmon in a gelatine matrix [291], however unpublished data indicated that gelatine matrices may themselves impact the severity of colitis as observed in rats administered with DSS (personal communication, Rachel Anderson, AgResearch Grasslands, New Zealand). The palatability of diets was based on the findings of Somers *et al.* [291] and Cleland *et al.* [292], who fed fish-fortified diets (20-30% fish flesh dry matter) without adverse effects on body weight or intake. It was further anticipated that a diet fortified with 45% salmon powder would provide approximately 3.7% total n-3 PUFA, with the estimation based on the lipid profile of farmed New Zealand Chinook salmon [293], and therefore similar to the amount of EPA in the "EPA time-course experiment". The high amount of fat from the salmon would not make it possible to adjust protein and carbohydrate for a nutritionally balanced rodent diet, with 45% salmon as upper limit without compromising nutritional adequacy of diets. Diets supplemented with 30% and 15% dry salmon by weight were included to establish a dose-response of the effects of salmon on colitis.

De-skinned and de-boned Chinook salmon fillets were provided by The New Zealand King Salmon Company (Nelson, New Zealand). The salmon fillets were minced, frozen and further lyophilised (FD18LT "ISLA", Cuddon Ldt., Blenheim, New Zealand). The lyophilised salmon fillets were analysed for macro- and micronutrient composition (Appendix I) and incorporated into modified AIN-76A diets at a concentration of 15%, 30% and 45% dry salmon by weight. For each of the salmon diets, a macronutrient-matched control diet was included in the experiment. These AIN-76A-based control diets did not contain salmon, and corn oil replaced salmon as fat source and casein as protein source (Table 2.2). Control diets were necessary to determine if any change in the intakes

observed were due to the high fat content of the salmon diet and/or its fishy smell/taste. Diets were prepared by Research Diets Inc. (New Jersey, USA) and vacuum sealed in 1 kg bags under nitrogen to prevent oxidation (personal communication, Lorene Leiter, Research Diets Inc., New Jersey, USA). Diets were stored at -20°C and food was thawed daily for feeding.

Analysis of experimental diets was performed by AsureQuality Ltd (Auckland, New Zealand). Primary lipid oxidation was measured using titrimetry after fat extraction (peroxide value; AOCS Cd 8b-90) and secondary oxidation using spectrophotometry (p-anisidine value; modified AOCS Cd 18-90). Fatty acid composition was measured by gas chromatography of fatty acid methyl esters [294]. Crude protein was determined using Kjeldahl digestion (AOAC 988.05). Ash residue was determined by gravimetric methods using a furnace at 550°C (AOAC 942.05), and moisture content determined using a convection oven at 135ºC (AOAC 930.15). Fat content was determined using an ether extraction based on AOCS 948.15. Carbohydrate content was calculated by difference. Energy content was calculated from protein, moisture, fat, carbohydrate and ash contents (ANZ Food Standards Code 2002 (Amendment No. 2)). Results of these analyses are given in Chapter 4.

2.3.4 Sampling procedure and tissue collection

Urine was collected from each mouse at 6.2, 9 and 11.5 weeks of age and stored at -80°C until analysis. Mice were euthanised at 12 weeks of age, when colitis was established in *Il10*$^{-/-}$ mice [116]. Before tissue collection, mice were subjected to a standardised feeding regime as outlined in Section 2.2.4. Mice were euthanised by CO_2 asphyxiation followed by cervical dislocation. The GIT was flushed with ice-cold 0.9% NaCl to remove digesta and sectioned into duodenum, jejunum, ileum, caecum and colon. All intestinal sections were fixed in 10% phosphate-buffered formalin for histological evaluation. A piece of colon was also stored in RNAlater overnight at 4°C and thereafter at -20°C (Ambion; Life Technologies, California, USA) to preserve RNA for simultaneous extraction of RNA and protein. Caecum digesta and liver were snap-frozen in liquid nitrogen and stored at -80°C.

Table 2.2 Formulation of salmon and control diets for the "salmon diet experiment".

	AIN-76A		*15% salmon*		*30% salmon*		*45% salmon*		*15% control*		*30% control*		*45% control*	
Component (%)	g	kcal	g	kcal	g	kcal	g	kcal	g	kcal	g	kcal	g	kcal
Protein	20	21	21	21	23	21	25	21	21	21	23	21	25	21
Carbohydrate	66	68	61	61	50	45	39	32	61	61	50	45	39	32
Fat	5	12	8	19	17	34	25	47	8	19	17	34	25	47
Total		100		100		100		100		100		100		100
Energy (kcal/g)	3.9		4.1		4.5		4.8		4.1		4.5		4.8	
Ingredient	g	kcal	g	kcal	g	kcal	g	kcal	g	kcal	g	kcal	g	kcal
Salmon total	0	0	145	0	265	0	365	0	0	0	0	0	0	0
Protein (from salmon)	0	0	64	255	117	468	161	644	0	0	0	0	0	0
Fat (from salmon)	0	0	81	728	148	1331	204	1833	0	0	0	0	0	0
Ash (from salmon; estimate)	0	0	0.2	0	0.2	0	0.3	0	0	0	0	0	0	0
Casein	200	800	136	544	83	332	39	156	200	800	200	800	200	800
DL-Methionine	3	12	3	12	3	12	3	12	3	12	3	12	3	12
Corn Starch	150	600	46	182	88	350	88	350	46	182	88	350	88	350
Maltodextrin	0	0	35	140	88	350	88	350	35	140	88	350	88	350
Sucrose	500	2000	500	2000	255	1019	129	517	500	2000	246	1019	129	517
Cellulose, BW200	50	0	50	0	50	0	50	0	50	0	50	0	50	0
Corn oil	50	450	0	0	0	0	0	0	81	728	148	1331	204	1833
Mineral Mix S10001	35	0	35	0	35	0	35	0	35	0	35	0	35	0
Vitamin Mix V10001	10	40	10	40	10	40	10	40	10	40	10	40	10	40
Choline Bitartrate	2	0	2	0	2	0	2	0	2	0	2	0	2	0
Total	1000	3902	962	3902	878	3902	808	3902	961	3902	878	3902	808	3902

De-boned and de-skinned salmon fillets were lyophilised and incorporated at 15%, 30% and 45% by dry weight into a modified AIN-76A diet. Three AIN-76A-based control diets were included to match the salmon diets in macronutrient composition, with corn oil as fat source and casein as protein source. An unmodified AIN-76A control diet was included as reference point to other studies. Diets were formulated by Research Diets Inc. (New Jersey, USA). All ingredients were sourced from Research Diets Inc., with the exception of salmon which was provided by the New Zealand King Salmon Company (Nelson, New Zealand). Weights do not add to 1000 g because the diet composition was calculated in terms of energy (as close as possible to 3902 kJ).

2.3.5 Statistical evaluation of growth performance

Statistical analyses of body weight and food intake were performed using the Predictmeans package written in R 2.13.1. For the intake data, a linear mixed model was fitted which incorporated a repeated measurements analysis of the intake for each mouse over the experimental period. A similar repeated measurements model was fitted for the body weight data for each mouse with incorporation of both a linear and quadratic trend over the experimental period. The models were visually checked for goodness of fit against individual mouse data. Predicted means of body weight and food intake were estimated from the model and significance evaluated using an ANOVA followed by an LSD post-hoc test. P-values less than 0.05 were considered significant and p-values between 0.05 and 0.1 were considered a trend.

2.4 Histopathological assessment

2.4.1 Tissue preparation and haematoxylin and eosin stain

Formalin-fixed intestinal samples (duodenum, jejunum, ileum, caecum and colon) were embedded in paraffin and cross-sectioned at a thickness of 5 μm. Three serial sections were cut with the final section at a tissue depth of 25 μm to display the depth of histological changes in the tissue. The sections were stained using haematoxylin and eosin (HE stain) for examination under the light microscope. HE staining is a common method used to highlight cell compartments within a tissue specimen. Haematoxylin forms oxidation-induced dye-metal complexes that bind and stain nucleic acids in shades of purple and blue (cell nucleus and ribosomes). The counterstain was performed with eosin, an acidic dye that stains eosinophilic structures in shades of pink and red (cytoplasm of cells and extracellular proteins such as collagen).

2.4.2 Histological injury score

The histological injury score (HIS), a measure of the degree of intestinal inflammation, was obtained by "blind" evaluation of tissue appearance and inflammatory cell infiltration across the three sections [295, 296]. The following characteristics for tissue appearance were scored from 0 (no change from normal tissue; no inflammation) to 10 (extreme changes in tissue; high levels of inflammatory features): changes specific to intestinal

crypts/villi (hyperplasia, aberrancy, injury, crypt loss, abscesses and goblet cell loss) and changes specific to the mucosa (lymphoid aggregates, mucosal aberrancy and surface loss). Additionally, the infiltration of inflammatory cells (monocytes/macrophages, plasma cells/lymphocytes and neutrophils) were evaluated in the same pattern, with scores from 0 (numbers of inflammatory cells in normal range) to 10 (highly elevated numbers of inflammatory cells). The infiltration of inflammatory cells was multiplied to give more weight to this value, representing a major feature during colitis. The total HIS was calculated as the sum of the individual features, with HIS = Σ [½ × (crypt and mucosal features) + ½ × ((monocytes/macrophages × 4) + (neutrophils × 2) + (plasma cells/lymphocytes × 4))].

2.4.3 Statistical evaluation of histopathological changes

In the "EPA time-course experiment", the differences in degree of inflammation in the individual intestinal sections were evaluated using a restricted maximum likelihood (REML) estimation in GenStat (17th Edition, VSN International, Hemel Hempstead, UK). The model included the total HIS from *Il10*$^{-/-}$ mice, using intestinal section and treatment (diet × sampling age) as factors and the individual mice were considered as random effects. Within *Il10*$^{-/-}$ mice, effects of dietary EPA on the severity of colitis were evaluated using an ANOVA. The residual plots were checked for all models.

In the "salmon diet experiment", histology data were analysed using a REML in GenStat (14th Edition[1]), with log-transformation to evaluate the differences between intestinal sections and genotypes. Log-transformation was necessary to compensate for differences between inflamed sections in *Il10*$^{-/-}$ mice (colon and caecum) and non-inflamed sections (small intestine). An ANOVA was used to evaluate differences within each intestinal section. P-values less than 0.05 were considered significant and p-values between 0.05 and 0.1 were considered a trend.

[1] The statistical analysis of histology data in the "salmon diet experiment" was carried out first, hence the version of GenStat varied between the experiments.

2.5 Isolation of peripheral blood mononuclear cells and RNA extraction

PBMCs are cells of the immune system characterised by a round nucleus, for example lymphocytes and monocytes. They infiltrate various tissues *via* the blood circulation, and might therefore contain information of metabolic or physiological changes that occur in various tissues [147]. The isolation of PBMCs from blood was performed using the density separation medium Lympholyte-Mammal (Cedarlane, Ontario, Canada). The Lympholyte-Mammal is designed to isolate viable lymphocytes and monocytes from peripheral blood but eliminates erythrocytes, dead cells and granulocytes (*e.g.* neutrophils). The elimination of granulocytes is necessary as these reflect acute inflammatory responses and granulocytes are therefore not ideal to characterise the long-term effects of dietary intervention.

Blood for isolation of PBMCs was collected post-mortem *via* cardiac puncture (as described in Section 2.2.4) and diluted at 1:1 with 1x sterile PBS. 3 ml Lympholyte-Mammal was carefully overlaid with diluted blood and centrifuged for 20 min at 800 × g to separate the blood components into layers of plasma, buffy coat and red blood cells. The buffy coat, containing platelets and PBMCs, was carefully removed by pipetting and transferred to a new tube for volume adjustment to 4 ml with 1x sterile PBS. The sample mixture was centrifuged at 800 × g for 10 min, the supernatant removed, and the remaining cell pellet resuspended in 2 ml PBS. This step was repeated until the resulting supernatant was visibly clear, indicating the complete removal of interfering platelets. After the final wash step, the remaining pellet was resuspended in 500 µl RNAprotect Cell Reagent (Qiagen Inc., California, USA) and mixed thoroughly to stabilise RNA. The resulting PBMC suspension was stored at -80°C until RNA extraction.

RNA was extracted from PBMC using the Qiagen RNeasy Plus Mini Kit according to the manufacturer's instructions including all optional steps (Qiagen Inc., California, USA). The PBMC suspension was centrifuged for 5 min at 5000 × g, the supernatant removed and the remaining cell pellet resuspended in 600 µl Buffer RLTplus containing 6 µl DL-Dithiothreitol to inhibit RNase activity (Sigma-Aldrich, Missouri, USA). The cell lysate was homogenised for approximately 30 s (OmniTH Homogenizer; Omni International, Georgia, USA). The homogenised cell lysate was transferred to a gDNA Eliminator spin column, centrifuged for 30 s at 13,000 × g, followed by the

addition of 1 volume of 70% ethanol to the flow through. 700 µl sample was transferred to an RNeasy spin column, placed in a 2 ml collection tube and centrifuged for 30 s at 13,000 × g. The flow-through was discarded and 700 µl Buffer RW1 was added to the RNeasy spin column and centrifuged for 30 s at 13,000 × g. The column was carefully removed to prevent the carryover of interfering substances. 500 µl Buffer RPE was added to the RNeasy spin column and centrifuged for 30 s at 13,000 × g. The spin column membrane was dried by adding another 500 µl Buffer RPE followed by a 2-min centrifugation at 13,000 × g, removal of the flow-through and a 1-min centrifugation at 13,000 × g. The RNeasy spin column was placed into a new 2 ml collection tube. To ensure complete elution of RNA from the membrane, 20-30 µl RNase-free water was directly pipetted onto the membrane, incubated for 1 min and further centrifuged for 1 min at 13,000 × g. The resulting RNA in 20-30 µl RNase-free water was stored at -80°C until analysis.

2.6 Extraction of RNA and protein from colon and liver

RNA and protein were extracted from colon and liver tissues using the Qiagen AllPrep DNA/RNA/Protein Mini Kit according to the manufacturer's instructions, including all optional steps (Qiagen Inc., California, USA). Approximately 10 mg (liver) or 30 mg (colon) tissue were submerged in 600 µl Buffer RLT containing 6 µl β-mercaptoethanol to inhibit RNase activity (BDH Middle East LLC, Dubai, United Arab Emirates). Tissues were homogenised for approximately 30 s (OmniTH Homogenizer; Omni International, Georgia, USA) until no visible pieces of tissue remained. After a 3-min centrifugation at 13,000 × g, the supernatant was carefully removed without disturbing the pellet, and applied to a DNA spin column placed in a 2 ml collection tube. The column was centrifuged for 30 s at 13,000 × g and, if necessary, re-spun until all liquid had passed through the membrane. The flow-through was further purified to obtain RNA and protein by adding 430 µl 96% ethanol. 700 µl sample was transferred to an RNeasy spin column placed in a 2 ml collection tube and centrifuged for 30 s at 13,000 × g. The flow-through-containing protein was transferred to a 2 ml tube and stored at -20°C until protein analysis. 700 µl Buffer RW1 was added to the RNeasy spin column and centrifuged for 30 s at 13,000 × g. The column was carefully removed to prevent the carryover of interfering substances. 500 µl Buffer RPE was added onto the RNeasy spin column and centrifuged for 30 s at 13,000 × g. The spin column membrane was dried by adding another 500 µl

Buffer RPE followed by a 2-min centrifugation at 13,000 × g, removal of the flow-through and a 1-min centrifugation at 13,000 × g. The RNeasy spin column was placed into a new 2 ml collection tube. To ensure complete elution of RNA from the membrane, the following steps were performed twice, using the same tube to collect the flow-through. 50 µl RNase-free water was directly pipetted onto the membrane, left to incubate for 1 min and further centrifuged for 1 min at 13,000 × g. The collection tube containing RNA in 100 µl RNase-free water was stored at -80°C until analysis.

2.7 Transcriptomic analysis of colon, liver and peripheral blood mononuclear cells

Transcriptomic analysis of colon, liver and PBMCs was performed to capture the expression of genes by measuring levels of mRNA transcripts *via* microarray technology. Whole mouse genome microarrays were used that contain the information for 39,430 Entrez Gene RNAs in form of DNA sequences (probes) on their surface [297].

2.7.1 Method overview

The workflow for transcriptomic analysis is illustrated in Figure 2.3. Briefly, extracted sample RNA (described in Sections 2.5 and 2.6) and reference RNA were transcribed into cRNA and simultaneously labelled with cyanine dyes Cy3 or Cy5. This reference design allowed an indirect gene expression comparison by hybridising sample RNA against the common reference RNA. Data were processed in R to calculate the intensities of the fluorescent signals which correspond to the extent of hybridisation to each gene-specific probe.

2.7.2 Sample preparation

RNA integrity was assessed using a RNA6000 Nano Labchip kit with an Agilent 2100 Bioanalyzer (Agilent Technologies, California, USA). The Bioanalyzer 28s/18s peak ratio must be greater than 1.2 to ensure intact RNA. An RNA integrity number (RIN) was calculated which reflects the presence or absence of degradation products, with 1 being the most degraded and 10 the most intact RNA [298]. Only RNA with a RIN greater than 6 was used; values less than 6 indicates that the RNA is degraded at least partly, which may lead to errors in subsequent analyses. RNA yield and purity were assessed using a NanoDrop ND-1000 spectrophotometer (Thermo Fisher Scientific, Delaware, USA).

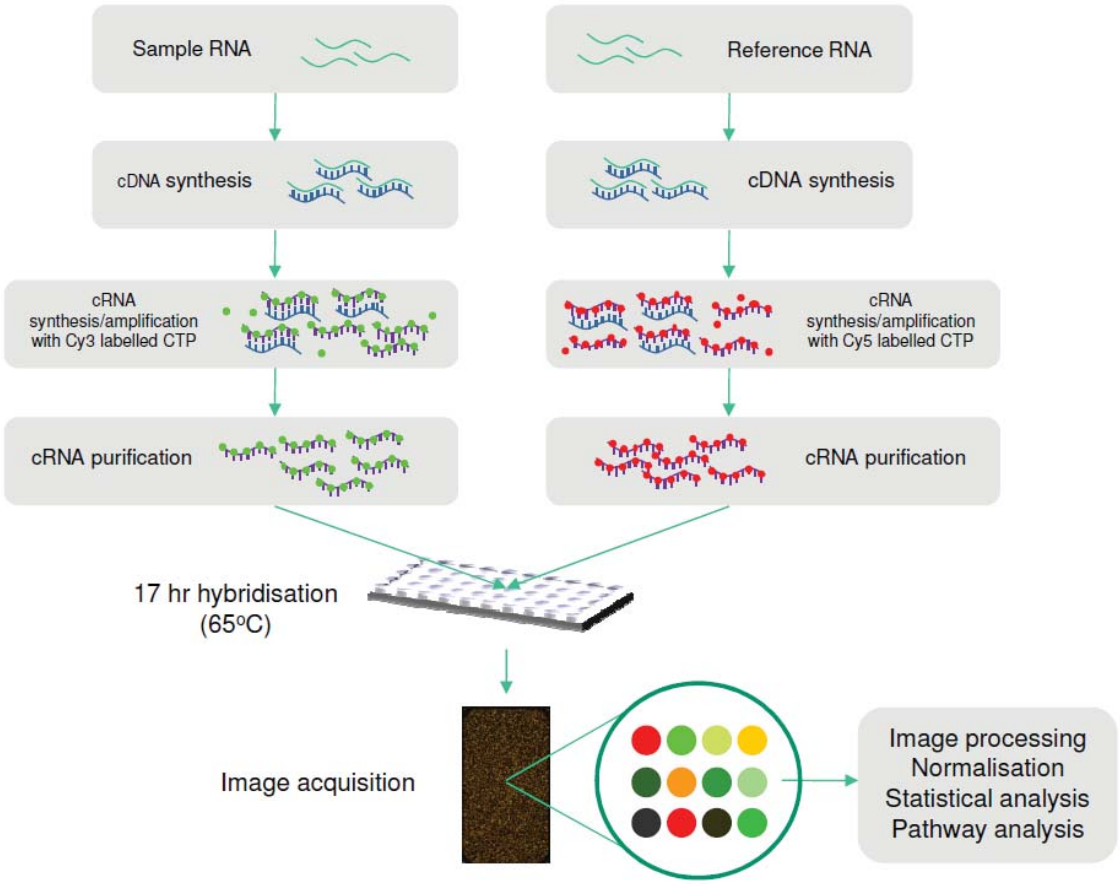

Figure 2.3 Transcriptomic analysis workflow applying a reference design. RNA was transcribed into cRNA and simultaneously amplified and labelled with Cy3 (sample RNA) or Cy5 (reference RNA). After purification, samples were co-hybridised on the same array. The intensities of the fluorescent signals corresponded to the extent of hybridisation to each gene-specific probe. Figure courtesy of Dr Wayne Young (AgResearch Grasslands).

Only RNA with an optical density ratio at 260/280 nm greater than 2.0 and a ratio at 260/230 nm greater than 1.6 were used. Where impurities in the sample were present (indicated by lower optical density ratios), samples required additional processing using the Qiagen RNeasy Mini Kit as per the manufacturer's instructions with all optional steps (Qiagen Inc., California, USA).

Briefly, after adjusting sample volume to 100 µl using RNase-free water, 350 µl Buffer RTL was added to the sample and mixed by vortexing. 250 µl 96% ethanol was added, mixed by pipetting and 700 µl sample was transferred to an RNeasy spin column placed in a 2 ml collection tube. After a 30-s centrifugation at 13,000 × g, the column was carefully removed to prevent carryover of interfering substances. 500 µl Buffer RPE was added to the RNeasy spin column and centrifuged for 30 s at 13,000 × g. The spin column membrane was dried by adding another 500 µl Buffer RPE followed by a 2-min centrifugation at 13,000 × g, removal of the flow-through and a 1-min centrifugation at 13,000 × g. The RNeasy spin column was placed into a new 2 ml collection tube. To ensure complete elution of RNA from the membrane, the following steps were carried out twice, using the same tube to collect the flow-through. 50 µl RNase-free water was directly pipetted onto the membrane, left to incubate for 1 min and centrifuged for 1 min at 13,000 × g. The collection tube containing RNA in RNase-free water was stored at -80°C until analysis.

2.7.3 CyDye-labelling and microarray hybridisation

Sample labelling and microarray processing were conducted according to the two-colour Quick Amp Labelling kit including all optional steps (Agilent Technologies, California, USA). RNA that met the quality criteria described in Section 2.7.2 was transcribed into complementary RNA (cRNA) using T7 RNA polymerase and simultaneously amplified and labelled with the green fluorescent dye Cy3 (sample RNA) or red fluorescent dye Cy5 (reference RNA). Amount of RNA starting material is indicated in the research chapters. Reference RNA was extracted from intestine, kidney, liver and foetus of Swiss mice. The quality of the amplification and incorporation of the dye were monitored using a NanoDrop ND-1000 spectrophotometer, excluding samples with a cRNA yield less than 825 ng and a specific activity less than 8 pmol Cy3 or Cy5 per µg cRNA. RNA Spike-in kits were included as instructed by the manufacturer (Agilent Technologies, California, USA).

In the "EPA time-course experiment", samples were hybridised onto Agilent Mouse Gene Expression 8x60K microarrays using four biological replicates per treatment group[2], with the exception of colon from C57BL/6J mice fed AIN-76A diet where n = 3. In the "salmon diet experiment", samples were hybridised onto Agilent Mouse Gene Expression 4x44K version 2 using six biological replicates per treatment group. Both microarray formats contain the same Entrez Gene information are fully compatible, while the 8x60K format also feature lincRNAs that were of interest to the study but beyond the scope of this dissertation. Gene expression hybridisation kits were used as instructed. Microarray slides were placed in a hybridisation oven set to 65°C and 10 rpm for 17 h. Thereafter, slides were washed in Wash Buffer 1 and 2 (Agilent Technologies, California, USA), acetonitrile, and Stabilisation and Drying solution (Agilent Technologies, California, USA). Immediately after washing, slides were scanned at 5 µm resolution using an Agilent Technologies Scanner G2505B with feature extraction software (version 10.10.1.1) to extract the raw microarray images.

2.7.4 Microarray data processing

Quality assessment of microarrays, normalisation and determination of differentially expressed genes were performed using the linear model for microarray (LIMMA) package within the Bioconductor project written in R 3.1.0 and for colon microarrays in the "salmon diet experiment" version 2.15.0 [299].

Microarray quality was visually assessed by checking red (reference RNA) and green (sample RNA) channel foreground and background signals. For individual arrays, image plots displayed spatial heterogeneity of background intensities from red and green channels. Boxplots illustrated the array-wide distribution of un-normalised background and foreground intensities from red and green channels. Spots that failed the quality assessment were excluded from analysis. Within-array normalisation was performed using local linear regression analysis (loess) of red and green channel signal intensities, followed by normalisation between arrays [300]. The performance of normalisation was visually assessed by plotting the $\log_2$-ratio of green-to-red channel intensities (M) against the average $\log_2$-intensity of red and green channels (A) for each dot in the plot (MA plot)

[2] The number of samples was restricted due to misplacement.

and by illustrating the distribution of the red and green channel signals for each array (density plots).

A $\log_2$-fold-change (logFC) was calculated for each probe, representing the ratio of red signal (reference RNA) to green signal (sample RNA). The significance of the logFC was evaluated by performing a moderated t-statistic using an empirical Bayes method [299]. Genes were defined as differentially expressed when FC ≥ |1.5| (logFC ≥ 0.583 for enhanced expression; logFC ≤ -0.583 for reduced expression) and a moderated p-value ≤ 0.005. Differentially expressed genes were uploaded into Ingenuity Pathway Analysis (IPA; Ingenuity Systems; www.ingenuity.com) to form networks and pathways of differentially expressed genes. In parallel, Gene Set Enrichment Analysis (GSEA [301]) was performed to identify Kyoto Encyclopedia of Genes and Genomes (KEGG) pathway gene sets that were responsive to the dietary treatments. Details of bioinformatic analyses are described in Section 2.11.

2.8 Proteomic analysis of colon tissue

2-dimensional (2D) sodium dodecyl sulphate polyacrylamide gel electrophoresis (SDS-PAGE) is a commonly used method to separate complex protein mixtures according to their differences in charge in first dimension and molecular weight in second (Figure 2.4) [302]. Proteomic analysis was performed according to the principle of difference gel electrophoresis (DIGE), an extension to the 2D SDS-PAGE [303]. This technique can reproducibly detect differences in protein expression between two protein samples using only one gel, not only reducing the numbers of gels required, but also limiting experimental variation. The two protein samples which are separated on the same gel are labelled with two different fluorescent dyes. An internal standard, labelled with a third dye, is used to normalise between gels, resulting in three protein samples on the same gel. In the first dimension (isoelectric focussing (IEF)), proteins are separated according to their isoelectric point (pI), a specific pH at which the net charge of the protein is zero. An electric potential is applied to create a positive charge on one end (anode) and a negative charge on the other end (cathode) of a gel strip which contains an immobilised pH gradient. The amino acid side chains and termini of proteins on the gel strip become charged, with the net charge of the protein depending on the pH of the surrounding environment. At pH values that are above a protein's pI, the protein has a negative net charge and at pH values below its pI, the protein has a positive net charge. Proteins with

a negative net charge migrate towards the anode and proteins with a positive net charge migrate towards the cathode of the gel strip, moving closer to a net charge of zero (equals the pI).

In the second dimension, proteins are separated according to their molecular weight. Immediately prior to the separation, the protein-containing gel strip is treated with sodium dodecyl sulphate (SDS) which forms a complex with the protein approximately proportional to the protein's mass, charging the SDS-protein-complex negative. The gel strip is then applied on top of a polyacrylamide gel perpendicular to the first dimension. An electric potential is applied and the negatively charged proteins migrate through the gel to the positive side. When the SDS-protein-complexes migrate through the gel, the polyacrylamide acts as a molecular sieve, retaining proteins with a larger molecular mass, but letting smaller ones pass. The resulting gel contains the immobilised proteins, arranged by molecular weight and charge, which can then be cut from the gel and identified using mass spectrometry (MS).

2.8.1 Method overview

The workflow for proteomic analysis is illustrated in Figure 2.5. Briefly, after extraction of protein from colon tissue (described in Section 2.6), samples were purified, labelled with CyDyes and further separated by 2D-DIGE. The scanned gel pictures were digitally overlaid and spot-features on the gels that met the cut-off criteria (FC $\geq$ |1.5| and p-value $\leq$ 0.05) were further excised from gels, digested and identified by LTQ linear ion trap MS with a nano-electrospray ionisation (ESI) interface. Proteins were identified using the Proteome Discoverer 1.4 protein identification software and MS spectra were searched against the National Center for Biotechnology Information (NCBI) *Mus musculus* database. The 2D-DIGE method used in the present dissertation was validated by Barraclough *et al.* [304] and previously used for protein extracted from whole colon tissue from mice [280, 286, 305].

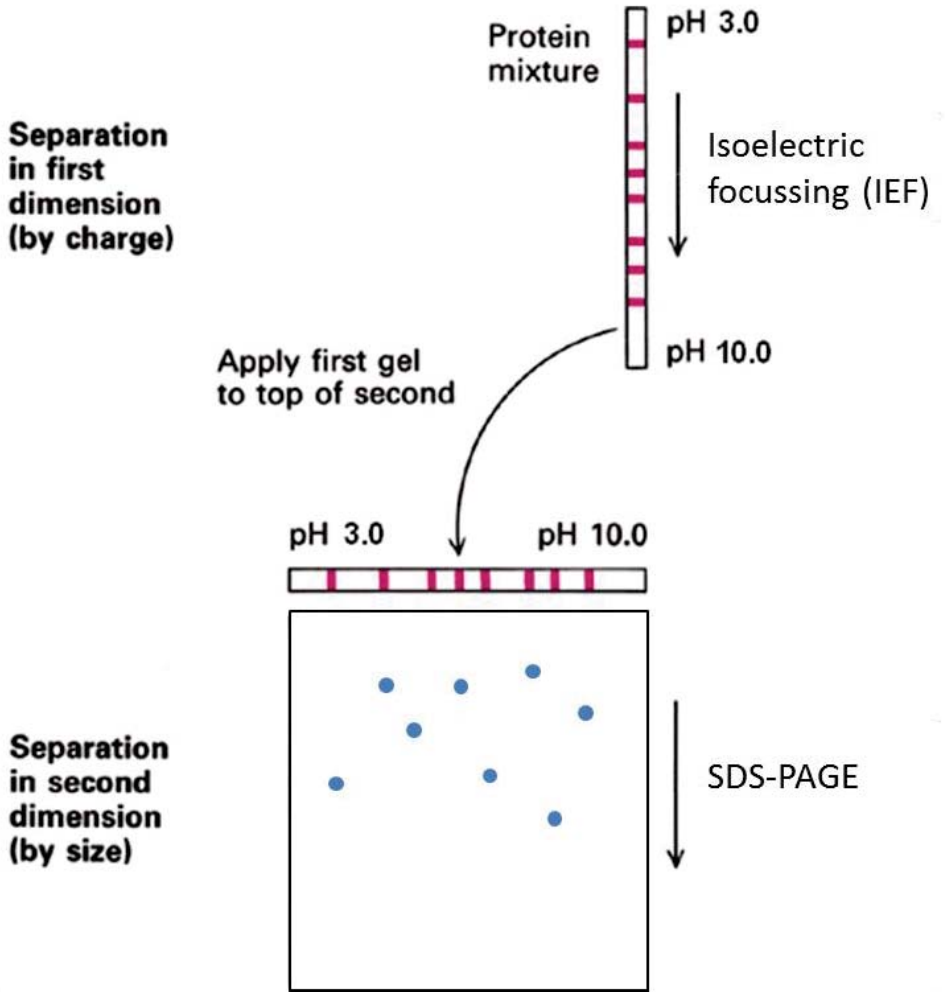

Figure 2.4 Principle of 2-dimensional (2D) gel electrophoresis with separation of the protein samples in first dimension by isoelectric focussing and second dimension by sodium dodecyl sulphate polyacrylamide gel electrophoresis (SDS-PAGE). The protein mixture is loaded onto a gel strip containing an immobilised pH gradient, and separated according to their isoelectric point. Thereafter, the gel strip is perpendicularly applied on top of a SDS polyacrylamide gel and proteins are separated according to their molecular weight.

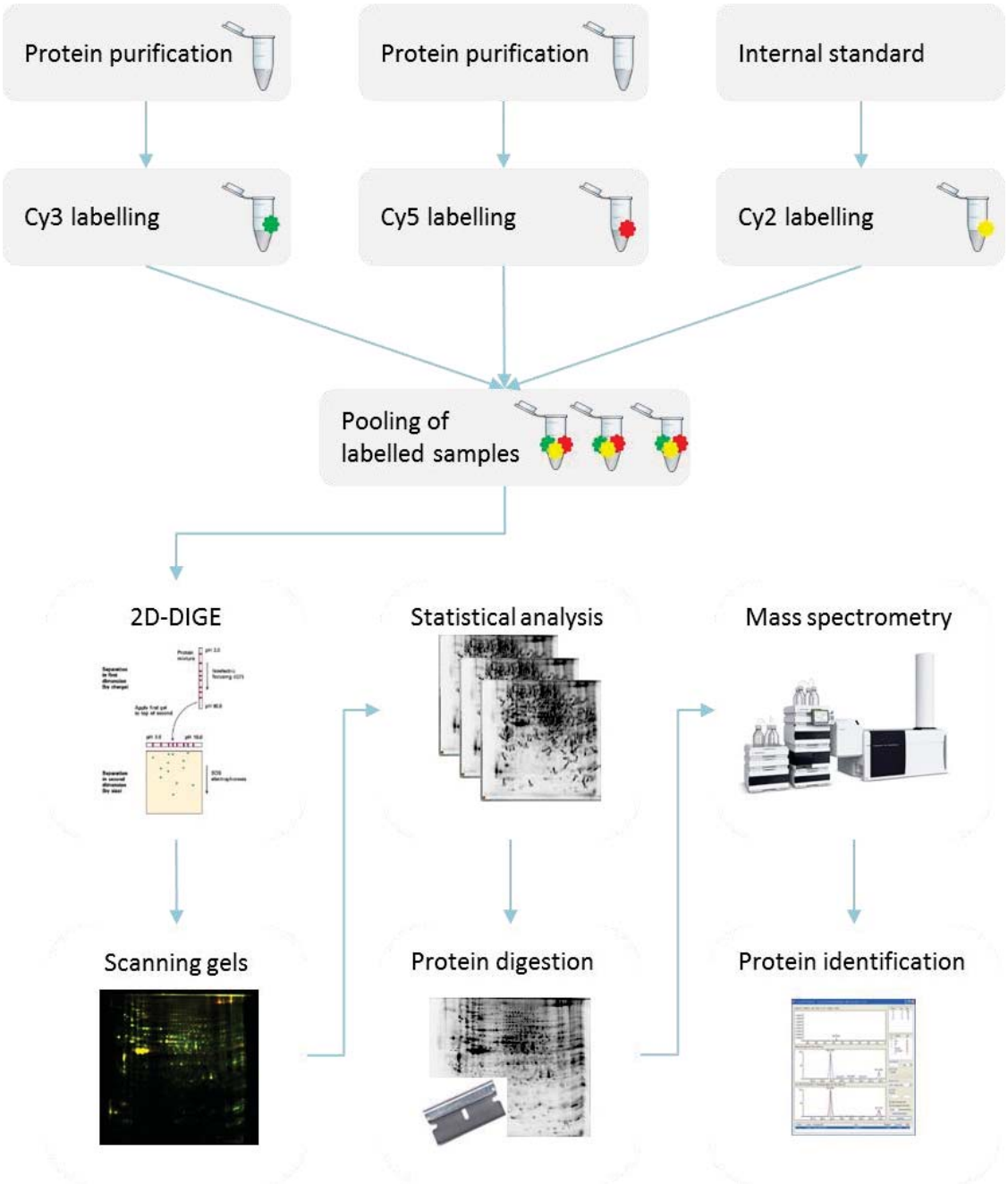

Figure 2.5 Proteomic analysis workflow. After extraction from colon tissue, sample protein was purified and labelled using either Cy3 or Cy5. An internal standard was prepared by pooling equal amounts of sample protein and labelled with Cy2. The separation of proteins according to charge and molecular weight was performed by two-dimensional difference gel electrophoresis (2D-DIGE). Spot-features on gel that met the cut-off criteria (FC $\geq$ |1.5| and p-value $\leq$ 0.05) were excised and digested from the gels and thereafter identified by liquid chromatography-mass spectrometry (LC-MS) with a nano-electrospray ionisation (ESI) interface. Proteins were identified using the Proteome Discoverer 1.4 protein identification software.

2.8.2 Sample preparation

Protein extracted from colon tissue (described in Section 2.6) of six biological replicates per treatment group was purified to remove interfering substances and non-protein impurities with the 2-D Clean-Up Kit as instructed by the manufacturer (GE Healthcare, Buckinghamshire, UK). 300 µl sample protein was mixed with 300 µl precipitant, vortexed and incubated on ice for 15 min. 300 µl co-precipitant was added to the mixture, vortexed and centrifuged for 5 min (13,000 × g, 4°C). The supernatant was discarded and the pellet briefly centrifuged to remove any remaining liquid by careful pipetting. 40 µl co-precipitant was added to the pellet, incubated on ice for 5 min and centrifuged for 5 min (13,000 × g, 4°C). The supernatant was carefully removed by pipetting and 25 µl ddH_2O added to the pellet. Each tube was vortexed for 5-10 s until the pellet was dispersed, then 1 ml pre-chilled wash buffer and 5 µl wash additive were added. This protein mixture was kept on ice for 30 min, vortexed for 30 s in 10-min intervals. The samples were then centrifuged for 5 min (13,000 × g, 4°C), the supernatant removed and the pellet air-dried for 5 min. The dried pellet was resuspended in 200 µl resolubilisation buffer (Table 2.3) and vortexed to fully dissolve the pellet. The samples were placed in a thermomixer (Eppendorf, Hamburg, Germany) for overnight incubation at 600 rpm and 22°C.

Protein concentration was determined by the Bradford [306] microplate assay. The Bradford working solution was prepared by diluting 5 ml Protein Assay Dye Reagent Concentrate (BioRad Laboratories, California, USA) in 15 ml ddH_2O. A standard was prepared by dissolving 2 mg albumin from bovine serum (BSA; Sigma Aldrich, Missouri, USA) in 1 ml resolubilisation buffer (Table 2.3). Serial dilutions of samples and standard were prepared in a 96-well microplate, followed by the addition of 200 µl Bradford working solution and 15-min incubation at room temperature. Absorbance at 595 nm was measured using a VICTOR X3 Multilabel Plate Reader (PerkinElmer, Massachusetts, USA) and protein concentration was determined against the BSA standard. Protein samples were stored at -80°C until CyDye-labelling.

Table 2.3 Preparation of solutions and buffers used for colon protein analysis

Solution	*Details*
Resolubilisation buffer	7 M urea[1] 2 M thiourea[2] 40 mM Tris[4] 4% (*v/v*) CHAPS[1]
2x sample buffer	7 M urea 2 M thiourea 130 mM DL-Dithiothreitol[3] 4% (*v/v*) CHAPS 2% (*v/v*) IPG buffer (pH range 3-11 nonlinear)[2]
Rehydration solution	7 M urea 2 M thiourea 65 mM DL-Dithiothreitol 4% (*v/v*) CHAPS 2% (*v/v*) IPG buffer (pH range 3-11 nonlinear) 10% (*v/v*) isopropanol[6] A few crystals of bromophenol blue (sodium salt)[3]
SDS equilibration buffer	50 mM Tris 6 M urea 30% (*v/v*) glycerol[6] 2% (*w/v*) SDS[5] pH adjusted to 8.8 A few crystals of bromophenol blue (sodium salt)
SDS tank buffer	25 mM Tris 192 mM glycine[1] 0.1% (*w/v*) SDS
Modified colloidal coomassie stain	17% (*w/v*) ammonium persulphate[6] 3% (*v/v*) ortho-phosphoric acid[7] 34% (*v/v*) methanol[8] 0.1% (*w/v*) Coomassie Brilliant Blue G-250[3]
30% acrylamide stock solution	30% (*v/v*) acrylamide monomer solution (40% (*w/v*))[1] 2.67% (*w/v*) Piperazine di-acrylamide[1]
Running gel buffer	3 M Tris pH adjusted to 8.8
10% PAGE Protean II gels (4 gels)	50 ml 30% acrylamide stock solution 18.75 ml Running gel buffer 37.5 ml 80% (*w/v*) Sucrose 42.18 ml ddH_2O 750 µl 10% (*w/v*) ammonium persulphate 75 µl TEMED[1]
Trypsin stock solution	25 µg modified trypsin[9] in 50 µl 1 mM HCl
Trypsin working solution	20 µl trypsin stock solution 200 µl 25 mM ammonium bicarbonate 10 µl 100% acetonitrile[10]

[1]BioRad (California, USA); [2]GE Healthcare (Buckinghamshire, UK); [3]Sigma-Aldrich (Missouri, USA); [4]Invitrogen (California, USA); [5]AppliChem (Darmstadt, Germany); [6]Merck (Darmstadt, Germany); [7]Ajax Finechem by Thermo Fisher Scientific (Sydney, Australia); [8]Honeywell (New Jersey, USA); [9]Roche (Basel, Switzerland); [10]Pierce by Thermo Scientific (Rockford, USA). SDS: Sodium dodecyl sulphate.

2.8.3 CyDye-labelling

Sample protein was labelled using the CyDye DIGE Fluor (minimal dyes) Labeling Kit (GE Healthcare, Buckinghamshire, UK). Before use, the CyDyes were reconstituted in 25 µl dimethylformamide (Thermo Scientific, Delaware, USA), mixed by vortexing and briefly centrifuged to obtain the final working solution. Sample protein that was run on the same gel was labelled with either green fluorescent dye Cy3 or red fluorescent dye Cy5. An internal standard was prepared by pooling equal amounts of all samples and further labelled with yellow fluorescent dye Cy2. 1 µl respective CyDye working solution was added per 33.3 µg protein, mixed and spun briefly. Samples were kept on ice for 30 min. The labelling reaction was stopped by adding 1 µl 10mM L-lysine (Sigma Aldrich, Missouri, USA), mixed and incubated on ice for 10 min. The final protein mixture was obtained by pooling 33.3 µg Cy3-labelled protein, 33.3 µg Cy5-labelled protein and 33.3 µg Cy2-labelled internal standard and the addition of an equal volume of 2x sample buffer (Table 2.3).

2.8.4 Separation in the first dimension

ReadyStrip IPG strips (17 cm, pH range 3-10 nonlinear (BioRad Laboratories, California, USA)) were rehydrated overnight in 350 µl rehydration solution (Table 2.3) and covered with paraffin oil. The first dimension was run on a Multiphor II Electrophoresis System with an EPS 3501 XL Power Supply (Amersham/GE Healthcare, Buckinghamshire, UK) and MultiTemp III Thermostatic Circulator set to 20°C. Rehydrated strips were gently washed with ddH_2O and placed on an Immobiline DryStrip aligner. The ends of the strips were partially covered with damp paper electrode wicks to collect salts and other contaminants eluting from the sample. The electrode bars were placed on the paper wicks, and the sample cup-bar and sample cups positioned. The strip tray was then overlaid with paraffin oil and a maximum of 100 µl sample loaded into sample cups. IEF was conducted by running a linear gradient from 0 to 200 V over 0.01 h, followed by 200 V for 2 h. The voltage was increased to 3500 V over 1 h, and held at 3500 V for 50 h. For samples that required loading of more than 100 µl, focussing was conducted in two steps. At first, 100 µl samples were loaded and focussing was run for 0.01 h (200V), 2 h (200V) and 1 h (3500V). The remainder of the sample was then loaded and focussing restarted. Gel strips were stored at -80°C until second dimension separation.

2.8.5 Equilibration

Immediately before separation in the second dimension, strips were equilibrated to solubilise focussed protein and allow SDS binding. The first equilibration step was performed for 12 min in 1% (*w/v*) DL-Dithiothreitol (Sigma Aldrich, Missouri, USA) in SDS equilibration buffer (Table 2.3). The second equilibration step was performed for 6 min in 4% (*w/v*) iodoacetamide (BioRad Laboratories, California, USA) in SDS equilibration buffer. After equilibration, strips were trimmed to 14.5 cm length to fit the 2D gels.

2.8.6 Separation in the second dimension

Laboratory-made gels were prepared as illustrated in Table 2.3. Poured gels were first overlaid with 50% isopropanol which was replaced by ddH_2O after 1 h. Full polymerisation was completed overnight at room temperature. Polymerised gels were fixed in an SDS-PAGE Protean II unit (BioRad Laboratories, California, USA), and the equilibrated and trimmed gel strips were positioned on the gel. After careful removal of air bubbles between the strip and the gel, the strips were fixed in place using hot agarose solution (0.25% (*w/v*) in SDS tank buffer (Table 2.3)). Precision Plus Protein standard plugs (BioRad Laboratories, California, USA) were used as molecular weight markers. After adding SDS tank buffer (Table 2.3) to the setup, the power pack was set to 900V, 96mA and 4 h for 4 gels. Thereafter, the gels were washed in ddH_2O to remove SDS residues which would compromise the scan quality. Gels were scanned on a Typhoon9410 scanner (Amersham/GE Healthcare, Buckinghamshire, UK) with the following settings: Cy2 images using a 540 nm laser and a 520 nm band pass 40 emission filter; Cy3 images using a 550 nm laser and a 580 nm band pass 30 emission filter; and Cy5 images using a 530 nm filter and a 670 nm band pass 30 emission filter. Resolution was set to 200 µm. After scanning, gels were stained in modified colloidal coomassie stain (Table 2.3 [307]) for a minimum of 24 h, followed by 24 h wash in ddH_2O to remove excess stain. Gels were dried between cellophane sheets and stored in a sealed plastic bag.

2.8.7 In-gel protein digestion

Scanned gel pictures were uploaded into Decodon Delta2D (Greifswald, Germany) to overlay and align gel images digitally. The software automatically identified and matched

the same spot across gels and generated a master image featuring all spots. Spot-features were normalised against the internal standard and the proteins corresponding to spots were considered significantly different when FC ≥ |1.5| and p-value ≤ 0.05.

Proteins of interest were excised from the gel using a razor blade (approximately 1 mm^3 piece) and rehydrated in 100 µl ddH_2O for 30 min. A similar size gel piece from a protein-free region was included to check for trypsin auto-proteolysis products. The rehydrated gel pieces were transferred to a fresh tube and 100 µl 25 mM ammonium bicarbonate (pH 8.0)/50% acetonitrile added (sterilised using Millipore FH 0.5 µm and HA 0.45 µm filters (Millipore by Merck, Darmstadt, Germany)). The tubes were placed in a thermomixer (Eppendorf, Hamburg, Germany) for 10 min at 1,400 rpm, briefly spun, and the supernatant discarded. This wash step was repeated twice. After the third wash step and removal of the supernatant, the gel particles were dried in a vacuum centrifuge for 10 min (SpeedVac Savant (Thermo Fisher Scientific, Delaware, USA)). Proteins were digested by adding 15 µl trypsin working solution (Table 2.3). After overnight incubation at 37°C and 600 rpm in a thermomixer, the tubes were briefly spun, 30 µl 5% formic acid/50% acetonitrile added, and sonicated for 5 min in a water bath. The solution was transferred to a fresh 0.65 ml tube. The step was repeated twice and the washes pooled to obtain a final volume of 90 µl 5% formic acid/50% acetonitrile. The recovered peptides were concentrated to 10-20 µl in a vacuum centrifuge for approximately 60 min. Samples were stored at -20°C until protein identification.

2.8.8 Protein identification

Tryptic peptides were separated and analysed using an EASY-nLC 1000 chromatography system coupled to a LTQ linear ion trap mass spectrometer with a nanospray ESI interface operating in positive ionisation mode (ThermoScientific, San Jose, CA, USA). 2 µl sample were injected onto an Acclaim® PepMap100 C18 75 µm internal diameter (i.d.) x 2 mm trap column for online desalting and separated on a nanoscale Acclaim® PepMap RSLC column 50 µm i.d. x 150 mm (ThermoScientific, California, USA). Samples were eluted at a constant flow rate of 300 nl/min of eluent A (0.1% formic acid in water) and eluent B (0.1% formic acid in acetonitrile) applying the following linear gradient: (1) 70% eluent A and 30% eluent B over 10 min; (2) 15% eluent A and 85% eluent B over 12 min, then held at 15% eluent A and 85% eluent B for 38 min. Data was acquired using a 'Top3' method in data-dependent mode with 'Dynamic Exclusion' enabled.

Proteins were identified using Proteome Discoverer^{TM} 1.4 protein identification software (Thermo Scientific, California, USA) applying a SEQUEST HT algorithm. MS spectra were compared against the NCBI *Mus musculus* database, with tolerance values of two dalton for precursor ions and one dalton for fragment ions, and allowable modifications included static carboxyamidomethylation (+57) of cysteine residues and dynamic oxidation (+16) of methionine residues. The protein identification was evaluated using a cross-correlation factor (XCorr; quality of the sequence-to-spectrum ratio) and delta Cn (dCn; indicating the difference between the top ranked match reported and the second ranked match). Positive identification was defined as dCn > 0.1 and either XCorr > 2.0 for doubly charged peptides or XCorr > 2.5 for triply charged peptides. All matched peptides were confirmed by visual examination of the spectra. Bioinformatic analysis was performed after removal of multiple isoforms of the same protein [268].

2.9 Metabolomic analysis of urine

The field of metabolomics aims to study the metabolome, *i.e.* the entire metabolic content of a cell or organism at any given time [136]. It represents a vast number of components that belong to a wide variety of compound classes, for example amino acids, lipids, nucleotides, etc. After the intake of specific foods, metabolites may arise from the absorption, digestion and metabolism of food components [139], or represent diet-induced changes in the endogenous metabolism, which may offer access to unexplored metabolic pathways that are affected by diet [140, 281].

At present, metabolomic analyses are approached in two ways: metabolic profiling and metabolic fingerprinting [132]. Although not a true 'Omics' approach, targeted metabolic profiling focusses on the analysis of a group of metabolites, for example amino acids, and can therefore provide insights into changes in disease mechanisms or diet-induced effects. In contrast, metabolic fingerprinting is the comprehensive analysis of the entire detectable metabolome in a given sample, with subsequent classification of samples (by their "fingerprint") followed by identification of the discriminating metabolites [132]. This untargeted approach can be used to identify changes in the metabolic "fingerprint" of a given sample. Most commonly, two technological platforms are used involving nuclear magnetic resonance (NMR) spectroscopy or MS, the latter usually coupled with the separation techniques gas chromatography or liquid chromatography. The advantage of liquid chromatography-

mass spectrometry (LC-MS) for the untargeted approach arises from the ease of sample preparation while retaining the possibility to detect a wide range of compound classes. Furthermore, as a "soft" ionisation, LC-MS has the advantage that metabolites reach the detector as fragmented ions, providing structural information about the metabolite and aiding initial identification [308].

2.9.1 Method overview

The workflow for the untargeted metabolite fingerprinting of mouse urine applied in the present thesis is illustrated in Figure 2.6. After sample preparation [309], samples were injected into an LC-MS operating in negative and positive ESI mode. MS data were processed using the XCMS package written in R [310]. Metabolite fingerprinting was focussed on the identification of metabolites which showed significant differences between treatments groups. These metabolites were annotated by comparing fragmentation patterns and mass-per-charge (*m/z*) ratios against literature and metabolite databases, including METLIN [311] and Human Metabolome Database (HMDB [312]).

2.9.2 Sample preparation and LC-MS analysis

Mouse urine was prepared according to Otter *et al.* [309] with a few modifications. Briefly, 4 µl urine was diluted with 200 µl 0.1% formic acid in a 250 µl glass vial. A quality control sample was prepared by pooling 4 µl from all urine samples and mixing thoroughly. This control sample was injected after every 15 to 30 samples and used to evaluate the stability and performance of each LC-MS run, providing information about the quality of the final data [313].

Sample urine from the "EPA time-course experiment" was analysed on a Thermo LC-MS/MS system (Thermo Fisher Scientific, Massachusetts, USA) fitted with an Accela 1250 quaternary UHPLC pump, auto-sampler and coupled to a Q Exactive Quadrupole-Orbitrap MS operating in both negative and positive ESI. Sample urine (5 µl) was injected in randomised order and resolved on an Agilent Zorbax SB-C18 column (2 x 50 mm, 1.8 µm (Agilent, California, USA)) using a mobile phase of 0.1% (*v/v*) formic acid in water (eluent A) and 0.1% (*v/v*) formic acid in acetonitrile (eluent B). At a constant flow rate of 400 µl/min, the following linear gradient was applied: (1) 95% eluent A and 5% eluent B over 1.5 min; (2) 100% eluent B over 8.5 min with a 1-min hold at 100%

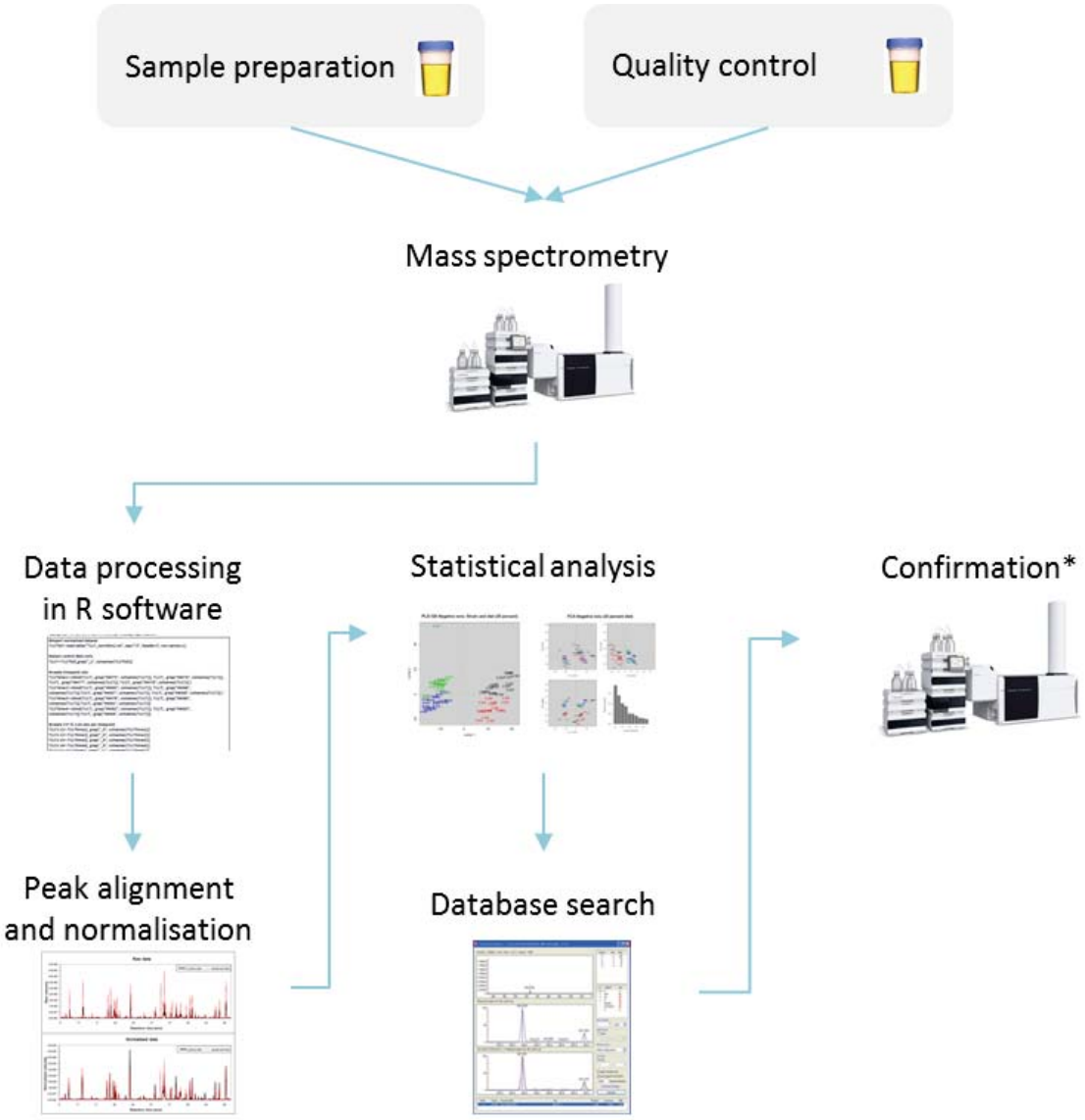

Figure 2.6 Metabolomic analysis workflow. Sample urine was prepared according to Otter *et al.* [309] and injected onto the HPLC system coupled with mass spectrometry (MS) operating in both positive and negative electrospray ionisation mode. A quality control sample comprising of mixed equal volumes of sample urine was injected every 15 to 30 samples. MSConvert software by ProteoWizard [314] was used to convert Thermo Fisher .raw data to .mzXML files. Data were normalised and correct for retention times using the XCMS package in R. Ions corresponding to metabolites were searched against publicly available databases. (*) the identity of selected ions from the "salmon diet experiment" were confirmed using high-resolution MS.

eluent B; (3) linear gradient to 95% eluent A and 5% eluent B over 1 min with a 3-min hold at 95% eluent A and 5% eluent B. Mass spectra were evaluated with XCalibur software (Thermo Electron Corporation, California, USA) and fragmentation patterns compared to the literature and databases.

In the "salmon diet experiment", sample urine collected from the respective collection days were run in separate analytical MS batches. Within each MS batch, sample urine was randomised and 2 µl injected into a UHPLC system and resolved on an SB-C18 column (50 x 2 x 1.8 µm). The UHPLC system was coupled to a Thermo LTQ XL linear ion trap MS (Thermo Electron Corporation, California, USA) operating in both negative and positive ESI and equipped with a Thermo Accela 1250 pump and an auto-sampler[3]. Samples were eluted from the column into the electrospray source at a constant flow rate of 400 µl/min of eluent A (0.1% (*v/v*) formic acid in water) and eluent B (0.1% (*v/v*) formic acid in acetonitrile) using the following linear gradient: (1) 95% eluent A and 5% eluent B over 1.5 min; (2) linear gradient to 100% eluent B over 8.5 min and a 1-min hold at 100% eluent B; (3) linear gradient to 95% eluent A and 5% eluent B over 1 min; and a 3-min hold at 95% eluent A and 5% eluent B. Mass spectra were evaluated with XCalibur software.

2.9.3 MS data processing and statistical analysis

The raw mass spectra data files were first converted to mzXML format using MSConvert by ProteoWizard [314, 315]. This was necessary to generate common text-based data that can be used for further processing and analysis. MSConvert was used with the following settings: Output format 'mzXML', Extension '32-bit', including 'Write index', 'Use zlib compression' and a 'PeakPicking filter' set from one. The XCMS package in the Bioconductor project written in R 3.1.2 ("EPA time-course experiment") and 3.0.1 ("salmon diet experiment") and was used for data pre-processing, quality assessment of MS runs, normalisation and metabolomic fingerprinting [310, 316]. Peaks of overlapping *m/z* bins were grouped, followed by retention time correction using loess smoothing, regrouping of peaks, and filling missed peaks. The codes applied in each experiment for data pre-processing are detailed in Appendix II. Un-normalised data were plotted as

[3] The analysis of sample urine from the "salmon diet experiment" was carried out first and the Thermo LC-MS/MS system as used in the "EPA time-course experiment" was not yet available.

heatmaps to detect effects related to sample injection order. The quality of the MS run was visually assessed by plotting total ion count intensities of quality control samples. Normalisation and log-transformation were applied to raw data. The final number of biological replicates per group is shown in Table 2.4 (EPA time-course experiment") and Table 2.5 ("salmon diet experiment"). For statistical evaluation of the metabolite data, each urine collection time-point was analysed separately.

Permutational multivariate analysis of variance using distance matrices (permutational MANOVA; from the Vegan package in R) was performed to evaluate differences in the urinary metabolite fingerprints between the treatment groups. Data were further visualised by Principal Component Analysis (PCA) and Partial Least Squares-Discriminant Analysis (PLS-DA). Analysis was first focussed on the ions with the ten highest PLS-DA loadings ("discriminant ions"; those that drive the separation between treatment groups) and statistical significance was evaluated using an ANOVA after log-transformation, followed by an LSD post-hoc test using a 5% significance level.

However, the identification of the "discriminant ions" based on database and literature search was largely not possible in the "EPA time-course experiment", therefore data was further evaluated by calculating p-values for all ionisation products using a Kruskal-Wallis test followed by multiple testing correction using the false discovery rate (FDR) estimation [317]. For metabolite identification, masses and fragmentation patterns of ions were searched against literature and databases, including METLIN [311] and HMDB [312].

In the "salmon diet experiment", "discriminant ions" with putative identification were analysed on a Thermo LC-MS/MS system (Thermo Fisher Scientific, Massachusetts, USA) to confirm their identity. The system was fitted with an Accela 1250 quaternary UHPLC pump, a 2 µl injection loop, and coupled to a Q Exactive Quadrupole-Orbitrap MS set to a resolution of 35,000. The sample urine for MS/MS identification was chosen based on the signal intensity detected by LC-MS. A high signal intensity of the ion implies a highly abundant metabolite and a good representation of the metabolite in the sample was needed to ensure detection above background signals. 10 µl sample was injected and resolved on an Agilent SB-C18 column (50 x 2 x 1.8 µm) using a mobile phase of 0.1% (*v/v*) formic acid in water (eluent A) and 0.1% (*v/v*) formic acid in acetonitrile (eluent B). At a constant flow rate of 400 µl/min, the following linear gradient

Table 2.4 Numbers of urine samples obtained from C57BL/6J mice and *Il10*$^{-/-}$ mice fed AIN-76A diets, either unmodified, or enriched with oleic acid (OA) or eicosapentaenoic acid (EPA), and included in metabolomic data analysis. Numbers of biological replicates were the same for positive and negative ionisation mode. Urine was collected at 7.1 (T1), 9 (T2), 10.1 (T3) and 12 (T4) weeks of age as part of the "EPA time-course experiment".

Genotype	*Diet*	*Scheduled sampling age (weeks)*	*T1*	*T2*	*T3*	*T4*
C57BL/6J	AIN-76A	12	5	4	4	4
	OA	9	10	8		
		12	9	8	7	9
	EPA	9	7	9		
		12	9	9	7	9
Il10$^{-/-}$	AIN-76A	12	10	9	7	6
	OA	9	10	9		
		12	9	9	7	9
	EPA	9	10	9		
		12	5	5	5	5

Table 2.5 Numbers of urine samples obtained from C57BL/6J mice and *Il10*$^{-/-}$ mice fed 30% salmon or 30% control diets and included in metabolomic data analysis. Numbers of biological replicates differed between positive and negative ionisation mode. Urine was collected at 6.2 (T1), 9 (T2), and 11.5 (T3) weeks of age as part of the "salmon diet experiment".

Ionisation mode	*Genotype*	*Diet*	*T1*	*T2*	*T3*
Positive	C57BL/6J	30% control	4	4	5
		30% salmon	2	4	7
	Il10$^{-/-}$	30% control	5	4	4
		30% salmon	6	4	7
Negative	C57BL/6J	30% control	5	4	5
		30% salmon	4	4	7
	Il10$^{-/-}$	30% control	5	4	4
		30% salmon	8	4	7

was applied: (1) 95% eluent A and 5% eluent B over 1.5 min; (2) 100% eluent B over 8.5 min with a 1-min hold at 100% eluent B; (3) linear gradient to 95% eluent A and 5% eluent B over 1 min with a 3-min hold at 95% eluent A and 5% eluent B. Mass spectra were evaluated with XCalibur software and fragmentation patterns compared to literature and databases.

2.10 Microbiomic analysis of caecum digesta

Microbiomics aims to capture genomic information from the microbiota present in an environment. With the invention of next-generation sequencing, for example, 454 pyrosequencing (Roche), SOLiD sequencing (Life Technologies) or Illumina sequencing (Illumina, Inc.), the exploration of the role of the microbiota in GIT homeostasis was enabled [318]. Roche's 454 FLX titanium sequencing targets the 16S gene region of the ribosomal RNA (rRNA) [319], a highly conserved gene in bacteria that consists of nine hyper-variable regions (V1-V9). During sequencing, the nucleotide sequences are read to a certain length and the reads are assigned to specific groups of organisms, the operational taxonomic units (OTUs). The advantage of Roche's 454 pyrosequencing compared to other methods is the capability to generate a relatively large amount of sequences with a good average read length (approximately 400 base pairs) despite relatively low costs [320]. Thus a good coverage of the microbial genome structure (average bacterial gene length approximately 950 base pairs [321]) can be achieved enabling more robust identification of the resident bacteria [322].

2.10.1 Method overview

The workflow for the microbiomic analysis from caecum digesta is illustrated in Figure 2.7. Briefly, DNA was extracted from caecum digesta and amplified using two sets of primers targeting the hyper-variable regions 1-3 (V123) and 4-6 (V456) of the 16S rRNA gene. Amplicons were purified and pyrosequenced on an FLX titanium sequencer (Roche, Connecticut, USA). Data was denoised and chimera-checked in Quantitative Insights Into Microbial Ecology (QIIME) software.

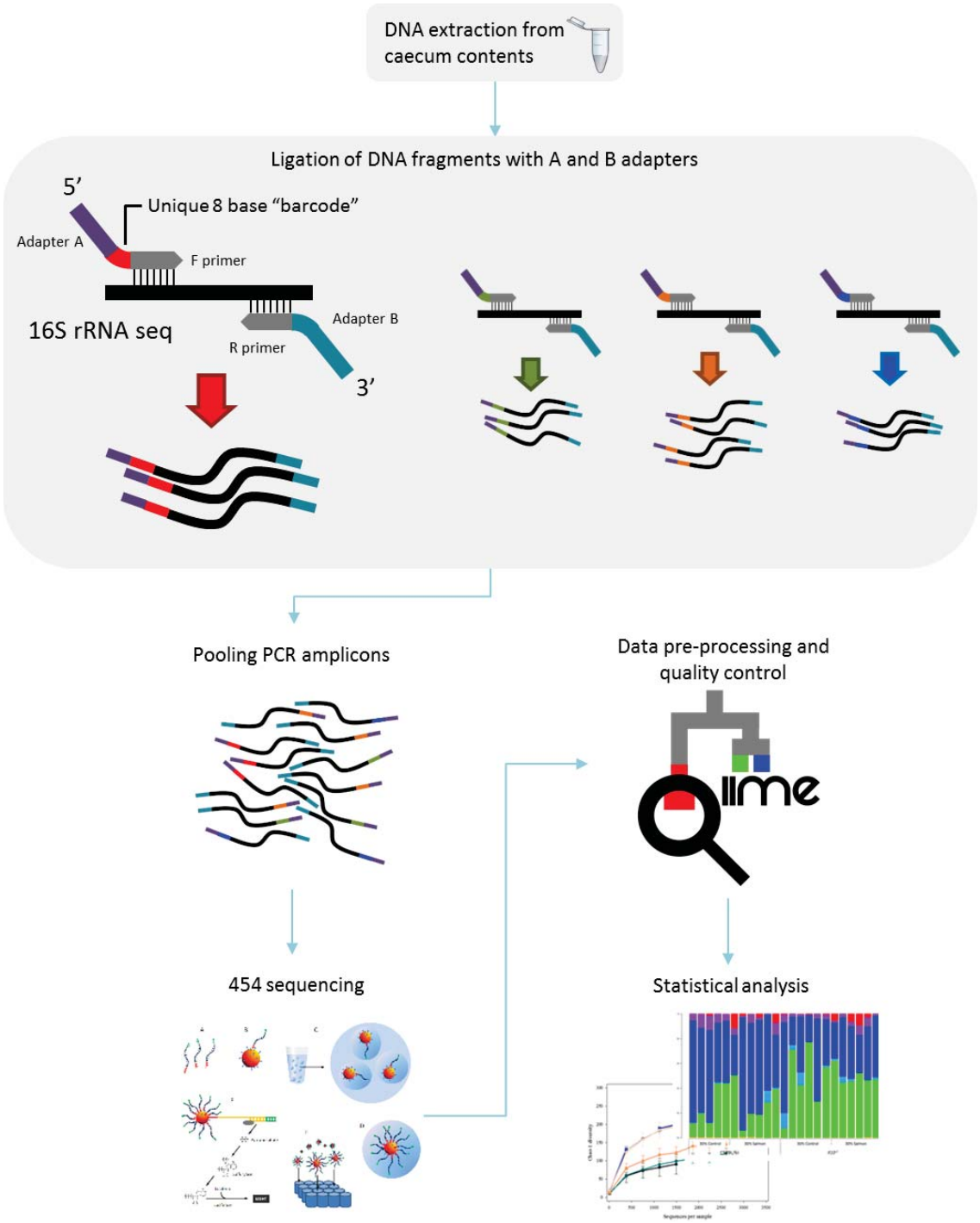

Figure 2.7 Microbiomic analysis workflow. After DNA extraction from caecum digesta, amplification of the 16S rRNA amplicons was performed using barcode-tagged primers. The community composition of the caecal microbiota was determined by 454 pyrosequencing on a FLX titanium sequencer (Roche). Quantitative Insights Into Microbial Ecology (QIIME 1.6) was used for sequence denoising, chimera-checking and statistical analysis.

2.10.2 Extraction of metagenomic DNA and 454 pyrosequencing

DNA was extracted from caecum digesta of six biological replicates per treatment group from the "salmon diet experiment", using the NucleoSpin Soil Kit as instructed (Macherey-Nagel, Dueren, Germany), quantified on a NanoDrop ND-1000 spectrophotometer (Thermo Fisher Scientific, Delaware, USA) and diluted to a concentration of 100 ng DNA in 10 µl RNAse-free water. This analysis was not carried out in the "EPA time-course experiment" because it has previously been reported [277]. The amplification of the regions V123 and V456 of the 16S rRNA gene was performed using a fixed primer on one end and a second primer carrying a unique barcode on the other (Microsynth, Balgach, Switzerland). The quality of amplification products was assessed by gel electrophoresis and amplicons were further purified using the High Pure PCR Product Purification Kit as instructed (Roche, Mannheim, Germany). Purification was performed to remove partial length PCR products and other impurities (*e.g.* enzymes and salts). Samples were pooled (500 ng per sample) and 454 pyrosequencing performed on a FLX titanium sequencer by Nestlé Research Center (Lausanne, Switzerland).

2.10.3 Data analysis

Denoised and chimera-checked sequences were analysed using QIIME 1.6. OTUs were clustered at a 97% sequence similarity using the UCLUST algorithm. Taxonomy was assigned to sequencing reads using the Ribosomal Database Project program at a default confidence score of 0.8. Community structure of the caecal microbiota was analysed as implemented in the QIIME pipeline [323, 324]: (1) species diversity (α-diversity) was estimated by rarefaction to illustrate differences between treatment groups [325] and statistically evaluated using an ANOVA in GenStat 15th edition; (2) within individual samples, the proportions of OTUs were calculated and further summarised by treatment groups to evaluate proportional shifts related to diet and/or genotype. Statistical significance was evaluated using a permutational MANOVA from the package Predictmeans in R 3.0.2 [326]; and (3) the level of phylogenetic (dis)similarity of microbiota in individual mice was visualised by Principal Coordinate Analysis (PCoA) using unweighted and weighted UniFrac distances as implemented in QIIME [327]. While the unweighted UniFrac distance only takes into account the presence or absence of taxa, a weighted UniFrac distance also considers abundance levels of the present taxa.

2.11 Bioinformatic analysis

The 'Omics'-technologies transcriptomics (gene expression), proteomics (protein expression), metabolomics (metabolite abundance) and microbiomics (microbiota) are high-throughput analyses that generate vast amounts of data, but extracting biologically meaningful information can be a challenge. Bioinformatic tools are essential in the analysis of these datasets, allowing an insight into the mechanisms by which the n-3 PUFA-enriched diets impact colitis in *Il10*$^{-/-}$ mice. Data from multiple 'Omics' platforms was further integrated to show biological pathways of interest with the aim to show "systemic" responses of the effects of n-3 PUFA-rich diets on colitis.

2.11.1 Ingenuity Pathway Analysis

Differentially expressed genes from the microarray dataset that passed the cut-off criteria (FC $\geq$ |1.5| and p-value $\leq$ 0.005) were uploaded into QIAGEN's Ingenuity Pathway Analysis (IPA, QIAGEN Redwood City, California, USA) to generate biological networks and to associate genes and proteins to functions and canonical pathways. 'Core analysis' was performed on datasets with default settings. For datasets with more than 1000 differentially regulated microarray probes, more stringent cut-off criteria were applied to reduce the dataset to approximately 1000 analysis-ready genes ('Best Practices for Expression Data Analysis' in the IPA handbook).

Differentially expressed genes and proteins were linked to their biological functions in the Ingenuity Knowledge Base. Biological functions were categorised into functional groups of *Diseases and Disorders*, *Molecular and Cellular Functions* and *Physiological System Development and Function*. Based on the direction of change of genes, a predicted activation state for each function was calculated, with *activation z-score* $\leq$ -2 for decreased state and $\geq$ 2 for increased state. P-values were calculated based on right-tailed Fisher's exact test. Biological functions were considered significantly affected when *activation z-score* $\geq$ |2| and p-value $\leq$ 0.05.

Canonical pathways are predefined metabolic and cell signalling pathways mapped by a number of molecules (genes/proteins and metabolites) that can affect its regulation. Based on the number of genes and direction of change, a ratio and a p-value are calculated for each pathway. By definition, the ratio indicates the number of genes that are affected, divided by the total number of molecules mapping the pathway.

Canonical pathways that show a low p-value combined with a high ratio are most likely affected in the dataset. Canonical pathways were considered significantly affected when p-value ≤ 0.05.

The *Upstream regulator analysis* in IPA is based on the expected interaction of an "upstream regulator" with its target molecules. The term "regulator" can cover different molecule types (transcription factors, cytokines, microRNAs, receptors, kinases, chemicals or drugs), but affects the expression of another molecule. The predicted activation state of a regulator is based on its known target molecules and their direction of change, whereby the gene expression of the upstream regulator is not taken into account. The *activation z-score* indicates the significance of the predicted activation state (activated or inhibited) and the *p-value of overlap* summarises the significance of genes that are downstream of the regulator, independently of the gene's direction of change. Analyses were focussed on transcription factors using the threshold *activation z-score* ≥ |2| and *p-value of overlap* ≤ 0.05.

2.11.2 Gene Set Enrichment Analysis

Parallel to the single-gene analysis, GSEA was performed with a focus on *a priori* defined sets of genes comprising KEGG pathways. KEGG is a publicly available database that contains information for 282 mouse-specific pathways [328]. The pathways in the database comprise of genes and proteins (the molecular building blocks), and metabolites and other small molecules, all of which are integrated to form biological interaction relationships. The information contained in the pathways is used to assign genes to sets and these gene sets can further be utilised for GSEA [301]. Genes are statistically evaluated in their biological context, for example within a KEGG pathway, and therefore GSEA may be biologically more relevant compared to single-gene analysis [329].

In GSEA, individual genes do not have to meet a significance value [301]. Reducing genes by applying a FC and p-value cut-off, thereby focussing on genes that show the largest difference between the treatment groups [301], could omit important information by setting arbitrary cut-offs [330]. GSEA may be a powerful tool when the microarray data generated appears to show subtle changes, but as a whole these changes are consistent and may explain an observed phenotype [331, 332]. Especially in metabolic

diseases, changes in gene expression are often subtle, but coordinated across members of shared biological functions [331, 332].

GSEA was used to collectively analyse sets of genes comprising KEGG pathways, and the statistical significance of gene sets was evaluated using Rotation gene set testing for linear models (ROAST) from the LIMMA package in R [333-335]. In ROAST, genes within a set were either increased in expression, contributing to the KEGG pathway being increased, or decreased in expression, contributing to the KEGG pathway being decreased. KEGG pathways were considered significant when p-value $\leq$ 0.01 (colon and PBMCs) and 0.05 (liver).

2.11.3 Integration of 'Omics' data

The integration of 'Omics' data aimed to establish a systemic response to the nutritional intervention with EPA and salmon. The integration of colon genes and proteins with urine metabolites associated with tryptophan metabolism was conducted utilising the WikiPathways application [336] in Cytoscape version 3.2.1 [337]. The correlation network comprising the caecal microbiota and urinary metabolites were generated using the mixOmics package in R 3.1.3 with a correlation threshold set to greater than 0.7 for positive correlation or less than -0.7 for negative correlation. Networks were generated for negative and positive ionisation mode separately and plotted in Cytoscape version 3.2.1. Ions with an ANOVA p-value less than 0.001 were defined as different between genotypes (*Il10*$^{-/-}$ vs. C57BL/6J mice fed 30% control) or between diets within *Il10*$^{-/-}$ mice (30% salmon vs. 30% control). Hepatic gene expression and urinary metabolites were correlated in R 3.1.3 using a Pearson correlation coefficient greater than 0.65 for positive correlation and less than -0.65 for negative correlation. The network was plotted in Cytoscape version 3.2.1.

2.12 Conclusion and outlook

The underlying molecular responses by which EPA- and salmon-containing diets influence colitis are largely unknown, but elucidating these responses may allow the mining of these datasets for biomarkers to predict their effects on colitis with minimally invasive methods. Two dietary intervention studies with n-3 PUFA-enriched diets were performed in *Il10*$^{-/-}$ mice, a model for human IBD ("EPA time-course experiment" and "salmon diet experiment"). An overview of data collected and measurements carried out

as part of these intervention studies is listed in Table 2.6, and of the work performed by the PhD candidate as well as collaborative contributions in Table 2.7. The 'Omics'-technologies transcriptomics (gene expression) and proteomics (protein expression) were used to identify metabolic pathways and key gene/protein regulatory "hubs" in the colon and/or PBMCs/liver of *Il10*$^{-/-}$ mice which were responsive to n-3 PUFA-enriched diets. A metabolomic approach was used to identify metabolites in mouse urine and microbiomics collected information about microbial changes in the caecum that were influenced by the n-3 PUFA-enriched diets.

Table 2.6 Overview of samples collected and measurements performed in the "EPA time-course experiment" and "salmon diet experiment"

EPA time-course experiment [4, 5]		*Salmon diet experiment* [6, 7]
Time-series Urine Metabolite abundance		*Time-series* Urine Metabolite abundance
Early colitis	*Established colitis*	*Established colitis*
Intestine Histopathology	Intestine Histopathology	Intestine Histopathology
Colon Gene expression	Colon Gene expression	Colon Gene and protein expression
PBMC Gene expression	PBMC Gene expression	
		Liver Gene expression
		Caecum Microbiota composition

[4] Colon protein samples were not available due to defrosting during transit.
[5] Effects of an EPA-enriched diet on microbial community profile previously shown [277].
[6] PBMCs for isolation from blood were not available in "salmon diet experiment".
[7] Samples for early colitis not collected, as the focus was on established colitis.

Table 2.7 Tasks performed in the "EPA time-course experiment" and "salmon diet experiment" including contributions by the PhD candidate.

Experiment and tasks performed
EPA time-course experiment
The experiment was organised by Dr Matt Barnett and animal husbandry and sample collection were performed by Ms Leigh Ryan (both AgResearch Grasslands).
Statistical evaluation of growth performance was conducted by Ms Lindy Guo (AgResearch Grasslands) after consultation with the candidate.
Histopathological assessment was performed by Mr Shuotun Zhu (University of Auckland, Auckland) and statistical evaluation of histology scores by Dr John Koolaard (AgResearch Grasslands) after consultation with the candidate.
Isolation of PBMCs from blood, extraction of RNA from PBMCs and colon, and microarray analysis were performed by Ms Kelly Armstrong (AgResearch Grasslands). Microarray data processing was performed by the candidate with the guidance of Mr Paul Maclean (AgResearch Ruakura).
Urine samples were collected by Ms Leigh Ryan, prepared for analysis by Drs Wayne Young and Anna Russ, and LC-MS was operated by Dr Don Otter (all AgResearch Grasslands). Statistical evaluation of metabolite data was conducted by the candidate with the guidance of Dr Jan Huege (AgResearch Grasslands).
Bioinformatic analysis and interpretation of results were performed by the candidate.
Salmon diet experiment
The candidate organised the experiment and performed animal husbandry and sample collection.
Statistical evaluation of growth performance was conducted by Dr John Koolaard after consultation with the candidate.
Histopathological assessment was performed by the candidate and Mr Shuotun Zhu (final scores reported in this dissertation were obtained by Mr Zhu). Statistical evaluation of histology scores was performed by Dr John Koolaard after consultation with the candidate.
Extraction of RNA from colon and liver was performed by the candidate. Microarray analysis of liver was performed by Ms Kelly Armstrong and the candidate performed microarray analysis of colon. Microarray data processing was performed by the candidate with the guidance of Dr Wayne Young. qPCR analysis was performed by the candidate.
Protein purification, 2D-DIGE and in-gel protein digestion were conducted by the candidate. Gel alignment and evaluation of significant spot-features were performed by Ms Di Brewster (Plant & Food Research, Auckland) and MS for protein identification was performed by Dr Janine Cooney (Plant & Food Research, Hamilton).
Urine samples were collected and prepared for analysis by the candidate and LC-MS was operated with the guidance of Dr Don Otter. Statistical evaluation was conducted by the candidate with the guidance of Dr Wayne Young. LC-MS/MS for the confirmation of putative identifications was performed by the candidate with the guidance of Dr Karl Fraser (AgResearch Grasslands).
Extraction of DNA from caecum digesta and PCR were performed by Ms Hetty KleinJan (AgResearch Grasslands) under the supervision of the candidate. QIIME analysis was performed by Dr Wayne Young. Statistical evaluation and visualisation were performed by the candidate with the guidance of Dr Wayne Young.
Bioinformatic analysis and interpretation of results were performed by the candidate.

Chapter 3

Effects of eicosapentaenoic acid-based diets on early and established colitis in the interleukin-10 gene-deficient mouse

3.1 Introduction

n-3 PUFA, in particular EPA, may be able to mitigate the course of IBD (including colitis) by interacting with and influencing the expression of genes in inflammatory pathways. Evidence of the beneficial effects of n-3 PUFA on colitis is inconsistent, potentially due to dose-responses, time-point of intervention (before/after clinical signs of colitis) and differences in bioavailability of lipids that are supplied for intervention [5, 7, 193-197]. In *Il10*$^{-/-}$ mice, a model of colitis similar to that occurring in IBD, feeding a diet enriched with pure EPA showed reduced colitis compared to those fed a control diet [6]. These studies have also shown that the molecular responses to dietary n-3 PUFA underlying any observed changes in colitis could be identified by the analysis of gene expression, which provides new insights on their effects. For example, pathways such as fatty acid metabolism, xenobiotic metabolism, oxidative stress and tryptophan metabolism that were altered in *Il10*$^{-/-}$ mice with established colitis were either increased or unaffected in these mice fed an EPA-rich diet [6].

Alterations in these colonic pathways in response to consuming a diet rich in n-3 PUFA may be *via* direct interaction with target genes or *via* intermediate molecules (such as the transcription factor PPARA) that subsequently alter gene expression [248]. EPA is a natural ligand of PPARs, which is an important transcriptional regulator of inflammatory genes. PPAR activation, observed in various animal models of colitis fed PUFA-rich diets [3, 6, 250, 252], can inhibit NFKB pathways and prevented the induction of inflammatory and immune response genes [338, 339]. These findings suggest that increased activity of PPARs and their impact on target genes in response to dietary EPA supplementation may have beneficial effects on several pathways related to inflammation and immune activation in the early stages of colitis and this may reduce the risk of developing colitis. The molecular responses to an EPA-rich diet in the colon of *Il10*$^{-/-}$ mice during the early stages of colitis remain to be elucidated.

Biomarkers are objective indicators of disease that in the case of IBD, are indicators of colitis, and changes in these biomarkers can provide evidence of the efficacy of, for example, nutritional intervention with EPA. Therefore, biomarkers may have an important role in translating fundamental research using animal models to a clinical setting. The minimally invasive nature of sample collection for urine and blood makes them convenient sources for identifying biomarkers of colitis. Differences in the urinary

metabolite profiles of mice with experimental colitis compared to non-inflamed mice [281, 340] and of IBD patients compared to healthy controls [156, 157, 341] have been linked to metabolites of the microbiota and of tryptophan metabolism in the colon. Lin *et al.* [281] highlighted tryptophan catabolites as early indicators of colitis in the urine of *Il10*$^{-/-}$ mice. Other authors have also reported increased activity of genes that mediate tryptophan catabolism in the caecum and colon of *Il10*$^{-/-}$ mice with established colitis [6, 342, 343]. The importance of tryptophan in inflammation and immune activation makes this pathway a target for candidate biomarkers of colitis [344, 345]. Understanding if an EPA-rich diet modulates tryptophan processes and associated urinary metabolites (as potential biomarkers) at an early stage of colitis is therefore essential.

Equally relevant for the identification of biomarker targets, PBMCs are inflammatory cells that infiltrate various tissues *via* the blood circulation. Transcriptomic profiling of PBMCs from IBD patients has highlighted that gene expression changes were largely associated with immune and inflammatory responses compared to healthy subjects [149, 346]. PBMCs have also increasingly been used to provide evidence of the effects of dietary n-3 PUFA on gene expression [151, 347], indicating reduced expression of NFKB target genes, inflammatory cytokines and genes involved in eicosanoid synthesis in healthy elderly subjects [151]. Given the relative ease of PBMC isolation from blood samples, PBMC gene expression responses to EPA-rich diets could provide targets to identify candidate biomarkers. This knowledge, together with that derived from urinary metabolites, could be used to identify biomarker targets to better translate the effects of diets rich EPA on colonic responses observed in experimental models such as *Il10*$^{-/-}$ mice to IBD patients.

3.2 Hypothesis and aim

The first hypothesis of this study was that the lower levels of colitis previously observed in 12-week-old *Il10*$^{-/-}$ mice (*i.e.,* with established colitis) in response to dietary EPA is also observed at 9 weeks of age (*i.e.*, during early stages of colitis). The second hypothesis was that PBMC gene expression and urinary metabolites from *Il10*$^{-/-}$ mice are reflective of these changes in colitis, both at an early stage of colitis and when it is established. To test these hypotheses, *Il10*$^{-/-}$ and C57BL/6J mice were fed one of three AIN-76A-based diets from five weeks of age: unmodified, supplemented with 3.7% OA (control fatty acid) or supplemented with 3.7% EPA. The unmodified AIN-76A diet enabled

comparison between previously published studies using the *Il10*$^{-/-}$ mouse model [116, 268, 277, 286, 348] and this study. The OA diet was chosen as an appropriate control diet due to the lipid profile similarity to the EPA diet relative to that of the AIN-76A diet [286]; this diet has been reported to have no effect on tissue lipid composition and eicosanoid production [287].

The colon and PBMC gene expression and urinary metabolites were compared at an early stage of colitis (9 weeks of age) and when colitis was established (12 weeks of age) in *Il10*$^{-/-}$ mice fed either control diet. This was (a) to confirm that the *Il10*$^{-/-}$ mouse model worked as expected, and (b) to identify potential biomarkers (PBMC genes and urinary metabolites) that reflected changes from early to established colitis. Then the effects of the EPA diet on the same parameters were assessed (a) to determine whether this diet resulted in lower levels of colitis during the early stages, and (b) to identify biomarkers of colitis responsive to an EPA diet at both early and established stages. Molecular analyses were conducted using 'Omics'-technologies described in Chapter 2.

3.3 Methods

A total of 50 male *Il10*$^{-/-}$ mice (C57BL/6J background, formal designation B6.129P2-Il10^{tm1Cgn}/J) and 46 male C57BL/6J control mice were sourced from Jackson Laboratory (Maine, USA). One C57BL/6J mouse was dead on arrival, limiting the number of C57BL/6J mice available at the start of the experiment to 45. A graphical illustration of the experimental design applied in this study is shown in Figure 3.1.

Ten *Il10*$^{-/-}$ mice and ten C57BL/6J mice were assigned to the following treatment groups (with the exception of the AIN-76A diet, where n = 5 for C57BL/6J mice): (i) unmodified AIN-76A diet and sampling at 12 weeks; (ii) modified AIN-76A diet with 3.7% OA and sampling at 9 weeks; (iii) modified AIN-76A diet with 3.7% EPA and sampling at 9 weeks; (iv) modified AIN-76A diet with 3.7% OA and sampling at 12 weeks; and (v) modified AIN-76A diet with 3.7% EPA and sampling at 12 weeks.[8]

[8] Five *Il10*$^{-/-}$ mice reached the maximum allowed weight loss as per Animal Ethics guidelines and were therefore euthanised prior to the scheduled sampling time (one mouse fed the OA diet and scheduled sampling time at 12 weeks; four mice fed the EPA diet and scheduled sampling time at 12 weeks). These mice were included in intake and body weight analyses after considering goodness of fit for the statistical models, but were disregarded for subsequent analyses due to age differences at time of euthanasia to other mice.

Bacterial inoculation was carried out (described in Section 2.2.2) and treatment diets were fed from 11 days after arrival (mean age 6.6 weeks) due to a delay in the shipment of the diets. Diet preparation is described in Section 2.2.3 and fresh diets were provided three times weekly. A detailed description of the histological assessment is included in Section 2.4, transcriptomic analysis[9] of colon and PBMCs in Sections 2.5 to 2.7, and urinary metabolite fingerprinting in Section 2.9.

3.4 Results

3.4.1 Growth performance

The dietary intake of mice was dependent on genotype, with higher estimated mean intakes observed in *Il10*$^{-/-}$ mice (6.6 g) compared to C57BL/6J mice (6.3 g; $P < 0.001$ (Table 3.1)). The type of diet had a significant influence on food intake ($P = 0.03$), but a genotype × diet interaction was not observed ($P = 0.22$). The highest intakes were observed in mice fed the OA and AIN-76A diets (approximately 6.5 g), regardless of genotype or age. The lowest intakes were observed for mice fed the EPA diet, with an estimated mean intake of 6.4 g (9 weeks of age) and 6.2 g (12 weeks of age) (Table 3.1).

The mean body weight was independent of genotype ($P = 0.15$), but differed between the diets (AIN-76A, OA and EPA; $P = 0.03$ (Figure 3.2 and Table 3.1)). No interaction between genotype × diet was observed ($P = 0.87$). Up until 9 weeks of age, the estimated mean body weights between mice were similar, regardless of the type of diet (EPA or OA (Table 3.1)). In the treatment groups that were sampled at 12 weeks of age, the lowest mean body weights were observed for mice fed the EPA diet (20.6 g), significantly lower compared to mice fed the AIN-76A diet (21.3 g) or the OA diet (21.1 g) irrespective of genotype (Table 3.1).

[9] The low RNA yield from PBMCs restricted starting material for microarrays to 43 ng RNA. LincRNAs are featured on 8x60K microarrays but are beyond the scope of this dissertation which focusses on the identification of biomarkers in accessible tissues and were removed prior to the analysis. For microarray analysis, four biological replicates per treatment group were used, with the exception of C57BL/6J mice fed the AIN-76A where n = 3.

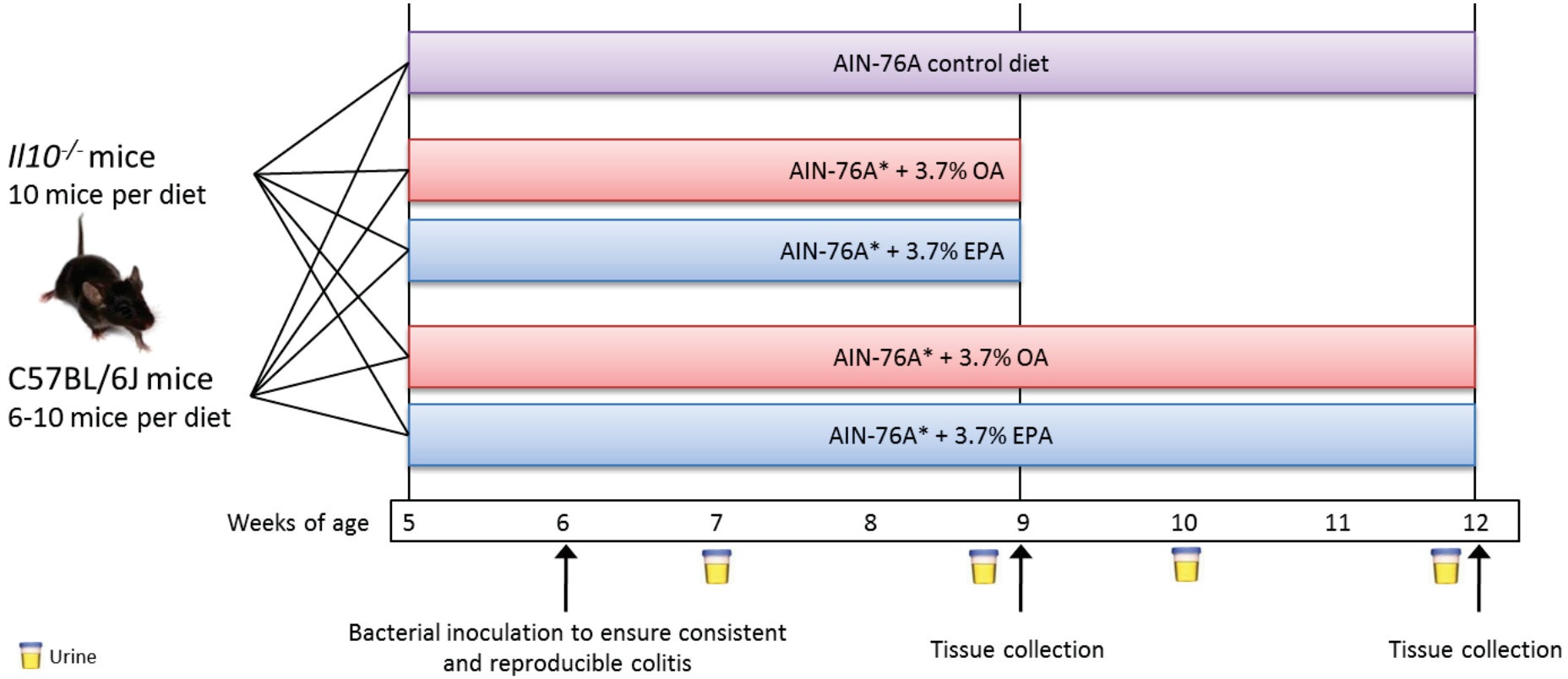

Figure 3.1 Design for the "EPA time-course experiment". 4-5-week-old *Il10*$^{-/-}$ mice (n=50) and C57BL/6J mice (n=46) were assigned to AIN-76A diets, either unmodified, or enriched with oleic acid (OA) or eicosapentaenoic acid (EPA). The OA diet was chosen as appropriate control diet for the EPA diet [286, 287] and the unmodified AIN-76A diet enabled comparison between previously published studies using the *Il10*$^{-/-}$ mouse model and this study. One C57BL/6J mouse was dead on arrival, limiting the number of C57BL/6J mice available at the start of the experiment to 45. Ten *Il10*$^{-/-}$ mice and ten C57BL/6J mice were assigned to each treatment group, with the exception of C57BL/6J mice fed the AIN-76A diet, where n = 5. Urine was collected at 7.1, 9, 10.1 and 12 weeks of age. Treatment diets were fed from 11 days after arrival (mean age 6.6 weeks) due to a delay in the shipment of the diets. Mice received a bacterial inoculation at 6.6 weeks of age and were sacrificed at 9 weeks (early colitis) or 12 weeks (established colitis) [116, 281]. (*) fat-free AIN-76A premix.

Table 3.1 Analysis of growth performance for "EPA time-course experiment". Dietary intake and body weights for C57BL/6J mice and *Il10*$^{-/-}$ mice fed AIN-76A diets, either unmodified, or enriched with oleic acid (OA) or eicosapentaenoic acid (EPA). Data represent estimated mean intakes (g) over 2-3 day periods or estimated mean body weights (g) and the 95% confidence interval. "Age" refers to scheduled sampling time (9 or 12 weeks) and unmodified AIN-76A diet and OA diet were included as control diets. P-values ≤ 0.05 were considered significant, and (*) denotes significance of the EPA diet to the AIN-76A diet with the same age at a 5% LSD level. Data represent ten biological replicates per treatment group, with the exception of C57BL/6J mice (AIN-76A) where n = 5.

Food intake (g)				*Body weight (g)*			
Genotype			*P-value*	*Genotype*			*P-value*
C57BL/6J		6.3 (6.2-6.4)	0.0001	C57BL/6J		20.8 (20.5-21.1)	0.154
Il10$^{-/-}$		6.6 (6.5-6.7)		*Il10*$^{-/-}$		21.0 (20.8-21.3)	
LSD (5%)		0.14		LSD (5%)		0.36	
Diet	*Age*			*Diet*	*Age*		
AIN-76A	12 weeks	6.5 (6.3-6.6)*	0.027	AIN-76A	12 weeks	21.3 (20.9-21.7)*	0.033
OA	9 weeks	6.5 (6.4-6.7)		OA	9 weeks	21.0 (20.6-21.4)	
EPA	9 weeks	6.4 (6.2-6.6)		EPA	9 weeks	20.6 (20.2-21.0)*	
OA	12 weeks	6.4 (6.3-6.6)		OA	12 weeks	21.1 (20.7-21.4)	
EPA	12 weeks	6.2 (6.1-6.4)*		EPA	12 weeks	20.6 (20.2-21.0)*	
LSD (5%)		0.22		LSD (5%)		0.54	

Significance was evaluated for the time comparison (9 vs. 12 weeks) in the same diet and for the diet comparison (EPA vs. OA; EPA vs. AIN-76A) at the same age.

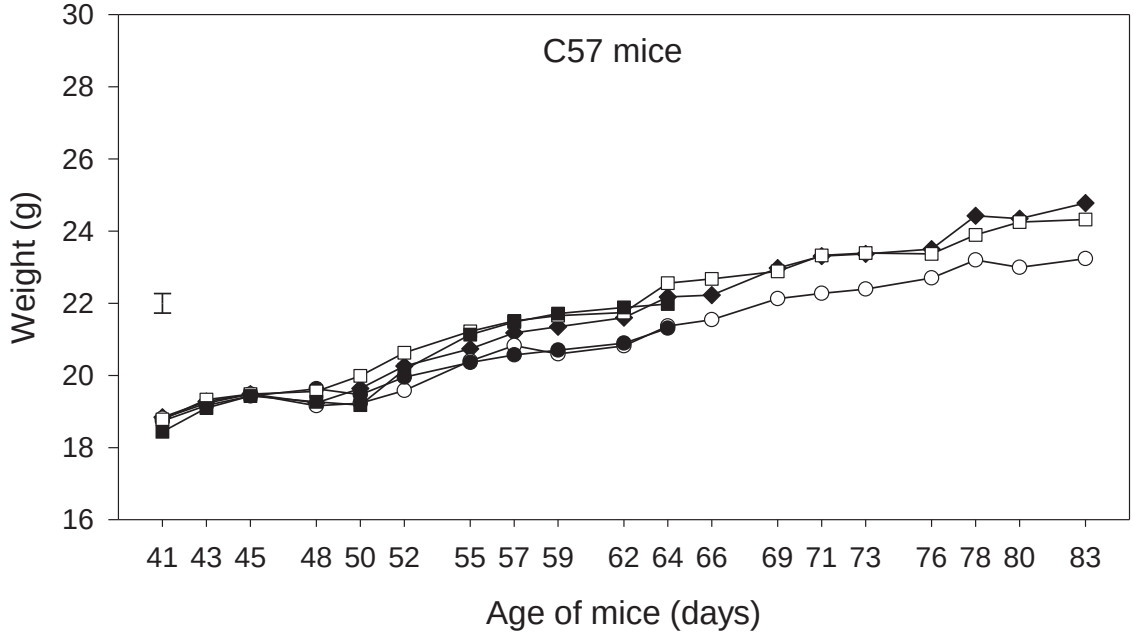

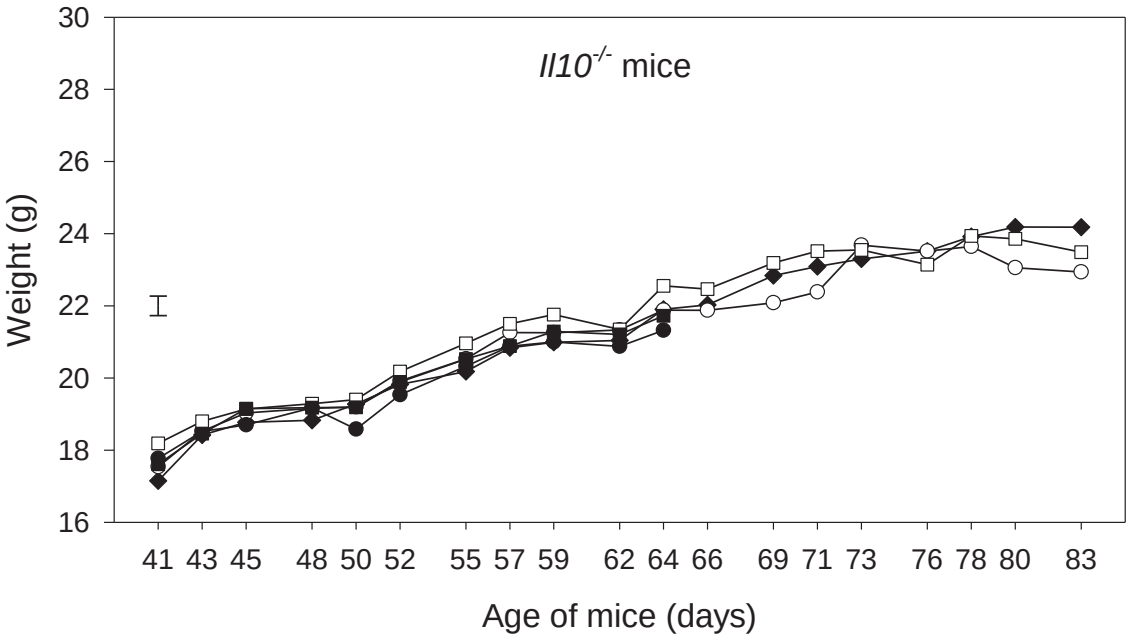

Figure 3.2 Mean body weights (g) for C57BL/6J and *Il10*$^{-/-}$ mice over the experimental period. The first measurement was taken five days after arrival, when the average age of the mice was 41 days of age and all mice were fed standard chow. Body weight was measured three times weekly thereafter. Mice were bacterially inoculated and fed treatment diets from 48 days of age. The final body weight was measured before a fast-feed period. Data represent five to ten biological replicates per treatment group. Error bar indicates the 5% LSD level.

◆ = AIN-76A diet (12 weeks); ■ = OA (9 weeks); □ = OA (12 weeks); ● = EPA (9 weeks); ○ = EPA (12 weeks).

3.4.2 Severity of intestinal inflammation at 9 and 12 weeks of age

No inflammation was observed in any section of the intestine in C57BL/6J mice (data not shown). Within *Il10*$^{-/-}$ mice, the degree of inflammation differed between the intestinal sections ($P < 0.001$), with lower HIS observed in the small intestine than the large intestine, irrespective of age (Table 3.2). The estimated mean HIS in the caecum and colon of *Il10*$^{-/-}$ mice at 9 weeks of age ranged from 12.7 to 16.3, and at 12 weeks of age from 14.1 to 20.7 (Table 3.2). Colitis in *Il10*$^{-/-}$ mice was characterised by infiltration of immune cells (primarily lymphocytes/plasma cells), aberrant crypts, and loss of crypts and these changes were independent of age or the type of diet (Figure 3.3).

At 9 weeks of age, the mean colon HIS was similar between *Il10*$^{-/-}$ mice fed the EPA diet and those fed the OA diet (Table 3.2) and no differences were observed in the individual histological features (Figure 3.3). At 12 weeks of age, the type of diet tended to affect the severity of colitis ($P = 0.1$), with highest mean colon HIS observed in *Il10*$^{-/-}$ mice fed the AIN-76A diet, followed by those fed the OA diet and the lowest scores for EPA-fed mice (estimated mean colon HIS of 20.7, 18.1 and 14.1, respectively (Table 3.2)). This reduction of colitis in *Il10*$^{-/-}$ mice fed the EPA diet was significant compared to those fed the AIN-76A diet, but not compared to those fed the OA diet (Table 3.2). However, in 12-week-old *Il10*$^{-/-}$ mice fed the EPA diet, reduced levels of crypt hyperplasia ($P = 0.06$) and infiltration of lymphocytes/plasma cells ($P = 0.006$), but increased lymphoid aggregates ($P = 0.02$), were observed compared to those fed either control diet (AIN-76A or OA (Figure 3.3)). Representative images of HE stained colon sections from C57BL/6J and *Il10*$^{-/-}$ mice fed the EPA diet can be found in Reference [6].

At 9 weeks of age, the total duodenal HIS was similar between *Il10*$^{-/-}$ mice fed the OA diet and those fed the EPA diet, with estimated mean scores of 3.1 and 3.7, respectively (Table 3.2). At 12 weeks of age, the degree of duodenal inflammation in *Il10*$^{-/-}$ mice fed the EPA diet was approximately 2-fold higher compared to those fed the OA diet, with estimated mean scores of 9.4 and 4.3, respectively (Table 3.2). This increase was mainly driven by the infiltration of inflammatory cells (primarily neutrophils and lymphocytes/plasma cells) and occurrence of aberrant villi in EPA-fed *Il10*$^{-/-}$ mice at 12 weeks (Appendix III).

Table 3.2 Estimated mean histological injury scores (HIS) obtained from intestinal sections of *Il10*$^{-/-}$ mice fed AIN-76A diets, either unmodified, or enriched with 3.7% oleic acid (OA) or 3.7% eicosapentaenoic acid (EPA). Mice were sampled at 9 or 12 weeks of age and the effects of the EPA diet compared to the AIN-76A and OA control diets. Data shown as predicted means using a restricted maximum likelihood (REML) estimation. Statistical significance was evaluated within the same tissue using an ANOVA and an LSD post-hoc test. Data represent ten (AIN-76A), ten (OA; 9 weeks of age), ten (EPA; 9 weeks of age), nine (OA; 12 weeks of age), and six (EPA; 12 weeks of age) biological replicates per treatment group.

Diet	*Age*	*Duodenum*	*Jejunum*	*Ileum*	*Caecum*	*Colon*
AIN-76A	12 weeks	4.7*	2.3	3.5	19.9	20.7*
OA	9 weeks	3.1	2.3	4.1	12.7*	15.4
OA	12 weeks	4.3*	2.1	3.0	17.6†	18.1
EPA	9 weeks	3.7*	2.2	3.0	16.2	16.3
EPA	12 weeks	9.4†	2.7	3.9	19.6	14.1†
LSD (5%)		1.6	n.d.	n.d.	4.8	5.2

Numbers not sharing a symbol differ at a 5% LSD level within the time comparison (9 vs. 12 weeks) in the same diet and within the diet comparison (EPA vs. OA; EPA vs. AIN-76A) at the same age. "n.d." not determined.

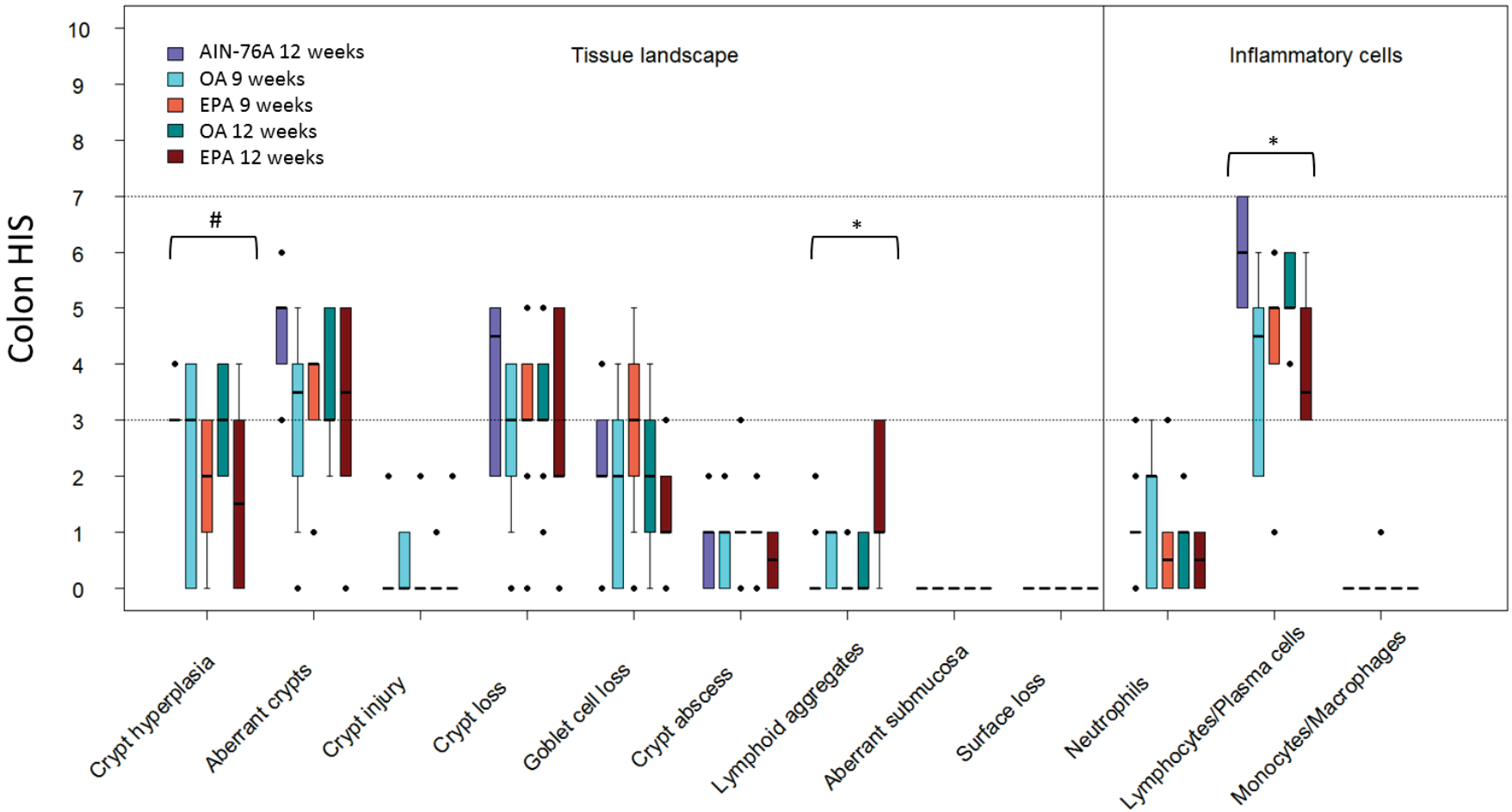

Figure 3.3 Histological injury scores (HIS) obtained from the colon of *Il10*$^{-/-}$ mice at 9 and 12 weeks of age. Mice were fed AIN-76A diets, either unmodified, or enriched with 3.7% oleic acid (OA) or 3.7% eicosapentaenoic acid (EPA). Individual features scored from 0 (no change from normal tissue) to 10 (extreme changes in tissue). Unmodified AIN-76A diet and OA diet were included as control diets. Data represent ten (OA; 9 weeks of age), ten (EPA; 9 weeks of age), nine (OA; 12 weeks of age), and six (EPA; 12 weeks of age) biological replicates per group. Statistical significance within each feature was calculated using Kruskal-Wallis one-way ANOVA in GenStat. (*) indicates significance $P < 0.05$; and (#) indicates a trend ($P < 0.1$).

3.4.3 Colon gene expression

Most changes in colon gene expression were observed between genotypes (*i.e. Il10*$^{-/-}$ vs. C57BL/6J mice), than within a genotype in response to the EPA supplementation (Table 3.3). This was also shown in Figure 3.4, with colon transcriptomic profiles clustering according to genotype, with *Il10*$^{-/-}$ and C57BL/6J mice showing a distinct separation based on gene expression profiles of the colon. The least changes in gene expression (approximately 25 genes) were observed in 9-week-old mice in response to the EPA supplementation, irrespective of genotype, compared to those fed the OA diet (Table 3.3). At a 0.5% significance level, the changes in these genes may be significant purely by chance and cannot be confidently linked to the influence of the EPA diet.

3.4.3.1 Comparison of colon gene expression between the AIN-76A and OA diet in *Il10*$^{-/-}$ mice

At 12 weeks of age, only 28 genes were differentially expressed between the colon of *Il10*$^{-/-}$ mice fed the OA diet and those fed the AIN-76A diet ($FC \geq |1.5|$ and $P \leq 0.005$), indicating that the OA diet affected gene expression similarly to the AIN-76A diet (Appendix IV). This result was supported by GSEA, with no KEGG pathway gene set differentially expressed in the colon of *Il10*$^{-/-}$ mice fed the OA diet compared to those fed the AIN-76A diet (data not shown). Thus the OA diet was considered an appropriate control to establish the effects of the EPA diet on colon gene expression in those mice and for the remainder of this chapter, the comparison will be presented in relation to the OA control diet unless stated otherwise.

3.4.3.2 Colon gene expression between mouse genotypes fed the OA diet

Approximately twice as many genes were differentially expressed in the colon of 12-week-old *Il10*$^{-/-}$ mice fed the OA diet (~2900 genes vs. 12-week-old C57BL/6J mice fed the same diet) than in 9-week-old *Il10*$^{-/-}$ mice fed the OA diet (~1400 genes vs. 9-week-old C57BL/6J mice fed the same diet) (Table 3.3). Most of the genes that were differentially expressed in OA-fed *Il10*$^{-/-}$ mice at 9 weeks of age were also differentially expressed at 12 weeks of age, with genes showing higher magnitude of absolute FC in 12-week-old *Il10*$^{-/-}$ mice (Table 3.4). As expected, among the genes with the largest FC were immune-regulatory genes, for example, regenerating islet-derived 3 gamma

Table 3.3 Numbers of differentially expressed genes in the colon of *Il10*$^{-/-}$ mice and C57BL/6J mice fed AIN-76A diets, either unmodified, or enriched with oleic acid (OA) or eicosapentaenoic acid (EPA). Samples were obtained at 9 or 12 weeks of age and the effects of the EPA diet compared to the AIN-76A and OA control diets. Genes passing a fold-change (≥ |1.5|) and p-value (≤ 0.005) cut-off were considered differentially expressed. Data represent four biological replicates per group, with the exception of C57BL/6J mice fed the AIN-76A diet where n = 3.

Contrast		*mRNA transcript levels*[1]		*Uploaded into Ingenuity Pathway Analysis*
		Increased	*Decreased*	*Analysis-ready molecules*[2]
Genotype comparison (Il10$^{-/-}$ *relative to C57)*				
9 weeks	OA	900	476	938
	EPA	1251	1269	820 (FC = 1.8 and P = 0.001)
12 weeks	AIN-76A	1455	1163	932 (FC = 1.8 and P = 0.001)
	OA	1558	1339	816 (FC = 2 and P = 0.001)
	EPA	1127	975	975 (FC = 1.5 and P = 0.001)
Diet comparison (EPA relative to OA)				
9 weeks	C57	22	2	13
	Il10$^{-/-}$	9	17	26
12 weeks	C57	113	57	133
	Il10$^{-/-}$	14	102	95

(1) FC ≥ |1.5| and p-value ≤ 0.005; genes may be represented with more than one probe on the array; (2) Reducing genes to 1000 genes for pathway analysis by applying more stringent FC and p-value as recommended in the IPA handbook.

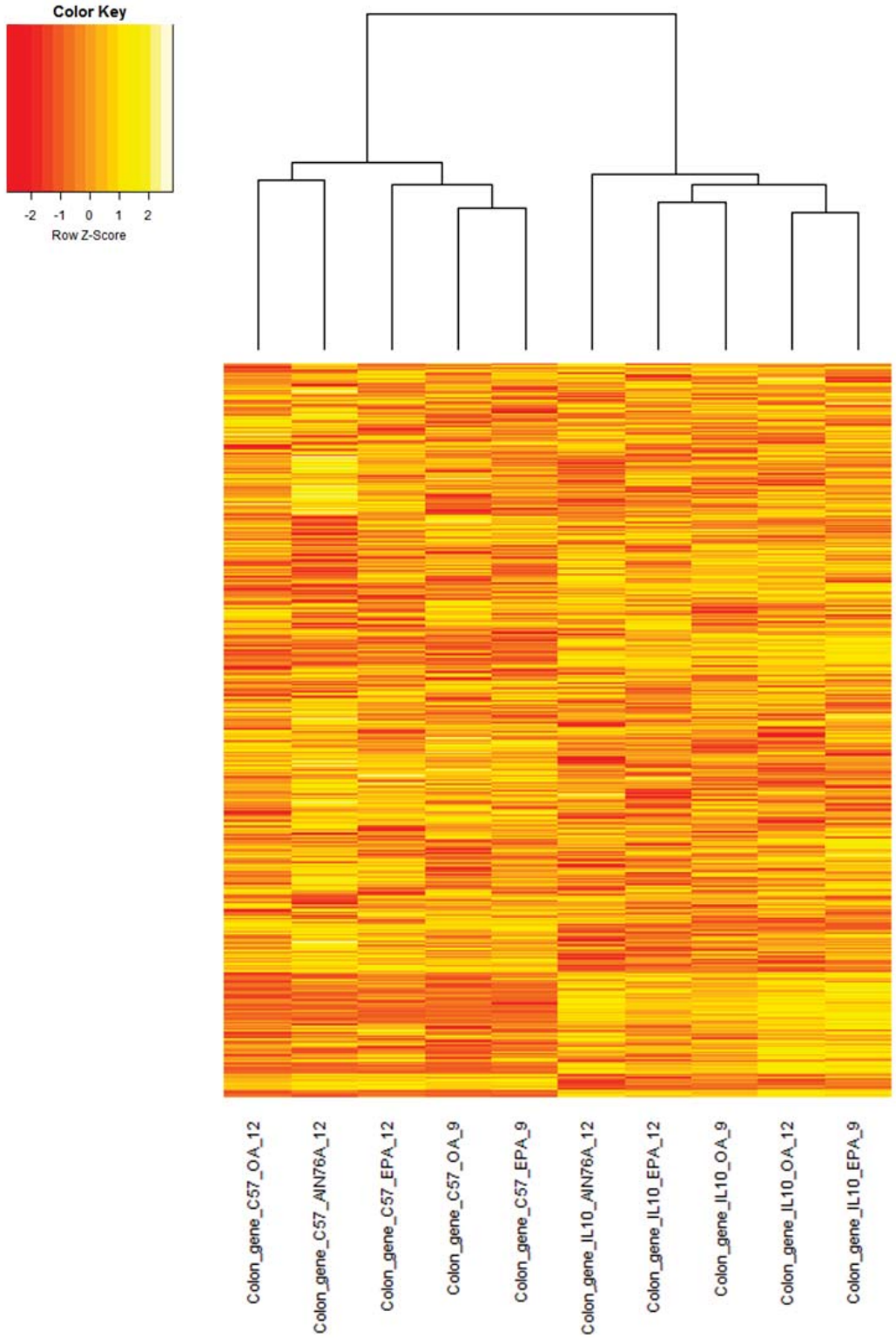

Figure 3.4 Heatmap of colon gene expression profiles in C57BL/6J mice and *Il10*$^{-/-}$ mice fed AIN-76A diets, either unmodified, or enriched with oleic acid (OA) or eicosapentaenoic acid (EPA). Colon samples were obtained at 9 or 12 weeks of age. The dendrogram above the heatmap was produced by hierarchical clustering of the treatment groups in the columns and illustrates the similarity of gene expression profiles, with higher similarity represented by closer relationship in the tree diagram. Rows indicate genes with the top 25% of variation across the treatment groups. Colour coding according to key. Data represent four biological replicates per group, with the exception of C57BL/6J mice fed the AIN-76A diet where n = 3.

(*REG3G*), indoleamine 2,3-dioxygenase 1 (*IDO1*), S100 calcium binding proteins A8 and A9 (*S100A8* and *S100A9*), and chemokine (C-X-C motif) ligands 6, 9, and 10 (*CXCL6*, *CXCL9* and *CXCL10*). The expression of these genes was increased in *Il10*$^{-/-}$ mice compared to C57BL/6J mice, with FC ranging from 3.7 to 23.2, irrespective of age (Table 3.4). Generally, the colon gene expression profiles of *Il10*$^{-/-}$ mice fed the OA diet at 9 and 12 weeks of age were similar (Pearson correlation coefficient = 0.98).

The ten highest p-value-ranked biological functions associated with the differentially expressed genes were similar between 9-week-old *Il10*$^{-/-}$ mice and 12-week-old *Il10*$^{-/-}$ mice fed the OA diet (vs. C57BL/6J mice) and mostly related to the cellular immune system (Table 3.5). These were for example "Activation" and "Quantity" of blood cells and "Activation", "Migration", "Movement", and "Quantity" of leukocytes, with the functions predicted to be increased in activity (*activation z-score* ≥ 2). At 9 weeks of age, the predictions for these 10 functions were based on 367 unique genes. Merging the genes into a biological interaction network (not shown due to the large number of genes) identified six central transcription regulators that affected the expression of many genes in the network. These were the interferon regulatory factor 1 and 8 (*IRF1* and *IRF8*), *TNF*, Spi-1 proto-oncogene (*SPI1*), *PPARA*, and spleen tyrosine kinase (*SYK*). The mRNA expression levels of these genes, except for *PPARA*, were increased by approximately 1.5 to 3.4-fold in *Il10*$^{-/-}$ mice compared to C57BL/6J mice, both fed the OA diet, indicating important roles in the regulation of the immune response in the colon of *Il10*$^{-/-}$ mice at 9 weeks of age.

At 12 weeks of age, the predictions for these ten functions were based on 376 unique genes. Merging the genes into a biological interaction network (not shown due to the large number of genes) identified five central transcription regulators that affected the expression of many genes in the network. These were *IRF1*, GATA binding protein 3 (*GATA3*), *PPARA*, FBJ murine osteosarcoma viral oncogene homolog (*FOS*), and lymphocyte-specific protein tyrosine kinase (*LCK*). The mRNA levels of these genes, except for *PPARA*, were increased by approximately 2.5-fold in *Il10*$^{-/-}$ mice compared to C57BL/6J mice, both fed the OA diet, indicating important roles in the regulation of the immune response in the colon of *Il10*$^{-/-}$ mice at 12 weeks of age.

Table 3.4 Genes with the highest fold-changes (FC) between the colon from *Il10*$^{-/-}$ mice and C57BL/6J mice fed the oleic acid (OA) diet (9 and 12 weeks of age). Ten genes with the highest positive FC and ten genes with the highest negative FC between 9-week-old *Il10*$^{-/-}$ mice vs. C57BL/6J mice and between 12-week-old *Il10*$^{-/-}$ mice vs. C57BL/6J mice are shown. Data represent four biological replicates per group.

Gene name (Gene ID)	*Il10*$^{-/-}$ *vs. C57BL/6J*	
	9 weeks of age	*12 weeks of age*
Genes with decreased expression		
Cytochrome P450, family 4, subfamily B, polypeptide 1 (*CYP4B1*)	-10.2	-16.6
Sulfotransferase family, cytosolic, 1C, member 2 (*SULT1C2*)	-5.6	-13.6
Galactose-3-O-sulfotransferase 2 (*GAL3ST2*)	-6.8	-12.5
Adiponectin, C1Q and collagen domain containing (*ADIPOQ*)	n.s.	-11.9
Carbonic anhydrase III, muscle specific (*CA3*)	n.s.	-11.9
Cytochrome P450, family 2, subfamily C, polypeptide 18 (*CYP2C18*)	n.s.	-11.0
Complement factor D (adipsin) (*CFD*)	n.s.	-8.8
Chromogranin B (secretogranin 1) (*CHGB*)	-2.9	-7.6
Chromogranin A (parathyroid secretory protein 1) (*CHGA*)	-3.1	-7.0
Resistin (*RETN*)	n.s.	-6.8
Colipase, pancreatic (*CLPS*)	-4.4	-5.6
Transient receptor potential cation channel, subfamily M, member 6 (*TRPM6*)	-3.6	-5.1
Protease, serine, 23 (*PRSS23*)	-4.2	-4.6
Neurexophilin and PC-esterase domain family, member 2 (*NXPE2*)	-5.3	-3.6
Metallothionein 1 (*Mt1*)	-4.5	n.s.
Metallothionein 2 (*Mt2*)	-5.3	n.s.
Phosphatidylinositol-4-phosphate 5-kinase, type I, alpha (*PIP5K1A*)	-4.9	n.s.
Genes with increased expression		
Indoleamine 2,3-dioxygenase 1 (*IDO1*)	6.7	23.2
S100 calcium binding protein A9 (*S100A9*)	5.6	22.2
Chemokine (C-X-C motif) ligand 9 (*CXCL9*)	11.5	19.5
Chemokine (C-X-C motif) ligand 10 (*CXCL10*)	8.1	13.8
Chemokine (C-X-C motif) ligand 6 (*CXCL6*)	4.0	13.0
Granzyme A (granzyme 1, cytotoxic T-lymphocyte-associated serine esterase 3) (*GZMA*)	8.2	12.9
Regenerating islet-derived 3 gamma (*REG3G*)	14.6	12.8
S100 calcium binding protein A8 (*S100A8*)	3.7	12.3
Interferon gamma induced GTPase (*Igtp*)	8.7	12.2
Nitric oxide synthase 2, inducible (*NOS2*)	8.0	12.0
T cell specific GTPase 1 (*Tgtp1*/*Tgtp2*)	8.1	10.1
Tripartite motif containing 15 (*TRIM15*)	7.5	9.4
Predicted gene 4951 (*Gm4951*)	6.9	8.8
Ubiquitin D (*UBD*)	8.7	7.0

"n.s." indicates a non-significant change in mRNA expression levels in the given contrast (FC < |1.5| and P > 0.005).

Table 3.5 Most significantly affected biological functions in the colon of *Il10*$^{-/-}$ mice compared to C57BL/6J mice fed the oleic acid (OA) diet (9 and 12 weeks of age). Functions with an *activation z-score* < |2| were excluded and biological functions limited to show the ten highest p-value-ranked functions. "# genes" indicates the number of genes associated with the biological function and individual genes may be represented in more than one function. Data represent four biological replicates per group.

Functions annotation		*P-value*	*# genes*	*Predicted activation state (activation z-score)*	*Category*
9 weeks of age					
Blood cells	Activation	1.73E-33	134	Increased (+4.9)	2, 5
	Quantity	1.42E-38	182	Increased (+2.6)	2 3
Leukocytes	Activation	1.86E-33	128	Increased (+4.8)	2, 5, 6, 7
	Migration	4.43E-37	159	Increased (+4.6)	6, 13
	Movement	4.67E-33	139	Increased (+4.4)	2, 6, 13
	Quantity	2.61E-41	173	Increased (+2.7)	2, 3
Lymphocytes	Quantity	5.51E-34	136	Increased (+3.6)	2, 3
Mononuclear leukocytes	Quantity	8.61E-34	139	Increased (+3.7)	2, 3
Glucose metabolism disorder		6.00E-44	205	Increased (+3.4)	12
Infection of mammalia		1.27E-38	96	Decreased (-5.3)	14
12 weeks of age					
Inflammatory response		9.17E-42	142	Increased (+4.0)	7
Cells	Activation	1.31E-41	162	Increased (+4.1)	5
Blood cells	Activation	1.43E-41	137	Increased (+4.7)	2, 5
	Quantity	2.33E-47	183	Increased (+3.2)	2, 3
Leukocytes	Activation	9.06E-43	133	Increased (+4.7)	2, 5, 6, 7
	Migration	3.93E-53	172	Increased (+5.0)	6, 13
	Movement	9.74E-47	150	Increased (+4.8)	6, 13
	Quantity	2.66E-51	176	Increased (+3.1)	2, 3
Glucose metabolism disorder		1.20E-54	207	Increased (+3.9)	12
Infection of mammalia		7.77E-48	101	Decreased (-5.2)	14

Categories: 1 Cellular Function and Maintenance; 2 Hematological System Development and Function; 3 Tissue Morphology; 4 Cellular Growth and Proliferation; 5 Cell-To-Cell Signalling and Interaction; 6 Immune Cell Trafficking; 7 Inflammatory Response; 8 Cell-mediated Immune Response; 9 Cellular Development; 10 Hematopoiesis; 11 Lymphoid Tissue Structure and Development; 12 Metabolic Disease; 13 Cellular Movement; 14 Infectious Disease; 15 Tissue Development; 16 Cell Morphology; 17 Cell Death and Survival; 18 Cellular Compromise; 19 Lipid Metabolism; 20 Small Molecules Biochemistry; 21 Organismal Survival; 22 Molecular Transport; 23 Organismal Development; 24 Cellular Assembly and Organisation; 25 Humoral Immune Response; 26 Protein Synthesis; 27 Immunological Disease; 28 Cardiovascular Disease.

GSEA supported the IPA results, showing that irrespective of age, the colon transcriptomic profile for *Il10*$^{-/-}$ mice fed the OA diet was associated with immune-related KEGG pathway gene sets compared to C57BL/6J mice fed the same diet ($P \leq 0.01$ (Table 3.6)). There was a good concordance of affected KEGG pathway gene sets between 9-week-old *Il10*$^{-/-}$ mice and 12-week-old *Il10*$^{-/-}$ mice, with 43 sets in common (Table 3.6). For example, within the biological process *Organismal systems* (function *Immune system*), the KEGG pathways *Antigen processing and presentation* and signalling pathways against bacteria and other pathogens such as *Intestinal immune network for IgA production*, *Cytosolic DNA-sensing pathway* and *Natural killer cell mediated cytotoxicity*, were increased in expression in the colon of *Il10*$^{-/-}$ mice (all $P \leq 0.01$ vs. C57BL/6J mice both fed the OA diet (Table 3.6)).

GSEA indicated decreased *PPAR signalling* in the colon of *Il10*$^{-/-}$ mice fed the OA diet (vs. C57BL/6J mice fed the same diet), but differences were dependent on age of mice (Table 3.6). At 9 weeks of age, *PPARA* mRNA expression levels were decreased 2.4-fold and at 12 weeks of age, a 4.3-fold decrease was detected ($P \leq 0.005$). As a gene set, the KEGG pathway *PPAR signalling* did not pass the significance criteria for differential expression in 9-week-old *Il10*$^{-/-}$ mice ($P = 0.05$, with 25% genes decreased). In 12-week-old *Il10*$^{-/-}$ mice, almost twice as many genes were affected in the *PPAR signalling* pathway (approximately 47% decreased ($P = 0.003$)), indicating a loss of functionality of *PPAR signalling* associated with the development of colitis in *Il10*$^{-/-}$ mice (Table 3.6).

Large increases in mRNA expression levels of the gene *IDO1* which catalyses the metabolism of tryptophan to kynurenine (Figure 3.6) has previously been observed in the large intestine of *Il10*$^{-/-}$ mice [6, 342] and was also shown in the current experiment, irrespective of age (Table 3.4). In contrast, the expression of genes that lead to the synthesis of tryptamine and tryptamine-derived metabolites (*e.g. DDC*, *INMT*, *AOC1*, *MAOA* and *MAOB*) and serotonin (*e.g. TPH* and *DDC*) were decreased in expression in the colon of *Il10*$^{-/-}$ mice fed the OA diet (vs. C57BL/6J mice fed the same diet (Figure 3.5 and Figure 3.6)). GSEA further supported these results, showing that the set of genes comprising the KEGG pathway *Tryptophan metabolism* was differentially expressed in the colon of 9-week-old *Il10*$^{-/-}$ mice fed the OA diet, with 25% genes decreased and 19% increased in expression compared to C57BL/6J mice fed the same diet (Table 3.6 and Figure 3.5). At 12 weeks of age, twice as many genes were decreased (30%) than

increased (14%) in expression in *Il10*$^{-/-}$ mice compared to C57BL/6J mice both fed the OA diet ($P \leq 0.01$ (Table 3.6)).

Within the biological processes *Organismal systems* and *Metabolism*, the expression of KEGG pathways associated with the digestion, absorption and metabolism of several nutrients was reduced in *Il10*$^{-/-}$ mice fed the OA diet compared to C57BL/6J mice fed the same diet (Table 3.6). These included for example, amino acids, carbohydrates, lipids, and cofactors and vitamins. This reduction in metabolism-related processes may indicate loss of functionality of biochemical pathways in the colon of *Il10*$^{-/-}$ mice and further point towards reduced energy levels for colonic mucosal cells. This was supported by reduced expression of two KEGG pathway gene sets related to *Energy metabolism* for *Il10*$^{-/-}$ mice fed the OA diet, regardless of age (9 or 12 weeks). Reduced functionality of pathways necessary for the detoxifications of xenobiotics in the colon was further observed, specifically by cytochrome P450, and may have been connected to the energy deficiency in those mice (Table 3.6). As these metabolism-related changes were not apparent in IPA, it may indicate that the metabolism-related genes show subtle, but coordinated changes in expression within a group of shared biological functions, rather than individual genes showing a high magnitude of fold-changes.

3.4.3.3 Effect of the EPA diet (vs. OA diet) on colon gene expression in *Il10*$^{-/-}$ mice

Within *Il10*$^{-/-}$ mice, colon gene expression changes were more pronounced at 12 weeks of age than at 9 weeks of age in response to EPA supplementation (vs. those fed the OA diet), with more differentially expressed genes in the colon of older mice (Table 3.3). However, the total number of differentially expressed genes in the colon was less than 200, irrespective of genotype. There was limited concordance between the differentially expressed genes, with only three genes (*MEP1A*, *CCL2*, and *IL1B*) in common between 9-week-old and 12-week-old *Il10*$^{-/-}$ mice fed the EPA diet (vs. those fed the OA diet (data not shown)). The direction of FC for these three genes was not consistent and potentially indicates that the EPA diet affected colon gene expression differently at early stages of colitis (9 weeks) compared to when colitis was established (12 weeks).

Table 3.6 KEGG pathway gene sets affected in the colon of *Il10*$^{-/-}$ mice compared to C57BL/6J mice fed the oleic acid (OA) diet and sampled at 9 or 12 weeks of age ($P \leq 0.01$). Numbers indicate the proportion of the KEGG pathway affected (%), with proportion of genes contributing to an increased KEGG pathway ("Up%") or proportion of genes contributing to a decreased KEGG pathway ("Down%"). Significance of changes in KEGG pathway expression was determined by GSEA using rotation gene set testing (ROAST function) in R. Data represent four biological replicates per treatment.

Biological process and function	*Pathway*	*9 weeks of age*			*12 weeks of age*		
		Down%	*Up%*	*P-value*	*Down%*	*Up%*	*P-value*
Cellular Processes							
Cell Communication	Gap junction	20.9	10.4	0.004	30.6	10.4	0.009
Transport and Catabolism	Phagosome	8.4	37.9	0.001	13.7	39.6	<0.001
Environmental Information Processing							
Signal Transduction	Hedgehog signalling	18.5	4.9	0.001	25.9	4.9	0.004
	Jak-STAT signalling			n.s.	11.1	27.1	0.001
Signalling Molecules and Interaction	Cell adhesion molecules (CAMs)	11.8	34.3	<0.001	17.2	35.3	<0.001
	Cytokine-cytokine receptor interaction	13.8	32.2	0.006	14.5	33.8	<0.001
	ECM-receptor interaction			n.s.	33.0	11.3	0.006
Genetic Information Processing							
Folding, Sorting and Degradation	Proteasome			n.s.	1.9	50.9	<0.001
Replication and Repair	Base excision repair			n.s.	2.0	29.4	0.003
	DNA replication			n.s.	2.1	35.4	0.004
Human Diseases							
Cancers	Basal cell carcinoma	14.3	3.9	0.004	27.3	2.6	0.007
Cardiovascular Diseases	Dilated cardiomyopathy			n.s.	29.1	12.8	0.001
	Hypertrophic cardiomyopathy (HCM)			n.s.	27.6	13.4	0.009
	Viral myocarditis	7.8	40.3	<0.001	7.8	40.3	<0.001
Endocrine and Metabolic Diseases	Type I diabetes mellitus	8.2	54.8	<0.001	9.6	58.9	0.001
Immune Diseases	Allograft rejection	3.3	67.2	<0.001	0.0	68.9	0.001
	Asthma	0.0	64.0	<0.001	0.0	56.0	<0.001
	Autoimmune thyroid disease	3.9	51.9	<0.001	1.3	53.2	<0.001
	Graft-versus-host disease	3.0	66.7	<0.001	0.0	68.2	<0.001
	Primary immunodeficiency	1.9	40.4	0.003	1.9	40.4	0.001

	Rheumatoid arthritis	8.4	42.1	0.001	13.7	47.4	<0.001
	Systemic lupus erythematosus	4.9	47.2	<0.001	9.7	45.8	<0.001
Infectious Diseases	African trypanosomiasis	17.9	38.5	0.003	20.5	43.6	<0.001
	Chagas disease (American trypanosomiasis)	10.4	27.8	0.006	13.9	34.0	<0.001
	Leishmaniasis	4.4	47.3	0.002	6.6	51.6	<0.001
	Malaria	21.6	37.3	0.008	25.5	39.2	0.003
	Staphylococcus aureus infection	1.6	59.4	<0.001	4.7	57.8	<0.001
	Toxoplasmosis			n.s.	13.9	37.0	0.002
Metabolism							
Amino Acid Metabolism	Cysteine and methionine metabolism			n.s.	22.8	10.5	0.010
	Histidine metabolism	19.4	6.5	0.003	35.5	16.1	0.008
	Phenylalanine, tyrosine and tryptophan biosynthesis	0.0	28.6	0.002	14.3	42.9	0.004
	Tryptophan metabolism	24.6	19.3	0.005	29.8	14.0	0.001
	Tyrosine metabolism	28.9	11.1	0.006	28.9	17.8	<0.001
	Valine, leucine and isoleucine degradation	25.4	6.3	0.008	46.0	6.3	0.001
Biosynthesis of Other Secondary Metabolites	Butirosin and neomycin biosynthesis	0.0	40.0	0.006	0.0	40.0	0.001
Carbohydrate Metabolism	Ascorbate and aldarate metabolism	27.3	9.1	0.006	50.0	4.5	0.008
	Butanoate metabolism			n.s.	34.1	4.9	0.008
	Glyoxylate and dicarboxylate metabolism			n.s.	25.0	0.0	0.009
	Pyruvate metabolism			n.s.	29.0	11.3	0.002
Energy Metabolism	Nitrogen metabolism	26.7	6.7	0.006	46.7	6.7	0.002
	Sulfur metabolism	30.8	0.0	0.005	53.8	0.0	0.004
Lipid Metabolism	alpha-Linolenic acid metabolism			n.s.	13.8	31.0	0.007
	Biosynthesis of unsaturated fatty acids			n.s.	23.5	11.8	0.002
	Ether lipid metabolism	11.8	25.5	0.001	17.6	33.3	0.006
	Fatty acid metabolism			n.s.	40.3	6.5	0.004
	Glycerolipid metabolism			n.s.	27.4	9.7	0.007
	Primary bile acid biosynthesis			n.s.	41.2	5.9	0.005
	Steroid biosynthesis			n.s.	4.2	50.0	0.009
Metabolism of Cofactors and Vitamins	Pantothenate and CoA biosynthesis			n.s.	36.8	5.3	0.009
	Retinol metabolism			n.s.	37.0	7.4	0.001
	Vitamin B6 metabolism	45.5	18.2	0.007	54.5	18.2	0.002
Metabolism of Other Amino Acids	beta-Alanine metabolism	22.6	9.7	0.009	32.3	9.7	0.004
	D-Glutamine and D-glutamate metabolism	50.0	0.0	0.002	66.7	0.0	<0.001
	Taurine and hypotaurine metabolism			n.s.	23.1	0.0	0.001

Metabolism of Terpenoids and Polyketides	Terpenoid backbone biosynthesis			n.s.	19.0	42.9	0.004
Xenobiotics Biodegradation and Metabolism	Drug metabolism - cytochrome P450	28.3	7.5	0.010	38.7	7.5	0.003
	Metabolism of xenobiotics by cytochrome P450			n.s.	36.6	8.6	0.006
Organismal Systems							
Circulatory System	Cardiac muscle contraction			n.s.	31.3	5.4	0.007
Development	Osteoclast differentiation	6.4	36.8	0.006	9.4	38.0	0.001
Digestive System	Protein digestion and absorption			n.s.	31.7	4.0	0.002
	Vitamin digestion and absorption	31.3	0.0	0.009	34.4	6.3	<0.001
Endocrine System	Adipocytokine signalling	22.5	19.6	0.008	33.3	20.6	0.009
	PPAR signalling			n.s.	47.3	4.5	0.003
Excretory System	Proximal tubule bicarbonate reclamation			n.s.	50.0	0.0	0.006
Immune System	Antigen processing and presentation	5.9	53.5	<0.001	6.9	51.5	0.001
	B cell receptor signalling			n.s.	10.7	39.3	0.002
	Chemokine signalling			n.s.	17.0	35.1	0.001
	Cytosolic DNA-sensing	1.5	44.1	0.003	2.9	39.7	<0.001
	Fc epsilon RI signalling	7.6	30.5	0.007	11.0	34.7	0.001
	Hematopoietic cell lineage	12.5	33.9	0.003	11.6	33.0	<0.001
	Intestinal immune network for IgA production	5.0	60.0	<0.001	6.7	56.7	<0.001
	Leukocyte transendothelial migration	8.9	29.7	0.004	13.9	29.1	0.007
	Natural killer cell mediated cytotoxicity	8.2	33.9	0.003	10.5	35.7	<0.001
	NOD-like receptor signalling			n.s.	9.9	33.3	0.001
	RIG-I-like receptor signalling			n.s.	6.1	27.6	0.003
	T cell receptor signalling			n.s.	10.9	33.3	<0.001
	Toll-like receptor signalling			n.s.	6.6	38.0	0.002
Sensory System	Taste transduction			n.s.	22.2	2.8	0.007

"n.s." indicates a non-significant change in the given comparison.

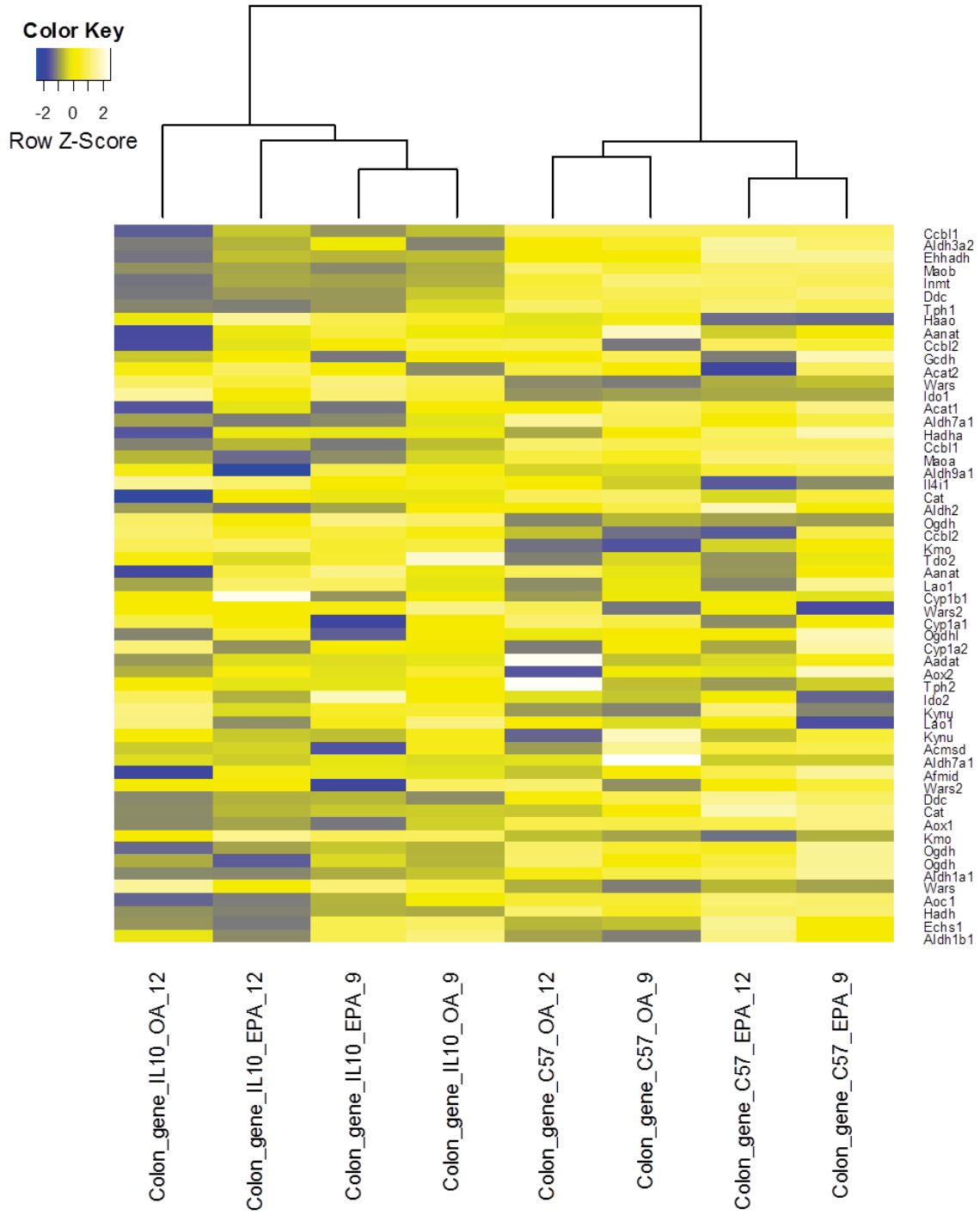

Figure 3.5 Heatmap showing the set of genes comprising the KEGG pathway *Tryptophan metabolism*. Colon obtained from *Il10*$^{-/-}$ mice and C57BL/6J mice fed the oleic acid (OA) diet or eicosapentaenoic acid (EPA) diet and sampled at 9 or 12 weeks of age ($P \leq 0.01$). The dendrogram above the heatmap was produced by hierarchical clustering of the treatment groups in the columns and illustrates the similarity of gene expression profiles, with higher similarity represented by closer relationship in the tree diagram. Rows indicate genes in the KEGG pathway. Colour coding as indicated in the key. Data represent four biological replicates per treatment.

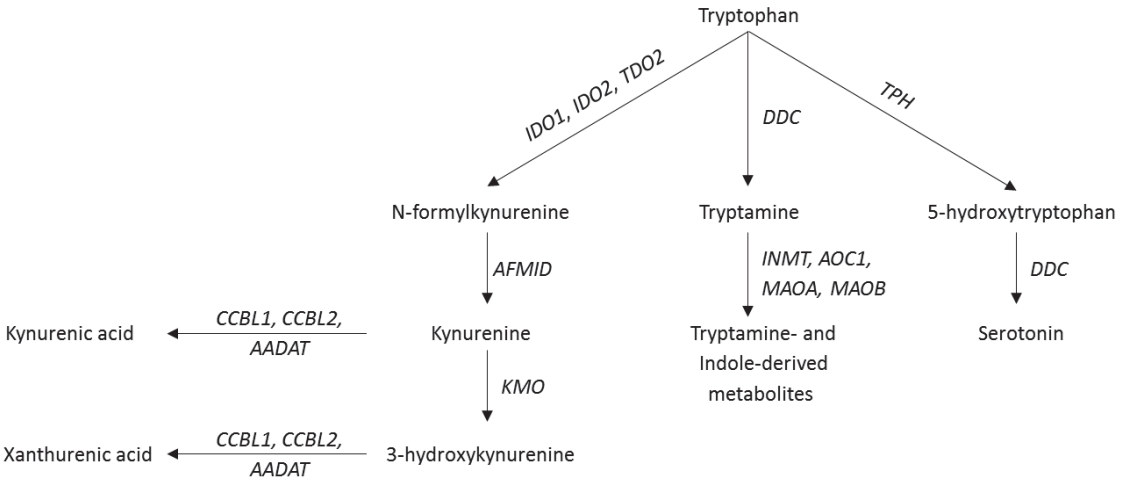

Figure 3.6 Metabolism of tryptophan to xanthurenic acid (*via* kynurenine), tryptamine and serotonin. Genes coding enzymes that catalyse the reactions are shown in italics. Information obtained from the KEGG database.

AADAT: Aminoadipate aminotransferase; AFMID: Arylformamidase; AOC1: Amine oxidase copper containing 1; CCBL1: Cysteine conjugate-beta lyase, cytoplasmic; CCBL2: Cysteine conjugate-beta lyase 2; DDC: Aromatic l-amino acid decarboxylase; IDO1: Indoleamine 2,3-dioxygenase 1; IDO2: Indoleamine 2,3-dioxygenase 2; INMT: Indolethylamine n-methyltransferase; KMO: Kynurenine 3-monooxygenase (kynurenine 3-hydroxylase); MAOA and B: Monoamine oxidase A and B; TDO2: Tryptophan 2,3-dioxygenase; TPH: Tryptophan hydroxylase.

At 9 weeks of age, the colon transcriptomic profile of *Il10*$^{-/-}$ mice fed the EPA diet (vs. OA diet) was associated with *Inflammatory response*, *Inflammation of body region* and *Inflammation of organ*, with the activation states of these functions predicted to be increased (Table 3.7). Furthermore, an increased "Adhesion" and "Proliferation" of immune cells, as well as "Accumulation" and "Recruitment" of leukocytes was predicted, indicating elevated cell-mediated immune responses in those mice (Table 3.7). These predictions were based on the expression of nine genes as indicated by a coloured border in Figure 3.7, with the central genes *IL1B* and chemokine (C-C motif) ligand 2 (*CCL2*), and the transcription regulator CCAAT/enhancer binding protein delta (*CEBPD*) (FC = 1.8 - 2.9).

At 12 weeks of age, the genes responsive to the EPA diet in the colon of *Il10*$^{-/-}$ mice were most significantly associated with "Quantity" and "Recruitment" of immune cells, specifically lymphocytes, compared to those fed the OA diet (Table 3.7). Based on the expression of target genes, these biological functions were predicted to be decreased in activation. Gene expression changes in *Il10*$^{-/-}$ mice fed the EPA diet were also associated with antigen-specific functions in the adaptive immune system, attributed to a predicted decrease in *Quantity of Immunoglobulin G (IgG)* compared to those fed the OA diet at 12 weeks of age (Table 3.7). The 46 genes linked to these ten functions were merged into a biological interaction network (Figure 3.8). The transcription regulators T-box 21 (*TBX21*) and *FOS* appeared to play a central role in regulating many of the genes in the network (Figure 3.8), for example, the cytokines *IL1B* and *CCL2*, and transmembrane receptor *CD40* (FC = -2 to -2.7). mRNA expression levels of both transcription regulators were decreased in the colon of *Il10*$^{-/-}$ mice fed the EPA diet at 12 weeks of age (FC = -1.6 and -2, respectively, vs. those fed the OA diet).

At 12 weeks of age, the canonical pathway *Eicosanoid signalling* was differentially expressed in the colon of *Il10*$^{-/-}$ mice in response to EPA supplementation ($P < 0.001$ vs. OA diet (data not shown)). This result was based on the genes phospholipase A2, group IID (*PLA2G2D*) and group III (*PLA2G3*), formyl peptide receptor 2 (*FPR2*), and thromboxane A synthase 1 (*TBXAS1*), all of which showed decreased mRNA expression levels in the colon of *Il10*$^{-/-}$ mice fed the EPA diet, and potentially demonstrating that the EPA diet influenced AA-mediated signalling pathways in the colon. This effect of the EPA diet on *Eicosanoid signalling* was not observed in 9-

Table 3.7 Most significantly affected biological functions in the colon of *Il10*$^{-/-}$ mice fed the eicosapentaenoic acid (EPA) diet compared to those fed the oleic acid (OA) diet (9 and 12 weeks of age). Functions with an *activation z-score* < |2| were excluded and biological functions limited to show the ten highest p-value-ranked functions (only eight functions passed the cut-off criteria for inclusion for 9-week-old *Il10*$^{-/-}$ mice). "# genes" indicates the number of genes associated with the biological function and individual genes may be represented in more than one function. Data represent four biological replicates per group.

Functions annotation		*P-value*	*# genes*	*Predicted activation state (activation z-score)*	*Category*
9 weeks of age					
Immune cells	Adhesion	9.20E-05	5	Increased (+2.2)	2, 5, 6, 15
	Proliferation	7.10E-04	6	Increased (+2.2)	2, 4, 9
Leukocytes	Accumulation	2.23E-05	5	Increased (+2.2)	2, 6, 7, 15
	Recruitment	6.04E-05	5	Increased (+2.2)	2, 5, 6, 13
Inflammatory response		7.36E-05	7	Increased (+2.4)	7
Inflammation of body region		1.28E-03	6	Increased (+2.1)	7
Inflammation of organ		6.81E-04	7	Increased (+2.1)	7
Atherosclerosis		4.04E-04	5	Increased (+2.2)	28
12 weeks of age					
Cells	Quantity	2.22E-13	38	Decreased (-2.6)	3
Leukocytes	Quantity	1.32E-20	36	Decreased (-2.9)	2, 3
	Recruitment	1.95E-10	15	Decreased (-2.4)	2, 5, 6, 13
Mononuclear leukocytes	Recruitment	2.11E-10	10	Decreased (-2.4)	2, 5, 6, 13
Lymphocytes	Quantity	4.27E-16	28	Decreased (-2.5)	2, 3
	Recruitment	4.83E-10	9	Decreased (-2.2)	2, 5, 6, 13
B lymphocytes	Quantity	6.36E-09	14	Decreased (-2.0)	2, 3, 25
IgG	Quantity	2.20E-10	13	Decreased (-2.4)	25, 26
Systemic autoimmune syndrome		1.48E-11	27	Increased (+2.1)	27
Infection of mammalia		1.31E-10	16	Increased (+2.4)	14

Categories: 1 Cellular Function and Maintenance; 2 Hematological System Development and Function; 3 Tissue Morphology; 4 Cellular Growth and Proliferation; 5 Cell-To-Cell Signalling and Interaction; 6 Immune Cell Trafficking; 7 Inflammatory Response; 8 Cell-mediated Immune Response; 9 Cellular Development; 10 Hematopoiesis; 11 Lymphoid Tissue Structure and Development; 12 Metabolic Disease; 13 Cellular Movement; 14 Infectious Disease; 15 Tissue Development; 16 Cell Morphology; 17 Cell Death and Survival; 18 Cellular Compromise; 19 Lipid Metabolism; 20 Small Molecules Biochemistry; 21 Organismal Survival; 22 Molecular Transport; 23 Organismal Development; 24 Cellular Assembly and Organisation; 25 Humoral Immune Response; 26 Protein Synthesis; 27 Immunological Disease; 28 Cardiovascular Disease.

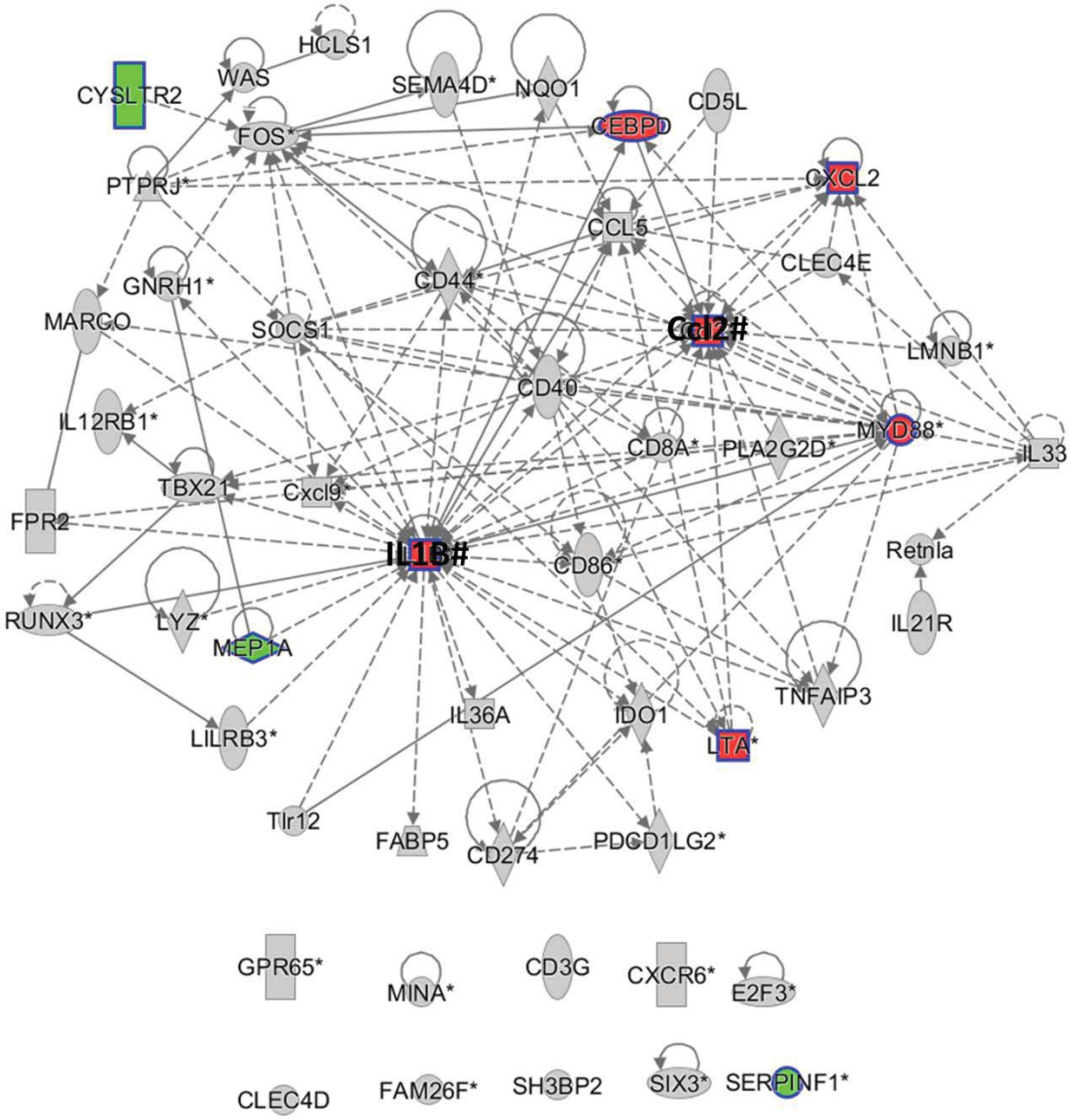

Figure 3.7 Colon gene expression changes in response to the eicosapentaenoic acid (EPA) diet (vs. oleic acid (OA) diet) in *Il10*$^{-/-}$ mice at early stages of colitis. The colour coding of genes indicates the direction of fold-change (FC) in 9-week-old EPA-fed *Il10*$^{-/-}$ mice, with red showing genes that are increased in expression, green showing decreased expression and genes shaded in grey are not differentially expressed. The network was generated by merging the genes associated with the ten most significant biological functions in the colon of *Il10*$^{-/-}$ mice fed the EPA diet compared to those fed the OA diet at 9 and 12 weeks of age. Genes with a coloured border were associated with biological functions in 9-week-old EPA-fed *Il10*$^{-/-}$ mice, and genes with non-coloured borders with 12-week-old EPA-fed *Il10*$^{-/-}$ mice. Two genes (indicated by "#") were in common between the two comparisons. The intensity of the colour of genes indicates the degree of FC, with greater intensity of colours pointing to higher levels of FC. Node shape indicates functional class of gene product as indicated in Appendix V. Data represent four biological replicates per group.

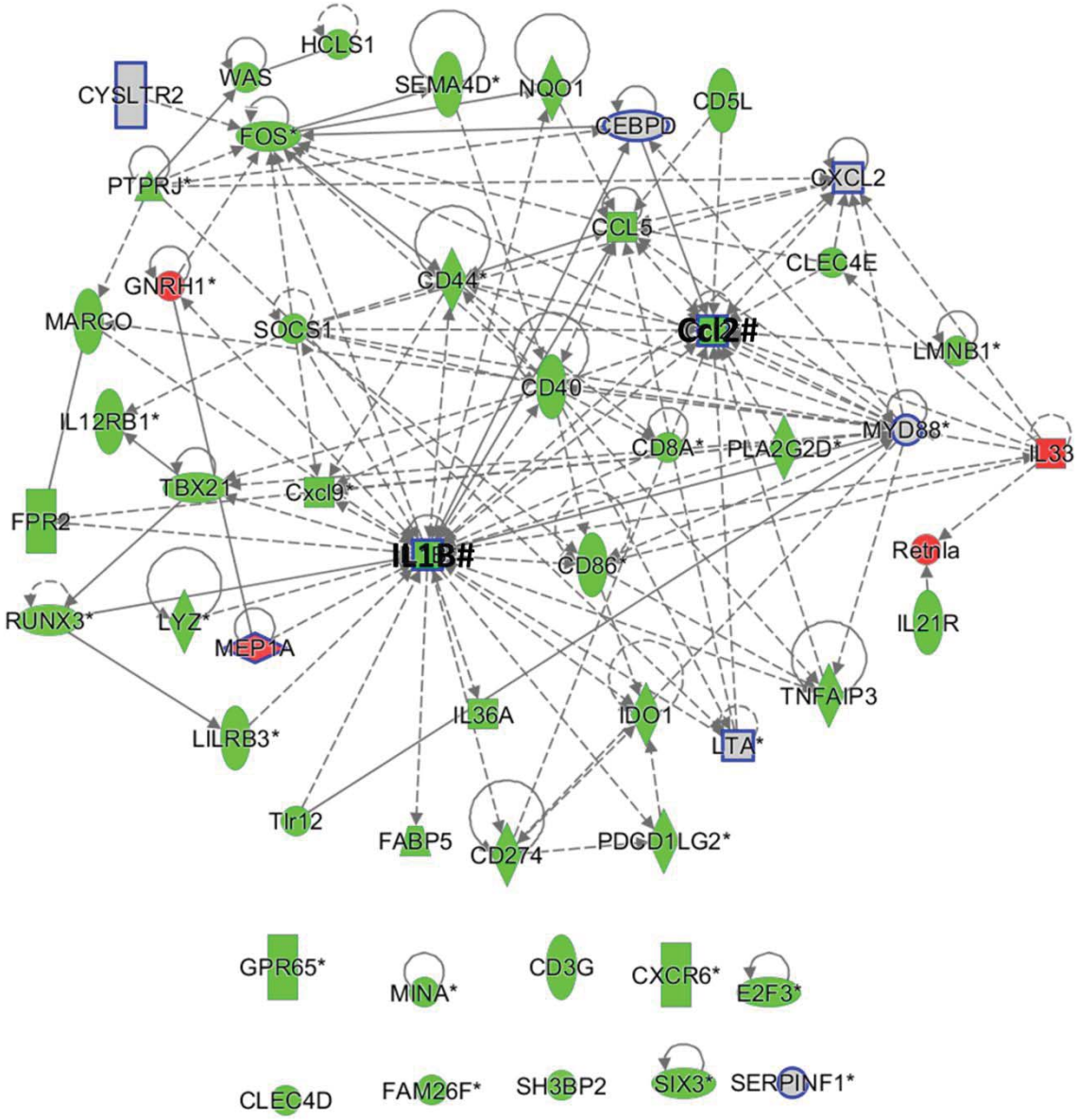

Figure 3.8 Colon gene expression changes in response to the eicosapentaenoic acid (EPA) diet (vs. oleic acid (OA) diet) in *Il10*$^{-/-}$ mice with established colitis. The colour coding of genes indicates the direction of fold-change (FC) in 12-week-old EPA-fed *Il10*$^{-/-}$ mice, with red showing genes that are increased in expression, green showing decreased expression and genes shaded in grey are not differentially expressed. The network was generated by merging the genes associated with the ten most significant biological functions in the colon of *Il10*$^{-/-}$ mice fed the EPA diet compared to those fed the OA diet at 9 and 12 weeks of age. Genes with a coloured border were associated with biological functions in 9-week-old EPA-fed *Il10*$^{-/-}$ mice, and genes with non-coloured borders with 12-week-old EPA-fed *Il10*$^{-/-}$ mice. Two genes (indicated by "#") were in common between the two comparisons. The intensity of the colour of genes indicates the degree of FC, with greater intensity of colours pointing to higher levels of FC. Node shape indicates functional class of gene product as indicated in Appendix V. Data represent four biological replicates per group.

week-old *Il10*$^{-/-}$ mice (P > 0.05 vs. OA diet (data not shown)), and may therefore depend on the duration of EPA supplementation. Furthermore, these changes were genotype-specific, and were not observed in C57BL/6J mice fed the EPA diet (data not shown).

The canonical pathway *PPAR signalling* was significantly affected in the colon of *Il10*$^{-/-}$ mice fed the EPA diet compared to those fed the OA diet, but only at 12 weeks of age (P = 0.001 (data not shown)). While the EPA diet did not affect *PPARA* mRNA expression levels, it may have affected the expression of *PPARG* in *Il10*$^{-/-}$ mice. This was attributed to the decreased mRNA expression levels of the transcription regulator *FOS*, a target gene that is inhibited by *PPARG* (FC = -2.2 and P = 0.004). This was further supported by the reduced mRNA expression levels of the cytokines *IL1B* and *IL36A* (Figure 3.8), both of which influence *NFKB* signalling, and thus may impact *PPARG* activity in the colon of EPA-fed *Il10*$^{-/-}$ mice at 12 weeks of age (vs. those fed the OA diet).

The canonical pathway *Tryptophan metabolism* was not differentially expressed in the colon of *Il10*$^{-/-}$ mice fed the EPA diet compared to those fed the OA diet, regardless of age (P > 0.1 (data not shown)). However, mRNA expression levels of *IDO1* were approximately 4-fold decreased in 12-week-old *Il10*$^{-/-}$ mice in response to EPA supplementation (Figure 3.8). At 9 weeks of age, no effect on *IDO1* gene expression was observed in *Il10*$^{-/-}$ mice fed the EPA diet (vs. those fed the OA diet (Figure 3.7)).

GSEA was carried out, but only one KEGG pathway (*ECM-receptor interaction*) passed the significance criteria in the colon of 9-week-old *Il10*$^{-/-}$ mice fed the EPA diet vs. OA diet, but none at 12-weeks of age (P ≤ 0.01(data not shown)).

3.4.4 PBMC gene expression

The highest number of differentially expressed genes were observed between *Il10*$^{-/-}$ mice and C57BL/6J mice, irrespective of whether mice were fed the EPA diet or the OA diet (Table 3.8). Within *Il10*$^{-/-}$ mice, more genes were differentially expressed in PBMCs of 12-week-old mice fed the EPA diet (463 genes compared to those fed the OA diet), than within 9-week-old mice (282 genes compared to those fed the OA diet). The least differences in gene expression were observed within C57BL/6J mice, irrespective of age, with approximately 140 to 170 genes differentially expressed in PBMCs of EPA-fed

Table 3.8 Numbers of differentially expressed genes in peripheral blood mononuclear cells (PBMCs) of *Il10*$^{-/-}$ mice and C57BL/6J mice fed the oleic acid (OA) or the eicosapentaenoic acid (EPA) diets. Samples were obtained at 9 or 12 weeks of age. Genes passing a fold-change (≥ |1.5|) and p-value (≤ 0.005) cut-off were considered differentially expressed. Data represent four biological replicates per treatment group.

Contrast		*mRNA transcript levels*[1]		*Uploaded into Ingenuity Pathway Analysis*
		Increased	*Decreased*	*Analysis-ready molecules*[2]
Genotype comparison (Il10$^{-/-}$ *relative to C57)*				
9 weeks	OA	277	179	308
	EPA	520	175	484
12 weeks	OA	222	143	248
	EPA	1516	462	997 (FC = 1.5 and P = 0.001)
Diet comparison (EPA relative to OA)				
9 weeks	C57	104	36	99
	Il10$^{-/-}$	173	109	217
12 weeks	C57	28	143	122
	Il10$^{-/-}$	372	91	346

(1) FC ≥ |1.5| and p-value ≤ 0.005; genes may be represented with more than one probe on the array; (2) Reducing genes to 1000 genes for pathway analysis by applying more stringent FC and p-value as recommended in the IPA handbook.

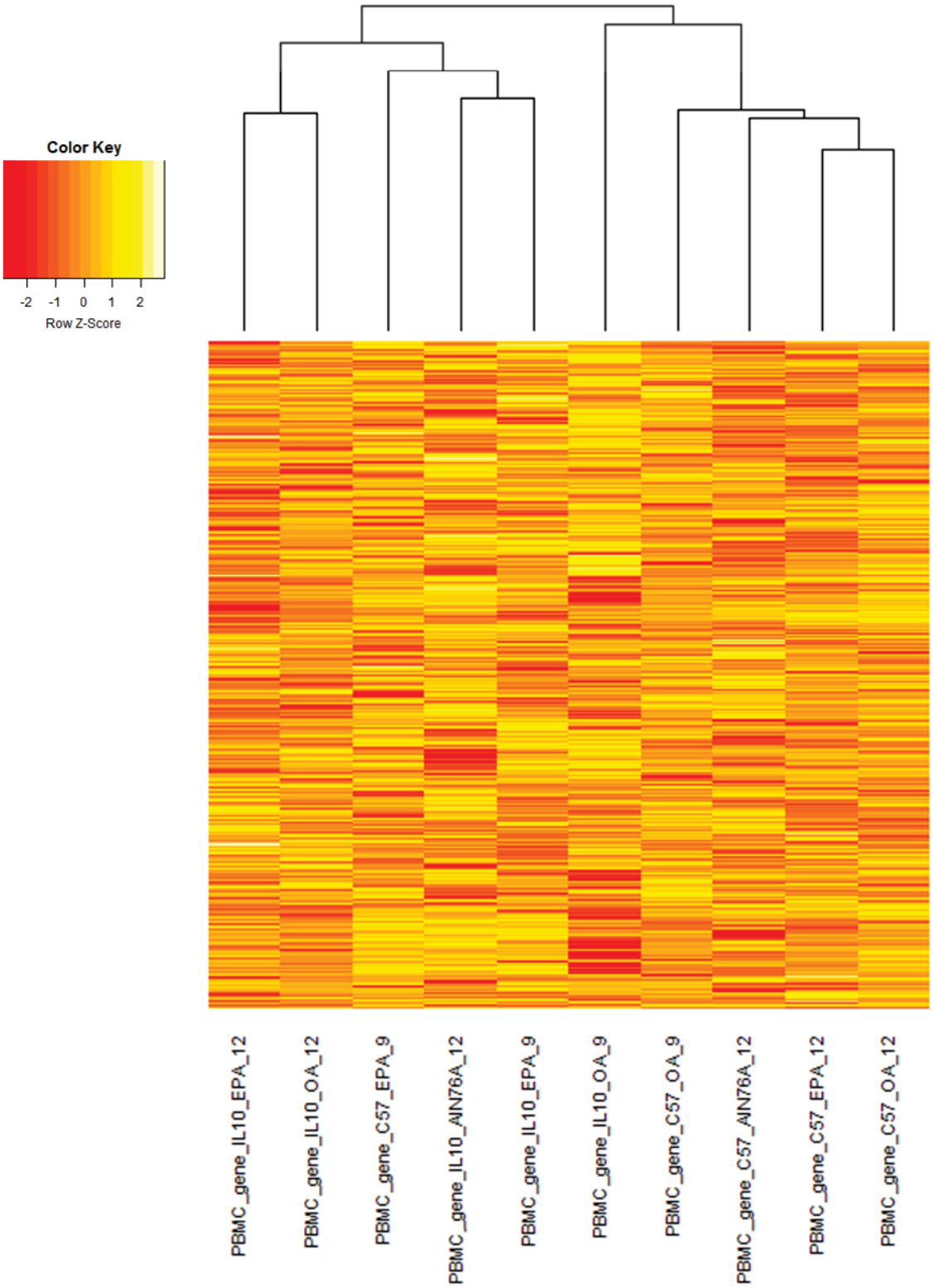

Figure 3.9 Heatmap of peripheral blood mononuclear cell (PBMCs) gene expression profiles from C57BL/6J mice and *Il10*$^{-/-}$ mice fed AIN-76A diets, either unmodified, or enriched with oleic acid (OA) or eicosapentaenoic acid (EPA). PBMC samples were obtained at 9 or 12 weeks of age. The dendrogram above the heatmap was produced by hierarchical clustering of the treatment groups in the columns and illustrates the similarity of gene expression profiles, with higher similarity represented by closer relationship in the tree diagram. Rows indicate genes with the top 25% of variation across the treatment groups. Colour coding according to key. Data represent four biological replicates per group.

C57BL/6J mice compared to those fed the OA diet (Table 3.8). This was also indicated in Figure 3.9, where the highest degree of similarity appeared to be between 12-week-old C57BL/6J mice fed the EPA diet and those fed the OA diet, indicating that diet type had limited impact on the transcriptomic profile of PBMCs in those mice.

3.4.4.1 PBMC gene expression between mouse genotypes fed the OA diet

Approximately 400 genes were differentially expressed in PBMCs from *Il10*$^{-/-}$ mice fed the OA diet compared to C57BL/6J mice fed the same diet, with approximately 60% of these genes increased in expression irrespective of age (FC $\geq$ 1.5 and P $\leq$ 0.005 (Table 3.8)). 72 genes differentially expressed in PBMCs from 9-week-old *Il10*$^{-/-}$ mice were also differentially expressed in 12-week-old *Il10*$^{-/-}$ mice (vs. C57BL/6J mice both fed the OA diet (Table 3.9)). Most of these shared genes were increased in expression, with similar FC between the contrasts (Table 3.9). These were for example, inflammatory genes *S100A8* and *S100A9*, *MMP8* and *MMP9*, and *LCN2*, all of which have been suggested as candidate biomarkers of IBD [143]. The PBMC gene expression profiles for *Il10*$^{-/-}$ mice fed the OA diet at 9 and 12 weeks of age were similar (Pearson correlation coefficient = 0.98). Expression levels of *PPARA* were not affected in PBMCs from *Il10*$^{-/-}$ mice relative to C57BL/6J mice fed the OA diet, irrespective of age.

As expected, gene expression changes in PBMCs from *Il10*$^{-/-}$ mice fed the OA diet were associated with biological functions affecting the inflammatory response and the cell-mediated immune response compared to C57BL/6J mice on the same diet (Table 3.10). These observations were made regardless of age and most apparent were predictions for the "Activation" and "Migration" of cells, specifically phagocytes, leukocytes and myeloid cells in PBMCs from *Il10*$^{-/-}$ mice, with these functions predicted to be increased at both 9 and 12 weeks of age (Table 3.10).

A total of 62 (9 weeks of age) and 94 (12 weeks of age) canonical pathways were differentially expressed in PBMCs from *Il10*$^{-/-}$ mice fed the OA diet compared to C57BL/6J mice fed the same diet (P $\leq$ 0.05 (Figure 3.10)). Regardless of age, the 15 highest p-value-ranked canonical pathways were mostly associated with the cellular immune response (*Dendritic cell maturation*, *Communication between innate and adaptive immune cells*, and *Granulocyte adhesion and diapedesis*), cytokine signalling (*IL-10 signalling*), and disease-specific signalling pathways (*Altered T cell and B cell signalling in rheumatoid arthritis*) (Figure 3.10). Specifically at 12 weeks of age,

decreased gene expression was associated with B cell development. For example, the canonical pathway *Primary immunodeficiency signalling* was affected in PBMCs from *Il10*$^{-/-}$ mice compared to C57BL/6J mice both fed the OA diet (P = 1.9E-07 (Figure 3.10)). As indicated in Figure 3.11, decreased mRNA expression levels were observed in *Il10*$^{-/-}$ mice for co-stimulatory molecules (*CD40*), transmembrane activator and cyclophilin ligand interactor (*TACI*), B-cell activating factor (*BAFFR*; labelled as *TNFRSF13C* in the figure), and Immunoglobulin heavy constant mu (*IGHM*) on the surface of B lymphocytes were observed. This gene expression pattern may indicate a defect in the development of B cells in those mice when colitis was established, but this effect was not observed at 9 weeks of age.

The large increase in mRNA expression levels of the *IDO1* gene that was shown in the colon of *Il10*$^{-/-}$ mice (vs. C57BL/6J mice) was not observed in PBMCs of those mice, irrespective of age (9 or 12 weeks of age). Furthermore, *IDO1* showed a low average expression value in PBMCs based on microarray analysis and was close to the detection limit (data not shown).

3.4.4.2 Effect of the EPA diet (vs. OA diet) on PBMC gene expression in *Il10*$^{-/-}$ mice

At 9 weeks of age, 282 genes were differentially expressed in PBMCs from *Il10*$^{-/-}$ mice fed the EPA diet compared to those fed the OA diet, with approximately 60% of these genes increased in expression (FC $\geq$ 1.5 and P $\leq$ 0.005 (Table 3.8)). At 12 weeks of age, 463 genes were differentially expressed in *Il10*$^{-/-}$ mice fed EPA diets (vs. OA diet), with 80% of these genes increased in expression in EPA-fed *Il10*$^{-/-}$ mice (Table 3.8). A limited number of genes (30) differentially expressed in PBMCs from *Il10*$^{-/-}$ mice fed the EPA diet (vs. OA diet) at 9 weeks were also differentially expressed in 12-week-old *Il10*$^{-/-}$ mice (Table 3.11). Of the genes that were in common, similar FCs were observed between these two time-points (Table 3.11). Two genes (*PLCD4* and *LILRB3*) showed increased expression in 9-week-old *Il10*$^{-/-}$ mice fed the EPA diet (vs. OA diet), but decreased expression in 12-week-old mice fed the EPA diet (vs. OA diet).

Table 3.9 Differentially expressed genes in peripheral blood mononuclear cells (PBMCs) from *Il10*$^{-/-}$ mice compared to C57BL/6J mice fed the oleic acid (OA) diet that were in common at 9 and 12 weeks of age (FC ≥ |1.5| and P ≤ 0.005). Data indicate fold-changes (FC) of genes, with positive values showing increased expression in *Il10*$^{-/-}$ mice and negative values indicating decreased expression. Data represent four biological replicates per group.

Entrez gene name	*Il10*$^{-/-}$ *vs. C57BL/6J mice*	
	9 weeks of age	*12 weeks of age*
Genes with decreased expression		
Deiodinase, iodothyronine, type I (*DIO1*)	-1.5	-1.6
Glutamine repeat protein 1 (*Glrp1*)	-2.0	-1.6
Gypsy retrotransposon integrase 1 (*GIN1*)	-2.6	-2.9
Interferon, gamma-inducible protein 16 (*IFI16*)	-2.0	-2.2
Minichromosome maintenance complex component 6 (*MCM6*)	-1.6	-1.8
RAB30, member RAS oncogene family (*RAB30*)	-1.5	-1.7
RELT-like 1 (*RELL1*)	-1.6	-1.7
Solute carrier family 25 (mitochondrial iron transporter), member 37 (*SLC25A37*)	-2.0	-2.1
Tumor necrosis factor receptor superfamily, member 13C (*TNFRSF13C*)	-1.7	-1.9
Zinc finger protein 318 (*ZNF318*)	-1.5	-1.8
Genes with increased expression		
Adrenoceptor beta 1 (*ADRB1*)	1.9	1.6
Annexin A1 (*ANXA1*)	1.8	2.1
Annexin A8-like 1 (*ANXA8*/*AXA8L1*)	2.5	2.2
Aspartic peptidase, retroviral-like 1 (*ASPRV1*)	4.9	3.4
Cathepsin E (*CTSE*)	9.5	10.2
CD300 molecule-like family member f (*CD300LF*)	3.1	2.2
CD33 antigen (*Cd33*)	2.0	2.2
Chemokine (C-X-C motif) receptor 2 (*CXCR2*)	6.4	4.6
Chitinase 3-like 1 (cartilage glycoprotein-39) (*CHI3L1*)	4.7	4.7
Chromosome 15 open reading frame 48 (*C15orf48*)	2.6	3.4
Colony stimulating factor 1 (macrophage) (*CSF1*)	1.8	2.3
Complement component 5a receptor 2 (*C5AR2*)	2.1	2.1
Cystatin A (stefin A) (*CSTA*)	5.4	6.1
Expressed sequence AI987944 (AI987944 (includes others))	1.8	1.8
Fc fragment of IgG, low affinity IIIa, receptor (*CD16a*) (*FCGR3A*/*FCGR3B*)	1.7	1.6
Formyl peptide receptor 1 (*FPR1*)	2.8	2.5
Formyl peptide receptor 2 (*FPR2*)	2.9	2.4
Free fatty acid receptor 2 (*FFAR2*)	2.5	2.3
G protein-coupled receptor 84 (*GPR84*)	2.1	2.5
Glucosaminyl (N-acetyl) transferase 2, I-branching enzyme (I blood group) (*GCNT2*)	1.8	1.7
Guanylate binding protein 2, interferon-inducible (*GBP2*)	1.6	1.6
Haptoglobin (*HP*)	2.1	2.1
Immunoresponsive 1 homolog (mouse) (*IRG1*)	3.8	5.6
Interferon induced transmembrane protein 1 (*Ifitm1*)	6.9	3.0
Interleukin 10 (*IL10*)	10.1	12.1

Interleukin 17 receptor E (*IL17RE*)	1.9	2.4
Interleukin 18 receptor accessory protein (*IL18RAP*)	2.5	2.3
Kinesin family member 4A (*KIF4A*)	1.5	1.5
Lactotransferrin (*LTF*)	3.1	5.6
Leucine-rich alpha-2-glycoprotein 1 (*LRG1*)	2.7	3.6
Lipocalin 2 (*LCN2*)	2.3	3.0
Lymphocyte antigen 6 complex, locus A (*Ly6a* (includes others))	2.5	1.6
MAS-related GPR, member X3 (*MRGPRX3*)	2.5	2.1
Matrix metallopeptidase 25 (*MMP25*)	2.3	2.3
Matrix metallopeptidase 8 (*MMP8*)	2.8	3.0
Matrix metallopeptidase 9 (*MMP9*)	3.2	2.9
Microsomal glutathione S-transferase 1 (*MGST1*)	1.9	1.9
Microtubule-associated protein 6 (*MAP6*)	1.6	1.9
Mitogen-activated protein kinase 13 (*MAPK13*)	2.3	2.1
Molybdenum cofactor sulfurase (*MOCOS*)	1.8	1.7
Nicotinamide nucleotide transhydrogenase (*Nnt*)	2.2	2.4
Paired immunoglobin-like type 2 receptor alpha (*PILRA*)	2.3	1.7
Paired immunoglobin-like type 2 receptor beta (*PILRB*)	2.1	1.6
Peptidylglycine alpha-amidating monooxygenase (*PAM*)	1.6	2.4
Phospholipase A2, group VII (platelet-activating factor acetylhydrolase, plasma) (*PLA2G7*)	2.2	1.9
Phosphorylase, glycogen, liver (*PYGL*)	2.3	2.0
PML-RARA regulated adaptor molecule 1 (*PRAM1*)	2.2	1.7
Pre-B-cell leukemia homeobox 1 (*PBX1*)	1.8	1.8
Predicted gene 14393 (*Gm14393*)	1.6	1.6
Programmed cell death 1 (*PDCD1*)	2.0	2.8
Proteinase 3 (*PRTN3*)	2.3	3.0
S100 calcium binding protein A8 (*S100A8*)	4.4	6.6
S100 calcium binding protein A9 (*S100A9*)	2.5	4.3
Stefin A1 (*Stfa1*)	5.1	4.4
Stefin A2 (*Stfa2*/*Stfa2l1*)	8.5	7.7
Suppressor of cytokine signaling 3 (*SOCS3*)	1.6	1.8
Transglutaminase 2 (*TGM2*)	2.2	2.0
WAP four-disulfide core domain 21 (*Wfdc21*)	5.7	5.8
Xanthine dehydrogenase (*XDH*)	1.6	1.6
Zinc finger protein 442 (*ZNF442*)	2.3	2.2
Genes with contrasting expression		
Immunoglobulin heavy constant alpha 1 (*IGHA1*)	-1.6	2.7
WD repeat and FYVE domain containing 1 (*WDFY1*)	-3.0	1.7

Table 3.10 Most significantly affected biological functions in peripheral blood mononuclear cells (PBMCs) from *Il10*$^{-/-}$ mice relative to C57BL/6J mice fed the oleic acid (OA) diet (9 and 12 weeks of age). Functions with an *activation z-score* < |2| were excluded and biological functions limited to show the ten highest p-value-ranked functions. "# genes" indicates the number of genes associated with the biological function and individual genes may be represented in more than one function. Data represent four biological replicates per group.

Functions annotation		*P-value*	*# genes*	*Predicted activation state (activation z-score)*	*Category*
9 weeks of age					
Cells	Activation	1.40E-08	43	Increased (+2.1)	5
	Migration	9.88E-09	68	Increased (+3.2)	13
	Movement	5.58E-09	74	Increased (+2.6)	13
Blood cells	Activation	1.04E-08	36	Increased (+2.7)	2, 5
Phagocytes	Activation	1.45E-08	23	Increased (+2.2)	2, 5, 6, 7
Leukocytes	Chemotaxis	1.03E-08	23	Increased (+2.8)	2, 6, 7, 13
	Homing	9.26E-09	24	Increased (+2.6)	2, 6, 13
	Migration	9.01E-12	47	Increased (+2.6)	6, 13
Myeloid cells	Activation	1.22E-08	22	Increased (+2.1)	2, 5, 6, 7
Inflammatory response		4.05E-10	40	Increased (+3.3)	7
12 weeks of age					
Cells	Activation	5.28E-14	47	Increased (+2.3)	5
Blood cells	Activation	1.43E-17	45	Increased (+2.5)	2, 5
	Adhesion	4.50E-11	25	Increased (+2.1)	15
Immune cells	Adhesion	4.22E-11	24	Increased (+2.3)	2, 6, 15
Phagocytes	Activation	4.00E-11	24	Increased (+2.3)	2, 5, 6, 7
Leukocytes	Activation	4.18E-18	44	Increased (+2.4)	2, 5, 6, 7
	Cell movement	1.23E-11	38	Increased (+2.2)	2, 6, 13
	Migration	1.79E-11	41	Increased (+2.8)	6, 13
Myeloid cells	Activation	5.47E-12	24	Increased (+2.1)	2, 5, 6, 7
Inflammatory response		1.60E-10	36	Increased (+3.3)	7

Categories: 1 Cellular Function and Maintenance; 2 Hematological System Development and Function; 3 Tissue Morphology; 4 Cellular Growth and Proliferation; 5 Cell-To-Cell Signalling and Interaction; 6 Immune Cell Trafficking; 7 Inflammatory Response; 8 Cell-mediated Immune Response; 9 Cellular Development; 10 Hematopoiesis; 11 Lymphoid Tissue Structure and Development; 12 Metabolic Disease; 13 Cellular Movement; 14 Infectious Disease; 15 Tissue Development; 16 Cell Morphology; 17 Cell Death and Survival; 18 Cellular Compromise; 19 Lipid Metabolism; 20 Small Molecules Biochemistry; 21 Organismal Survival; 22 Molecular Transport; 23 Organismal Development; 24 Cellular Assembly and Organisation.

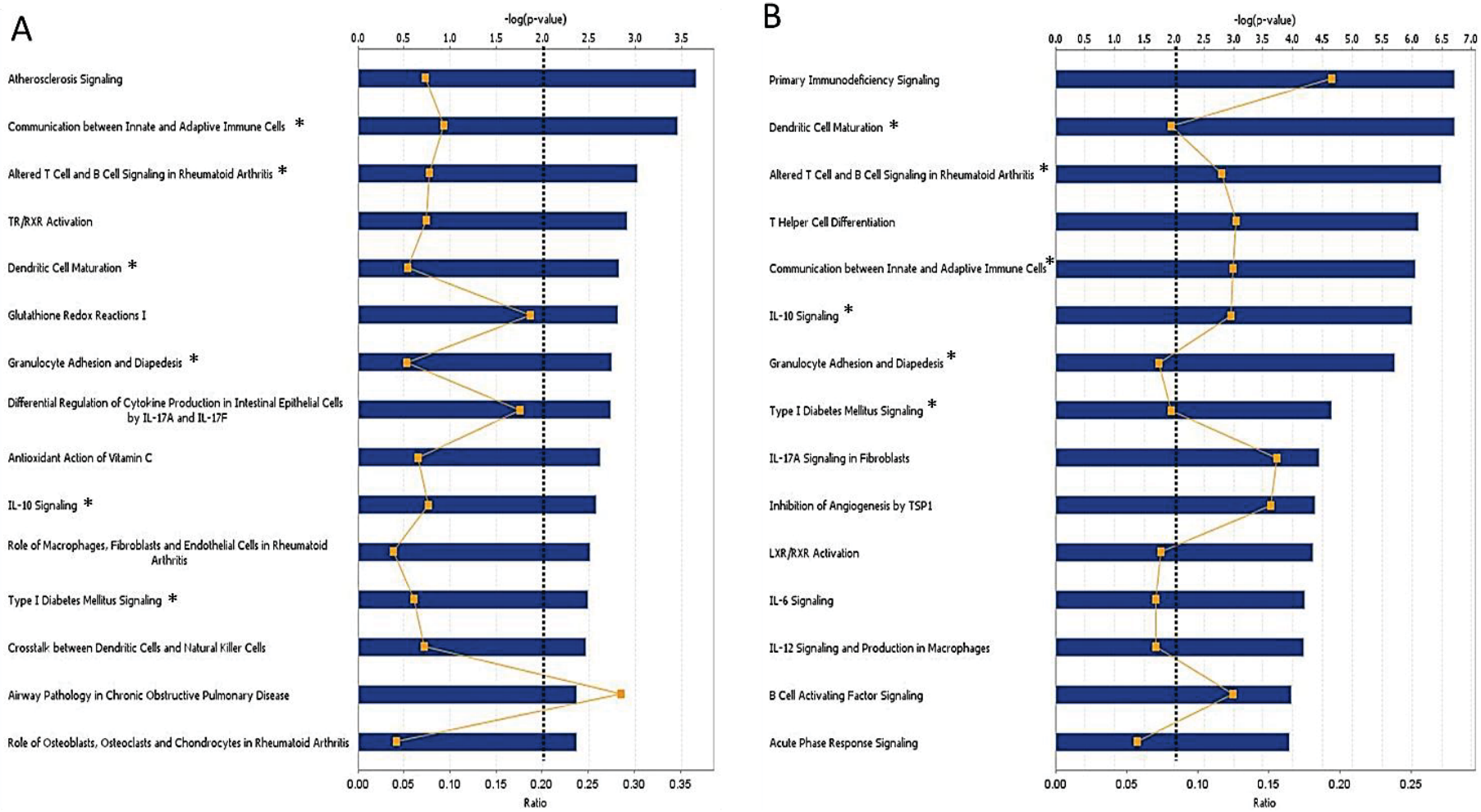

Figure 3.10 15 highest p-value-ranked canonical pathways in peripheral blood mononuclear cells (PBMCs) from *Il10*$^{-/-}$ mice compared to C57BL/6J mice both fed the oleic acid (OA) diet at 9 (A) and 12 (B) weeks of age. Bars indicate the significance of the canonical pathway (top axis), shown as log-transformed p-value for each pathway. All pathways are significant at a p-value ≤ 0.01 (dotted vertical line at -log(P-value) = 2). (*) indicates pathways that are significantly different at 9 and 12 weeks of age. (■) indicates the ratio of the pathway affected (bottom axis). Data represent four biological replicates per group.

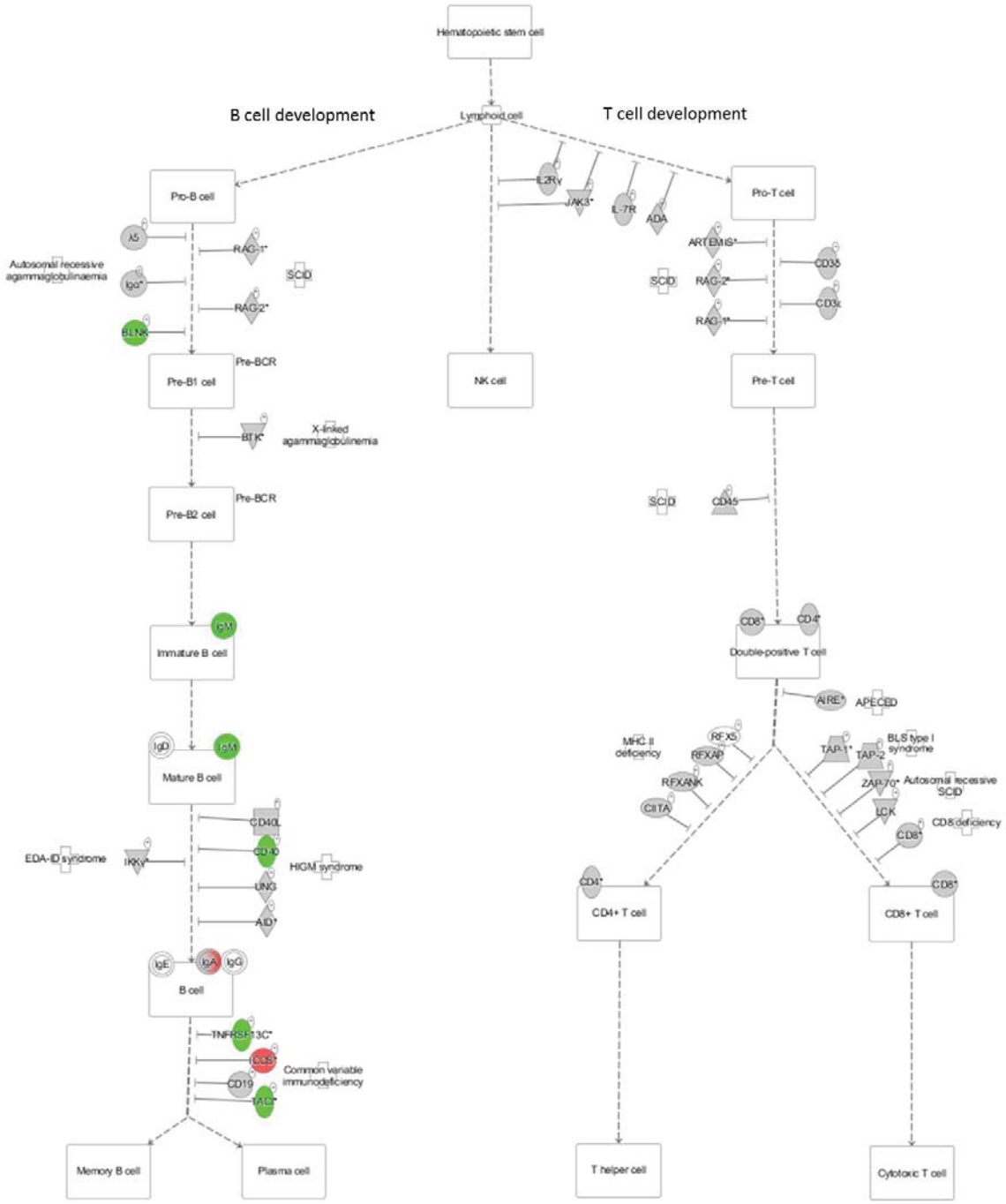

Figure 3.11 Ingenuity pathway for *Primary immunodeficiency signalling* indicating molecular events that lead to maturation of B and T cells. Nodes represent genes and red (green) colour coding of nodes indicates increased (decreased) expression levels in peripheral blood mononuclear cells (PBMCs) from *Il10*$^{-/-}$ mice fed the oleic acid (OA) diet at 12 weeks of age (relative to C57BL/6J mice fed the same diet). The intensity of the colour of nodes indicates the degree of fold-change (FC), with greater intensity of colours pointing to higher levels of FC. Node shape indicates functional class of gene product as indicated in Appendix V. Data represent four biological replicates per group.

Regardless of age, gene expression changes in PBMCs from *Il10*$^{-/-}$ mice fed the EPA diet were associated with biological functions of inflammatory cells compared to those fed the OA diet (Table 3.12). At 9 weeks of age, the PBMC transcriptomic profile from *Il10*$^{-/-}$ mice fed the EPA diet was associated with "Chemotaxis", "Cell movement", and "Influx" of immune cells, while at 12 weeks of age, biological functions such as "Activation" and "Adhesion" of immune cells were more apparent (Table 3.12). The activation states of these functions were predicted to be increased based on the expression of genes (*activation z-score* ≥ 2 and $P \leq 0.05$). The differentially expressed genes associated with these ten biological functions from 9-week-old *Il10*$^{-/-}$ mice (29 genes) and 12-week-old *Il10*$^{-/-}$ mice (106 genes) were merged to show biological interaction (Figure 3.12 and Figure 3.13). Central genes that connected many of the differentially expressed genes were peptidases *MMP2* and *MMP9*, cytokines transforming growth factor beta 1 (*TGFB1*) and *IL10*, and transmembrane receptors integrin beta 1 and 3 (*ITGB1* and *3*). At 12 weeks of age, these central genes, except for *IL10*, were increased in expression (FC = 1.5-2.3 vs. OA diet). At 9 weeks of age, only *MMP9* was differentially expressed in response to the EPA diet in PBMCs from *Il10*$^{-/-}$ mice (Figure 3.12 and Figure 3.13).

At 9 weeks of age, the canonical pathway *Acute phase signalling* was differentially expressed in *Il10*$^{-/-}$ mice fed the EPA diet compared to those fed the OA diet ($P = 0.0002$ (data not shown)). Increases in mRNA expression levels were observed for several genes encoding acute phase proteins, for example, mitogen-activated protein kinase 13 (*MAPK13*), and serpin peptidase inhibitor, clade A (alpha-1 antiproteinase, antitrypsin), member 1 (*SERPINA1*) and 3 (*SERPINA3*) (Figure 3.12). These changes were not observed in 12 week-old *Il10*$^{-/-}$ mice fed the EPA diet (Figure 3.13), thus the effects of the EPA diet on acute phase proteins might be specific to early stages of colitis in these *Il10*$^{-/-}$ mice. However, irrespective of age, increases in genes that regulate immune cell trafficking were evident, as shown by differential expression of canonical pathways *Granulocyte adhesion and diapedesis* and *Leukocyte extravasation signalling* in PBMCs from EPA-fed *Il10*$^{-/-}$ mice ($P \leq 0.05$ vs. *Il10*$^{-/-}$ mice fed the OA diet (data not shown)).

mRNA expression levels of *PPARA* and *PPARG* were not affected in PBMCs of *Il10*$^{-/-}$ mice fed the EPA diet compared to those fed the OA diet, irrespective of age. However, in 12-week-old *Il10*$^{-/-}$ mice, the *PPARG* coactivator 1 alpha (*PPARGC1A*)

Table 3.11 Differentially expressed genes in peripheral blood mononuclear cells (PBMCs) from *Il10*$^{-/-}$ mice fed the eicosapentaenoic acid (EPA) diet compared to those fed the oleic acid (OA) diet that are in common at 9 and 12 weeks of age (FC ≥ |1.5| and P ≤ 0.005). Data indicate fold-changes (FC), with positive values indicating increased expression of genes in EPA-fed mice and negative values indicating decreased expression. Data represent four biological replicates per group.

Entrez gene name	*EPA vs. OA in Il10*$^{-/-}$	
	9 weeks of age	*12 weeks of age*
Genes with increased expression		
Annexin A1 (*ANXA1*)	2.3	1.6
Aspartic peptidase, retroviral-like 1 (*ASPRV1*)	3.0	3.2
CAP, adenylate cyclase-associated protein, 2 (yeast) (*CAP2*)	1.6	2.5
Carcinoembryonic antigen-related cell adhesion molecule 10 (*Ceacam10*)	3.3	2.5
CD63 molecule (*CD63*)	1.6	1.6
Copine II (*CPNE2*)	1.5	1.6
C-type lectin domain family 4, member D (*CLEC4D*)	1.9	2.0
Cystatin A (stefin A) (*CSTA*)	4.7	2.9
Cysteine-rich secretory protein LCCL domain containing 2 (*CRISPLD2*)	2.8	2.5
Formyl peptide receptor 1 (*FPR1*)	2.0	2.6
G protein-coupled receptor 97 (*GPR97*)	2.0	3.3
Glutaredoxin (thioltransferase) (*GLRX*)	1.6	1.5
Interleukin 1 receptor, type II (*IL1R2*)	3.7	3.5
Lipocalin 2 (*LCN2*)	2.0	1.8
MAS-related GPR, member X3 (*MRGPRX3*)	2.3	3.0
Matrix metallopeptidase 9 (gelatinase B, 92kDa gelatinase, 92kDa type IV collagenase) (*MMP9*)	2.6	2.3
MAX dimerization protein 1 (*MXD1*)	1.9	2.0
Mitogen-activated protein kinase 13 (*MAPK13*)	2.2	2.8
Perilipin 5 (*PLIN5*)	1.8	1.7
S100 calcium binding protein A8 (*S100A8*)	2.2	2.2
Stefin A1 (*Stfa1*)	3.5	4.0
Stefin A2 (*Stfa2*/*Stfa2l1*)	3.0	3.7
Stefin A3 (*Stfa3*)	2.9	2.3
Stimulator of chondrogenesis 1 (*SCRG1*)	2.2	2.1
Transglutaminase 1 (*TGM1*)	1.7	1.6
Troponin T type 1 (skeletal, slow) (*TNNT1*)	2.2	2.1
Tubulin tyrosine ligase-like family, member 1 (*TTLL1*)	1.6	1.8
WAP four-disulfide core domain 21 (*Wfdc21*)	3.1	4.5
Genes with contrasting expression		
Leukocyte immunoglobulin-like receptor, subfamily B (with TM and ITIM domains), member 3 (*LILRB3*)	1.8	-1.6
Phospholipase C, delta 4 (*PLCD4*)	1.6	-1.5

Table 3.12 Most significantly affected biological functions in peripheral blood mononuclear cells (PBMCs) from *Il10*$^{-/-}$ mice fed the eicosapentaenoic acid (EPA) diet relative to those fed the oleic acid (OA) diet (9 and 12 weeks of age). Functions with an *activation z-score* < |2| were excluded and biological functions limited to show the ten highest p-value-ranked functions. "# genes" indicates the number of genes associated with the biological function and individual genes may be represented in more than one function. Data represent four biological replicates per group.

Functions annotation		*P-value*	*# genes*	*Predicted activation state (activation z-score)*	*Category*
9 weeks of age					
Cells	Chemotaxis	5.19E-05	18	Increased (+2.1)	13
Phagocytes	Chemotaxis	5.05E-06	14	Increased (+2.5)	2, 6, 7, 13
	Migration	5.74E-05	12	Increased (+2.2)	2, 6, 7, 13
Leukocytes	Chemotaxis	1.04E-05	15	Increased (+2.2)	2, 6, 7, 13
	Influx	5.69E-04	5	Increased (+2.2)	2, 6, 13
	Migration	1.48E-05	27	Increased (+2.5)	6, 13
Mononuclear leukocytes	Chemotaxis	1.09E-05	10	Increased (+2.4)	2, 6, 7, 13
Peripheral blood monocytes	Chemotaxis	7.46E-06	4	Increased (+2.0)	2, 6, 7, 13
Monocytes	Cell movement	6.99E-07	11	Increased (+2.5)	2, 6, 7, 13
	Chemotaxis	1.41E-07	9	Increased (+2.4)	2, 6, 7, 13
12 weeks of age					
Cells	Activation	1.69E-13	56	Increased (+2.7)	5
	Quantity	3.52E-14	83	Increased (+3.1)	3
Blood cells	Activation	1.44E-16	52	Increased (+2.3)	2, 5
	Adhesion	6.62E-13	32	Increased (+2.9)	5, 15
Immune cells	Adhesion	3.45E-13	31	Increased (+3.1)	2, 5, 15
Phagocytes	Activation	1.36E-15	34	Increased (+2.1)	2, 5, 6, 7
Leukocytes	Activation	5.14E-14	46	Increased (+2.3)	2, 5, 6, 7
	Migration	4.14E-12	51	Increased (+3.0)	6
Myeloid cells	Activation	5.50E-16	33	Increased (+2.5)	2, 5, 6, 7
Inflammatory response		2.06E-12	47	Increased (+2.5)	7

Categories: 1 Cellular Function and Maintenance; 2 Hematological System Development and Function; 3 Tissue Morphology; 4 Cellular Growth and Proliferation; 5 Cell-To-Cell Signalling and Interaction; 6 Immune Cell Trafficking; 7 Inflammatory Response; 8 Cell-mediated Immune Response; 9 Cellular Development; 10 Hematopoiesis; 11 Lymphoid Tissue Structure and Development; 12 Metabolic Disease; 13 Cellular Movement; 14 Infectious Disease; 15 Tissue Development; 16 Cell Morphology; 17 Cell Death and Survival; 18 Cellular Compromise; 19 Lipid Metabolism; 20 Small Molecules Biochemistry; 21 Organismal Survival; 22 Molecular Transport; 23 Organismal Development; 24 Cellular Assembly and Organisation.

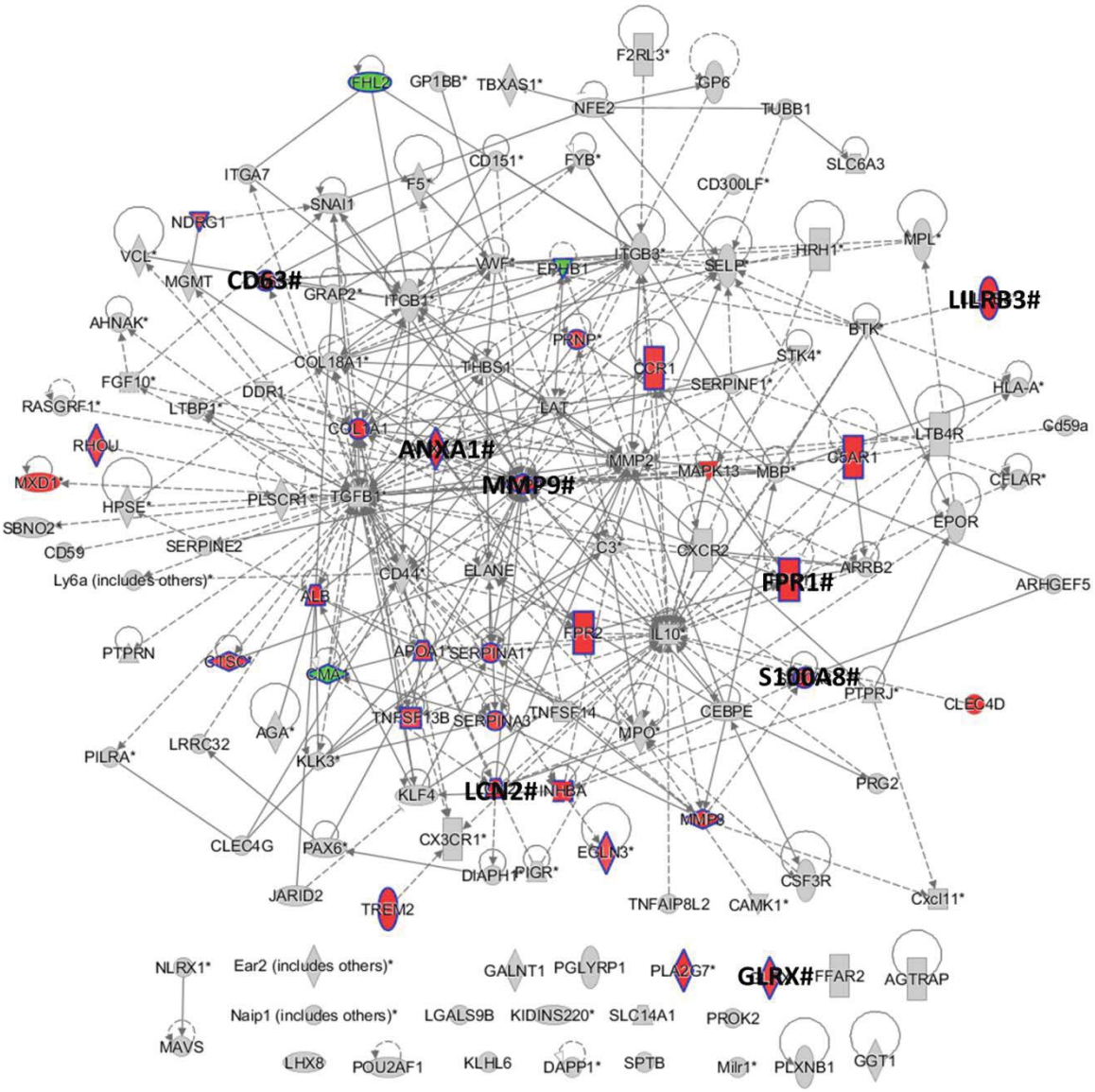

Figure 3.12 PBMC gene expression changes in response to the eicosapentaenoic acid (EPA) diet (vs. oleic acid (OA) diet) in *Il10*$^{-/-}$ mice at early stages of colitis. The colour coding of genes indicates the direction of fold-change (FC) in 9-week-old EPA-fed *Il10*$^{-/-}$ mice, with red showing genes that are increased in expression, green showing decreased expression and genes shaded in grey are not differentially expressed. The network was generated by merging the genes associated with the ten most significant biological functions in PBMCs of *Il10*$^{-/-}$ mice fed the EPA diet compared to those fed the OA diet at 9 and 12 weeks of age. Genes with a coloured border were associated with biological functions in 9-week-old EPA-fed *Il10*$^{-/-}$ mice, and genes with non-coloured borders with 12-week-old EPA-fed *Il10*$^{-/-}$ mice. Eight genes (indicated by "#") were in common between the two comparisons. The intensity of the colour of genes indicates the degree of FC, with greater intensity of colours pointing to higher levels of FC. Node shape indicates functional class of gene product as indicated in Appendix V. Data represent four biological replicates per group.

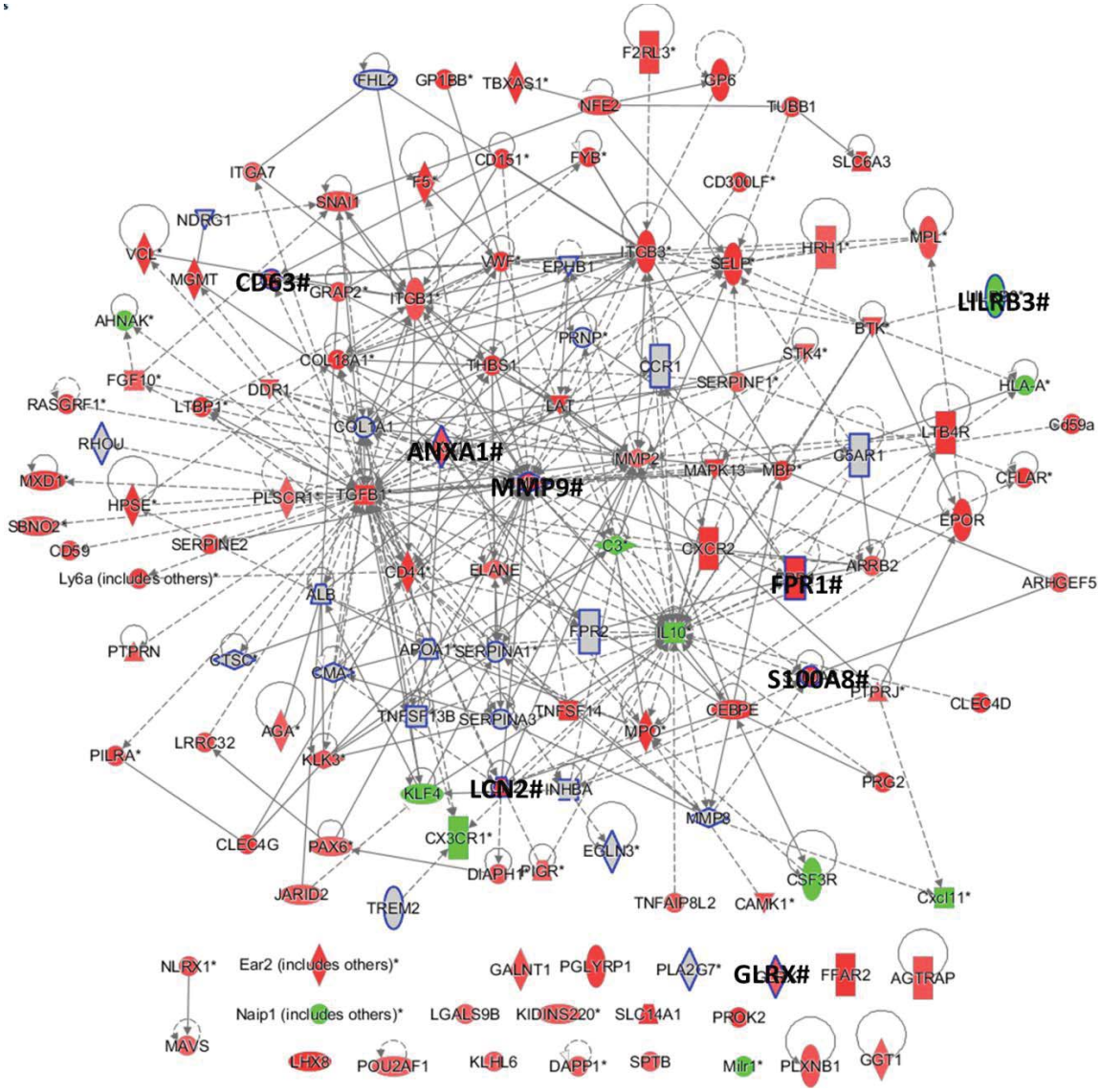

Figure 3.13 PBMC gene expression changes in response to the eicosapentaenoic acid (EPA) diet (vs. oleic acid (OA) diet) in *Il10*$^{-/-}$ mice with established colitis. The colour coding of genes indicates the direction of fold-change (FC) in 12-week-old EPA-fed *Il10*$^{-/-}$ mice, with red showing genes that are increased in expression, green showing decreased expression and genes shaded in grey are not differentially expressed. The network was generated by merging the genes associated with the ten most significant biological functions in PBMCs of *Il10*$^{-/-}$ mice fed the EPA diet compared to those fed the OA diet at 9 and 12 weeks of age. Genes with a coloured border were associated with biological functions in 9-week-old EPA-fed *Il10*$^{-/-}$ mice, and genes with non-coloured borders with 12-week-old EPA-fed *Il10*$^{-/-}$ mice. Eight genes (indicated by "#") were in common between the two comparisons. The intensity of the colour of genes indicates the degree of FC, with greater intensity of colours pointing to higher levels of FC. Node shape indicates functional class of gene product as indicated in Appendix V. Data represent four biological replicates per group.

was predicted to be increased in mice fed the EPA diet compared to those fed the OA diet (*activation z-score* = 2.2 and P = 0.01 (data not shown)). This prediction was based on the *PPARGC1A* target genes complement component 3 (*C3*), carnitine palmitoyltransferase 1B muscle (*CPT1B*), *CYP11A1*, *IL10*, myelin basic protein (*MBP*), perilipin 5 (*PLIN5*), and peroxidoredoxin 3 (*PRDX3*), all of which are associated with the metabolism of lipids, specifically "concentration of lipids". *PPARGC1A* increases the transcriptional activity of *PPARG,* hence EPA may have affected *PPARG* gene expression indirectly. However, this effect of the EPA diet was not specific to colitis in *Il10*$^{-/-}$ mice, with increased expression of *PPARG* mRNA transcript levels also in PBMCs of C57BL/6J mice, irrespective of age (FC = 1.8 at 9 weeks of age and FC = 2.5 at 12 weeks of age vs. OA diet).

3.4.5 Comparison of colon and PBMC gene expression

3.4.5.1 Colon and PBMC gene expression between mouse genotypes fed the OA diet

A network of differentially expressed genes that were in common between PBMCs and colon of *Il10*$^{-/-}$ mice fed the OA diet (vs. C57BL/6J mice) is shown in Figure 3.14 and Figure 3.15 for 9 weeks of age, and Figure 3.16 and Figure 3.17 for 12 weeks of age (FC $\geq |1.5|$ and $P \leq 0.005$).

Approximately 3000 genes were changed in expression in the colon of *Il10*$^{-/-}$ mice compared to C57BL/6J mice, both fed the OA diet (12 weeks of age). Of these genes, only a small number (80) were also differentially expressed in PBMCs of those mice as shown in Figure 3.16 and Figure 3.17. Nevertheless, many of the common genes were associated with leukocyte function as indicated in the figures by a coloured border, *e.g. ICOS*, *S100A8* and *S100A9*, formyl peptide receptor 1 and 2 (*FPR1* and *2*), cathepsin E (*CTSE*), and suppressor of cytokine signaling 3 (*SOCS3*). Regardless of tissue type, these genes were increased in expression in *Il10*$^{-/-}$ mice with established colitis (vs. C57BL/6J mice). Similar observations were made in *Il10*$^{-/-}$ mice at 9 weeks of age as shown in Figure 3.14 and Figure 3.15. A summary of the gene expression responses in colon and PBMCs can be found in Table 3.13.

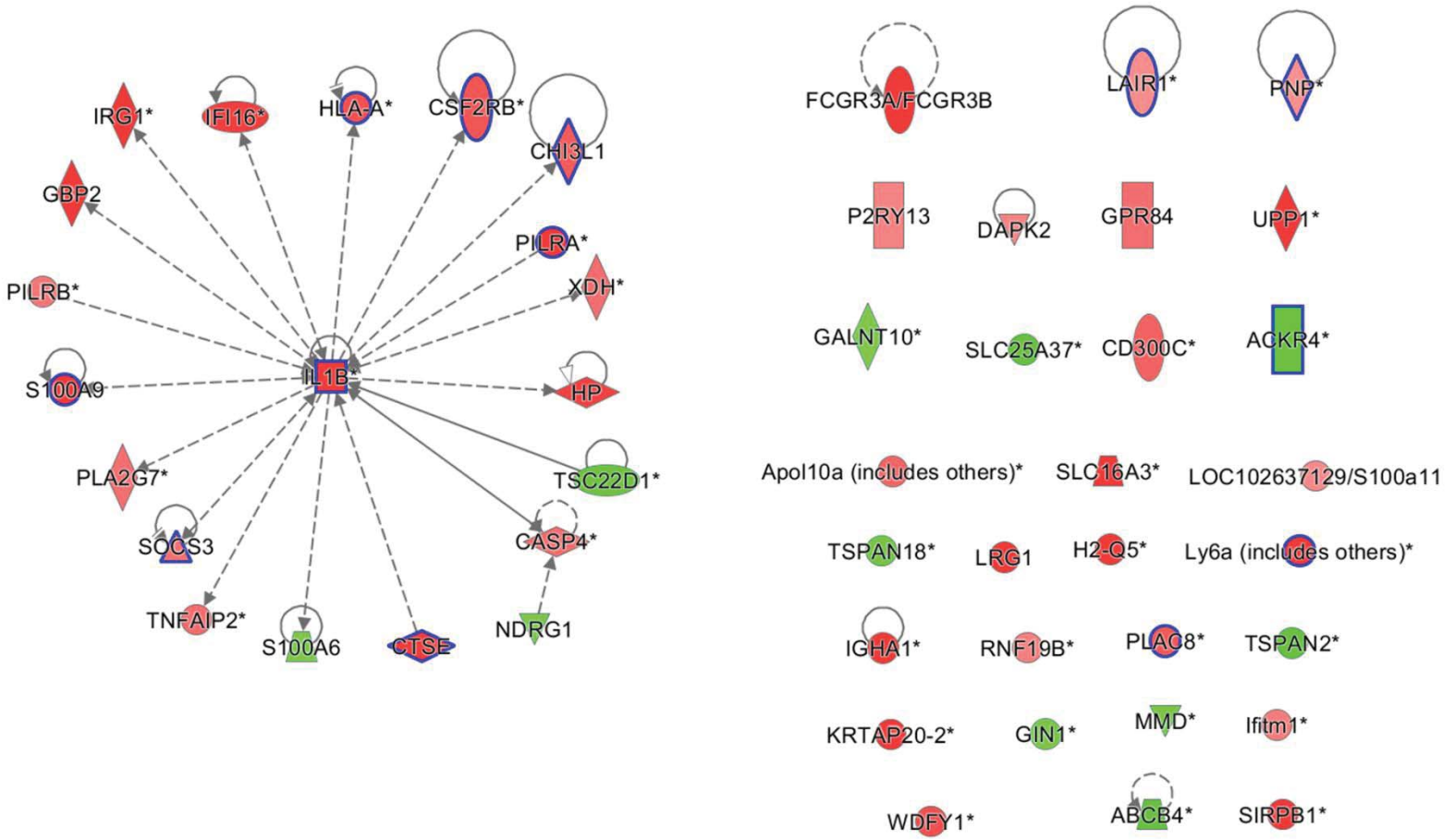

Figure 3.14 Colon gene expression associated with early stages of colitis in *Il10*$^{-/-}$ mice. The network includes genes that were differentially expressed in colon and peripheral blood mononuclear cells (PBMCs) of *Il10*$^{-/-}$ mice fed the oleic acid (OA) diet compared to C57BL/6J mice at 9 weeks of age. The colour coding of nodes indicate the direction of fold-change (FC) in the colon of *Il10*$^{-/-}$ mice, with red showing genes that are increased in expression and green showing decreased mRNA expression levels. The intensity of the colour of nodes indicates the degree of FC, with greater intensity of colours pointing to higher levels of FC. Node shape indicates functional class of gene product as indicated in Appendix V. Genes with a coloured border indicate association with *quantity of leukocytes*. Data represent four biological replicates per treatment group.

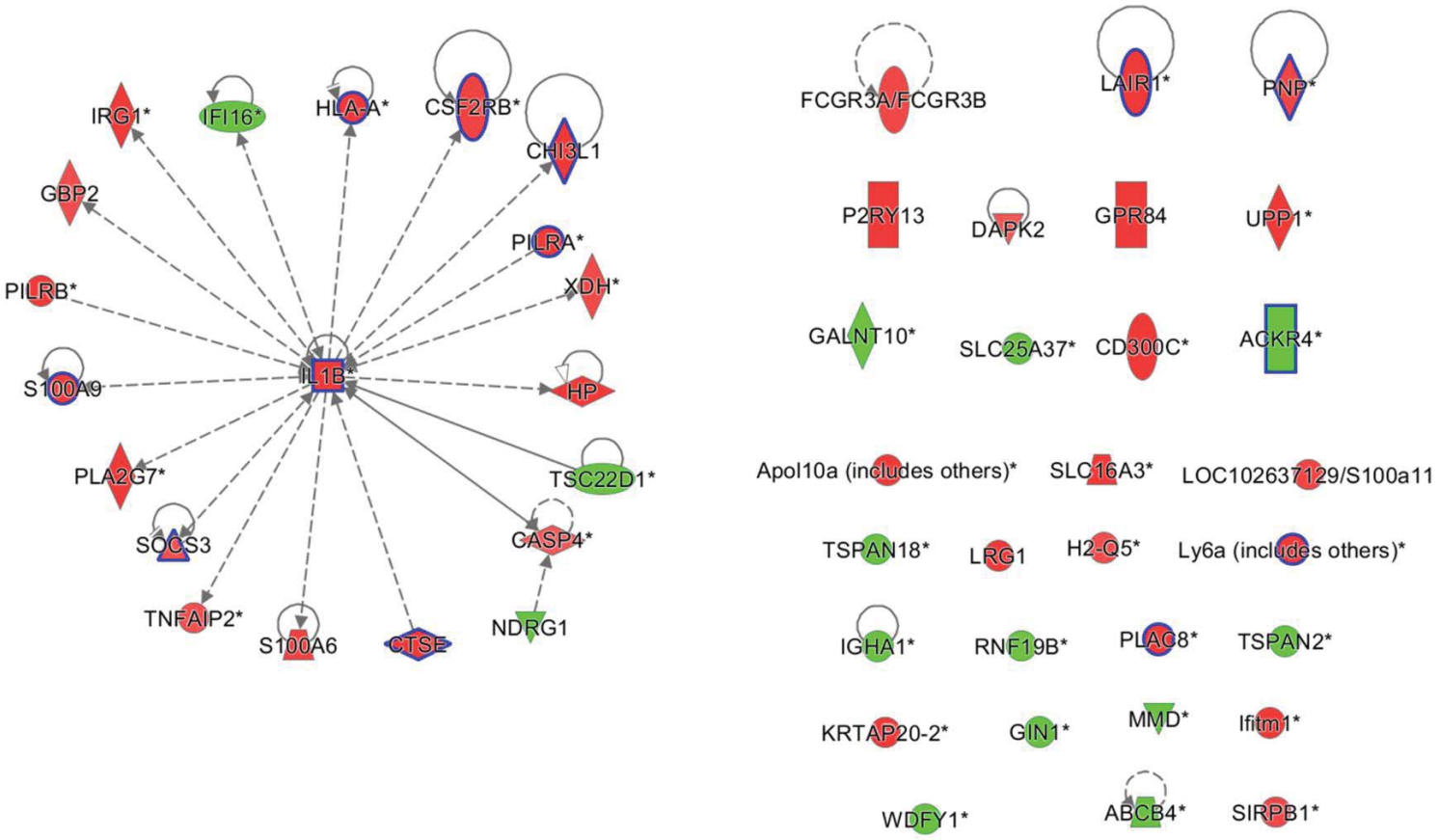

Figure 3.15 Peripheral blood mononuclear cell (PBMC) gene expression associated with early stages of colitis in *Il10*$^{-/-}$ mice. The network includes genes that were differentially expressed in colon and PBMCs of *Il10*$^{-/-}$ mice fed the oleic acid (OA) diet compared to C57BL/6J mice at 9 weeks of age. The colour coding of nodes indicate the direction of fold-change (FC) in PBMCs of *Il10*$^{-/-}$ mice, with red showing genes that are increased in expression and green showing decreased mRNA expression levels. The intensity of the colour of nodes indicates the degree of FC, with greater intensity of colours pointing to higher levels of FC. Node shape indicates functional class of gene product as indicated in Appendix V. Genes with a coloured border indicate association with *quantity of leukocytes*. Data represent four biological replicates per treatment group.

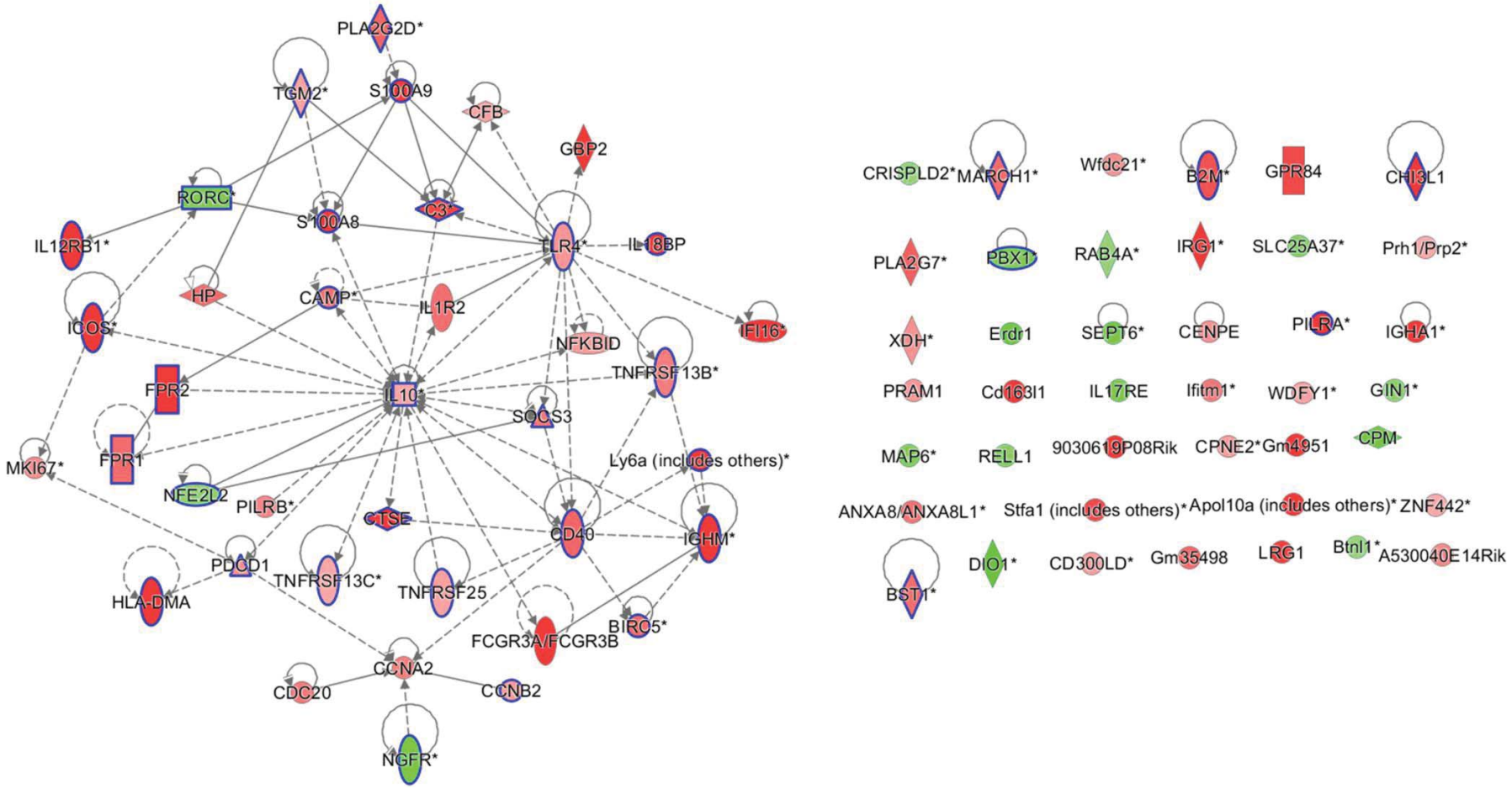

Figure 3.16 Colon gene expression associated with established colitis in *Il10*$^{-/-}$ mice. The network includes genes that were differentially expressed in colon and peripheral blood mononuclear cells (PBMCs) of *Il10*$^{-/-}$ mice fed the oleic acid (OA) diet compared to C57BL/6J mice at 12 weeks of age. The colour coding of nodes indicate the direction of fold-change (FC) in the colon of *Il10*$^{-/-}$ mice, with red showing genes that are increased in expression and green showing decreased mRNA expression levels. The intensity of the colour of nodes indicates the degree of FC, with greater intensity of colours pointing to higher levels of FC. Node shape indicates functional class of gene product as indicated in Appendix V. Genes with a coloured border indicate association with *quantity of leukocytes*. Data represent four biological replicates per treatment group.

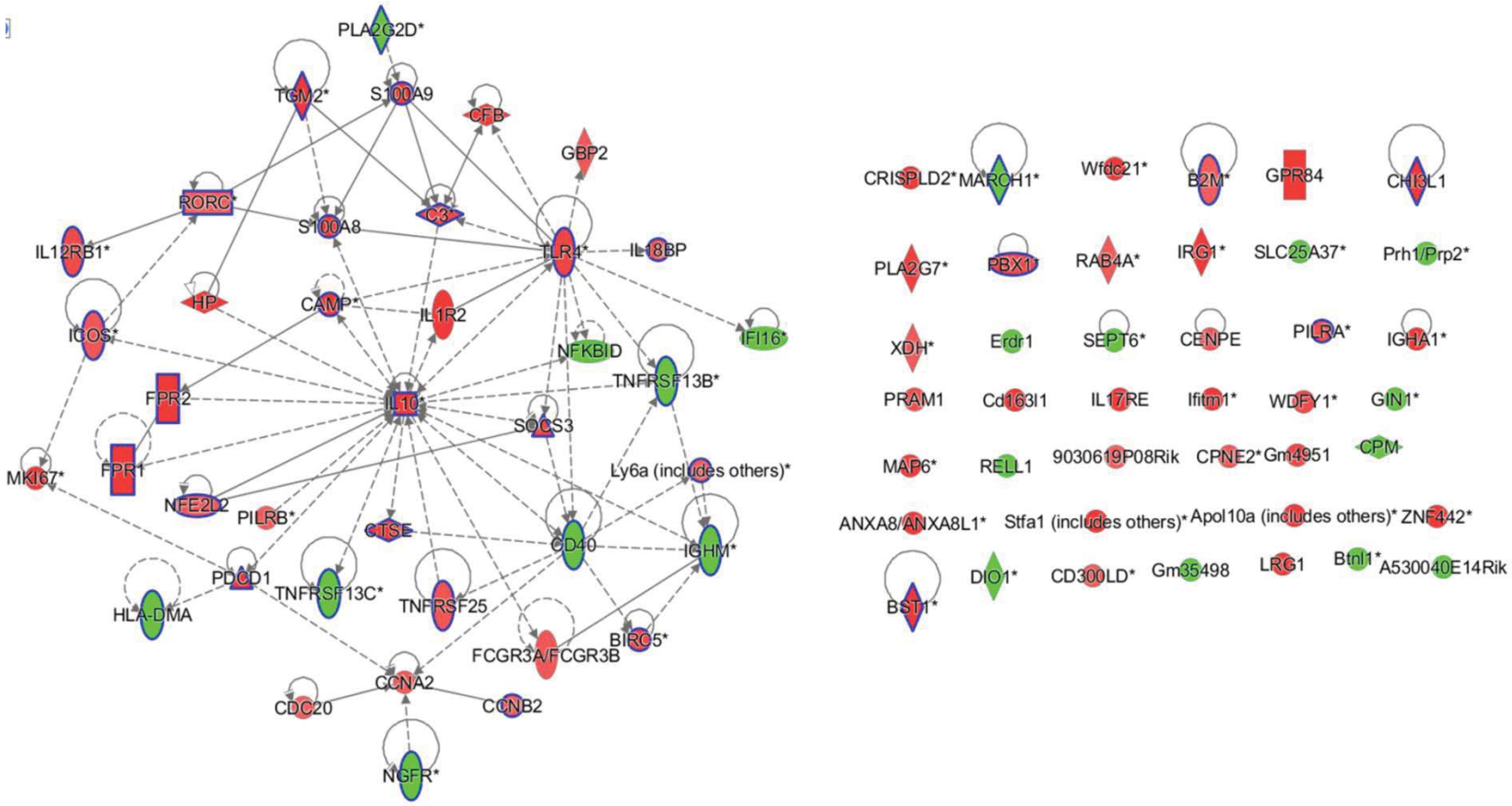

Figure 3.17 Peripheral blood mononuclear cell (PBMC) gene expression associated with established colitis in *Il10*$^{-/-}$ mice. The network includes genes that were differentially expressed in colon and PBMCs of *Il10*$^{-/-}$ mice fed the oleic acid (OA) diet compared to C57BL/6J mice at 12 weeks of age. The colour coding of nodes indicate the direction of fold-change (FC) in PBMCs of *Il10*$^{-/-}$ mice, with red showing genes that are increased in expression and green showing decreased mRNA expression levels. The intensity of the colour of nodes indicates the degree of FC, with greater intensity of colours pointing to higher levels of FC. Node shape indicates functional class of gene product as indicated in Appendix V. Genes with a coloured border indicate association with *quantity of leukocytes*. Data represent four biological replicates per treatment group.

Table 3.13 Summary of gene expression changes in the colon and peripheral blood mononuclear cells (PBMCs) from *Il10*$^{-/-}$ and C57BL/6J mice fed AIN-76A diets, either unmodified (AIN), or enriched with oleic acid (OA) or eicosapentaenoic acid (EPA). Mice were sampled at 9 or 12 weeks of age and AIN-76A and OA diet were included as control diets. (↑) indicates increased expression, (↓) decreased expression, and (-) a non-significant result using the cut-off criteria FC ≥ |1.5| and P ≤ 0.005. Data represent four biological replicates per group (except colon from C57BL/6J mice fed the AIN-76A diet where n=3).

			Colon					*PBMC*				
			Il10$^{-/-}$ *vs. C57*			*EPA vs. OA*		*Il10*$^{-/-}$ *vs. C57*			*EPA vs. OA*	
	Gene	*Age*	*AIN*	*OA*	*EPA*	*Il10*$^{-/-}$	*C57*	*AIN*	*OA*	*EPA*	*Il10*$^{-/-}$	*C57*
A	*LILRB3*	9		↑	↑	-	-		-	↑	↑	-
		12	↑	↑	↑	↓	-	↑	-	↓	↓	-
	TBXAS1	9		↑	↑	-	-		-	-	-	-
		12	↑	↑	-	↓	-	-	-	↑	↑	-
	GPR65	9		↑	↑	-	-		-	-	-	-
		12	↑	↑	↑	↓	-	-	-	↑	↑	-
	CLEC4D	9		↑	↑	-	-		-	-	↑	-
		12	↑	↑	↑	↓	-	↑	-	↑	↑	-
	PTPRJ	9		-	-	-	-		-	-	-	-
		12	-	-	-	↓	-	-	-	↑	↑	-
	CD44	9		-	-	-	-		-	-	-	-
		12	-	-	-	↓	-	-	-	↑	↑	-
	Gm19958	9		-	-	-	-		-	-	-	-
		12	-	-	-	↑	-	-	-	-	↑	-
B	*S100A8*	9		-	↑	-	-		↑	↑	↑	-
		12	↑	↑	↑	-	-	↑	↑	↑	↑	↑
	S100A9	9		↑	↑	-	-		↑	↑	-	-
		12	↑	↑	↑	-	-	↑	↑	↑	-	↑
	Cxcl13	9		↑	↑	-	-		-	-	-	-
		12	↑	↑	-	-	-	-	-	-	-	-
	MMP7	9		↑	↑	-	-		-	-	-	-
		12	↑	↑	↑	-	-	-	-	-	-	-
	MMP8	9		-	-	-	-		↑	↑	↑	-
		12	-	-	-	-	-	↑	↑	↑	-	-
	MMP9	9		-	-	-	-		↑	↑	↑	-
		12	-	-	-	-	-	↑	↑	↑	↑	-
	LCN2	9		-	↑	-	-		↑	↑	↑	-
		12	↑	-	↑	-	-	↑	↑	↑	↑	-
	LTF	9		-	-	-	-		↑	↑	-	-
		12	↑		↑	-	-	↑	↑	↑	-	↑
C	*IL36A*	9		-	↑	-	-		-	-	-	-
		12	↑	↑	↑	↓	-	-	-	-	-	-
	IL1B	9		↑	↑	↑	-		↑	↑	-	-
		12	↑	↑	↑	↓	-	↑	-	↑	-	-
	PPARG	9		-	-	-	-		↑	-	-	↑
		12	-	-	-	-	-	-	-	-	-	↑
	PPARA	9		↓	↓	-	-		-	-	-	-
		12	↓	↓	↓	-	-	-	-	-	-	-
	FOS	9		-	-	-	-		-	-	-	-
		12	-	↑	↑	↓	-	↑	-	-	-	-
D	*IDO1*	9		↑	↑	-	-		-	-	-	-
		12	↑	↑	↑	↓	-	-	-	-	-	-

Genes in bold are represented more than once on the microarray.

(A) denotes genes with EPA-induced expression changes in both colon and PBMCs of *Il10*$^{-/-}$ mice with established colitis (vs. OA diet), (B) proposed candidate biomarkers of IBD [143], (C) genes related to PPAR, and (D) genes related to tryptophan metabolism.

3.4.5.2 Effect of the EPA diet (vs. OA diet) on colon and PBMC gene expression in *Il10*$^{-/-}$ mice

Within *Il10*$^{-/-}$ mice, only a limited number of genes (7) were differentially expressed in response to the EPA diet (vs. OA diet) in the colon as well as in PBMCs of those mice at 12 weeks of age (in Table 3.13 listed under "A"). Of these seven genes, only two genes (*LILRB3* and *Gm19958* predicted gene) showed similar direction of change. At 9 weeks of age, no gene was differentially expressed in the colon in response to the EPA diet that was also affected in PBMCs within *Il10*$^{-/-}$ mice (vs. OA diet (data not shown)). Furthermore, as shown in Table 3.7, the transcriptomic profile of colon was associated with a reduction in immune cell function at 12 weeks of age in response to the EPA diet in *Il10*$^{-/-}$ mice, however, the transcriptional profile of PBMCs did not reflect these changes, pointing towards increases in immune cell trafficking in those mice (vs. OA diet (Table 3.12)).

3.4.6 Urinary metabolites

The urine obtained from 242 mice was analysed by untargeted metabolite fingerprinting using an LC-MS/MS system operating in positive and negative ionisation mode. Peak detection and alignment produced 19109 (positive) and 14706 (negative) mass ions with a mean retention time between 100 and 800 sec. Irrespective of ionisation mode, the urinary metabolite fingerprints were dependent on age at urine collection, genotype, treatment (diet and age at euthanasia), and indicated an interaction of genotype × age at urine collection (Table 3.14). These genotype-specific differences may be attributed to the presence of inflammatory metabolites in urine of *Il10*$^{-/-}$ mice during development of colitis that were absent in C57BL/6J mice. There was no interaction of genotype × treatment (Table 3.14), suggesting that *Il10*$^{-/-}$ mice showed similar urinary metabolite fingerprints to C57BL/6J mice in response to diet.

The metabolite fingerprint of urine collected at 7.1 weeks of age appeared to be different to the other time-points, irrespective of ionisation mode, while urine collected at 9, 10.1 and 12 weeks clustered more closely (Figure 3.18). The first urine was collected two days after the commencement of dietary treatments and bacterial inoculation, when *Il10*$^{-/-}$ mice did not show histopathological signs of colitis. A Kruskal Wallis test supported these findings, showing that the total numbers of significantly different ions

Table 3.14 Permutation MANOVA of the urinary metabolite fingerprints. C57BL/6J mice and *Il10*$^{-/-}$ mice were fed AIN-76A diets, either unmodified, or enriched with oleic acid (OA) or eicosapentaenoic acid (EPA), and euthanised at 9 or 12 weeks of age. Unmodified AIN-76A diet and OA diet were included as control diets. Urine was collected at 7.1, 9, 10.1 and 12 weeks of age. Data represent five to nine biological replicates per treatment group. P-values ≤ 0.05 were considered significant.

Ionisation mode	*Factor*	*P-value*
Positive	Genotype	<0.001
	Time-point	<0.001
	Treatment[#]	<0.001
	Time-point × Genotype	0.006
	Time-point × Treatment	0.139
	Genotype × Treatment	0.389
	Genotype × Time-point × Treatment	0.997
Negative	Genotype	<0.001
	Time-point	<0.001
	Treatment[#]	<0.001
	Time-point × Genotype	0.001
	Time-point × Treatment	0.255
	Genotype × Treatment	0.316
	Genotype × Time-point × Treatment	0.976

[#] Treatment refers to "Diet" and "age at euthanasia".

Positive ionisation mode

Negative ionisation mode

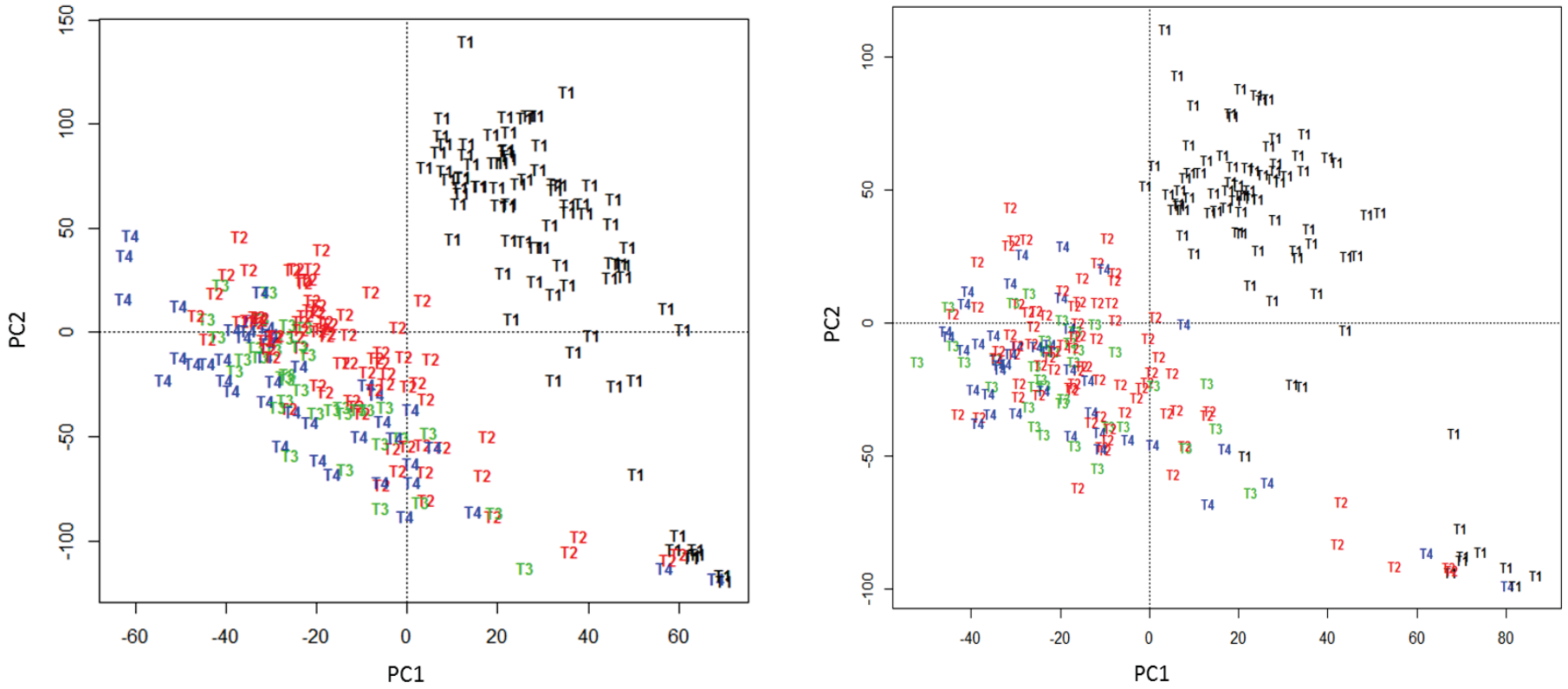

Figure 3.18 Partial Least Squares-Discriminant Analysis (PLS-DA) of metabolite fingerprint from urine in positive and negative ionisation mode at 7.1 (T1), 9 (T2), 10.1 (T3) and 12 (T4) weeks of age. Colour coding according to urine collection time-point (T1, T2, T3, or T4) and symbols indicate individual mice. Data represent 84 (T1), 79 (T2), 37 (T3) and 42 (T4) mice.

between genotypes (*Il10*$^{-/-}$ vs. C57BL/6J) and between diets (EPA vs. OA, irrespective of genotype) approximately doubled from the first to the second collection time-point (as shown in Figure 3.19 for genotype and in Figure 3.20 for diet). The separation between the second and fourth urine collection time-points as indicated in Figure 3.18 was marginally improved by plotting in three dimensions (data not shown), while data from both time-points (second and fourth) remained overlapping with the third time-point. Furthermore, the total number of differential ions was on average 4.5-times higher between the diets (Figure 3.20) than between the genotypes (Figure 3.19), indicating that diet had more impact on the urinary metabolome than genotype.

Figure 3.22 shows that the type of diet (AIN-76A, OA or EPA) had more impact on the urinary metabolite fingerprints than age at euthanasia (9 or 12 weeks), and metabolite fingerprints from urine of mice fed the AIN-76A diet were more similar to those fed the OA diet than the EPA diet. At the early urine collection time-points (7.1 and 9 weeks), the urinary metabolite fingerprint of 9-week-old mice was similar to 12-week-old mice and data from 9-week-old mice was therefore removed before analysis to improve statistical balance.

3.4.6.1 Urinary metabolites between mouse genotypes irrespective of diet

As expected, the urinary metabolite fingerprint was dependent on genotype ($P < 0.001$ (Table 3.14 and Figure 3.21)). These differences between *Il10*$^{-/-}$ mice and C57BL/6J mice became more pronounced from the first urine collection time-point at 7.1 weeks of age until the last collection time-point at 12 weeks of age, attributed to the total number of significantly different ions that increased over the experimental period (Figure 3.19). At 7.1 weeks of age, the lowest number of differential ions was observed (161 positive mode and 141 negative mode) in the urine of *Il10*$^{-/-}$ mice vs. C57BL/6J mice and at 9, 10.1 and 12 weeks of age, the total number of differential ions increased to 570/347, 655/1097, and 1148/950 in positive/negative ionisation mode, respectively (FDR ≤ 0.05). In positive ionisation mode 44 ions, and in negative mode 33 ions, were significant at every time-point (Figure 3.19). Of these ions, metabolites associated with tryptophan metabolism were most apparent (Table 3.15 and Table 3.16).

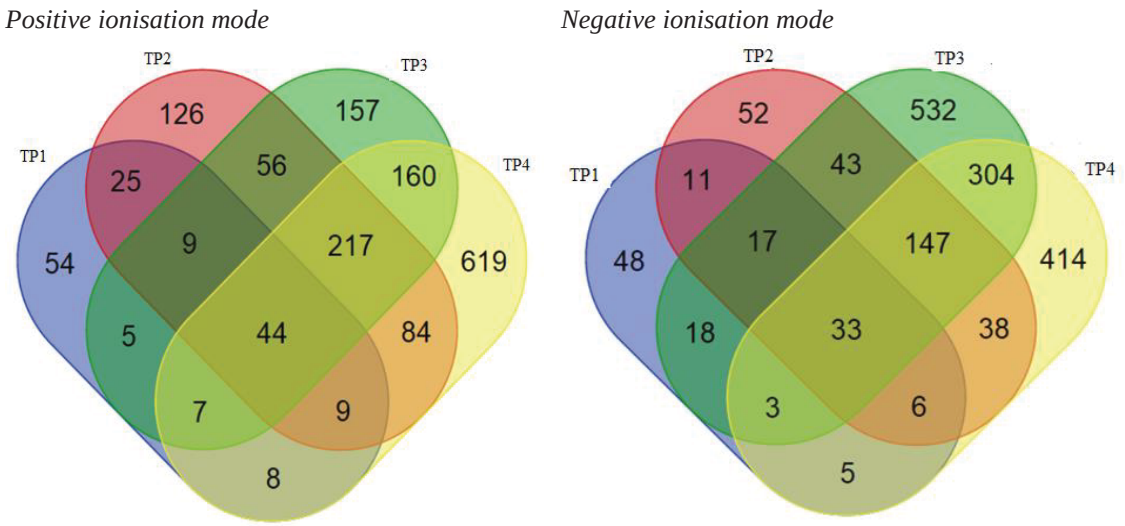

Figure 3.19 Venn diagram indicating numbers of significantly different ionisation products in the urine of *Il10*$^{-/-}$ mice compared to C57BL/6J mice (FDR ≤ 0.05). Mice were fed either a diet enriched with eicosapentaenoic acid (EPA) or oleic acid (OA) and euthanised at 12 weeks of age. Numbers may also include isotopologues, salt adducts or neutral loss fragments, which can make up a large proportion of the ionisation products [349]. Urine was collected when mice were 7.1 (TP1), 9 (TP2), 10.1 (TP3) and 12 (TP4) weeks of age. Data represent five to nine biological replicates per treatment group.

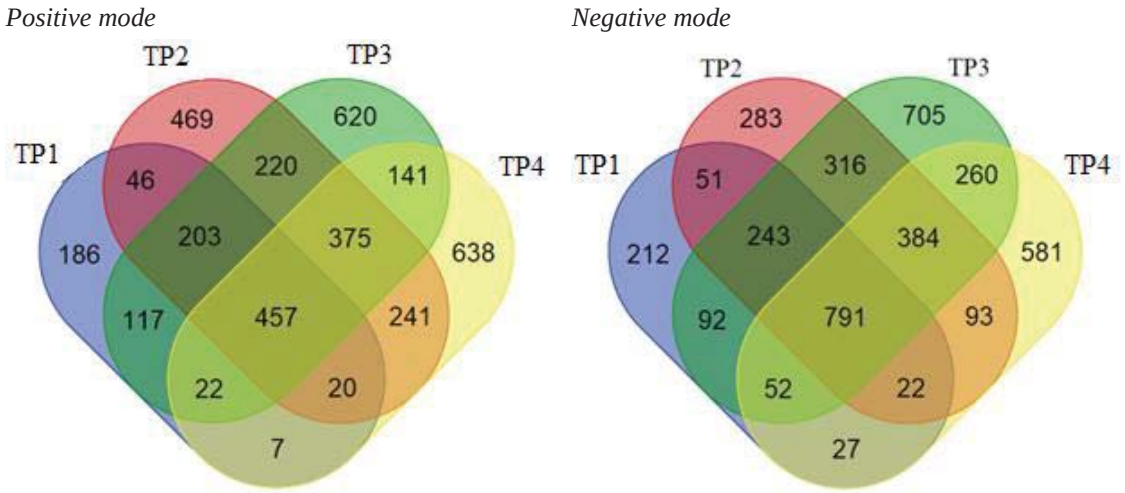

Figure 3.20 Venn diagram indicating numbers of significantly different ionisation products in the urine of mice fed the eicosapentaenoic acid (EPA) diet compared to those fed the oleic acid (OA) diet, irrespective of genotype (FDR ≤ 0.05). Numbers may also include isotopologues, salt adducts or neutral loss fragments, which can make up a large proportion of the ionisation products [349]. Urine was collected when mice were 7.1 (TP1), 9 (TP2), 10.1 (TP3) and 12 (TP4) weeks of age and mice were euthanised at 12 weeks of age. Data represent five to nine biological replicates per treatment group.

Positive ionisation mode

Negative ionisation mode

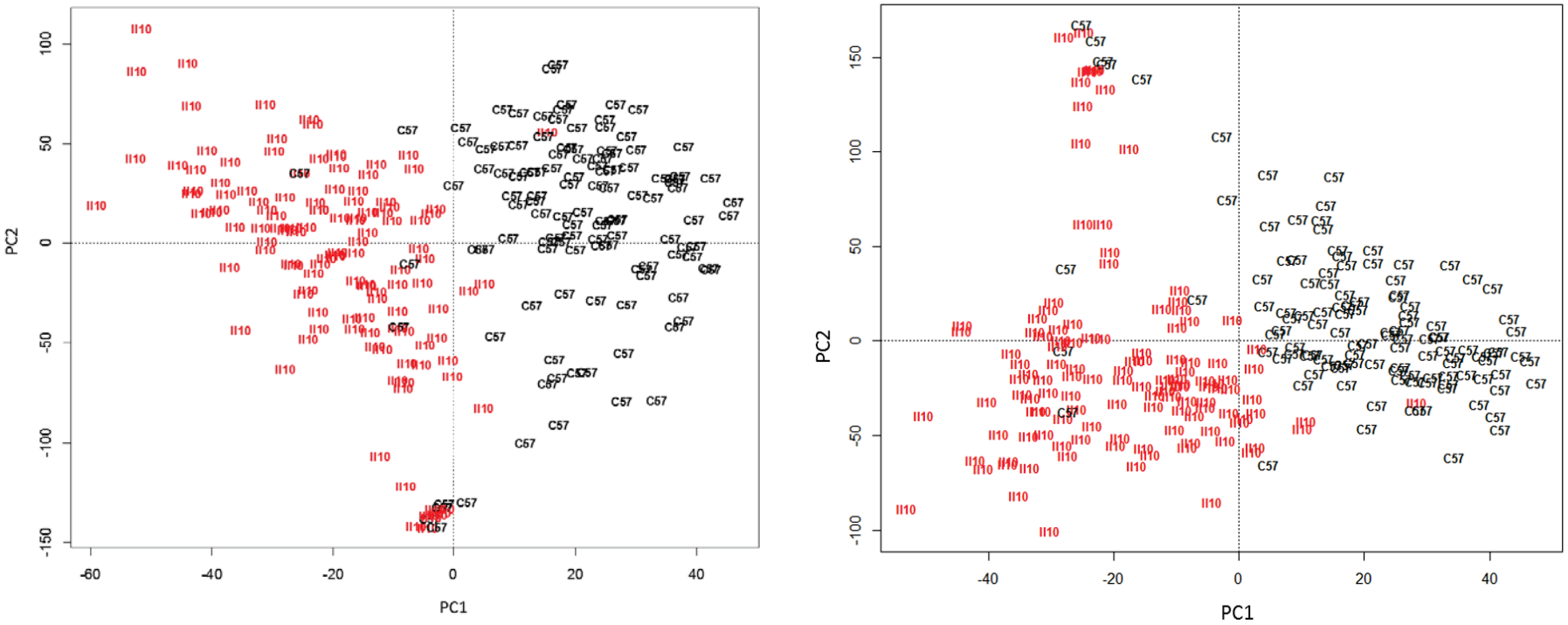

Figure 3.21 Partial Least Squares-Discriminant Analysis (PLS-DA) of metabolite fingerprint from urine of *Il10*$^{-/-}$ mice and C57BL/6J mice in positive and negative ionisation mode. Colour coding according to genotype (C57BL/6J or *Il10*$^{-/-}$) and symbols indicate individual mice. Data represent 118 (C57BL/6J) and 124 (*Il10*$^{-/-}$) mice.

Positive ionisation mode

Negative ionisation mode

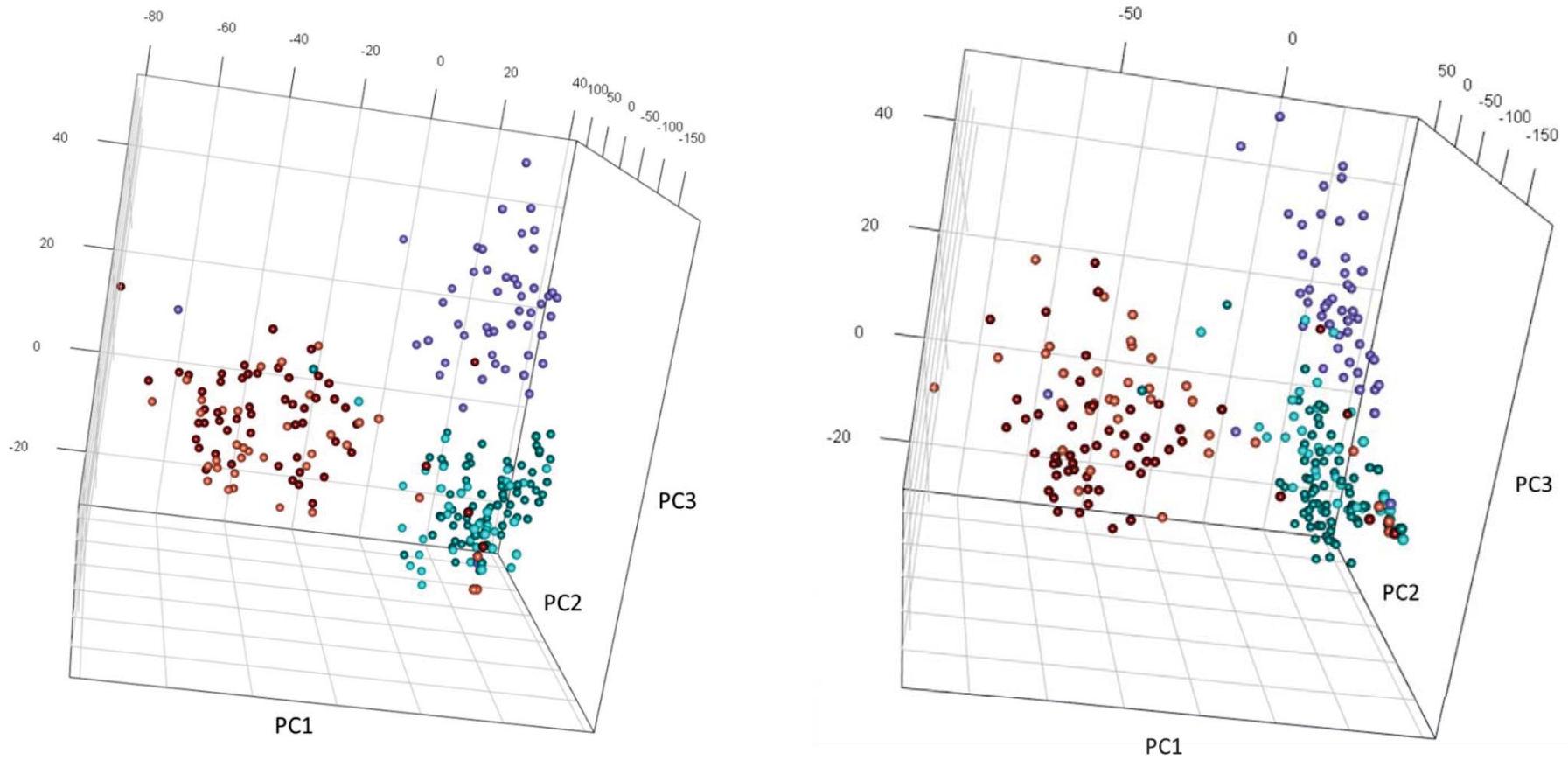

Figure 3.22 Partial Least Squares-Discriminant Analysis (PLS-DA) of metabolite fingerprint from urine in positive and negative ionisation mode, with mice sampled either at 9 weeks of age and fed oleic acid (OA) or eicosapentaenoic acid (EPA) diets, or at 12 weeks of age and fed AIN-76A, OA or EPA diets. Data represent 49 (AIN-76A), 37 (OA; 9 weeks), 67 (OA; 12 weeks), 35 (EPA; 9 weeks), and 54 (EPA; 12 weeks) mice. Data points indicate individual mice.
Violet: AIN-76A + sampling 12 weeks; Light blue: OA + sampling 9 weeks; Dark blue: OA + sampling 12 weeks; Brown: EPA + sampling 9 weeks; Orange: EPA + sampling 12 weeks.

Table 3.15 Positive ionisation products significantly different in the urine from *Il10*$^{-/-}$ mice compared to C57BL/6J mice (FDR ≤ 0.05). Differential ions in common to every collection time-point (7.1, 9, 10.1 and 12 weeks of age) or at the last three collection time-points (9, 10.1 and 12 weeks of age). Mice were fed a diet enriched either with eicosapentaenoic acid (EPA) or oleic acid (OA), and euthanised at 12 weeks of age. Arrows represent direction of change in *Il10*$^{-/-}$ mice for each ion. "RT" indicates the retention time in seconds. Only products with putative identification listed (METLIN and HMDB search with 5 ppm mass accuracy and adducts M+H, M+Na and M+NH_4 enabled). Metabolites in bold are discussed. Data represent five to nine biological replicates per treatment group.

Ion (M/Z)	*RT*	*Entries*	*Adduct*	*Putative identification*	*Metabolite information*	*Il10*$^{-/-}$ *vs. C57BL/6J*
In common at 7.1, 9, 10.1 and 12 weeks of age						
231.0436	211	1	M+NH_4	Indoxyl sulfate	Tryptophan metabolism	↑
291.1188	235	1	M+H	N-Succinyl-L,L-2,6-diaminopimelate	Lysine biosynthesis	↑
192.0655	**246**	5	M+H	5-Hydroxyindoleacetic acid	Tryptophan metabolism	↑
368.2794	495	8	M+NH_4	Tetrahydrocorticosterone	Major urinary metabolite from corticosterone	↑
In common at 9, 10.1 and 12 weeks of age						
575.1946	101	2	M+Na	Deoxycholic acid disulfate	Bile acid	↓
				Chenodeoxycholic acid disulfate		
489.1145	109	4	M+H	Citicoline	Biosynthesis of structural phospholipids in cell membranes	↓
506.1409	110	1	M+NH_4	Adduct ion of 489.1145/109		↓
225.0868	**112**	6	M+H	L-3-Hydroxykynurenine	Tryptophan metabolism	↑
				Hydroxykynurenine		
				5-Hydroxykynurenine		
				4-(2-Aminophenyl)-2,4-dioxobutanoic acid		
329.0293	139	2	M+Na	4-Hydroxy-5-(dihydroxyphenyl)-valeric acid-O-sulphate	Metabolite of valeric acid	↓
352.1031	**176**	3	M+H	Indole-3-acetic-acid-O-glucuronide	Tryptophan metabolism	↓
237.0871	**179**	4	M+H	N-Formylkynurenine	Tryptophan metabolism	↑
				L-Formylkynurenine		
			M+NH_4	8-Methoxykynurenate		
				Methyl 2,6-dihydroxy-4-quinolinecarboxylate		
379.0888	228	1	M+H	7-Methylguanosine 5'-phosphate	Purine nucleotide; RNA degradation	↓

308.1355	229	3	M+H	1,N2-propanodeoxyguanosine	Purine nucleoside	↑
229.1185	249	7	M+H	Prolyl-Hydroxyproline	Protein	↑
				Hydroxyprolyl-Proline		
			$M+NH_4$	Methyldopa		
				3-Methoxytyrosine	Serotonin and dopamine biosynthesis	
				3-O-Methyl-a-methyldopa		
343.1136	253	5	$M+NH_4$	Dihyroxy-1H-indole glucuronide I	Tryptophan metabolism	↓
311.0479	256	1	M+Na	Orotidine	Pyrimidine nucleotide	↓
206.0450	**268**	3	M+H	Xanthurenic acid	Tryptophan metabolism	↑
				4,6-Dihydroxy-2-quinolinecarboxylic acid		
222.0394	269	1	M+H	7,8-Dihydroxykynurenate	Tryptophan metabolism	↑
411.0820	269	2	M+H	4,6-Dihydroxy-2-quinolinecarboxylic acid	Tryptophan metabolism	↑
202.0696	270	4	M+Na	7-Aminomethyl-7-carbaguanine	Pyrrolopyrimidine; precursors of nucleoside Q (queuosine) biosynthesis	↑
				Glucosamine	Amino sugar	
				beta-D-Glucosamine		
				Fructosamine	Monosaccharide	
160.0757	**286**	1	M+H	Indoleacetaldehyde	Tryptophan metabolism	↓
457.7328	295	4	M+Na	1-Nitro-5-hydroxy-6-glutathionyl-5,6-dihydronaphthalene	Metabolism of xenobiotics by cytochrome P450	↑
				1-Nitro-7-hydroxy-8-glutathionyl-7,8-dihydronaphthalene		
				1-Nitro-5-glutathionyl-6-hydroxy-5,6-dihydronaphthalene		
				1-Nitro-7-glutathionyl-8-hydroxy-7,8-dihydronaphthalene		
514.1606	300	4	$M+NH_4$	Adduct of ion 457.7328/295		
482.1772	301	1	M+Na	5-Methyl-THF	Biologically active form of the folic acid	↓
206.0449	322	3	M+H	Xanthurenic acid	Tryptophan metabolism	↑
				6-Hydroxykynurenic acid (tautomer)		
337.0550	418	2	M+H	Nicotinate beta-D-ribonucleotide	Cofactor biosynthesis; Nicotinate and nicotinamide metabolism	↓

Table 3.16 Negative ionisation products significantly different in the urine from *Il10*$^{-/-}$ mice compared to C57BL/6J mice (FDR ≤ 0.05). Differential ions in common to every collection time-point (7.1, 9, 10.1 and 12 weeks of age) or at the last three collection time-points (9, 10.1 and 12 weeks of age). Mice were fed a diet enriched with either eicosapentaenoic acid (EPA) or oleic acid (OA), and euthanised at 12 weeks of age. Arrows represent direction of change in *Il10*$^{-/-}$ mice for each ion. "RT" indicates the retention time in seconds. Only products with putative identification listed (METLIN and HMDB search with 5 ppm mass accuracy and adduct M-H enabled). Metabolites in bold are discussed. Data represent five to nine biological replicates per treatment group. (A) Information from [309, 350]

Ion (M/Z)	*RT*	*Entries*	*Putative identification*	*Metabolite information*	*Il10*$^{-/-}$ *vs. C57BL/6J*
In common at 7.1, 9, 10.1 and 12 weeks of age					
196.0247	222	1	3-Hydroxy-2-methylpyridine-4,5-dicarboxylate	Vitamin B6 metabolism	↓
366.0841	**247**	2	Xanthurenate-8-O-beta-D-glucoside		↑
204.0296	**265**	3	Xanthurenic acid	Tryptophan metabolism	↑
			4,6-Dihydroxy-2-quinolinecarboxylic acid		
453.1775	**357**	1[A]	α-CEHC glucuronide	Metabolite of alpha tocopherol	↓
In common at 9, 10.1 and 12 weeks of age					
216.0332	108	1	Tyramine-O-sulfate	Sulfate derivative of tyramine	↑
487.0998	109	1	Citicoline	Biosynthesis of structural phospholipids in cell membranes	↓
214.1083	170	1	2-amino-8-oxo-9,10-epoxy-decanoic acid	Oxo fatty acid	↓
334.1511	234	1	Isopentenyl adenosine	Biosynthesis of secondary metabolites	↓
249.0073	250	3	3,4-Dihydroxyphenylglycol O-sulfate	Norepinephrine metabolite	↑
409.0686	268	2	4,6-Dihydroxy-2-quinolinecarboxylic acid	Tryptophan metabolism	↑
204.0302	308	4	Xanthurenic acid 6-Hydroxykynurenate 6-Hydroxykynurenic acid	Tryptophan metabolism	↑
425.1831	**341**	12	Gamma-CEHC glucoside	Metabolite of gamma tocopherol	↓
			Abscisic acid glucose ester	Carotenoid biosynthesis; Biosynthesis of secondary metabolites	
401.1106	422	2	4-Hydroxy-5-(3',4'-dihydroxyphenyl)-valeric acid-O-glucuronide 4-Hydroxy-5-(3',5'-dihydroxyphenyl)-valeric acid-O-glucuronide	Microbiota	↓
247.1203	431	1	Histidylproline diketopiperazine	Metabolite of thyrotropin releasing hormone	↓

Irrespective of ionisation mode, differential ions at 7.1, 9, 10.1 and 12 weeks of age mostly corresponded to metabolites of tryptophan metabolism (Table 3.15 and Table 3.16), highlighting the importance of this pathway underlying colitis in *Il10*$^{-/-}$ mice. Tryptophan is metabolised to either xanthurenic acid *via* kynurenine (Figure 3.23), or melatonin *via* serotonin (Figure 3.24). The pathway leading to the synthesis of melatonin (*via* serotonin) appeared to be decreased in *Il10*$^{-/-}$ mice, likely attributed to reduced levels of melatonin glucuronide ($[M+NH_4]^+$ 426.1886/342) at 9 and 12 weeks of age (FDR = 0.05), irrespective of the type of diet (EPA or OA). At 10.1 weeks of age, urinary abundance of melatonin glucuronide between *Il10*$^{-/-}$ mice and C57BL/6J mice was dependent on the type of diet, with both genotypes showing similar levels when fed the EPA diet, but lower levels in *Il10*$^{-/-}$ mice when they were fed the OA diet (FDR = 0.01 (Figure 3.24)).

The enzymatic conversion of tryptophan to either kynurenic acid/xanthurenic acid occurs *via* kynurenine, or to indoleacetaldehyde and indoleacetic acid with typtamine as an intermediate (Figure 3.23). Reduced levels of the ions putatively identified as indoleacetaldehyde ($[M+H]^+$ 160.0757/286) and indole-3-acetic-acid-O-glucuronide ($[M+H]^+$ 352.1031/176) were observed in the urine of *Il10*$^{-/-}$ mice from 9 until 12 weeks of age compared to C57BL/6J mice. The first step in the conversion to kynurenine is the synthesis of N-formylkynurenine from tryptophan by the enzyme IDO1. The differences in urinary N-formylkynurenine between *Il10*$^{-/-}$ mice and C57BL/6J mice became more pronounced with increasing colitis in *Il10*$^{-/-}$ mice, ranging from similar levels at 7.1 weeks of age (FDR = 1) to significantly higher levels in *Il10*$^{-/-}$ mice at 10.1 and 12 weeks of age (FDR $\leq$ 0.05). The urinary abundance of L-3-hydroxykynurenine ($[M+H]^+$ 225.0868/112) showed similarities to N-formylkynurenine, with increased abundance in urine of *Il10*$^{-/-}$ mice at 9, 10.1 and 12 weeks of age (FDR < 0.05 for all three time-points). The increased urinary abundance of xanthurenic acid ($[M-H]^-$ 204.0296/265) was independent of the type of diet in *Il10*$^{-/-}$ mice from 7 until 10.1 weeks of age (FDR $\leq$ 0.05), but showed a diet-specific effect at 12 weeks of age.

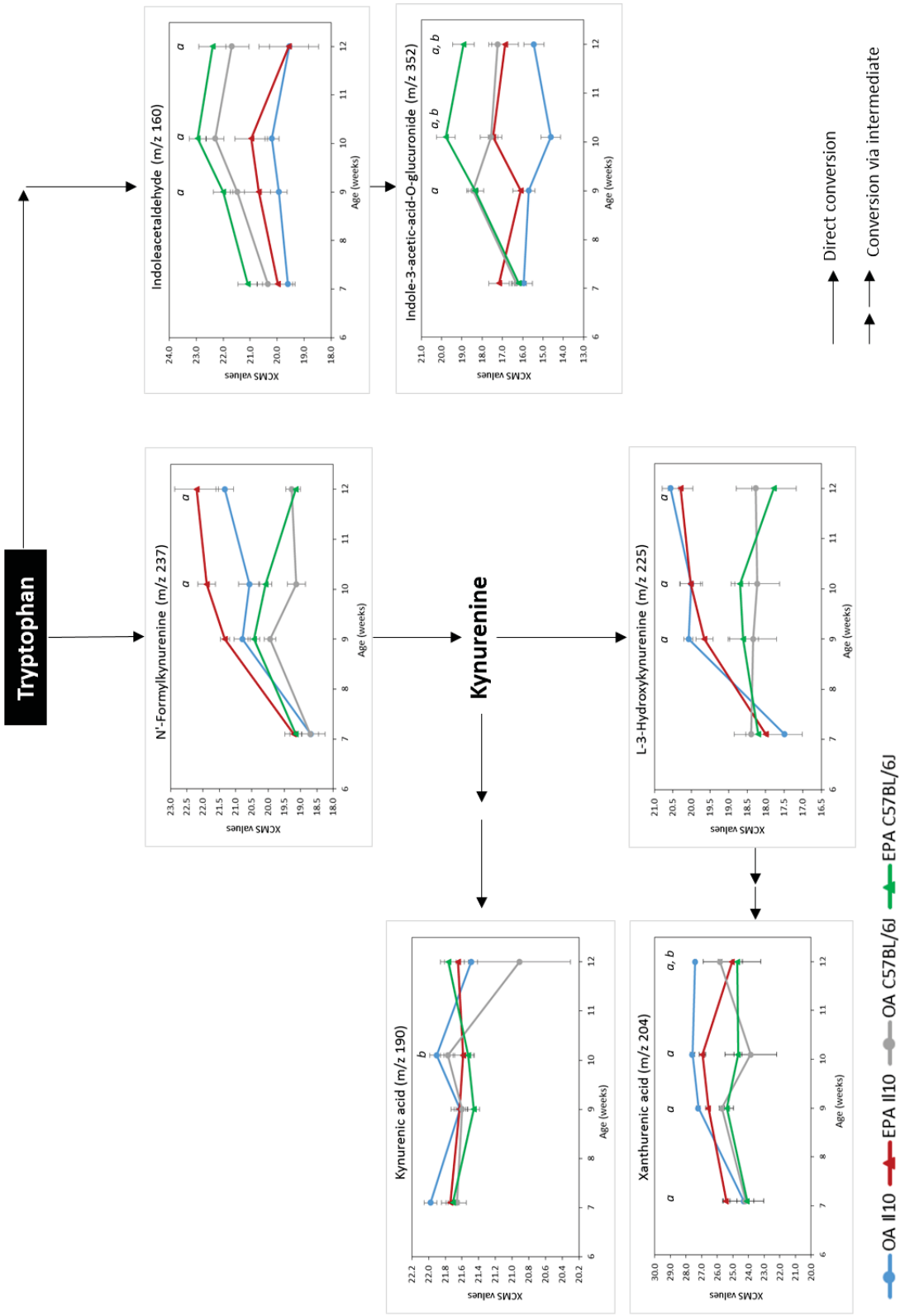

Figure 3.23 Urinary metabolites associated with metabolism of tryptophan *via* kynurenine and indoleacetaldehyde. C57BL/6J mice and *Il10*$^{-/-}$ mice were fed an oleic acid (OA) or eicosapentaenoic acid (EPA) diet, urine was collected at 7.1, 9, 10.1 and 12 weeks of age, and mice were euthanised at 12 weeks of age. Metabolites are putative identifications from METLIN and HMDB with 5 ppm mass accuracy. Data represent mean XCMS values ± SEM with five to nine biological replicates per treatment group. Significance indicated by (a) for genotype (*Il10*$^{-/-}$ vs. C57BL/6J); and (b) for diets (EPA vs. OA) (FDR ≤ 0.05). Information for the pathway obtained from the KEGG database.

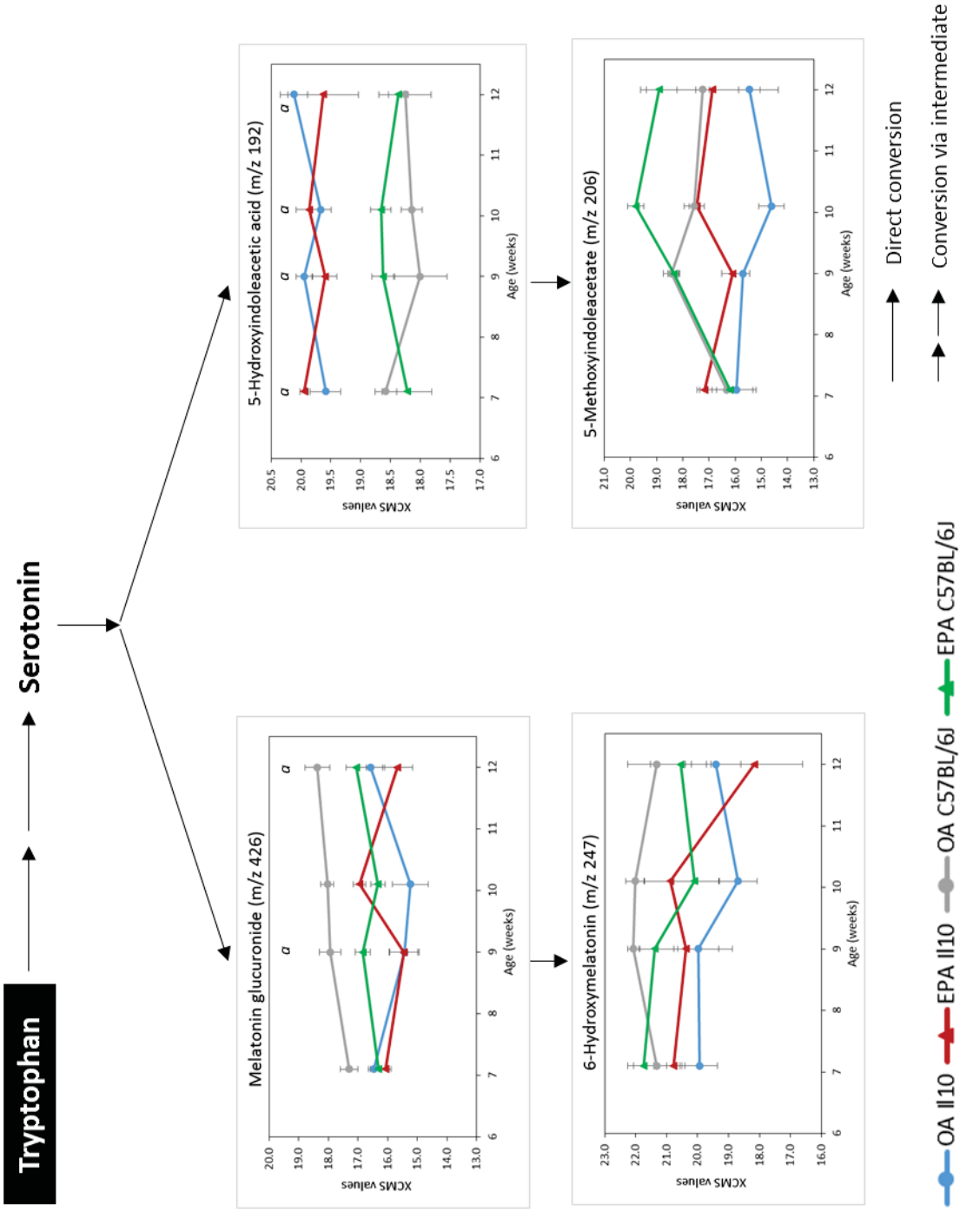

Figure 3.24 Urinary metabolites associated with metabolism of tryptophan *via* serotonin. C57BL/6J mice and *Il10*$^{-/-}$ mice were fed an oleic acid (OA) or eicosapentaenoic acid (EPA) diet, urine was collected at 7.1, 9, 10.1 and 12 weeks of age, and mice were euthanised at 12 weeks of age. Metabolites are putative identifications from METLIN and HMDB with 5 ppm mass accuracy. Data represent mean XCMS values ± SEM with five to nine biological replicates per treatment group. Significance indicated by (a) for genotype (*Il10*$^{-/-}$ vs. C57BL/6J); and (b) for diets (EPA vs. OA) (FDR ≤ 0.05). Information for the pathway obtained from the KEGG database.

3.4.6.2 Effect of the EPA diet (vs. OA diet) on urinary metabolites irrespective of genotype

The type of diet contributed to the urinary metabolite fingerprint ($P < 0.001$), with mice fed the EPA diet showing distinct differences to those fed the OA diet irrespective of genotype (Figure 3.22). These differences became more pronounced from the first urine collection time-point at 7.1 weeks of age until the last collection time-point at 12 weeks of age, attributed to the total number of significantly different ions that increased with the age of mice (Figure 3.20). At 7.1 weeks of age, metabolite differences were already established, with approximately 1000 (positive) and 1500 (negative) ions differing between mice fed the EPA diet compared to those fed the OA diet, and increased to approximately 2000 (positive) and 2500 (negative), respectively, compared to those fed the OA diet (9, 10.1 and 12 weeks of age; FDR ≤ 0.05).

375 (positive) and 384 (negative) ions were in common to the second, third and fourth time-points, reflecting changes in the urinary metabolite profile affected by the type of diet (EPA or OA (Figure 3.20)). Irrespective of ionisation mode, metabolites corresponding to the differential ions were mostly related to phospholipids (*i.e.* phosphatidylcholine and phosphatidylethanolamine) and their breakdown products (lysophosphatidylcholine (lysoPC) and lysophosphatidylethanolamine (lysoPE)), amino acid and lipid metabolism, microbial metabolism, and lipid mediators (FDR ≤ 0.05 (Table 3.17 and Table 3.18)).

The abundance of lipid mediators affected in the urine of mice fed the EPA diet was attributed to the significant increases of metabolites putatively identified as those derived from EPA (vs. mice fed the OA diet). Increases were observed irrespective of ionisation mode, however, with current methods few of the isomers could be distinguished. With the increased intake of the EPA diet, increased EPA-derived lipid mediators were detected, *e.g.*, E-series resolvins (RvE1 $[M+H]^+$ 367.2115/350 and $[M-H]^-$ 349.2024/425), and series-3 prostaglandins (PGE3, PGH3, or PGD3 $[M-H]^-$ 349.2024/425) and thromboxanes (TXB3 $[M+Na]^+$ 391.2092/392). The abundances of these metabolites were significantly elevated from 9.1 weeks of age in EPA-fed mice and remained higher until 12 weeks of age (FDR ≤ 0.05 vs. OA diet (Table 3.17 and Table 3.18)).

Table 3.17 Positive ionisation products with differential abundance in the urine of mice fed the eicosapentaenoic acid (EPA) diet compared to those fed the oleic acid (OA) diet and were in common at 9, 10.1 and 12 weeks of age (FDR ≤ 0.05). *Il10*$^{-/-}$ and C57BL/6J mice were euthanised at 12 weeks of age. Arrows represent the direction of change in EPA-fed mice. "RT" indicates retention time in seconds. Products with putative identification listed, searching METLIN and HMDB with 5 ppm mass accuracy and adducts M+H, M+Na and M+NH_4 enabled. Metabolites in bold are discussed. Data represent five to nine biological replicates per treatment group.

Ion (M/Z)	*RT*	*Entries*	*Adduct*	*Putative identification*	*EPA vs. OA*
Phospholipids; Lysophospholipids[B]					
826.6308	338	21	M+Na M+H	Phosphatidylethanolamine Phosphatidylcholine	↓
502.2930	**533**	5	M+H	LysoPE(0:0/20:4n-6) LysoPE(20:4n-6/0:0) LysoPE(0:0/20:4n-3) LysoPE(20:4n-3/0:0)	↓
503.2965	533			Isotope of 502.293/533	
524.2751	533			Na-adduct of 502.2930/533	
454.2928 [A]	560	4	M+H	LysoPE(0:0/16:0) LysoPE(16:0/0:0)	↓
568.3399	571	5	M+H	LysoPC(22:6n-3) Phosphatidylcholine (22:6n-3/0:0)[U] Phosphatidylcholine (22:6n-3/0:0)	↓
480.3085	579	4	M+H	LysoPE(18:1n-9/0:0) LysoPE(0:0/18:1n-9) LysoPE(18:1n-7/0:0) LysoPE(0:0/18:1n-7)	↓
544.3401	**583**	2	M+H	LysoPC(20:4n-6) LysoPC(20:4n-3)	↓
530.3242	584	5	M+H	LysoPE(0:0/22:4n-6) LysoPE(22:4n-6/0:0)	↓
Lipid mediators					
367.2115	**350**	16	M+H	12-oxo-20-dihydroxy-leukotriene B4 12-oxo-10,11-dihydro-20-COOH-LTB4 20-Carboxy-leukotriene B4 11-dehydro-TXB3 19-hydroxy-Resolvin E1 (RvE1) 20-hydroxy-Resolvin E1 ox-LGD2 2,3-Diketo-13,14-dihydro-PGF1a 6k-PGF1α-d4	↑
317.2111[C]	390	25	M+H	15-Deoxy-d-12,14-PGJ2	↑
391.2092	**392**	11	M+Na	20-COOH-10,11-dihydro-LTB4 Prostaglandin G2 19-Hydroxy-PGE2 20-Hydroxy-PGE2 6-Ketoprostaglandin E1 5(6)-Epoxy Prostaglandin E1 Thromboxane B3 11-Dehydro-thromboxane B2	↑

Microbial metabolism					
306.0645	225	1	$M+NH_4$	5'-(3',4'-Dihydroxyphenyl)-gamma-valerolactone sulfate	↓
308.0799	252	2	$M+NH_4$	4-Hydroxy-5-(4'-hydroxyphenyl)-valeric acid-4'-O-sulphate 4-Hydroxy-5-(3'-hydroxyphenyl)-valeric acid-3'-O-sulphate	↓
311.0201	236	1	M+Na	5'-(3',4'-Dihydroxyphenyl)-gamma-valerolactone sulfate	↓
240.123	260	12	$M+NH_4$	5'-(3'-Methoxy-4'-hydroxyphenyl)-gamma-valerolactone	↑
320.1851	438	5	$M+NH_4$	Enterodiol	↑
Amino acid metabolism					
350.1017	137	4	M+H	S-(Formylmethyl)glutathione	↑
177.0759	166	5	M+H	3-Isopropylmalate	↑
190.0712	184	4	M+H	N-Acetylglutamic acid Glutarylglycine	↑
213.0366[E]	217	2	M+Na	3-Dehydroquinate	↓
145.0491[D]	233	8	M+H	3-Methylglutaconic acid	↑
339.1413	369	3	$M+NH_4$	S-Glutaryldihydrolipoamide	↓
406.1318	379	4	M+Na	N-Acetyllactosamine Beta-1,4-mannose-N-acetylglucosamine	↓
118.0654	**427**	2	M+H	Indole	↑
Lipid metabolism					
232.1545	213	4	M+H	Isobutyryl-L-carnitine Butyrylcarnitine	↓
213.0366[E]	217	2	M+Na	2-Hydroxy-2-(2-oxopropyl)butanedioic acid	↓
145.0491[D]	233	8	M+H	3-Hexenedioic acid	↑
260.1856	320	4	M+H	L-Hexanoylcarnitine Hexanoylcarnitine	↓
133.0649	322	4	M+H	Indanone	↑
Vitamin derivatives					
319.1517	323	5	M+Na	Alpha-tocopheronic acid	↑
317.2111[C]	390	25	M+H	Retinoic acid derivative	↑
307.1903	392	1	M+H	5'-Carboxy-gamma-chromanol	↑
271.1303	538	28	M+Na	Gamma-CEHC	↑
569.3434	571		M+Na	16-Glutaryloxy-1α,25-dihydroxyvitamin D3 16-Glutaryloxy-1α,25-dihydroxy-20-epivitamin D3	↓
Not categorised					
308.1212	347	1	M+Na	Glycylprolylhydroxyproline	↓
489.2527	355	1	M+H	7-Sulfocholic acid	↑
216.0871	359	7	$M+NH_4$	3-(3,4-Dihydroxyphenyl)lactic acid	↓

				Syringic acid	
				Vanillylmandelic acid	
				3-Hydroxy-4-methoxymandelate	
				3,4-O-Dimethylgallic acid	
184.0970	367	28	M+Na	Nicotine imine	↑
			$M+NH_4$	3-Phenoxypropionic acid	
			$M+NH_4$	Desaminotyrosine	
			$M+NH_4$M+H	Homovanillin	
				Normetanephrine	
				Epinephrine	
			$M+NH_4$	3-(3-Hydroxyphenyl)propanoic acid	
			$M+NH_4$	L-3-Phenyllactic acid	
				D-Phenyllactic acid	
				Phenyllactic acid	

[A] Also detected in negative ionisation mode, therefore putative ID lysoPE while rejecting salt adduct.
[B] With current methods few isoforms (*i.e.* n-3, n-6, n-7, or n-9) could be distinguished.
[C-E] Metabolites corresponding to the same ion clustered in different groups.
LysoPC: Lysophosphatidylcholine; LysoPE: Lysophosphatidylethanolamine.

Table 3.18 Negative ionisation products with differential abundance in the urine of mice fed the eicosapentaenoic acid (EPA) diet compared to those fed the oleic acid (OA) diet, and were in common at 9, 10.1 and 12 weeks of age (FDR ≤ 0.05). *Il10*$^{-/-}$ and C57BL/6J mice were euthanised at 12 weeks of age. Arrows represent the direction of change in EPA-fed mice. "RT" indicates retention time in seconds. Products with putative identification listed, searching METLIN and HMDB with 5 ppm mass accuracy and adduct M-H enabled. Metabolites in bold are discussed. Data represent five to nine biological replicates per treatment group.

Ion (M/Z)	*RT*	*Entries*	*Compound*	*EPA vs. OA*
Phospholipids; Lysophospholipids[A]				
424.2094	388	2	Phosphatidylcholine (5:0/5:0)	↑
500.279	533	5	LysoPE(20:4n-3/0:0) LysoPE(0:0/20:4n-3) LysoPE(0:0/20:4n-6) LysoPE(20:4n-6/0:0)	↓
452.2789	559	3	LysoPE(0:0/16:0) LysoPE(16:0/0:0)	↓
478.2946	579	4	LysoPE(18:1n-9/0:0) LysoPE(0:0/18:1n-9) LysoPE(18:1n-7/0:0) LysoPE(0:0/18:1n-7)	↓
528.3099	584	2	LysoPE(0:0/22:4n-6) LysoPE(22:4n-6/0:0)	↓
613.3352	570	13	Phosphatidylinositol (19:0/0:0)	↓
Lipid mediators				
297.1710	392	8	Tetranor-PGE1 Tetranor-PGD1 13,14-dihydro-15-keto-tetranor PGD2 13,14-dihydro-15-keto-tetranor PGE2	↑
349.2024	**425**	14	(ent-6alpha,7alpha,12alpha)-6,7,12-Trihydroxy-16-kauren-19-oic acid Prostaglandin H3 (PGH3) Resolvin E1 (RvE1) Prostaglandin E3 (PGE3) 5,12,18R-TriHEPE 15-Epi-lipoxin B5 15-Keto-prostaglandin E2 20-oxo-leukotriene B4 12-Oxo-20-hydroxy-leukotriene B4 8-iso-15-keto-PGE2 Prostaglandin D3 (PGD3) 15-Oxo-lipoxin A4	↑
Microbial metabolism				
283.0825	346	3	p-Cresol glucuronide	↑
223.0609	367	4	5-(3',4',5'-Trihydroxyphenyl)-gamma-valerolactone	↑
397.1143	378	5	5-(3',5'-Dihydroxyphenyl)-gamma-valerolactone-O-glucuronide-O-methyl 5-(3',4'-Dihydroxyphenyl)-gamma-valerolactone-3'-O-methyl-4'-O-glucuronide 5-(3',4'-Dihydroxyphenyl)-gamma-valerolactone-4'-O-methyl-3'-O-glucuronide	↓

			5-(3',4'-Dihydroxyphenyl)-gamma-valerolactone-3'-O-glucuronide	
Metabolic pathways				
216.0332	145	1	Tyramine-O-sulfate	↓
258.1711	275	2	L-Hexanoylcarnitine Hexanoylcarnitine	↓
280.0827	316	1	4-Hydroxyphenylacetylglutamine	↓
216.1237	338	1	Propionylcarnitine	↓
222.0774	382	2	N-Acetyl-L-tyrosine Salsolinol 1-carboxylate	↑
365.2335	390	5	5a-Tetrahydrocortisol 3b-Allotetrahydrocortisol Beta-Cortolone Tetrahydrocortisol	↑
261.0811	418	1	Thiamine aldehyde	↑
Not categorised				
237.0436	229	2	L-4-Chlorotryptophan	↑
239.997	254	1	Indole-3-carboxilic acid-O-sulphate	↓
185.0714	376	1	1-Methoxy-1H-indole-3-acetonitrile	↑
407.2807	421	22	Alpha-Muricholic acid Cholic acid 3b,7b,12a-Trihydroxy-5a-Cholanoic acid Hyocholic acid 3a,6b,7b-Trihydroxy-5b-cholanoic acid 1b,3a,12a-Trihydroxy-5b-cholanoic acid Ursocholic acid	↓

[A] With current methods few isoforms (*i.e.* n-3, n-6, n-7, or n-9) could be distinguished.
LysoPE: Lysophosphatidylethanolamine.

The two ions $[M+H]^+$ 569.2895/387 and $[M-H]^-$ 385.2235/355 were putatively identified as AA-derived leukotrienes F4 (LTF4) and 10,11-dihydro-20-trihydroxy-leukotriene B4 (Appendix VI and Appendix VII). The metabolites corresponding to these ions were elevated at 7.1 weeks of age in the urine of all mice fed the EPA diet compared to those fed the OA diet and remained significantly elevated until 12 weeks of age (FDR $\leq$ 0.05). As the abundance of the ions was affected from only two days after commencement of dietary treatment diets, it may indicate a rapid effect of the EPA diet on AA-derived eicosanoids.

Several ions detected in the urine of mice were putatively identified as lysophospholipids lysoPE and lysoPC (Table 3.17 and Table 3.18), which are intermediates in phospholipid metabolism and turnover [351] and generated by phospholipase A2 activity [352]. The intake of the EPA diet resulted in decreased urinary abundance of lysophospholipids lysoPE and lysoPC with varying lengths and saturation in all mice compared to those fed the OA diet from 9 weeks of age and remained significantly lower until 12 weeks, irrespective of genotype (Table 3.17 and Table 3.18). For example, the ions $[M+H]^+$ 502.293/533 and $[M+H]^+$ 544.3401/583 which were putatively identified as lysoPE(20:4) and lysoPC(20:4) were highest in mice fed the OA diet (Table 3.17).

Concomitantly to the decrease of lysophospholipids(20:4), the ions $[M+H]^+$ 500.2773/503 and $[M-H]^-$ 498.2634/502 which were putatively identified as lysoPE(20:5n-3) showed increased abundance in the urine of mice fed the EPA diet compared to those fed the OA diet, irrespective of genotype (Appendix VI and Appendix VII). Increases of lysoPE(20:5n-3) were observed from 7.1 weeks of age, and remained significant until 12 weeks of age (FDR $\leq$ 0.05). This suggests that the EPA diet affected the phospholipids rapidly, with effects measurable two days after the commencement of treatment diets.

The metabolism of tryptophan was affected by the EPA diet towards the later stages of the experiment. This was attributed to increased abundance of the metabolite putatively identified as indole-3-acetic-acid-O-glucuronide ($[M+H]^+$ 352.1031/176 (Figure 3.23)), decreased xanthurenic acid ($[M-H]^-$ 204.0296/265 (Figure 3.23)), and increased abundance of indole ($[M+H]^+$ 118.0654/427 (Table 3.17)) in the urine of EPA-fed mice, irrespective of genotype (FDR $\leq$ 0.05 vs. OA diet). This suggests that the

metabolism of tryptophan was affected by the EPA diet by decreasing the synthesis of xanthurenic acid from tryptophan and concomitantly elevating the tryptamine pathway towards later stages of the experiment.

As shown in Table 3.17 and Table 3.18, ions putatively identified as metabolites of microbial metabolism, such as enterodiol, valeric acid and valerolactone conjugates, and p-cresol glucuronide, were significantly different between mice fed the EPA diet and those fed the OA diet from 9 weeks of age. There was no clear direction of change, with some metabolites increased, while others were decreased. This abundance pattern in the urine may follow adaptations of the microbial community profile in response to the EPA diet, irrespective of genotype.

3.4.6.3 Effect of the EPA diet (vs. OA diet) on urinary metabolites in *Il10*$^{-/-}$ mice

Table 3.19 shows that the intake of the EPA diet affected lysophospholipid abundance in the urine of all mice, regardless of genotype and are therefore an effect of diet, rather than specific to colitis in *Il10*$^{-/-}$ mice. While this was mostly similar for lipid mediators, metabolites putatively identified as E-series resolvins ($[M+H]^+$ 367.2115/350), series-3 prostaglandins ($[M-H]^-$ 349.2024/425) and thromboxane B3 (TXB3 $[M+Na]^+$ 391.2092/392) showed genotype-specific responses to the EPA diet at 12 weeks of age (Table 3.19). The urinary abundances of these three lipid mediators were, in EPA-fed *Il10*$^{-/-}$ mice, increased from 9 until 12 weeks of age compared to those fed the OA diet. Within C57BL/6J mice, increases of these three lipid mediators were only observed at 9 and 10.1 weeks of age in response to the EPA diet (vs. OA diet), while no effect was shown at 12 weeks of age (Table 3.19). It remains to be established whether an EPA-rich food also exerts these effects on lipid mediator abundance.

At 12 weeks of age, genotype-specific effects of the EPA diet (vs. OA diet) were observed on urinary tryptophan metabolites (Table 3.19). Increased abundances were shown in EPA-fed *Il10*$^{-/-}$ mice for metabolites putatively identified as N-formylkynurenine ([M+H] 237.0871/179) and indole ($[M+H]^+$ 118.0654/427), but reduced abundance of xanthurenic acid ($[M-H]^-$ 204.0296/265). The effects of the EPA diet on indole and xanthurenic acid abundances were not observed at earlier urine collection time-points and therefore indicates a modulation of tryptophan metabolism by dietary EPA in *Il10*$^{-/-}$ mice with established colitis (Table 3.19). Therefore, tryptophan

Table 3.19 Summary of urinary metabolites detected in *Il10*$^{-/-}$ and C57BL/6J mice fed AIN-76A-based diets, either enriched with eicosapentaenoic acid (EPA) or oleic acid (OA). *Il10*$^{-/-}$ and C57BL/6J mice were euthanised at 12 weeks of age and urine was collected at 7.1, 9, 10.1 and 12 weeks of age (referred to as 1st, 2nd, 3rd and 4th time-point in the table). "XCMS ion" shows the mass-per-charge ratio and retention time, with "metabolite" indicating the putative identification. "ESI" indicates the electrospray ionisation mode (positive or negative). Arrows indicate the direction of change within the comparison. P-values were calculated using permutation ANOVA of the log transformed, normalised peak intensities as per XCMS at each time-point independently. (↑) indicates increased expression, (↓) decreased expression, and (-) a non-significant result using a permutation p-value ≤ 0.05. Data represent five to nine biological replicates per treatment group.

XCMS ion	*ESI*	*Metabolite*	*Il10*$^{-/-}$ *vs. C57BL/6J mice* *OA diet*				*EPA vs. OA* *Il10*$^{-/-}$ *mice*				*EPA vs. OA* *C57BL/6J mice*			
			1st	*2nd*	*3rd*	*4th*	*1st*	*2nd*	*3rd*	*4th*	*1st*	*2nd*	*3rd*	*4th*
Tryptophan														
225.0868/112	+	L-3-hydroxykynurenine	-	↑	↑	↑	-	-	-	-	-	-	-	-
352.1031/176	+	Indole-3-acetic-acid-O-glucuronide	-	↓	↓	↓	↑	-	↑	-	-	-	↑	↑
237.0871/178	+	N-Formylkynurenine	-	↑	↑	↑	-	-	-	↑	-	-	-	-
192.0655/246	+	5-Hydroxyindoleacetic acid	↑	↑	↑	↑	-	-	-	-	-	-	↑	-
160.0757/286	+	Indoleacetaldehyde	-	↑	↑	↑	-	-	-	-	-	-	-	-
222.0394/269	+	7-8-Dihydroxykynurenate	-	↑	↑	↑	-	-	-	↓	-	-	↓	↓
204.0296/265*	-	Xanthurenic acid	-	↑	↑	↑	-	-	-	↓	-	-	-	-
204.0302/308	-	4,6-Dihydroxy-2-quinolinecarboxylic acid Xanthurenic acid 6-Hydroxykynurenate 6-Hydroxykynurenic acid	↑	↑	↑	↑	-	↓	-	↓	-	-	-	-
118.0654/427	+	Indole	-	-	-	-	-	↑	↑	↑	↑	↑	↑	-
Lysophospholipids														
500.2773/503	+	LysoPE(20:5n-3)	-	-	-	-	↑	↑	↑	↑	↑	↑	↑	↑
454.2928/560	+	LysoPE(16:0)	-	-	-	-	-	-	↓	-	-	↓	↓	↓
480.3085/579	+	LysoPE(18:1n-9)	-	-	-	-	-	-	-	↓	↓	↓	↓	↓
502.2930/533	+	LysoPE(20:4n-6)	-	-	-	-	-	↓	↓	↓	-	↓	↓	↓
530.3242/584	+	LysoPE(20:4n-3) LysoPE(22:4n-6)	-	-	-	↓	-	-	↓	↓	-	↓	↓	↓

544.3401/583	+	LysoPC(20:4n-6) LysoPC(20:4n-3)	-	-	-	-	-	↓	↓	↓	-	↓	↓	↓
568.3399/571	+	LysoPC(22:6n-3)	-	-	-	-	-	↓	↓	↓	-	-	↓	↓
452.2789/559	-	LysoPE(0:0/16:0)	-	-	-	-	-	↓	↓	↓	↓	↓	↓	↓
478.2946/579	-	LysoPE(18:1n-9)	-	-	-	-	-	↓	↓	↓	↓	-	↓	↓
498.2634/502	-	LysoPE(20:5n-3) PE(20:5n-3)	↑	-	-	-	↑	↑	↑	↑	↑	↑	↑	↑
500.279/533	-	LysoPE(20:4n-3)	-	-	-	-	-	↓	↓	↓	-	↓	↓	↓
528.3099/584	-	LysoPE(22:4n-6)	-	-	-	-	↓	-	-	↓	-	-	↓	↓
Lipid mediators														
459.2160/322	+	18-Carboxy-dinor-LTE4	↓	-	-	-	↑	↑	↑	↑	↑	↑	↑	↑
368.2433/372	+	Resolvin E1 Prostaglandin E3 5,12,18R-TriHEPE 15-Epi-lipoxin B5 15-Keto-prostaglandin E2 20-oxo-leukotriene B4 12-Oxo-20-hydroxy-leukotriene B4 8-iso-15-keto-PGE2 Prostaglandin D3 15-Oxo-lipoxin A4 PGH3	↑	-	-	-	↑	↑	↑	↑	↑	↑	↑	↑
569.2895/387	+	Leukotriene F4 (LTF4)	-	-	-	-	↑	↑	↑	↑	↑	↑	↑	↑
367.2115/350	+	19-hydroxy-Resolvin E1 (RvE1) 20-hydroxy-Resolvin E1	-	-	-	↓	-	↑	↑	↑	-	↑	↑	-
391.2092/392	+	Thromboxane B3	-	-	↓	-	-	↑	↑	↑	-	↑	↑	-
317.2111/390	+	15-Deoxy-d-12,14-PGJ2	-	-	-	-	-	↑	↑	↑	-	↑	-	↑
297.1710/392	-	Tetranor-PGE1 Tetranor-PGD1 13,14-dihydro-15-keto-tetranor PGD2 13,14-dihydro-15-keto-tetranor PGE2	-	-	-	-	↑	↑	↑	↑	-	-	↑	↑

349.2024/425	-	Prostaglandin H3 (PGH3) Resolvin E1 (RvE1) Prostaglandin E3 (PGE3) Prostaglandin D3 (PGD3)	-	-	-	↓	-	↑	↑	↑	-	↑	↑	-
351.2182/398	-	Prostaglandin E2 Prostaglandin D2	-	-	-	-	↑	↑	↑	↑	↑	↑	↑	↑

* Xanthurenic acid: closer to expected retention time.

LysoPC: Lysophosphatidylcholine; LysoPE: Lysophosphatidylethanolamine; PE: Phosphatidylethanolamine.

metabolism may be a candidate biomarker of colitis responsive to dietary EPA, but it remains to be established whether an EPA-rich food also exerts these effects.

3.5 Discussion

The inflammatory phenotype of the *Il10*$^{-/-}$ mouse model was as expected and findings were comparable to other studies using *Il10*$^{-/-}$ mice. Colitis in *Il10*$^{-/-}$ mice was characterised by infiltration of lymphocytes/plasma cells into colon tissue, loss of goblet cells, and crypt hyperplasia, showing a higher degree of colitis at 9 and 12 weeks of age compared to C57BL/6J mice. The colon transcriptomic profile was associated with increased immune regulatory mechanisms and cell-mediated immune system, while reduced functionality of metabolic processes were observed, irrespective of the type of diet or age. These findings were supported by other studies using *Il10*$^{-/-}$ mice as a model for IBD [6, 95, 109, 116, 305, 342, 343, 348, 353]. In addition, this study reports for the first time the PBMC gene expression profile in *Il10*$^{-/-}$ mice reflects the profile of the colon in early stages of colitis and when it was established. Urine appeared to be a suitable surrogate for changes in the colon gene expression profiles associated with tryptophan metabolism in *Il10*$^{-/-}$ mice during colitis and was characterised by decreased melatonin biosynthesis but elevated urinary abundance of xanthurenic acid compared to C57BL/6J mice.

Similar to a previous study, the EPA diet reduced levels of lymphocyte infiltration and crypt hyperplasia in the colon of 12-week-old *Il10*$^{-/-}$ mice compared to those fed the OA diet [6]. The colon transcriptomic profile of these mice indicated reduced expression of genes associated with lymphocyte function, eicosanoid signalling, but elevated *PPARG* signalling pathways. However, contrary to the hypothesis but a novel finding was that these EPA-induced effects were not observed in *Il10*$^{-/-}$ mice at 9 weeks of age, with unchanged severity of colitis (histological analysis) and the aforementioned molecular pathways (gene expression) compared to those fed the OA diet.

Unexpectedly, the results presented in this chapter did not support the hypothesis that the transcriptomic profile of PBMCs reflect the reduced severity of colitis and most of the colon gene expression changes (except for *PPARG*) in *Il10*$^{-/-}$ mice fed the EPA diet. The concordance of PBMC and colon *PPARG* gene expression in *Il10*$^{-/-}$ mice fed the EPA

diet at 12 weeks of age was attributed to an increase in *PPARGC1A* target genes. However, regardless of age of *Il10*$^{-/-}$ mice, PBMC gene expression showed primarily elevated immune cell activation in response to the EPA diet compared to those fed the OA diet.

The urinary abundance of the metabolite putatively identified as xanthurenic acid, N-formylkynurenine and indole may be a reflection of reduced colonic *IDO1* gene expression in *Il10*$^{-/-}$ mice fed the EPA diet (vs. OA diet) at 12 weeks of age, therefore supporting the stated hypothesis that urine could be used as surrogate for EPA-induced gene expression changes in the colon. This study is the first to show these effects of dietary EPA *in vivo*, but these observations were not made at early stages of colitis in *Il10*$^{-/-}$ mice. Additionally, in agreement with the literature [98, 243, 244, 354, 355], dietary EPA affected lipid mediator synthesis, but this study was the first to link an increased urinary abundance of metabolites putatively identified as pro-resolution RvE1, and anti-inflammatory series-3 prostaglandins (PGE3, PGH3, or PGD3) and TXB3 with reduced colitis in *Il10*$^{-/-}$ mice compared to those fed the control OA diet.

3.5.1 Growth performance

Despite a higher mean food intake for *Il10*$^{-/-}$ mice, their body weights were similar to C57BL/6J mice and in agreement to observations made in previous studies using *Il10*$^{-/-}$ mice [95, 290]. Growth retardation in *Il10*$^{-/-}$ mice is commonly observed [95, 109], and may be linked to an impaired ability to absorb nutrients along the small intestine and colon due to alterations in its microstructure and physiology [95, 266]. Aside from genotype-specific differences, all 12-week-old mice fed the EPA diet had lower dietary intakes and body weights irrespective of genotype, albeit similar levels of energy per gram between the experimental diets. This was reported in other studies, for example, in *Il10*$^{-/-}$ mice fed an EPA-enriched diet [6] and in International Cancer Research mice fed a DHA-enriched diet [356]. This effect was not apparent in mice that were sampled at 9 weeks of age, a difference in palatability between the diets is therefore unlikely, and as this was observed in both the *Il10*$^{-/-}$ mice and C57BL/6J mice, it may be independent of colitis development.

3.5.2 Severity of colitis in *Il10*$^{-/-}$ mice

The severity of colitis was higher in *Il10*$^{-/-}$ mice compared to C57BL/6J mice, irrespective of age or the type of diet (AIN-76A, OA or EPA), and characterised by infiltration of lymphocytes/plasma cells, loss of goblet cells, and crypt hyperplasia, indicating that the *Il10*$^{-/-}$ mouse model performed as expected [95, 109]. At 9 weeks of age, the intake of the EPA diet did not have an effect in *Il10*$^{-/-}$ mice, showing a similar degree of colitis to *Il10*$^{-/-}$ mice fed the AIN-76A and OA diets. At 12 weeks of age, supplementation with dietary EPA resulted in lower levels of colonic crypt hyperplasia and infiltration of lymphocytes/plasma cells in *Il10*$^{-/-}$ mice compared to those fed either type of control diet (AIN-76A or OA). These findings that EPA reduced the severity of colitis were supported by other studies in mice with experimental colitis [5-7, 357]. However it is of note that four *Il10*$^{-/-}$ mice in the EPA diet group reached the maximum allowed weight loss according to Animal Ethics guidelines and were therefore euthanised prior to their scheduled sampling time. It cannot be excluded that this excess weight loss was linked to adverse effects of dietary EPA on inflammatory processes in those mice.

3.5.3 Transcriptomic profiling of PBMCs and colon tissue

Irrespective of diet or age, more genes were differentially expressed in the colon than in PBMCs of *Il10*$^{-/-}$ mice (vs. C57BL/6J mice) within the same diet. The opposite was observed in response to the EPA supplementation, with more genes differentially expressed in PBMCs from mice fed the EPA diet (vs. OA diet) within a genotype than in the colon. This indicates that PBMCs were more responsive to the EPA diet in terms of gene expression changes compared to the OA diet than colon tissue, irrespective of inflammatory status (*i.e.* within *Il10*$^{-/-}$ mice or within C57BL/6J mice). The higher degree of gene expression changes in PBMCs is likely reflective of the increase in EPA incorporation into PBMCs and further migration to peripheral tissues *via* the blood circulation. It has previously been reported that PBMC gene expression showed distinctive changes upon PUFA supplementation in healthy male individuals compared to those who received a diet enriched with saturated fatty acids [358].

3.5.3.1 Colon transcriptomic profile during colitis

The colon transcriptomic profile of *Il10*$^{-/-}$ mice was associated with immune regulatory mechanisms and cell-mediated immune responses compared to C57BL/6J mice,

irrespective of the type of diet or age. These findings were supported by other studies using *Il10*$^{-/-}$ mice [6, 116, 305, 342, 343, 353]. The induced expression of genes such as *REG3B*, *S100A9* and multiple members of the C-X-C chemokine subfamily in the colon of *Il10*$^{-/-}$ mice has also been shown in UC patients compared to healthy subjects [359]. Calprotectin is a complex formed by the proteins S100A8 and S100A9, highly abundant in the cytosolic fraction of neutrophils [360], and are elevated at local sites of inflammation. Faecal calprotectin was suggested as a biomarker of IBD [143], however, the EPA diet did not have an effect on the expression of genes *S100A8* or *S100A9* in the colon of *Il10*$^{-/-}$ mice.

The induction of genes in inflammatory pathways in the colon of *Il10*$^{-/-}$ mice was also associated with antigen presentation in those mice compared to C57BL/6J mice, regardless of diet or age. The antigen presentation pathway is vital for the development of innate and adaptive immunity, and a dysregulation in these responses has been suggested to be part of the pathogenesis in IBD [361]. The loss of intestinal barrier integrity in IBD may result in increased infiltration of bacteria into the mucosa, which could increase antigen presentation (MHC class II) by antigen presenting cells to $CD4^+$ T cells [362]. Following activation, $CD4^+$ T cells differentiate into one of several Th cells that further drive the immune response by releasing cytokines, recruiting other immune cells to the site and assisting in maturation of other white blood cells such as B cells. Another study in *Il10*$^{-/-}$ mice reported an abnormally high number of colonic mucosal $CD4^+$ cells, with predominant Th1 activity that produced large amounts of cytokines [109], thus supporting the current findings.

Myeloid differentiation primary response gene 88 (*MYD88*), an important regulator of the commensal microbiota along the GIT [271], was increased in expression in the colon of 9-week-old *Il10*$^{-/-}$ mice compared to C57BL/6J mice, irrespective of the type of diet (OA or EPA). This increase in the early stages of colitis may indicate early responses to the commensal microbiota, potentially connected to the antimicrobial genes *REG3G*, which is dependent on *MYD88* signalling in the colon [271]. At 9 weeks of age, colonic *REG3G* was the gene with the largest increase in expression in *Il10*$^{-/-}$ mice compared to C57BL/6J mice. *REG3G* controls the physical separation of the microbiota from the epithelial surface [363], and in their absence, commensal and pathogenic microbiota increasingly colonise the epithelial surface, triggering the activation of the immune response [364]. Therefore increased *MYD88* gene expression in the colon of

Il10$^{-/-}$ mice at 9 weeks of age, as observed here, may be an attempt to control the separation of microbiota and the epithelial surface during early stages of colitis.

Genes involved in digestive/absorptive processes and related to metabolism of, for example, amino acids, carbohydrates, lipids, and cofactors and vitamins were decreased in expression in the colon of *Il10*$^{-/-}$ mice. This may suggest perturbations of numerous biochemical processes underlying colitis [266] and has been reported in other studies using mice with experimental colitis [6, 265, 268, 343]. Similar observations were made in the colon of IBD patients, where decreased expression of several genes involved in metabolism of fatty acids was reported (*e.g. FATP 3* and *4* and *FABP 2* and *6* [267]). Martínez-Augustin *et al.* [265] suggested that the reduced functionality of various metabolic processes in colitis may result in an energy deficiency for mucosal cells. This was supported by decreased expression of genes in energy metabolism in the colon of *Il10*$^{-/-}$ mice, regardless of age, and also reported in other studies [265, 268]. It is further proposed that this may cause a shortage of energy for processes which are energy-demanding, for example, selective permeability or xenobiotic metabolism.

The KEGG pathway *Metabolism of xenobiotics by cytochrome P450* was decreased in expression in the colon of *Il10*$^{-/-}$ mice compared to C57BL/6J mice when both were fed the OA diet. The GIT surface is the largest interface between the body and the outside environment and is constantly exposed to foreign substances. The CYP-mediated metabolism of xenobiotics is crucial to detoxify these foreign substances which could otherwise lead to severe destruction of the tissue [262, 264]. In *Il10*$^{-/-}$ mice, loss of detoxification could further result in increased epithelial permeability, triggering the inflammatory response by infiltrating toxins and bacteria.

The metabolism of tryptophan was affected in the colon of *Il10*$^{-/-}$ mice compared to C57BL/6J mice at 9 and 12 weeks of age, with increased *IDO1*-mediated degradation of tryptophan to xanthurenic acid *via* kynurenine, but reduced genes that mediate the synthesis of tryptamine and serotonin. *IDO1* was among the genes with the largest increase in the colon of *Il10*$^{-/-}$ mice and has reportedly been elevated in expression in lesional biopsies from CD patients [365, 366]. It has been suggested that an increased *IDO1* gene expression by antigen-presenting cells of the lamina propria may suppress T cell responses to induce immune tolerance, while in epithelial cells, *IDO1* expression may specifically be induced to limit microbial invasion as a result of ongoing inflammation

[366]. Concomitantly with the induction of *IDO1* gene expression, the expression of genes that lead to the synthesis of tryptamine and tryptamine-derived metabolites from tryptophan (*e.g. DDC*, *INMT*, *AOC1*, *MAOA* and *MAOB*), and serotonin from tryptophan (*e.g. TPH1* and *DDC* [367-369]), were decreased in expression in the colon of *Il10*$^{-/-}$ mice (vs. C57BL/6J mice), regardless of age. Similar observations were made in another study among UC patients, where levels of serotonin in colon biopsies were reduced compared to healthy control subjects [370]. The authors attributed these reductions to the gene *TPH1*, the rate-limiting enzyme in the biosynthesis of serotonin. Together this supports the findings of increased *IDO1*-mediated catabolism of kynurenine from tryptophan, concomitantly with lowered expression of genes along the serotonin and tryptamine pathways.

3.5.3.2 Colon transcriptomic profile in response to the EPA diet (vs. OA diet) in *Il10*$^{-/-}$ mice

Dietary EPA did not affect *PPARA* expression in the colon of *Il10*$^{-/-}$ mice compared to those fed the OA diet, but may have affected *PPARG* signalling pathways at 12 weeks of age. This was attributed to reduced expression of the pro-inflammatory cytokines *IL1B* and *IL36A*, and decreased expression of *FOS* gene in EPA-fed *Il10*$^{-/-}$ mice. As a natural ligand of PPARs, purified EPA reportedly increased *PPARG* expression in a mouse model of experimental cardiac transplantation and induced anti-inflammatory gene expression in this tissue [250]. In a pig model with DSS-induced colitis, an increase in colonic *PPARG* gene expression in response to linoleic acid supplementation was linked to a delayed onset of colitis [3]. A delay in colitis onset was not observed in *Il10*$^{-/-}$ mice in the current study, with similar severity of colitis between *Il10*$^{-/-}$ mice fed the EPA diet and those fed the OA diet at 9 weeks of age, and may be linked to the differences in animal model (pig vs. mouse) or induction model (acute DSS model vs. genetic model).

It was shown that IL1B and IL36A signalling cascades are mediated *via* NFKB [371], which inhibits the binding of PPARG and its target genes [372], thus a reduction in *IL1B* and *IL36A* in EPA-fed *Il10*$^{-/-}$ mice may have increased the transcriptional activity of *PPARG*. There is limited evidence regarding the impact of dietary n-3 PUFA on *IL36A* gene expression, but studies in other mouse models of IBD showed reduced expression of *IL1B* after DHA supplementation [260], but not after EPA supplementation [6]. Downstream of *PPARG*, increased transcriptional activity was reported to inhibit the

Activator protein 1 (AP1) complex, formed by FOS and Jun proto-oncogene (JUN) in the nucleus of cells [373]. It is possible that inhibition of the transcriptional activity of AP1 may have affected *COX2* gene expression, a target gene of AP1 [373], influencing lipid mediator synthesis in *Il10*$^{-/-}$ mice fed the EPA diet.

The intake of the EPA diet may have affected eicosanoid signalling in the colon of 12-week-old *Il10*$^{-/-}$ mice (vs. OA diet). The genes *PLA2G2D* and *PLA2G3* encode the protein phospholipase 2 (PLA2) and were decreased in expression in response to the EPA diet in *Il10*$^{-/-}$ mice. PLA2 catalyses cleavage of AA from cell membrane phospholipids [374] thereby releasing it as substrate for lipid mediators. Supporting this, the gene *TBXAS1* that codes a protein located in the endoplasmic reticulum membrane catalysing the conversion of AA-derived prostaglandin H2 to thromboxane A2, was reduced in expression in *Il10*$^{-/-}$ mice in response to EPA supplementation. This was supported by reduced expression of the receptor for AA-derived lipoxin (*FPR2*) in the colon of *Il10*$^{-/-}$ mice fed the EPA diet compared to those fed the OA diet at 12 weeks of age. These findings were in agreement with those reported in another study [151], where eicosanoid signalling was shown to decrease in PBMCs from healthy elderly subjects after fish oil supplementation for 26 weeks and may have reduced the age-related low-grade inflammation [375]. It is known that an increased intake of EPA-rich diets replaces AA in cell membrane phospholipids, thus affecting lipid mediator synthesis by producing less potent and anti-inflammatory eicosanoids from EPA compared to those derived from AA [243].

In the colon of *Il10*$^{-/-}$ mice, the expression of *IDO1* was reduced by feeding the EPA diet at 12 weeks of age (vs. the OA diet). Only a limited number of studies have reported an effect of EPA on gene expression associated with the metabolism of tryptophan. For example, an *in vitro* study showed an inhibitory effect of EPA on IDO1 activity in human acute leukemic cells, indicated by reduced production of kynurenine after exposure to the cytokine INFG in those cells [376]. *In vivo* studies noted that genes with multiple functional roles in metabolic processes, *e.g.* the gene families of CYP or aldehyde dehydrogenase (ALDH), were responsive to dietary n-3 PUFA in the colon of *Il10*$^{-/-}$ mice [6] or liver of healthy mice [377], but *IDO1* gene expression was unchanged. It is possible that changes in gene expression in tryptophan metabolism are the result of reduced pro-inflammatory cytokines, such as IFNG [376] in EPA-fed *Il10*$^{-/-}$ mice, rather than a direct interaction of EPA with genes that metabolise tryptophan, and the result of

a less inflammatory phenotype in those mice (vs. *Il10*$^{-/-}$ mice fed the OA diet). At 9 weeks of age, no effect of the EPA diet on metabolism of tryptophan was observed in *Il10*$^{-/-}$ mice.

At 9 weeks of age, the EPA diet had limited effects on gene expression in the colon of *Il10*$^{-/-}$ mice compared to those fed the OA diet. Considering that the severity of colitis was similar between these mice, the low number of differentially expressed genes between these treatment groups is expected. Nevertheless, at 9 weeks of age, the genes with altered expression pointed towards an elevated inflammatory response in the colon of *Il10*$^{-/-}$ mice fed the EPA diet compared to those fed the OA diet (*e.g.* increased genes *IL1B,* lymphotoxin alpha (*LTA*), *MYD88*, and *CEBPD*). This indicates that the EPA diet may have exaggerated pro-inflammatory gene expression in the colon of *Il10*$^{-/-}$ mice during early stages of colitis. Some studies suggested that feeding pure EPA or fish oil increased colonic injury and delayed repair mechanisms compared to control diets during an acute inflammatory response in the colon [259, 378], associated with the suppression of signalling pathways mediated by epidermal growth factor receptor and downstream cytoskeletal remodelling in response to an EPA diet [259]. Furthermore, it was postulated that specifically during colitis, delayed mucosal healing may allow increased bacterial infiltration into the colonic mucosa and exacerbated immune responses. Yet in the current experiment, colon gene expression did not specifically show changes in wound healing events, such as the expression of epidermal growth factor receptor, in EPA-fed *Il10*$^{-/-}$ mice at 9 weeks of age. In bacterially inoculated *Il10*$^{-/-}$ mice (as used in the current study), loss of intestinal barrier integrity and subsequent accumulation of bacteria in the mucosa may have occurred as early as 7 weeks of age [277]. This increased bacterial infiltration (not measured here) may explain the induction of colonic *MYD88* in 9-week-old *Il10*$^{-/-}$ mice fed the EPA diet compared to those fed the OA diet.

Changes in eicosanoid signalling were not observed in *Il10*$^{-/-}$ mice fed the EPA diet at 9 weeks of age. EPA replaces AA in cell membrane phospholipids in a time-dependent manner and it may be possible that the duration of EPA supplementation was too short to have an effect. In animal studies, daily feeding of n-3 PUFA-rich diets showed that DHA was incorporated into membrane phospholipids of liver, heart and adipose tissue of mice as early as four days after the initiation of increased DHA intake, but colonic mucosal cell incorporation was not measured [356]. In DSS-administered mice, incorporation of EPA and DHA into colonic mucosal cell phospholipids was reported after three weeks, mostly at the expense of AA, but no information on earlier time-points

were provided [259]. In human studies, supplementation with fish oil capsules showed that the incorporation of EPA and DHA into human immune cells peaked four weeks after commencing increased intake [221, 379]. However, not all studies confirmed these findings, for example, Browning *et al.* [380] indicated slower incorporation into PBMCs (approximately eight months), while most rapid incorporation was detected in plasma phospholipids (one to two weeks). In the current experiment, the incorporation of EPA into cell phospholipids was not measured and no conclusion can be drawn about its enrichment in colonic cells, but with the late arrival of the experimental diets, the EPA diet was fed approximately two weeks before the samples for the early time-points were collected.

3.5.3.3 PBMC transcriptomic profile during colitis

The PBMC transcriptomic profile of *Il10*$^{-/-}$ mice was associated with immune-regulatory mechanisms and cell-mediated immune system compared to C57BL/6J mice, irrespective of the type of diet or age. In agreement with the literature, genes such as *S100A8*, *S100A9*, *MMP8*, *MMP9*, and *LCN2* have previously been suggested as biomarkers of IBD in faeces or serum [143] and have also been increased in expression in the current experiment in PBMCs during early and established colitis in *Il10*$^{-/-}$ mice. The genome-wide gene expression profiling of PBMCs from IBD patients identified increased expression of genes associated with immune and inflammatory response, and cell proliferation [149, 346], further supporting current findings.

Gene expression changes in PBMCs from *Il10*$^{-/-}$ mice fed the OA diet compared to C57BL/6J mice showed an effect on B lymphocytes, where co-stimulatory molecules (*e.g. CD40* and *CD83*), immunoglobulin (*IGHM*), and receptors for TNF-related ligands (*e.g. TACI* and *BAFFR*) were decreased at 12 weeks of age. This may be explained by a decrease of lymphocytes in the purified PBMC fraction, which has been reported in IBD patients compared to healthy subjects [149]. Hence the decrease in mRNA expression levels may reflect the decline in a certain cell type in the PBMC fraction of *Il10*$^{-/-}$ mice compared to those of healthy C57BL/6J mice, rather than active changes in gene expression by a cell type. However, defective expression of *TACI* and *ICOS*, reduced serum immunoglobulins (*e.g.* IgM), are also associated with common variable immunodeficiency, a defect reported in IBD [as reviewed in 381], and may explain the observed changes in PBMCs from *Il10*$^{-/-}$ mice at 12 weeks of age. Despite a normal

number of circulating B cells, the cells present may be unable to mount protective antibody responses [382] contributing to the development of colitis in *Il10*$^{-/-}$ mice.

The *IL10 signalling* pathway was differentially expressed and *IL10* mRNA levels increased in PBMCs from *Il10*$^{-/-}$ mice, irrespective of the type of diet (OA or EPA), as was observed by other studies using *Il10*$^{-/-}$ mice [286, 383]. In the adaptive immune system, only effector T cells produce and secrete IL10 and the cytokine pattern that regulates the differentiation of naïve T cells to effector T cells also regulates the initiation of IL10 production. This represents a feedback loop to prevent excessive inflammatory processes, hence an increase in *IL10* expression may represent an attempt to dampen the inflammatory cascade in *Il10*$^{-/-}$ mice. It was however shown that in *Il10*$^{-/-}$ mice, the protein IL10 was not functional [95].

The importance of *Tryptophan metabolism* was shown in the colon of *Il10*$^{-/-}$ mice, but the pathway did not appear to be affected in PBMCs compared to C57BL/6J mice. Only approximately 3% of PBMCs express the *IDO1* gene, with the majority being plasmacytoid dendritic cells [384]. This may explain the low expression of *IDO1* in PBMCs from all mice, as indicated by microarray analysis, and the non-differential expression of the gene between *Il10*$^{-/-}$ and C57BL/6J mice, irrespective of age or the type of diet. Thus PBMCs are not suitable to monitor the gene expression changes in tryptophan metabolism.

3.5.3.4 PBMC transcriptomic profile in response to the EPA diet (vs. OA diet) in *Il10*$^{-/-}$ mice

Transcriptomic analysis of PBMCs obtained from *Il10*$^{-/-}$ mice fed the EPA diet indicated elevated tissue homing, as shown by increased expression of chemokine receptors [385], integrins [386], and cell activation markers [387] irrespective of age (vs. OA diet). While it has been demonstrated that chronic intestinal inflammation in IBD patients is characterised by increased activation and migration of immune cells to the inflamed intestine [362, 385], it appears counterintuitive that this was also observed in 12-week-old *Il10*$^{-/-}$ mice with reduced colitis when fed the EPA diet (vs. OA diet). It is possible that the PBMC transcriptomic profile reflected cell signalling that lead to the proliferation of myeloid-derived suppressor cells, which can suppress T cell responses [388], or trafficking of Treg cells to the colon to reduce colitis [389]. However, the number of myeloid-derived suppressor cells and Treg cells in the PBMC fraction are generally low

[389, 390] and may not have been detected in the overall PBMC transcriptomic profile. Alternatively, when considering PBMCs as a reflection of the physiological state of subjects [151, 391], the elevated duodenal inflammation in 12-week-old EPA-fed *Il10*$^{-/-}$ mice (vs. OA diet) may explain the current findings.

The EPA diet did not affect *PPARA* gene expression in PBMCs from *Il10*$^{-/-}$ mice, but may have induced the expression of *PPARGC1A* (a co-activator of *PPARG*) at 12 weeks of age. This increase was linked to changes in expression of the *PPARGC1A* target genes *C3*, *CPT1B*, *CYP11A1*, *IL10*, *MBP*, *PLIN5*, and *PRDX3*. These genes are associated with "lipid concentration" and may indicate changes in PBMC fatty acid metabolism induced by the EPA diet in mice. In rats with DSS-induced colitis, feeding a krill oil-enriched diet for one month resulted in an increased expression of *PPARGC1A* in the colon compared to a control diet, therefore reversing the observed decrease that was underlying colitis in DSS-administered rats [252]. However, an increased expression of *PPARG* was also observed in PBMCs of C57BL/6J mice in the current study, and therefore these effects of EPA on *PPARG* are a dietary effect rather than a specific effect of EPA on colitis.

3.5.4 Urine metabolomics

3.5.4.1 Urine metabolomic profile during colitis

Urinary metabolites that differed between *Il10*$^{-/-}$ and C57BL/6J mice were mostly associated with metabolism of tryptophan, while only a limited number of other metabolites were detected, *e.g.* bile acids, norepinephrine derivatives, and valeric acid conjugates. Of the urinary metabolites that differed between *Il10*$^{-/-}$ and C57BL/6J mice at 7 weeks of age, 5-hydroxyindoleacetic acid has previously been associated with the *Il10*$^{-/-}$ genotype [281], while xanthurenate-8-O-beta-D-glucoside (xanthurenic acid glucoside) is reportedly a regulator of sodium excretion by the kidneys [392].

The metabolism of tryptophan was modulated in *Il10*$^{-/-}$ mice, indicated by increased urinary abundance of xanthurenic acid and decreased abundance of melatonin compared to C57BL/6J mice. These differences were observed from 9 weeks of age and remained significant until 12 weeks of age. Xanthurenic acid is a product of metabolism of tryptophan, whereupon tryptophan is metabolised to kynurenine as an intermediate molecule, yielding final products of niacin, CO_2, kynurenic acid and xanthurenic acid. In

Il10$^{-/-}$ mice, elevated levels of urinary xanthurenic acid are indicative of early stages of colitis [281, 309, 393], and linked to increased colonic *IDO1* gene activity. In the current study, *IDO1* was the gene with the largest increase in expression in the colon of *Il10*$^{-/-}$ mice with established colitis (vs. C57BL/6J mice). In antigen-presenting cells, the induction of *IDO1* gene expression has been suggested to suppress T cell responses towards immune tolerance, while in epithelial cells, *IDO1* gene expression may be induced to limit bacterial invasion in the small intestine and colon [366]. Furthermore, it has been shown that melatonin itself protects against oxidative DNA damage and stimulates its repair in colonocytes of UC patients [394] while reduced levels of melatonin were reported in plasma from UC patients [395], supporting the findings of the current study. Metabolism of tryptophan in relation to colitis is further discussed in Chapter 6.

3.5.4.2 Urine metabolomic profile in response to the EPA diet (vs. OA diet) irrespective of genotype

Several lysophospholipids (lysoPE and lysoPC) with varying chain lengths and degrees of saturation were detected in the urine of mice, and their abundance was affected by the EPA diet. Lysophospholipids are, in addition to free fatty acids, the result of enzymatic activity of PLA2 on regular phospholipids such as phosphatidylcholine, phosphatidylethanolamine, or phosphatidic acid [351, 396] and have previously been detected in urine [397, 398]. The results from the current study indicated the replacement of AA and other SCFA from membrane phospholipids with EPA in all mice, irrespective of genotype. This was attributed to a higher level of lysoPE(20:5n-3) in urine, but lower levels of other (non-EPA-containing) lysophospholipids, *e.g.* lysoPC(20:4), and lysoPEs 16:0, 18:1, 20:4, and 22:4n-6. The increased level of lysoPE(20:5n-3) was detected only two days after the initial feeding of dietary treatments, while decreases of lysophospholipids not containing EPA were detected two weeks thereafter, and remained decreased until 12 weeks of age. The incorporation of n-3 PUFA into phospholipids in response to n-3 PUFA-rich diets was also reported by others [399], where fish oil intervention increased plasma phospholipids containing LC n-3 PUFA in healthy subjects compared to a control diet after 3 weeks. Thus, the EPA diet may have resulted in a remodelling of the membrane phospholipid composition and may have affected signalling pathways in those mice [351].

Irrespective of genotype, the AA-derived metabolite LTF4 was increased in EPA-fed mice compared to those fed the OA diet, was one of the metabolites earliest to change and remained elevated until 12 weeks of age. As an AA-derived metabolite, urinary abundance of LTF4 was expected to be reduced in response to the EPA diet, or at least remain at the same level compared to mice fed the OA diet. It was however reported that LTF4 is a less potent mediator than its precursor leukotrienes (*e.g.* LTC4 and LTE4) [400], further supporting the influence of dietary EPA on lipid mediator synthesis.

3.5.4.3 Urine metabolomic profile in response to the EPA diet (vs. OA diet) in *Il10*$^{-/-}$ mice

The intake of the EPA diet (vs. OA diet) may have affected metabolism of tryptophan in *Il10*$^{-/-}$ mice with established colitis, indicated by increased urinary abundance of metabolites putatively identified as N-formylkynurenine and indole, but reduced abundance of xanthurenic acid. This study is the first to show these effects of dietary EPA on tryptophan metabolism associated with colitis. The reduction of xanthurenic acid may have been the result of lower levels of pro-inflammatory cytokines and decreased *IDO1* gene expression [401] and subsequently lowered production of xanthurenic acid. The transformation of indole from tryptophan in the colon is associated with the microbiota [402], rather than host metabolism, and may indicate changes in the microbial community profile in response to the EPA supplementation in *Il10*$^{-/-}$ mice (vs. OA diet), which has previously been reported [6].

In agreement with the literature [98, 243, 245, 354, 355], the EPA diet increased the abundance of metabolites putatively identified as anti-inflammatory and pro-resolving E-series resolvin (RvE1) and series-3 prostaglandin (PGE3, PGH3, or PGD3) and thromboxane (TXB3). Synthetic RvE1 (administered by intraperitoneal injection) has previously been shown to reduce leukocyte infiltration into the colon of mice with TNBS-induced colitis [403], but the current study is the first to link dietary EPA-induced changes in urinary lipid mediator abundance to reduced colitis in *Il10*$^{-/-}$ mice. Lipid mediators derived from AA mainly exert pro-inflammatory effects and an increased intake of LC n-3 PUFA is suggested to replace AA in immune cell membranes. After cleavage from the membrane by the enzyme PLA2, LC n-3 PUFA is substrate for anti-inflammatory and pro-resolving mediators. In a chronic inflammatory state such as IBD, these lipid mediators from LC n-3 PUFA may act as potent initiators and regulators of inflammatory

resolution in the colon of *Il10*$^{-/-}$ mice. A fish oil intervention in an adoptive transfer mouse model of colitis increased the abundance of colonic PGE3 and TXB3 after eight weeks [98]. Bosco *et al.* [98] further demonstrated that in the adoptive transfer mouse model of colitis, n-3 PUFA-derived lipid metabolites were between 10 to 100-fold lower than n-6 PUFA-derived counterparts in the colon, despite a higher intake of n-3 PUFA for eight weeks. The authors observed a lower amount of free AA in the colon, but concluded that this may not result in a reduction of AA-derived mediators. Thus, despite a higher intake of EPA, a decrease of colitis may not have been detectable in *Il10*$^{-/-}$ mice at 9 weeks of age.

3.6 Conclusion and outlook

The reported beneficial effects of a diet enriched with purified EPA on colitis were age-dependent in *Il10*$^{-/-}$ mice, and only observed at 12 weeks of age as assessed by colon histological analysis and colon transcriptomic profiling. The hypothesis that the transcriptional profile of PBMCs reflects the profile from colon was limited to *PPARG* signalling in *Il10*$^{-/-}$ mice with established colitis. However, PBMC gene expression did not reflect the molecular responses to the EPA diet observed in the inflamed colon, such as genes that regulate immune cell trafficking which were increased in expression in PBMCs when colitis was established. Urine may be a useful surrogate to monitor EPA-induced effects in *Il10*$^{-/-}$ mice, in particular tryptophan catabolites and lipid mediators. These findings provide knowledge that could support the evaluation of food such as EPA-rich salmon to determine if it reduces the risk of developing colitis.

Chapter 4

Dose-response of salmon-based diets on established colitis and associated colonic gene expression in the interleukin-10 gene-deficient mouse

4.1 Introduction

The immune-modulatory properties of the LC n-3 PUFA EPA, DHA and DPA may be able to mitigate the course of IBD, a disorder characterised by chronic inflammation of the GIT, including the colon (colitis). In humans, foods containing LC n-3 PUFA may be an option to reduce the risk of IBD development. Using a food frequency questionnaire, it was shown that salmon was perceived to be one of the most beneficial foods for New Zealand IBD patients to alleviate disease symptoms [9]. Dietary intervention studies among IBD patients showed that the weekly intake of two portions of salmon reduced a systemic inflammation marker in serum and disease activity, and may have promoted an anti-inflammatory phenotype by increasing the plasma n-3/n-6 ratio in patients [146, 161]. No study has reported the effects of dietary salmon on metabolic pathways such as those linked to tryptophan or fatty acids during colitis that may be linked to activation of PPARs as shown by a diet containing purified EPA in Chapter 3 and other published studies [3, 6, 250, 251, 347].

Immune-modulatory properties of pure LC n-3 PUFA may function differently when in a food matrix. Bioavailability of LC n-3 PUFA may be higher when consumed as a part of fish compared to PUFA supplements [204, 205], as the ingestion of whole foods is followed by more efficient digestion and absorption in the small intestine. Salmon also contains amino acids (*e.g.* taurine, arginine and glutamine) and micronutrients (iron, selenium, and vitamins C, D and E) and these may potentially induce synergistic effects in combination with other nutrients such as LC n-3 PUFA [184, 185]. Several of these micronutrients, for example vitamin D [166], calcium [166], selenium [167] and vitamin E [170] have been reported to suppress inflammation in rodents with experimental colitis.

Evidence of the effects of n-3 PUFA on colitis is inconsistent, with some studies showing detrimental effects [193, 194], while others reported a positive response and reduced colitis [5-7, 195-197, 404]. It has been suggested that the level of n-3 PUFA may explain some of the inconsistent evidence. Trebble *et al.* [198] demonstrated that the production of the pro-inflammatory cytokines TNF and IL6 by PBMCs after LPS stimulation followed a "U-shaped" dose-response during a supplementation study of DHA and EPA in the form of fish oil in healthy humans. Decreased TNF and IL6 production by PBMCs were observed at the lowest supplementation level (0.3 g n-3

PUFA per day). A maximum inhibition was observed at intermediate levels (1.0 g n-3 PUFA per day), but the least inhibition was seen at the highest supplementation levels (2.0 g n-3 PUFA per day). It was suggested that the molecular mechanisms by which n-3 PUFA influences cell function (*i.e.* altered eicosanoid synthesis, signal transduction or gene expression) could have maximum effects at different levels of n-3 PUFA and the combined effects could produce this "U-shaped" dose-response curve [198]. As these observations were made for LC n-3 PUFA extracts, it remains to be determined whether foods containing LC n-3 PUFA, such as salmon, show similar effects on colitis.

4.2 Hypothesis and aim

The hypothesis of this study was that salmon-based diets reduce colitis and affect the expression of genes in metabolic pathways such as fatty acid metabolism, xenobiotic metabolism, tryptophan metabolism and *PPAR* signalling in the colon in a dose-dependent manner. To test this hypothesis, *Il10*$^{-/-}$ and C57BL/6J mice were fed one of seven AIN-76A-based diets from five weeks of age: unmodified, supplemented with controlled amounts (15%, 30% and 45%) of lyophilised Chinook salmon fillets (*Oncorhynchus tshawytscha*) or modified to match the salmon diets in macronutrient composition. The unmodified AIN-76A diet enabled comparison between previously published studies using the *Il10*$^{-/-}$ mouse model and this study. The effects of the salmon-enriched diets on the severity of colitis and colon gene expression were compared to the matched control diets at 12 weeks of age.

4.3 Methods

A total of 56 male *Il10*$^{-/-}$ mice (C57BL/6J background, formal designation B6.129P2-Il10^{tm1Cgn}/J) and 56 male C57BL/6J control mice were sourced from Jackson Laboratory (Maine, USA) at 4 to 5 weeks of age. Mice received a bacterial inoculation five days after arrival (mean age 5.5 weeks). A graphical illustration of the experimental design applied in this study is shown in Figure 4.1.

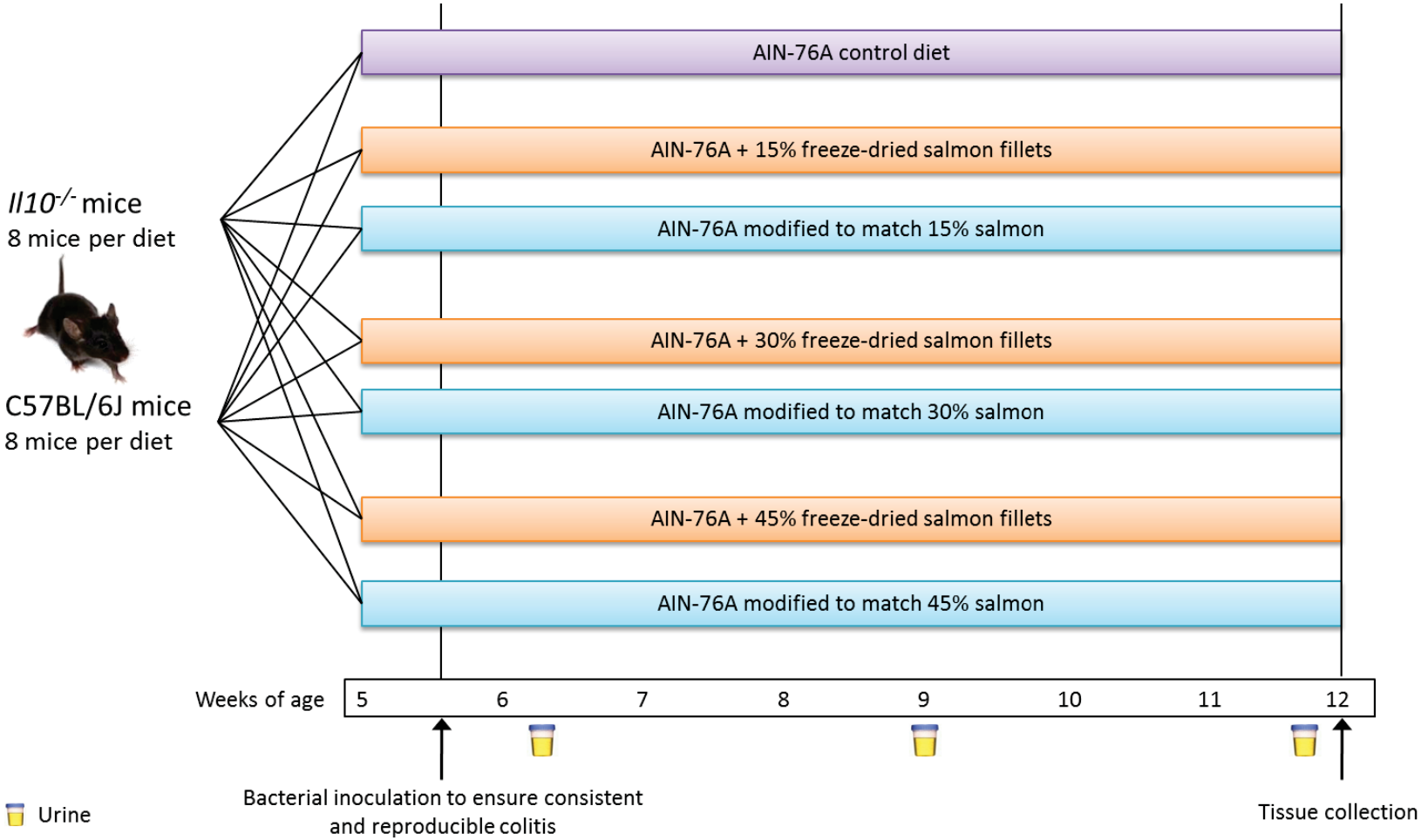

Figure 4.1 Design for the "salmon diet experiment". 4-5-week-old *Il10*$^{-/-}$ mice (n=56) and C57BL/6J mice (n=56) were assigned to AIN-76A diets, either unmodified, enriched with lyophilised salmon fillets (15%, 30% and 45% by dry weight), or modified to match the corresponding salmon diet in macronutrient composition. Urine was collected at 6.2, 9 and 11.5 weeks of age (urine results are presented in Chapter 5). Mice received a bacterial inoculation at 5.5 weeks of age and were euthanised at 12 weeks of age [116, 290].

Eight *Il10*$^{-/-}$ and eight C57BL/6J mice were randomly assigned to the following diets: (i) unmodified AIN-76A; (ii) basal AIN-76A with 15% lyophilised salmon fillets; (iii) modified AIN-76A to match the 15% salmon diet; (iv) basal AIN-76A with 30% lyophilised salmon fillets; (v) modified AIN-76A to match the 30% salmon diet; (vi) basal AIN-76A with 45% lyophilised salmon fillets; and (vii) modified AIN-76A to match the 45% salmon diet. Diet preparation is described in Section 2.3.3. Mice were euthanised and samples collected at 12 weeks of age. An early sample collection time-point at 9 weeks of age was not included in this study, due to the lack of effects observed by the EPA-enriched diet in *Il10*$^{-/-}$ mice at this early stage of colitis (shown in Chapter 3). A detailed description of the histological assessment is included in Section 2.4 and colon gene expression analysis[10] in Sections 2.6 and 2.7.

4.4 Results

4.4.1 Experimental diet composition

The nutritional analysis of experimental diets is given in Table 4.1. As anticipated, the lowest amount of LC n-3 PUFA was detected in the 15% salmon diet, with similar amounts of EPA and DHA (approximately 0.5% each per 100 g diet). The 30% salmon diet provided intermediate amounts of LC n-3 PUFA, with approximately 1% of each, EPA and DHA. The 45% salmon diet provided the highest levels of LC n-3 PUFA. DPA ranged from approximately 0.2% to 0.5% in the salmon diets. Levels of EPA, DHA and DPA were below the detection limit for all of the AIN-76A-based control diets. The n-6 PUFA AA was highest in the 45% salmon diet, followed by the 30% salmon diet and lowest levels in the 15% salmon diet (0.13% to 0.05% (Table 4.1)). AA was below the detection limit for the AIN-76A-based control diets. The resulting n-3/n-6 ratio was 1.6 in the 15% salmon diet, 1.8 in the 30% salmon diet and 1.7 in the 45% salmon diet (Table 4.1).

[10] Microarray analysis was performed using 500 ng RNA obtained from six biological replicates per treatment group. One microarray slide was removed prior to analysis due to an error in the feature extraction, which contained one *Il10*$^{-/-}$ mouse fed the 30% salmon diet. qPCR was performed as described in Appendix XI and confirmed the expression of selected genes.

Table 4.1 Nutritional composition of diets salmon and control diets. Lyophilised salmon fillets were incorporated at 15%, 30% and 45% by dry weight into a basal AIN-76A diet. The 15%, 30% and 45% control diets were based on the AIN-76A formulation and modified to match the corresponding salmon diet in macronutrient composition. Components shown as % (*w/w*) of diet.

	AIN-76A	*15%*		*30%*		*45%*	
		Control	*Salmon*	*Control*	*Salmon*	*Control*	*Salmon*
Component (%)							
Protein	17.9	19.0	18.8	19.5	20.6	21.6	22.9
Carbohydrates	69.8	65.3	62.9	53.8	50.5	42.9	40.8
Fat	6.3	9.4	10.2	17.1	17.0	25.8	24.9
Polyunsaturated	3.61	5.46	2.96	9.94	4.92	15.06	6.80
Omega-3	0.05	0.08	1.51	0.15	2.70	0.22	3.62
ALA	0.05	0.08	0.11	0.14	0.19	0.22	0.29
EPA	<0.05	<0.05	0.54	<0.05	0.96	<0.05	1.31
DHA	<0.05	<0.05	0.51	<0.05	0.95	<0.05	1.14
DPA	<0.05	<0.05	0.19	<0.05	0.32	<0.05	0.47
Omega-6	3.33	5.08	0.96	9.32	1.47	14.13	2.19
AA	<0.05	<0.05	0.05	<0.05	0.10	<0.05	0.13
LA	3.33	5.08	0.81	9.32	1.22	14.13	1.84
GLA	<0.05	<0.05	<0.05	<0.05	<0.05	<0.05	0.06
Monounsaturated	1.82	2.67	4.57	4.84	7.57	7.26	11.38
OA	1.61	2.40	2.99	4.42	4.96	6.66	7.57
Palmitoleic	<0.05	<0.05	0.71	<0.05	1.22	<0.05	1.84
Saturated	0.87	1.27	2.55	2.31	4.29	3.48	6.43
Palmitic	0.66	0.97	1.59	1.78	2.65	2.71	3.97
Stearic	0.11	0.15	0.42	0.28	0.67	0.42	1.00
Energy (kJ/100g)	1720	1780	1770	1880	1840	2050	2000
n-3/n-6 ratio	0.02	0.02	1.6	0.02	1.8	0.02	1.7
Oxidation							
Peroxide (meq O_2/kg fat)	<0.1	<0.1	6.2	2.6	2.4	1.3	1.2
p-Anisidine	78	13.6	420.2	9.9	23.8	12.4	3.9

AA: Arachidonic acid; ALA: Alpha-linolenic acid; DHA: Docosahexaenoic acid; DPA: Docosapentaenoic acid; EPA: Eicosapentaenoic acid; GLA: Gamma-linolenic acid; LA: Linoleic acid; OA: Oleic acid.

The oxidation state of the lyophilised salmon and AIN-76A-based control diets were evaluated using the peroxide test for primary oxidation products, and the p-anisidine test for secondary oxidation products [405]. Peroxide values below 10 and p-anisidine values below 30 are recommended for foods safe for human consumption [405]. The oxidation state of the lyophilised salmon indicated no oxidation prior to diet preparation (peroxide value = 1.3 meq O_2/kg fat and p-anisidine value = 9.1 (Appendix I)). In the salmon diets, the peroxide value decreased with increasing amounts of salmon (15% salmon, 30% salmon and 45% salmon: 6.2, 2.4 and 1.2 meq O_2/kg fat, respectively (Table 4.1)). This was also observed for secondary oxidation products, with highest values in the 15% salmon diet (420 units), followed by 30% salmon and 45% salmon (both < 25 units). No oxidation was measured in the matched control diets, with levels of primary oxidation below 5 meq O_2/kg fat and secondary oxidation below 15 units in each diet (Table 4.1). In the AIN-76A diet, primary oxidation products were not detected (< 0.1 meq O_2/kg fat) but secondary oxidation products were above the recommended value with 78 units (Table 4.1).

4.4.2 Growth performance

Food intake and body weight data are shown in Table 4.2 and Figure 4.2. There was no effect of genotype (*Il10*$^{-/-}$ compared to C57BL/6J) on food intake ($P > 0.1$), therefore *Il10*$^{-/-}$ and C57BL/6J mice were not separated for analysis of dietary intake. Dietary intake was not affected by the experimental duration of seven weeks ($P > 0.1$). With increasing amounts of fat in the diet, mean intakes were reduced ($P < 0.001$). Salmon-fed mice had a higher average intake ($P < 0.001$) than mice on the corresponding control diets. Mean body weights increased over time for all treatments (Figure 4.2). Salmon-fed mice were heavier than mice on corresponding control diets ($P = 0.01$) and C57BL/6J mice tended to have higher mean body weight than *Il10*$^{-/-}$ mice ($P = 0.08$). As the amount of fat provided from the diets increased, mean body weight increased ($P = 0.008$).

Table 4.2 Analysis of growth performance for "salmon diet experiment". The dietary intake for *Il10*$^{-/-}$ and C57BL/6J mice was similar and therefore not separated for analysis. Food intake was measured daily and values shown in grams (g) per day. Significance was evaluated between a salmon diet and its corresponding control diet, with (*) indicating p-values lower than 0.05 and considered significant, and (#) indicating p-values between 0.1 and 0.05. Data shown as means estimated from the repeated measures analysis and represent eight biological replicates per treatment group.

Food intake (g per day)				*Body weight (g)*					
Diet		*Il10*$^{-/-}$ *and C57BL/6J*	*P-value*	*Diet*		*C57BL/6J*	*P-value*	*Il10*$^{-/-}$	*P-value*
15%	Control	2.87	0.07$^{\#}$	15%	Control	20.77	0.05*	21.22	0.93
	Salmon	2.99			Salmon	22.97		22.00	
30%	Control	2.70	0.02*	30%	Control	22.37	0.81	22.00	1.00
	Salmon	2.85			Salmon	23.32		22.28	
45%	Control	2.55	0.09$^{\#}$	45%	Control	23.13	0.97	22.46	1.00
	Salmon	2.67			Salmon	23.73		22.79	
	LSD (5%)	0.11			LSD (5%)	1.62			

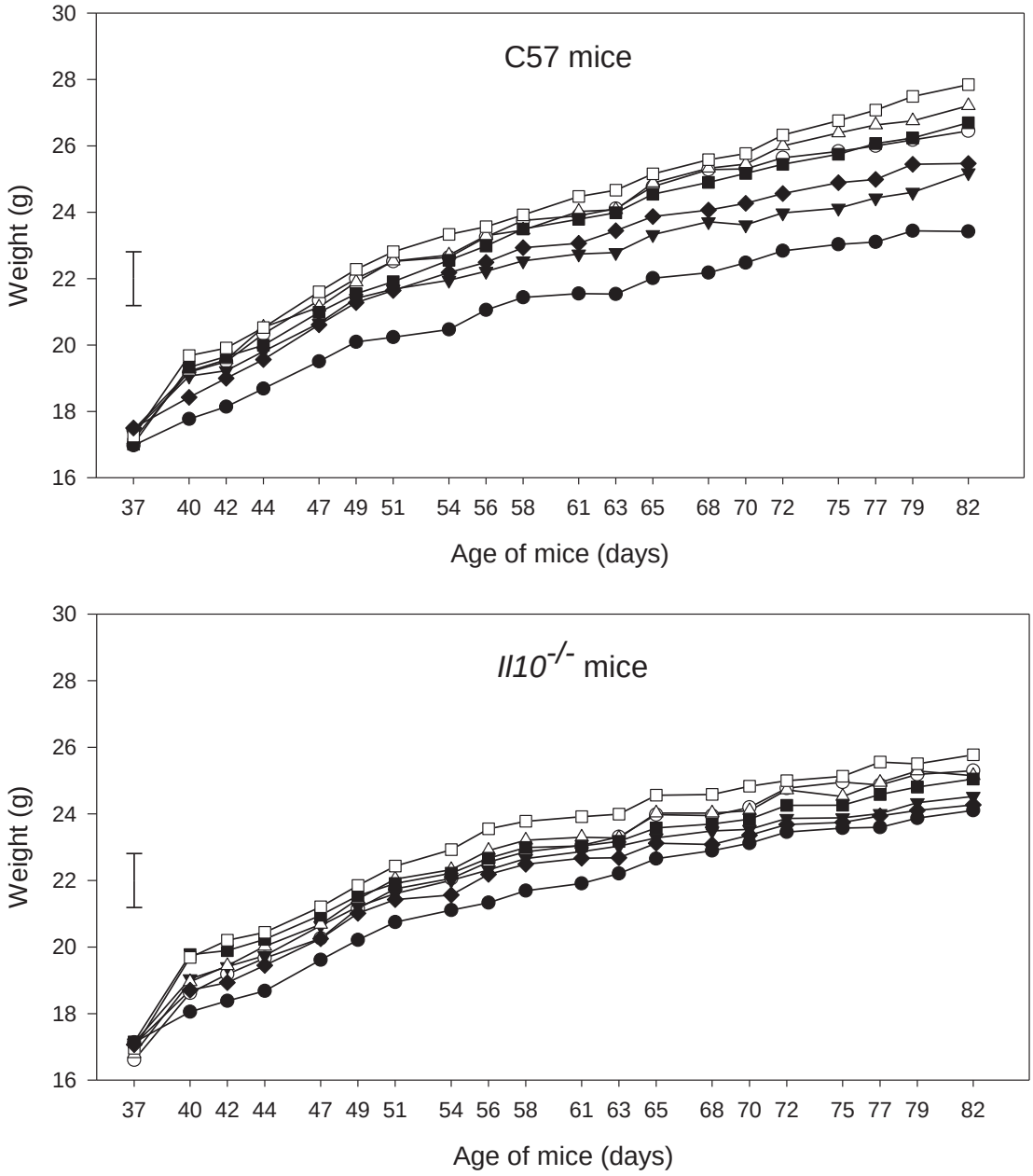

Figure 4.2 Mean body weights (g) for *Il10*$^{-/-}$ and C57BL/6J mice over the experimental period. The first measurement was taken on the second day after arrival, when the average age of mice was 37 days and fed standard chow. Mice were assigned to treatment groups on the same day and body weight was measured three times weekly thereafter. The final body weight was measured before a fast-feed period. Data represent eight biological replicates per group. Error bar indicates 5% LSD level.
● = 15% control diet; ○ = 15% salmon diet; ▼ = 30% control diet; △ = 30% salmon diet; ■ = 45% control diet; □ = 45% salmon diet; ◆ = AIN-76A diet.

4.4.3 Severity of intestinal inflammation

No signs of inflammation were observed in the small intestinal sections (duodenum, ileum and jejunum) within *Il10*$^{-/-}$ or C57BL/6J mice on all diets. On average, C57BL/6J mice showed normal intestinal morphology. In the caecum and colon, the mean HIS in *Il10*$^{-/-}$ mice was higher ($P < 0.001$) compared to C57BL/6J mice and this effect was independent of the type of diet. The greatest histopathological changes (highest mean HIS) were observed in the caecum of *Il10*$^{-/-}$ mice, followed by the colon with the second highest total HIS. Colitis in *Il10*$^{-/-}$ mice was characterised by infiltration of inflammatory cells, especially lymphocytes and plasma cells (Figure 4.3 D and E), goblet cells loss (Figure 4.3 B, D and E), and crypt hyperplasia and aberrancy (Figure 4.3 D and E). Appendix X shows the HIS in all intestinal sections of *Il10*$^{-/-}$ and C57BL/6J mice across salmon and control diets.

Within *Il10*$^{-/-}$ mice, the 15% and 45% salmon diets had no effect on mean colon HIS compared to *Il10*$^{-/-}$ mice fed their respective control diets (mean colon HIS = 12.1/10.6 for 15% salmon/15% control diets, and 15.6/14.6 for 45% salmon/45% control diets, respectively ($P > 0.1$)). No differences in the individual histopathological features were observed in the colon of *Il10*$^{-/-}$ mice fed the 15% and 45% salmon diet compared to the corresponding control diets (data not shown). *Il10*$^{-/-}$ mice fed the 30% salmon diet showed reduced colitis compared to *Il10*$^{-/-}$ mice fed the 30% control diet (mean colon HIS = 10.8 and 17.1, respectively ($P = 0.03$)). Figure 4.4 illustrates the individual histological features of *Il10*$^{-/-}$ mice fed 30% salmon and 30% control diets. Compared to *Il10*$^{-/-}$ mice fed the 30% control diet, those fed the 30% salmon diet were less affected by crypt loss, goblet cell loss and infiltration of lymphocyte/plasma cells into colon tissue (all $P \leq 0.05$). Crypt hyperplasia and crypt aberrancy tended to be reduced in 30% salmon-fed *Il10*$^{-/-}$ mice ($P = 0.08$) and numbers of lymphoidal aggregates increased ($P = 0.06$) compared to those fed the 30% control diet.

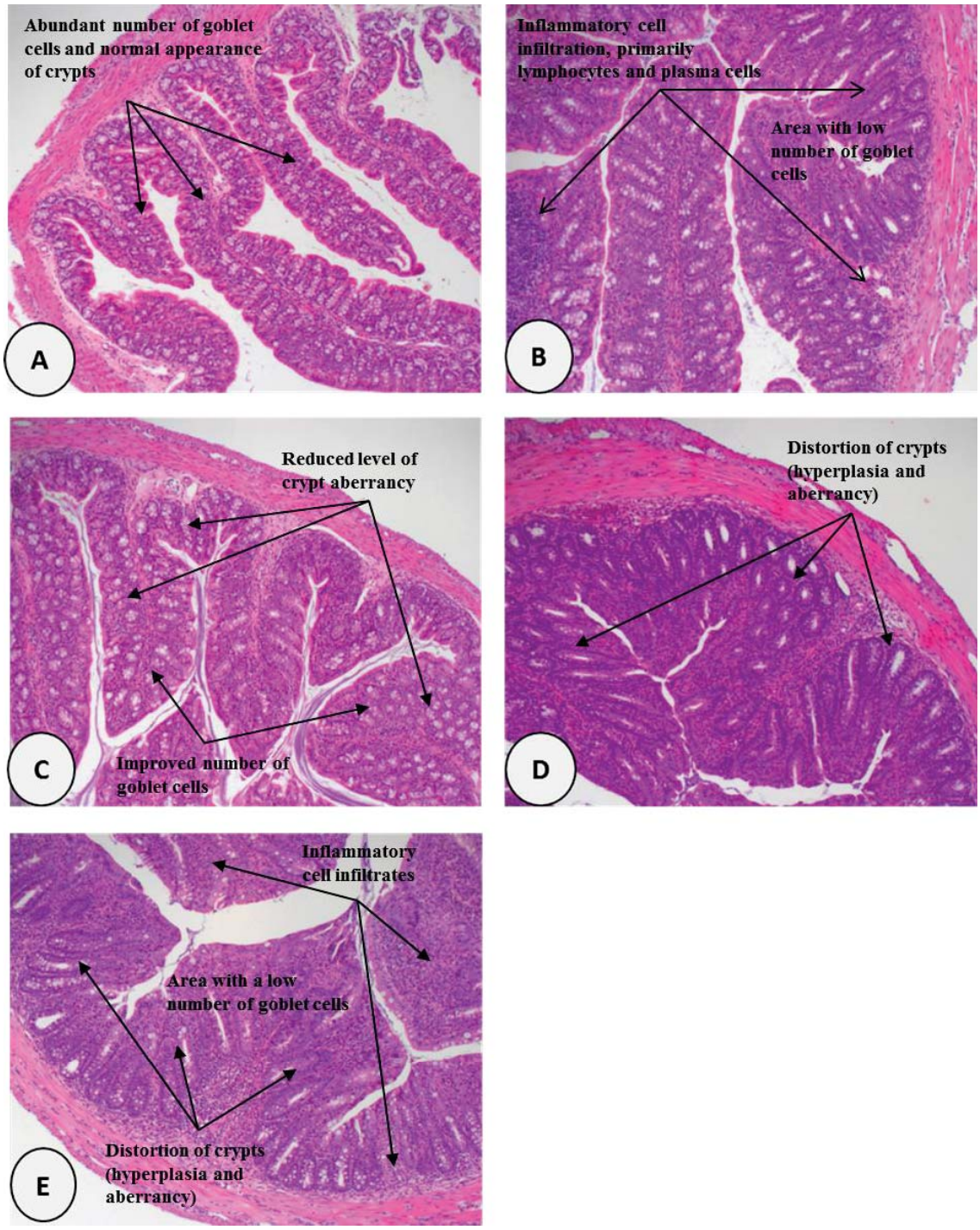

Figure 4.3 Representative images of colon sections stained with haematoxylin and eosin (×100 magnification). (A) C57BL/6J mouse fed a 30% salmon diet: non-inflamed tissue with abundant goblet cells and normal appearance of colonic crypts; (B) *Il10*$^{-/-}$ mouse fed an AIN-76A control diet: sample indicates goblet cell loss but inflammatory cells, especially lymphocytes and plasma cells, are elevated; (C) *Il10*$^{-/-}$ mouse fed a 30% salmon diet, showing lower signs of colitis; goblet cells are higher in number and crypt aberrancy reduced; (D) *Il10*$^{-/-}$ mouse fed a 30% control diet: sample shows colonic crypt hyperplasia and aberrancy; goblet cells are lower in number but inflammatory cells, especially lymphocytes and plasma cells, are elevated. (E) *Il10*$^{-/-}$ mice fed a 15% salmon diet: sample indicates a high infiltration of inflammatory cells and loss of goblet cells with crypt aberrancy and hyperplasia.

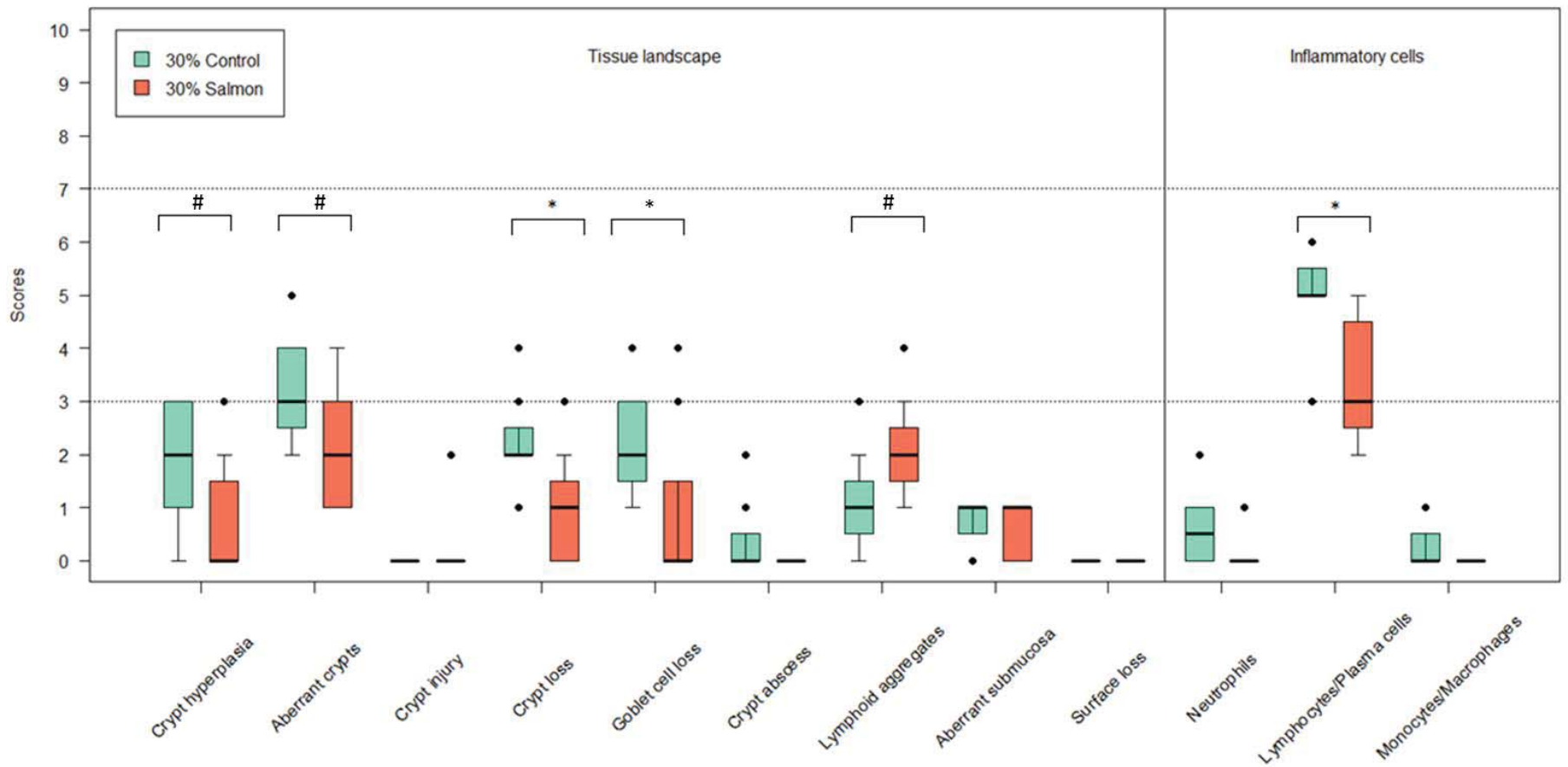

Figure 4.4 Scores of individual histological features in colon tissue of *Il10*$^{-/-}$ mice fed the 30% salmon diet and 30% control diet. The individual features in tissue landscape and inflammatory cell infiltration were scored from 0 (no change from normal tissue) to 10 (extreme changes). The boxplots were created in R, and statistical significance within each feature was calculated using the Wilcoxon test from the EMA package in R. (*) indicates significance $P < 0.05$; and (#) indicates a trend ($P < 0.1$). Data represent eight biological replicates per treatment group.

4.4.4 Colon gene expression

Microarray analysis was carried out to show changes in the transcriptomic profile in the colon of *Il10*$^{-/-}$ mice compared to that of C57BL/6J mice and in response to varying levels of dietary salmon (15%, 30% or 45%). Table 4.3 provides an overview of the total number of differentially expressed genes in the different comparisons (FC ≥ |1.5| and p-value ≤ 0.005). The highest number of differentially expressed genes was between *Il10*$^{-/-}$ mice and C57BL/6J mice, both fed the 30% control diet. This was followed by the comparison of *Il10*$^{-/-}$ mice compared to C57BL/6J mice, both fed the 45% salmon diet, then the 15% salmon diet and AIN-76A diet (Table 4.3). Both the 15% salmon diet and the 45% salmon diet had greater influences on colon gene expression within C57BL/6J mice (compared to those fed the corresponding control diets), than within *Il10*$^{-/-}$ mice (compared to those fed the respective control diets). The 45% salmon diet only had a limited effect on gene expression in *Il10*$^{-/-}$ mice when compared to those fed the 45% control diet (15 genes differentially expressed).

4.4.4.1 Colon gene expression between mouse genotypes fed the AIN-76A diet

2063 genes were differentially expressed between *Il10*$^{-/-}$ and C57BL/6J mice fed the AIN-76A diet. Of these, the mRNA levels of 1124 genes were decreased (FC ≤ -1.5) and 939 mRNA transcript levels increased (FC ≥ 1.5 and P ≤ 0.005). Pathway analysis was performed after reducing the number of genes < 1000 by increasing the stringency as stated in Table 4.3. Among the genes with the largest fold-changes were those regulating immune responses, for example, regenerating islet-derived 3 beta (*REG3B*), ubiquitin D (*UBD*), S100 calcium binding proteins A8 and A9 (*S100A8* and *S100A9*), chemokine (C-X-C motif) ligands 6, 9, and 10 (*CXCL6*, *CXCL9* and *CXCL10*). The expression of these genes were increased in *Il10*$^{-/-}$ mice compared to C57BL/6J mice with FC ranging from approximately 10 to 21, indicating that the *Il10*$^{-/-}$ mouse model performed as expected.

Table 4.3 Numbers of differentially expressed genes in the colon of C57BL/6J and *Il10*$^{-/-}$ mice. Genes passing a fold-change (≥ |1.5|) and p-value (≤ 0.005) cut-off were considered differentially expressed. Data represent six biological replicates per group, with the exception of *Il10*$^{-/-}$ mice fed the 30% salmon diet where n = 5.

Contrast	*mRNA transcript levels*[1]		*Uploaded into Ingenuity Pathway Analysis*
	Decreased	*Increased*	*Analysis-ready molecules*[2]
Genotype comparison (Il10$^{-/-}$ *relative to C57 mice)*			
AIN-76A	1124	939	902 (FC 1.6 and p-value 0.001)
15% Control	320	207	526
30% Control	1568	1956	968 (FC 2 and p-value 0.001)
45% Control	554	870	969
15% Salmon	668	1739	959 (FC 1.6 and p-value 0.001)
30% Salmon	74	305	252
45% Salmon	1076	1613	911 (FC 1.7 and p-value 0.001)
Diet comparison (Salmon relative to control diet)			
C57BL/6J mice			
15% Salmon vs. 15% Control	493	118	484
30% Salmon vs. 30% Control	90	64	134
45% Salmon vs. 45% Control	159	224	295
Il10$^{-/-}$ mice			
15% Salmon vs. 15% Control	87	203	202
30% Salmon vs. 30% Control	177	131	235
45% Salmon vs. 45% Control	8	7	13

(1) FC ≥ |1.5| and p-value ≤ 0.005; genes may be represented with more than one probe on the array; (2) Reducing genes to 1000 genes for pathway analysis by applying more stringent FC and p-value as recommended in the IPA handbook.

The ten highest p-value-ranked biological functions associated with the differentially expressed genes are listed in Table 4.4. These functions were mostly related to cells, blood cells or leukocytes, with the functions predicted to be increased in activity (*activation z-scores* ≥ 2). The predictions for these ten functions were based on 386 unique genes. Merging the genes into a biological interaction network (not shown due to the large number of genes) identified four central genes that connected many of the differentially expressed genes. These were the transcription regulators V-myc avian myelocytomatosis viral oncogene homolog (*MYC*), nuclear factor of kappa light polypeptide gene enhancer in B-cells inhibitor alpha (*NFKBIA*), *CEBPD*, and Signal transducer and activator of transcription 1 (*STAT1*). The mRNA levels of these transcription regulators were increased by approximately 2-3-fold in *Il10*$^{-/-}$ mice fed the AIN-76A diet compared to C57BL/6J mice fed the same diet, indicating important roles in the regulation of the immune response in the colon of *Il10*$^{-/-}$ mice.

In *Il10*$^{-/-}$ mice fed the AIN-76A diet, sets of genes comprising 69 KEGG pathways were significantly affected compared to C57BL/6J mice fed the same diet ($P \leq 0.01$ (Figure 4.5)). Of these, 32 gene sets were decreased and 37 increased in expression, with most of the gene sets associated with biological processes in *Organismal systems*, *Metabolism*, *Human diseases*, and *Environmental information processing* (Figure 4.5).

The enhanced gene sets in the colon of *Il10*$^{-/-}$ mice were mostly immune-related (versus C57BL/6J mice both fed the AIN-76A diet), supporting the findings from IPA. KEGG pathways in *Immune system* were increased, for example the pathways *Antigen processing and presentation* (60% genes increased) and *T cell receptor signalling pathway* (31% genes increased) (Figure 4.5). Furthermore, signalling pathways against bacteria and other pathogens were increased, for example, *Intestinal immune network for IgA production* (58% genes increased), *NOD-like receptor signalling pathway* (30% genes increased) and *Toll-like receptor signalling pathway* (37% genes increased) (all $P < 0.001$). Further pathways that were increased in the colon of *Il10*$^{-/-}$ mice fed the AIN-76A diet compared to C57BL/6J mice were those associated with *Signal transduction* and *Signalling molecules and interaction* (*e.g. Cell adhesion molecules (CAMs)*, *Jak-STAT signalling pathway*, and *Cytokine-cytokine receptor interaction*) which are important for immune-related signalling pathways (Figure 4.5).

Table 4.4 Most significantly affected biological functions in the colon of *Il10*$^{-/-}$ mice relative to C57BL/6J mice (both fed the AIN-76A diet). Functions with an *activation z-score* < |2| were excluded and biological functions limited to show the ten highest p-value-ranked functions. "# genes" indicates the number of genes associated with the biological function and individual genes may be represented in more than one function. Data represent six biological replicates per group.

Functions annotation		*P-value*	*# genes*	*Predicted activation state (activation z-score)*	*Category*
Cells	Activation	1.22E-26	144	Increased (+3.4)	5
	Movement	6.37E-25	236	Increased (+2.1)	13
	Migration	5.37E-23	214	Increased (+2.3)	13
Blood cells	Quantity	5.09E-26	156	Increased (+2.7)	2, 3
Leukocytes	Activation	1.51E-23	109	Increased (+4.1)	2, 5, 6, 7
	Movement	1.48E-25	124	Increased (+3.4)	2, 6, 13
	Migration	3.75E-27	139	Increased (+3.7)	6, 13
	Quantity	7.81E-29	149	Increased (+2.5)	2, 3
Infection of mammalia		1.31E-22	74	Decreased (-5.1)	14
Glucose metabolism disorder		1.50E-31	117	Increased (+3.1)	12

Categories: 1 Cellular Function and Maintenance; 2 Hematological System Development and Function; 3 Tissue Morphology; 4 Cellular Growth and Proliferation; 5 Cell-To-Cell Signalling and Interaction; 6 Immune Cell Trafficking; 7 Inflammatory Response; 8 Cell-mediated Immune Response; 9 Cellular Development; 10 Hematopoiesis; 11 Lymphoid Tissue Structure and Development; 12 Metabolic Disease; 13 Cellular Movement; 14 Infectious Disease; 15 Tissue Development; 16 Cell Morphology; 17 Cell Death and Survival; 18 Cellular Compromise.

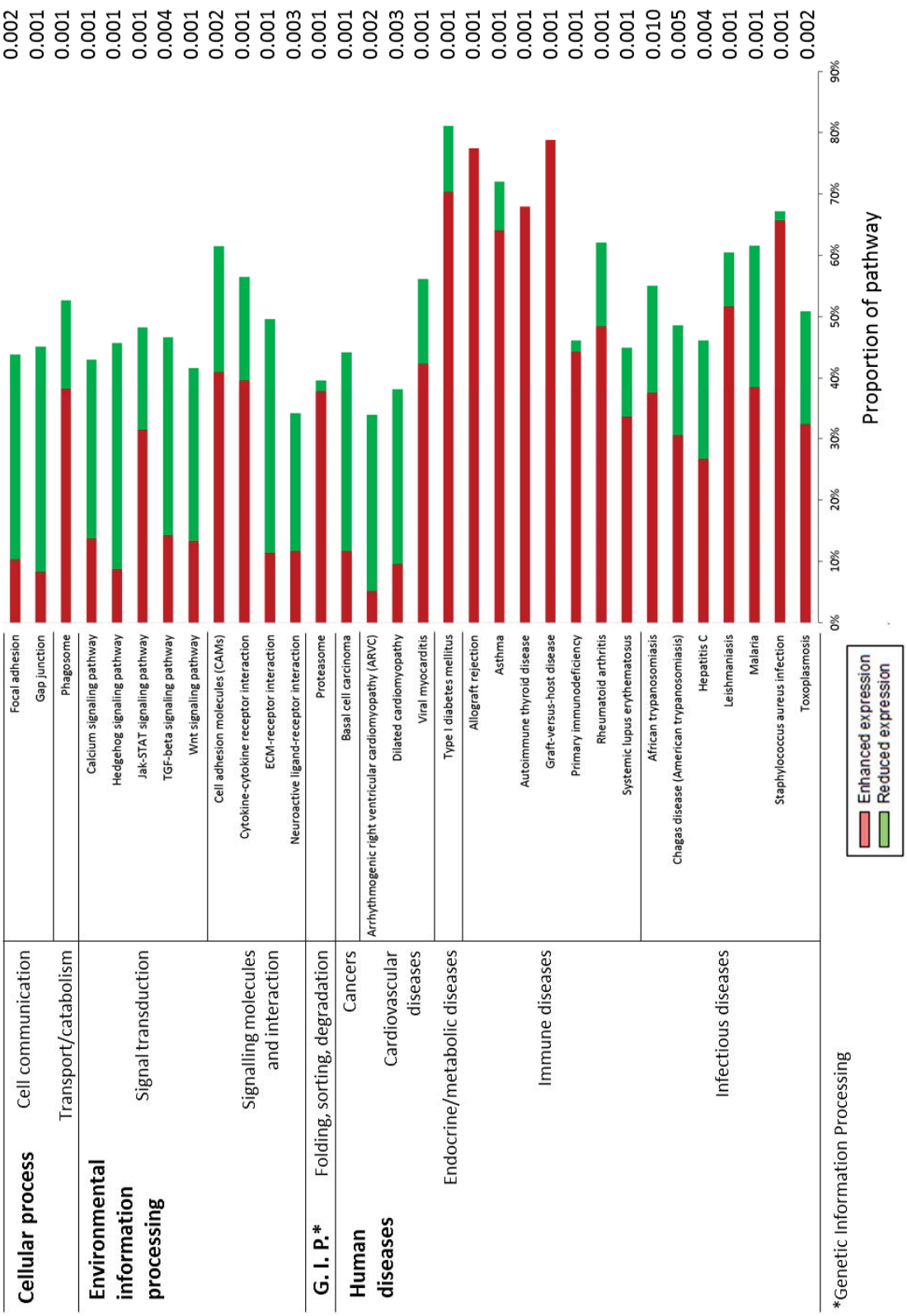

Figure 4.5 KEGG pathway gene sets affected in the colon of *Il10*$^{-/-}$ mice compared to C57BL/6J mice (both fed the AIN-76A diet) ($P < 0.01$). Bars indicate the proportion of the KEGG pathway affected (%): red bars are the proportion of genes contributing to an increased KEGG pathway and green bars are the proportion of genes contributing to a decreased KEGG pathway. Significance of changes in KEGG pathway expression was determined by GSEA using rotation gene set testing (ROAST function) in R. The p-value significance is indicated by numbers next to bars. Data represent six biological replicates per treatment group.

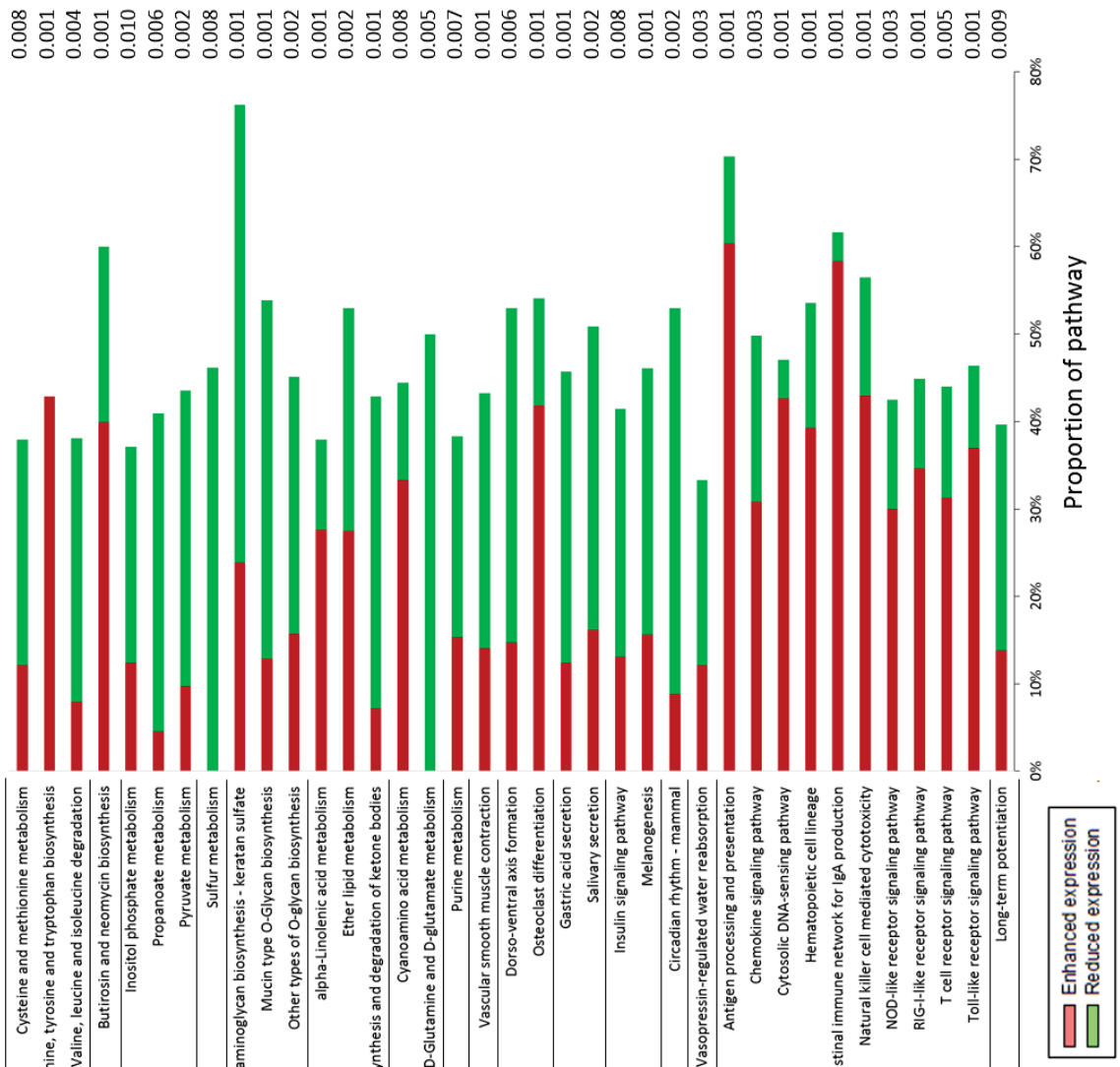

Figure 4.5 continued.

A general decrease in expression of KEGG pathways related to *Metabolism* was observed in *Il10*$^{-/-}$ mice compared to C57BL/6J mice fed the AIN-76A diet (Figure 4.5). In *Il10*$^{-/-}$ mice, decreased expressions of genes in the metabolism of, for example, amino acids, carbohydrates, and lipids were observed compared to C57BL/6J mice fed the AIN-76A diet, indicating an effect on metabolic gene expression in *Il10*$^{-/-}$ mice with established colitis.

4.4.4.2 Colon gene expression in mice fed the 15% salmon and 15% control diets

In the treatment groups that were fed the 15% diets, the highest number of differentially expressed genes were observed in *Il10*$^{-/-}$ mice fed the 15% salmon diet compared to C57BL/6J mice on the same diet (approximately 2400 genes with ~70% genes showing increased expression (Table 4.3)). 527 genes were changed in expression in *Il10*$^{-/-}$ versus C57BL/6J mice fed the 15% control diet (320 genes decreased and 207 genes increased). Changes in gene expression modulated by the intake of the 15% salmon diet (compared to those fed the 15% control diet) were more pronounced within C57BL/6J mice (611 genes, mostly decreased in expression) than within *Il10*$^{-/-}$ mice (290 genes, mostly increased in expression).

4.4.4.2.1 Colon gene expression between mouse genotypes fed the 15% control diet

Among the genes with the largest FC in *Il10*$^{-/-}$ mice (versus C57BL/6J mice) were the genes *CXCL9*, major histocompatibility complex, class II, DM alpha and beta (*HLA-DMA* and *HLA-DMB*), and histocompatibility 2, class II antigen A, alpha (*HLA-DQA1*), and *UBD*. These genes showed higher expression in *Il10*$^{-/-}$ mice compared to C57BL/6J mice regardless of whether mice were fed 15% control or 15% salmon diets (data not shown).

The ten highest p-value-ranked biological functions associated with the differentially expressed genes between *Il10*$^{-/-}$ mice and C57BL/6J mice fed the 15% control diet are listed in Table 4.5. These functions were mostly associated with blood cells and more specifically with the morphology of leukocytes and T lymphocytes, with functions predicted to be decreased in activation state (*activation z-score* $\leq$ -2). Several genes which were associated with the activation of leukocytes were increased in *Il10*$^{-/-}$ mice compared to C57BL/6J mice (both fed the 15% control diet), with an *activation z-score* of +2.2 (Table 4.5). Merging the 93 unique genes that were associated

with these ten functions into a biological interaction network (not shown due to the large number of genes) identified four central genes that connected many of the differentially expressed genes. These were the transcription regulator *NOTCH1*, *MMP9*, nitric oxide synthase 2 inducible (*NOS2*), and *IL10*. The mRNA expression levels of these genes were increased, indicating important roles in the regulation of the immune response in the colon of *Il10*$^{-/-}$ mice fed the 15% control diet (FC = 1.7-2.9 vs. C57BL/6J mice). The expression of three of four central genes (*NOTCH1*, *NOS2*, and *IL10*) was also increased in *Il10*$^{-/-}$ mice compared to C57BL/6J when mice were fed 15% salmon diets (approximately 4.5-fold). *MMP9* was not differentially expressed when *Il10*$^{-/-}$ mice were fed the 15% salmon diet compared to C57BL/6J mice on the same diet, indicating a complex interaction of this gene.

In *Il10*$^{-/-}$ mice fed the 15% control diet, sets of genes comprising 26 KEGG pathways were significantly affected compared to C57BL/6J mice on the same diet ($P < 0.01$ (Figure 4.6)). Of these, ten gene sets were decreased and 16 increased in expression, with most of the gene sets associated with biological processes in *Human diseases*, *Metabolism*, *Organismal systems*, and *Genetic information processing* (Figure 4.6). The enhanced gene sets were mostly immune-related, supporting the findings from IPA. For example, increases were observed in KEGG pathways in *Immune system* and *Immune diseases*, such as *Antigen processing and presentation*, *Allograft rejection*, and *Graft-versus-host disease* (more than 50% genes increased in each pathway ($P < 0.01$)). Further increases were observed in KEGG pathways related to *Genetic information processing* in *Il10*$^{-/-}$ mice compared to C57BL/6J mice both fed the 15% control diet (Figure 4.6). These were specifically genes in *Replication and repair* (*DNA replication* and *Mismatch repair*), and *Folding, sorting and degradation* (*Proteasome*).

A further three gene sets were linked to functions of *Metabolism*, with several functions related to *Glycan biosynthesis and metabolism* reduced in *Il10*$^{-/-}$ mice fed the 15% control diet compared to C57BL/6J mice on the same diet, for example, the KEGG pathways *Mucin type O-glycan biosynthesis* and *Glycosaminoglycan biosynthesis* (Figure 4.6).

Table 4.5 Most significantly affected biological functions in the colon of *Il10*$^{-/-}$ mice relative to C57BL/6J mice (both fed the 15% control diet). Functions with an *activation z-score* < |2| were excluded and biological functions limited to show the ten highest p-value-ranked functions. "# genes" indicates the number of genes associated with the biological function and individual genes may be represented in more than one function. Data represent six biological replicates per group.

Functions annotation		*P-value*	*# genes*	*Predicted activation state (activation z-score)*	*Category*
Blood cells	Morphology	6.80E-07	31	Decreased (-3.2)	16
Leukocytes	Activation	3.53E-06	39	Increased (+2.2)	2, 5, 6, 7
	Morphology	2.46E-07	28	Decreased (-3.1)	16
Mononuclear leukocytes	Morphology	4.55E-08	21	Decreased (-3.1)	16
Lymphocytes	Morphology	9.24E-08	20	Decreased (-3.1)	16
T lymphocytes	Morphology	8.37E-09	17	Decreased (-3.1)	2, 16
	Lack	3.59E-07	8	Decreased (-2.8)	2, 16
CD8+ T lymphocyte	Lack	1.17E-07	6	Decreased (-2.4)	2, 16
Cytotoxic T cells	Cytotoxicity	5.24E-06	7	Increased (+2.6)	17, 18
Glucose metabolism disorder		1.96E-09	69	Increased (+2.1)	12

Categories: 1 Cellular Function and Maintenance; 2 Hematological System Development and Function; 3 Tissue Morphology; 4 Cellular Growth and Proliferation; 5 Cell-To-Cell Signalling and Interaction; 6 Immune Cell Trafficking; 7 Inflammatory Response; 8 Cell-mediated Immune Response; 9 Cellular Development; 10 Hematopoiesis; 11 Lymphoid Tissue Structure and Development; 12 Metabolic Disease; 13 Cellular Movement; 14 Infectious Disease; 15 Tissue Development; 16 Cell Morphology; 17 Cell Death and Survival; 18 Cellular Compromise; 19 Lipid Metabolism; 20 Small Molecules Biochemistry; 21 Organismal Survival; 22 Molecular Transport; 23 Organismal Development; 24 Cellular Assembly and Organisation.

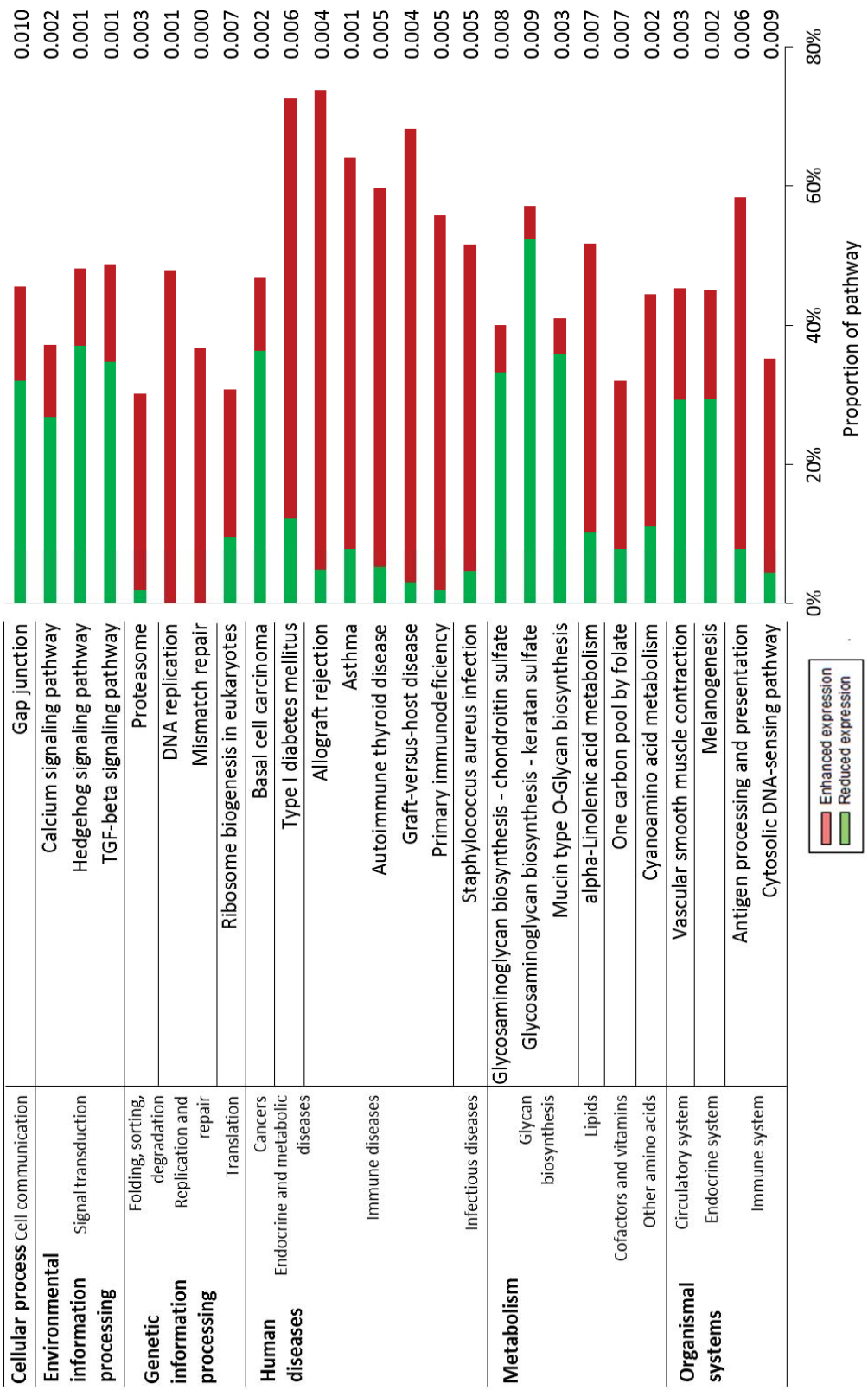

Figure 4.6 KEGG pathway gene sets affected in the colon of *Il10*$^{-/-}$ mice compared to C57BL/6J mice (both fed the 15% control diet) ($P < 0.01$). Bars indicate the proportion of the KEGG pathway affected (%): red bars are the proportion of genes contributing to an increased KEGG pathway and green bars are the proportion of genes contributing to a decreased KEGG pathway. Significance of changes in KEGG pathway expression was determined by GSEA using rotation gene set testing (ROAST function) in R. The p-value significance is indicated by numbers next to bars. Data represent six biological replicates per treatment.

Some differences in colon gene expression were observed when *Il10*$^{-/-}$ and C57BL/6J mice were fed the 15% salmon diet compared to when mice were fed the 15% control diet (data not shown). For example, inflammatory genes *S100A8* and *S100A9* were only increased in expression in *Il10*$^{-/-}$ mice fed the 15% salmon diet (vs. C57BL/6J mice on the same diet), but were unchanged in *Il10*$^{-/-}$ mice fed the 15% control diet (vs. C57BL/6J mice on the same diet). Furthermore, mRNA levels of *PPARA* gene were decreased approximately 3-fold in *Il10*$^{-/-}$ mice fed the 15% salmon diet compared to C57BL/6J mice on the same diet. *PPARA* was unchanged in *Il10*$^{-/-}$ mice fed the 15% control diet compared to C57BL/6J mice on the same diet. Thus it appeared that the 15% salmon diet exacerbated pro-inflammatory gene expression in the colon of *Il10*$^{-/-}$ mice relative to when mice were fed the 15% control diet.

4.4.4.2.2 Effect of the 15% salmon diet (vs. 15% control diet) on colon gene expression in *Il10*$^{-/-}$ mice

The gene expression changes in the colon of *Il10*$^{-/-}$ mice fed the 15% salmon diet were generally immune-related compared to those fed the 15% control diet. Increases in expression levels were observed in the immune-regulatory genes *MMP3*, *MMP7*, *IRG1*, *Igtp*, *IL12B*, and *TNF* (FC = 2-6 and $P \leq 0.005$). Among the ten most significant biological functions associated with the gene expression profile in the colon of 15% salmon-fed *Il10*$^{-/-}$ mice were the development, proliferation and generation of immune cells, specifically leukocytes, mononuclear leukocytes, and lymphocytes compared to those fed the 15% control diet (Table 4.6). The activation states of these ten highest p-value-ranked biological functions were predicted to be increased (*activation z-score* ≥ 2 and $P < 0.05$) based on the expression of 44 unique genes that were further merged to show biological interaction (Figure 4.7). Genes that were central in connecting many of the differentially expressed genes were *TNF*, colony stimulating factor 2 (*CSF2*), *STAT4* and *CXCL10*, all of which are potent inflammatory regulators. These four central genes were increased in expression by approximately 2-fold in *Il10*$^{-/-}$ mice fed the 15% salmon diet compared to those fed the 15% control diet. None of these changes were observed in C57BL/6J mice compared to those fed the 15% control diet (data not shown), hence this pattern indicates an induction of pro-inflammatory gene expression by the 15% salmon diet that is specific to *Il10*$^{-/-}$ mice.

Table 4.6 Most significantly affected biological functions in the colon of *Il10*$^{-/-}$ mice fed the 15% salmon diet relative to those fed the 15% control diet. Functions with an *activation z-score* < |2| were excluded and biological functions limited to show the ten highest p-value-ranked functions. "# genes" indicates the number of genes associated with the biological function and individual genes may be represented in more than one function. Data represent six biological replicates per group.

Functions annotation		*P-value*	*# genes*	*Predicted activation state (activation z-score)*	*Category*
Blood cells	Development	4.90E-09	27	Increased (+3.0)	2, 9, 10
Immune cells	Proliferation	3.06E-09	30	Increased (+2.0)	2, 4, 9
Leukocytes	Development	8.43E-09	25	Increased (+3.0)	2, 9, 10, 11
	Generation	5.47E-10	14	Increased (+3.0)	4, 15
Mononuclear leukocytes	Generation	1.36E-08	12	Increased (+2.6)	4, 15
Lymphocytes	Homeostasis	1.38E-09	25	Increased (+2.7)	1
	Proliferation	7.13E-09	28	Increased (+2.2)	2, 4, 9
	Stimulation	1.05E-08	11	Increased (+2.6)	2, 4, 5
T cells	Development	1.34E-09	24	Increased (+2.6)	1, 2, 8, 9
Antigen presenting cells	Quantity	8.87E-15	23	Increased (+2.2)	2, 3

Categories: 1 Cellular Function and Maintenance; 2 Hematological System Development and Function; 3 Tissue Morphology; 4 Cellular Growth and Proliferation; 5 Cell-To-Cell Signalling and Interaction; 6 Immune Cell Trafficking; 7 Inflammatory Response; 8 Cell-mediated Immune Response; 9 Cellular Development; 10 Hematopoiesis; 11 Lymphoid Tissue Structure and Development; 12 Metabolic Disease; 13 Cellular Movement; 14 Infectious Disease; 15 Tissue Development; 16 Cell Morphology; 17 Cell Death and Survival; 18 Cellular Compromise; 19 Lipid Metabolism; 20 Small Molecules Biochemistry; 21 Organismal Survival; 22 Molecular Transport; 23 Organismal Development; 24 Cellular Assembly and Organisation.

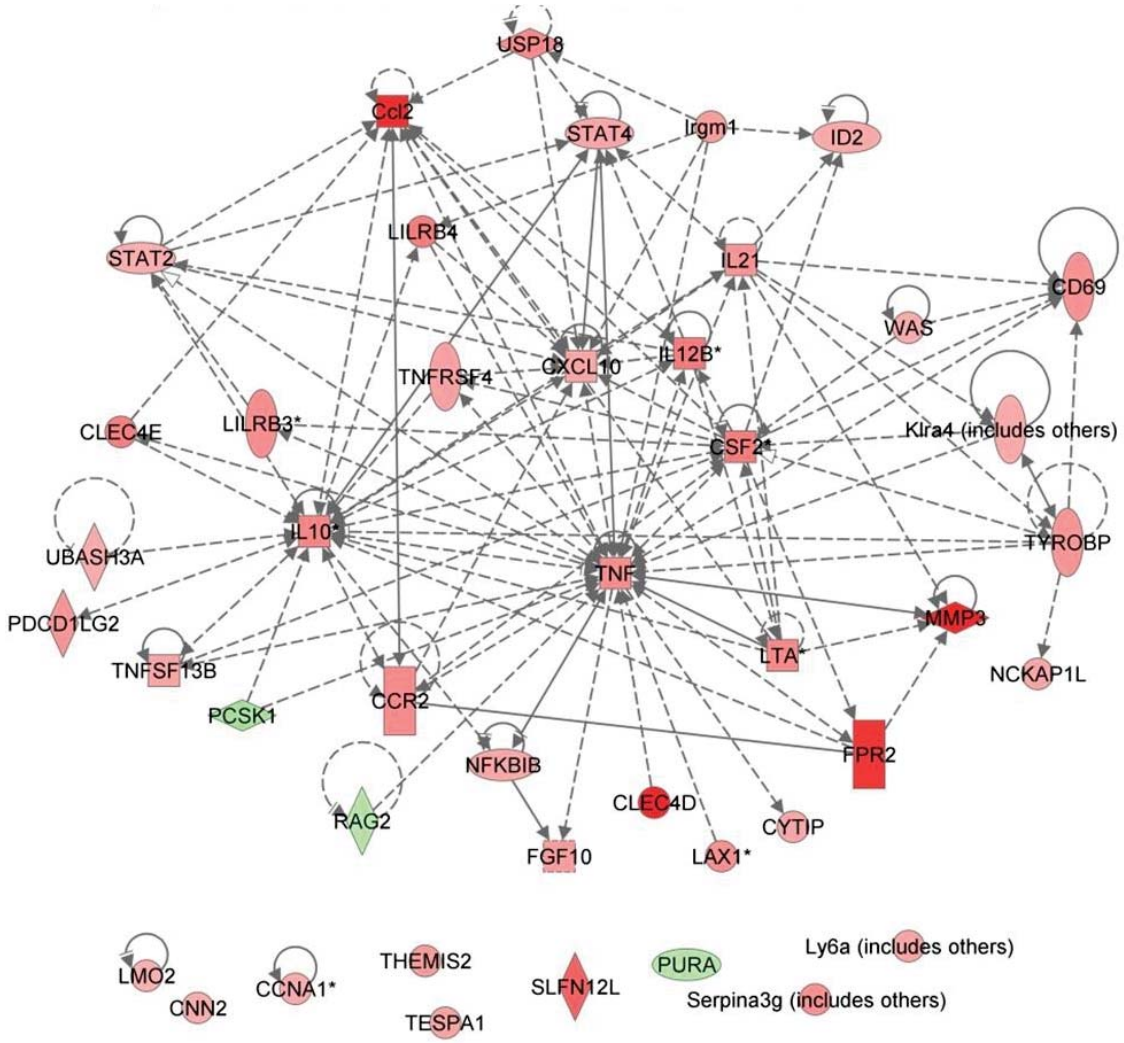

Figure 4.7 Biological interaction network of differentially expressed genes associated with the ten most significant biological functions in *Il10*$^{-/-}$ mice fed the 15% salmon diet relative to those fed the 15% control diet. Nodes represent genes and edges represent direct (full line) and indirect (dotted line) interactions of genes. The colour coding of nodes indicate the direction of fold-change (FC), with red showing genes that are increased in expression in 15% salmon-fed *Il10*$^{-/-}$ mice and green showing decreased gene expression. The intensity of the colour of nodes indicates the degree of FC, with greater intensity of colours pointing to higher levels of FC. Node shape indicates functional class of gene product as indicated in Appendix V. Data represent six biological replicates per treatment group.

GSEA was performed, but showed limited changes in *Il10*$^{-/-}$ mice fed the 15% salmon diet compared to those fed the 15% control diet, with only two gene sets differentially expressed in the colon ($P \leq 0.01$). These were *Biotin metabolism* (Function: *Metabolism of cofactors and vitamins*), with approximately 33% genes decreased in the gene set, and *p53 signalling pathway* (Function: *Cell Growth and Death*), with approximately 20% genes increased in the gene set (data not shown).

4.4.4.3 Colon gene expression in mice fed the 30% salmon and 30% control diets

In the treatment groups that were fed the 30% diets, the highest number of differentially expressed genes were detected in the colon of *Il10*$^{-/-}$ mice fed the 30% control diet compared to C57BL/6J mice fed the same diet (3524 genes (Table 4.3)). When mice were fed the 30% salmon diet, only 379 genes were differentially expressed in *Il10*$^{-/-}$ mice compared to C57BL/6J mice. In *Il10*$^{-/-}$ mice fed the 30% salmon diet, 308 genes were differentially expressed relative to those fed the 30% control diet (Table 4.3), and of those, 177 were decreased and 131 were increased. A moderated effect by the 30% salmon diet was observed in C57BL/6J mice, with only 154 genes differentially expressed compared to those fed the 30% control diet.

4.4.4.3.1 Colon gene expression between mouse genotypes fed the 30% control diet

Pathway analysis was performed after reducing the number of genes < 1000 by increasing the stringency as stated in Table 4.3. The gene expression changes in the colon of *Il10*$^{-/-}$ mice fed the 30% control diet were generally immune-related compared to C57BL/6J mice, and approximately one third of the differentially expressed genes were associated with functional roles in inflammatory responses. Increased genes included for example *S100A9*, *CXCL9*, *CXCL10*, *Igtp*, and *IDO1* (FC = 8.5-16.1), all of which are known to be important inflammatory regulators. *PPARA* and *PPARGC1A* transcript levels were reduced approximately 2-fold in *Il10*$^{-/-}$ mice compared to C57BL/6J both fed the 30% control diet (data not shown).

Most significantly affected were the activation and quantity of cells and blood cells, specifically leukocytes (including mononuclear) and lymphocytes (Table 4.7). The activation states of these functions were predicted to be increased based on the expression of genes (*activation z-score* ≥ 2 and $P < 0.05$). Due to the high number of genes involved,

the gene network is not shown. However, four genes that were central in connecting many of the differentially expressed genes were *STAT1*, *IRF1*, *LCK* and v-yes-1 Yamaguchi sarcoma viral related oncogene homolog (*LYN*). The transcript levels of these genes were increased approximately 2.5-fold in *Il10*$^{-/-}$ mice relative to C57BL/6J mice both fed the 30% control diet.

In *Il10*$^{-/-}$ mice fed the 30% control diet, sets of genes comprising 84 KEGG pathways were significantly affected compared to C57BL/6J mice fed the same diet ($P \leq 0.01$ (Figure 4.8)). Of these, 41 gene sets were decreased and 43 increased in expression, with most of the gene sets associated with biological processes in *Organismal systems*, *Metabolism* and *Human diseases* (Figure 4.8).

The enhanced gene sets in the colon of *Il10*$^{-/-}$ mice were mostly immune-related (versus C57BL/6J mice both fed the 30% control diet), supporting the findings from IPA. KEGG pathways in *Immune system* were increased (within the biological process *Organismal systems*), for example the pathways *Antigen processing and presentation* (65% genes increased), *B cell receptor signalling pathway* (49% genes increased) and *T cell receptor signalling pathway* (46% genes increased) (Figure 4.8). Furthermore, signalling pathways against bacteria and other pathogens were increased, for example, *Intestinal immune network for IgA production* (68% genes increased), *NOD-like receptor signalling pathway* (50% genes increased) and *Toll-like receptor signalling pathway* (44% genes increased) (all $P < 0.001$). The highest ratio of genes affected divided by total numbers of genes in the pathway were the KEGG pathways *Allograft rejection signalling* and *Graft-versus-host disease signalling*, with 79% and 74% genes contributing to the increased set ($P < 0.001$ (Figure 4.8)). Both pathways were among the most significantly affected in *Il10*$^{-/-}$ mice fed the 30% control diet compared to C57BL/6J mice fed the same diet as per single-gene analysis in IPA (data not shown).

A further 11 gene sets were linked to functions of *Organismal systems*, with several functions related to *Digestive system* reduced in *Il10*$^{-/-}$ mice fed the 30% control diet compared to C57BL/6J mice fed the same diet (Figure 4.8). The KEGG pathways *Vitamin digestion and absorption* and *Protein digestion and absorption* were also affected, with 59% and 39% genes contributing to a decrease in function ($P = 0.002$ and 0.01, respectively).

Table 4.7 Most significantly affected biological functions in the colon of *Il10*$^{-/-}$ mice relative to C57BL/6J mice (both fed the 30% control diet). Functions with an *activation z-score* < |2| were excluded and biological functions limited to show the ten highest p-value-ranked functions. "# genes" indicates the number of genes associated with the biological function and individual genes may be represented in more than one function. Data represent six biological replicates per group.

Functions annotation		*P-value*	*# genes*	*Predicted activation state (activation z-score)*	*Category*
Cells	Activation	2.34E-64	203	Increased (+5.2)	5
Blood cells	Activation	1.93E-64	174	Increased (+5.7)	2, 5
	Quantity	6.08E-61	214	Increased (+3.9)	2, 3
Mononuclear leukocytes	Quantity	1.12E-60	176	Increased (+4.7)	2, 3
Leukocytes	Function	3.64E-77	170	Increased (+2.4)	1
	Quantity	2.12E-67	208	Increased (+3.7)	2, 3
	Activation	5.98E-65	163	Increased (+5.8)	2, 5, 6
Lymphocytes	Activation	1.41E-54	124	Increased (+4.9)	2, 5, 6, 7
	Quantity	1.13E-62	175	Increased (+4.8)	2, 3
Glucose metabolism disorder		2.35E-65	216	Increased (+2.1)	12

Categories: 1 Cellular Function and Maintenance; 2 Hematological System Development and Function; 3 Tissue Morphology; 4 Cellular Growth and Proliferation; 5 Cell-To-Cell Signalling and Interaction; 6 Immune Cell Trafficking; 7 Inflammatory Response; 8 Cell-mediated Immune Response; 9 Cellular Development; 10 Hematopoiesis; 11 Lymphoid Tissue Structure and Development; 12 Metabolic disease.

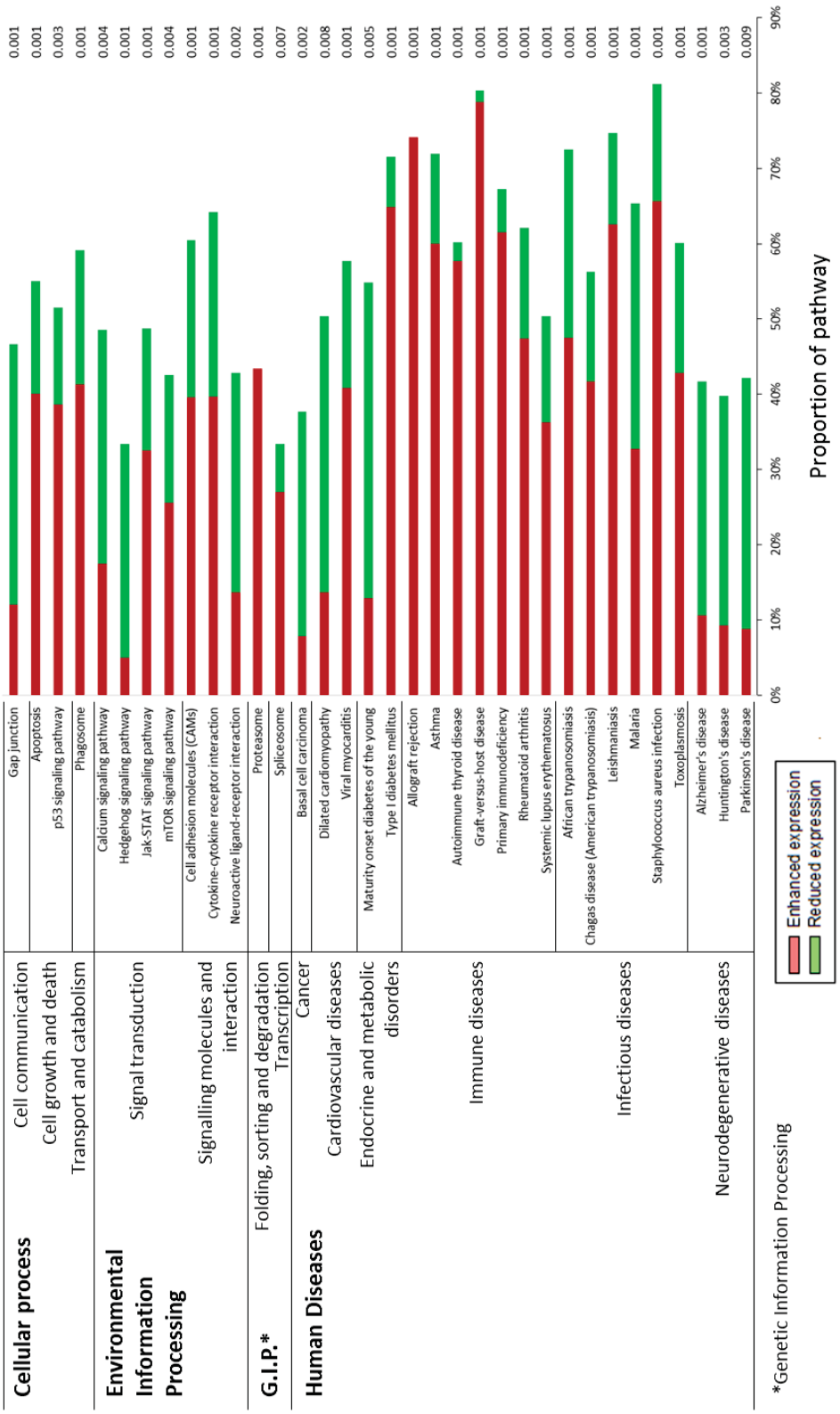

Figure 4.8 KEGG pathway gene sets affected in the colon of *Il10*$^{-/-}$ mice compared to C57BL/6J mice (both fed the 30% control diet) ($P \leq 0.01$). Bars indicate the proportion of the KEGG pathway affected (%): red bars are the proportion of genes contributing to an increased KEGG pathway and green bars are the proportion of genes contributing to a decreased KEGG pathway. Significance of changes in KEGG pathway expression was determined by GSEA using rotation gene set testing (ROAST function) in R. The p-value significance is indicated by numbers next to bars. Data represent six biological replicates per treatment.

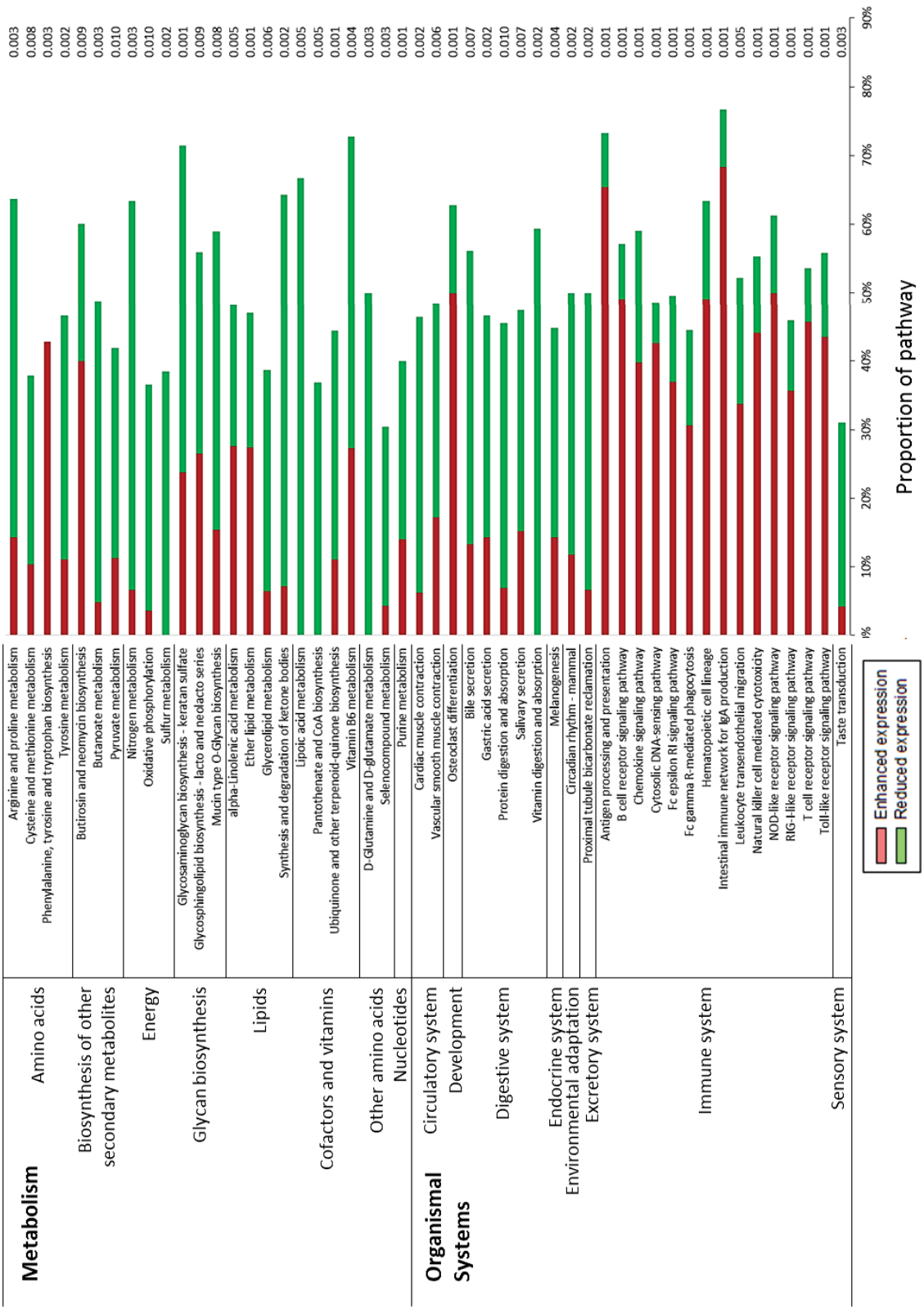

Figure 4.8 continued.

A general decrease in expression of KEGG pathways related to *Metabolism* was observed in *Il10*$^{-/-}$ mice compared to C57BL/6J mice, both fed the 30% control diet (Figure 4.8). In *Il10*$^{-/-}$ mice, decreased expressions of genes in the metabolism of, for example, amino acids (*e.g.* arginine and proline, and phenylalanine, tyrosine and tryptophan), lipids (glycerolipid and ketone bodies), cofactors and vitamins (*e.g.* Vitamin B6 and ubiquinone) were observed compared to C57BL/6J mice fed the 30% control diet. Furthermore, three KEGG pathways related to *Energy metabolism* were decreased in *Il10*$^{-/-}$ mice (*Nitrogen metabolism*, *Sulphur metabolism* and *Oxidative phosphorylation*), further indicating reduced energy levels in the colon of *Il10*$^{-/-}$ mice fed the 30% control diet.

4.4.4.3.2 Effect of the 30% salmon diet (vs. 30% control diet) on colon gene expression in *Il10*$^{-/-}$ mice

Gene expression changes in *Il10*$^{-/-}$ mice fed the 30% salmon diet were associated with the development, homeostasis, quantity and stimulation of several types of blood cells, specifically lymphocytes, compared to those fed the 30% control diet (Table 4.8). The activation states of these functions were predicted to be decreased based on the expression of 52 unique genes (*activation z-score* $\leq$ -2 and $P < 0.05$) which were further merged to show biological interaction as shown in Figure 4.9. Compared to *Il10*$^{-/-}$ mice fed the 30% control diet, those fed the 30% salmon diet showed decreased mRNA expression levels of interleukins (*e.g. IL10*, *IL12B*, *IL21*, and *IL36A*) and cell-surface receptors (*e.g. CD28*, *CD86*, *CD69*, *ITGA4*, and *ICOS*) (Figure 4.9). The changes in mRNA expression levels of these genes may be attributed to the transcription regulators *CEBPB* and early growth response 2 (*EGR2*), all of which were decreased in expression in the colon of 30% salmon-fed *Il10*$^{-/-}$ mice (FC = -2 and $P < 0.005$ vs. 30% control diet).

The *Upstream regulator analysis* of differentially expressed genes in the colon of *Il10*$^{-/-}$ mice fed the 30% salmon diet predicted an inhibition of transcription factors *STAT1*, *STAT3*, *IRF7*, *RELA*, *NFKBIA*, *CEBPB*, and *PRDM1*, but enhanced activation states of *PPARA* and *PPARGC1A* compared to those fed the 30% control diet (*activation z-score* $\geq |2|$ and *p-value of overlap* ≤ 0.01 (Figure 4.10)). The predicted activation of the *PPARA* nuclear receptor (*activation z-score* = 2.3 and *p-value of overlap* = 9.8E-04) was based on target genes with functional roles in fatty acid metabolism (*ACAA2*, *ACOT2*, *Acot5*, *UCP3*, *CPT1A*). Additionally it was shown that the transcription factor *CEBPD*

was associated with these transcription factors and reduced 1.9-fold in response to the 30% salmon supplementation in *Il10*$^{-/-}$ mice compared to those fed the 30% control diet (Figure 4.10). Thus it appears that the intake of the 30% salmon diet induced an anti-inflammatory gene expression in the colon of *Il10*$^{-/-}$ mice compared to those fed the 30% control diet.

In *Il10*$^{-/-}$ mice fed the 30% salmon diet, GSEA revealed differential expression of 25 KEGG pathway gene sets compared to those fed the 30% control diet ($P \leq 0.01$ (Figure 4.11)). Of these, six gene sets were decreased and 19 were increased in expression ($P \leq 0.01$). Most pathways affected by the 30% salmon diet in *Il10*$^{-/-}$ mice were associated with *Metabolism* and *Organismal systems*. Only a limited number of KEGG pathways in *Environmental information processing* and *Genetic information processing* were affected in those mice.

Within the biological processes *Organismal systems* and *Metabolism*, the expression of KEGG pathways associated with the digestion, absorption and metabolism of several nutrients was enhanced in *Il10*$^{-/-}$ mice by the 30% salmon diet relative to those fed the 30% control diet (Figure 4.11). The set of genes comprising the KEGG pathway *Vitamin digestion and absorption* was increased in expression in *Il10*$^{-/-}$ mice fed the 30% salmon diet compared to those fed the 30% control diet ($P = 0.008$) and the proportion of genes in the set contributing to the increase was with 56% the largest proportion in the comparison (Figure 4.11). Furthermore, *Il10*$^{-/-}$ mice fed the 30% salmon diet showed a significant increase in expression of genes in the KEGG pathway *PPAR signalling*, with 45% of genes in the set contributing compared to those fed the 30% control diet ($P = 0.002$ (Figure 4.11)). This increase supports the predicted activation of *PPARA* and *PPARGC1A* transcriptional activity in the colon of 30% salmon-fed *Il10*$^{-/-}$ mice as shown by IPA *Upstream regulator analysis* and shown in Figure 4.10. Within C57BL/6J mice, these effects on *PPARA* and *PPARGC1A* were not observed (30% salmon vs. 30% control (data not shown)).

Compared to *Il10*$^{-/-}$ mice fed the 30% control diet, those fed the 30% salmon diet showed increased expression of genes in KEGG pathways associated with *Metabolism* (metabolism of amino acids, lipids, and cofactors/vitamins (Figure 4.11)). *Il10*$^{-/-}$ mice fed the 30% salmon diet showed increases in expression of genes associated with lipid-related KEGG pathways: *Arachidonic acid metabolism*, *Biosynthesis of unsaturated fatty acids*,

Fatty acid degradation and *Glycerolipid metabolism*, with 37-42% of genes contributing to the increases ($P < 0.01$ compared to *Il10*$^{-/-}$ mice fed the 30% control diet). Sets of genes comprising two KEGG pathways in *Vitamin metabolism* were increased: *Retinol metabolism* (52% of genes in the set increased) and *Pantothenate and Coenzyme A biosynthesis* (37% of genes in the set increased). The KEGG pathway *Metabolism of xenobiotics by cytochrome P450*, as well as other drug-related metabolism pathways, was also increased in *Il10*$^{-/-}$ mice fed the 30% salmon diet, with 41% of genes in the set contributing to the increased expression ($P = 0.006$ compared to *Il10*$^{-/-}$ mice fed the 30% control diet). However, the 30% salmon diet did not affect the KEGG pathway *Tryptophan metabolism* in the colon of *Il10*$^{-/-}$ mice ($P > 0.01$ vs. 30% control diet).

Most gene sets affected by the 30% salmon diet (vs. 30% control diet) in *Il10*$^{-/-}$ mice were associated with metabolic KEGG pathways, but three pathways associated with *Immune system* were reduced in expression in these mice (biological process *Organismal systems* (Figure 4.11)). These were pathways *T cell receptor signalling*, *NOD-like receptor signalling*, and *Chemokine signalling*, with approximately 30% decreased genes in each pathway in 30% salmon-fed *Il10*$^{-/-}$ mice ($P < 0.01$), indicating that the 30% salmon diet may have reduced in receptor-mediated signalling pathways.

4.4.4.4 Colon gene expression in mice fed the 45% salmon and 45% control diets

In the treatment groups that were fed the 45% diets, the lowest number of differentially expressed genes was observed in the comparison of 45% salmon vs. 45% control within *Il10*$^{-/-}$ mice, with only 15 genes differentially expressed ($FC \geq |1.5|$ and $P \leq 0.005$ (Table 4.3). At a 0.5% significance level, the changes in these genes may be significant purely by chance and cannot be confidently linked to the influence of the 45% salmon diet. Within C57BL/6J mice, the expression of 383 genes were affected by the 45% salmon diet compared to those fed the 45% control diet. 2689 genes were differentially expressed between *Il10*$^{-/-}$ and C57BL/6J mice both fed the 45% salmon diet, approximately twice as many when these mice were fed the 45% control diet. Regardless of whether mice were fed the 45% salmon diet or the 45% control diet, genes were mostly increased in expression in *Il10*$^{-/-}$ mice (vs. C57BL/6J mice). Pathway analysis was performed after reducing the number of genes < 1000 by increasing the stringency as stated in Table 4.3.

Table 4.8 Most significantly affected biological functions in the colon of *Il10*$^{-/-}$ mice fed the 30% salmon diet relative to those fed the 30% control diet. Functions with an *activation z-score* < |2| were excluded and biological functions limited to show the ten highest p-value-ranked functions. "# genes" indicates the number of genes associated with the biological function and individual genes may be represented in more than one function. Data represent six (*Il10*$^{-/-}$ mice 30% control) and five (*Il10*$^{-/-}$ mice 30% salmon) biological replicates.

Functions annotation		*P-value*	*# genes*	*Predicted activation state (activation z-score)*	*Category*
Blood cells	Development	1.91E-12	34	Decreased (-2.6)	2, 9, 10
	Quantity	1.23E-11	44	Decreased (-2.5)	2, 3
Leukocytes	Stimulation	2.48E-11	16	Decreased (-3.5)	2, 4, 5
Mononuclear leukocytes	Stimulation	2.60E-12	15	Decreased (-3.3)	2, 4, 5
	Quantity	1.34E-11	36	Decreased (-2.0)	2, 3
Lymphocytes	Homeostasis	1.56E-13	32	Decreased (-2.3)	1
	Quantity	1.97E-11	35	Decreased (-2.0)	2, 3
	Development	3.40E-13	32	Decreased (-2.5)	2, 9, 10, 11
T lymphocytes	Stimulation	6.48E-13	14	Decreased (-3.0)	2, 4, 5
T cell	Development	6.41E-13	30	Decreased (-2.4)	1, 2, 8, 9, 10, 11

Categories: 1 Cellular Function and Maintenance; 2 Hematological System Development and Function; 3 Tissue Morphology; 4 Cellular Growth and Proliferation; 5 Cell-To-Cell Signalling and Interaction; 6 Immune Cell Trafficking; 7 Inflammatory Response; 8 Cell-mediated Immune Response; 9 Cellular Development; 10 Hematopoiesis; 11 Lymphoid Tissue Structure and Development; 12 Metabolic disease.

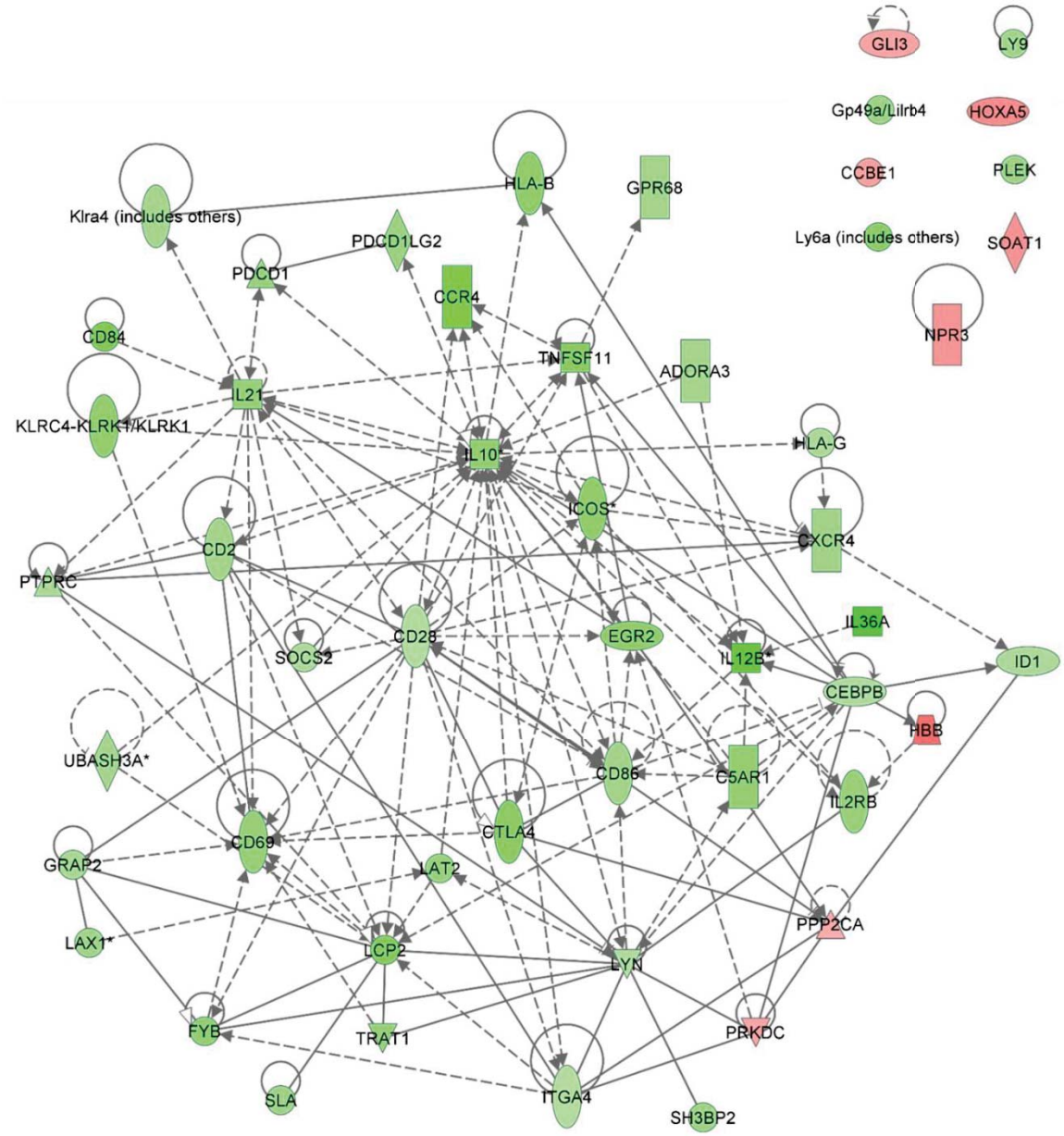

Figure 4.9 Biological interaction network of differentially expressed genes associated with the ten most significant biological functions in the colon of *Il10*$^{-/-}$ mice fed the 30% salmon diet compared to those fed the 30% control diet. Nodes represent genes and edges represent direct (full line) and indirect (dotted line) interactions of genes. The colour coding of nodes indicate the direction of fold-change (FC), with red showing genes that are increased in expression and green showing decreased expression in the colon of 30% salmon-fed *Il10*$^{-/-}$ mice. The intensity of the colour of nodes indicates the degree of FC, with greater intensity of colours pointing to higher levels of FC. Node shape indicates functional class of gene product as indicated in Appendix V. Data represent six (*Il10*$^{-/-}$ mice 30% control) and five (*Il10*$^{-/-}$ mice 30% salmon) biological replicates.

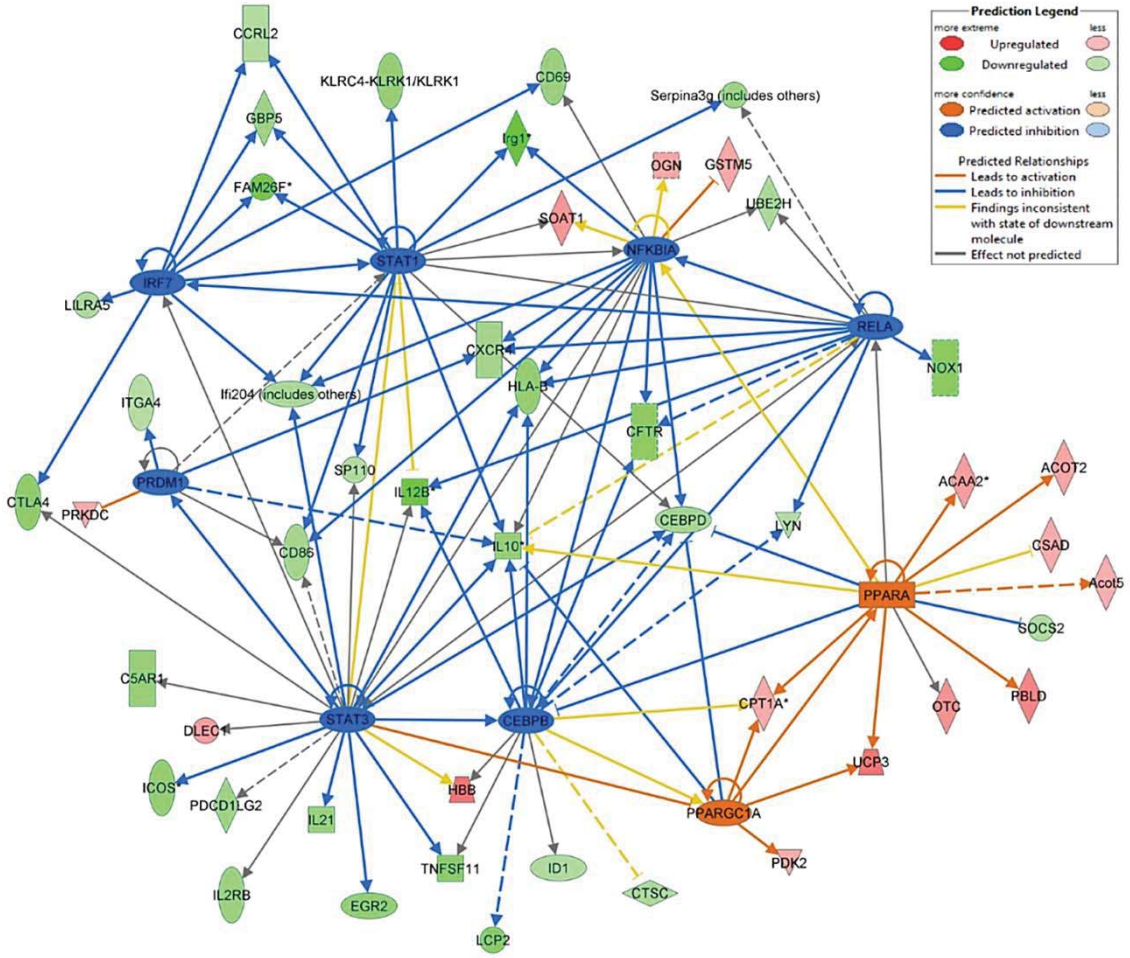

Figure 4.10 Biological interaction network of transcription factors that were predicted to be inhibited or activated in the colon of *Il10*$^{-/-}$ mice fed the 30% salmon diet compared to those fed the 30% control diet (*activation z-score* $\geq |2|$ and *p-value of overlap* ≤ 0.005). Nodes represent genes and edges represent direct (full line) and indirect (dotted line) interactions of genes. The activation state is predicted for the activity of the regulator protein, with blue shading of regulators indicating predicted inhibition and orange indicating predicted activation in 30% salmon-fed *Il10*$^{-/-}$ mice. The colour coding of genes indicate the direction of fold-change (FC), with red showing genes that are increased in expression and green showing decreased expression in the colon of 30% salmon-fed *Il10*$^{-/-}$ mice. The intensity of the colour of nodes indicates the degree of FC, with greater intensity of colours pointing to higher levels of FC. Node shape indicates functional class of gene product as indicated in Appendix V. Data represent six (*Il10*$^{-/-}$ mice 30% control), and five (*Il10*$^{-/-}$ mice 30% salmon) biological replicates.

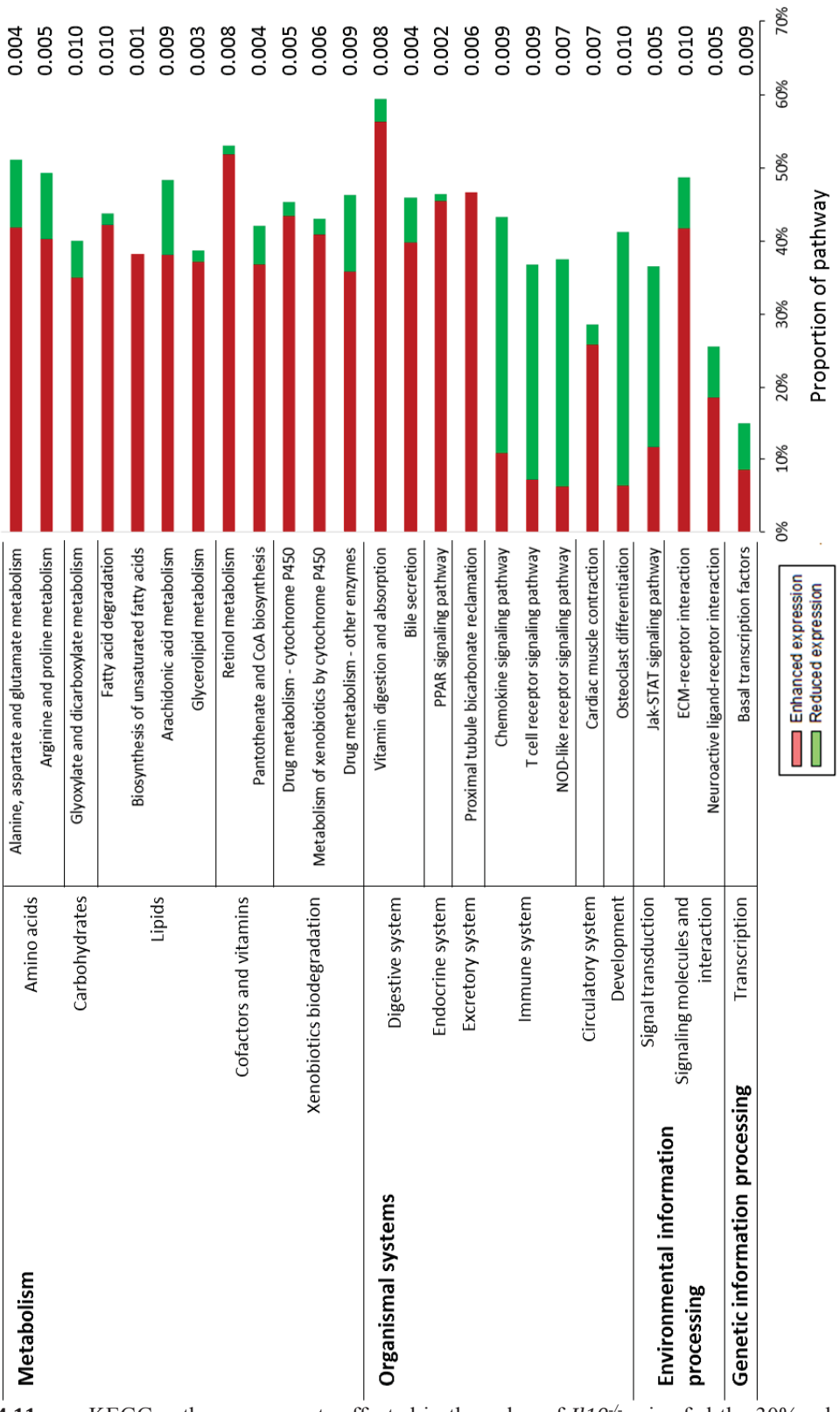

Figure 4.11 KEGG pathway gene sets affected in the colon of *Il10*$^{-/-}$ mice fed the 30% salmon diet compared to those fed the 30% control diet ($P \leq 0.01$). Bars indicate the proportion of the KEGG pathway affected (%): red bars are proportion of genes increased in expression and green bars are the proportion of genes decreased in expression. Significance of changes in KEGG pathway expression was determined by GSEA using rotation gene set testing (ROAST function) in R. The p-value significance is indicated by the number next to the bars. Data represent six (*Il10*$^{-/-}$ mice 30% control), and five (*Il10*$^{-/-}$ mice 30% salmon) biological replicates.

4.4.4.4.1 Colon gene expression between mouse genotypes fed the 45% control diet

The gene expression changes in the colon of *Il10*$^{-/-}$ mice fed the 45% control diet were generally immune-related compared to C57BL/6J mice fed the same diet, and approximately 30% of the differentially expressed genes were linked to functional roles in the inflammatory response. As shown in Table 4.9, the differentially expressed genes were mostly associated with the activation and quantity of several types of inflammatory cells, for example leukocytes and lymphocytes. The activation states of these ten highest p-value-ranked functions were predicted to be increased based on the expression of 242 unique genes (*activation z-score* ≥ 2 and $P < 0.05$). Merging these genes into a biological interaction network (not shown due to the large number of genes) identified four genes that were central in connecting many of the differentially expressed genes. These genes were transcription factor *STAT1*, cytokines *TNF*, *IL1B*, and *IL10*. The expression of these genes were increased in expression in *Il10*$^{-/-}$ mice fed the 45% control diet compared to C57BL/6J mice fed the same diet (FC = 2.2-4.8), and are known to play important roles in the regulation of the immune system.

Changes in gene expression in the colon of *Il10*$^{-/-}$ mice fed the 45% control diet were associated with *Free Radical Scavenging* compared to C57BL/6J mice fed the same diet. This included the functions *Synthesis of Reactive Oxygen Species (ROS)* and *Production of ROS* with activation states predicted to be increased in both functions (*activation z-scores* = 2.5 and $P < 0.001$ (data not shown)). As shown in Figure 4.12, the canonical pathway *Production of Nitric Oxide and Reactive Oxygen Species in macrophages* was increased in expression, with 11% of the canonical pathway increased in *Il10*$^{-/-}$ mice relative to C57BL/6J mice fed the 45% control diet ($P < 0.001$). Increases in genes associated with ROS production were also observed in *Il10*$^{-/-}$ mice fed the 45% salmon diet compared to C57BL/6J mice fed the same diet (data not shown), therefore the impact on *Free Radical Scavenging* processes by the 45% diets appeared to be independent of the type of 45% diet (salmon or control).

Table 4.9 Most significantly affected biological functions in the colon of *Il10*$^{-/-}$ mice relative to C57BL/6J mice (both fed the 45% control diet). Functions with an *activation z-score* < |2| were excluded and biological functions limited to show the ten highest p-value-ranked functions. "# genes" indicates the number of genes associated with the biological function and individual genes may be represented in more than one function. Data represent six biological replicates per group.

Functions annotation		*P-value*	*# genes*	*Predicted activation state (activation z-score)*	*Category*
Cells	Activation	1.09E-22	136	Increased (+3.1)	5
Blood cells	Quantity	6.41E-27	158	Increased (+3.0)	2, 3
Mononuclear leukocytes	Quantity	6.08E-27	126	Increased (+3.8)	2, 3
Leukocytes	Activation	1.67E-23	109	Increased (+3.4)	2, 5, 6, 7
	Cell movement	5.61E-25	123	Increased (+4.5)	2, 6, 13
	Migration	1.40E-26	138	Increased (+4.2)	6, 13
	Quantity	2.38E-30	152	Increased (+3.1)	2, 3
Lymphocytes	Quantity	3.93E-28	125	Increased (+4.1)	2, 3
T lymphocytes	Quantity	1.67E-25	101	Increased (+3.9)	2, 3
Infection of mammalia		3.06E-23	75	Decreased (-5.3)	14

Categories: 1 Cellular Function and Maintenance; 2 Hematological System Development and Function; 3 Tissue Morphology; 4 Cellular Growth and Proliferation; 5 Cell-To-Cell Signalling and Interaction; 6 Immune Cell Trafficking; 7 Inflammatory Response; 8 Cell-mediated Immune Response; 9 Cellular Development; 10 Hematopoiesis; 11 Lymphoid Tissue Structure and Development; 12 Metabolic disease; 13 Cellular Movement; 14 Infectious Disease; 15 Tissue Development; 16 Cell Morphology; 17 Cell Death and Survival; 18 Cellular Compromise; 19 Lipid Metabolism; 20 Small Molecules Biochemistry; 21 Organismal Survival; 22 Molecular Transport; 23 Organismal Development; 24 Cellular Assembly and Organisation.

In *Il10*$^{-/-}$ mice fed the 45% control diet, sets of genes comprising 37 KEGG pathways were significantly affected compared to C57BL/6J mice fed the same diet ($P < 0.01$ (Figure 4.13)). Of these, with most of the gene sets associated with biological processes in *Human diseases*, *Organismal systems*, *Metabolism*, and *Environmental information processing* (Figure 4.13). The increased gene sets in the colon of *Il10*$^{-/-}$ mice fed the 45% control diet (vs. C57BL/6J mice fed the same diet) were mostly immune-related. As shown in Figure 4.13, KEGG pathways in *Immune system* (within the biological process *Organismal systems*) were increased, for example the pathways *Antigen processing and presentation*, *B cell receptor signalling pathway* and *T cell receptor signalling pathway* (40%-59% genes increased in pathways). Furthermore, signalling pathways against bacteria and other pathogens were increased, for example, *Intestinal immune network for IgA production*, *NOD-like receptor signalling pathway* and *Toll-like receptor signalling pathway* (37-68% genes increased) (all $P < 0.001$). Within the biological process *Human diseases*, those KEGG pathways associated with *Immune diseases* (*e.g. Allograft rejection*, *Asthma*, and *Graft-versus-host disease*) were among the pathways with the highest ratio of affected genes (Figure 4.13).

There was an increase in expression of KEGG pathways related to *Environmental information processing* in *Il10*$^{-/-}$ mice compared to C57BL/6J mice fed the 45% control diet (Figure 4.13). In *Il10*$^{-/-}$ mice, increased expressions of genes in *Signal transduction* (*Jak-STAT signalling pathway* and *VEGF signalling pathway*) and *Signalling molecules and interaction* (*Cell adhesion molecules* and *Cytokine-cytokine receptor interaction*) were observed compared to C57BL/6J mice fed the 45% control diet.

4.4.4.4.2 Effect of the 45% salmon diet (vs. 45% control diet) on colon gene expression irrespective of genotype

Due to the low number of differentially expressed genes in the colon of *Il10*$^{-/-}$ mice fed the 45% salmon diet compared to those fed the 45% control diet (15 genes (Table 4.3)), pathway analysis in IPA was restricted and no common biological function associated with these genes. GSEA supported these results, with no KEGG pathway gene set differentially expressed between these two treatment groups.

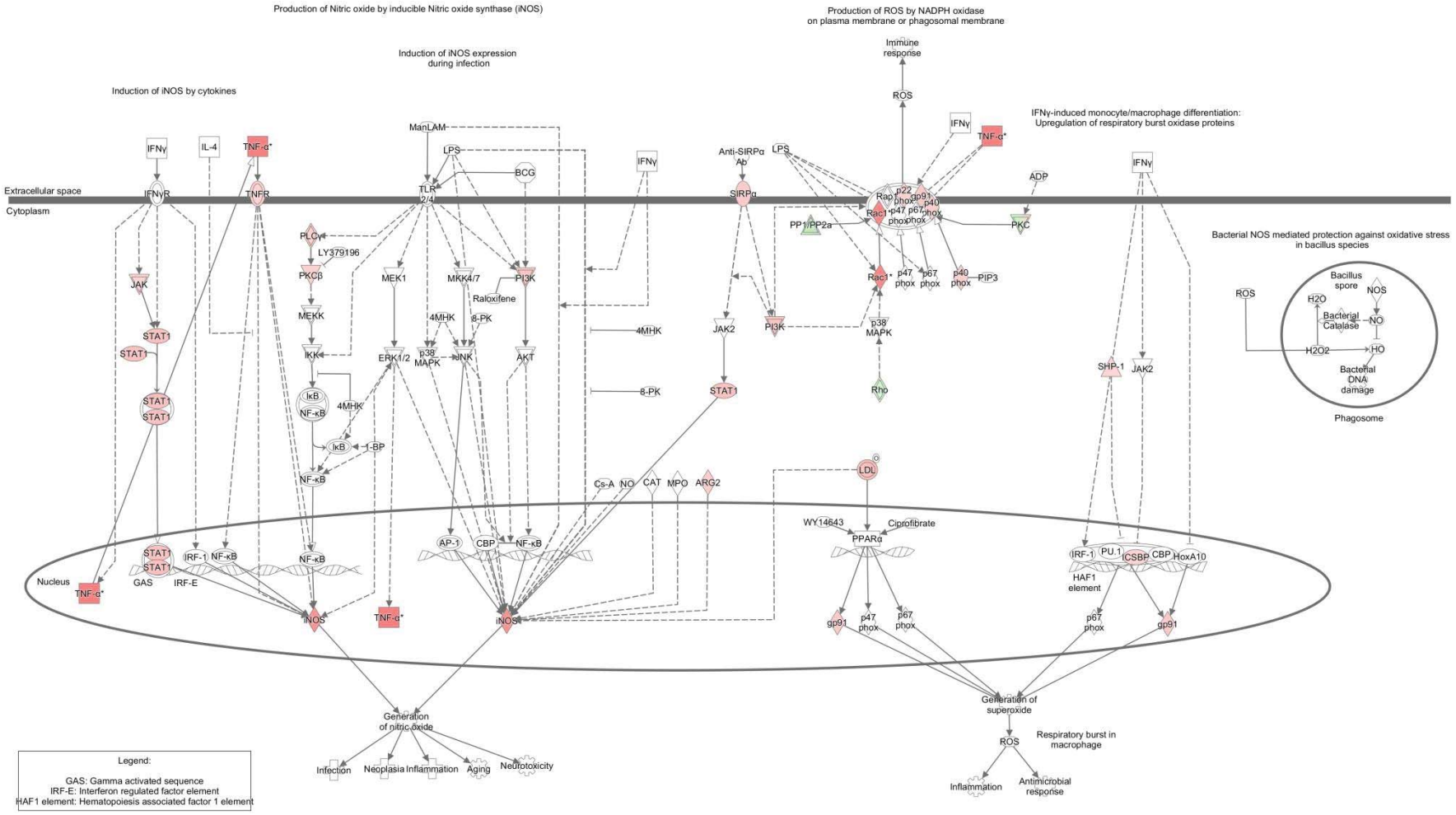

Figure 4.12 Ingenuity pathway for *Production of Nitric Oxide and Reactive Oxygen Species in macrophages*. Nodes represent genes and red colour coding of nodes indicates increased mRNA expression levels and green colour coding decreased levels in the colon of *Il10*$^{-/-}$ mice fed the 45% control diet (compared to C57BL/6J mice fed the same diet). The intensity of the colour of nodes indicates the degree of fold-change (FC), with greater intensity of colours pointing to higher levels of FC. Node shape indicates functional class of gene product as indicated in Appendix V. Data represent six biological replicates per group.

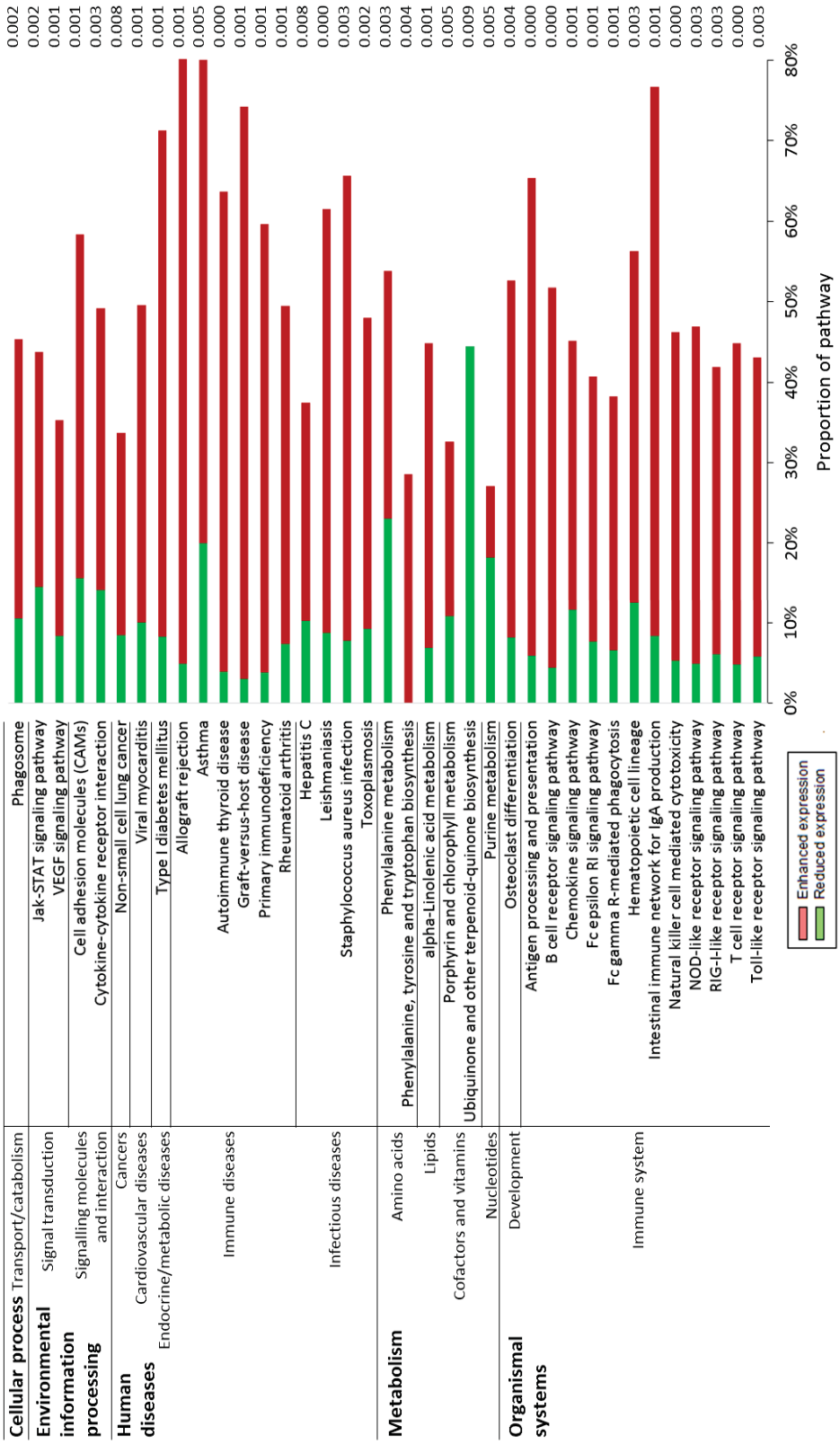

Figure 4.13 KEGG pathway gene sets affected in the colon of *Il10*$^{-/-}$ mice compared to C57BL/6J mice (both fed the 45% control diet) ($P < 0.01$). Bars indicate the proportion of the KEGG pathway affected (%): red bars are the proportion of genes contributing to an increased KEGG pathway and green bars are the proportion of genes contributing to a decreased KEGG pathway. Significance of changes in KEGG pathway expression was determined by GSEA using rotation gene set testing (ROAST function) in R. The p-value significance is indicated by numbers next to bars. Data represent six biological replicates per treatment.

However, within C57BL/6J mice, the intake of the 45% salmon diet affected the expression of 383 genes compared to those fed the 45% control diet (FC ≥ |1.5| and P ≤ 0.005 (Table 4.3)). The ten highest p-value-ranked biological functions associated with the differentially expressed genes in the colon of C57BL/6J mice fed the 45% salmon diet are listed in Table 4.10 (vs. 45% control diet). Two of these ten functions were lipid-related processes (*Fatty acid metabolism* and *Transport of lipid*) and predicted to be increased in activation state. The effect of the 45% salmon diet on lipid-related processes in C57BL/6J mice was further supported by the increased expression of the canonical pathway *Fatty acid β-oxidation* (13% of the canonical pathway increased; P = 0.007 compared to C57BL/6J mice fed the 45% control diet (data not shown)). The genes associated with these ten highest p-value-ranked biological functions were merged into biological interaction (Figure 4.14). The genes that connected many of the differentially expressed genes were amyloid beta precursor protein (*APP*), integrin beta 1 (*ITGB1*), forkhead box O1 (*FOXO1*), and sterol regulatory element binding transcription factor 2 (*SREBF2*). All of these genes were increased in expression in C57BL/6J mice fed the 45% salmon diet (vs. 45% control diet). None of these genes was differentially expressed in *Il10*$^{-/-}$ mice fed the 45% salmon diet (vs. 45% control diet), thus these changes in gene expression by the 45% salmon diet in C57BL/6J mice may indicate effects of this diet specific to healthy mice.

GSEA revealed differential expression of 29 gene sets in C57BL/6J mice fed the 45% salmon diet compared to those fed the 45% control diet (P ≤ 0.01 (data not shown)). Of these, 21 sets of genes comprising KEGG pathways were related to *Metabolism* and increased in expression (*e.g.* metabolism of amino acids, carbohydrates, lipids, and cofactors and vitamins). C57BL/6J mice fed the 45% salmon diet showed increases in expression of genes in lipid-related KEGG pathways: *Biosynthesis of unsaturated fatty acids*, *Fatty acid metabolism*, *Fatty acid biosynthesis*, and *Steroid hormone biosynthesis*, with 32-55% of genes contributing to the increase in each pathway (P < 0.01 compared to C57BL/6J mice fed the 45% control diet). The increase in KEGG pathways associated with lipid metabolism supported the results from single-gene analysis in IPA. Furthermore, sets of genes comprising two KEGG pathways associated with *Vitamin metabolism* were increased in 45% salmon-fed C57BL/6J mice: *Retinol metabolism* (33% of genes in the set increased) and *Pantothenate and Coenzyme A biosynthesis* (26% of genes in the set increased) vs. those fed the 45% control diet.

Table 4.10 Most significantly affected biological functions in the colon of C57BL/6J mice fed the 45% salmon diet relative to those fed the 45% control diet. Functions with an *activation z-score* < |2| were excluded and biological functions limited to show the ten highest p-value-ranked functions. "# genes" indicates the number of genes associated with the biological function and individual genes may be represented in more than one function. Data represent six biological replicates per group.

Functions annotation		*P-value*	*# genes*	*Predicted activation state (activation z-score)*	*Category*
Lipid	Transport	8.23E-04	9	Increased (+2.4)	19, 20, 22
	Fatty acid metabolism	3.27E-05	23	Increased (+2.4)	19, 20
Organism	Death	9.71E-05	65	Decreased (-4.3)	21
	Mass	9.11E-04	14	Increased (+2.3)	23
	Survival	1.87E-03	22	Increased (+2.6)	21
Lymphocyte	Migration	1.70E-03	13	Increased (+2.2)	2, 6, 13
	Cell movement	2.50E-03	14	Increased (+2.4)	2, 6, 13
Cell death of kidney cell lines		2.05E-03	12	Increased (+2.1)	17
Infection by HIV-1		2.69E-03	20	Increased (+2.3)	14
Organisation of cytoskeleton		3.06E-03	34	Increased (+2.0)	1, 24

Categories: 1 Cellular Function and Maintenance; 2 Hematological System Development and Function; 3 Tissue Morphology; 4 Cellular Growth and Proliferation; 5 Cell-To-Cell Signalling and Interaction; 6 Immune Cell Trafficking; 7 Inflammatory Response; 8 Cell-mediated Immune Response; 9 Cellular Development; 10 Hematopoiesis; 11 Lymphoid Tissue Structure and Development; 12 Metabolic Disease; 13 Cellular Movement; 14 Infectious Disease; 15 Tissue Development; 16 Cell Morphology; 17 Cell Death and Survival; 18 Cellular Compromise; 19 Lipid Metabolism; 20 Small Molecules Biochemistry; 21 Organismal Survival; 22 Molecular Transport; 23 Organismal Development; 24 Cellular Assembly and Organisation.

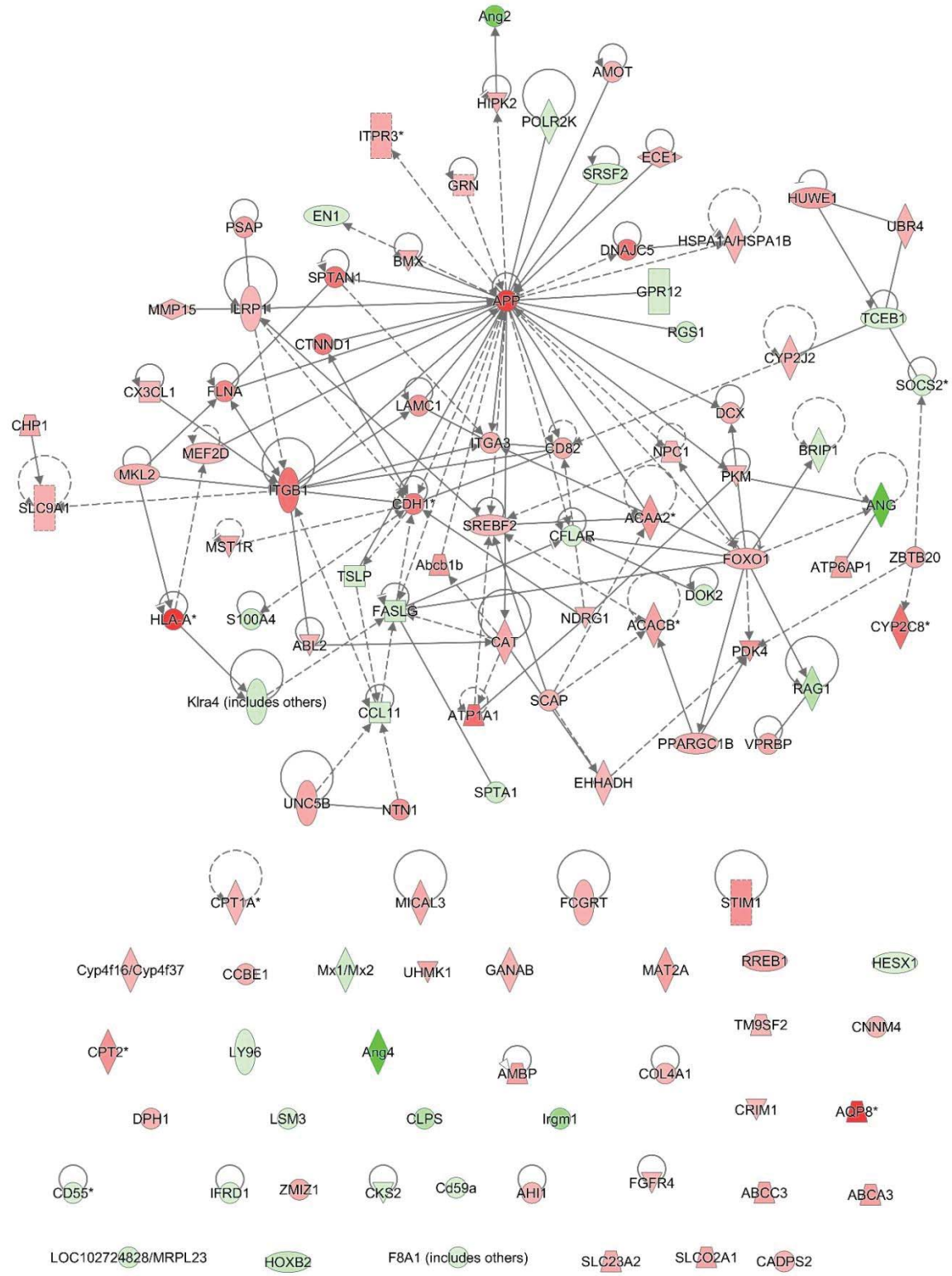

Figure 4.14 Biological interaction network of differentially expressed genes associated with the ten most significant biological functions in the colon of C57BL/6J mice fed the 45% salmon diet compared to those fed the 45% control diet. Nodes represent genes and edges represent direct (full line) and indirect (dotted line) interactions of genes. The colour coding of nodes indicate the direction of fold-change (FC), with red showing genes that are increased in mRNA expression levels and green showing decreased levels in 45% salmon-fed C57BL/6J mice. The intensity of the colour of nodes indicates the degree of FC, with greater intensity of colours pointing to higher levels of FC. Node shape indicates functional class of gene product as indicated in Appendix V. Data represent six biological replicates per group.

While *PPARA* mRNA expression levels were unaffected in the colon of 45% salmon-fed C57BL/6J mice, *PPARGC1B* gene expression was increased 1.6-fold compared to those fed the 45% control diet (Figure 4.14). GSEA further highlighted differential expression of the KEGG pathway *PPAR signalling*, with 27% of genes in the set increased (P = 0.004 (data not shown)).

4.5 Discussion

The inflammatory phenotype of *Il10*$^{-/-}$ mice, as a model of IBD, was as expected. A higher degree of colitis was observed at 12 weeks of age compared to C57BL/6J mice. Similar to the observations in Chapter 3 and published data [6, 95, 109, 116, 305, 348], colitis was characterised by infiltration of lymphocytes/plasma cells into colon tissue, loss of goblet cells, and crypt hyperplasia and aberrancy, irrespective of the type of diet. Also in agreement, the transcriptomic profiling of the colon indicated elevated immune-related events in *Il10*$^{-/-}$ mice [342, 343, 353].

The results presented in this chapter support the hypothesis that the effects on histopathological signs of colitis and associated immune and metabolic pathways were dependent on the amount of salmon included in the diet of *Il10*$^{-/-}$ mice.

Histological analysis of colon tissue showed no effect of a diet enriched with 15% salmon on the severity of colitis in *Il10*$^{-/-}$ mice compared to the corresponding control diet. However, the 15% salmon diet induced the expression of immune-related pathways in the colon of *Il10*$^{-/-}$ mice compared to those fed the 15% control diet, with the pro-inflammatory effects potentially explained by the increased oxidation state of the 15% salmon diet.

This is the first *in vivo* study to show lower levels of colitis in *Il10*$^{-/-}$ mice fed a diet enriched with 30% salmon compared to those fed a macronutrient-matched control diet. This reduction of colitis in 30% salmon-fed *Il10*$^{-/-}$ mice was linked to decreased crypt loss, goblet cells loss and lymphocyte infiltration into the colon tissue. Colon gene expression showed reduced expression of genes associated with lymphocyte function, and enhanced expression of genes comprising metabolism-related KEGG pathways, specifically associated with xenobiotics, amino acids, lipids, and cofactors/vitamins in 30% salmon-fed *Il10*$^{-/-}$ mice (vs. 30% control diet) that may have partly been mediated by *PPARA* transcriptional activity. The effects on colon tissue morphology and gene

expression were not observed in C57BL/6J mice fed the 30% salmon diet, and therefore specific to *Il10*$^{-/-}$ mice.

The 45% salmon diet did not affect the severity of colitis or gene expression profile in *Il10*$^{-/-}$ mice compared to those fed the 45% control diet. The 45% salmon diet provided a similar amount (3.6%) of total n-3 PUFA as the EPA diet (3.7%) in Chapter 3, but did not alter the colon gene expression profile in *Il10*$^{-/-}$ mice in a similar way. This could potentially be due to the high amount of fat provided by salmon (approximately 47% energy as fat in the 45% salmon diet compared to 12% in the EPA diet) which may have diminished the beneficial effects of n-3 PUFA provided by the 45% salmon diet to *Il10*$^{-/-}$ mice. It was further shown that the 45% salmon diet enhanced the expression of metabolic pathways in energy production and lipid metabolism in the colon of healthy C57BL/6J mice compared to those fed the 45% control diet.

4.5.1 Levels of LC n-3 PUFA

The dietary intake for C57BL/6J and *Il10*$^{-/-}$ mice was affected by the type of diet (the intake of the salmon diets was higher compared to corresponding controls) and percentage of fat (decreased intake with increasing amount of fat). These observations may be due to the energy density in the diets, which increased with the fat content. The percentages of n-3 PUFA provided by the salmon-enriched diets were 1.5%, 2.7% and 3.6% (15%, 30% and 45% salmon diet, respectively). The dose of n-3 PUFA in the 45% salmon-enriched diet was similar to the 3.7% EPA experiment described in Chapter 3. On average, the mice fed the 45% salmon diet ingested approximately 78 mg LC n-3 PUFA per day (DHA, EPA and DPA), while mice fed the 30% salmon diet ingested 64 mg per day and 37 mg per day for the 15% salmon diet. These levels of n-3 PUFA are within the range of those used in other rodent colitis experiments [for example references 6, 197, 252, 259, 378, 406]. Chapter 3 and other published studies have shown that feeding pure EPA led to less severe colitis in *Il10*$^{-/-}$ mice at 3.7% in the diet [6] and reduced the risk of colorectal cancer in a mouse model at 3.1% [406] and 5% [407].

Using a formula to model the daily ingested doses from mice to humans [408], the mean intakes of LC n-3 PUFA for a 60 kg human per day would be approximately 9 g (15% salmon), 15.5 g (30% salmon) and 19 g (45% salmon). A human would have to consume approximately 500 g salmon per day to reach the LC n-3 PUFA provided by the

30% salmon diet. Fish oil capsules provide varying amounts of DHA and EPA and usually range from 0.2 to 1 g DHA plus EPA [as reviewed in 409]. Recommendations for dietary n-3 PUFA intake vary between countries and the desired biological outcome (*i.e.* prevention vs. treatment) [as reviewed in 409]. In New Zealand, the recommended dietary intake is approximately 0.5 g per day of LC n-3 PUFA to reduce the risk of chronic diseases, which approximately translates to two portions of fish per week, one of which should be oily such as salmon [410]. With the mean intakes of LC n-3 PUFA in the present study ranging from 37 to 78 mg per day (9 to 19 g for humans), the recommended daily intake of 0.5 g per day above is exceeded by at least 18-fold. As reviewed by Calder [411] and Kim *et al.* [412], in dietary intervention studies among healthy individuals, as well as IBD patients, LC n-3 PUFA doses typically average approximately 5 g per day (range from 1 to 9 g). To date there is no recommended upper limit of n-3 PUFA [413]. Interestingly, the diet of Greenland Inuit was reported to contain approximately 14 g n-3 PUFA per day, slightly less than the 30% salmon diet, and chronic diseases are uncommon in Greenland Inuit [159, 414].

4.5.2 Severity of colitis in *Il10*$^{-/-}$ mice

As expected, the severity of colitis was higher in *Il10*$^{-/-}$ mice compared to C57BL/6J mice and characterised by infiltration of lymphocytes/plasma cells, loss of goblet cells, and crypt hyperplasia, indicating that the *Il10*$^{-/-}$ mouse model performed as expected. The lowest (15%) and highest (45%) doses of salmon did not reduce the severity of colitis in *Il10*$^{-/-}$ mice compared to their corresponding control diets, whereas feeding a diet containing 30% salmon resulted in decreased colitis. This may indicate that the effects of salmon diets are dependent on dose of salmon provided.

In a study performed by Woodworth *et al.* [194], mice with experimental colitis were fed four different concentrations of fish oil. The most inflamed caeca and colons were observed in the group with the highest levels of fish oil (6% fish oil; the diet provided 0.3% EPA and 3.2% DHA). The mice fed the lowest amount of fish oil (0.75% fish oil; the diet provided 0.04% EPA and 0.4% DHA) showed reduced severity of colitis compared to those fed the highest amount of fish oil. The mice from the groups fed the medium amount of fish oil (3.75% and 2.25% fish oil; the diets provided 0.2% EPA and 2% DHA, and 0.1% EPA and 1.2% DHA, respectively) showed intermediate levels of colitis. Apart from differences in mouse model and lipid source, the LC n-3 PUFA

provided by Woodworth *et al.* [194] was mostly in the form of DHA and therefore differed to the salmon diets used in this study which provided approximately equal amounts of DHA and EPA.

Another study tested the incorporation of EPA and DHA into erythrocyte phospholipids by supplementation of fish oil capsules to healthy subjects for 12 weeks [198]. The doses of fish oils were equivalent to 0.3 g, 1 g or 2 g of EPA plus DHA per day, approximately two thirds of which was EPA. It was reported that the incorporation of EPA and DHA into erythrocyte phospholipids showed a positive dose-dependent relationship, but reaching a plateau at the highest levels. Furthermore, the cytokine production by cultured and LPS-stimulated PBMCs from those subjects showed that intermediate concentrations of fish oil were associated with a greater inhibitory effect on TNF production than higher concentrations. However, in the experiment of Trebble *et al.* [198], the highest concentration of LC n-3 PUFA from fish oil (2 g) was approximately four times lower than that provided by the 15% salmon diet in the current study (9 g LC n-3 PUFA). The incorporation of EPA and DHA into cell membrane phospholipids was not tested in the current study thus it remains unknown whether cell membrane phospholipids responded differently to the varying doses.

The 15% salmon diet provided the lowest levels of LC n-3 PUFA, as well as the lowest levels of fat. An unusually high measure of lipid oxidation was noted in the 15% salmon diet, with more than ten times the recommended values [405, 415]. LC n-3 PUFA is highly susceptible to oxidation, and its oxidation products may trigger inflammatory processes [416]. The lipid oxidation state of the salmon and control diets was measured using the p-anisidine and peroxide values [405]. While the p-anisidine tests for secondary oxidation products, the peroxide level indicates primary oxidation. The European Food Safety Authority [405] recommends the peroxide level to be below ten and the p-anisidine level below 30 for foods to be safe for human consumption. During the feeding stages of the experiment, the salmon and corresponding control diets were stored identically at -20°C in vacuum-sealed bags. Peroxide values between five to ten meqO_2/kg have an oxidised aroma and flavour [405]. However, during the experiment, “off smells” were undetectable from any of the diets. Before the preparation of the diets, the lyophilised salmon was tested for oxidation status, with p-anisidine value and peroxide value within the normal range. It is possible that oxidation of the 15% salmon diet occurred during the extraction and analysis process at, or during transport to or storage at the AsureQuality

laboratory where the analysis was performed. The oxidation state of the 15% salmon diet cannot be ruled out as a contributing factor for the limited effects of this diet on the severity of colitis in *Il10*$^{-/-}$ mice.

4.5.3 Transcriptomic profiling of colon tissue

As expected, the transcriptional profile in the colon of *Il10*$^{-/-}$ mice compared to C57BL/6J mice was characterised by increased expression of genes in inflammatory processes, specifically pointing to an increase in quantity and function of immune cells (specifically lymphocytes), and reduced expression of metabolism-related genes. This gene expression profile was similar between the control diets (AIN-76A, 15% control, 30% control and 45% control) and comparable to other studies in *Il10*$^{-/-}$ mice [116, 286, 342, 343, 348, 353]. Furthermore, there was good concordance between the colon gene expression profiles observed in *Il10*$^{-/-}$ mice fed the AIN-76A diet described in Chapter 3 and the findings in the present chapter.

4.5.3.1 Pro-inflammatory gene expression in *Il10*$^{-/-}$ mice fed the 15% salmon diet (vs. 15% control diet)

Transcriptomic profiling of colon tissue showed that the pro-inflammatory gene expression of *Il10*$^{-/-}$ mice relative to C57BL/6J mice was exacerbated when mice were fed the 15% salmon diet compared to when mice were fed the 15% control diet. The analysis of the 15% salmon diet indicated elevated levels of lipid oxidation, and may explain the pro-inflammatory effect on colon gene expression in *Il10*$^{-/-}$ mice. Awada *et al.* [416] demonstrated that in healthy mice, the expression of heat shock 70kDa protein 5 (*HSPA5* gene; also known as *GRP78*) increased in the duodenum and jejunum by oxidised PUFA and their end-products, but not in more distal regions of the small intestine (*i.e.* ileum; large intestine not assessed). Increased *HSPA5* expression may act as a protective mechanism against oxidative stress by impairing essential ER functions in order to maintain cell viability [417]. In the present study, *HSPA5* was increased in expression in the colon of *Il10*$^{-/-}$ mice fed the 15% salmon diet compared to C57BL/6J mice fed the same diet, but unchanged when *Il10*$^{-/-}$ mice were fed the 15% control diet and may indicate increased oxidative stress in 15% salmon-fed *Il10*$^{-/-}$ mice.

4-Hydroxynonenal and 4-hydroxyhexanal are products of lipid oxidation, with the former being an end-product of n-6 fatty acids, and the latter from n-3 fatty acids

[418]. 4-Hydroxynonenal and 4-hydroxyhexanal are highly reactive with cellular components (*e.g.* proteins and DNA) and can damage genetic material [419]. The protein p53 plays an important contribution to maintaining genomic integrity by inducing signalling pathways involved in DNA repair [420, 421] and apoptosis [422]. It has been shown that 4-hydroxynonenal can induce the p53 signalling pathway [423, 424], and may explain the observed increase in the gene set comprising the KEGG pathway *p53 signalling* in the colon of *Il10*$^{-/-}$ mice fed the 15% salmon diet compared to those fed the 15% control diet.

An unexpected induction of *TNF* and other pro-inflammatory genes and immune-related pathways was observed in the colon of 15% salmon-fed *Il10*$^{-/-}$ mice compared to those fed the 15% control diet. *TNF* was central in connecting many of the differentially expressed genes, while other studies showed reduced expression of this gene following n-3 PUFA supplementation [3, 249, 357]. The *TNF* gene modulating effect by dietary n-3 PUFA was attributed to the activation of *PPARG* gene expression and a subsequent reduced *NFKB* activity that affects *TNF* expression [249]. In *Il10*$^{-/-}$ mice fed the 15% salmon diet increased *TNF* gene expression appeared to be independent of *PPAR* compared to those fed the 15% control diet, but an increase in *TNF* gene expression may have inhibited *NFKBIB* activity. As an inhibitor of *NFKB*, reduced *NFKBIB* gene expression would consequently allow increased translocation of *NFKB* into the nucleus and increased transcription of pro-inflammatory genes [as reviewed in 425, 426].

4.5.3.2 Enhanced metabolic pathways in *Il10*$^{-/-}$ mice fed the 30% salmon diet (vs. 30% control diet)

The intake of the 30% salmon diet (vs. 30% control diet) increased the expression of genes involved in digestion and absorption of vitamins in the colon of *Il10*$^{-/-}$ mice. These effects on vitamin-related gene expression may be attributed to the commensal microbiota [271], and potentially indicate an increase of specific microbial strains that favour the nutrient-rich environment. For example, *Bacteroides* are associated with biosynthesis of pantothenate, biotin, riboflavin, and ascorbate, while *Prevotella* and *Desulfovibrio* are specialised in thiamine and folate synthesis [276]. A recent study has shown that colon epithelial cells absorb water-soluble vitamins synthesised by the microbiota, such as niacin, and are directly available for cellular nutrition [427]. Thus an increase in vitamin-related pathways may have contributed energy to colonic epithelial cells (reduced genes

in metabolic pathways in *Il10*$^{-/-}$ mice with established colitis that may affect energy levels for colonocytes in those mice), potentially enabling better tissue repair, an important aspect of mucosal healing in IBD. This may have partly contributed to the observed reduction in severity of colitis in *Il10*$^{-/-}$ mice fed the 30% salmon diet compared to those fed the 30% control diet. Whether the colon gene expression changes in *Il10*$^{-/-}$ mice fed 30% salmon are related to the microbiota cannot be confirmed without determining the microbial community composition of the colon.

An increased expression of genes in metabolic pathways in *Il10*$^{-/-}$ mice fed the 30% salmon diet compared to those fed the 30% control diet was observed. These metabolic pathways were associated with *Lipid metabolism* such as *Fatty acid metabolism*, *Biosynthesis of unsaturated fatty acids*, and *Glycerolipid metabolism*. A similar observation was made in *Il10*$^{-/-}$ mice fed an AA-enriched diet, where the expression of proteins in metabolic processes was increased, potentially contributing to the reduced severity of colitis in those mice [268]. The salmon diet provided a mixture of fatty acids with varying lengths and saturation, thus the changes in lipid metabolism cannot be attributed to a specific fatty acid. The changes in expression of genes may be due to direct interaction with n-3 PUFA, or *via* interaction with PPARA transcription factor [428]. The induction of *PPARA* and *PPARGC1A* activity in *Il10*$^{-/-}$ mice fed the 30% salmon diet was shown by IPA *Upstream regulator analysis* which indicated an increase of their target genes, and further the induction of the KEGG pathway gene set *PPAR signalling*, compared to those fed the 30% control diet. The increase of *PPAR* has previously been reported in other studies feeding n-3 PUFA to mice with experimental colitis [3, 6, 250] and was also observed in Chapter 3. An increase of *PPARG* target gene expression was indicated in the colon of *Il10*$^{-/-}$ mice with established colitis and an increase of *PPARGC1A* target gene expression in PBMCs in response to the EPA supplementation.

PPARA and *PPARG* are widely distributed through tissues and are expressed throughout the GIT [253]. The induction of *PPAR* (shown specifically for *PPARA*) was associated with enhanced fatty acid β-oxidation in the colon of *Il10*$^{-/-}$ mice [6] and the liver of healthy mice [377]. It was suggested that dietary fatty acids may influence lipid homeostasis *via PPARG* and *PPARA* and affect overall energy balance [428], which may be especially important in IBD, an energy-deficiency disease [429]. Furthermore, the alteration of genes regulating the metabolism of fatty acid was suggested to contribute to

the pathophysiology, as shown in UC patients [267]. Thus the induction of fatty acid metabolism, potentially via *PPARA*, may have contributed to the reduced severity of colitis in *Il10*$^{-/-}$ mice in response to 30% salmon diet.

PPARA and *PPARG* can further affect the expression of genes in immune and inflammatory pathways, for example, *via* interaction with the transcription factor *CEBPD* [430, 431]. *CEBPB* and *CEBPD* were decreased in expression in the colon of *Il10*$^{-/-}$ mice fed the 30% salmon diet compared to those fed the 30% control diet. *CEBPB* has been suggested to play a role in the transcription of pro-inflammatory genes such as *IFNG* [432, 433] and *IL6* [431]. An *in vitro* study postulated that the anti-inflammatory effects of EPA may have been mediated *via* negative autoregulation of *CEBP* by transactivation of *PPARG* in a cell model system for neurodegenerative disorders [434], thus providing a feedback mechanism that decreased transcription of inflammatory gene expression [431]. This was also shown in mice with TNBS-induced colitis, where a diet supplemented with a ginger extract reduced severity of colitis and may have partially explained the decreased pro-inflammatory gene expression *via CEBPB* activation [435]. Similarly in a DSS model, parsley supplementation reduced expression of *CEBPB* in the colon, potentially contributing to reduced colitis in those mice [436]. Thus the reduction in severity of colitis may have been mediated by suppression of the transcriptional regulators *CEBPD* and *CEBPB*, potentially *via* activation of *PPARA*, and subsequent decreased expression of pro-inflammatory cytokines in response to the 30% salmon diet in the colon of *Il10*$^{-/-}$ mice.

Genes associated with the KEGG pathway *Metabolism of xenobiotics by cytochrome P450* were enhanced in expression in 30% salmon-fed *Il10*$^{-/-}$ mice compared to those fed the 30% control diet and has previously been reported in *Il10*$^{-/-}$ mice fed an EPA diet [6]. Increased expression of genes in the detoxification pathway may be connected to the increased expression of genes in metabolic pathways and the impact on the energy levels for mucosal cells in these mice. In IBD, the loss of detoxification of xenobiotics is suggested to expose the intestinal mucosal cells to toxins, leading to severe tissue destruction [264]. The increased biotransformation of xenobiotics in the colon tissue may have resulted in lower levels of toxins exposed to the colon epithelium and potentially a diminished immune response in those mice. These observations were supported by the reduction of genes in inflammatory pathways, such as *T cell receptor signalling*, *NOD-like receptor signalling*, and *Chemokine signalling* in 30% salmon-fed

Il10$^{-/-}$ mice. An excessive infiltration of immune cells into inflamed colon tissue is characteristic in IBD, and elevated detoxification of toxins may have reduced inflammatory agents towards a restoration of colonic homeostasis in 30% salmon-fed *Il10*$^{-/-}$ mice.

As shown in Chapter 3, the EPA-enriched diet (vs. OA diet) reduced the expression of *IDO1*, the gene that mediates the rate-limiting step in the metabolism of tryptophan to xanthurenic acid, in the colon of *Il10*$^{-/-}$ mice with established colitis. However, the 30% salmon diet did not affect colonic *IDO1* gene expression in *Il10*$^{-/-}$ mice. These differences may be related to the level of EPA in the diets, and the 30% salmon diet only provided 1% EPA, compared to 3.7% in Chapter 3.

4.5.3.3 Effect of the 45% salmon diet (vs. 45% control diet) dependent on genotype

The amount of n-3 PUFA provided by the 45% salmon diet (3.6%) was similar to the level of EPA (3.7%) provided to *Il10*$^{-/-}$ and C57BL/6J mice in Chapter 3. However, while the EPA diet reduced the expression of genes associated with lymphocyte function, eicosanoid signalling and elevated *PPARG* signalling pathways in the colon of *Il10*$^{-/-}$mice (vs. OA diet), no biological function was associated with the colon transcriptomic profile of *Il10*$^{-/-}$ mice fed the 45% salmon diet (vs. 45% control diet). These differences in gene expression changes between dietary EPA in *Il10*$^{-/-}$ mice (results presented in Chapter 3) and the 45% salmon diet may be related to the levels of fat associated with the 45% salmon diet rather than differences in the types of fatty acids (EPA as ethyl ester vs. mainly triglyceride in salmon) that may affect bioavailability [437].

Transcriptomic profiling of the colon from *Il10*$^{-/-}$ mice fed the 45% salmon or control diets showed increased expression of genes in pathways related to the production of ROS (compared to C57BL/6J mice fed the same diet). ROS production by immune cells such as activated neutrophils and macrophages (mechanism *via* NADPH oxidase) is considered part of the innate immune system and crucial for host defence against microbial infections [438]. However, in the colonic mucosa of IBD patients, elevated ROS production has been linked to increased tissue damage [439, 440]. It has been shown that diets with high levels of lard enhanced NADPH oxidase activity, and overproduction of ROS in a mouse model of dementia, which subsequently triggered NFKB activation [441]. This potentially provides an explanation for the detrimental effects of high levels

of dietary fat in IBD [442]. However, it is suggested that the type of fatty acid plays a role, and in the study of Bamba *et al.* [442], the diets provided mostly n-6 PUFA LA. In the current study, it is unlikely that the increased expression of genes associated with ROS production is attributed to dietary LA. The 15% and 30% control diets provided more LA than the 45% salmon diets, but no effects of these control diets were observed on genes associated with ROS production in *Il10*$^{-/-}$ mice. Hence the effects on colon gene expression in *Il10*$^{-/-}$ mice fed the 45% diets may be connected to overproduction of ROS and activation of NADPH oxidase, triggering NFKB activation and exacerbating inflammatory processes in those mice [441].

The limited changes in colon gene expression in *Il10*$^{-/-}$ mice fed the 45% salmon diet (compared to those fed the 45% control diet) further supports the supposition that the high fat content of the 45% salmon diet may have diminished the anti-inflammatory benefits of LC n-3 PUFA observed with the 30% salmon diet. However, the high levels of fat from the 45% salmon diet did not affect genes associated with ROS production in C57BL/6J mice, with the colon transcriptomic profile of C57BL/6J mice showing increased expression of genes in *PPAR signalling* compared to those fed the 45% control diet (similar to the effects of the EPA diet in Chapter 3). This indicates beneficial effects on colon gene expression induced by the 45% salmon diet in healthy mice.

4.6 Conclusion and outlook

The reported beneficial effects of salmon on colitis were dose-dependent in *Il10*$^{-/-}$ mice, and only the intermediate amount of salmon (30%) reduced colitis as assessed by histological analysis and colon transcriptomic profiling. However, gene expression only partly explains the observed phenotype as several post-translational processes can affect protein abundance. Therefore, linking gene expression changes to protein expression was anticipated to provide novel insights into the beneficial effects of a diet enriched with 30% salmon. The liver is the central site for lipid metabolism and understanding changes in gene expression in the liver in response to a diet containing salmon, rich in LC n-3 PUFA, may support the identification of candidate biomarkers from urine. Furthermore, signature shifts in the community profile of the large intestinal microbiota are anticipated to provide evidence of the effects of the 30% salmon diet that could be mined for candidate biomarkers of colitis in accessible “tissues” such as faeces.

Chapter 5

Multi-‘Omics’ approach to investigate the effects of a diet containing 30% salmon on the microbial community in the caecum and immune and metabolic pathways in colon and liver in the interleukin-10 gene-deficient mouse

5.1 Introduction

Most research has focussed on the effects of diet on gene expression in colitis that occurred in IBD, but this approach has limited success in identifying biomarkers of colitis to monitor efficacy of dietary intervention. By using a multi-'Omics' approach, an advanced method that aims to increase the coverage of dietary effects in a high-throughput "unbiased" manner, the identification of novel pathways/regulatory processes is possible. Mining these resulting datasets for biomarkers of colitis and determining how these candidate biomarkers can predict the effects of diet on colitis are important for research translation to humans.

The increase or decrease of expression levels of a gene that codes for a certain protein does not necessarily result in changed protein abundance due to several post-transcriptional processes that can influence protein abundance [119, 120]. The combined analysis of genes and proteins provided novel insights into the modulation of PPARA activity by dietary EPA, which increased expression of *PPARA* mRNA transcript levels in the colon [6], and decreased abundance of HSP90AB1, a protein that represses PPARA activity [268]. *PPARA* activation may have inhibited NFKB pathways and prevented the induction of inflammatory and immune response genes [338]. These findings highlight the importance of a combined pathway analysis to provide novel insights into underlying molecular events in colitis and diet-induced alterations.

The liver is the central organ to regulate metabolic processes and connected to the GIT *via* the enterohepatic cycle, crucial for transporting nutrients and metabolites from the GIT to the liver, and bile from the liver to the GIT [443]. In IBD, hepatic inflammation is attributed to the translocation of various bacterial species to the liver [444-446], potentially caused by a disruption in the GIT epithelial barrier integrity [447]. The transcriptional profile of the liver may provide further evidence of changes in expression of genes in metabolic pathways in subjects with colitis. Furthermore, new insights into hepatic lipid metabolism that may be affected in these subjects when fed a diet supplemented with salmon may be gained. This is supported by findings in mice fed DHA-enriched diets that showed hepatic *PPARA* activation [377].

The general inaccessibility of the human colon necessitates biomarkers in accessible surrogate "tissues" (*e.g.* urine, blood or faeces) to monitor the efficacy of

dietary intervention on colitis. In healthy individuals, untargeted metabolomic analysis of urine after the consumption of smoked salmon identified several metabolites arising from the digestion and absorption of salmon, including trimethylamine N-oxide, anserine and 1-methylhistidine [139]. However, no study has looked into the effects of dietary salmon on urinary metabolites in subjects with colitis. In Chapter 3, an EPA-enriched diet modulated the metabolism of tryptophan in *Il10*$^{-/-}$ mice as shown by a reduction of the metabolite putatively identified as xanthurenic acid in the urine, but it remains to be established whether salmon, an EPA-rich food which was shown to reduce colitis at 30% in the diet, also exerts these effects on these urinary metabolites. In addition, the large intestinal microbiota plays an important role in the development of IBD, and metabolites of bacterial metabolism can provide information about shifts in the microbial community profile in urine [140, 156, 340].

Signature shifts in the community profile of the faecal microbiota as a proxy of changes in the large intestine in humans may provide insights into host-microbe interactions and/or may be a valuable biomarker of the response to dietary salmon in colitis. While studies showed the long-term intake of specific diets modulates the faecal microbial community structure [123], the composition of the faecal microbiota from healthy female individuals was not affected by the intake of two portions of farmed salmon per week after nine months [448]. Bacterial "dysbiosis" is commonly observed in intestinal biopsies and faeces from IBD patients and characterised by complex shifts in the microbial community profile, combined with a loss of microbial diversity [449]. It has previously been shown that an EPA-enriched diet affects the microbial community composition in the caecum of *Il10*$^{-/-}$ mice potentially by affecting the fatty acid composition of the epithelial cell membrane and allowing colonisation of beneficial bacteria [277], but it is unknown if a 30% salmon diet (rich in EPA and other LC n-3 PUFA (reported in Chapter 4)) would shape the microbial community structure in a dysbiotic environment that is characteristic of colitis.

5.2 Hypothesis and aim

The main hypothesis of this study was that the analysis of protein expression provides novel molecular pathways underlying the improvements in colitis of *Il10*$^{-/-}$ mice fed a 30% salmon diet. The second hypothesis was that the liver gene expression profile, urinary metabolite profile and caecal microbial community structure in *Il10*$^{-/-}$ mice fed a

30% salmon diet are distinct from those fed a macronutrient-matched control diet. To test these hypotheses, changes in protein expression in the colon and gene expression in the liver of *Il10*$^{-/-}$ mice with established colitis were determined and further responses in these tissues to a 30% salmon diet analysed. *Il10*$^{-/-}$ and C57BL/6J mice were fed either a 30% salmon diet or a macronutrient-matched control diet for 7 weeks (described in Chapter 4). Pathway analysis of colon protein expression and hepatic transcriptional profile, urinary metabolite fingerprint and caecal microbiota were carried out at 12 weeks of age to identify (a) changes when colitis was established and (b) diet-induced alterations (beneficial or adverse) of these parameters. All molecular analyses were conducted using the 'Omics'-technologies described in Chapter 2.

5.3 Methods

The mouse experiment was conducted according to the methods described in Chapter 2, with proteomic analysis of colon tissue detailed in Section 2.8, hepatic transcriptional profiling[11] in Section 2.7, urine metabolite analysis in Section 2.9, and next-generation sequencing of caecum digesta in Section 2.10.

5.4 Results

5.4.1 Colon protein expression

5.4.1.1 Identification of proteins

A representative image of the 42 spot-features that were selected for identification is shown in Figure 5.1 (FC $\geq$ |1.5| and p-value $\leq$ 0.05). Of these, 27 spot-features were successfully identified by MS corresponding to a single protein and for 12 spot-features, the identification lead to two or more protein matches.[12] Three spot-features remained unidentified. An additional five spot-features were identified by comparison to a reference gel compiled from previous Nutrigenomics New Zealand experiments with *Il10*$^{-/-}$ and C57BL/6J mice (unpublished data) and shown in Appendix XIII. Identified proteins were linked to biological pathways as illustrated in Table 5.1.

[11] 195 ng RNA starting material.
[12] Seven of the 42 for identification selected proteins were matched to more than one spot-feature and most likely represent multiple isoforms due to post-translational modifications.

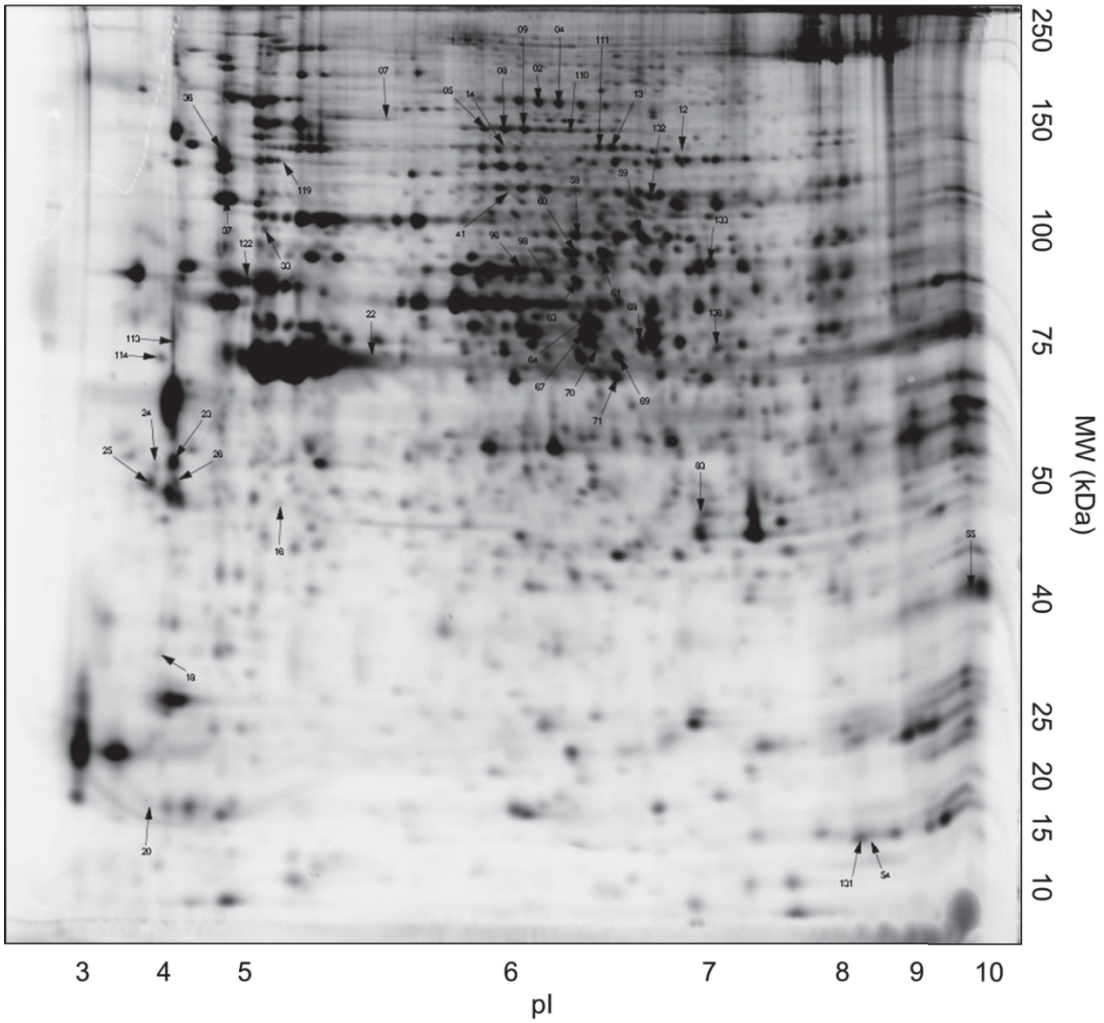

Figure 5.1 Representative gel image with selected spot-features corresponding to proteins for identification. The separation of proteins according to the isoelectric point (pI) and molecular weight (MW) was performed by two-dimensional difference gel electrophoresis (2D-DIGE). Spot-features on gel that met the cut-off criteria (FC $\geq$ |1.5| and p-value $\leq$ 0.05) were excised and digested from the gels for identification. A total of 47 spot-features are labelled, with 42 of those relevant for the current comparisons.

Table 5.1 List of differentially expressed proteins in the colon of *Il10*$^{-/-}$ and C57BL/6J mice fed the 30% control or 30% salmon diet (FC ≥ |1.5| and p-value ≤ 0.05). Values indicate fold-changes and "n.s." denotes a non-differential expression in the comparison listed. "A" or "B" indicates more than one protein was identified for a spot-feature on the gel. Proteins listed with an asterisk (*) are associated with more than one biological function in the KEGG database. Spot-features that remained unidentified were not listed.

Protein within biological function	*Protein identified*	*Spot-feature*	*Il10*$^{-/-}$ *vs. C57 (control)*	*Il10*$^{-/-}$ *vs. C57 (salmon)*	*Salmon vs. control (Il10*$^{-/-}$*)*	*Salmon vs. control (C57)*
Signal transduction						
COL6A2*	Collagen alpha-2(VI) chain	2	2.47	n.s.	-3.01	n.s.
COL6A2*	Collagen alpha-2(VI) chain	4	3.74	n.s.	-3.31	n.s.
CTNNA1*	Catenin alpha-1	7.A	n.s.	n.s.	-3.30	n.s.
CTNNA1*	Catenin alpha-1	14.A	4.25	n.s.	-4.99	n.s.
ACTB*	Actin, cytoplasmic 1	22.A	-2.10	n.s.	n.s.	n.s.
YWHAE*	14-3-3 protein epsilon	24	3.56	n.s.	n.s.	n.s.
YWHA Q or Z*	14-3-3 protein isoforms theta or zeta	25	2.05	n.s.	n.s.	n.s.
YWHA G, B, Z or H*	14-3-3 protein isoforms	26	1.80	n.s.	n.s.	n.s.
HSP90AA1 or HSP90AB1*	Heat shock protein 90kDa alpha (cytosolic), class A or B member 1	36	n.s.	n.s.	n.s.	-2.04
ENO1*	Enolase 1, alpha non-neuron	70	2.89	n.s.	n.s.	n.s.
MAPK3*	Mitogen-activated protein kinase 3	71	2.11	n.s.	n.s.	n.s.
PREDICTED: similar to alpha-enolase*		68	2.43	n.s.	n.s.	2.28
PREDICTED: similar to alpha-enolase*		136	n.s.	n.s.	2.04	n.s.
Cell communication						
COL6A2*	Collagen alpha-2(VI) chain	2	2.47	n.s.	-3.01	n.s.
COL6A2*	Collagen alpha-2(VI) chain	4	3.74	n.s.	-3.31	n.s.
CTNNA1*	Catenin alpha-1	7.A	n.s.	n.s.	-3.30	n.s.
VCL*	Vinculin	8	3.36	n.s.	n.s.	n.s.
CTNNA1*	Catenin alpha-1	14.A	4.25	n.s.	-4.99	n.s.
ACTB*	Actin, cytoplasmic 1	22.A	-2.10	n.s.	n.s.	n.s.
MAPK3*	Mitogen-activated protein kinase 3	71	2.11	n.s.	n.s.	n.s.
Cell growth and death						
YWHAE*	14-3-3 protein epsilon	24	3.56	n.s.	n.s.	n.s.
YWHA Q or Z*	14-3-3 protein isoforms theta or zeta	25	2.05	n.s.	n.s.	n.s.
YWHA G, B, Z or H*	14-3-3 protein isoforms	26	1.80	n.s.	n.s.	n.s.
MAPK3*	Mitogen-activated protein kinase 3	71	2.11	n.s.	n.s.	n.s.

Regulation of cytoskeleton/actin binding						
VCL*	Vinculin	8	3.36	n.s.	n.s.	n.s.
ACTB*	Actin, cytoplasmic 1	22.A	-2.10	n.s.	n.s.	n.s.
TPM3*	Tropomyosin alpha-3 chain	23	2.68	n.s.	-1.52	n.s.
EZR*	Ezrin	41.A	2.79	n.s.	-2.50	n.s.
TAGLN	Transgelin	55.A	-2.13	n.s.	n.s.	-2.10
WDR1	WD repeat-containing protein 1	58.A	3.23	n.s.	n.s.	n.s.
LMNA	Prelamin-A/C	58.B	3.23	n.s.	n.s.	n.s.
WDR1	WD repeat-containing protein 1	59.B	2.48	n.s.	n.s.	n.s.
TPM2	Tropomyosin beta chain	113	n.s.	n.s.	-2.67	n.s.
Endocytosis/Peroxisome/Phagosome						
ACTB*	Actin, cytoplasmic 1	22.A	-2.10	n.s.	n.s.	n.s.
PRDX1*	Peroxiredoxin-1	55.B	-2.13	n.s.	n.s.	-2.10
EHD4	EH domain-containing protein 4	59.A	2.48	n.s.	n.s.	n.s.
CORO1A*	Coronin-1A	63	4.81	n.s.	n.s.	n.s.
PITPNA	Phosphatidylinositol transfer protein alpha	77	2.05	n.s.	n.s.	n.s.
CALR*	Calreticulin	114	n.s.	n.s.	-3.02	n.s.
Proteasome/protein processing/RNA degradation						
GANAB	Neutral alpha-glucosidase AB	7.B	n.s.	n.s.	-3.30	n.s.
LONP1	Lon protease homolog, mitochondrial	9	3.94	n.s.	n.s.	2.55
PSMB9*	Proteasome subunit beta type-9	18	2.10	n.s.	-1.72	n.s.
HSP90AA1 or HSP90AB1*	Heat shock protein 90kDa alpha (cytosolic), class A or B member 1	36	n.s.	n.s.	n.s.	-2.04
HSPA5*	78 kDa glucose-regulated protein	37	2.07	n.s.	n.s.	n.s.
PREDICTED: similar to alpha-enolase*		68	2.43	n.s.	n.s.	2.28
ENO1*	Enolase 1, alpha non-neuron	70	2.89	n.s.	n.s.	n.s.
PDIA3*	Protein disulfide-isomerase A3	96	2.18	n.s.	n.s.	n.s.
CCT2	T-complex protein 1 subunit beta	98	2.61	n.s.	n.s.	n.s.
CALR*	Calreticulin	114	n.s.	n.s.	-3.02	n.s.
PREDICTED: similar to alpha-enolase*		136	n.s.	n.s.	2.04	n.s.
Cancer pathways						
CTNNA1*	Catenin alpha-1	7.A	n.s.	n.s.	-3.30	n.s.
CTNNA1*	Catenin alpha-1	14.A	4.25	n.s.	-4.99	n.s.
ACTB*	Actin, cytoplasmic 1	22.A	-2.10	n.s.	n.s.	n.s.
TPM3*	Tropomyosin alpha-3 chain	23	2.68	n.s.	-1.52	n.s.

YWHAE*	14-3-3 protein epsilon	24	3.56	n.s.	n.s.	n.s.
YWHA Q or Z*	14-3-3 protein isoforms theta or zeta	25	2.05	n.s.	n.s.	n.s.
YWHA G, B, Z or H*	14-3-3 protein isoforms	26	1.80	n.s.	n.s.	n.s.
HSP90AA1 or HSP90AB1*	Heat shock protein 90kDa alpha (cytosolic), class A or B member 1	36	n.s.	n.s.	n.s.	-2.04
EZR*	Ezrin	41.A	2.79	n.s.	-2.50	n.s.
MAPK3*	Mitogen-activated protein kinase 3	71	2.11	n.s.	n.s.	n.s.
ALDH1B1*	Aldehyde dehydrogenase X, mitochondrial	64	2.46	n.s.	n.s.	n.s.
ALDH1B1*	Aldehyde dehydrogenase X, mitochondrial	133	n.s.	n.s.	2.88	n.s.
Infectious diseases						
CTNNA1*	Catenin alpha-1	7.A	n.s.	n.s.	-3.30	n.s.
VCL*	Vinculin	8	3.36	n.s.	n.s.	n.s.
CTNNA1*	Catenin alpha-1	14.A	4.25	n.s.	-4.99	n.s.
ACTB*	Actin, cytoplasmic 1	22.A	-2.10	n.s.	n.s.	n.s.
YWHAE*	14-3-3 protein epsilon	24	3.56	n.s.	n.s.	n.s.
YWHA Q or Z*	14-3-3 protein isoforms theta or zeta	25	2.05	n.s.	n.s.	n.s.
YWHA G, B, Z or H*	14-3-3 protein isoforms	26	1.80	n.s.	n.s.	n.s.
CORO1A*	Coronin-1A	63	4.81	n.s.	n.s.	n.s.
MAPK3*	Mitogen-activated protein kinase 3	71	2.11	n.s.	n.s.	n.s.
CALR*	Calreticulin	114	n.s.	n.s.	-3.02	n.s.
Antigen processing and presentation						
PSMB9*	Proteasome subunit beta type-9	18	2.10	n.s.	-1.72	n.s.
HSP90AA1 or HSP90AB1*	Heat shock protein 90kDa alpha (cytosolic), class A or B member 1	36	n.s.	n.s.	n.s.	-2.04
PDIA3*	Protein disulfide-isomerase A3	96	2.18	n.s.	n.s.	n.s.
CALR*	Calreticulin	114	n.s.	n.s.	-3.02	n.s.
Leukocyte transendothelial migration						
CTNNA1*	Catenin alpha-1	7.A	n.s.	n.s.	-3.30	n.s.
VCL*	Vinculin	8	3.36	n.s.	n.s.	n.s.
CTNNA1*	Catenin alpha-1	14.A	4.25	n.s.	-4.99	n.s.
ACTB*	Actin, cytoplasmic 1	22.A	-2.10	n.s.	n.s.	n.s.
EZR*	Ezrin	41.A	2.79	n.s.	-2.50	n.s.

Tryptophan metabolism						
OGDH	2-oxoglutarate dehydrogenase, mitochondrial	13	3.70	n.s.	-3.18	n.s.
ALDH1B1*	Aldehyde dehydrogenase X, mitochondrial	64	2.46	n.s.	n.s.	n.s.
ALDH2*	Aldehyde dehydrogenase, mitochondrial	67	2.43	n.s.	n.s.	n.s.
OGDH	2-oxoglutarate dehydrogenase, mitochondrial	111	n.s.	n.s.	-3.26	n.s.
ALDH1B1*	Aldehyde dehydrogenase X, mitochondrial	133	n.s.	n.s.	2.88	n.s.
Nitrogen metabolism						
CA1 or 2	Carbonic anhydrase, isoform 1 or 2	83	-2.41	n.s.	2.21	n.s.
CA3	Carbonic anhydrase 3	84	-2.52	n.s.	n.s.	n.s.
Lipid metabolism						
Sult1d1	Sulfotransferase 1 family member D1	29	2.04	n.s.	n.s.	n.s.
ALDH1B1*	Aldehyde dehydrogenase X, mitochondrial	64	2.46	n.s.	n.s.	n.s.
ALDH2*	Aldehyde dehydrogenase, mitochondrial	67	2.43	n.s.	n.s.	n.s.
ALDH1B1*	Aldehyde dehydrogenase X, mitochondrial	133	n.s.	n.s.	2.88	n.s.
^ TPI1	Triosephosphate isomerase 1	135	n.s.	n.s.	2.06	n.s.
Protein digestion and absorption						
COL6A2*	Collagen alpha-2(VI) chain	2	2.47	n.s.	-3.01	n.s.
COL6A2*	Collagen alpha-2(VI) chain	4	3.74	n.s.	-3.31	n.s.
Endocrine system						
EEF2	Elongation factor 2	12	3.26	n.s.	n.s.	n.s.
ACTB*	Actin, cytoplasmic 1	22.A	-2.10	n.s.	n.s.	n.s.
HSP90AA1 or HSP90AB1*	Heat shock protein 90kDa alpha (cytosolic), class A or B member 1	36	n.s.	n.s.	n.s.	-2.04
MAPK3*	Mitogen-activated protein kinase 3	71	2.11	n.s.	n.s.	n.s.
Excretory system						
ARHGDIA	Rho GDP-dissociation inhibitor 1	16.A	2.64	2.31	n.s.	n.s.
ARHGDIA	Rho GDP-dissociation inhibitor 1	17	1.87	n.s.	n.s.	n.s.
MAPK3*	Mitogen-activated protein kinase 3	71	2.11	n.s.	n.s.	n.s.
CA2*	Carbonic anhydrase 2	83.B	-2.41	n.s.	2.21	n.s.
Oxidative stress						
TXN	Thioredoxin	20	2.46	n.s.	-2.28	2.45
ALDH16A1	Aldehyde dehydrogenase family 16 member A1	41.B	2.79	n.s.	-2.50	n.s.

PRDX1*	Peroxiredoxin-1	55.B	-2.13	n.s.	n.s.	-2.10
No pathway information						
ERAP1	Endoplasmic reticulum aminopeptidase 1	14.B	4.25	n.s.	-4.99	n.s.
UCHL1	Ubiquitin carboxyl-terminal hydrolase isozyme L1	16.B	2.64	2.31	n.s.	n.s.
ACTC1	Actin, alpha cardiac muscle 1	22.B	-2.10	n.s.	n.s.	n.s.
LMNB1	Lamin-B1	33.A	2.52	n.s.	n.s.	n.s.
LCP1	Lymphocyte cytosolic protein 1/Plastin-2	33.B	2.52	n.s.	n.s.	n.s.
S100A9	S100 calcium binding protein A9	54	n.s.	n.s.	n.s.	2.04
DYPSL2	Dihydropyrimidinase-related protein 2	60	2.62	n.s.	n.s.	n.s.

^ Information from [450]

5.4.1.2 Colon protein expression between mouse genotypes fed the 30% control diet

35 proteins were differentially expressed between *Il10*$^{-/-}$ mice fed the 30% control diet and C57BL/6J mice on the same diet (4 decreased and 31 increased). The biological functions associated with the differentially expressed proteins mostly clustered into *Immune system* (KEGG pathways *Antigen processing and presentation* and *Leukocyte transendothelial migration*), *Infectious diseases*, *Genetic information processing* (*Protein processing* and *Proteasome*), *Cancer*, and *Metabolism* (*Tryptophan*, *Nitrogen* and *Lipid*) in the colon of *Il10*$^{-/-}$ mice fed the 30% control diet compared to C57BL/6J mice (Table 5.1).

Within the KEGG pathway *Oxidative stress*, the induction of proteins TXN and ALDH16A1 in the colon of *Il10*$^{-/-}$ mice fed the 30% control diet compared to C57BL/6J mice (approximately 2.5-fold) indicated elevated levels of oxidative stress in those mice. PRDX1 showed lower expression in the same comparison, however, it appears two proteins co-migrated as one overlapping spot on the gel (spot-feature 55) and PRDX1 protein expression changes are therefore uncertain (Table 5.1). Elevated oxidative stress can increase protein misfolding in the ER, which was indicated by the higher expression levels of the proteins LONP1 and HSPA5, two proteins that process proteins that are degraded, misfolded or oxidatively damaged (FC = 3.9 and 2.1, respectively, in *Il10*$^{-/-}$ mice vs. C57BL/6J mice both fed the 30% control diet).

The processing of functional proteins in the ER is an important aspect to the presentation of antigens in immune cells. As shown in Figure 5.2, the proteins PSMB9 (labelled as LMP2 in the figure) and PDIA3 were increased in expression in *Il10*$^{-/-}$ mice fed the 30% control diet (approximately 2-fold vs. C57BL/6J mice). These changes in molecular events leading to antigen presentation in the colon of *Il10*$^{-/-}$ mice were supported by transcriptomic analysis (as presented in Chapter 4), indicating an important role underlying colitis in *Il10*$^{-/-}$ mice. The increase in immune-related processes was further supported by the elevated expression of MAPK3, a ubiquitous protein involved in several inflammatory processes (KEGG pathway *Endocrine system*), in the colon of *Il10*$^{-/-}$ mice fed the 30% control diet (FC = 2.1 vs. C57BL/6J mice (Table 5.1)).

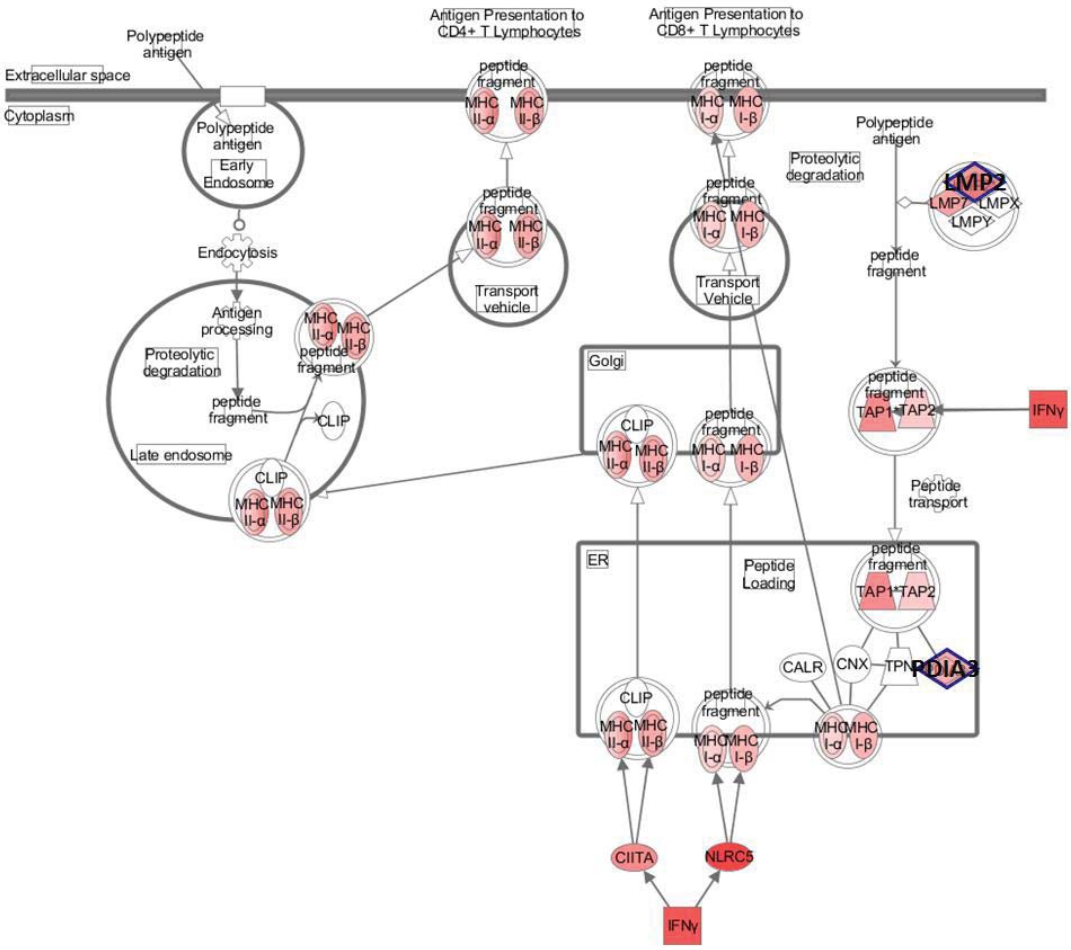

Figure 5.2 Ingenuity pathway for *Antigen presentation* indicating molecular events that lead to the presentation of antigens to $CD4^+$ and $CD8^+$ T cells during colitis. Nodes represent genes and red colour coding of nodes indicates increased expression in the colon of *Il10*$^{-/-}$ mice fed the 30% control diet (relative to C57BL/6J mice fed the same diet). Expression data were established by either transcriptomic analysis of colon tissue, or proteomic analysis as indicated by a coloured border of nodes. For proteomic data, the protein was linked to its coding gene in IPA before pathway analysis. The intensity of the colour of nodes indicates the degree of fold-change (FC), with greater intensity of colours pointing to higher levels of FC. Node shape indicates functional class of gene product as indicated in Appendix V. Molecules with contrasting border indicate those discussed in the text. Data represent six biological replicates per group.

Several proteins related to *Metabolism* (KEGG pathways *Nitrogen metabolism*, *Tryptophan metabolism* and *Lipid metabolism*) were affected in the colon of *Il10*$^{-/-}$ mice compared to C57BL/6J mice (both fed the 30% control diet), largely attributed to increased expression of the mitochondrial dehydrogenase proteins ALDH1B1, ALDH2, and OGDH (FC = 2.4 to 3.7 (Table 5.1)).

5.4.1.3 Effect of the 30% salmon diet (vs. 30% control diet) on colon protein expression in *Il10*$^{-/-}$ mice

16 proteins were differentially expressed between the colon of *Il10*$^{-/-}$ mice fed the 30% salmon diet and those fed the 30% control diet (4 increased and 12 decreased (Table 5.1)). Increases in metabolic pathways in the colon of *Il10*$^{-/-}$ mice fed the 30% salmon diet were observed compared to those fed the 30% control diet, attributed to changes in expression levels of proteins CA1 or 2, OGDH, ALDH1B1, TPI1, and a protein predicted to be similar to ENO1. These proteins mostly clustered in metabolism of lipids, tryptophan and nitrogen (Table 5.1).

In the KEGG pathway *Tryptophan metabolism*, increased expression of ALDH1B1 suggested elevated melatonin biosynthesis from tryptophan in the colon of 30% salmon-fed *Il10*$^{-/-}$ mice, while reduced expression of OGDH may indicate reduction in tryptophan catabolism *via* kynurenine. It is of note that ALDH1B1 was linked to two spot-features on the gel (#64 and #133), and while spot #133 was increased approximately 3-fold in *Il10*$^{-/-}$ mice fed the 30% salmon diet (vs. those fed the 30% control diet), spot #64 was not differentially expressed and may indicate a post-translational modification (Table 5.1). The expression of TPI1 was also increased in the colon of 30% salmon-fed *Il10*$^{-/-}$ mice compared to those fed the 30% control diet (Table 5.1). As part of fatty acid β-oxidation, TPI1 catalyses the conversion of glycerol to glyceraldehyde-3-phosphate. Thus the intake of the 30% salmon diet may have influenced the degradation of fatty acids in the colon of *Il10*$^{-/-}$ mice compared to those fed the 30% control diet.

Two proteins associated with oxidative stress were decreased in expression in *Il10*$^{-/-}$ mice fed the 30% salmon diet compared to those fed the 30% control diet (Table 5.1). These were TXN and ALDH16A1, with approximately 2 to 2.5-fold decrease in *Il10*$^{-/-}$ mice fed 30% salmon ($P = 0.01$), and may indicate a reduction in oxidative stress in these mice.

In contrast to the colon transcriptomic profile reported in Chapter 4, the proteomic profile from *Il10*$^{-/-}$ mice fed the 30% salmon diet did not provide evidence that *PPAR signalling* was affected compared to those fed the 30% control diet. However within C57BL/6J mice, the expression of HSP90 (isoform AA1 or AB1) was reduced in those fed 30% salmon diet compared to the control diet (FC = -2 (Table 5.1)) and indicates an effect of the 30% salmon diet on *PPAR signalling* in healthy mice.

The intake of the 30% salmon diet affected protein expression associated with *Antigen presentation* in the colon of *Il10*$^{-/-}$ mice compared to those fed the 30% control diet (Table 5.1), with reduced expression of PSMB9 (labelled as LMP2 in Figure 5.3) and the chaperone protein calreticulin (CALR) in 30% salmon-fed *Il10*$^{-/-}$ mice. These findings were supported by transcriptomic profiling, showing differential expression of two genes that encode major histocompatibility complex (MHC) class I molecules (*HLA-G* and *HLA-B*), with 2-fold decrease within the same comparison. Thus it appears that the intake of the 30% salmon diet specifically affected the processing of antigens (degradation and loading) in the colon of *Il10*$^{-/-}$ mice, and expression of genes encoding MHC class I molecules in the $CD8^+$ T lymphocyte pathway (Figure 5.3).

5.4.2 Liver gene expression

Microarray analysis was performed to elucidate changes in gene expression in the liver from *Il10*$^{-/-}$ mice (compared to C57BL/6J mice) and to reveal gene expression changes that were modulated by the intake of a diet enriched with 30% salmon (compared to those fed the 30% control diet). Table 5.2 provides an overview of the total number of differentially expressed genes in the different comparisons (FC $\geq$ |1.5| and p-value $\leq$ 0.005). The highest number of differentially expressed genes were measured in the liver from *Il10*$^{-/-}$ mice versus C57BL/6J mice fed the 30% control diet and these genes were mostly increased in expression. The intake of the 30% salmon diet affected the expression of more genes in the liver from C57BL/6J mice (vs. C57BL/6J mice fed the 30% control diet) than within *Il10*$^{-/-}$ mice (vs. *Il10*$^{-/-}$ mice fed the 30% control diet (Table 5.2)).

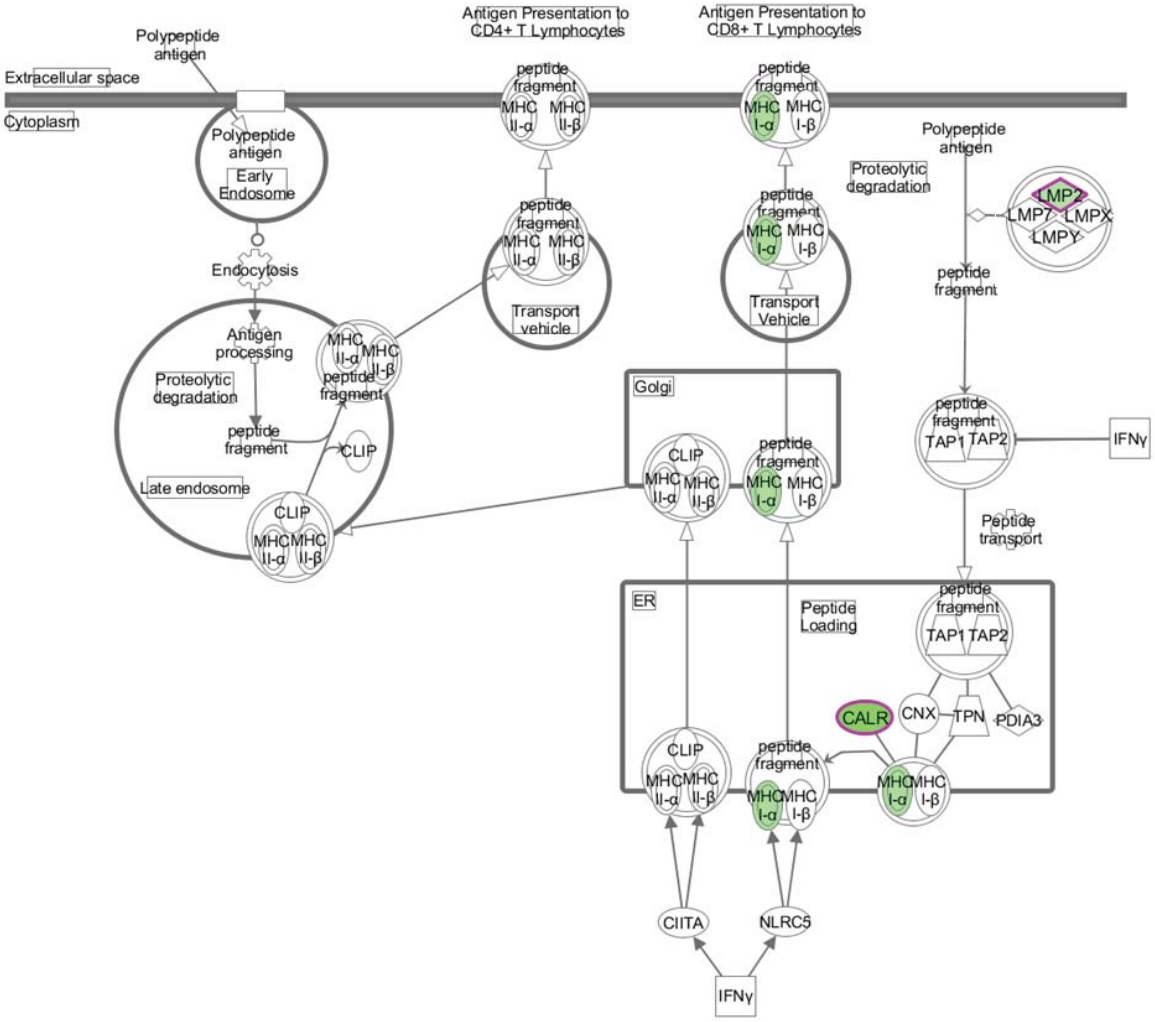

Figure 5.3 Ingenuity pathway for *Antigen presentation* indicating molecular events that lead to the presentation of antigens to $CD4^+$ and $CD8^+$ T cells in *Il10*$^{-/-}$ mice fed the 30% salmon diet. Nodes represent genes and green colour coding of nodes indicate decreased expression in the colon of *Il10*$^{-/-}$ mice fed the 30% salmon diet (relative to *Il10*$^{-/-}$ mice fed the 30% control diet). Expression data were established by either transcriptomic analysis of colon tissue, or proteomic analysis as indicated by a coloured border of nodes. For proteomic data, the protein was linked to its gene in IPA before pathway analysis. The intensity of the colour of nodes indicates the degree of fold-change (FC), with greater intensity of colours pointing to higher levels of FC. Node shape indicates functional class of gene product as indicated in Appendix V. Transcriptomic data represent six (*Il10*$^{-/-}$ mice 30% control) and five (*Il10*$^{-/-}$ mice 30% salmon) biological replicates. Molecules with contrasting border indicate those discussed in the text. Proteomic data represent six biological replicates per group.

Table 5.2 Numbers of differentially expressed genes in the liver of C57BL/6J and *Il10*$^{-/-}$ mice. Genes passing a fold-change (≥ |1.5|) and p-value (≤ 0.005) cut-off were considered differentially expressed. Data represent six biological replicates per group.

Contrast	*mRNA transcript levels*[1]	
	Decreased	*Increased*
Genotype comparison (Il10$^{-/-}$ *relative to C57BL/6J mice)*		
30% Control	107	313
30% Salmon	95	137
Diet comparison (Salmon relative to control diet)		
C57BL/6J mice	117	120
Il10$^{-/-}$ mice	38	37

(1) FC ≥ |1.5| and p-value ≤ 0.005; genes may be represented with more than one probe on the array.

5.4.3.1 Liver gene expression between mouse genotypes fed the 30% control diet

In the liver of *Il10*$^{-/-}$ mice fed the 30% control diet, differentially expressed genes were mostly associated with the cell-mediated immune response (Table 5.3), and among the genes with the largest FC were those related to the immune system, for example, *S100A8* and *S100A9* (4-fold increased) compared to C57BL/6J mice fed the same diet. The ten highest p-value-ranked biological functions were mostly linked to cells, blood cells, myeloid cells, leukocytes and phagocytes, with the functions predicted to be increased in activation states (*activation z-score* ≥ 2 (Table 5.3)). These functions were based on 79 unique genes that were further merged into a biological interaction network (Figure 5.4). Central genes that connected many genes in the network were transcription factors *NOTCH1* (FC = 2.4), *CEBPD* (FC = 1.8) and interferon gamma-inducible protein 16 (*IFI16*; FC = -1.6), and cytokine *IL1B* (FC = 2.1), indicating key roles for these genes in inflammatory processes in the liver of *Il10*$^{-/-}$ mice fed the 30% control diet compared to C57BL/6J mice (Figure 5.4).

Increased signalling pathways associated with the *Immune system* were also shown by GSEA (Figure 5.5), with elevated expression of KEGG pathways *Cytosolic DNA-sensing* and *NOD-like receptor signalling* indicating changes specifically in host defence by receptor recognition and other immune-related pathways in *Il10*$^{-/-}$ mice compared to C57BL/6J mice both fed the 30% control diet.

In the liver of *Il10*$^{-/-}$ mice fed the 30% control diet (vs. C57BL/6J mice), the KEGG pathway *Xenobiotics biodegradation and metabolism* was decreased (P = 0.019 (Figure 5.5)). As shown in Table 5.4, the expression of genes that mediate the phase I (family of CYPs) and phase III (*ABCC3*) biotransformation of xenobiotics was reduced in those mice. Genes coding phase II enzymes showed contrasting expression levels, with reductions observed for glutathione S-transferases (*GST*) but increases for UDP glucuronosyltransferase 1 family, polypeptide A8 (*UGT1A9*) and heparan sulfate (glucosamine) 3-O-sulfotransferase 6 (HS3ST6 (Table 5.4)). This may suggest reduced functionality of CYPs in the liver of *Il10*$^{-/-}$ mice which potentially affects the metabolism of xenobiotics in those mice.

Table 5.3 Most significantly affected biological functions in the liver of *Il10*$^{-/-}$ relative to C57BL/6J mice (both fed the 30% control diet). Functions with an *activation z-score* < |2| were excluded and biological functions limited to show the ten highest p-value-ranked functions. "# genes" indicates the number of genes associated with the biological function and individual genes may be represented in more than one function. Data represent six biological replicates per group.

Functions annotation		*P-value*	*# genes*	*Predicted activation state (activation z-score)*	*Category*
Inflammatory response		1.42E-16	47	Increased (+3.9)	7
Cells	Activation	4.81E-17	55	Increased (+4.1)	5
Blood cells	Activation	3.05E-16	46	Increased (+4.1)	2, 5
	Adhesion	3.07E-16	33	Increased (+2.9)	5, 15
Myeloid cells	Activation	5.88E-17	31	Increased (+3.0)	2, 5, 6, 7
Leukocytes	Activation	9.08E-17	45	Increased (+3.9)	2, 5, 6, 7
	Cell movement	4.27E-19	52	Increased (+3.2)	2, 6, 13
	Immune response	1.78E-17	31	Increased (+2.9)	5, 7
	Migration	8.54E-20	57	Increased (+3.0)	6, 13
Phagocytes	Cell movement	1.44E-18	43	Increased (+3.4)	2, 6, 7, 13

Categories: 1 Cellular Function and Maintenance; 2 Hematological System Development and Function; 3 Tissue Morphology; 4 Cellular Growth and Proliferation; 5 Cell-To-Cell Signaling and Interaction; 6 Immune Cell Trafficking; 7 Inflammatory Response; 8 Cell-mediated Immune Response; 9 Cellular Development; 10 Hematopoiesis; 11 Lymphoid Tissue Structure and Development; 12 Metabolic disease; 13 Cellular Movement; 14 Infectious Disease; 15 Tissue Development; 16 Cell Morphology; 17 Cell Death and Survival; 18 Cellular Compromise; 19 Lipid Metabolism; 20 Small Molecules Biochemistry; 21 Organismal Survival; 22 Molecular Transport; 23 Organismal Development; 24 Cellular Assembly and Organisation.

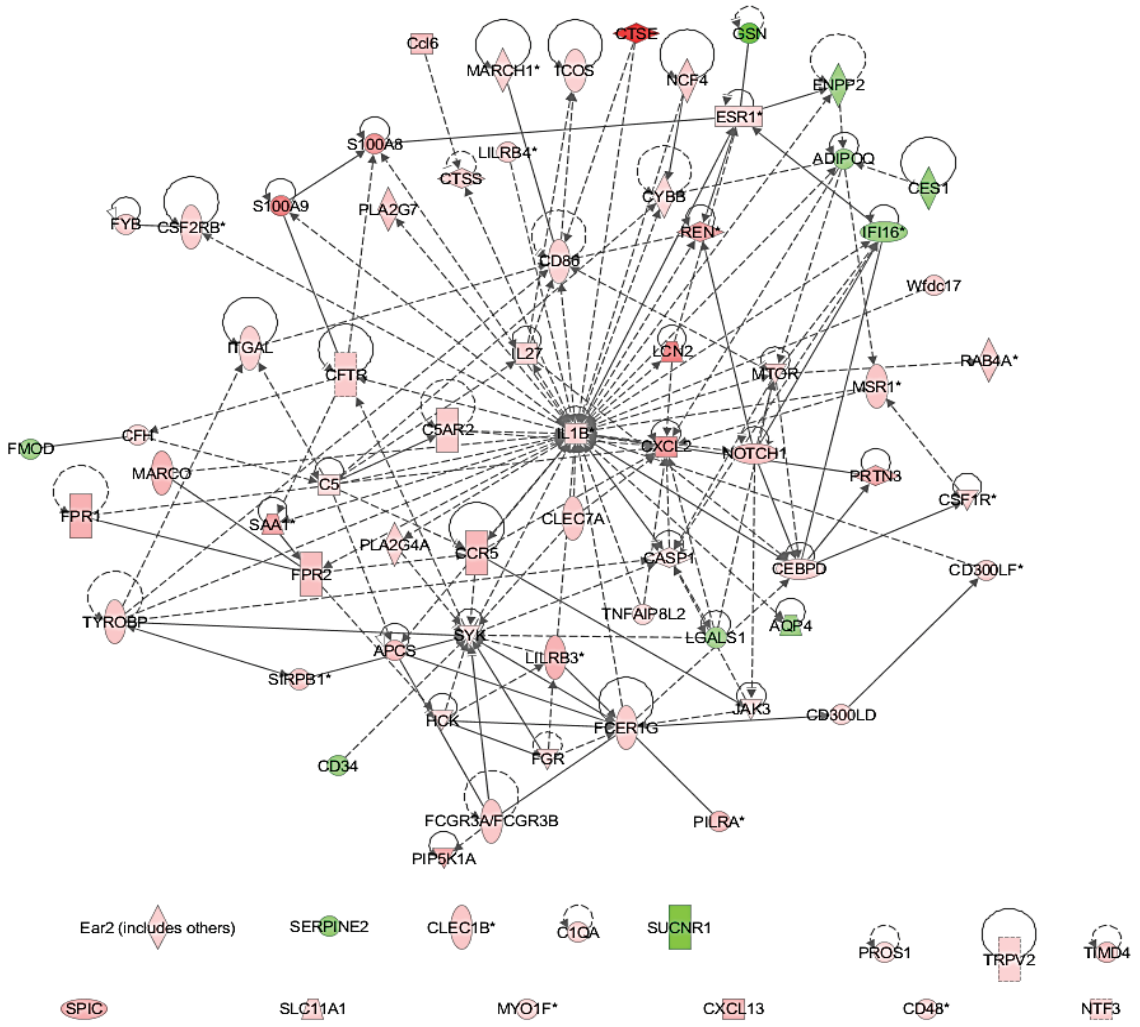

Figure 5.4 Biological interaction network of differentially expressed genes associated with the ten most significant biological functions in the liver of *Il10*$^{-/-}$ mice compared to C57BL/6J mice both fed the 30% control diet. Nodes represent genes and edges represent direct (full line) and indirect (dotted line) interactions of genes. The colour coding of nodes indicate the direction of fold-change (FC), with red showing genes that are increased in expression and green showing decreased mRNA expression levels in liver of *Il10*$^{-/-}$ mice. The intensity of the colour of nodes indicates the degree of FC, with greater intensity of colours pointing to higher levels of FC. Node shape indicates functional class of gene product as indicated in Appendix V. Data represent six biological replicates.

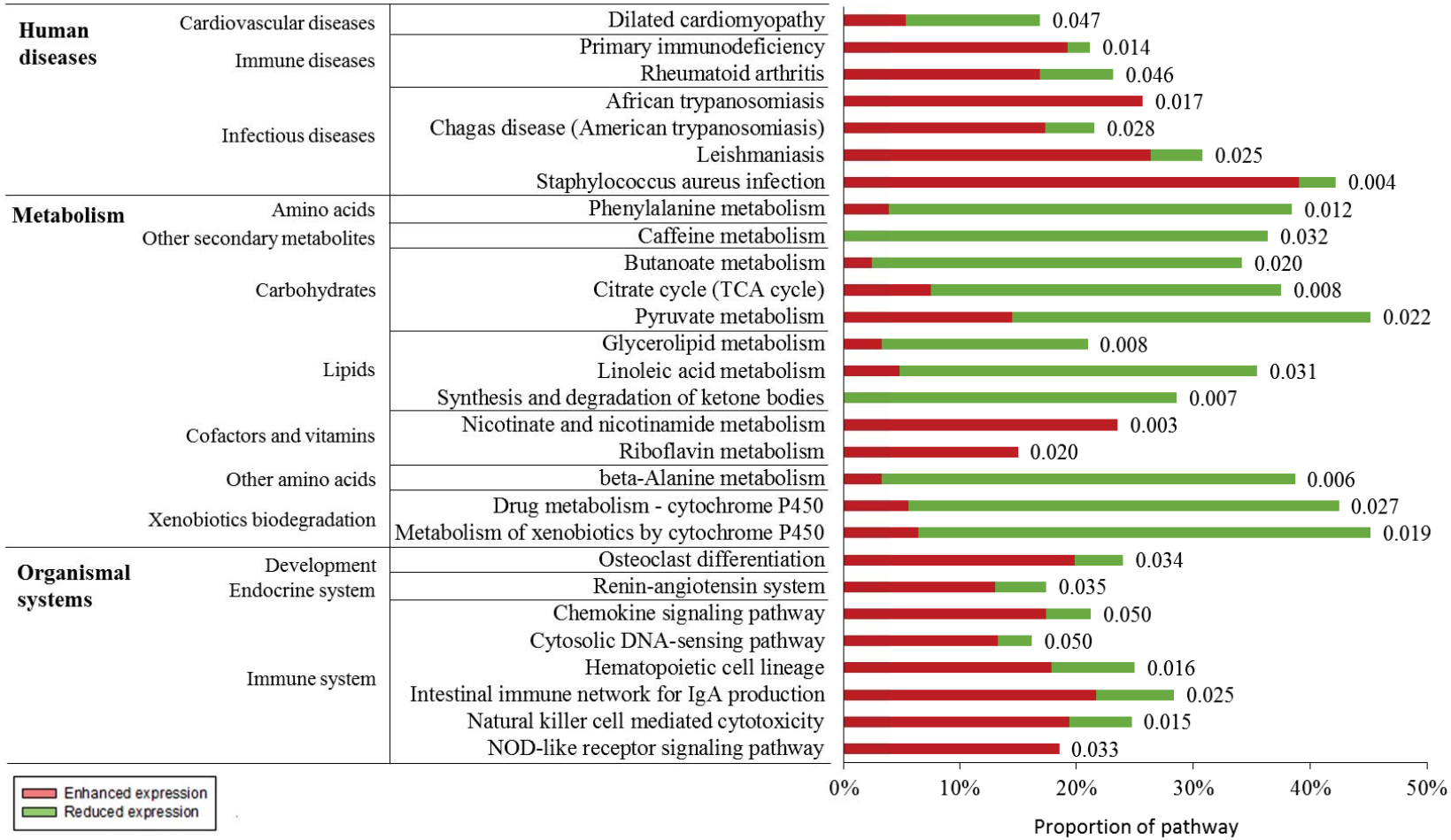

Figure 5.5 KEGG pathway gene sets differentially expressed in the liver of *Il10*$^{-/-}$ mice compared to C57BL/6J mice fed the 30% control diet ($P \leq 0.05$). Bars indicate the proportion of the KEGG pathway affected (%): red bars are the proportion of genes contributing to an increased KEGG pathway and green bars are the proportion of genes contributing to a decreased KEGG pathway. Significance of changes in KEGG pathway expression was determined by GSEA using rotation gene set testing (ROAST function) in R. The p-value significance is indicated by numbers next to bars. Data represent six biological replicates per treatment group.

Table 5.4 Differentially expressed genes associated with *Xenobiotic metabolism* in the liver of *Il10*$^{-/-}$ mice compared to C57BL/6J mice, both fed either the 30% control diet, or the 30% salmon diet. Values indicate fold-changes (FC) or p-values as per microarray analysis and are shown for *Il10*$^{-/-}$ mice fed the 30% control diet or for *Il10*$^{-/-}$ mice fed the 30% salmon diet (vs. C57BL/6J mice fed the same diet). Data represent six biological replicates per treatment.

Genes associated with xenobiotic metabolism	*30% control*		*30% salmon*	
	FC	*P-value*	*FC*	*P-value*
Phase I				
CYP3A5 (mouse ortholog *Cyp3a11*)	-5.9	5.9E-09	-5.0	6.3E-07
CYP3A7 (mouse ortholog *Cyp3a13*)	1.5	2.4E-03	-1.0	7.6E-01*
Cytochrome P450, family 3, subfamily a, polypeptide 16 (*Cyp3a16*)	-5.5	1.2E-04	-2.8	1.2E-02*
Cytochrome P450, family 3, subfamily a, polypeptide 41B (*Cyp3a41b*)	-11.5	1.9E-06	-7.3	4.5E-05
Phase II				
Glutathione S-transferase, alpha 2 (*GSTA2*)	-2.6	6.0E-04	-2.1	3.9E-03
Glutathione S-transferase, alpha 4 (*GSTA4*)	-1.7	3.2E-04	-1.7	7.7E-05
Glutathione S-transferase, mu 1 (*GSTM1*)	-1.5	4.1E-05	-1.1	3.3E-01*
Glutathione S-transferase, theta 1 (*GSTT1*)	-1.6	1.2E-04	-1.2	1.1E-01*
Heparan sulfate (glucosamine) 3-O-sulfotransferase 6 (*HS3ST6*)	1.9	6.1E-04	1.0	9.6E-01*
UDP glucuronosyltransferase 1 family, polypeptide A8 (*UGT1A9* (includes others))	3.8	6.9E-07	3.3	5.6E-06
Phase III				
ATP-binding cassette, sub-family C (CFTR/MRP), member 3 (*ABCC3*)	-1.6	6.4E-04	-1.6	8.0E-04

(*) not considered differentially expressed by microarray analysis (FC $\geq$ 1.5 and P $\leq$ 0.005).

GSEA further showed 12 KEGG pathways were decreased in expression in the liver of *Il10*$^{-/-}$ mice compared to C57BL/6J mice both fed the 30% control diet, and were mostly metabolism-related pathways, *e.g.* lipids, carbohydrates and amino acids ($P \leq 0.05$ (Figure 5.5)). Dysregulation of metabolic pathways may indicate reduced energy production in livers of *Il10*$^{-/-}$ mice, also shown by reduced gene expression in the KEGG pathway gene set *Citrate cycle* ($P = 0.008$). As this was not shown by single-gene analysis in IPA, the dysregulation appears to include many genes with subtle mRNA expression level changes, rather than a limited number of genes with large fold-changes.

5.4.3.2 Effect of the 30% salmon diet (vs. 30% control diet) on liver gene expression in *Il10*$^{-/-}$ mice

Despite the lowest number of differentially expressed genes, the hepatic transcriptomic profile of *Il10*$^{-/-}$ mice fed the 30% salmon diet showed many of those genes were associated with metabolic pathways compared to those fed the 30% control diet (Figure 5.6), specifically *Xenobiotic metabolism* and *Lipid metabolism* (Table 5.5). These findings were irrespective of the type of transcriptomic analysis (single-gene or GSEA).

Genes associated with the metabolism of xenobiotics were among those with the largest FC, for example, genes encoding phase I (*CYP26A1*, *CYP2B9*, *CYP2B13*), phase II (*GSTA1* and *GSTA2*), and phase III (*ABCC3*) detoxification enzymes (FC = 1.6-5.3; $P < 0.005$ (Table 5.5)). As a gene set, the KEGG pathway *Metabolism of xenobiotics by cytochrome P450* showed approximately 45% of genes were increased in the liver of 30% salmon-fed *Il10*$^{-/-}$ mice ($P = 0.02$), further confirming enhanced detoxification processes mediated by CYPs compared to those fed the 30% control diet (Figure 5.6). The regulation of xenobiotic gene expression may have been mediated by the ligand-dependent Nuclear receptor subfamily 1, group I, member 3 (*NR1I3*; also known as *CAR*). *NR1I3* mRNA expression levels did not pass the significance cut-off in 30% salmon-fed *Il10*$^{-/-}$ mice based on microarray data (Table 5.5), but the nuclear receptor was significantly associated with the dataset as shown by *Upstream regulator analysis* in IPA (*p-value of overlap* = 1.2E-09). As this increase in *NR1I3* was also observed in C57BL/6J mice fed the 30% salmon diet (FC = 1.7 vs. C57BL/6J mice fed the 30% control diet (Table 5.5)), this effect was not specific to colitis.

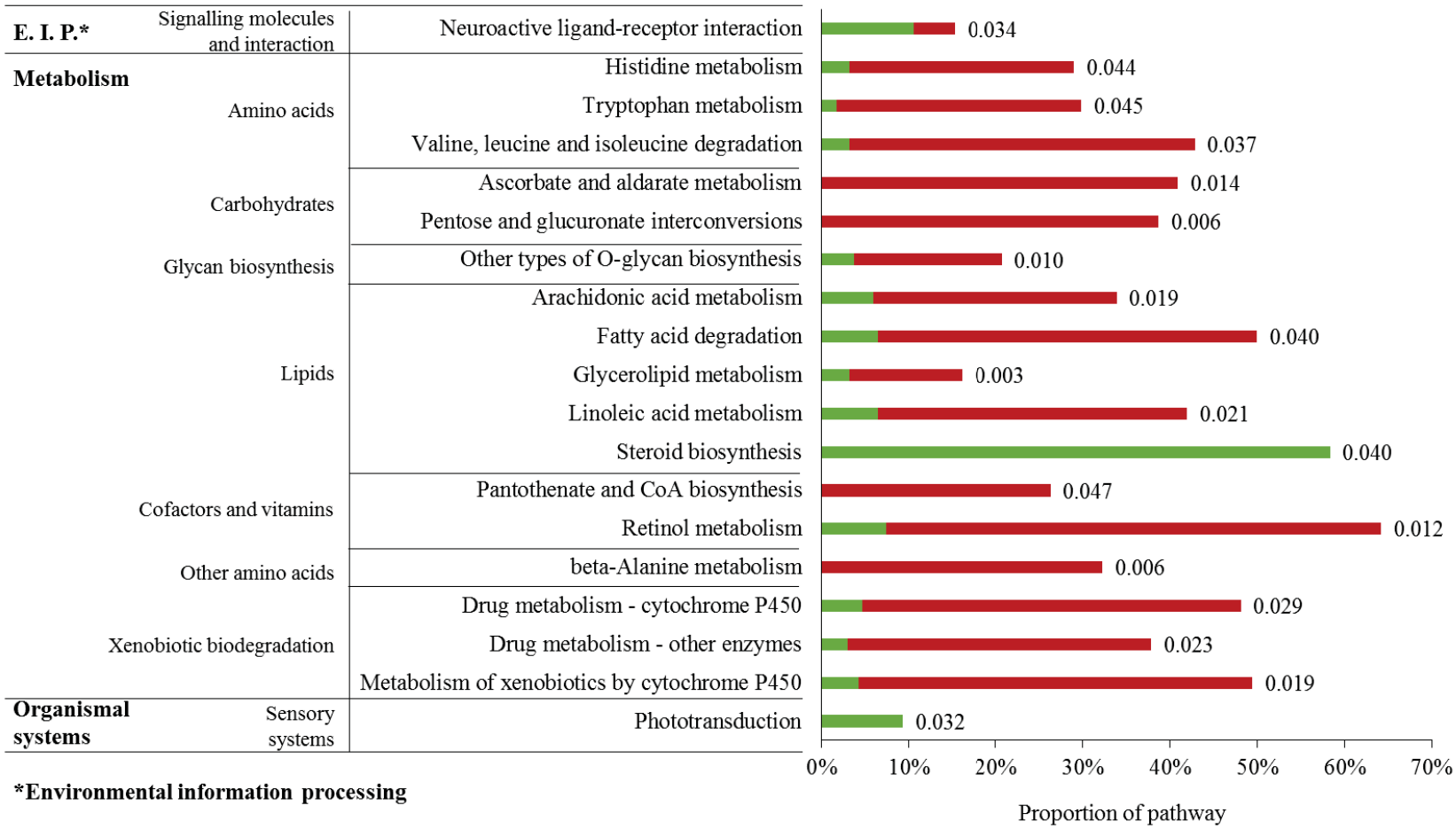

Figure 5.6 KEGG pathway gene sets differentially expressed in the liver of *Il10*$^{-/-}$ mice fed the 30% salmon diet compared to those fed the 30% control diet ($P \leq 0.05$). Bars indicate the proportion of the KEGG pathway affected (%): red bars are the proportion of genes contributing to an increased KEGG pathway and green bars are the proportion of genes contributing to a decreased KEGG pathway in 30% salmon-fed *Il10*$^{-/-}$ mice. Significance of changes in KEGG pathway expression was determined by GSEA using rotation gene set testing (ROAST function) in R. The p-value significance is indicated by numbers next to bars. Data represent six biological replicates per treatment group.

Table 5.5 Differentially expressed genes associated with *Lipid metabolism* and *Xenobiotics metabolism* in the liver of C57BL/6J mice or *Il10*$^{-/-}$ mice fed the 30% salmon diet compared to those fed the 30% control diet. Values indicate fold-changes (FC) or p-values as per microarray analysis and are shown for either C57BL/6J mice (30% salmon *vs.* 30% control) or *Il10*$^{-/-}$ mice (30% salmon *vs.* 30% control). Data represent six biological replicates per group.

Genes within biological pathway	*C57BL/6J*		*Il10*$^{-/-}$	
	FC	*P-value*	*FC*	*P-value*
Lipid metabolism				
Nuclear receptor subfamily 1, group I, member 3 (*NR1I3*; *CAR*)	1.7	4.5E-03	-1.0	8.9E-01*[#]
Nuclear receptor subfamily 1, group I, member 2 (*NR1I2*; *PXR*)	2.0	2.0E-02	1.3	3.8E-01*[^]
ELOVL Fatty acid elongase 2 (*ELOVL2*)	-1.6	1.6E-05	-1.6	1.6E-05
ELOVL fatty acid elongase 5 (*ELOVL5*)	-1.7	4.0E-05	-1.4	2.8E-03*
Stearoyl-CoA desaturase (delta-9-desaturase) (*SCD*)	-2.7	1.3E-03	-3.8	6.4E-05
CCAAT/enhancer binding protein delta (*CEBPD*)	-1.3	1.0E-01*	-1.9	6.1E-04
Acyl-CoA thioesterase 2 (*ACOT2*)	2.4	3.8E-04	2.0	5.7E-03*
Acyl-CoA thioesterase 3 (*Acot3*)	2.3	1.2E-03	2.7	2.1E-04
Acyl-CoA thioesterase 4 (*ACOT4*)	1.6	8.7E-04	1.6	2.1E-03
Acyl-CoA synthetase long-chain family member 1 (*ACSL1*)	-1.1	6.9E-02*	1.6	1.2E-03
1-acylglycerol-3-phosphate O-acyltransferase 9 (*AGPAT9*)	2.1	9.0E-09	2.0	1.1E-07
Solute carrier family 13 (sodium-dependent citrate transporter), member 5 (*SLC13A5*)	-1.3	8.4E-02*	-1.7	4.0E-04
Epoxide hydrolase 1, microsomal (*EPHX1*)	1.6	5.1E-05	1.5	8.7E-05
Renin 2 tandem duplication of Ren1 (*Ren2*)	-1.1	6.2E-01*	-2.3	2.2E-03
Xenobiotic metabolism				
Phase I				
Cytochrome P450, family 26, subfamily A, polypeptide 1 (*CYP26A1*)	5.5	2.3E-04	5.3	5.0E-04
Cytochrome P450, family 39, subfamily A, polypeptide 1 (*CYP39A1*)	-2.5	2.7E-05	-1.8	1.0E-03
Cytochrome P450, family 2, subfamily b, polypeptide 9 (*CYP2B9*)	1.5	2.6E-02*	1.7	1.4E-03
Cytochrome P450, family 2, subfamily b, polypeptide 13 (*CYP2B13*)	1.5	5.7E-04	1.6	1.5E-04
Phase II				
Glutathione S-transferase, alpha 1 (*GSTA1*)	2.0	6.1E-03*	2.3	1.4E-03
Glutathione S-transferase, alpha 2 (*GSTA2*)	2.2	2.5E-03	2.7	3.9E-04
Phase III				
ATP-binding cassette, sub-family C (CFTR/MRP), member 3 (*ABCC3*)	1.7	6.1E-05	1.7	1.5E-04

(*) not considered differentially expressed by microarray analysis (FC ≥ 1.5 and P ≤ 0.005).

([#]) IPA "Upstream regulator analysis" *p-value of overlap* = 1.18E-09.

(^) IPA "Upstream regulator analysis" *p-value of overlap* = 1.65E-04.

The metabolism of lipids was affected by the intake of the 30% salmon diet in the liver of *Il10*$^{-/-}$ mice, attributed to changes in mRNA expression levels of genes from the families of fatty acid elongases and acyl-CoA thioesterases, and a stearoyl-CoA desaturase (*SCD*) (Table 5.5). Supporting this data, the hepatic gene expression in *Il10*$^{-/-}$ mice fed the 30% salmon diet was associated with the biological function *Oxidation of fatty acid* compared to those fed the 30% control diet (P = 0.006), with a predicted increase in activation (*activation z-score* = 2 (data not shown)). KEGG pathway gene sets supported these effects of the 30% salmon diet, showing increased expression in *Fatty acid degradation*, *Glycerolipid metabolism*, *Arachidonic acid metabolism*, and *Linoleic acid metabolism* (Figure 5.6). Within C57BL/6J mice, similar changes were observed in the liver of mice fed the 30% salmon diet compared to the 30% control diet (Table 5.5), and may indicate that hepatic regulation of genes associated with lipid metabolism in response to the 30% salmon diet occurs irrespective of the inflammatory state in the colon.

Immune and inflammatory pathways appeared largely unaffected in the liver of *Il10*$^{-/-}$ mice fed the 30% salmon diet (vs. those fed the 30% control diet). However, the mRNA expression levels of *CEBPD*, a transcription regulator of acute phase proteins, was decreased in the liver of *Il10*$^{-/-}$ mice fed the 30% salmon diet (Table 5.5). The gene further indicated genotype-specific expression changes, with *CEBPD* gene expression unchanged in C57BL/6J mice fed the 30% salmon diet (vs. those fed the 30% control diet (Table 5.5)).

5.4.4 Urinary metabolites

5.4.4.1 Metabolite identification

The untargeted metabolite fingerprinting of mouse urine highlighted a differential metabolite occurring at a RT of 200 to 201 sec in positive and negative ionisation mode. Initial comparison of the detected mass and in-source fragmentation pattern of the molecular ion *m/z* 205.9 (positive ionisation mode) indicated similarities to xanthurenic acid, as detected in Chapter 3 and other published studies in *Il10*$^{-/-}$ mice [281, 309]. Further MS/MS structural elucidation revealed the molecular ion $[M+H]^+$ 205.9 fragmented to give major ions at *m/z* 188.0714, 178.0493, 160.0373, 132.0445, 104.0498 and 77.0390 (Figure 5.7). This fragmentation pattern matched xanthurenic acid as observed by Otter *et al.* [309], confirming the identification of the metabolite. In negative

ionisation mode, targeted analysis of the corresponding molecular ion *m/z* 204 (RT 201 sec) revealed a closely eluting metabolite that interfered with the molecular ion [supported by 309]. However, the fragment ion *m/z* 176 was putatively identified as corresponding to xanthurenic acid (RT 200 sec).

A lowly abundant ion *m/z* 366 corresponding to the metabolite eluting at 123 sec (negative mode) indicated differences between *Il10*$^{-/-}$ and C57BL/6J mice. MS/MS structural elucidation of the molecular ion $[M-H]^-$ 366 resulted in the fragment ion *m/z* 204.2730 (Figure 5.8), indicating a metabolite similar to xanthurenic acid. The fragmentation pattern and the earlier elution of the metabolite relative to xanthurenic acid suggested xanthurenate-8-O-beta-D-glucoside (xanthurenic acid glucoside), a metabolite which was also putatively identified in Chapter 3 and in agreement with published data [309].

The untargeted metabolic fingerprinting of urine highlighted a differential metabolite eluting at 334 sec in positive and negative ionisation mode. Initial comparison of in-source fragmentation patterns of the ions *m/z* 444.1 and 449.2 were matched to the NH_4^+ and Na^+ adducts of γ-carboxyethylhydroxychroman (γ-CEHC) glucoside, a metabolite of γ-tocopherol [350]. MS/MS fragmentation of the ion $[M+NH_4]^+$ 444.2219 resulted in the major daughter ions *m/z* 265.1432, 247.1327 and 151.0752 (Figure 5.9). This fragmentation pattern confirmed γ-CEHC glucoside [350].

The untargeted metabolic fingerprinting of urine highlighted a differential metabolite eluting at 347 to 348 sec in positive and negative ionisation mode. Initial comparison of in-source fragmentation patterns of ions *m/z* 472 and 477 were matched to the NH_4^+ and Na^+ adducts of α-carboxyethylhydroxychroman (α-CEHC) glucuronide, a metabolite of α-tocopherol [350]. MS/MS fragmentation of the ion $[M-H]^-$ 453.1761 resulted in the major daughter ions *m/z* 276.1373, 233.1540 and 113.0230 (Figure 5.10). This fragmentation pattern confirmed α-CEHC glucuronide [309, 350].

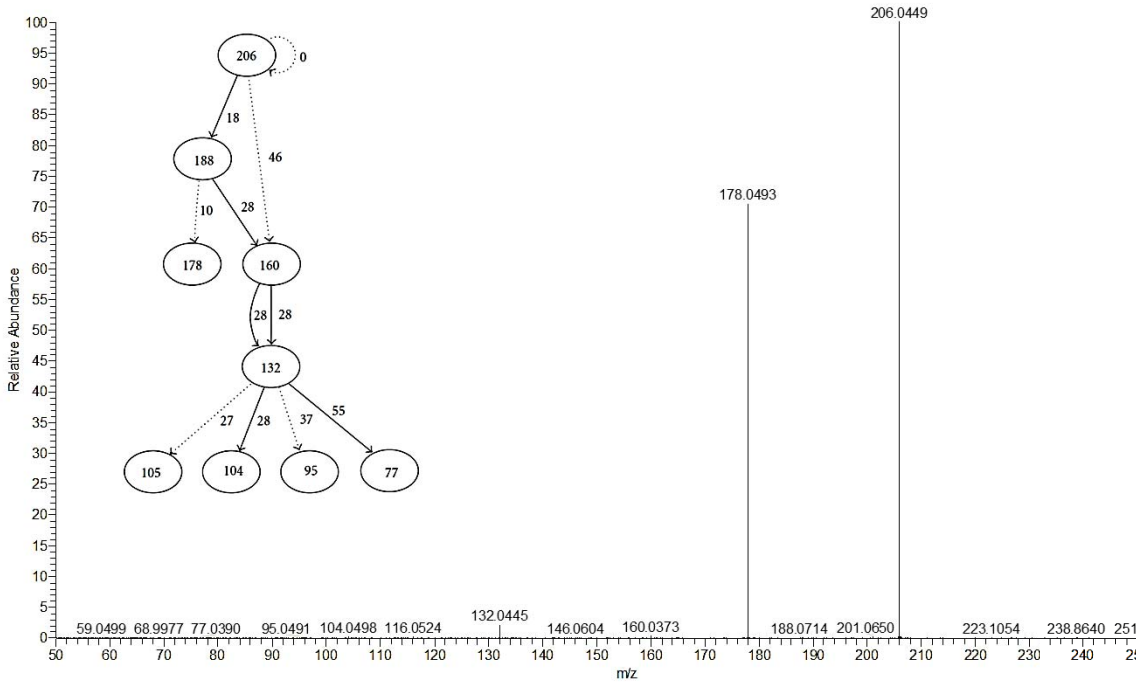

Figure 5.7 Structural elucidation of xanthurenic acid $[M+H]^+$ 206 on a Thermo Scientific Q Exactive Quadrupole-Orbitrap mass spectrometer in positive electrospray ionisation mode. The interpretation of the major daughter ions is shown in the inlaid diagram [309]. Reference urine sample obtained from an *Il10*$^{-/-}$ mouse at 11.5 weeks of age.

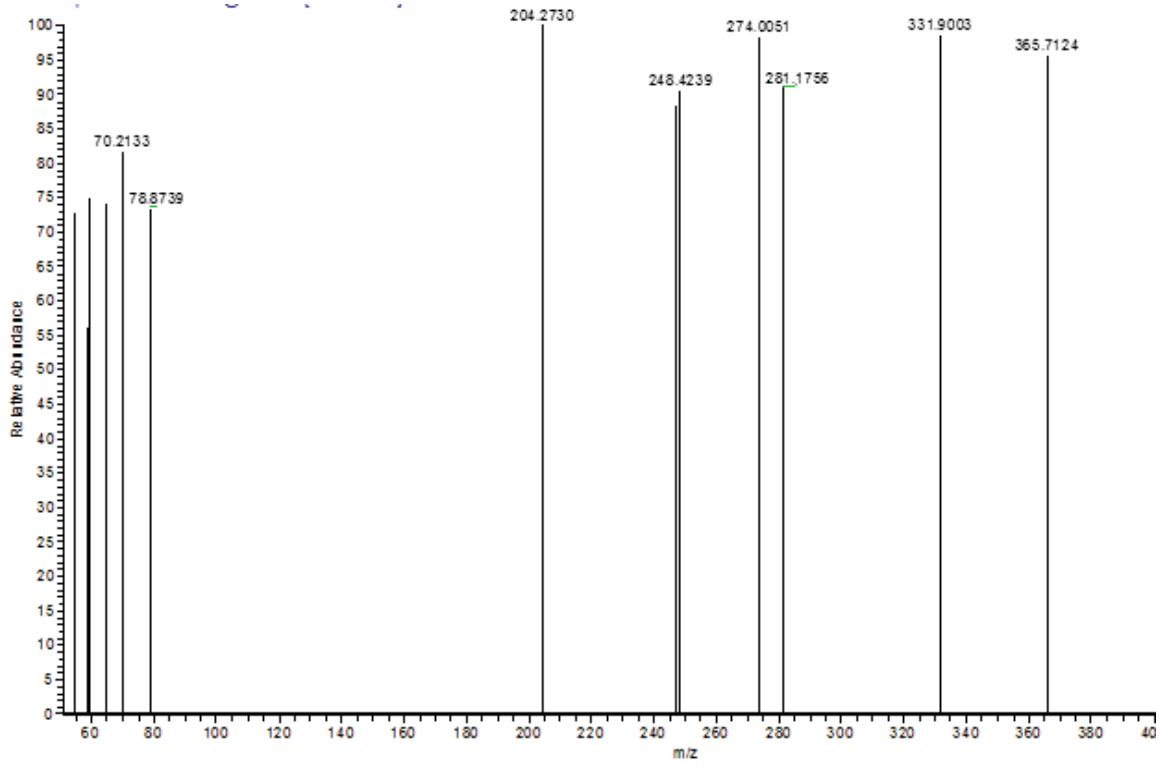

Figure 5.8 Structural elucidation of xanthurenic acid glucoside $[M-H]^-$ 366 on a Thermo Scientific Q Exactive Quadrupole-Orbitrap mass spectrometer in negative electrospray ionisation mode. Reference urine sample obtained from an *Il10*$^{-/-}$ mouse at 11.5 weeks of age.

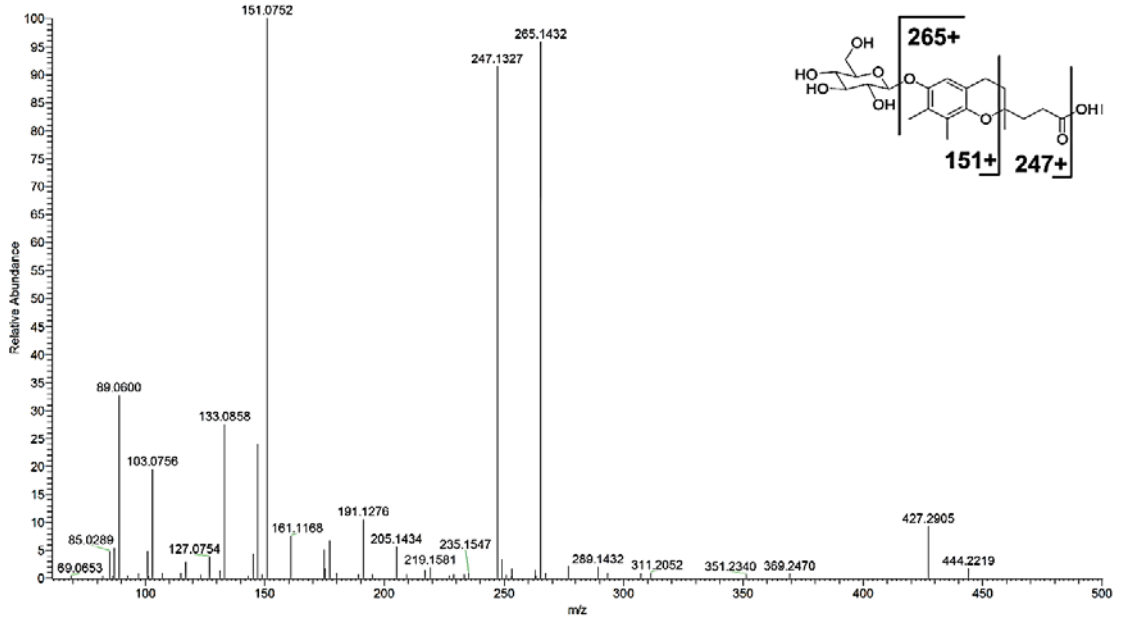

Figure 5.9 Structural elucidation of γ-CEHC glucoside $[M+NH_4]^+$ 444.1 on a Thermo Scientific Q Exactive Quadrupole-Orbitrap mass spectrometer in positive electrospray ionisation mode. The interpretation of the major daughter ions is shown in the inlaid structural diagram [350]. Reference urine sample obtained from a C57BL/6J mouse at 11.5 weeks of age.

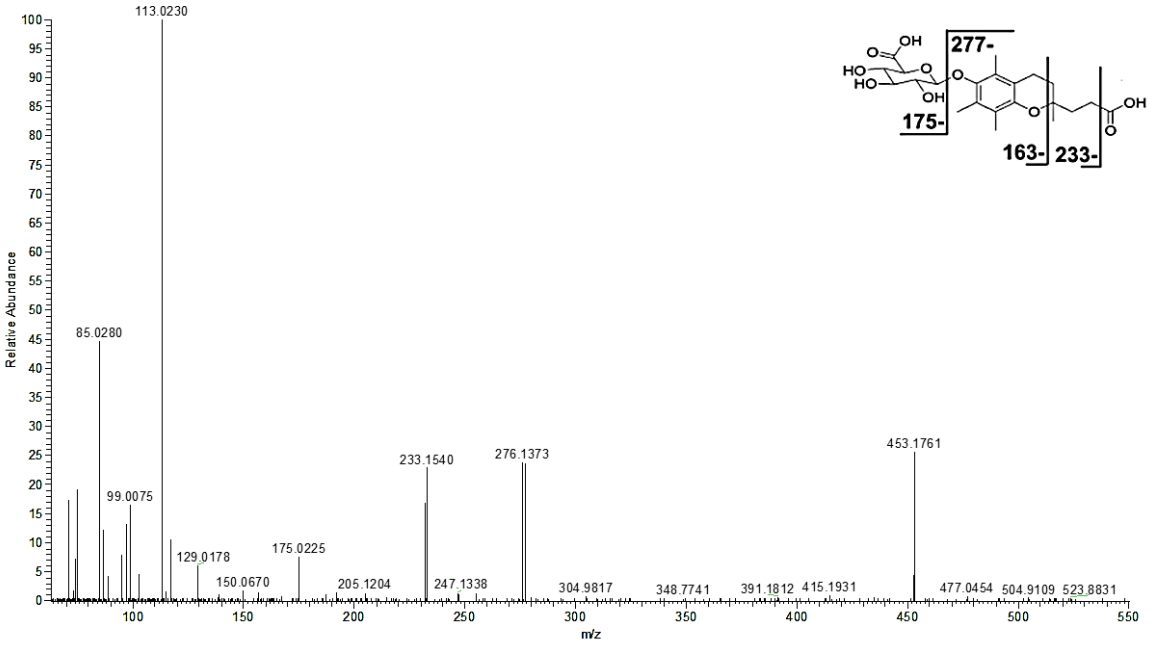

Figure 5.10 Structural elucidation of α-CEHC glucuronide $[M-H]^-$ 453.1 on a Thermo Scientific Q Exactive Quadrupole-Orbitrap mass spectrometer in negative electrospray ionisation mode. The interpretation of the major daughter ions is shown in the inlaid structural diagram [350]. Reference urine sample obtained from a C57BL/6J mouse at 11.5 weeks of age.

5.4.4.2 Metabolomic fingerprinting

Peak detection and alignment produced 2431 (positive) and 2076 (negative) mass ions with mean retention times between 12 and 800 sec. Irrespective of ionisation mode, the urinary metabolite fingerprint was dependent on diet (30% salmon vs. 30% control) at every collection time-point (6.2, 9 and 11.5 weeks of age (Table 5.6)). The significance of genotype (*Il10*$^{-/-}$ vs. C57BL/6J) differed between the time-points and ionisation modes (Table 5.6). At 6.2 weeks of age, the metabolite fingerprint of urine from *Il10*$^{-/-}$ mice already differed significantly to C57BL/6J mice in positive ionisation mode, while a trend was detected in negative mode (Table 5.6). However, at 9 weeks of age, no difference between the genotypes was detected in positive mode, but they significantly differed in negative mode ($P = 0.03$). At 11.5 weeks of age, when colitis in *Il10*$^{-/-}$ mice is established, the genotype contributed significantly to the urinary metabolite fingerprint (Table 5.6). Similar observations were made in Chapter 3, where the age at urine collection time-point significantly affected the urinary metabolite fingerprint, and differences between *Il10*$^{-/-}$ and C57BL/6J mice become more pronounced towards later stages of the experiment. Furthermore, this data suggests that the intake of the salmon diet affected the urinary metabolite fingerprint earlier than genotype, similar to the findings of Chapter 3, and overall had more impact on the urinary metabolome than genotype.

No interaction of genotype × diet was observed at 6.2 and 9 weeks of age, suggesting that *Il10*$^{-/-}$ mice showed similar urinary metabolite fingerprints to C57BL/6J mice in response to either diet before colitis development (6.2 weeks) and at early stages (9 weeks). At 11.5 weeks of age, when colitis was established in *Il10*$^{-/-}$ mice, the positive ionisation mode showed a significant interaction of genotype × diet, while a trend was detected in negative ionisation mode (Table 5.6). This was also shown in Figure 5.11, where the separation of the urinary metabolite fingerprints was more pronounced towards later stages of the experiment.

The ions with the ten highest PLS-DA loadings are shown in Table 5.7 and Appendix XII. These "discriminant ions" were most significant for the separation of the urinary metabolite fingerprint between the treatment groups, and involved ions corresponding to the metabolites γ-CEHC glucoside, α-CEHC glucuronide, xanthurenic acid and its glucoside (Table 5.7). None of the other discriminant ions were identified.

Table 5.6 Permutation MANOVA of the urinary metabolite fingerprints. C57BL/6J mice and *Il10*$^{-/-}$ mice were fed 30% control or 30% salmon diets and urine was collected at 6.2, 9 and 11.5 weeks of age. Data represent two to eight biological replicates per treatment group. P-values ≤ 0.05 were considered significant and between 0.05 and 0.1 a trend.

Ionisation mode	*Factor*	*Age (weeks)*	*P-value*
Positive	Diet	6.2	0.001
		9	0.002
		11.5	0.001
	Genotype	6.2	0.036
		9	0.527
		11.5	0.010
	Diet × Genotype	6.2	0.657
		9	0.550
		11.5	0.037
Negative	Diet	6.2	0.001
		9	0.001
		11.5	0.001
	Genotype	6.2	0.095
		9	0.031
		11.5	0.018
	Diet × Genotype	6.2	0.747
		9	0.473
		11.5	0.061

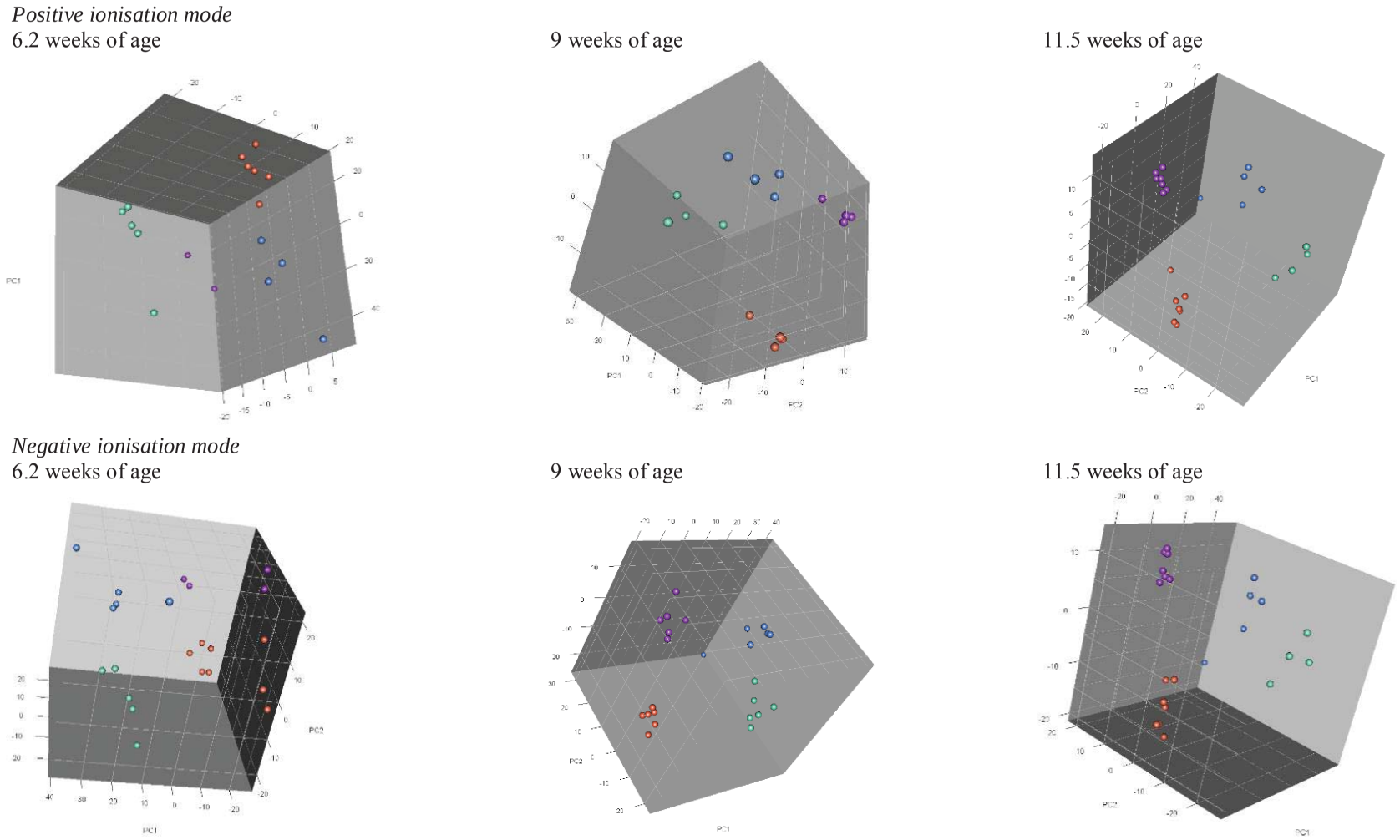

Figure 5.11 Partial Least Squares-Discriminant Analysis (PLS-DA) of mouse urine in negative and positive ionisation mode at 6.2, 9 and 11.5 weeks of age. Individual mice are shown as points, with C57BL/6J mice fed 30% control diet (blue), C57BL/6J mice fed 30% salmon diet (violet), *Il10*$^{-/-}$ mice fed 30% control diet (turquoise) and *Il10*$^{-/-}$ mice fed 30% salmon diet (orange). Data represent two to eight biological replicates per treatment group.

Table 5.7 Ions with the ten highest Partial Least Squares-Discriminant Analysis (PLS-DA) loadings in *Il10*$^{-/-}$ and C57BL/6J mice fed 30% control or 30% salmon diets. For negative and positive ionisation mode, loadings were obtained by PLS-DA at 6.2, 9 and 11.5 weeks of age (referred to as 1st, 2nd and 3rd time-point in the table). Arrows indicate direction of fold-change (FC) in *Il10*$^{-/-}$ mice compared to C57BL/6J mice (irrespective of diet), or 30% salmon-fed mice vs. 30% control diet (irrespective of genotype). Data shown as p-values of the log-transformed, normalised peak intensities as per XCMS, with significance evaluated by ANOVA at each time-point independently. Interaction p-value (genotype × diet) given for the third time-point only. "n.s." indicates ions that are not significantly different between a given comparison. Data represent two to eight biological replicates per treatment group. Only ions with confident identifications listed and ions without identification shown in Appendix XII. P-values ≤ 0.001 were considered significant.

XCMS RT	*XCMS ions (m/z)*[1]	*Discriminant time-point*	*Metabolite*	*Ion quantitated*	*Il10*$^{-/-}$ *vs. C57BL/6J*				*30% salmon vs. 30% control*				*Interaction*[2]
					FC	*1st*	*2nd*	*3rd*	*FC*	*1st*	*2nd*	*3rd*	*3rd*
Positive ionisation													
200-1	**177.9**, **205.9**	2	Xanthurenic acid	205.9 $[M+H]^+$	↑	n.s.	2.1E-07	6.7E-07		n.s.			n.s.
334	**151**, **265**, **444.1**, **445.1**, **449.2**	1, 3	Gamma CEHC glucoside	444.1 $[M+NH_4]^+$	↓	2.0E-06	8.2E-05	1.3E-10	↓	3.5E-10	1.8E-08	4.3E-16	1.0E-03
347	**472.1**, 477.1	1	Alpha CEHC glucuronide	472 $[M+NH_4]^+$	↓	1.7E-05	3.9E-06	6.2E-09	↑	1.8E-05	4.4E-05	5.5E-05	n.s.
Negative ionisation													
123	**366**	2, 3	Xanthurenic acid glucoside	366 $[M-H]^-$	↑	7.2E-05	8.2E-08	2.6E-07		n.s.			n.s.
201	**159.9**, 176, 204	2, 3	Xanthurenic acid	159.9[3]	↑	2.5E-05	3.3E-07	1.4E-07		n.s.			n.s.
2134	**453.1**, **454.1**	2, 3	Alpha CEHC glucuronide	453.1 $[M-H]^-$	↓	1.1E-08	5.7E-08	1.6E-08	↑	2.8E-07	3.4E-05	1.8E-03	n.s.

RT: Retention time in seconds as per XCMS; *m/z*: Mass-per-charge ratio.

[1] Values in bold are discriminant ions; [2] As per permutation MANOVA, interaction of genotype × diet is only significant at 11.5 weeks of age; [3] Fragment ion of xanthurenic acid, a closely eluting metabolite interfered with the molecular ion *m/z* 204.

5.4.4.2.1 Urinary metabolites between mouse genotypes fed the 30% control diet

The abundance of xanthurenic acid was higher in urine of *Il10*$^{-/-}$ mice compared to C57BL/6J mice at 9 and 11.5 weeks of age, independent of the type of diet (30% salmon or 30% control (Table 5.7)). At 6.2 weeks of age, no difference was detected in positive mode, while in negative mode, the fragment ion of xanthurenic acid (*m/z* 159.9) was significantly elevated in *Il10*$^{-/-}$ mice (vs. C57BL/6J mice). Furthermore, the differences between the genotypes became more pronounced over the experimental period, with relative peak intensities between *Il10*$^{-/-}$ and C57BL/6J mice increasing from approximately 3-fold (6.2 weeks of age) to 8-fold (11.5 weeks) when both were fed the 30% control diet (Figure 5.12). This pattern of xanthurenic acid in the urine may be attributed to increasing severity of colitis in *Il10*$^{-/-}$ mice, and the elevated presence of xanthurenic acid in the urine of those mice.

The abundance of urinary xanthurenic acid glucoside (*m/z* 366) was significantly different between *Il10*$^{-/-}$ and C57BL/6J mice at all time-points (Table 5.7), with approximately 3-fold more xanthurenic acid glucoside in the urine of *Il10*$^{-/-}$ mice at the first time-point and remaining at this level until 11.5 weeks of age (Figure 5.12). Thus, the relative differences between the genotypes was unaffected by colitis development in *Il10*$^{-/-}$ mice. Compared to other metabolites, xanthurenic acid glucoside showed low abundance in urine.

The urinary abundance of vitamin E metabolites (*i.e.*, γ-CEHC glucoside and α-CEHC glucuronide) was dependent on genotype (*Il10*$^{-/-}$ vs. C57BL/6J mice), with lower levels in *Il10*$^{-/-}$ mice at all time-points (Table 5.7 and Figure 5.12). At 6.2 and 9 weeks of age, the abundance of ions corresponding to the metabolite γ-CEHC glucoside was approximately 3 to 5-fold lower in the urine of *Il10*$^{-/-}$ mice compared to C57BL/6J mice and irrespective of the type of 30% diet (salmon or control (Figure 5.12)). However, when colitis was established in *Il10*$^{-/-}$ mice (11.5 weeks of age), the abundance of γ-CEHC glucoside was approximately 5 to 6-fold lower in *Il10*$^{-/-}$ mice fed the 30% control diet compared to C57BL/6J mice fed the same diet (Figure 5.12).

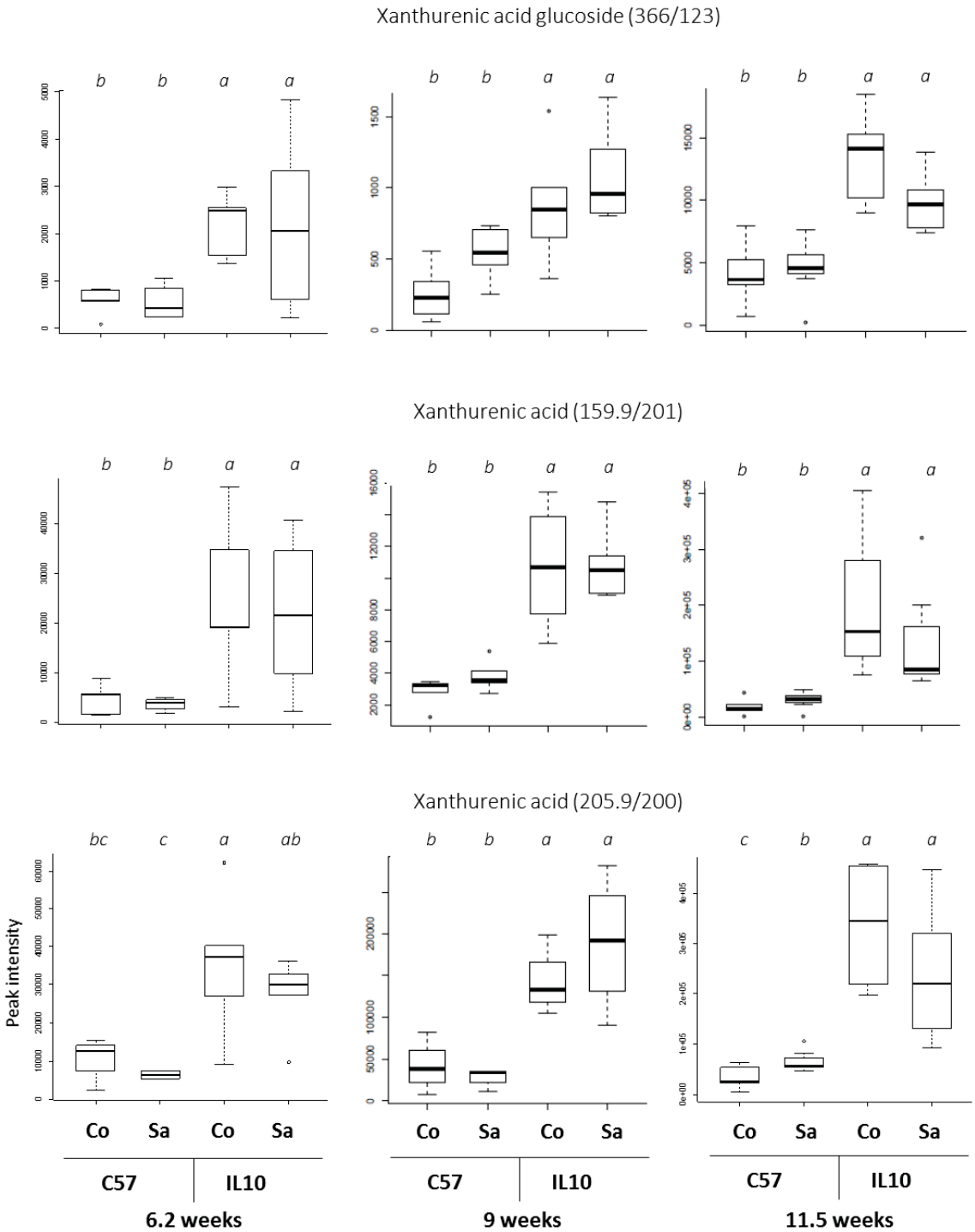

Figure 5.12 Peak intensities of the molecular ions corresponding to the urinary metabolites xanthurenic acid glucoside (negative ionisation mode) and xanthurenic acid (positive and negative). *Il10*$^{-/-}$ and C57BL/6J (C57) mice were fed a 30% salmon (Sa) or 30% control (Co) diet and urine was collected at 6.2, 9 and 11.5 weeks of age. Numbers in parentheses next to metabolite names refers to mass-to-charge ratio and retention time in seconds. Boxplots indicate unnormalised peak intensity values. Boxes that share the same letter are not significantly different at a 5% LSD within a time-point, evaluated by ANOVA of log-transformed, normalised peak intensities as per XCMS. Data represent two to eight biological replicates per treatment.

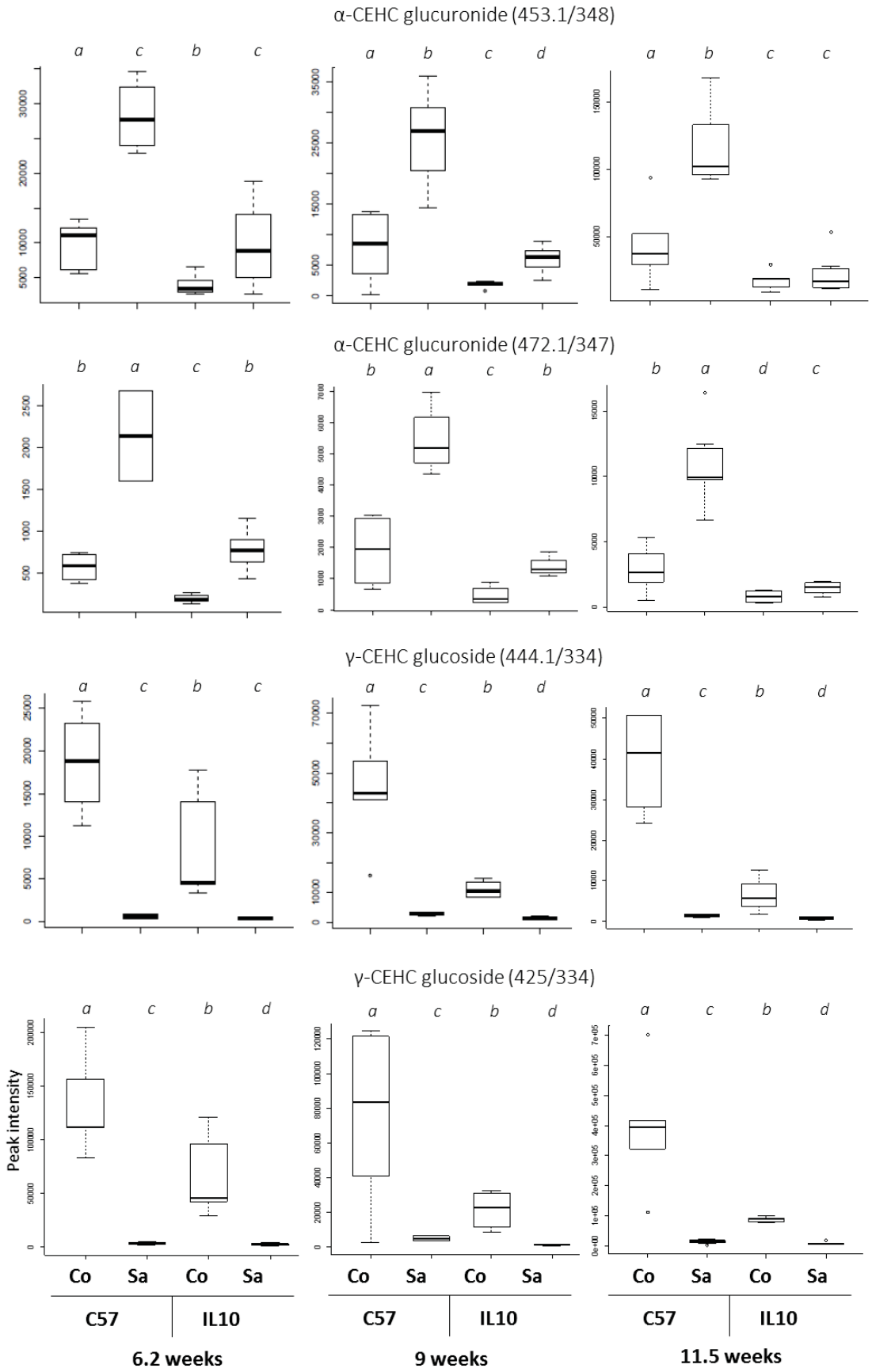

Figure 5.12 continued. Peak intensities of the molecular ions corresponding to the urinary metabolites α-CEHC glucuronide and γ-CEHC glucoside (negative and positive modes).

The differences in urinary abundance of α-CEHC glucuronide between *Il10*$^{-/-}$ mice and C57BL/6J mice both fed the 30% control diet was most pronounced at 9 weeks of age, with approximately 5-fold less in the urine of *Il10*$^{-/-}$ mice (Figure 5.12 and Table 5.7). These relative differences between *Il10*$^{-/-}$ and C57BL/6J mice were reduced at 6.2 and 11.5 weeks of age (approximately 3-fold; 30% control diet), with lower abundance in *Il10*$^{-/-}$ mice.

5.4.4.2.2 Effect of the 30% salmon diet (vs. 30% control diet) on urinary metabolites in *Il10*$^{-/-}$ mice

Irrespective of age, the intake of the 30% salmon diet did not affect the abundance of xanthurenic acid, or xanthurenic acid glucoside, in the urine of *Il10*$^{-/-}$ mice compared to those fed the 30% control diet (Table 5.7 and Figure 5.12).

The intake of the 30% salmon diet affected the abundance of α-CEHC glucuronide in the urine of *Il10*$^{-/-}$ mice, with 2 to 3-fold more α-CEHC glucuronide detected compared to those fed the 30% control diet at 6.2 and 9 weeks of age (Table 5.7 and Figure 5.12). At 11.5 weeks of age, those differences in *Il10*$^{-/-}$ mice depended on ionisation mode and were only significantly elevated in those fed the 30% salmon diet in positive mode (*m/z* 472 (Table 5.7 and Figure 5.12)). Furthermore, the interaction of genotype × diet was not significant for α-CEHC glucuronide at any time-point during the experiment, indicating that the 30% salmon diet affected its abundance similarly in *Il10*$^{-/-}$ and C57BL/6J mice, thus may be reflecting dietary intake rather than a specific effect on colitis.

The difference in γ-CEHC glucoside abundance between all mice fed the 30% salmon diet and those fed the 30% control diet was substantial, with mice fed the 30% salmon diet excreting approximately 25 to 35-fold less at 6.2 and 9 weeks of age, irrespective of genotype (Figure 5.12 and Table 5.7). At 11.5 weeks of age, the abundance of γ-CEHC glucoside showed contrasting responses to the 30% salmon diet based on genotype ($P = 0.001$ in both ionisation modes). When *Il10*$^{-/-}$ mice were fed the 30% salmon diet, the urinary metabolite abundance was approximately 10-fold lower compared to those fed the 30% control diet (Figure 5.12). However, within C57BL/6J mice, approximately 21 to 37-fold less γ-CEHC glucoside was detected in urine in those fed the 30% salmon diet (Figure 5.12). It appears that the intake of the 30% salmon diet

reduced the urinary abundance of γ-CEHC glucoside, and may be a candidate biomarker of colitis to monitor the effects of a diet containing salmon.

5.4.5 Analysis of microbiota from caecum digesta

The analysis of microbiota was carried out using caecum digesta obtained from *Il10*$^{-/-}$ and C57BL/6J mice fed the 30% diets. After DNA extraction from digesta and amplification, the barcode-tagged PCR amplicons with primers targeting the bacterial 16S rRNA were pyrosequenced, resulting in 87079 sequence reads with an average sequence length of 442 nucleotides for 23 samples. The mean number of sequence reads within treatment groups were 3015 (C57BL/6J 30% control), 3328 (C57BL/6J 30% salmon), 3738 (*Il10*$^{-/-}$ 30% control), and 4011 (*Il10*$^{-/-}$ 30% salmon).

5.4.5.1 Species diversity estimate

The microbiota in the caecum of *Il10*$^{-/-}$ mice was less diverse based on a lower Chao1 index compared to C57BL/6J mice, irrespective of the type of 30% diet ($P < 0.001$ (Figure 5.13)). At the lowest common sequence read (1494 per sample), the intake of the 30% salmon diet did not affect the diversity in *Il10*$^{-/-}$ mice ($P = 0.497$), with similar Chao1 indices for *Il10*$^{-/-}$ mice fed the 30% salmon diet (122) and the 30% control diet (99) (Figure 5.13).

5.4.5.2 Taxonomic differences

The 16S rRNA sequences of caecal digesta DNA obtained from mice fed the 30% control or 30% salmon diet were assigned to eight bacterial phyla at an 80% confidence cut-off. Prevalent phyla included *Firmicutes* (53% of total sequence reads), *Bacteroidetes* (38%), *Proteobacteria* (4.7%), *Deferribacteres* (2.3%) and *Verrucomicrobia* (2.1%) (Figure 5.14). Phyla with less than 0.5% population size across treatment groups are labelled as "Others" in Figure 5.14.

Dominant phyla

In C57BL/6J mice fed the 30% control diet, the caecal microbiota was dominated by *Firmicutes* with 63.8% of total sequence reads, followed by *Bacteroidetes* with 26.1% (ratio *Firmicutes* to *Bacteroidetes* = 2.5:1 (Figure 5.14)). In *Il10*$^{-/-}$ mice fed the 30% control diet, the proportions of *Bacteroidetes* were almost 2-fold higher than in C57BL/6J

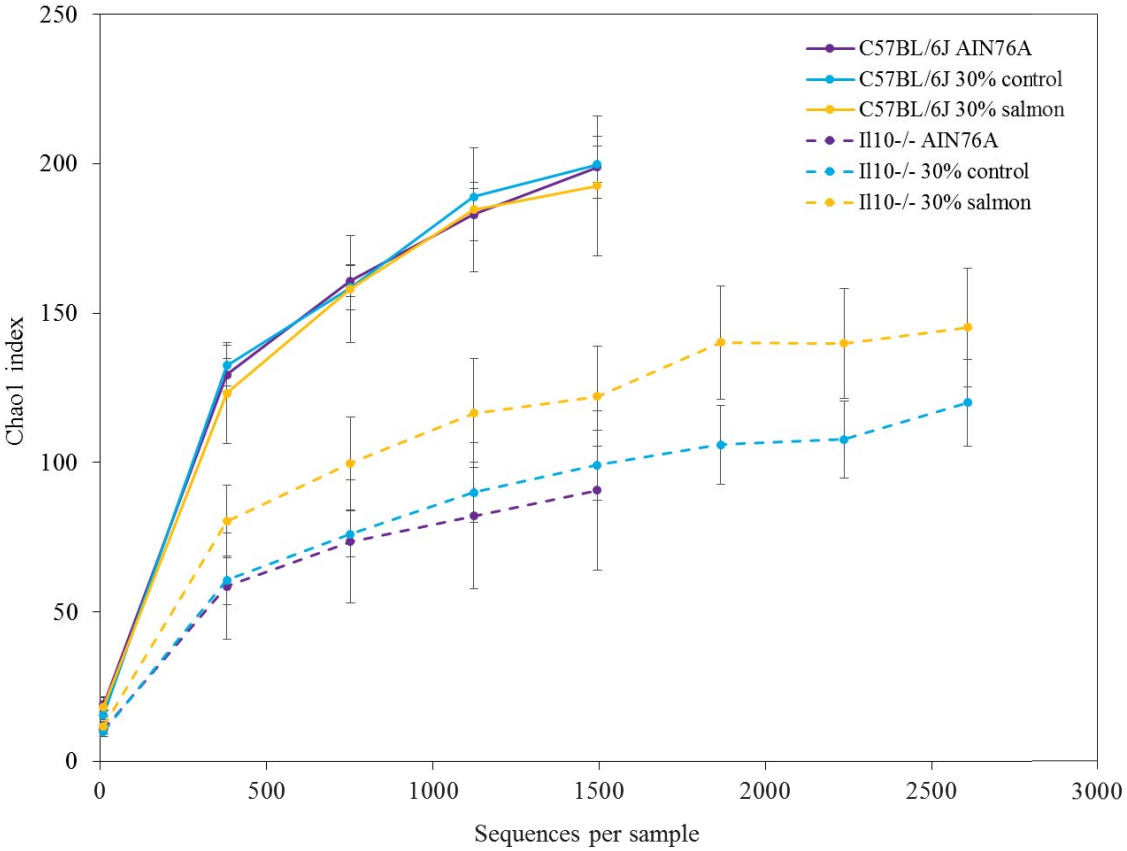

Figure 5.13 Chao1 index [325] of caecal microbiota from C57BL/6J mice and *Il10*$^{-/-}$ mice fed either an AIN-76A diet, a 30% salmon diet or a 30% control diet. Data represent six biological replicates per treatment, with the exception of C57BL/6J mice fed the 30% control diet where n = 5. Data shown as means ± SEM.

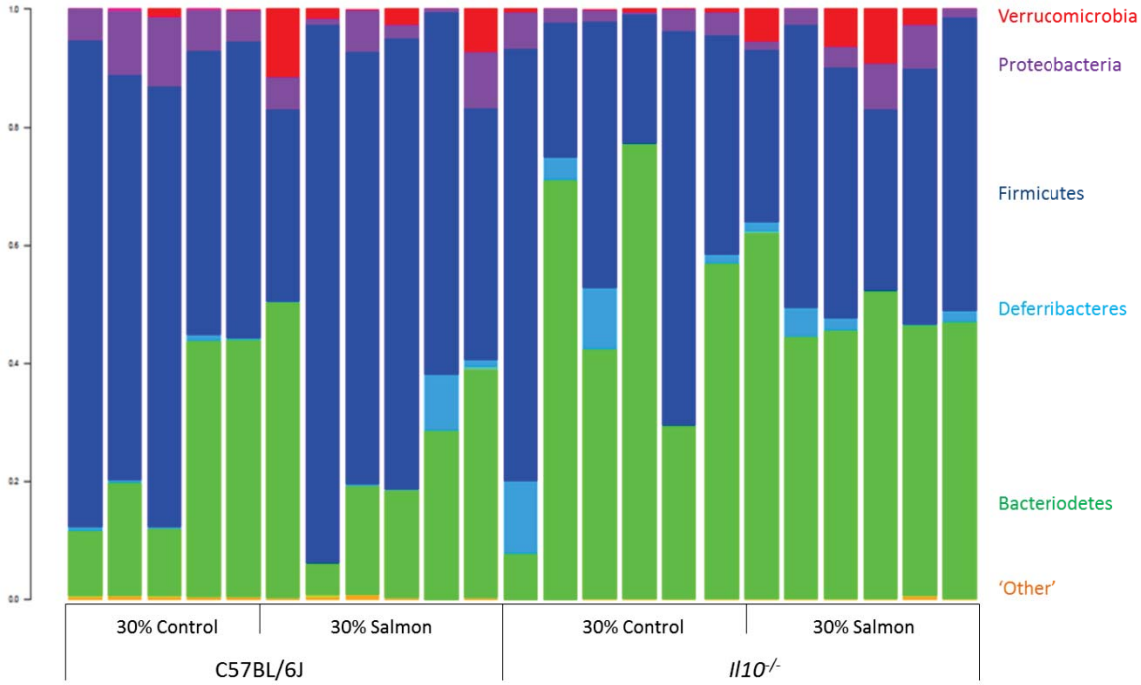

Figure 5.14 Dominant phyla in the caeca of C57BL/6J mice and *Il10*$^{-/-}$ mice fed the 30% control diet and the 30% salmon diet. Each bar represents the microbial community structure in the caecum digesta of an individual mouse. Data represent six biological replicates per treatment, with the exception of C57BL/6J mice fed the 30% control diet where n = 5. Phyla with a population size greater than 0.5% of total sequence reads are listed by name while "Other" refers to the sum of less dominant phyla.

mice fed the same diet (P = 0.004), while *Firmicutes* was lower (P = 0.01). This increase of *Bacteroidetes*, but decrease of *Firmicutes*, resulted in a ratio of approximately 1:1 in the caecum of *Il10*$^{-/-}$ mice (Figure 5.14). The dietary intake of the 30% salmon diet did not affect the abundances of *Firmicutes* or *Bacteroidetes* in *Il10*$^{-/-}$ mice compared to those fed the 30% control diet (ratio approximately 1:1).

The highest proportion of *Proteobacteria* was detected in C57BL/6J mice fed the 30% control diet (7.9%), while *Il10*$^{-/-}$ mice fed the same diet showed decreased proportion of 3% (P = 0.06 (Figure 5.14)). No effect of the 30% salmon diet on *Proteobacteria* proportions were observed within *Il10*$^{-/-}$ mice or C57BL/6J mice compared to those fed the 30% control diet (P = 0.3).

Dominant genera

Within the five most prevalent phyla (Figure 5.14), 18 genera were dominant at a mean population size greater than 0.5% of total sequence reads. Of these, 12 were assigned to known genera and six remained unclassified at the genus level using an 80% confidence cut-off (Table 5.8). Most differences in the microbial community composition were observed between C57BL/6J mice and *Il10*$^{-/-}$ mice, rather than as a response to dietary intake within the same genotype (30% salmon diet vs. 30% control diet (Table 5.8)).

The observed increase in sequence reads belonging to the phylum *Bacteroidetes* was mainly driven by *Bacteroides* spp. in *Il10*$^{-/-}$ mice. While *Bacteroides* spp. only comprise approximately 14% of the caecal microbiota in C57BL/6J mice, proportions of approximately 40% were detected in *Il10*$^{-/-}$ mice, regardless of whether mice were fed the 30% salmon or 30% control diet (Table 5.8).

The decrease in the phylum *Firmicutes* in *Il10*$^{-/-}$ mice compared to C57BL/6J mice was driven by the depletion of *Allobaculum* spp. (P = 0.007). On average, approximately one third of detected sequences in C57BL/6J mice were assigned to *Allobaculum* spp., with numbers reduced to 3.7% in *Il10*$^{-/-}$ mice fed the 30% control diet. Concomitantly with decreased *Allobaculum* spp., the decreased abundance of *Firmicutes* in *Il10*$^{-/-}$ mice were further driven by reductions of unclassified *Lachnospiraceae* (P = 0.002), *Ruminococcus* spp. (P = 0.02) and *Oscillospira* spp. (P = 0.02) (Table 5.8). The

Table 5.8 Average proportions of dominant genera in caecal digesta of C57BL/6J and *Il10*$^{-/-}$ mice fed the 30% control diet or the 30% salmon diet (minimum population size larger than 0.5% of total sequence reads). Data represent six biological replicates per treatment group, with the exception of C57BL/6J mice fed the 30% control diet where n = 5.

Phylum	*Family*	*Genus*	*C57BL/6J mice*		*Il10*$^{-/-}$ *mice*		*P-values*		
			Control	*Salmon*	*Control*	*Salmon*	*Genotype (Il10*$^{-/-}$ *vs. C57)*	*Diet (Salmon vs. Control)*	*Genotype × diet*
Bacteroidetes	Unclassified	Unclassified	2.6 ± 2	4.1 ± 1.9	1.5 ± 0.6	3.1 ± 2.1	0.535	0.396	0.994
	Bacteroidaceae	*Bacteroides*	13.6 ± 6.1	14.1 ± 4.1	43.2 ± 10.6	37 ± 3.1	0.002	0.667	0.623
	Porphyromonadaceae	*Parabacteroides*	1.1 ± 0.4	1.4 ± 0.6	1.4 ± 0.5	2 ± 0.4	0.308	0.367	0.785
	Rikenellaceae	Unclassified	2.4 ± 0.6	2.3 ± 0.8	0.6 ± 0.2	3.2 ± 0.7	0.478	0.044	0.039
	S24-7	Unclassified	4.3 ± 0.8	3.4 ± 1.6	0.5 ± 0.2	2.7 ± 0.6	0.020	0.490	0.122
Deferribacteres	*Deferribacteraceae*	*Mucispirillum*	0.5 ± 0.1	1.9 ± 1.6	4.7 ± 2.2	1.8 ± 0.7	0.215	0.582	0.175
Firmicutes	*Coprobacillaceae*	Unclassified	0.8 ± 0.5	6 ± 5.7	9.7 ± 2.8	9.2 ± 5.3	0.217	0.646	0.508
	Clostridiaceae	*Clostridium*	0.0	0.0	4 ± 3.2	0.1 ± 0	0.195	0.150	0.142
	Enterococcaceae	*Enterococcus*	0.0	0.8 ± 0.8	0.8 ± 0.2	0.6 ± 0.4	0.674	0.659	0.382
	Erysipelotrichaceae	*Eubacterium*	0.0	0.0	3.2 ± 0.9	0.6 ± 0.3	0.002	0.010	0.011
		Allobaculum	33.5 ± 3.3	30.1 ± 12.1	3.7 ± 1.1	13.3 ± 5.1	0.007	0.664	0.364
	Lachnospiraceae	Unclassified	15.9 ± 4.9	7.1 ± 1.9	2.6 ± 1.1	3.5 ± 1.4	0.002	0.169	0.066
		Ruminococcus	2.4 ± 0.4	2.1 ± 0.5	0.8 ± 0.2	1.5 ± 0.5	0.020	0.673	0.225
	Peptostreptococcaceae	Unclassified	0.7 ± 0.4	4.6 ± 2.2	14.2 ± 6.7	4.2 ± 2.6	0.132	0.445	0.091
	Ruminococcaceae	*Oscillospira*	1.9 ± 0.5	2.6 ± 1.2	0.9 ± 0.3	0.6 ± 0.3	0.021	0.880	0.579
Proteobacteria	*Desulfovibrionaceae*	*Desulfovibrio*	4 ± 0.3	3.3 ± 1.3	1.3 ± 0.8	2.3 ± 0.9	0.070	0.840	0.370
	Helicobacteraceae	*Helicobacter*	3.6 ± 1.3	0.9 ± 0.3	1.1 ± 0.5	0.4 ± 0.2	0.030	0.008	0.165
Verrucomicrobia	*Verrucomicrobiaceae*	*Akkermansia*	0.3 ± 0.2	3.8 ± 1.9	0.3 ± 0.1	3.9 ± 1.5	0.932	0.014	0.949

Data indicate % ± SEM.

intake of the 30% salmon diet did not affect the abundances of these genera (P = 0.7 (Table 5.8)).

The abundance of *Eubacterium* spp. was dependent on genotype (*Il10*$^{-/-}$ vs. C57BL/6J; P = 0.002), the type of diet (30% salmon vs. 30% control; P = 0.01), and showed contrasting responses to diet based on genotype (P = 0.01 (Table 5.8)). While sequences of *Eubacterium* spp. were not detected in the caecum of C57BL/6J mice on either diet, *Eubacterium* spp. was detected in *Il10*$^{-/-}$ mice fed the 30% control diet (3.2%), and *Il10*$^{-/-}$ mice fed the 30% salmon diet (0.6%). The 16S rRNA gene sequence was most closely associated with *Eubacterium dolichum* (data not shown).

The abundance of sequence reads belonging to *Akkermansia* spp. were higher in mice fed the 30% salmon diet compared to those fed the 30% control diet (P = 0.01 (Table 5.8)). This effect was independent of genotype (P = 0.9), with *Il10*$^{-/-}$ mice and C57BL/6J mice showing almost identical numbers of abundance when fed the 30% control diet (0.3%) and when fed the 30% salmon diet (3.8-3.9%). The 16S rRNA gene sequence was most closely associated with *A. muciniphila* (data not shown).

An unclassified *Rikenellaceae* was detected in *Il10*$^{-/-}$ mice fed the 30% salmon diet (3.2%), and was higher than in those fed the 30% control diet (0.6%) (Table 5.8). The sequence counts in C57BL/6J mice were unaffected by the 30% salmon diet (similar to C57BL/6J mice fed 30% control diet: approximately 2.4%), indicating a genotype-specific effect of *Rikenellaceae* sequences in response the 30% salmon diet (P = 0.04). However, compared to other genera, the abundance of sequence reads belonging to the unclassified *Rikenellaceae* was generally low.

The abundance of *Helicobacter* spp. was approximately 3-fold higher in *Il10*$^{-/-}$ mice fed the 30% control diet compared to C57BL/6J mice fed the same diet (Table 5.8). The abundance of *Helicobacter* spp. was also affected by the intake of the 30% salmon diet, with sequence reads reduced in mice fed 30% salmon compared to those fed the 30% control diet, regardless of genotype (P = 0.008). However, compared to other genera, the abundance of sequence reads belonging to *Helicobacter* spp. was generally low.

5.4.5.3 Beta diversity

PCoA of unweighted UniFrac distances, which are a measure of the phylogenetic similarity between communities, showed differences between the microbial community structure of digesta from *Il10*$^{-/-}$ mice compared to C57BL/6J mice (Figure 5.15). These genotype-related differences were mainly observed along the first principal coordinate (PC1) and explained 30.3% of the total variation (Figure 5.15). Based on unweighted UniFrac distances, there was limited effect of the 30% salmon diet on the microbial community structure compared to mice fed the 30% control diet, irrespective of genotype (C57BL/6J mice or *Il10*$^{-/-}$ mice). The differences in diet were mainly explained along PC2 (8.5% of variation (Figure 5.15)).

While the unweighted UniFrac method only takes the presence or absence of taxa into account, the community similarities were also assessed using a weighted UniFrac distance, which further considers the abundance of the specific taxa (Figure 5.15). It was shown that the microbial communities in the caecum of *Il10*$^{-/-}$ mice were more similar to C57BL/6J mice when they were fed the 30% salmon diet than when they were fed the 30% control diet (Figure 5.15). Therefore it appears that the 30% salmon diet affected the growth of resident bacteria similarly in both mouse genotypes, but this did not occur when mice were fed the 30% control diet.

5.5 Discussion

The hypothesis that protein expression provided novel molecular mechanisms of the effects of the 30% salmon diet in the colon of *Il10*$^{-/-}$ mice appeared to be limited to oxidative stress responses. It did support the effects of the 30% salmon diet on antigen presentation and lipid metabolism reported in Chapter 4. Lower levels of oxidative stress in the colon of 30% salmon-fed *Il10*$^{-/-}$ mice may be attributed to anti-oxidative properties of tocopherols provided by the salmon diet (vs. 30% control diet), however markers of ER stress were not affected in those mice. The expression of two antigen-processing proteins were reduced in 30% salmon-fed *Il10*$^{-/-}$ mice and specifically indicated reduced proteasome-mediated antigen processing and generation of class I binding peptides compared to those fed the control diet.

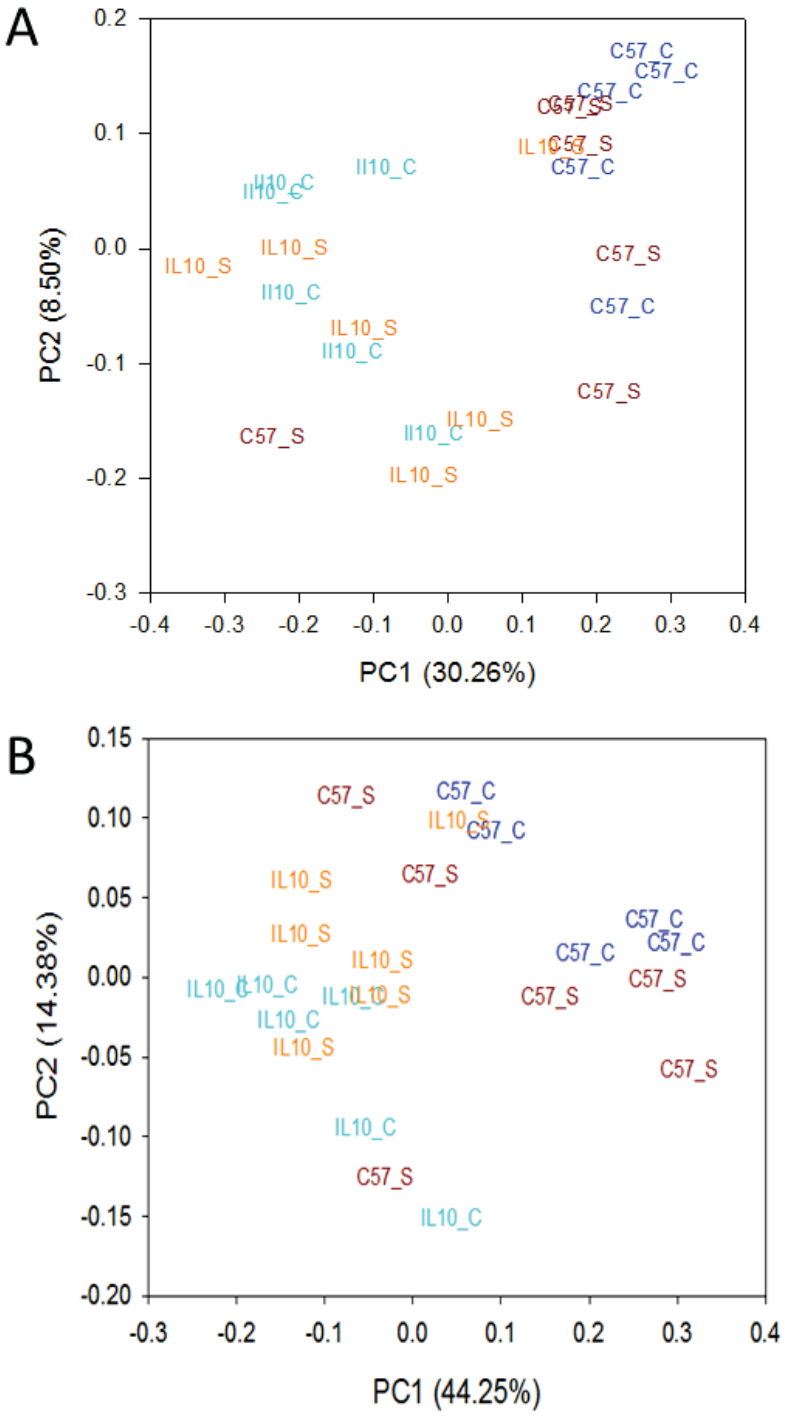

Figure 5.15 Principal Coordinate Analysis (PCoA) using (A) an unweighted UniFrac method and (B) a weighted UniFrac method to show (dis)similarities of the microbial community structure based on phylogenetic information [327]. Caecal digesta obtained from C57BL/6J mice and *Il10*$^{-/-}$ mice fed either a 30% control diet or 30% salmon diet. Data represent six biological replicates per treatment, with the exception of C57BL/6J mice fed the 30% control diet where n = 5. Numbers in parentheses indicate amount of variance explained by the principal coordinates (PC).
"C57_C" = C57BL/6J mice fed 30% control; "C57_S" = C57BL/6J mice fed 30% salmon; "Il10_C" = *Il10*$^{-/-}$ mice fed 30% control; "IL10_S" = *Il10*$^{-/-}$ mice fed 30% salmon.

The transcriptomic profiling of liver tissue supported the stated hypothesis that the 30% salmon diet affected the expression of genes in *Il10*$^{-/-}$ mice compared to those fed the 30% control diet, with metabolism of lipids and xenobiotics affected. A novel finding was that the liver reflected the reduced mRNA expression of colonic *CEBPD* (findings presented in Chapter 4) in *Il10*$^{-/-}$ mice fed the 30% salmon diet compared to those fed the 30% control diet, further reversing the increases in *CEBPD* expression underlying colitis in *Il10*$^{-/-}$ mice (vs. C57BL/6J mice).

The analysis of urine obtained from *Il10*$^{-/-}$ mice highlighted the potential of xanthurenic acid as a biomarker of colitis and was consistent with the findings presented in Chapter 3 and published data [281, 309]. However, the intake of the 30% salmon diet did not have an impact on the abundance of xanthurenic acid in the urine of *Il10*$^{-/-}$ mice (vs. 30% control diet). Two vitamin E metabolites (*i.e.* α-CEHC glucuronide and γ-CEHC glucoside) were also identified as metabolites responsive to the 30% salmon diet. Promising results were initially obtained with observed increases of urinary α-CEHC glucuronide in response to 30% salmon, previously suggested as a biomarker of colitis in *Il10*$^{-/-}$ mice [309], but as this was irrespective of genotype, it may be a biomarker of dietary exposure rather than of function. However, this is the first study to show urinary γ-CEHC glucoside responses to the 30% salmon diet were genotype-specific and may be a candidate biomarker of colitis to monitor the effects of salmon.

The intake of the 30% salmon diet did not affect the loss of microbial species diversity associated with colitis in *Il10*$^{-/-}$ mice. However, it was shown that the intake of the 30% salmon diet modulated the abundances of some of the resident bacteria (*e.g. Verrucomicrobia akkermansia*), an effect which was mostly independent of genotype, causing the community profiles of the microbiota of *Il10*$^{-/-}$ mice to be more similar to C57BL/6J mice when mice were fed the 30% salmon diet compared to when they were fed the 30% control diet. The expansion of *Eubacterium* spp. (most closely associated with *Eubacterium dolichum*) in *Il10*$^{-/-}$ mice fed the 30% control diet was reduced by the intake of the 30% salmon diet in those mice. *E. dolichum* was not detected in C57BL/6J mice on either diet. Genotype-specific effects were also associated with an unclassified *Rikenellaceae*, which was depleted in *Il10*$^{-/-}$ mice fed the 30% control diet, but not in those fed the 30% salmon diet. However, compared to other genera, the abundances of *Eubacterium* spp. and the unclassified *Rikenellaceae* were generally low.

5.5.1 Proteomic profiling of colon tissue

5.5.1.1 Colon proteomic profile during colitis

Elevated TXN and ALDH16A1 expression in the colon of *Il10*$^{-/-}$ mice fed the 30% control diet (vs. C57BL/6J mice) may be indicative of increased oxidative stress and is in agreement with published studies among IBD patients, where increased serum TXN has been shown compared to healthy controls [451]. Oxidative stress is defined as imbalance between the production of free radicals/reactive metabolites such as ROS and their elimination by antioxidants which can ultimately lead to apoptosis [as reviewed in 452]. TXN is an intracellular redox-regulating molecule [453] and its expression can be induced by oxidative stress, acting as a potent chemotactic for inflammatory cells [454]. However, prolonged oxidative stress can lead to misfolding of proteins in the ER or oxidative damage of proteins. The elevated oxidative stress in *Il10*$^{-/-}$ mice may further increase levels of misfolded proteins in the ER, commonly known as ER stress [as reviewed in 455], and indicated by the increased abundance of protein HSPA5 in the colon of *Il10*$^{-/-}$ mice compared to C57BL/6J mice fed the 30% control diet, also reported in another study using *Il10*$^{-/-}$ mice [456]. The increase of LONP1 expression in the colon of *Il10*$^{-/-}$ mice further supported these findings. LONP1 is a regulatory protein that mediates selective degradation of misfolded and oxidatively damaged polypeptides in the mitochondrial matrix, however, the exact mechanism of action remains unknown [457].

Abnormalities in epithelial antigen presentation have been linked to the pathogenesis of IBD [458], attributed to the enhanced presentation of antigens in the inflamed colon tissue which further attracts immune cells and drives the immune response. The MHC class I signalling pathway (specific to CD8$^+$ T cells) is associated with intracellular peptides that are at the end of their functional lives, while the MHC class II signalling pathway is associated with exogenous sources and specific to CD4$^+$ T cells [for a review on antigen presentation see 56]. In agreement with the literature [343, 348], increased antigen presentation was observed in the colon of *Il10*$^{-/-}$ mice, with transcriptomic profiling indicating an increase in expression of genes that code MHC class I and class II molecules. The analysis of genes and proteins showed an involvement of proteasome-mediated degradation of proteins, attributed to the increase of two members of the proteasome PSMB8 and PSMB9 (also known as LMP7 and LMP2, respectively), which catalyse the degradation of intracellular proteins to fragments for

further processing of the antigen in the ER. Furthermore, it was shown that peptide transport and loading in the ER was increased in the colon of *Il10*$^{-/-}$ mice compared to C57BL/6J mice (chaperone proteins such as CALR and PDIA3 that stabilise MHC class I molecules for assembly in the ER), thus further supporting elevated antigen-presentation, specifically to CD8^{+} T cells, in the colon of *Il10*$^{-/-}$ mice fed the 30% control diet (vs. C57BL/6J mice).

Differential regulation of genes associated with tryptophan metabolism has been reported in IBD patients [366] and was also shown in Chapters 3 and 4 and other studies using *Il10*$^{-/-}$ mice [281, 393, 459]. Protein expression in the colon of *Il10*$^{-/-}$ mice showed increases in the mitochondrial dehydrogenases ALDH1B1 and ALDH2. Increased expression of ALDH1B1 has been observed in human adenocarcinomas [460], however, these findings are in contrast to Cooney *et al.* [268] who reported decreased expression of ALDH1B1 and ALDH2 in the colon of *Il10*$^{-/-}$ mice compared to C57BL/6J mice. As part of the tryptophan metabolism pathway, the family of ALDH proteins metabolise indole-3-acetaldhyde to indole-3-acetic acid (*via* indolepyruvate), and 5-hydroxyindole-acetaldehyde to 5-hydroxy-indoleacetate (*via* serotine) [461]. The biosynthesis of melatonin *via* serotonin is likely to be reduced in *Il10*$^{-/-}$ mice (reduced gene expression and metabolites (Chapters 3 and 4)), and is supported by others [395]. Thus increases of ALDH1B1 and ALDH2 may therefore be more likely connected to the metabolism of tryptophan to indolic acid derivatives *via* indolepyruvate.

5.5.1.2 Colon proteomic profile in response to the 30% salmon diet (vs. 30% control diet) in *Il10*$^{-/-}$ mice

Proteomic analysis of colon tissue highlighted an increase in expression of proteins associated with metabolic pathways, including metabolism of lipids and tryptophan, but a reduction of proteins associated with oxidative stress and antigen presentation, in *Il10*$^{-/-}$ mice fed the 30% salmon diet (vs. those fed the 30% control diet).

ALDH1B1 is a protein associated with several metabolic processes (*e.g.* tryptophan, lipids and carbohydrates), and metabolises a wide range of substrates including acetaldehyde, products of lipid oxidation [460] and other ROS [462]. In the colon of *Il10*$^{-/-}$ mice fed the 30% salmon diet, ALDH1B1 protein expression was increased compared to those fed the 30% control diet, and was similar to another study in *Il10*$^{-/-}$ mice, where AA-enriched diets increased its expression in the colon compared to a

control diet [268]. However, as the concentration of AA in the 30% salmon diet was similar to the 30% control diet (approximately 0.1%), and lower than 3.7% in the study of Cooney *et al.* [268], ALDH1B1 expression was most likely not affected by dietary AA provided by the salmon diet. Nevertheless, an increase in ALH1B1 was also observed in *Il10*$^{-/-}$ mice compared to C57BL/6J mice as discussed above, and may have been linked to the metabolism of tryptophan in those mice. Furthermore, elevated levels of ALDH1B1 have been suggested as biomarkers of human colon cancer [460]. Due to the wide range of substrates, it is not possible to confidently link ALDH1B1 protein expression to a specific metabolic process.

The intake of the 30% salmon diet may have increased fatty acid β-oxidation in the colon of *Il10*$^{-/-}$ mice compared to those fed the 30% control diet, attributed to elevated protein expression of TPI1. There is limited evidence on the effects of PUFA on TPI1 expression, and the results presented in Chapter 3 and other published studies [268] did not support this increase of TPI1 by an EPA-enriched diet. It has been reported that TPI1 specifically catabolises β-oxidative processes from saturated fatty acids [450], which were approximately twice the amount in the 30% salmon diet (4.3%) compared to the 30% control diet (2.3%), and may explain the elevated TPI1 protein expression in the colon of 30% salmon-fed *Il10*$^{-/-}$ mice. As IBD is an energy-deficiency disease, an increase in β-oxidation and therefore increased energy production is favourable.

Nutrients in salmon that possess antioxidant activity (*e.g.* vitamin E) may have protected against the inflammation-induced oxidative stress that was observed in the colon of *Il10*$^{-/-}$ mice (compared to C57BL/6J mice) and commonly reported in IBD patients [439, 440, 463]. In *Il10*$^{-/-}$ mice fed the 30% salmon diet, TXN protein was decreased in colon tissue compared to those fed the 30% control diet, and may have been the result of increased vitamin E intake provided by the 30% salmon diet (5.3 mg vitamin E in 100 g fresh salmon fillet). Supplementation with vitamin E (in the form of α-tocopherol) has been linked to decreased oxidative stress in patients with coronary spastic angina [464] and viral Hepatitis C [465] and was attributed to decreased serum levels of TXN. Nevertheless, lower levels of ER stress were not observed in the colon of *Il10*$^{-/-}$ mice fed the 30% salmon diet (attributed to unchanged expressions of proteins HSPA5 and LONP1) compared to those fed the 30% control diet.

The association of the intake of 30% salmon by *Il10*$^{-/-}$ mice and antigen presentation pathways was shown by transcriptomic and proteomic profiling of colon tissue compared to those fed the 30% control diet. No effect of dietary DHA [260] or EPA as shown in Chapter 3 and published studies [6, 268] were observed on genes and/or proteins related to antigen presentation pathways in mice with experimental colitis. It appears that in *Il10*$^{-/-}$ mice fed the 30% salmon diet, the proteasome-mediated antigen presentation to $CD8^+$ T cells was decreased, mediated by proteins PSMB9 and CALR (reduced in expression) and genes that code for MHC class I molecules (reduced in expression). This pathway is specifically associated with the intracellular degradation of proteins that are at the end of their functional lives [as reviewed in 56]. It is possible that lower levels of oxidative stress in 30% salmon-fed *Il10*$^{-/-}$ mice may have resulted in reduced protein misfolding in the ER, thus further explaining reduced antigen processing and presentation. However, the evidence regarding misfolded proteins and antigen presentation remains unclear, with some studies suggesting that misfolded proteins can lead to increased presentation of MHC class I antigens [466], while others do not support this view [467].

The transcription factors *PPARA* and *PPARG* have repeatedly been reported to be activated by n-3 PUFA-enriched diets in animal models of colitis [3, 6, 252] and in agreement with Chapter 3. The transcriptomic analysis of colon tissue from *Il10*$^{-/-}$ mice fed the 30% salmon diet indicated enhanced expression of KEGG pathway *PPAR signalling* compared to those fed the 30% control diet (findings presented in Chapter 4). However, proteomic analysis of the colon from *Il10*$^{-/-}$ mice did not support these responses to the 30% salmon diet and is in contrast with published data showing reduced expression of HSP90AB1 protein by dietary EPA (vs. OA control diet) [268]. The protein HSP90AB1 is a repressor of PPARA activity [270], thus decreased expression of HSP90AB1 protein may have resulted in increased activity of PPARA and subsequent transcription of PPARA target genes [268]. In the current study, reduced HSP90 (isoform AA1 or AB1) was however observed in healthy C57BL/6J mice fed the 30% salmon diet (vs. 30% control diet).While this may indicate an effect specific to heathy mice, Chapter 4 did not indicate gene expression changes associated with *PPAR signalling* in those mice and was also not show by published data [268] and may indicate that increased HSP90 (as a molecular chaperone) was not associated with *PPAR signalling*.

5.5.2 Transcriptomic profiling of liver tissue

5.5.2.1 Liver transcriptomic profile during colitis

Compared to C57BL/6J mice, elevated inflammatory processes were detected in the liver of *Il10*$^{-/-}$ mice fed the 30% control diet and similar to other studies using mice with experimental colitis [444, 447, 468, 469]. In IBD, hepatic inflammation is attributed to the translocation of various bacterial species to the liver [444-446], potentially caused by a disruption in the epithelial barrier integrity [447]. In *Il10*$^{-/-}$ mice, the hepatic transcriptomic profile showed elevated host defence mechanisms by receptor recognition, for example, NOD-like receptor signalling, thus potentially indicating increased microbial translocation. In the bloodstream, bacterial endotoxins (*e.g.* lipopolysaccharide (LPS)) and endotoxin-containing complexes can activate monocytes and macrophages, which at high LPS doses was reported to trigger *NFKB* signalling pathways, while at low LPS doses, inflammatory responses were mediated by the transcription regulator *CEBPD* [470]. Gene expression levels of hepatic *CEBPD* were increased in *Il10*$^{-/-}$ mice compared to C57BL/6J mice fed the 30% control diet, thus may indicate increased endotoxemia in *Il10*$^{-/-}$ mice.

CEBPD was further one of the central transcription factors that regulated many of the differentially expressed genes in the liver of *Il10*$^{-/-}$ mice fed the 30% control diet (vs. C57BL/6J mice), and was associated with the predicted increases in inflammatory cell activation in those mice. IL17, a cytokine produced and secreted by activated T cells [471], can trigger CEBPD-mediated transcription of *IL6* and subsequent B cell development [472], thus may represent a link between T cell activation and colitis in *Il10*$^{-/-}$ mice. Downstream of CEBPD, the gene *SAA3* (coding for the acute phase protein serum amyloid α; a major acute-phase protein synthesised and secreted mainly by the liver) is one of the target genes of CEBPD [473], and was increased in expression in *Il10*$^{-/-}$ mice compared to C57BL/6J mice. Serum amyloid α has been reported to be increased in mice with experimental colitis [6, 109, 474, 475] and IBD patients [143, 476], further supporting the observed gene expression changes.

The hepatic transcriptomic profile of *Il10*$^{-/-}$ mice fed the 30% control diet showed that genes coding for phase I (family of CYPs), phase II (*e.g.* family of glutathione S-transferases, and *UGT1A9* and *HS3ST6*), and phase III (membrane-bound transporter

ABCC3) detoxification enzymes were affected compared to C57BL/6J mice fed the same diet. The liver is a central organ for xenobiotic metabolism, and it has previously been reported that reduced functionality of hepatic CYP enzymes may be the result of increased bacterial translocation and endotoxemia as a consequence of chronic inflammation in the intestine [445, 477]. This might explain the observed reductions in expression of CYPs in the liver of *Il10*$^{-/-}$ mice compared to C57BL/6J mice, in common to other mouse models of experimental colitis [444, 478]. Decreased detoxification of xenobiotics in the colon of IBD patients is well known [264], and has been observed in the colon of *Il10*$^{-/-}$ mice (Chapters 3 and 4, and Knoch *et al.* [6]), including other mouse models of colitis, *e.g.* TNBS [468] and DSS [444] thus supporting the current findings.

5.5.2.2 Liver transcriptomic profile in response to the 30% salmon diet (vs. 30% control diet) irrespective of genotype

The intake of the 30% salmon diet induced the expression of genes associated with xenobiotic metabolism in the liver of mice compared to those fed the 30% control diet, irrespective of genotype. This was attributed to increased genes coding phase I (family of CYPs), phase II (glutathione S-transferases), and phase III (membrane-bound transporter *ABCC3*) detoxification enzymes. The genes *NR1I3* and pregnane X receptor (*PXR*; also known as *NR1I2*) encode nuclear receptors that are central in hepatic xenobiotic metabolism and further regulate homeostasis of lipids, vitamins and other endogenous hydrophobic molecules [443, 479]. The induction of xenobiotic-related gene expression may have been moderated by *NR1I3* and *PXR* in response to the 30% salmon diet, as both nuclear receptors were shown to be associated with the differentially expressed genes by IPA *Upstream regulator analysis*. While hepatic transcriptomic profiling indicated a non-differential expression of the nuclear receptors in 30% salmon-fed *Il10*$^{-/-}$ mice (vs. 30% control diet), within C57BL/6J mice, hepatic *NR1I3* was increased compared to those fed the 30% control diet. *PXR* and *NR1I3* regulate their own expression [479] by inhibiting their transcription and limiting the induction of target genes [480]. This may reduce the mRNA expression levels of a transcriptional regulator while its protein product is still active [481].

Increased mRNA expression levels of hepatic CYPs in all 30% salmon-fed mice irrespective of genotype (vs. 30% control diet) may indicate elevated hepatic metabolism of nutrients provided by the salmon, such as vitamins E [482] and A [483]. This is

supported by current knowledge about metabolism of retinoic acid (vitamin A) in the liver, which is primarily mediated by CYP26A1 [483]. Compared to mice fed the 30% control diet, *CYP26A1* was among the genes with the highest increase in expression in the liver of those fed the 30% salmon diet, irrespective of genotype. Retinoic acid may exert its functions *via* nuclear receptors (especially RXR) [as reviewed in 484]. Vitamin A cannot be synthesised by animals, hence observed increases in metabolism of retinol is attributed to dietary sources. In farmed salmon (as was used in the current experiment), the retinoic acid astaxanthin is one of the primary forms of pigmentation used in salmon feed [485, 486], thus is the primary carotenoid present in muscle of salmon [487]. In mice, astaxanthin can be converted to retinol *via* β-carotene [488] and may therefore provide substrate for *CYP26A1*.

Vitamin E is among the vitamins with the highest concentration in muscle of salmon [178], and the liver regulates α-tocopherol concentration by increasing genes coding for phase I, II, and III detoxification enzymes [482], involving a series of enzymatic conversions that yield α-CEHC as a major metabolite [489]. *NR1I3* and *PXR* were shown to be involved in the regulation of gene transcription in all three phases of biotransformation of α-tocopherol [482]. It is possible that the elevated expression of xenobiotic genes is indicative of increased metabolism of α-tocopherol in the liver after salmon intake, irrespective of genotype.

The hepatic transcriptomic profile of all mice fed the 30% salmon diet was associated with fatty acid metabolism compared to those fed the 30% control diet, irrespective of genotype. The observations were based on increased expression of acyl-coenzyme A thioesterases (*ACOT2*, *3*, and *4*), but reduced expression of ELOVL fatty acid elongases (*ELOVL2* and 5), and stearoyl-CoA desaturase (*SCD*) in mice on the 30% salmon diet. Due to the mixture of fatty acids in salmon, it is difficult to attribute effects to specific types of fatty acids. A study in mice fed high-fat diets reported reduced expression and activity of ELOVL5, however, the diets provided 60% of the energy from fat, approximately double the amount compared to the 30% salmon diet, and did not contain LC n-3 PUFA [192]. It is therefore more likely that reduced hepatic mRNA expression of *ELOVL5* in mice fed the 30% salmon diet was linked to feedback regulation of fatty acid elongases by the LC n-3 PUFA in the salmon [192]. *ELOVL2* and *ELOVL5* contribute to the *de novo* PUFA synthesis, *i.e.* the conversion of LA to AA (n-6 pathway) and ALA to DHA (n-3 pathway), by elongating 20- and 22-carbon PUFA (*ELOVL2*) and

18- and 20-carbon PUFA (*ELOVL5*) [192, 490]. The 30% salmon diet provided more EPA and DHA than their precursor ALA (n-3 pathway), therefore a reduction in expression of fatty acid elongases (*ELOVL2* and *ELOVL5*) may have occurred compared to those mice fed the 30% control diet.

Compared to mice fed the 30% control diet, those fed the 30% salmon diet showed increased utilisation of fatty acids for energy production in the liver. SCD is the rate-limiting enzyme in the biosynthesis of MUFA in the liver (*e.g.* palmitoleic acid (16:1n-7) and oleic acid (18:1n-9) from palmitate (16:0) and stearate (18:0)), and was decreased in 30% salmon-fed mice irrespective of genotype. MUFA are the preferred fat storage in liver cells [377, 491, 492], thus reduced expression of *SCD* may have reduced the hepatic lipid content, as observed in another study in C57BL/6J mice where fish oil diets decreased hepatic *SCD* gene expression relative to those fed a control diet, resulting in a reduction of hepatic lipid stores [480]. Additionally, the gene *ACSL1*, involved in the activation of fatty acids for degradation by β-oxidation, was increased in expression but only in the liver of *Il10*$^{-/-}$ mice fed the 30% salmon diet (vs. those fed the 30% control diet). Furthermore, the increased KEGG pathway gene set *Fatty acid degradation* in the liver of mice fed the 30% salmon diet, and increased expression of hepatic *ACOT* genes which regulate and terminate reactions in the fatty acid β-oxidation [493], supports these findings. As similar observations were made in the liver of C57BL/6J mice fed a fish oil diet for six weeks [494], the induction of genes associated with hepatic mitochondrial fatty acid β-oxidation cannot be specifically attributed to colitis in *Il10*$^{-/-}$ mice.

5.5.2.3 Liver transcriptomic profile in response to the 30% salmon diet (vs. 30% control diet) in *Il10*$^{-/-}$ mice

The intake of the 30% salmon diet reduced hepatic expression of *CEBPD* in *Il10*$^{-/-}$ mice compared to those fed the matched control diet, but these effects were not observed in C57BL/6J mice. There is limited evidence of the regulation of hepatic *CEPBD* by dietary n-3 PUFA. Inflammatory cytokines such as IL1B can induce transcriptional activity of *CEBPD* [495], but *IL1B* was not differentially expressed in liver tissues of 30% salmon-fed *Il10*$^{-/-}$ mice (vs. 30% control diet). As discussed earlier, increased hepatic *CEBPD* may be indicative of endotoxemia, therefore the reduced expression of *CEBPD* in 30% salmon-fed *Il10*$^{-/-}$ mice may be attributed to a reduction of circulating endotoxins compared to those fed the 30% control diet. While *CEBPD* regulates the transcription of

acute phase proteins such as serum amyloid α in the liver [496], the reduction of *CEBPD* gene expression did not result in reduced expression of *SAA* genes in *Il10*$^{-/-}$ mice fed the 30% salmon diet (vs. 30% control diet).

5.5.3 Urine metabolomics

The differences in the urinary metabolite fingerprint between all treatment groups became more pronounced with increasing age and therefore increasing colitis in *Il10*$^{-/-}$ mice. A similar result was shown in Chapter 3, where the total number of significantly different ions between the treatment groups increased over the experimental period. At the first time-point (6.2 weeks of age), when *Il10*$^{-/-}$ mice do not show signs of colitis based on histological analysis [280], the clusters of specific treatment groups were not well established. This may potentially be attributed to the lack of inflammatory metabolites in the urine of *Il10*$^{-/-}$ mice at this stage. However, Lin *et al.* [393] reported that xanthurenic acid, the main metabolite associated with early stages of colitis in *Il10*$^{-/-}$ mice, was elevated as early as 5.5 weeks of age compared to C57BL/6J mice.

It is not possible here to draw conclusions regarding changes in the abundances of the individual metabolites over the experimental period. This is due to the fact that the urine collected was analysed in three MS analytical batches specific to their collection time-points and without the inclusion of a common reference sample. After pre-processing and normalisation of MS data, a clear separation of the metabolomic fingerprints were shown to be based on time of urine collection, but may have been artefacts of the analytical batches.

5.5.3.1 Urine metabolomic profile during colitis

In the urine of *Il10*$^{-/-}$ mice, xanthurenic acid glucoside and its aglycone were detected. As observed in Chapter 3 and in agreement with published data [281], increased urinary xanthurenic acid was associated with colitis in *Il10*$^{-/-}$ mice and a side-product of tryptophan catabolism, a pathway shown to be enhanced in lesional biopsies from CD patients [365]. In *Il10*$^{-/-}$ mice, the abundance of urinary xanthurenic acid was elevated from 6.2 weeks of age, which is before signs of colitis are present in *Il10*$^{-/-}$ mice [280], and remained higher compared to C57BL/6J mice until 11.5 weeks of age when colitis was established in *Il10*$^{-/-}$ mice. This is in agreement with other studies using *Il10*$^{-/-}$ mice [281, 309, 393]. The detection of xanthurenic acid was only possible in positive mode. In

negative mode, the molecular ion was absent from the XCMS table (theoretical molecular ion *m/z* 204), but a targeted search of the *m/z* 204 ion confirmed its presence in the MS spectrum. As suggested by Otter *et al.* [309], a closely eluting metabolite interfered with the molecular ion corresponding to xanthurenic acid in negative ionisation mode. In Chapter 3, a different mass spectrometer was used for metabolomic fingerprinting compared to the current chapter and Otter *et al.* [309], enabling the detection of the molecular ion *m/z* 204 in negative mode.

The abundance of xanthurenic acid glucoside was higher in urine of *Il10*$^{-/-}$ mice compared to C57BL/6J at all time-points (in agreement with the findings presented in Chapter 3). Cain *et al.* [392] associated xanthurenic acid glucoside in human urine as a natriuretic hormone that regulates sodium excretion by the kidney. The abundance of this metabolite in the urine was low, which can make it difficult to detect above background signals in untargeted metabolomic fingerprinting.

The metabolites α-CEHC glucuronide and γ-CEHC glucoside were decreased in abundance in the urine of *Il10*$^{-/-}$ mice compared to C57BL/6J mice, both fed the 30% control diet. Both metabolites were also putatively identified in Chapter 3, with reduced abundances in the urine of *Il10*$^{-/-}$ mice compared to C57BL/6J mice. α-CEHC glucuronide and γ-CEHC glucoside are the water-soluble forms of vitamin E, formed from α-tocopherol and γ-tocopherol by glucuronidation in the liver [350, 497]. Serum concentrations of α-tocopherol may be a marker for the status of vitamin E in the liver [498], and its metabolised form, α-CEHC glucuronide, has previously been suggested as a biomarker of colitis in *Il10*$^{-/-}$ mice [309]. These metabolites (xanthurenic acid, α-CEHC glucuronide and γ-CEHC glucoside) were considered candidate biomarkers of colitis and are further discussed in Chapter 6.

5.5.3.2 Urine metabolomic profile in response to the 30% salmon diet (vs. 30% control diet) irrespective of genotype

The urinary abundance of the vitamin E metabolite α-CEHC glucuronide was dependent on diet at all time-points, with higher abundance in all salmon-fed mice, regardless of genotype. This increase in response to the 30% salmon diet may be due to the amount of α-tocopherol that was provided by the salmon compared to the 30% control diet, as the majority of tocopherol in salmon are in the alpha homologue [168]. This was supported by a study in healthy male Japanese adults, where a positive correlation between the

intake of α-tocopherol as part of a controlled diet and urinary abundance of α-CEHC was reported [499]. The standard vitamin mixture added to the experimental diets contained vitamin E in the form of α-tocopherol (personal communication, Lorene Leiter, Research Diets Inc, and Anonymous [285]) and was equally incorporated into control and salmon diet, thus differences in α-tocopherol abundance in urine should be independent of other dietary factors than salmon. Thus, the higher urinary abundance of α-CEHC glucuronide may be attributed to the α-tocopherol provided by the 30% salmon diet, but its metabolism in the liver remains to be established.

5.5.3.3 Urine metabolomic profile in response to the 30% salmon diet (vs. 30% control diet) in *Il10*$^{-/-}$ mice

γ-CEHC glucoside, a metabolite of γ-tocopherol showed a genotype-specific response to the 30% salmon diet, with the urinary abundance in 30% salmon-fed *Il10*$^{-/-}$ mice further reduced (vs. 30% control diet). Considering that the salmon diet provided tocopherol mostly in the alpha homologue [168], the levels of γ-tocopherol metabolites should be similar between mice fed the 30% salmon diet and those fed the 30% control diet. However, it was shown that α-tocopherol can affect metabolism of γ-tocopherol in the liver [500, 501] and may offer an explanation for the reduced level of γ-CEHC glucoside in the urine of *Il10*$^{-/-}$ mice fed the 30% salmon diet (vs. 30% control diet).

It is yet to be clarified whether α-tocopherol is more anti-inflammatory than γ-tocopherol, however, it is suggested that their effects may be dose-dependent and may reach cytotoxicity at high levels [502]. Jiang *et al.* [503] tested the inflammatory response to α- and γ-tocopherols in LPS-stimulated human macrophages and IL1B-treated human epithelial cancer cells. They specifically measured the synthesis of PGE2, a lipid mediator that is synthesised *via* the COX2-catalysed oxidation of AA during inflammation. It was reported that γ-tocopherol and its metabolite γ-CEHC reduced the synthesis of PGE2 in macrophages and epithelial cells, whereas α-tocopherol only reduced PGE2 synthesis in macrophages, but not in epithelial cancer cells. The effects of γ-tocopherol and γ-CEHC in macrophages were linked to the "inhibition of COX2 activity, rather than affecting protein expression or substrate availability, and appeared to be independent of antioxidant activity". An *in vivo* study among patients with Metabolic Syndrome showed that the combined administration of α- and γ- tocopherol was superior in reducing markers of

oxidative stress and inflammation (*e.g.* plasma TNF and CRP) than supplementation of either one alone [504].

The 30% salmon diet did not affect the abundance of xanthurenic acid in the urine of *Il10*$^{-/-}$ mice (vs. 30% control diet) and is in contrast to the observations of Chapter 3, where a genotype-specific reduction of the metabolite was observed in the urine of *Il10*$^{-/-}$ mice with established colitis (vs. OA diet).

5.5.4 Microbiomic analysis of caecum digesta

5.5.4.1 Microbial community profile during colitis

In the caecum of *Il10*$^{-/-}$ mice, decreased microbial diversity was observed compared to C57BL/6J mice. The *Firmicutes*/*Bacteroidetes* ratio was shown to be reduced in faecal samples of patients with active IBD, mainly driven by a reduction of the species *F. prausnitzii* in the phylum *Firmicutes* [505]. Similar observations were made in the caecum of *Il10*$^{-/-}$ mice in the current study, where the ratio decreased to approximately 1:1 from 2.5:1 in C57BL/6J mice. The increase in *Bacteroidetes* in *Il10*$^{-/-}$ mice was mainly attributed to elevated proportions of *Bacteroides* spp., which is commonly reported in IBD patients [506, 507] and in other studies using *Il10*$^{-/-}$ mice [277, 508].

In the caecum of C57BL/6J mice, the dominant species was *Allobaculum* spp. in the phylum *Firmicutes*, a SCFA-producing bacterium [509] and *in vitro* it has been demonstrated that SCFAs may exert anti-inflammatory effects by inhibition of the NFKB cascade *via* TNF [510]. Furthermore, SCFAs (in particular butyrate) are the main energy source for colonocytes [511], and depletion of SCFA-producing bacteria may provide a further link between the suggested energy deficiency of mucosal cells and chronic intestinal inflammation [429]. *F. prausnitzii* was not detected in the current study and may have been below the detection limited therefore no conclusion can be reached about its levels.

5.5.4.2 Microbial community profile in response to the 30% salmon diet (vs. 30% control diet) irrespective of genotype

It is known that dietary choices shape the microbiota [123], and an increase, or depletion, of a specific bacteria due to dietary changes is linked to the ability of the bacterial community to metabolise the nutrients offered. By comparing the microbial profile in the

caecum of mice fed a 30% salmon diet to those fed the 30% control diet, changes can be related to the effect of the nutrient profile of salmon. Results showed that the intake of the 30% salmon diet did not change which taxa were present in the caecum of mice, but instead affected the abundance of some of the resident bacteria (*e.g. V. akkermansia*), an effect which was independent of genotype.

In the caecum of mice that were fed the 30% salmon diet, the abundance of *V. akkermansia* was increased compared to the 30% control diet, regardless of genotype. *Akkermansia muciniphila*, the only sequenced strain in the phylum *Verrucomicrobia*, is a mucin-degrading bacterium that resides in the mucus layer [512] and abundantly colonises in a nutrient-rich environment. The mucus is a substrate for commensal microbiota and a loss of goblet cell-containing crypts and goblet cells may therefore result in a loss of substrate. Evidence showed that *A. muciniphila* was depleted in faeces [513] and mucosal biopsies [514] of patients with active IBD compared to healthy controls. While the intake of dietary PUFA has previously not been associated with altered abundance of *A. muciniphila*, the bacterium has been shown to be increased by administration of prebiotics (oligofructose) in genetically obese mice [515]. Nevertheless, there is controversy regarding *A. muciniphila*, as it exacerbated large intestinal inflammation in typhimurium-infected gnotobiotic mice [516], while Everard *et al.* [275] attributed increased abundance of *V. akkermansia* to a restoration of the colonic barrier function by increasing mucus layer thickness. An increase of *A. muciniphila* was observed irrespective of genotype, however, it is possible that *A. muciniphila* favourably influenced the colonic barrier function in 30% salmon-fed *Il10*$^{-/-}$ mice and contributed to the reduced severity of colitis in those mice compared to the 30% control diet.

5.5.4.3 Microbial community profile in response to the 30% salmon diet (vs. 30% control diet) in *Il10*$^{-/-}$ mice

The 30% salmon diet did not affect the loss of bacterial diversity associated with colitis in *Il10*$^{-/-}$ mice compared to those fed the 30% control diet. However, in *Il10*$^{-/-}$ mice fed the 30% salmon diet, *Eubacterium* spp. was decreased compared to those fed the 30% control diet, with the 16S rRNA gene sequence most closely associated with *Eubacterium dolichum*. *E. dolichum* has previously not been associated with IBD. However, an increase of *E. dolichum* was reported in a mouse model of obesity induced by Western-type diets which were high in fat (41% energy as fat compared to 34% in the 30% salmon

diet) [517]. *E. dolichum* abundance did not increase in the caecum of C57BL/6J mice on either diet, the effect cannot be entirely attributed to the differences in lipid profiles between the 30% salmon diet and the 30% control diet. The genotype-specific changes indicate an effect of either the *Il10*$^{-/-}$ genotype or inflammation-related differences, for example, increased intestinal permeability is linked to both obesity and IBD. Nevertheless, compared to other genera, the abundance of this bacterium was generally low and can make it difficult to detect.

5.6 Conclusion and outlook

The use of a multi-'Omics' approach allowed the identification of novel pathways/ regulatory processes by which a diet containing 30% salmon reduced the severity of colitis in *Il10*$^{-/-}$ mice and integrating these resulting datasets (gene, protein, metabolite and microbiota) may enable the identification of biomarkers of colitis that are specifically responsive to dietary salmon in *Il10*$^{-/-}$ mice. Diet-induced changes in the colon, microbiota and/or liver may result in differential abundance of metabolites (*e.g.* α-CEHC glucuronide and γ-CEHC glucoside) which could potentially be detected in surrogate "tissues" such as urine.

Chapter 6

Integration of ‘Omics’ data to characterise the systemic responses to a diet containing 30% salmon in the interleukin-10 gene-deficient mouse

6.1 Introduction

The integration of 'Omics' data enables the interpretation of complex, individual datasets, *e.g.* transcriptomics, proteomics, metabolomics and microbiomics, to understand the biology behind a complex system such as IBD and how diet might decrease this disease risk. For example, the combination of large-scale profiling of genes, proteins and metabolites in blood, urine, and adipose tissue provided evidence for the anti-inflammatory and anti-oxidative properties of a dietary supplement containing n-3 PUFA-rich fish oil, green tea extract, resveratrol, α-tocopherol, vitamin C and tomato extract in overweight, but otherwise healthy, subjects [518]. The integration of gene expression data from blood and adipose tissue showed that increased fatty acid oxidation, reduced triacylglycerol synthesis in the liver, as well as *PPARG* activation in adipose tissue, were linked to decreased plasma triacylglycerol concentrations in subjects receiving the supplement [518]. This shows the potential of a systems biology approach to explain changes in plasma lipid biomarkers with molecular responses in the liver and adipose tissues following nutritional intervention. Such systems biology approach may allow a more targeted strategy to monitor the efficacy of dietary intervention studies in humans to reduce risk of colitis that occurred in IBD.

In this dissertation, a diet containing EPA (vs. control OA diet) was confirmed, as expected from previous studies, to reduce colitis in *Il10*$^{-/-}$ mice, a model of colitis, when colitis was established, but not at an early time-point of colitis (Chapter 3). While transcriptomic analysis of PBMCs showed similarity of gene expression of colon in *Il10*$^{-/-}$ mice and published studies in IBD human subjects [143], it was not the case for the comparison of the EPA diet in *Il10*$^{-/-}$ mice (Chapter 3). Urinary metabolites for the colitis comparison and EPA comparison were more informative and provided a focal point for exploring potential tissue (colon and liver) pathways in Chapters 4 and 5. In Chapter 4, a diet containing 30% salmon was shown to reduce the symptoms of colitis in *Il10*$^{-/-}$ mice compared to those fed a matched control diet. This effect was associated with changes in expression of colonic genes (and for some proteins) linked to lymphocyte function and metabolism-related KEGG pathways, specifically lipid metabolism, in the colon and liver of these mice (Chapters 4 and 5). The changes in colonic gene expression were similar to those shown in Chapter 3 for the EPA diet. Furthermore, the profile of the caecal microbiota was modulated with altered abundances of *Eubacterium* spp. and an

unclassified *Rikenellaceae* (Chapter 5). Feeding a 30% salmon diet to *Il10*$^{-/-}$ mice indicated some candidate biomarkers in urine (α-CEHC glucuronide and γ-CEHC glucoside, the latter showing a genotype-specific response to salmon) (Chapter 5). The integration of the urine metabolomics data with the large intestinal and liver 'Omics' data could provide new insights into the effects of this diet on colitis and identify candidate biomarkers correlated to these responses.

6.2 Hypothesis and aim

The hypothesis of this study was that the integration of 'Omics' data provides additional insights into the colitis phenotype of *Il10*$^{-/-}$ mice and the systemic responses to a diet supplemented with 30% salmon that was associated with improved colitis in *Il10*$^{-/-}$ mice. To test this hypothesis, data from multiple 'Omics'-technologies were integrated to identify how altered colon and liver metabolic pathways, and the caecal microbial community profile could represent changes in urinary metabolite profiles in *Il10*$^{-/-}$ mice with established colitis and their responses when these mice were fed a 30% salmon-enriched diet. To this end, 'Omics' datasets were integrated as follows: (a) colon transcriptomic and proteomic data with urine metabolomic data, (b) liver transcriptomic data with urine metabolomic data, and (c) caecal microbiomic data with urine metabolomic data.

6.3 Methods

The mouse experiment was conducted according to methods described in Chapter 2. Transcriptomic and proteomic analyses of colon tissue and transcriptomic analysis of liver were described in Sections 2.6 to 2.8, urine metabolite analysis in Section 2.9, and next-generation sequencing of caecum digesta in Section 2.10. The integration of these 'Omics' data is described in Section 2.11. All individual datasets used for the integration or supporting information were presented in Chapter 3 (EPA: colon transcriptomics, urinary metabolomics), Chapter 4 (Salmon: colon transcriptomics), Chapter 5 (Salmon: colon proteomics, liver transcriptomics, urinary metabolomics, caecal microbiomics).

6.4 Results

6.4.1 Tryptophan metabolism between mouse genotypes fed the 30% control diet

The combined analysis of colon gene expression and urinary metabolite data indicated changes in the metabolism of tryptophan with increased colitis, as shown by the comparison of *Il10*$^{-/-}$ mice fed the 30% control diet with C57BL/6J mice fed the same diet. As shown in Figure 6.1, the expression of genes that lead to the synthesis of tryptamine and tryptamine-derived metabolites from tryptophan (*e.g. INMT*, *MAOA* and *MAOB*), and serotonin from tryptophan (*e.g. TPH1*) were reduced, contrasting the increase of genes that mediate the production of xanthurenic acid. mRNA expression levels of *IDO1*, the gene that codes for the enzyme that catalyses the rate-limiting step in the conversion of tryptophan to xanthurenic acid, was approximately 10-fold higher in the colon of *Il10*$^{-/-}$ mice compared to C57BL/6J mice, both fed the 30% control diet. Concomitantly, increased abundance of urinary xanthurenic acid was observed in *Il10*$^{-/-}$ mice with established colitis. Similar changes were observed in *Il10*$^{-/-}$ mice compared to C57BL/6J mice, both fed the OA diet (data from Chapter 3; Appendix VIII). This suggests that urinary xanthurenic acid concentration may be representative of the changes in tryptophan metabolism occurring when colitis was established.

6.4.2 Tocopherol metabolism between mouse genotypes fed the 30% control diet

The abundance of ions corresponding to the metabolites γ-CEHC glucoside and α-CEHC glucuronide in the urine correlated with several genes that regulate the biotransformation of xenobiotics in the liver (Figure 6.2). In *Il10*$^{-/-}$ mice fed the 30% control diet, reduced levels of both metabolites were detected in the urine compared to C57BL/6J mice. The lower level of α-CEHC glucuronide may partly be attributed to reduced expression of genes involved in phase I (*Cyp3a11* and *Cyp3a16*), phase II (*Gsta4*) and phase III (*Abcc3*) biotransformation in the liver of *Il10*$^{-/-}$ mice (Figure 6.2). *Ugt1a10*, a gene that mediates the glucuronidation of α-CEHC to α-CEHC glucuronide, showed increased mRNA transcript levels in the liver, and negatively correlated with the metabolites in urine (all Pearson correlation coefficient ≥ |0.65|) (Figure 6.2).

Furthermore, as illustrated in Figure 6.2, several genes correlated with the abundance of γ-CEHC glucoside in urine, but none of these genes was differentially expressed in the liver of *Il10*$^{-/-}$ mice fed the 30% control diet compared to C57BL/6J mice. This may indicate that the lower urinary abundance of γ-CEHC glucoside observed in *Il10*$^{-/-}$ mice during colitis may not be attributed to changes in hepatic expression of xenobiotic genes (Figure 6.2), or alternatively may be attributed to changes in protein activity which were not measure in this study.

6.4.3 Microbial community profile between mouse genotypes fed the 30% control diet

Changes in the microbial community composition in the caecum of *Il10*$^{-/-}$ mice compared to C57BL/6J mice, specifically for *Bacteroides* spp. (phylum *Bacteroidetes*) and two members of the phylum *Firmicutes* (*Allobaculum* spp. and an unclassified *Coprobacillaceae*), were linked to changes in the abundance of urinary metabolites (Figure 6.3).

In the caecum of *Il10*$^{-/-}$ mice fed the 30% control diet, the decreased sequence counts of the phylum *Firmicutes* was driven by the depletion of *Allobaculum* spp. Only approximately 10% of the total number of sequences were assigned to *Allobaculum* spp., compared to approximately 30% for C57BL/6J mice ($P < 0.05$). As indicated by an asterisk in Figure 6.3, the sequence counts of *Allobaculum* spp. were positively correlated with the urinary abundance of an unidentified metabolite eluting at 373 sec in positive and negative ionisation mode, indicating that the depletion of *Allobaculum* spp. in *Il10*$^{-/-}$ mice was associated with lower abundance of this metabolite in the urine.

An approximate 3-fold increase in sequence counts of *Bacteroides* spp. was observed in the caecum of *Il10*$^{-/-}$ mice fed the 30% control diet compared to C57BL/6J mice fed the same diet. As shown in Figure 6.3, this increase correlated with the abundance of several urinary metabolites, including xanthurenic acid (ions "M159.9T201", "M177.9T201" and "M205.9T200"). The positive correlation of *Bacteroides* spp. with xanthurenic acid may indicate a link between the commensal microbiota and alterations in metabolism of tryptophan when colitis was established.

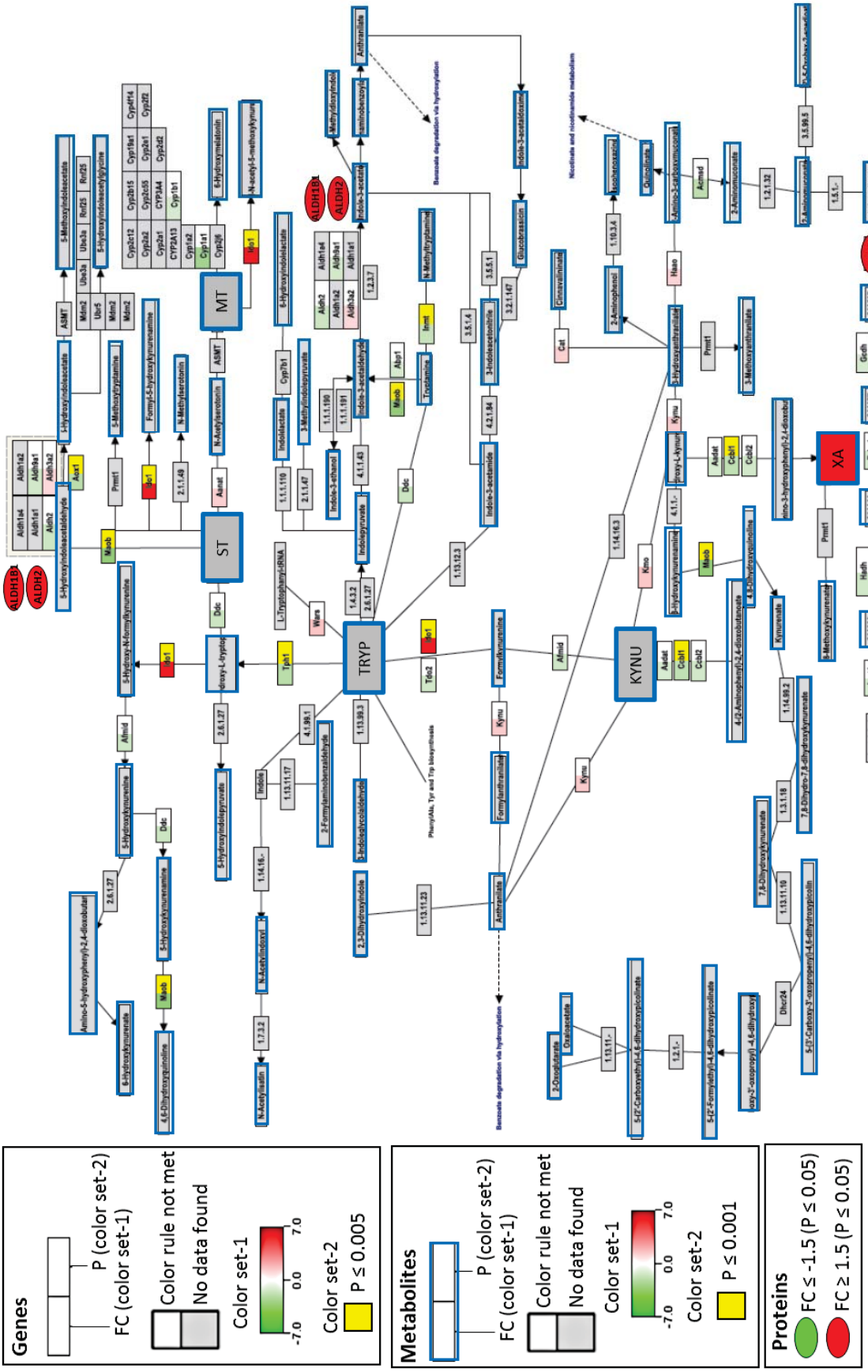

Figure 6.1 Biological pathway for *Tryptophan metabolism* indicating molecular events that lead to the biosynthesis of melatonin from tryptophan (*via* serotonin), or xanthurenic acid (*via* kynurenine) in *Il10*$^{-/-}$ mice fed the 30% control diet compared to C57BL/6J mice fed the same diet.

Figure 6.1 continued. Nodes represent genes (rectangles), proteins (ovals), or metabolites (rectangles with a coloured border). Colour coding of nodes indicates increased (red) or decreased (green) levels, as illustrated in the legend. Data for genes and metabolites shaded in grey not considered or measured. Gene expression data were established by microarray analysis of colon tissue from *Il10*$^{-/-}$ mice, protein expression data by 2D-DIGE, and metabolomics data by untargeted LC-MS of urine. Pathway information obtained from Kanehisa *et al.* [328] and Ferrante *et al.* [519].
KYNU: Kynurenine; MT: Melatonin; ST: Serotonin; TRYP: Tryptophan; XA: Xanthurenic acid.

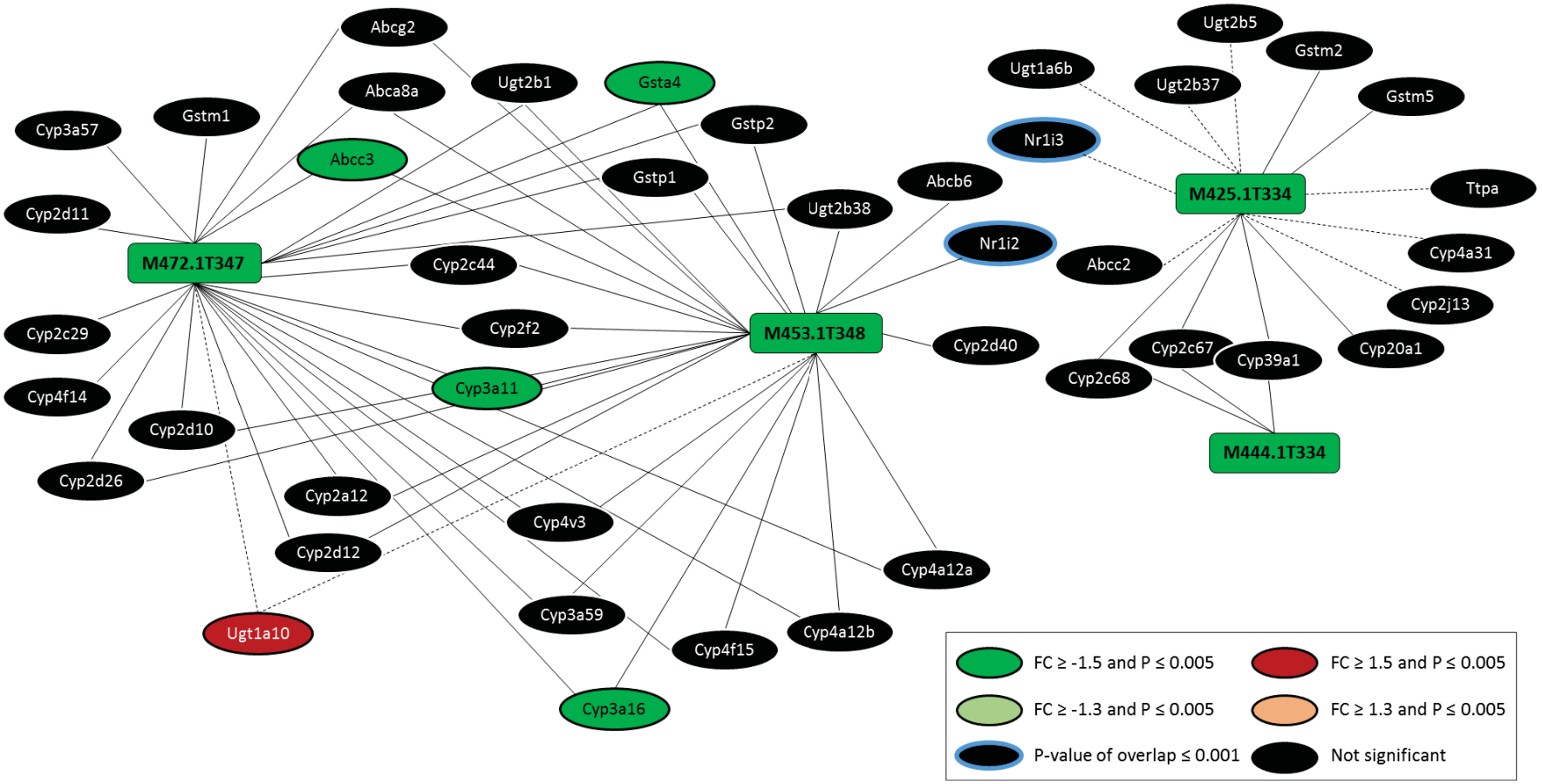

Figure 6.2 Correlation of urinary α-CEHC glucuronide ("M453.1T348" and "M472.1T347") and γ-CEHC glucoside ("M425.1T334" and "M444.1T334") abundance with hepatic expression of genes associated with phase I, phase II and phase III biotransformation of xenobiotics. The gene names are indicated in oval shapes, with colour coding referring to expression values of 12-week-old *Il10*$^{-/-}$ mice fed the 30% control diet (vs. C57BL/6J mice fed the same diet). Genes not differentially expressed defined as FC < |1.3| or P > 0.005 ("not significant"). "P-value of overlap" refers to IPA *Upstream regulator analysis*. A positive correlation was defined as Pearson correlation coefficient ≥ 0.65 (solid line) and a negative correlation as ≤ -0.65 (dashed line).

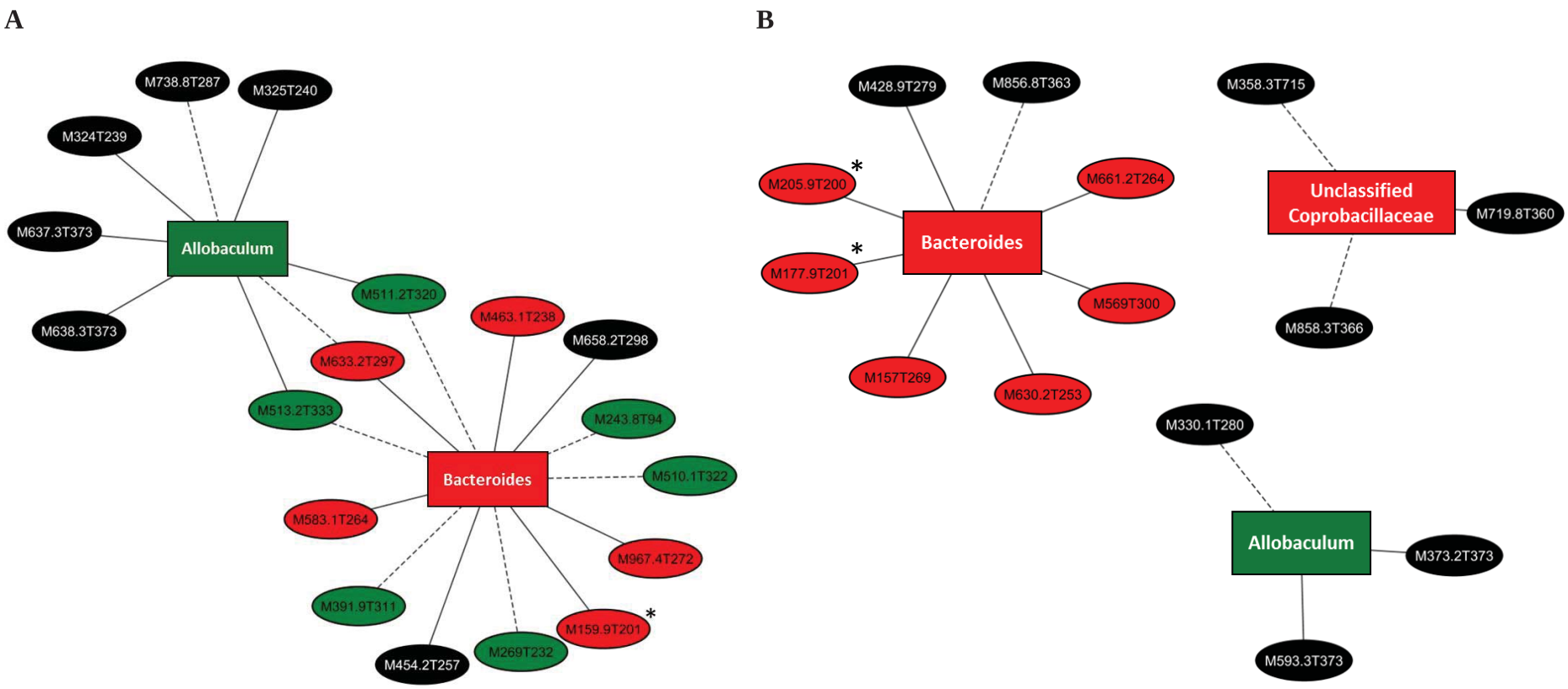

Figure 6.3 Relevance network indicating correlation of (A) negative and (B) positive ions and the caecal microbiota, with expression values of *Il10*$^{-/-}$ mice fed a 30% control diet (vs. C57BL/6J mice) overlaid. The ions corresponding to urinary metabolites are illustrated in mass-per-charge ratio (M) and retention time (T), and the colour refers to increased (red), decreased (green), or non-differential (black) abundance in the urine of *Il10*$^{-/-}$ mice ($P \leq 0.001$). The abundance of each ion was correlated to the abundance of microbial sequences from the caecum using data from the same mice, with correlation classified above 0.7 (positive) or below -0.7 (negative) and represented with a solid (positive) or dashed (negative) line. (*) denotes a metabolite with confirmed identification.

6.4.4 Colon and hepatic gene expression and microbial community profile and their relationship to the urinary metabolite profile in *Il10*$^{-/-}$ mice fed the 30% salmon diet (vs. 30% control diet)

The 30% salmon diet had limited effects on genes involved in tryptophan metabolism in *Il10*$^{-/-}$ mice compared to those fed the 30% control diet (Figure 6.4). The abundance of colonic proteins ALH1B1 and OGDH was affected, but the expression levels of key colonic genes such as *IDO1* were not ($P > 0.005$). Concomitantly, levels of xanthurenic acid in urine were unchanged in these mice. This was in contrast to the effects mediated by the EPA diet, where a reduction of mRNA expression levels were observed in *Il10*$^{-/-}$ mice (vs. OA diet) when colitis was established and a lower level of the metabolite putatively identified as xanthurenic acid in urine (Chapter 3, Appendix IX).

The intake of the 30% salmon diet increased the level of urinary α-CEHC glucuronide in *Il10*$^{-/-}$ mice, but reduced the level of γ-CEHC glucoside compared to those fed the 30% control diet (Figure 6.5). The increased abundance of α-CEHC glucuronide in urine was linked to increased hepatic expression of phase II (*Gsta4*) and phase III (*Abcc3* and *Abcg2*) genes. Reduced urinary γ-CEHC glucoside levels were positively correlated to decreased mRNA expression levels of phase I (*Cyp39a1*) glucuronidation enzymes, and negatively correlated to increased expression of phase II (*Ugt2b5* and *Ugt2b37*) glucuronidation enzymes (all Pearson correlation coefficient $\geq |0.65|$) (Figure 6.5). Within C57BL/6J mice, the expression of these genes was also affected in the liver of mice fed the 30% salmon diet, with similar expression values as in *Il10*$^{-/-}$ mice and increased urinary α-CEHC glucuronide but reduced γ-CEHC glucoside compared to C57BL/6J mice fed the 30% control diet (data not shown). Nevertheless, urinary γ-CEHC glucoside abundance showed genotype-specific effects in response to the 30% salmon diet as shown in Table 5.7 and Figure 5.12 and may be a candidate biomarker of colitis.

As indicated in Figure 6.6, the intake of the 30% salmon diet did not affect sequence abundances of caecal *Allobaculum*, *Bacteroides* or unclassified *Coprobacillaceae*, and the urinary abundance of correlating metabolites (*e.g.* xanthurenic acid) were unchanged in *Il10*$^{-/-}$ mice compared to those fed the 30% control diet.

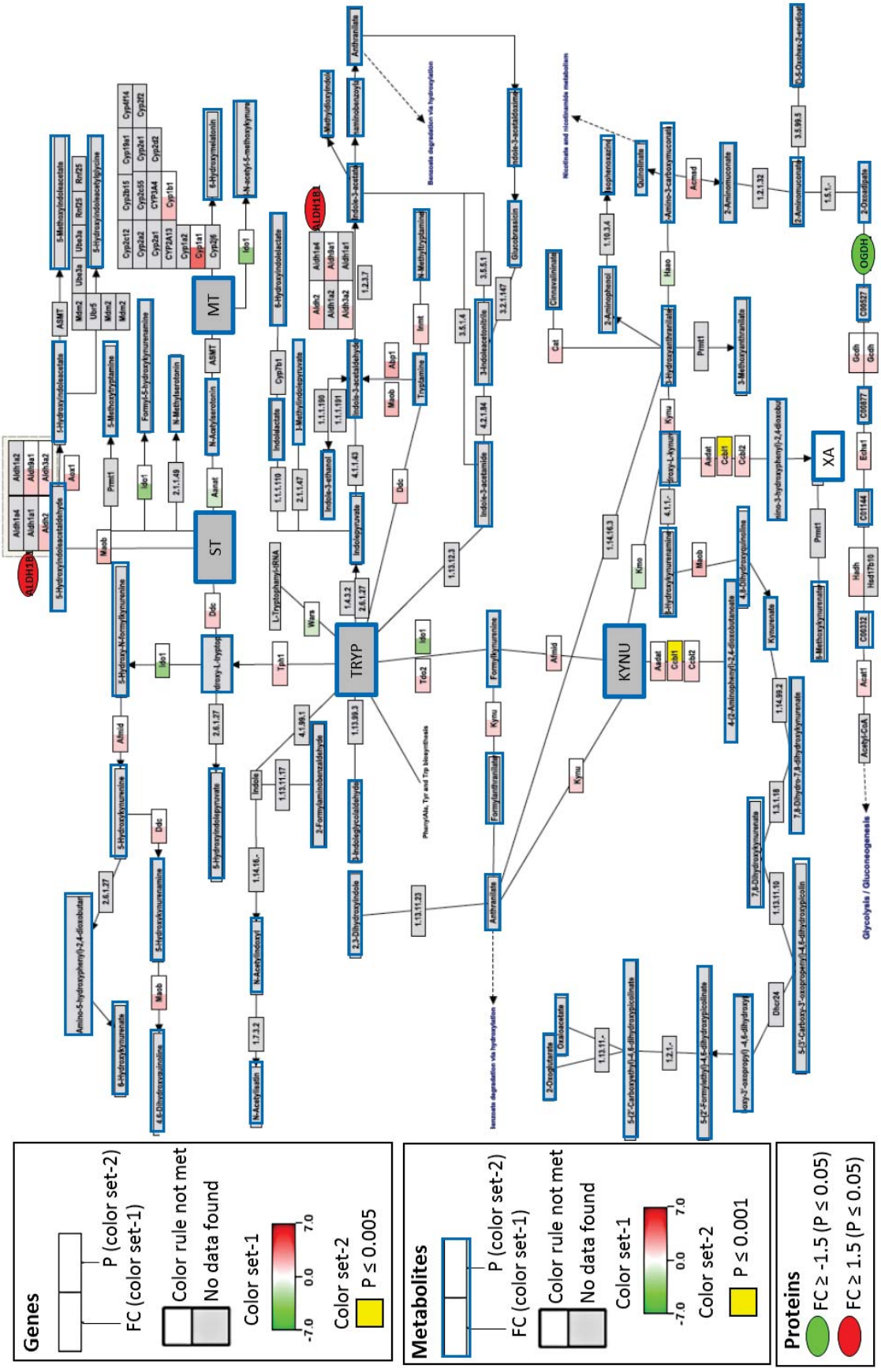

Figure 6.4 Biological pathway for *Tryptophan metabolism* indicating molecular events that lead to the biosynthesis of melatonin from tryptophan (*via* serotonin), or xanthurenic acid (*via* kynurenine) in *Il10*$^{-/-}$ mice fed the 30% salmon diet compared to those fed the 30% control diet.

Figure 6.4 continued. Nodes represent genes (rectangles), proteins (ovals), or metabolites (rectangles with a coloured border). Colour coding of nodes indicate increased (red) or decreased (green) levels, as illustrated in the legend. Data for genes and metabolites shaded in grey not considered or measured. Gene expression data were established by microarray analysis of colon tissue from *Il10*$^{-/-}$ mice, protein expression data by 2D-DIGE, and metabolomics data by untargeted LC-MS of urine. Pathway information obtained from Kanehisa *et al.* [328] and Ferrante *et al.* [519].
KYNU: Kynurenine; MT: Melatonin; ST: Serotonin; TRYP: Tryptophan; XA: Xanthurenic acid.

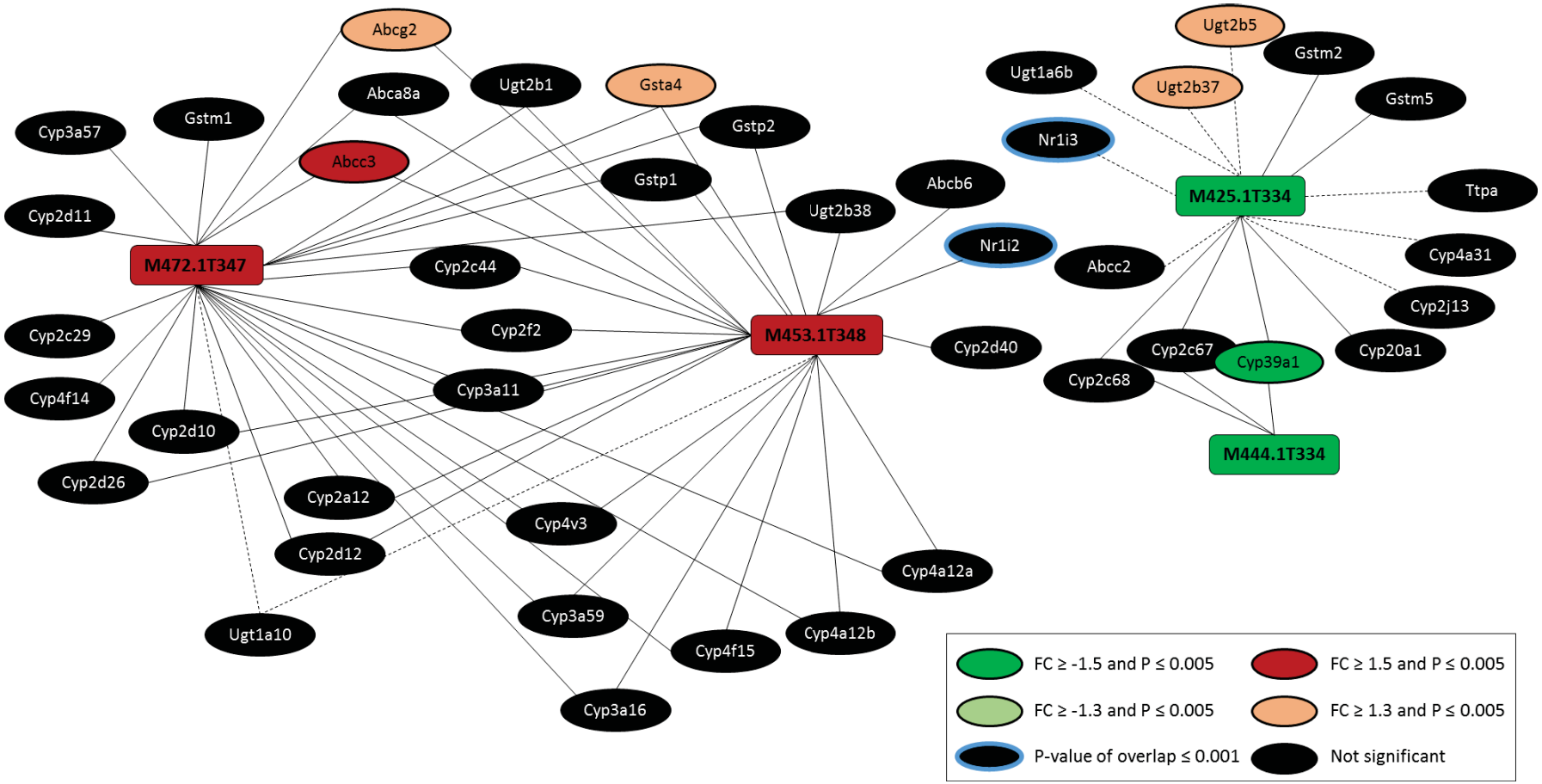

Figure 6.5 Correlation network of urinary α-CEHC glucuronide ("M453.1T348" and "M472.1T347") and γ-CEHC glucoside ("M425.1T334" and "M444.1T334") abundance with hepatic expression of genes associated with phase I, phase II and phase III biotransformation of xenobiotics. The gene names are indicated in oval shapes, with colour coding referring to expression values of 12-week-old *Il10*$^{-/-}$ mice fed the 30% salmon diet (vs. *Il10*$^{-/-}$ mice fed the 30% control diet). Genes not differentially expressed defined as FC < |1.3| or P > 0.005 ("not significant"). "*P-value of overlap*" refers to IPA *Upstream regulator analysis*. A positive correlation was defined as Pearson correlation coefficient ≥ 0.65 (solid line) and a negative correlation as ≤ -0.65 (dashed line).

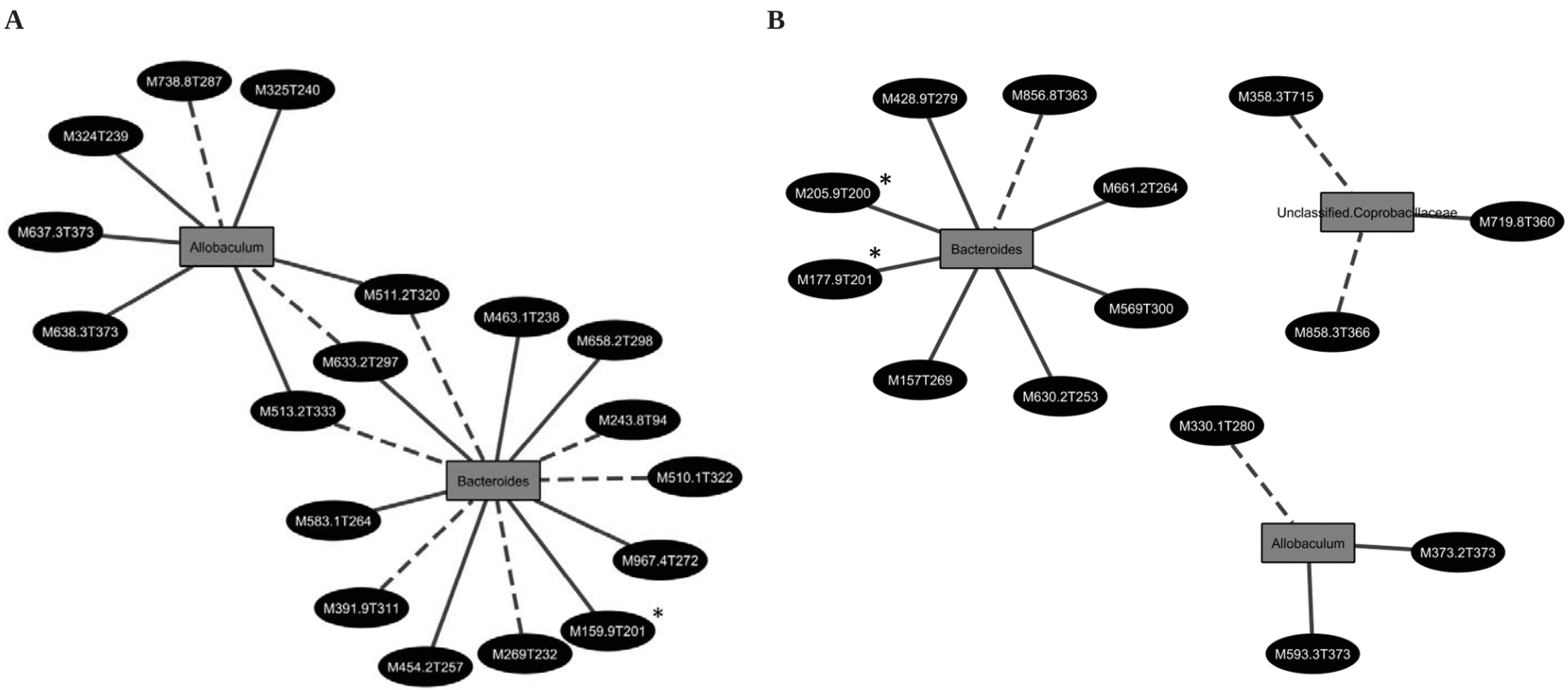

Figure 6.6 Relevance network indicating correlation of (A) negative and (B) positive ions and the caecal microbiota, with expression values of *Il10*$^{-/-}$ mice fed the 30% salmon diet compared to those fed the 30% control diet overlaid. The ions corresponding to urinary metabolites are illustrated in mass-per-charge ratio (M) and retention time (T), and the colour refers to increased (red), decreased (green), or non-differential (black) abundance in the urine of *Il10*$^{-/-}$ mice ($P \leq 0.001$). The abundance of each ion was correlated to the abundance of microbial sequences from the caecum using data from the same mice, with correlation classified above 0.7 (positive) or below -0.7 (negative) and represented with a solid (positive) or dashed (negative) line. (*) denotes a metabolite with confirmed identification.

6.5 Discussion

The hypothesis that the integration of 'Omics' data provided additional insights into the systemic responses to colitis in *Il10*$^{-/-}$ mice appeared to be limited to large intestinal (caecum/colon) tryptophan metabolism and hepatic tocopherol metabolism. Consistent with the literature, the integration of colon gene/protein expression data and urinary metabolites highlighted the importance of tryptophan metabolism, specifically pointing towards increased xanthurenic acid levels and identified a novel link to *Bacteroides* spp. in colitis. Additionally, new insights into inflammation in this model were obtained by correlating the urinary metabolites α-CEHC glucuronide and γ-CEHC glucoside with expression of hepatic genes regulating xenobiotic metabolism during colitis. Consistent with the stated hypothesis, the integration of 'Omics' data also provided novel insights into the systemic responses associated with the reduced colon inflammatory phenotype of *Il10*$^{-/-}$ mice fed the 30% salmon diet. While the 30% salmon diet had limited effects on tryptophan metabolism, it increased the urinary abundance of α-CEHC glucuronide, but lowered the level of γ-CEHC glucoside.

6.5.1 Novel insights into tryptophan metabolism during colitis

Findings from integration of colon gene expression and urinary metabolomic data showed increased production of xanthurenic acid from tryptophan *via* kynurenine during colitis, as shown by the comparison of *Il10*$^{-/-}$ mice (vs. C57BL/6J mice), both fed the 30% control diet. These observations are consistent with previous studies in *Il10*$^{-/-}$ mice [281, 309, 393] and human IBD patients [365, 366, 395]. The largest increase in mRNA transcript levels in the colon were observed for *IDO1*, the gene that codes for the enzyme catalysing the first step in the catabolism of tryptophan to xanthurenic acid. *IDO1* mRNA and protein levels are expressed in all parts of the small intestine and colon [520-522], but in the inflamed intestine, elevated *IDO1* activity may be an attempt to limit ongoing inflammation [365, 366, 521, 522].

In IBD, antigen-presenting cells of the lamina propria may increase expression of *IDO1* to induce immune tolerance by suppressing T cell responses [521, 522]. For example, in lamina propria dendritic cells, the activity of IDO1 inhibited their ability to drive the differentiation of naïve T cells to Th1 and Th17 cells [521, 522]. It has further been suggested that in intestinal epithelial cells, elevated IDO1 activity may be increased

to limit microbial invasion [366], with anti-microbial effects specifically shown by 3-hydroxykynurenine and kynurenine in a human myeloid cell line infected with *Listeria monocytogenes* [523]. Thus, the large number of cells that induce *IDO1* gene expression along the length of the GIT may have been sufficient to cause the changes in tryptophan catabolite levels that were detected in plasma [281], serum [366], and urine [281, 309] in other studies. In the current study, plasma levels of tryptophan catabolites were not assessed, however in a similar *Il10*$^{-/-}$ model, plasma kynurenine and 3-hydroxykynurenine were elevated during colitis [281]. Xanthurenic acid was largely undetected in the plasma of *Il10*$^{-/-}$ mice, but a positive correlation to plasma kynurenine suggested a transformation from kynurenine to xanthurenic acid in the kidneys [281].

Adding to the importance of tryptophan in colitis, in the current study, a positive correlation between the abundance of caecal *Bacteroides* spp. and urinary xanthurenic acid was indicated during colitis (*Il10*$^{-/-}$ mice vs. C57BL/6J mice, both fed the 30% control diet). The degradation of tryptophan by bacteria is catalysed by tryptophanase [524], an enzyme commonly found in anaerobes such as *Bacteroides fragilis* and *B. thetaiotaomicron* that are present in the large intestine [525]. Interestingly, both *Bacteroides* species have previously been associated with increased risk of colitis development, as shown for *B. thetaiotaomicron* in a genetically susceptible mouse model [526] and for enterotoxigenic *B. fragilis* (a molecular subtype of *B. fragilis*) in a DSS-administered mouse model [527].

The importance of tryptophan metabolism makes this pathway an important target for the mining of candidate biomarkers of dysbiosis processes occurring during colitis. These candidate biomarkers could be monitored in surrogate "tissues" such as urine (and likely other "tissues" like plasma and faeces) to indicate IDO1 activity in the inflamed colon of experimental models or in human subjects at risk of developing colitis symptoms such as IBD.

6.5.2 Novel insights into tocopherol metabolism during colitis

The urinary metabolites α-CEHC glucuronide and γ-CEHC glucoside were decreased in abundance during colitis, as shown by the comparison of *Il10*$^{-/-}$ mice fed the 30% control diet with C57BL/6J mice. A correlation between α-CEHC glucuronide and hepatic expression of phase I (decreased *Cyp3a11* and *3a16*), phase II (increased *Ugt1a10*), and

phase III (decreased *Abcc3*) detoxification enzymes was observed. Reduced functionality of hepatic cytochrome P450 enzymes has commonly been observed in rodent models of experimental colitis [444, 468] and may be the result of increased bacterial translocation and endotoxemia as a consequence of chronic inflammation in the GIT [445, 477]. Specifically, the *CYP3A* family (including *Cyp3a11* and *3a16*) was reportedly decreased in expression due to the occurrence of pro-inflammatory cytokines that can activate NFKB and subsequently inhibit transcriptional regulators of *CYP3A* (*PXR* and *NR1I3*) in the liver [444]. These findings are supported by the results from IPA *Upstream regulator analysis* which showed *PXR* was associated with differentially expressed genes in the liver during colitis (results presented in Chapter 5). Reduced abundance of γ-CEHC glucoside in the urine correlated with hepatic genes coding phase I, phase II and phase III detoxification enzymes, but no differential expression of these genes was observed with established colitis (Chapter 5), although hepatic protein expression was not measured. These results suggest that γ-CEHC glucoside and α-CEHC glucuronide as candidate biomarkers of colitis, but further studies are required to explain their reduction in urine of *Il10*$^{-/-}$ mice with established colitis.

6.5.3 Novel insights into tocopherol metabolism in response to the 30% salmon diet (vs. 30% control diet) in *Il10*$^{-/-}$ mice

The integration of transcriptomic and metabolomic data showed an effect of the 30% salmon diet on hepatic tocopherol metabolism, as shown by the comparison of *Il10*$^{-/-}$ mice fed the 30% salmon diet to those fed the 30% control diet. In contrast to the changes observed with colitis, the level of α-CEHC glucuronide, a metabolite of α-tocopherol, was increased in the urine of *Il10*$^{-/-}$ mice fed the 30% salmon diet, while γ-CEHC glucoside, a metabolite of γ-tocopherol, was further decreased. It has previously been shown that the intake of α-tocopherol as part of a controlled diet positively correlated with the urinary abundance of α-CEHC [499], thus the higher abundance of α-CEHC glucuronide in response to the 30% salmon diet may be due to the amount of α-tocopherol that was provided in the diet compared to the control diet. Salmon contains approximately 5 mg vitamin E per 100 g fresh fillets [178], mainly in form of α-tocopherol, and only minor amounts of β-, γ- and δ-tocopherols [168].

Considering that the salmon diet provided tocopherol mostly in the alpha homologue [168], the levels of γ-tocopherol metabolites should be similar between mice

fed the 30% salmon diet and those fed the 30% control diet. Reduced abundance of γ-CEHC glucoside was detected in 30% salmon-fed *Il10*$^{-/-}$ mice (vs. those fed the 30% control diet) and may be attributed to the absorption of γ-tocopherol in the jejunum compared to α-tocopherol. Some studies have shown that α-tocopherol might impair the bioavailability of γ-tocopherol, as both are transported through the epithelium by the scavenger receptor class B type 1 [528]. However, the molecular mechanisms of vitamin E uptake by enterocytes in the jejunum has not been fully elucidated [529], and in the current experiment, these measurements were not performed thus no conclusion can be made. Alternatively, it was shown that α-tocopherol can affect metabolism of γ-tocopherol in the liver [500, 501] and may offer an explanation for the reduced level of γ-CEHC glucoside in the urine of *Il10*$^{-/-}$ mice fed the 30% salmon diet.

The degradation of α- and γ-tocopherol in the liver involves a series of metabolic reactions that yield α-CEHC and γ-CEHC as end products (Figure 6.7). The increased abundance of α-CEHC glucuronide in 30% salmon-fed *Il10*$^{-/-}$ mice may be attributed to changes in hepatic phase II (increased *Gsta4*) and phase III (increased *Abcg2* and *Abcc3*) genes compared to those fed the 30% control diet. This was supported by a study in rats, where an increase in hepatic ABC-transporters (including *Abcg2* and *Abcc3*) were observed following α-tocopherol injections [530]. However, another study suggested that *in vivo*, the hepatic metabolism of vitamin E may occur non-specifically, *i.e.* increased tocopherol supplementation may simply increase the activity of xenobiotic pathways, rather than mechanisms specific to tocopherols [531].

PXR and *NR1I3* transcriptional regulators may regulate genes that mediate the biotransformation of xenobiotics [479], and correlation analysis indicated that α-CEHC glucuronide abundances were linked to *PXR*, while γ-CEHC glucoside appeared to be linked to *NR1I3*. This is supported by Landes *et al.* [532] who showed that α-tocopherol binds *PXR* with greater affinity then γ-tocopherol in a human liver carcinoma cell culture system. As indicated by IPA *Upstream regulator analysis*, *PXR* was associated with the hepatic transcriptional prolife of 30% salmon-fed *Il10*$^{-/-}$ mice (results presented in Chapter 5). Literature evidence regarding the effects of α-tocopherol supplementation on hepatic *PXR* expression is inconclusive, with studies reporting no effect [533, 534], increased expression [530], and one study reporting an increase using microarray technology which could not be confirmed by qPCR analysis [482]. It was further

suggested that *PXR* transcriptional activity may also depend on other factors than hepatic α-tocopherol concentration [530], for example, abundance of bile acids [535].

Alternatively, a decrease in hepatic *SCD1* gene expression in 30% salmon-fed *Il10*$^{-/-}$ mice (compared to *Il10*$^{-/-}$ mice fed a matched control diet) may have affected hepatic lipoprotein metabolism [492, 536] and caused reduced binding capacity of α-tocopherol. This is supported by current knowledge about the degradation of α-tocopherol in the liver, which is triggered when the binding capacity to its transporter (lipoproteins) is reached, thus plasma lipid concentrations are an important factor in the elimination of α-CEHC [537]. It was reported that reduced accumulation of α-tocopherol occurred in humans with low plasma lipid concentrations, and the urinary excretion of α-CEHC occurred earlier than those with higher plasma lipid levels [537]. Therefore it may be possible that the higher excretion of α-CEHC glucuronide may be a result of the decreased hepatic *SCD1* gene expression in *Il10*$^{-/-}$ mice fed the 30% salmon diet compared to those fed the 30% control diet.

6.6 Conclusion and outlook

This chapter detailed the integration of multi-'Omics' datasets such as 1) colon transcriptomic and proteomic data with urine metabolomic data, 2) liver transcriptomic data with urine metabolomic data, and 3) caecal microbiomic data with urine metabolomic data confirmed earlier findings. This integration provided new insights underlying the colitis phenotype in *Il10*$^{-/-}$ mice, as a model of IBD. Overall urine appeared to be a suitable surrogate "tissue" to predict changes in tryptophan metabolism that occur in the colon of *Il10*$^{-/-}$ mice and changes in metabolites associated with this pathway may be useful biomarkers of colitis. Other candidate biomarkers include the tocopherol metabolites α-CEHC glucuronide and γ-CEHC glucoside, but their reduced urinary abundance in *Il10*$^{-/-}$ mice requires further studies. Knowledge derived from the integrated datasets also enabled the characterisation of systemic responses to a diet containing 30% salmon in the *Il10*$^{-/-}$ mouse model of IBD at a time-point when colitis was established. Transcriptomic analyses of colon (and to a lesser extent proteomic) and hepatic tissues, and microbiota analysis of the large intestine provided new insights and were representative of the changes in metabolite profiles of the urine, both for colitis and for salmon-fed *Il10*$^{-/-}$ mice. Overall, the integration of 'Omics' datasets showed while the 30% salmon diet had limited effects on tryptophan metabolism in *Il10*$^{-/-}$ mice, its impact

on hepatic tocopherol metabolism was detected in urine and correlated with the urinary abundance of a metabolite previously suggested as biomarker of colitis in *Il10*$^{-/-}$ mice. These candidate biomarkers of colitis or the response to a 30% salmon diet in an animal model of colitis needs to be further investigated in a dose-response and larger study before these could be considered targets for IBD cohort characterisation or nutrition management in IBD patients.

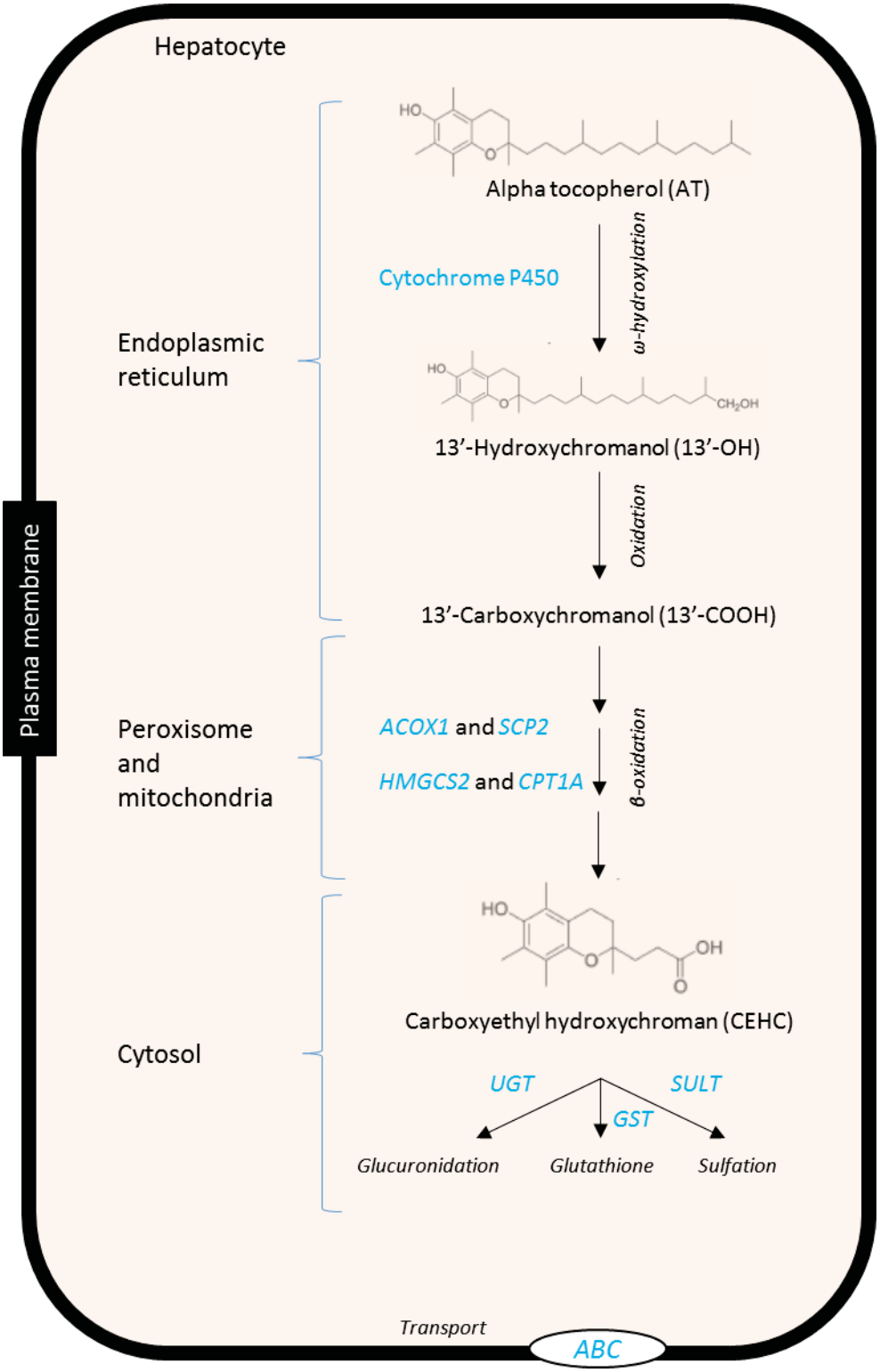

Figure 6.7 Proposed hepatic molecular mechanisms that lead to the elimination of α-tocopherol in the form of α-CEHC glucuronide. The initial ω-hydroxylation, mediated by the family of cytochrome P450 genes, is followed by β-oxidation (phase I), glucuronidation (phase II), and finally transport from the liver (phase III) by the family of ATP-binding cassettes. Genes or gene families are indicated in blue. Illustrated with information from [350, 482, 489, 530, 533, 534, 538, 539].

Chapter 7

General discussion

Manuscripts for potential publication in:

The Journal of Nutritional Biochemistry for results from the “EPA time-course experiment”

The Journal of Proteomic Research for results from the “salmon diet experiment”

7.1 Background

IBD are a group of disorders characterised by chronic inflammation of the GIT including the colon (colitis) and while the exact aetiology of IBD remains unknown, it is generally accepted that the microbiota, an exaggerated immune response, genetic susceptibility, and environmental factors play a role. IBD was recently identified as an emerging disease globally [1] and with severe symptoms, the disorder can often affect a patient's quality of life. To date there is no cure and many patients require medications which are often anti-inflammatory agents that inhibit inflammatory pathways. However, these immune suppressants cannot be considered a long-term solution due to their significant negative side effects [2]. An alternative or complementary treatment option is desirable.

As described in Chapter 1, dietary salmon has frequently been associated with beneficial effects in chronic diseases, as well as in IBD. Studies reported that increased dietary intake of salmon lowered disease activity in UC patients [161], was perceived to be well tolerated in a New Zealand CD population compared to other food groups [9], and reduced the systemic inflammation marker CRP in serum of patients with previous colorectal adenomas or inactive UC [146]. While some of this data was self-reported using food frequency questionnaires [9], it indicates the potential for targeted nutritional intervention in the management of human IBD. The lack of experimental evidence however highlights the necessity of identifying and validating objective markers (biomarkers) to predict metabolic or physiological changes associated with increased or decreased disease state that are responsive to targeted nutritional intervention.

Studies suggested that the n-3 PUFA provided by salmon is the main factor that reduced colitis by modulating molecular processes, specifically the expression of genes in inflammatory and signalling pathways [146, 161]. Linking these specific changes in the inflamed colon with systemic characterisation of blood immune genes (from PBMCs) and urinary metabolites using 'Omics'-technologies will likely provide new insights into the underlying mechanism of colitis and how a diet enriched in EPA, in purified form or provided as part of a food, can reduce the risk of colitis development. Using only one or two 'Omics', the often subtle effects of dietary intervention on molecular mechanisms underlying phenotypical changes might be missed. The integration of transcriptomic and proteomic datasets of the host colon responses on the microbiomic dataset of caecal microbial community profile changes with the metabolomic dataset of urinary

metabolites is a powerful approach to identify potential biomarkers to be used, once validated, in nutritional intervention studies with IBD patients. These potential biomarkers could allow early detection of the responses to intervention with n-3 PUFA-rich foods such as salmon, and potentially enable a complementary nutritional solution to current treatments of IBD.

The central hypothesis of this dissertation was that dietary salmon reduces the severity of colitis by altering the expression of genes and/or proteins in the colon (and/or liver) and that biomarkers (*e.g.* genes and metabolites) that predict these physiological changes are detectable in "tissues" that can be obtained minimally invasive such as blood, urine and faeces (or a proxy of faeces).

7.2 Summary of results

The studies undertaken in this dissertation use a multi-'Omics' approach to investigate the effects of dietary n-3 PUFA, either in a purified form (EPA) or in a food matrix like salmon, on colitis. Changes in colon/PBMC gene expression (transcriptomics), colon protein expression (proteomics), urinary metabolite abundance (metabolomics) and caecal microbial community profile (microbiomics) were assessed in the *Il10*$^{-/-}$ mouse model of colitis as observed in IBD (and healthy control mice). These 'Omics' datasets were further mined to identify candidate biomarkers of colitis in surrogate "tissues" and then, their responses to diets rich in EPA or salmon were evaluated.

The minimally invasive nature of blood, urine and faecal sample collection makes them convenient sources for biomarkers. Urine requires less complex sample preparation due to lower levels of protein compared to other materials (*e.g.* faeces) or fluids (*e.g.* serum [540]). As a result, sample preparation time is reduced, and due to less sample modification, the range of detectable metabolites for untargeted metabolomics is increased (as applied in this study).

In addition to urine, other candidate "tissues" such as PBMCs isolated from blood using minimally invasive sampling methods were evaluated. PBMCs are important factors of the immune system that can perpetuate the immune response by secreting cytokines and cell adhesion molecules and infiltrate various tissues (including the colon) *via* blood circulation. Powell *et al.* [541] showed that PBMCs are a suitable "tissue" to monitor changes associated with lipid metabolism in the liver. PBMCs have been used as

surrogates for molecular responses during colitis in humans [149, 346], but not in *Il10*$^{-/-}$ mice, and no study has looked into their potential as surrogate "tissue" for the effects of n-3 PUFA-enriched diets that occur in the inflamed colon of *Il10*$^{-/-}$ mice, as a model of colitis that occurred in IBD.

The aim of Chapter 3 was to define whether dietary intervention with purified EPA results in lower levels of colitis in *Il10*$^{-/-}$ mice during the early stages of disease onset and to identify biomarkers of colitis in accessible "tissues" (*i.e.* PBMCs and urine) which are responsive to an EPA-rich diet at both early and established stages. The dietary EPA (vs. OA diet) was confirmed, as expected from previous studies, to reduce colitis in *Il10*$^{-/-}$ mice when colitis was established. Contrary to the hypothesis, but a novel finding was that the reduction of colitis was not observed at early stages of colitis. The transcriptomic profiling of colon tissue provided a more detailed characterisation of molecular mechanisms underlying this reduction and also confirmed those previously reported [3, 6]. These include changes in expression of genes associated with lymphocyte function, eicosanoid signalling, and *PPARG* signalling.

This study is the first to show that while the transcriptomic profile of PBMCs is similar to colon in *Il10*$^{-/-}$ mice with established colitis and published studies in human IBD subjects [143], this was not the case for the comparison of the EPA diet (vs. OA diet) in *Il10*$^{-/-}$ mice. The EPA diet affected *PPARG* signalling linked to increased expression of target genes of *PPARGC1A*, an activator of *PPARG* [542] in PBMCs of *Il10*$^{-/-}$ mice with established colitis, similar to the colon. However, the transcriptional profile of PBMCs did not further predict the molecular responses to the EPA diet observed in the inflamed colon, such as genes that regulate immune cell trafficking which were increased in expression in PBMCs when colitis was established (Chapter 3).

In addition, in Chapter 3, the use of accessible, surrogate "tissues" such as urine for metabolomic fingerprinting showed for the first time that dietary EPA (vs. OA diet) reduced colon *IDO1* gene expression in *Il10*$^{-/-}$ mice with established colitis, linked to lower urinary levels of xanthurenic acid, but increased N-formylkynurenine and indole, in those mice. These findings supported urine as surrogate "tissue" for EPA-induced colonic gene expression changes associated with colitis in *Il10*$^{-/-}$ mice.

Based on histological assessment and gene expression profiling of colon tissue, and urinary metabolomic fingerprinting (Chapter 3), it was concluded that purified EPA

reduced the severity of colitis in *Il10*$^{-/-}$ mice. These effects were not apparent at early stages of colitis. While PBMC gene expression profiles were not a suitable predictor for the responses to dietary EPA when colitis was established, metabolite fingerprinting of urine appeared to be a useful surrogate "tissue" to monitor the reduction of colitis by dietary EPA (Chapter 3). Therefore, the focus of the research reported in the subsequent chapters (4, 5 and 6) focussed on a nutritional intervention study with diets enriched in salmon and its effects on colitis, colonic immune and metabolic pathways (gene in Chapter 4; protein in Chapter 5), hepatic lipid metabolism (gene in Chapter 5), caecal microbiota profile (Chapter 5) and their relationships with the presence or absence of relevant metabolites in urine (Chapters 5 and 6).

To evaluate whether an EPA-rich food such as salmon reduces the risk of developing colitis compared to when provided as a pure form, Chapter 4 focussed on the impact of dietary salmon on colitis. The salmon diets were prepared by lyophilisation of Chinook salmon fillets (*Oncorhynchus tshawytscha*) and incorporation of the powder into AIN-76A-based formulations at 15, 30 and 45% by dry weight. These diets were fed to *Il10*$^{-/-}$ and C57BL/6J mice for seven weeks, with effects of the salmon-based diets assessed when colitis was established at 12 weeks of age, by comparing the severity of colitis and colon gene expression profiles to *Il10*$^{-/-}$ mice fed macronutrient-matched control diets. The results of these analyses indicated that dietary salmon modulated the severity of colitis and underlying molecular mechanisms in a dose-dependent manner, with only the intermediate amount of salmon (30%) effective in reducing colitis. Similar to the results for the EPA diet in Chapter 3, in *Il10*$^{-/-}$ mice fed the 30% salmon diet, reduced expression of genes associated with lymphocyte function and enhanced expression of genes in metabolic KEGG pathways that may have partly been mediated *via PPARA* was observed compared to those fed the 30% matched control diet (Chapter 4).

In Chapter 5, further molecular insights were gained by measuring the protein expression profile of the colon (proteomics) to support and/or add strength to the colon gene expression data. This is because gene expression data only partly explains the observed phenotype as several post-translational processes can affected protein abundance [119]. Thus, it was hypothesised that the combined analysis of gene and protein expression data from the same colon samples provides further insights into the reduced inflammatory phenotype of *Il10*$^{-/-}$ mice fed the 30% salmon diet. The results

showed that the abundance of proteins with functional roles in antigen presentation and oxidative stress responses was decreased, while proteins associated with lipid metabolism increased in the colon of *Il10*$^{-/-}$ mice fed the 30% salmon diet (vs. 30% control diet). The expression of *CEBPD*, a transcription regulator of acute phase proteins was decreased in the liver of 30% salmon-fed *Il10*$^{-/-}$ mice, however, the expression of acute phase proteins was unchanged compared to those fed the 30% control diet (Chapter 5).

The microbiota contributes to the development of IBD and profiling of the microbial community structure (microbiomics) from faeces, a proxy of the large intestinal microbiota, could be done in human IBD subjects minimally invasive. In agreement with published data from human IBD patients [543] and *Il10*$^{-/-}$ mice [544], the loss of microbial diversity associated with colitis in *Il10*$^{-/-}$ mice was largely attributed to a depletion of the phylum *Firmicutes*, specifically the SCFA-producing bacterium *Allobaculum* spp. (Chapter 5). Further in agreement with the literature [277, 506-508] was the colitis-associated increase of *Bacteroidetes* proportions, predominantly *Bacteroides* spp., in the caecum of *Il10*$^{-/-}$ mice. Previously not associated with IBD, the abundance of *Eubacterium* spp. (most closely associated with *Eubacterium dolichum*), was increased in *Il10*$^{-/-}$ mice fed the 30% control diet with established colitis, but was not detected in C57BL/6J mice fed the same diet. However, its abundance compared to other genera was generally low.

Additionally, in Chapter 5, new knowledge of the effects of a 30% salmon diet on the caecal microbiota composition was obtained. This study is the first to show elevated sequence counts of *V. akkermansia* in response to a salmon-enriched diet in mice, irrespective of genotype. *V. akkermansia* stimulates host mucus turnover [545] which may have been beneficial specifically in *Il10*$^{-/-}$ mice by improving mucus thickness and its associated barrier function to reduce bacterial translocation into mucosa [275]. A reduced number of *V. akkermansia* has previously been reported in mucosal biopsies of human IBD patients [514] and *V. akkermansia* may be a candidate biomarker to predict the effects of dietary salmon on colitis. However, due to the lack of specificity of and the remaining controversy about *V. akkermansia* (*e.g.* disturbing mucus layer homeostasis in an infectious mouse model, thereby exacerbating colitis by increasing translocation of *Salmonella typhimurium* into mucosa [516]), further work is required to confirm its role in colitis. To date, there are no published studies to show the effects of dietary salmon intake on the microbial community structure in a dysbiotic environment such as IBD. The

findings that the intake of the 30% salmon diet reduced the abundance of *Eubacterium* spp., but increased an unclassified *Rikenellaceae* in *Il10*$^{-/-}$ mice (vs. 30% control diet), may represent novel candidate biomarkers of colitis.

In Chapter 6, the 'Omics' datasets were integrated as follows: 1) colon transcriptomic and proteomic data with urine metabolomic data, 2) liver transcriptomic data with urine metabolomic data, and 3) caecal microbiomic data with urine metabolomic data. These integrated datasets allow to relate changes in molecular responses occurring in the colon and liver, as well as the caecal microbiota, to urinary metabolites of *Il10*$^{-/-}$ mice, and establish the effects of the 30% salmon diet on these. These analyses highlighted the importance of tryptophan metabolism associated with colitis in *Il10*$^{-/-}$ mice, similar to other studies using *Il10*$^{-/-}$ mice [281, 309, 393] and human IBD patients [365, 366, 395]. Increased abundance of xanthurenic acid in urine was attributed to the elevated expression of *IDO1* gene in the colon. Additionally, a positive correlation between caecal *Bacteroides* spp. abundance and the urinary tryptophan metabolite xanthurenic acid was established in colitis.

While the 30% salmon diet did not reduce the IDO1-mediated catabolism of xanthurenic acid in *Il10*$^{-/-}$ mice, it increased the urinary abundance of α-CEHC glucuronide, a metabolite of α-tocopherol previously suggested as a biomarker of colitis [309]. However, increased abundance of α-CEHC glucuronide was also measured in 30% salmon-fed C57BL/6J mice (vs. 30% control diet) and may therefore be a dietary effect (linked to α-tocopherol in the salmon) rather than specific to colitis in *Il10*$^{-/-}$ mice. In agreement, published data that showed urinary α-CEHC positively correlated with dietary α-tocopherol in healthy male subjects [499]. A novel finding was that the 30% salmon diet reduced the urinary abundance of γ-CEHC glucoside only in *Il10*$^{-/-}$ mice (vs. 30% control diet) and may therefore be a suitable biomarker of colitis to monitor effects of a diet enriched in salmon, but further studies are required to explain their reduction in urine of *Il10*$^{-/-}$ mice with established colitis. A summary of the main biological functions and the microbiota affected by the EPA and 30% salmon diets is shown in Table 7.1.

Table 7.1 Summary of the main biological functions and microbiota affected in *Il10*$^{-/-}$ mice fed diets containing either 3.7% eicosapentaenoic acid (EPA) ("EPA time-course experiment") or 30% salmon ("salmon diet experiment"). The variables were measured in the tissues stated (colon, peripheral blood mononuclear cells (PBMCs), liver, urine and caecum). Arrows indicate the direction of change, with (↑) showing an increase, (↓) a decrease, (↑ ↓) an affected function/microbiota, and (-) a non-significant change compared to a matched control diet. A shaded square indicates that the function/microbiota was not measured (black square) or that the data is not available (grey square). Effects indicate those observed at 12 weeks of age.

	EPA time-course			*Salmon diet*			
	Colon	*PBMCs*	*Urine*	*Colon*	*Liver*	*Urine*	*Caecum*
Biological functions							
Lymphocyte function	↓	↑		↓	-		
PPAR signalling	↑	↑		↑	-		
Antigen presentation	-	-		↓	-		
Oxidative stress	-	-		↓	-		
Metabolic pathways	-	-		↑	↑		
Tocopherol metabolism	-	-		-	↑ ↓	↑ ↓	
Tryptophan metabolism	↓	-	↑ ↓	-	-	-	
Lipid mediator metabolism	↓	-	↑ ↓	-	-		
Microbiota			↑ ↓				↑ ↓

7.3 General discussion

The *Il10*$^{-/-}$ mouse model shows several characteristics of human IBD, such as increased intestinal permeability [546-548], microbial dysbiosis [544], and similar colonic gene expression profiles [116], thus making it a suitable model to explore molecular responses to dietary intervention. The importance of the GIT microbiota in the development of IBD was highlighted in rodent models, as most models fail to develop IBD when raised under germ-free conditions [110-114]. In *Il10*$^{-/-}$ mice, the manifestation of colitis is further attributed to the large number and diversity of microbiota compared to other sections of the GIT [109, 549]. Bacterial inoculation of *Il10*$^{-/-}$ mice on this particular genetic background (C57BL/6J), as used in the studies reported in Chapters 3 and 4, is required to accelerate the onset of colitis [116].

The main site for the digestion and absorption of dietary PUFA are the duodenum and jejunum (presented in Chapter 1) and in this context, it remains to be discussed how PUFA or salmon-containing diets exert their effects on colitis in *Il10*$^{-/-}$ mice. After uptake in enterocytes, fatty acids are incorporated into TG and transported out of the enterocyte *via* chylomicrons which enter first the lymphatic capillaries in the villi and are then released into the blood stream. Once in the circulatory system, the chylomicrons enriched with PUFA increase their distribution to peripheral tissues (including the colon). The fatty acids are hydrolysed from chylomicrons and taken up by cells which affect biophysical properties of cell membranes, lipid mediator production, and intracellular gene and protein expression and further alter signalling pathways in those cells. The increased intake of n-3 PUFA potentially affects the membrane fatty acid composition of bacterial adhesion sites on epithelial cells [227] and the adhesion of bacterial strains to the mucosal surface in the GIT [228], hence impacting on the microbial community structure and its function.

To allow the identification of signalling and metabolic pathways responsive to dietary intervention with EPA or salmon-rich diets, the current dissertation focussed on untargeted analyses of molecular responses using a multi-'Omics' approach. The analysis of gene expression (transcriptomics) was performed on colon and PBMCs using microarray technology. At least in *Il10*$^{-/-}$ mice, the use of PBMCs as surrogate "tissue" to predict EPA-induced effects in the colon did not appear suitable. The EPA diet induced anti-inflammatory gene expression in the colon of *Il10*$^{-/-}$ mice when colitis was

established (vs. OA diet), but it was unexpected that the PBMC transcriptomic profile indicated increased immune cell activation in these mice. For this reason, the PBMC gene expression profile was not used as an outcome measure for the following study with the salmon-enriched diet. The unexpected PBMC profile might be linked to elevated duodenal inflammation (primarily associated with inflammatory cell infiltrates) which was observed in these mice. Published data indicated that, specifically in the duodenum, lipid oxidation products can damage the mucosa by inducing oxidative stress in cells [416]. The oxidation state of the EPA diets was not measured, but may offer an explanation for the increased duodenal inflammation in *Il10*$^{-/-}$ mice.

This is the first *in vivo* study to show a reduction of colon gene expression associated with lymphocyte function, but increased genes in metabolic KEGG pathways, specifically lipid metabolism that may have been mediated by *PPARA* activity, in 30% salmon-fed *Il10*$^{-/-}$ mice compared to those fed a macronutrient-matched control diet. Proteomic analysis of colon tissue from the same mice further supported elevated lipid metabolism, but suggested limited new targets by which the 30% salmon diet influenced molecular mechanisms in the inflamed colon. The limited concordance between individual gene transcript and protein expression levels has previously been reported [268, 550, 551] and was therefore not unexpected.

The analysis of protein expression is more challenging than gene expression due to the complexity of the proteome (*e.g.* post-translational modifications) and technical factors such as issues with poor resolution for lowly abundant proteins in mixtures with highly abundant proteins. Several spot-features on the gel that passed the cut-off criteria for differential expression remained unidentified, primarily low-abundance proteins (*e.g.* transcription factors [552]) that could not be excised from the gel due to failed visualisation after coomassie staining. Nandal *et al.* [553] proposed an extension to 2D-DIGE using a computerised method that utilises the information from identified proteins to construct a protein-protein interaction network, thereby creating a list of candidate proteins for these non-visible (but differentially expressed) spots that match their location on the gel and could further be confirmed by Western blotting. Alternatively, gel-free methods that combine a separation technique such as HPLC with high-resolution MS after direct injection of protein mixtures (*e.g.* shotgun proteomics [554]) can also be used to help identify proteins with low expression levels and those that traditionally are not amenable to 2D-electrophoresis, including large or hydrophobic proteins or proteins

which are poorly soluble. Combining methods such as untargeted analysis (2D-DIGE or shotgun) with targeted Western blotting, or a workflow incorporating pre-fractionation prior to 2D-electrophoresis, may be necessary to achieve greater coverage of the proteome influenced by diet.

While changes in gene and protein expression are considered a snapshot for what may be occurring in a biological system, metabolites are definite products of metabolism [120, 121]. The untargeted analysis of metabolites in surrogate "tissues" such as urine provided further insights into the effects of n-3 PUFA-rich diets that occurred in the colon (EPA, salmon), liver and microbiota (salmon). The untargeted analysis of urine poses its own challenges, not only due to many unknown metabolites in the urine, but also the unpredictable degree of urinary dilution related to the different levels of water intake and urine collection volume. Results can be improved by using a normalisation method that adjusts peak intensities between samples to a common scale and therefore reduces dilution-induced variation of urine samples [555].

In the current study, a common reference sample was not included in the untargeted analysis of urine and it has recently been shown that results are still satisfactory [556]. A distinct separation of the urinary metabolite fingerprints was apparent in the current experiments and observed by others [156, 158, 281, 340], with differences between *Il10*$^{-/-}$ and C57BL/6J mice largely attributed to changes associated with tryptophan metabolism, α-CEHC glucuronide and γ-CEHC glucoside. The integration of urinary metabolomic data and colon gene expression data related to tryptophan metabolism highlighted increased *IDO1*-mediated catabolism of kynurenine (and subsequently xanthurenic acid) from tryptophan, concomitantly with decreased expression of genes along the serotonin and tryptamine pathways. This study is the first to show reduced *IDO1* gene expression in the colon of *Il10*$^{-/-}$ mice in response to EPA supplementation (vs. OA diet), concomitantly with a decrease of the ion putatively identified as xanthurenic acid along with increases of indole and N-formylkynurenine in urine when colitis was established.

However, the effects of salmon on colitis might not be able to be predicted by changes in tryptophan metabolism as the gene expression of colonic *IDO1*, or the abundance of urinary xanthurenic acid, was unchanged in *Il10*$^{-/-}$ mice fed the salmon diet compared to those fed the corresponding control diet. The 30% salmon diet did not

contain the same amount of EPA compared to the EPA diet (1.0% vs. 3.7%), and these differences may explain the lack of effect on *IDO1* gene expression.

Promising results were initially obtained with observed changes in urinary α-CEHC glucuronide, a metabolite of α-tocopherol, previously suggested as a biomarker of colitis in *Il10*$^{-/-}$ mice [309]. As expected, the levels of α-CEHC glucuronide in urine were lower in *Il10*$^{-/-}$ mice compared to C57BL/6J mice (Chapters 3 and 4). However, increased abundance of α-CEHC glucuronide was detected in the urine of all mice fed the 30% salmon diet, irrespective of genotype, and was linked to the higher α-tocopherol content in this diet [499] and/or increased hepatic xenobiotic metabolism [531]. These results might mean that α-CEHC glucuronide in the urine is a biomarker of dietary exposure rather than a biomarker of function. The genotype-specific response of urinary γ-CEHC glucoside to dietary salmon suggests this metabolite may be a candidate biomarker of colitis. Interestingly, a recent study in a hamster atherosclerosis model showed an inverse correlation of urinary γ-CEHC with disease risk. This reduction in atherosclerosis risk was linked to a diet low in cholesterol and saturated fatty acids [557] and supports the findings of γ-CEHC glucoside (and potentially its aglycone [557]) as a candidate biomarker to monitor the effects of dietary lipids. However, it also indicates the possibility that γ-CEHC glucoside (as a derivative of γ-CEHC) may show limited specificity to colitis. There are to date no published studies that confirm the presence (or absence) of α-CEHC glucuronide or γ-CEHC glucoside in urine of human IBD patients. This gap in knowledge represents opportunities for further research.

In the current study, the microbial community structure was determined from digesta of the caecum, rather than the colon, because the small size of the colon in mice restricted collection of sample material. Other studies have reported that the caecal microbiota is similar to the colonic microbiota, with *Firmicutes* and *Bacteroidetes* dominating either section of the large intestine in mice [558, 559] and humans [560]. The salmon-enriched diets showed limited impact specific to colitis, and those genera affected (*Eubacterium* spp. and an unclassified *Rikenellaceae*) were, compared to other genera, only lowly abundant. They may present novel targets for further research into biomarkers of colitis to monitor the effects of salmon.

7.4 Future perspectives

Salmon is one of the richest natural sources of n-3 PUFA and may be a nutritional option to help with the management of the symptoms of colitis as observed in IBD. To use diet as a complementary solution to conventional treatments, any effects of diet need to be monitored using biomarkers that predict (specifically and sensitively) metabolic or physiological changes associated with increased or decreased risk of colitis that occurred in IBD. Key features are that these biomarkers can be detected at an early stage of colitis in surrogate "tissues" that can be sampled with minimally invasive methods. Temporal monitoring of these biomarkers will allow time for prevention, thus reducing the risk to develop colitis before its onset.

Whole colon tissue contains a variety of cell types which may not necessarily respond uniformly to dietary intervention. Therefore the use of specific cell fractions instead of whole colon tissue may offer novel insights into the effects of dietary n-3 PUFA. Transcriptomic profiling of whole colon tissue largely showed increased immune cell function, possibly from infiltrating immune cells directing the inflammatory response, while more subtle (albeit important) gene expression changes from small populations of cells may have not been detected due to noise from more abundant cell types. This may be relevant especially during early stages of colitis, when loss of epithelial barrier function or regulation of the commensal microbiota contribute to the perpetuation of disease [561, 562]. As described by Russ *et al.* [348], the use of laser microdissection followed by microarray analysis of colon epithelial cells may provide more information about the impact of the EPA diet on early stages of colitis compared to the analysis of whole colon tissue. Additionally, the transcriptomic profile from the colonic epithelium may have provided further information about the cross-talk between *V. akkermansia* and the epithelial cells in *Il10*$^{-/-}$ mice in response to the 30% salmon diet. However, laser microdissection requires invasive sampling methods (biopsies) and may be of limited use in dietary intervention studies among human IBD patients.

In *Il10*$^{-/-}$ mice fed the EPA diet, changes in gene expression indicated reduced signalling processes associated with AA-derived lipid mediators in the colon. The characterisation of the lipid mediator profile in the colon of EPA-fed *Il10*$^{-/-}$ mice could be performed using a targeted analysis of lipids based on LC-MS/MS (lipidomics) [for example, references 563, 564]. It was shown that the severity of colitis in UC patients

correlated with an AA-derived mucosal lipid mediator profile [564], and an increased intake of fish oil resulted in an adaptation of the lipid mediators towards elevated n-3 PUFA-derived mediators in the colonic mucosa of an adoptive transfer mouse model [98]. While lipidomics of the colonic mucosa requires invasive sampling methods (biopsies), these measurements could be extended to surrogate "tissues" such as urine that could be accessed minimally invasive in humans to provide evidence of n-3 PUFA or salmon intervention [565]. As shown in the EPA experiment, changes in the lipid mediator profile occurred in the urine of all mice fed the EPA diet, and indicated an increase in pro-resolution mediators that may have contributed to the beneficial effect of the EPA diet in *Il10*$^{-/-}$ mice at 12 weeks of age. The resolution of the LC-MS used in the "salmon diet experiment" was not high enough to identify lipid mediators in the urine of mice fed the 30% salmon diet and there was no conclusive evidence of their presence (or absence).

There is currently no standardised method to perform the integration of 'Omics' data in experiments where multiple sources of data are available. The integration of colon gene expression data and urinary metabolomic data may provide another opportunity to show how changes in colonic gene expression mediated by the EPA and salmon diets are associated with metabolite abundance in the urine compared to those fed the control diets. This may have highlighted a connection between genes affecting eicosanoid signalling in the colon that correlate with lipid mediator abundance in the urine of *Il10*$^{-/-}$ mice fed the EPA diet compared to those fed the OA diet. However, colonic eicosanoid metabolism was not affected by the salmon diet in *Il10*$^{-/-}$ mice and therefore the effect of dietary EPA on lipid mediators was not of immediate interest. Additionally, while the integration of microbial abundances and colon gene expression data may have provided information about the cross-talk between host colonic cells and the commensal microbiota, it would have been of limited use for identifying candidate biomarkers.

7.5 Conclusion

In conclusion, diets enriched in EPA (3.7%) or salmon (30%) were able to reduce the severity of colitis in *Il10*$^{-/-}$ mice, however these effects were subtle and dependent on stage of colitis (for the EPA diet) or on dose (for the salmon diet). While gene expression in PBMCs did not predict reduced colitis in response to the EPA diet in *Il10*$^{-/-}$ mice, urine metabolites appeared to be a suitable surrogate "tissue" for biomarkers associated with the molecular responses underlying colitis. Urinary metabolites of tryptophan metabolism

were detected, and characterised by elevated *IDO1*-mediated catabolism of kynurenine (and subsequently xanthurenic acid in urine) from tryptophan, concomitantly with decreased expression of genes in the serotonin and tryptamine pathways in the inflamed colon. Other candidate biomarkers are α-CEHC glucuronide and γ-CEHC glucoside, two metabolites of tocopherol with reduced urinary abundance in *Il10*$^{-/-}$ mice with established colitis; the former is a metabolite previously suggested as a biomarker of colitis in *Il10*$^{-/-}$ mice [309]. The 30% salmon diet had limited effects on tryptophan metabolism in *Il10*$^{-/-}$ mice compared to the corresponding control diet. However, its impact on hepatic tocopherol metabolism was detected in urine, as shown by increased abundance of α-CEHC glucuronide and reduced γ-CEHC glucoside.

The experiments described in this dissertation provide the foundation for further research to better monitor and predict the effects of dietary intervention on colitis. Previous evidence of the immune-modulatory properties of n-3 PUFA such as EPA suggested the relevance of foods rich in such compounds for reducing colitis, with studies among IBD patients reporting beneficial effects of n-3 PUFA-rich salmon [9, 146, 161, 185]. The current experimental approach was designed to advance the understanding of the effects of the pure compound of interest (EPA) on the severity of colitis, and the underlying molecular responses that lead to phenotypic changes. This knowledge was then applied to a whole food rich in EPA (salmon) and to the identification of candidate biomarkers of these responses. A key challenge remaining is the validation of these candidate biomarkers of colitis. A valid biomarker should not only reflect the metabolic or physiological changes associated with increased or decreased risk of IBD, it also needs to be predictive of future health status [566].

High-throughput characterisation of biological samples using 'Omics'-technologies, as used for the studies described in this PhD dissertation, provides significant opportunities to identify candidate biomarkers. The development of powerful data analysis tools that is needed to derive knowledge from complex multidimensional datasets is rapidly advancing, and this should result in an increased number of specific and sensitive candidate biomarkers available to monitor biological responses [566]. These biomarkers could be tested and validated in a dose-response and larger study with animal models of IBD before their use for IBD cohort characterisation and, subsequently, for nutritional management of IBD symptoms with foods rich in EPA such as salmon.

Triggs *et al.* [9] highlighted that other oily fish (tuna) and lean fish (white fish) were perceived to be well tolerated by people with CD in the New Zealand population, and these may present opportunities for further fish-based nutritional intervention studies for subjects with colitis symptoms similar to those found in IBD. The use of multiple 'Omics' platforms has allowed the exploration of previously unknown signalling and metabolic pathways responsive to dietary intervention, and will be an important approach for future studies.

APPENDICES

Appendix I Analysis of lyophilised salmon fillets (de-skinned and de-boned) by AsureQuality (Auckland, New Zealand).

Component (%)	
Protein	44
Carbohydrates	<0.5
Fat	56
Energy (kJ/100g)	2730
Lipid profile (%)	
Polyunsaturated	
Omega-3	7.3
EPA (20:5n-3)	3.0
DHA (22:6n-3)	2.5
DPA (22:5n-3)	1.1
ALA (18:3n-3)	0.7
Omega-6	4.5
AA (20:4n-6)	0.3
LA (18:2n-6)	4.1
GLA (18:3n-6)	0.1
Monounsaturated	
OA (18:1n-9)	17.0
Palmitoleic (16:1n-7)	4.1
Saturated	
Palmitic (16:0)	9.0
Stearic (18:0)	2.3
n-3/n-6 ratio	1.6
Oxidation	
Peroxide (meq O_2/kg fat)	1.3
p-Anisidine	9.1

AA: Arachidonic acid; ALA: Alpha-linolenic acid; DHA: Docosahexaenoic acid; DPA: Docosapentaenoic acid; EPA: Eicosapentaenoic acid; GLA: Gamma-linolenic acid; LA: Linoleic acid; OA: Oleic acid.

Appendix II R codes applied for pre-processing of metabolomics data from the (A) "EPA time-course experiment" and (B) "salmon diet experiment".

A

```
#=== peak detection ===========================================
xset <- xcmsSet(files = filenames$FileName, snames = paste(filenames$Sample),
        sclass = paste(filenames$Strain,filenames$Diet,filenames$Urine_sample_time,sep="_"),
        method = "centWave", ppm = 2.5, peakwidth =c (5,20),
        prefilter = c(3,5000), snthresh = 10, integrate = 1, noise = 100)
#=== peak grouping ============================================
xs.grp <- group.density(xset, bw = 10, mzwid = 0.015, minfrac = 0.75)
#=== Retention Time correction ================================
xs.grp.rt <- retcor.obiwarp(xs.grp, plottype = "deviation")
#=== regrouping ===============================================
xs.regrp <- group.density(xs.grp.rt, bw = 10, mzwid = 0.015, minfrac = 0.75)
#=== fill peaks ===============================================
xs.fill <- fillPeaks(xs.regrp)
#==== peak table ==============================================
Peak.Table <- peakTable(xs.fill)
values.raw <- PeakTable[which(PeakTable$rt > 100 & PeakTable$rt < 800),colnames(PeakTable) %in%
filenames$Sample]
```

B

```
xset <-xcmsSet(files = filenames$Filenames, snames = filenames$Index, sclass =
        paste(filenames$Strain,filenames$Diet,filenames$Sampling.day,sep="_"), fwhm=6)
xset <- group(xset)
xset2 <- retcor(xset, method="loess", plottype = "deviation", span=0.5)
xset2 <- group(xset2, bw=10)
xset3 <- fillPeaks(xset2)
PeakTable <- peakTable(xset3)
values.raw <- groupval(xset3, value="into",method="medret")
```

Appendix III Histological injury scores (HIS) obtained from the duodenum of C57BL/6J and *Il10*$^{-/-}$ mice at 9 and 12 weeks of age. Mice were fed AIN-76A diets, either unmodified, or enriched with 3.7% oleic acid (OA) or 3.7% eicosapentaenoic acid (EPA). Individual features scored from 0 (no change from normal tissue) to 10 (extreme changes in tissue). Unmodified AIN-76A diet and OA diet were included as control diets. Data represent five to ten biological replicates per treatment group.

Genotype	*Histological feature*	*9 weeks*		*12 weeks*		
		OA	*EPA*	*AIN-76A*	*OA*	*EPA*
C57BL/6J	Crypt hyperplasia	0	0	0	0	0
	Aberrant villi	0.8 ± 0.2	1 ± 0.2	0.2 ± 0.2	0.4 ± 0.2	0.2 ± 0.1
	Crypt injury	0	0.2 ± 0.2	0	0	0
	Crypt loss	0	0	0	0	0
	Goblet cell loss	0	0	0	0	0
	Crypt abscess	0	0	0	0	0
	Lymphoid aggregates	0.4 ± 0.3	0.2 ± 0.1	0.2 ± 0.2	0	0
	Aberrant submucosa	0	0	0	0	0
	Surface loss	0	0	0	0	0
	Neutrophils	0	0	0	0	0
	Lymphocytes/plasma cells	1.1 ± 0.1	1.1 ± 0.1	1 ± 0	1 ± 0	1 ± 0
	Monocytes/macrophages	0	0	0	0	0
Il10$^{-/-}$	Crypt hyperplasia	0	0	0.1 ± 0.1	0	1.2 ± 0.4
	Aberrant villi	1.2 ± 0.2	1.2 ± 0.2	1.1 ± 0.2	1.1 ± 0.3	2.5 ± 0.2
	Crypt injury	0	0	0	0	0
	Crypt loss	0	0	0	0	0
	Goblet cell loss	0	0	0	0	0
	Crypt abscess	0	0	0	0.1 ± 0.1	0.2 ± 0.2
	Lymphoid aggregates	0.1 ± 0.1	0.1 ± 0.1	0.1 ± 0.1	0.2 ± 0.1	0
	Aberrant submucosa	0	0	0	0	0
	Surface loss	0	0	0	0	0
	Neutrophils	0	0	0.2 ± 0.2	0	1.8 ± 0.7
	Lymphocytes/plasma cells	1.2 ± 0.1	1.4 ± 0.2	1.9 ± 0.2	1.8 ± 0.1	2.8 ± 0.2
	Monocytes/macrophages	0	0.1 ± 0.1	0	0	0

Data represent means ± SEM.

Appendix IV Differentially expressed genes in the colon of *Il10*$^{-/-}$ mice fed the oleic acid (OA) diet compared to those fed the AIN-76A diet at 12 weeks of age. Genes considered differentially expressed when passing the cut-off fold-change (FC) ≥ |1.5| and p-value < 0.005. Data represents four biological replicates per treatment group.

Gene name	*Description*	*FC*	*P-value*
Dph1	DPH1 homolog (S. cerevisiae)	-1.52	0.005
Klhl1	Kelch-like 1	-1.59	0.002
Cav2	Caveolin 2	-1.50	0.005
Ahcyl1	S-adenosylhomocysteine hydrolase-like 1	-4.40	0.001
Cspp1	Centrosome and spindle pole associated protein 1	-1.50	0.005
Clptm1l	CLPTM1-like	-1.53	0.005
Gm6792	Predicted gene 6792	-1.69	<0.001
Isl1	ISL1 transcription factor, LIM/homeodomain	2.32	0.001
Slc30a9	Solute carrier family 30 (zinc transporter) member 9	-1.68	0.004
TC1700876	NA	-1.88	0.002
Col9a1	Collagen, type IX, alpha 1	-1.52	0.004
Frs3	Fibroblast growth factor receptor substrate 3	-1.55	0.003
Vmn2r70	Vomeronasal 2, receptor 70	-1.54	0.004
Clec10a	C-type lectin domain family 10, member A	-2.01	0.003
ENSMUST00000098110	NA	1.55	0.005
Mgll	Monoglyceride lipase	-1.55	0.001
NAP061934-1	NA	-1.64	<0.001
Pkp4	Plakophilin 4	-1.62	0.001
ENSMUST00000086868	NA	-1.84	0.001
LOC676689	H-2 class I histocompatibility antigen, L-D alpha chain precursor-like	-1.72	0.001
ENSMUST00000105696	NA	-1.56	0.001
Gm3993	Predicted gene 3993	-1.58	<0.001
Gm11127	Predicted gene 11127	-1.65	0.003
Nckap1	NCK-associated protein 1	-1.67	0.001
Sypl	Synaptophysin-like protein	1.55	0.005
Chrd	Chordin	1.51	0.001
1700028M03Rik	RIKEN cDNA 1700028M03 gene	-1.77	0.002
4930447K03Rik	RIKEN cDNA 4930447K03 gene	1.68	0.001

Appendix V Molecule shapes and relationship types used by Ingenuity Pathway Analysis to present gene and protein expression data (IPA; Ingenuity Systems; www.ingenuity.com).

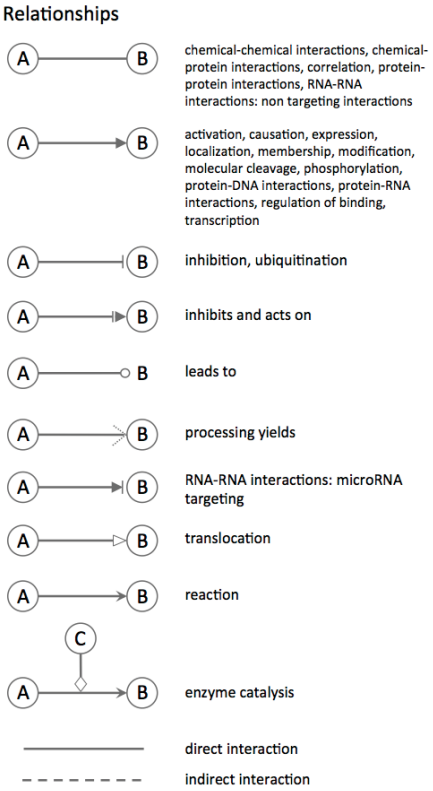

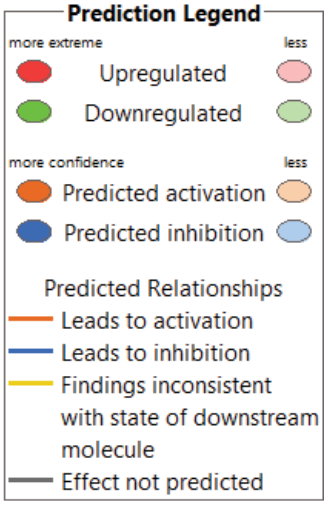

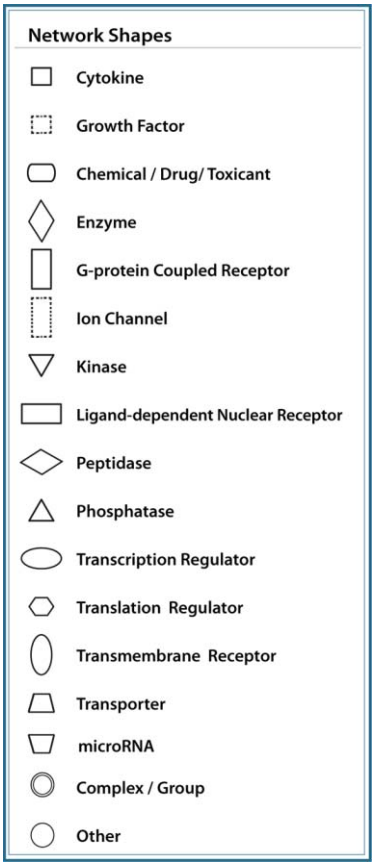

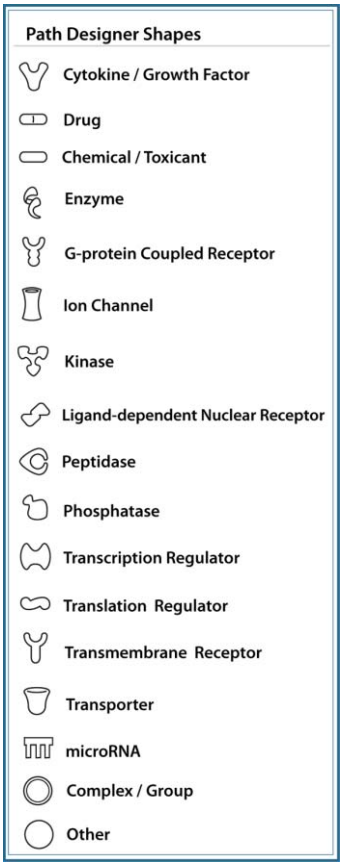

Appendix VI Positive ionisation products with differential abundance in the urine of mice fed the eicosapentaenoic acid (EPA) diet compared to those fed the oleic acid (OA) diet, and in common at 7.1, 9, 10.1 and 12 weeks of age (FDR ≤ 0.05). Mice euthanised at 12 weeks of age. Arrows represent the direction of change in EPA-fed mice. "RT" indicates the retention time in seconds. Products with putative identification listed, searching METLIN and HMDB with 5 ppm mass accuracy and adducts M+H, M+Na and M+NH_4 enabled. Metabolites in bold are discussed. Data represent five to nine biological replicates per treatment group.

Ion (M/Z)	*RT*	*Entries*	*Adduct*	*Putative identification*	*EPA vs. OA*
258.1337	106	3	M+NH_4	3-Carboxy-4-methyl-5-propyl-2-furanpropionic acid	↑
232.1180	193	2	M+H	Suberylglycine	↑
				Isovalerylglutamic acid	
162.0760	234	11	M+NH_4	trans-2-Hexenedioic acid	↑
				3-Hexenedioic acid	
			M+NH_4	Maleic acid homopolymer	
			M+H	Aminoadipic acid	
206.1388	238	11	M+NH_4	Diethyl glutarate	↑
				Diethyl methylsuccinate	
				2,4-Dimethylpimelic acid	
				Azelaic acid	
				Nonate	
				3-Methylsuberic acid	
215.1391	258	6	M+NH_4	Metanephrine	↑
220.1545	277	7	M+NH_4	Sebacic acid	↑
152.1071	281	2	M+H	N-Methylphenylethanolamine	↑
			M+NH_4	Indan-1-ol	
309.1558	281	1	M+NH_4	Serinyl-tryoptophan	↑
332.0953	282	3	M+Na	N-Acetylneuraminic acid	↓
				N-Acetyl-a-neuraminic acid	
169.0496	289	13	M+H	Isovanillic acid	↑
				3,4-Dihydroxybenzeneacetic acid	
				p-Hydroxymandelic acid	
				Homogentisic acid	
				3,4-Dihydroxymandelaldehyde	
				Vanillic acid	
				3-Hydroxymandelic acid	
214.1075	298	14	M+NH4	Homoveratric acid	↑
215.1390	299	6	M+NH_4	Metanephrine	↑
238.1050	309	1	M+Na	Propenoylcarnitine	↑
268.1542	309	4	M+NH_4	Ubiquinone-1	↑
				3,4-Dihydro-6-hydroxy-2,5,7,8-tetramethyl-2H-1-benzopyran-2-carboxylic acid	
				Helinorbisabone	
				Delta-CEHC	
136.0475	313	1	M+Na	Creatinine	↑
459.2160	323	5	M+NH_4	18-Carboxy-dinor-LTE4	↑
261.1485	324	1	M+H	10-Hydroxy-3-methoxy-1,3,5,7-cadinatetraen-9-on	↑
299.1470	324	5	M+NH_4	1-Methyladenosine	↑
				N6-Methyladenosine	
214.1073	329	14	M+NH_4	Homoveratric acid	↑
361.1398	330	16	M+H	Dityrosine	↑
			M+NH4	Caffeoyl tyrosine	
152.1071	348	2	M+H	N-Methylphenylethanolamine	↑

			$M+NH_4$	Indan-1-ol	
213.0951	349	3	M+Na	N-(o)-Hydroxyarginine	↑
333.1309	352	1	M+H	Tryptophyl-Glutamate	↑
486.1124	362	2	M+Na	Isopeonidin 3-galactoside Isopeonidin 3-glucoside	↓
368.2433	372	14	$M+NH_4$	Resolvin E1 Prostaglandin E3 5,12,18R-TriHEPE 15-Epi-lipoxin B5 15-Keto-prostaglandin E2 20-oxo-leukotriene B4 12-Oxo-20-hydroxy-leukotriene B4 8-iso-15-keto-PGE2 Prostaglandin D3 15-Oxo-lipoxin A4 PGH3	↑
331.1905	374			11b-Hydroxyprogesterone Carnosic acid 7'-Carboxy-gamma-tocotrienol	↑
558.2914	386	1	$M+NH_4$	Tetrahydroaldosterone-3-glucuronide	↑
569.2895	**387**	1	M+H	Leukotriene F4	↑
333.2060	391	14	M+H	(1(10)E,4E,6a,9b)-9-(2-Methylbutanoyloxy)-1(10),4,11(13)-germacratrien-12,6-olide ent-15-Kaurene-17,19-dioic acid (1(10)E,4E,6a,9b)-9-(3-Methylbutanoyloxy)-1(10),4,11(13)-germacratrien-12,6-olide 6-Angeloylfuranofukinol 11b-Hydroxyprogesterone (9Z,11S,16S)-1-Acetoxy-9,17-octadecadiene-12,14-diyne-11,16-diol Carnosic acid 7'-Carboxy-gamma-tocotrienol Petasitin 7,18-Dihydroxykaurenolide ent-7alpha,12beta-Dihydroxy-16-kauren-19,6beta-olide	↑
312.1806	392	2	$M+NH_4$	Tocopheronic acid	↑
377.1569	394	4	$M+NH_4$	Epinephrine glucuronide L-DOPA 3'-glucoside	↑
164.0376	397	1	M+H	Acetylcysteine	↑
378.2275	404	6	$M+NH_4$	Cortisone	↑
380.2434	422	1	$M+NH_4$	Cortisol	↑
500.2773	**503**	2	M+H	LysoPE(20:5n-3)	↑

Appendix VII Negative ionisation products with differential abundance in the urine of mice fed the eicosapentaenoic acid (EPA) diet compared to those fed the oleic acid (OA) diet, and in common at 7.1, 9, 10.1 and 12 weeks of age (FDR ≤ 0.05). *Il10*$^{-/-}$ and C57BL/6J mice were euthanised at 12 weeks of age. Arrows represent direction of change in EPA-fed mice. "RT" indicates the retention time in seconds. Products with putative identification listed, searching METLIN and HMDB with 5 ppm mass accuracy and adduct M-H enabled. Metabolites in bold are discussed. Data represent five to nine biological replicates per group.

Ion (M/Z)	*RT*	*Entries*	*Putative identification*	*EPA vs. OA*
337.0602	111	1	N-(Carbomethoxyacetyl)-4-S-chlorotryptophan	↑
175.0606	171	5	2,3-Dimethyl-3-hydroxyglutaric acid 2-Isopropylmalic acid 3-Isopropylmalate	↑
172.0608	222	1	N-Acetyl-L-glutamate 5-semialdehyde	↑
230.1032	236	2	Isovalerylglutamic acid Suberylglycine	↑
350.1470	245	1	Zeatin	↑
155.0706	256	2	8-Hydroxy-5,6-octadienoic acid	↑
373.1869	263	1	6-Epi-7-isocucurbic acid glucoside	↑
331.1770	267	2	Tryptophyl-Lysine Lysyl-Tryptophan	↑
197.0814	276	6	2,3-Methylene suberic acid 3,4-Methylene suberic acid	↑
245.1392	293	1	3-Hydroxydodecanedioic acid	↑
199.0970	295	8	cis-5-Decenedioic acid (±)-Camphoric acid 5-Pentyltetrahydro-2-oxo-3-furancarboxylic acid alpha-Carboxy-delta-nonalactone cis-4-Decenedioic acid	↑
196.0970	309	3	Metanephrine	↑
169.0498	311	4	3,4-Dihydroxyphenylglycol	↑
156.0660	312	3	Tiglylglycine 3-Methylcrotonylglycine	↑
315.1392	324	2	11,11,11,12,12-Pentafluoro-9Z-dodecenyl acetate 4,7,10,13,16,19-Docosahexaynoic acid	↑
297.1707	328	7	13,14-dihydro-15-keto-tetranor Prostaglandin D2 Tetranor-PGE1 Tetranor-PGD1 13,14-dihydro-15-keto-tetranor PGE2	↑
269.0675	328	2	Phenylglucuronide Phenol glucuronide	↑
196.0613	330	4	2-Hydroxy-3-(3,4-dihydroxyphenyl)propanamide N-Hydroxy-L-tyrosine DL-Dopa L-Dopa	↑
397.1140	335	6	5-(3',5'-Dihydroxyphenyl)-gamma-valerolactone-O-glucuronide-O-methyl 5-(3',4'-Dihydroxyphenyl)-gamma-valerolactone-4'-O-methyl-3'-O-glucuronide 5-(3',4'-Dihydroxyphenyl)-gamma-valerolactone-3'-O-methyl-4'-O-glucuronide 5-(3',4'-dihydroxyphenyl)-gamma-valerolactone-3'-O-glucuronide	↑
737.1720	346	1	3-O-beta-D-Galactopyranosylproanthocyanidin A5'	↓
196.0974	348	1	Metanephrine	↑
196.0974	348	3	Metanephrine	↑

373.1872	353	1	6-Epi-7-isocucurbic acid glucoside	↑
385.2235	**355**	1	10,11-dihydro-20-trihydroxy-leukotriene B4	↑
513.2709	357	4	Cinncassiol D1 glucoside Cinncassiol D4 2-glucoside Cofaryloside Capsianoside V	↑
182.0817	371	5	Normetanephrine Levonordefrin Epinephrine Methylnoradrenaline	↑
177.0914	378	20	5-Phenylvaleric acid	↑
196.0976	379	3	Metanephrine	↑
242.1402	379	1	Tiglylcarnitine	↑
177.0914	379	2	5-Phenylvaleric acid	↑
274.1203	388	3	Alanyl-Tryptophan Tryptophyl-Alanine Alanyltryptophan	↑
320.1000	392	1	S-Glutaryldihydrolipoamide	↑
337.1664	397	4	Omega-Carboxy-trinor-leukotriene B4 2,3-Dinor-6,15-diketo-13,14-dihydro-PGF1a	↑
351.2182	398	3	Prostaglandin E2 Prostaglandin D2	↑
328.1036	401	1	Dopamine glucuronide	↑
367.2129	403	28	Thromboxane B3 6,15-Diketo,13,14-dihydro-PGF1a Cinncassiol D2 20-COOH-10,11-dihydro-LTB4 5(6)-Epoxy Prostaglandin E1 Prostaglandin G2 19-Hydroxy-PGE2 20-Hydroxy-PGE2 6-Ketoprostaglandin E1 11-Dehydro-thromboxane B2 Cinncassiol D3 6-keto PGE1 13,14-dihydro-6,15-diketo-PGF1alpha Δ17-6-keto PGF1α 5,12-dihydroperoxy-6,8,10,14-eicosatetraenoic acid 5,15-dihydroperoxy-6,8,11,13-eicosatetraenoic acid 8,15-dihydroperoxy-5,9,11,13-eicosatetraenoic acid 15(R),19(R)-hydroxy Prostaglandin E2 20-hydroxy-PGD2 15S-hydroperoxy-PGE2 15S-hydroperoxy-PGD2 5,12-diHPETE 5,15-diHPETE 8,15-diHPETE 5S,15S-diHPETE 8S,15S-diHPETE	↑
367.1533	413	13	PA(6:0/6:0)	↑
228.0780	421	1	Endalin	↓
277.1446	432	4	Alpha-CEHC	↑
498.2634	**502**	3	LysoPE(20:5(n-3)/0:0) LysoPE(0:0/20:5(n-3))	↑

Appendix VIII Biological pathway for *Tryptophan metabolism* indicating molecular events that lead to the biosynthesis of melatonin from tryptophan (*via* serotonin), or xanthurenic acid (*via* kynurenine) in *Il10*$^{-/-}$ mice fed the oleic acid (OA) diet compared to C57BL/6J mice fed the same diet at 12 weeks of age.

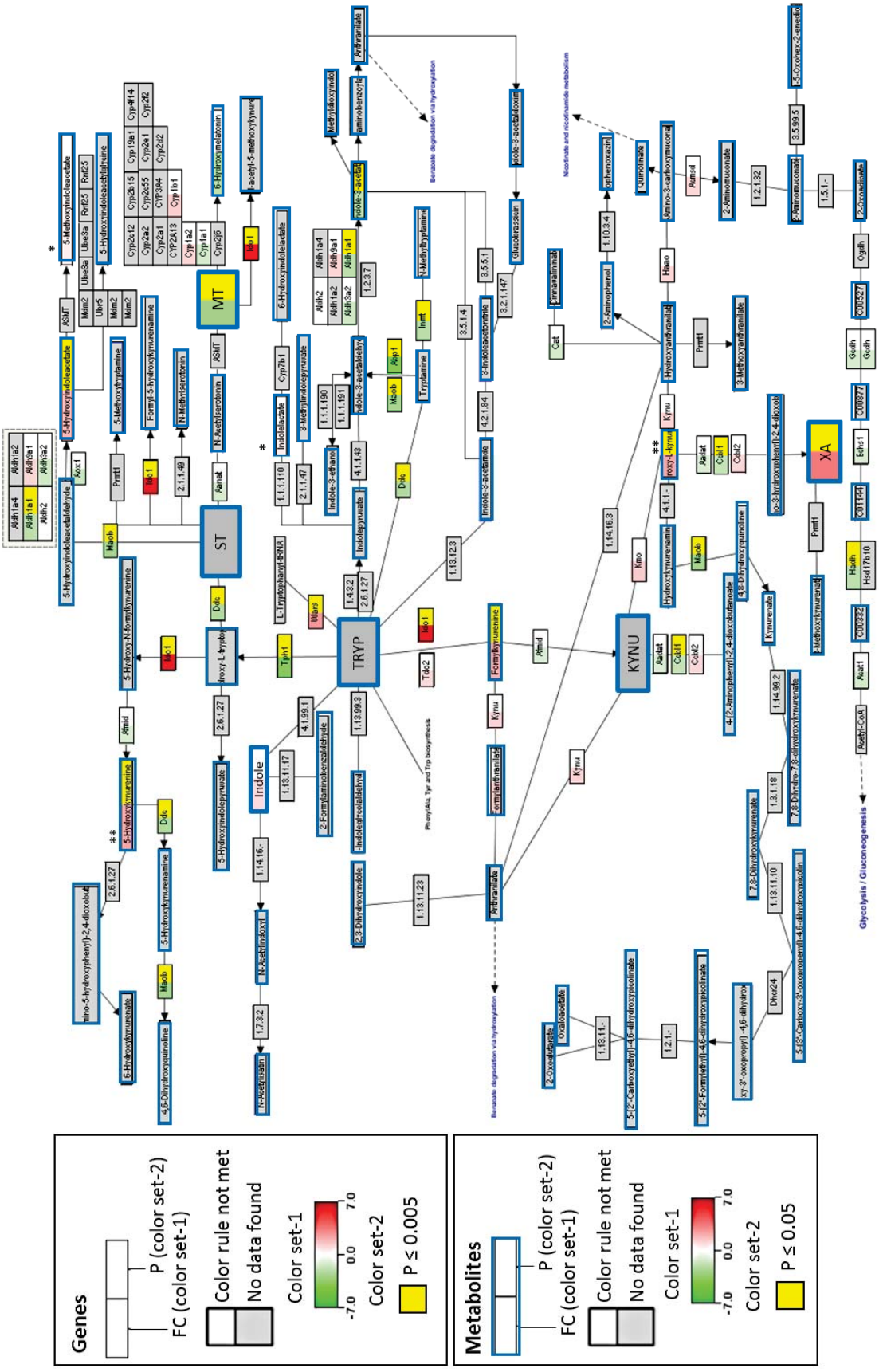

Appendix VIII continued. Nodes represent genes and metabolites (coloured border). Colour coding of nodes indicate increased (red) or decreased (green) levels as illustrated in the legend. Data for genes and metabolites shaded in grey not considered or measured. Gene expression data were established by microarray analysis of colon tissue from *Il10*$^{-/-}$ mice and metabolomics data by untargeted MS of urine (putative identifications). Metabolites marked with asterisk were putatively identified for the same ion. Pathway information obtained from Kanehisa *et al.* [328] and Ferrante *et al.* [519].
KYNU: Kynurenine; MT: Melatonin; ST: Serotonin; TRYP: Tryptophan; XA: Xanthurenic acid.

Appendix IX Biological pathway for *Tryptophan metabolism* indicating molecular events that lead to the biosynthesis of melatonin from tryptophan (*via* serotonin), or xanthurenic acid (*via* kynurenine) in *Il10*$^{-/-}$ mice fed the eicosapentaenoic acid (EPA) diet compared to those fed the oleic acid (OA) diet.

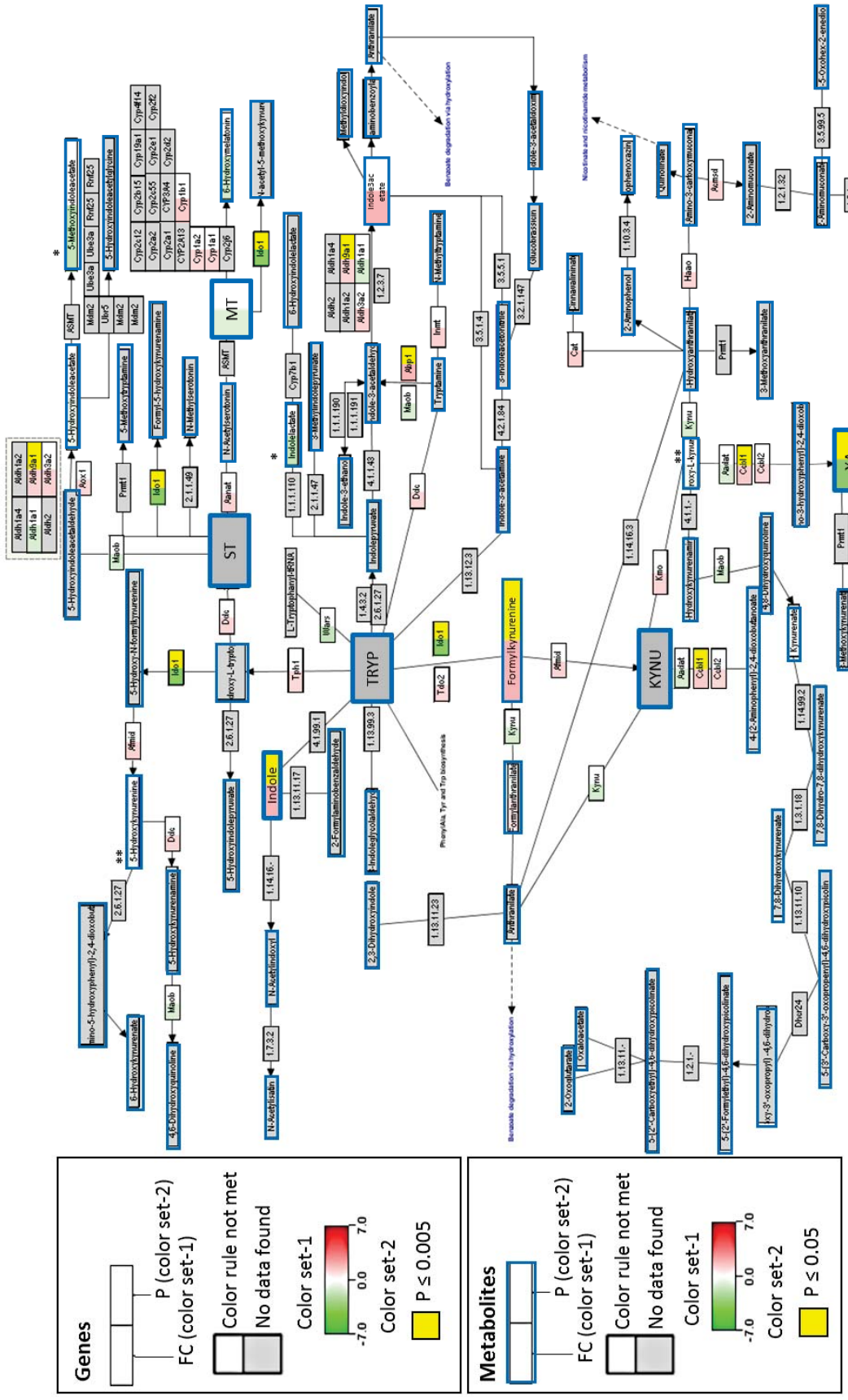

Appendix IX continued. Nodes represent genes or metabolites as indicated by a coloured border. Colour coding of nodes indicate increased (red) or decreased (green) levels as illustrated in the legend. Data for genes and metabolites shaded in grey not considered or measured. Gene expression data were established by microarray analysis of colon tissue from *Il10*$^{-/-}$ mice and metabolomics data by untargeted MS of urine (putative identifications). Metabolites marked with asterisk were putatively identified for the same ion. Pathway information obtained from Kanehisa *et al.* [328] and Ferrante *et al.* [519].
KYNU: Kynurenine; MT: Melatonin; ST: Serotonin; TRYP: Tryptophan; XA: Xanthurenic acid.

Appendix X Histology scores from (A) C57BL/6J mice and (B) *Il10*$^{-/-}$ mice fed diets supplemented with 15%, 30% or 45% salmon and corresponding macronutrient-matched control diets. Intestinal sections (caecum, colon, duodenum, ileum and jejunum) were obtained from eight biological replicates per group, fixed in formalin and stained with haematoxylin and eosin. The tissue appearances were scored from 0 (no change from normal tissue; no inflammation) to 10 (extreme changes; highly inflamed tissue): changes specific to intestinal crypts (hyperplasia, aberrancy and injury), changes in tissue landscape (goblet cell loss, crypt loss, crypt abscess, lymphoid aggregates and sub-mucosal thickening) and changes specific to epithelial cells (surface loss). The infiltration of inflammatory cells (monocytes, neutrophils, macrophages, plasma cells and lymphocytes) was scored from 0 (numbers of inflammatory cells in normal range) to 10 (highly elevated numbers of inflammatory cells). The total HIS was calculated as the sum of the individual features.

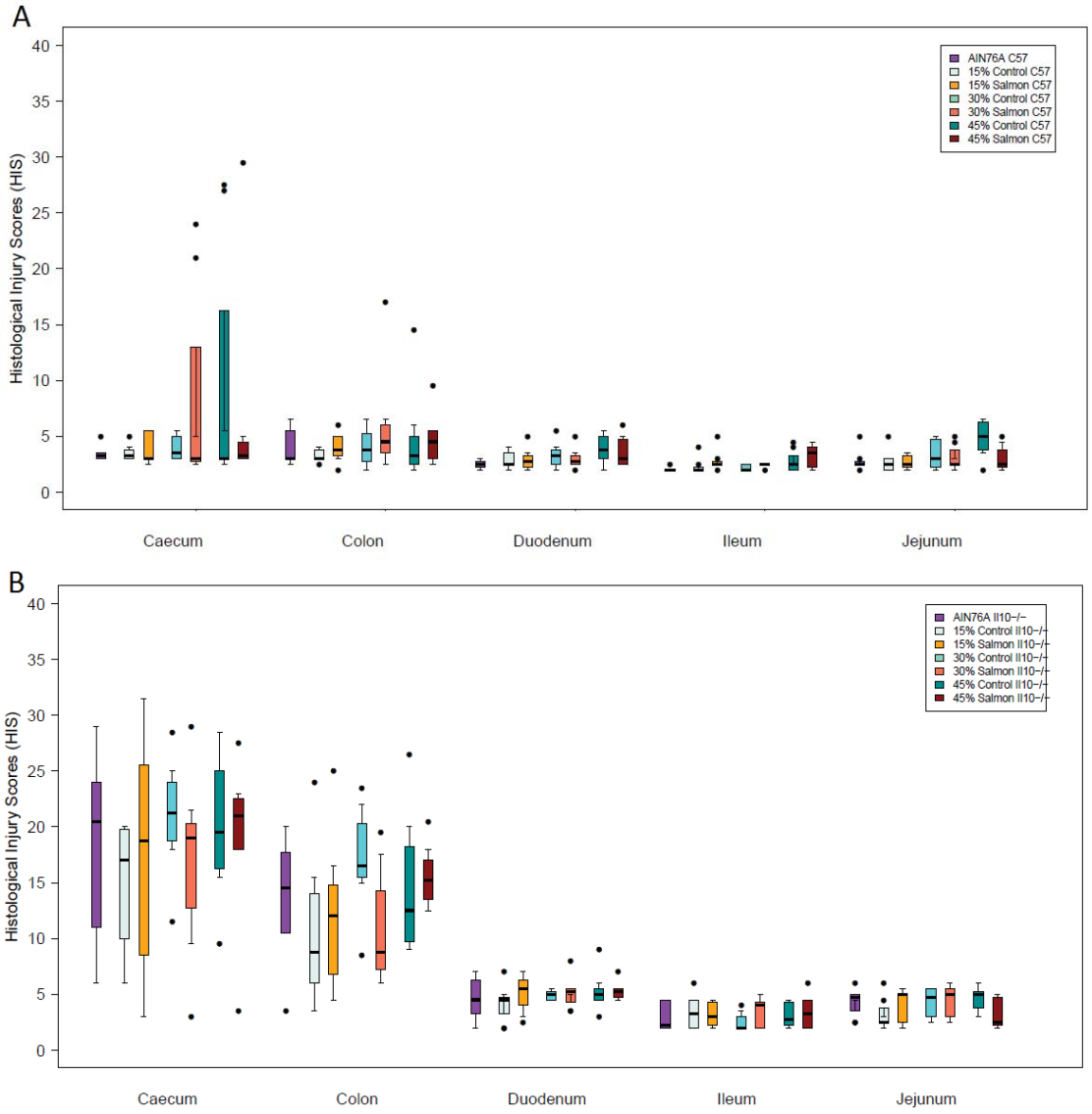

Method

Target genes were chosen based on expression FC and associated relevance in intestinal inflammation: *CXCL5* (RefSeq number NM_009141), *CYP26B1* (NM_001177713), *S100A9* (NM_009114), *IL12B* (NM_008352), *SULT1C2* (NM_026935), *KCNN2* (NM_080465), *ICOS* (NM_017480) and *GAL3ST2* (NM_199366). Calnexin (*CANX*; NM_007597) was selected as a housekeeping gene as it was not differentially expressed between the treatment groups and showed low variance across microarrays. *CANX* was also used as a housekeeping gene in previous experiments with *Il10*$^{-/-}$ mice [6, 305, 567].

The Universal mouse reference RNA (Agilent Technologies, California, USA) and sample RNA (30% salmon and 30% control diets) were reverse-transcribed using the High Capacity RNA-to-cDNA Kit (Applied Biosystems by Life Technologies, California, USA). 1000 ng RNA were brought to a volume of 9 µl with nuclease-free water, followed by the addition of 10 µl 2x reverse-transcription buffer and 1 µl 20x reverse-transcription enzyme mix. Samples were mixed gently and put on ice until loaded into the RotorGene 6000 qPCR instrument (Qiagen, distributed by Bio-Strategy Ltd, Auckland, New Zealand). Thermal cycling was set to 37°C for 60 min, followed by 95°C for 5 min. cDNA samples were stored at -20°C until further processing.

PrimeTime qPCR assays, containing the gene-specific primers, were sourced from Integrated DNA Technologies (Iowa, USA) and resuspended in 500 µl nuclease-free water before use. For each target and housekeeping gene, a master mix was prepared comprising of 5 µl 2x Universal qPCR Master Mix (Kapa Biosystems, Massachusetts, USA), 0.5 µl resuspended PrimeTime qPCR assay and 3.5 µl nuclease-free water.

Each qPCR analysis was designed using a no-template control, a calibrator and the sample templates. The no-template control enabled monitoring the reaction for contamination of the components. The calibrator was necessary for subsequent extraction of results from the software and was prepared using the housekeeping gene and reference cDNA. The final qPCR reactions were set up using the following design: (1) no-template control (9 µl gene-specific master mix, 1 µl nuclease-free water); (2) calibrator (9 µl Canx master mix, 1 µl reference cDNA at a 1:20 dilution); (3) sample cDNA (9 µl gene-specific master mix, 1 µl cDNA at a 1:20 dilution). All samples were represented in duplicates

and each qPCR was run twice to increase confidence in the data. The thermal cycling profile was set to 95°C for 3 min, followed by 40 cycles of 95°C for 3 s and 60°C for 30 s. The results were uploaded into the Relative Expression Software Tool (REST, version 2.0.13 [568]). Genes were defined as differentially expressed when FC ≥ |1.5| and p-value ≤ 0.05.

Result

The direction of FC for all selected genes was consistent between qPCR and microarrays, confirming the expression of these genes: *ICOS*, *IL12B*, *KCNN2*, *CYP26B1*, *S100A9*, *CXCL5*, *GAL3ST2*, and *SULT1C2* (Table.A 1). Five expression FC were not considered significantly different based on microarray analysis, but showed differential expression in qPCR. These were *KCNN2* (*Il10*$^{-/-}$ vs. C57BL/6J mice fed the AIN-76A diet), and in the comparison 30% salmon vs. 30% control in *Il10*$^{-/-}$ mice the genes *S100A9*, *CXCL5*, *GAL3ST2* and *SULT1C2*. qPCR is considered the more sensitive method [569] and this result was not unexpected.

Table.A 1 qPCR validation of selected genes from microarray analysis. The genes were selected based on fold-change (FC) and p-value, using sample RNA from the same mice included for microarray analysis. qPCR data was analysed by REST software [568] and a FC ≥ |1.5| and p-value ≤ 0.05 were regarded as significant. On a microarray level, genes were considered differentially expressed when FC ≥ |1.5| and p-value ≤ 0.005.

Comparison	*Gene*	*qPCR*			*Microarray*		
		FC	*P-value*		*FC*	*P-value*	
Il10$^{-/-}$ vs. C57BL/6J 30% control	*ICOS*	+ 4.67	< 0.001		+ 3.9	< 0.005	^
	IL12B	+ 7.35	< 0.001		+ 3.6	< 0.005	^
	KCNN2	- 3.29	< 0.001		- 3.2	< 0.005	^
	CYP26B1	- 1.45	< 0.001		- 1.7	0.083	†
	S100A9	+ 11.76	< 0.001		+ 8.5	< 0.005	
	CXCL5	+ 8.49	< 0.001		+ 9.6	< 0.005	
	GAL3ST2	- 6.94	< 0.001		- 4.9	< 0.005	^
	SULT1C2	- 7.46	< 0.001		- 8.0	< 0.005	
30% salmon vs. 30% control *Il10*$^{-/-}$	*ICOS*	- 1.48	< 0.001		- 2.2	< 0.005	^
	IL12B	- 1.63	0.001		- 2.9	< 0.005	^
	KCNN2	+ 1.92	< 0.001		+ 2.3	< 0.005	^
	CYP26B1	+ 2.72	< 0.001		+ 2.7	< 0.005	
	S100A9	- 1.81	0.024	#	- 3.6	0.050	
	CXCL5	- 1.78	0.027	#	- 4.5	0.020	
	GAL3ST2	+ 2.40	< 0.001	#	+ 2.0	0.032	^
	SULT1C2	+ 2.21	< 0.001	#	+ 2.3	0.034	

^ Presented more than once on microarray therefore average FC of probes with specified p-value calculated.
† Not considered differentially expressed by microarray analysis and qPCR.
# Differentially expressed by qPCR, but not by microarray analysis.

Appendix XII Unidentified ions with the ten highest Partial Least Squares-Discriminant Analysis (PLS-DA) loadings ("discriminant ions") in *Il10*$^{-/-}$ and C57BL/6J mice fed 30% control or 30% salmon diets. For negative and positive ionisation mode, loadings were obtained by PLS-DA at 6.2, 9 and 11.5 weeks of age (referred to as 1st, 2nd and 3rd time-point in the table). Arrows indicate direction of fold-change (FC) in *Il10*$^{-/-}$ mice (compared to C57BL/6J mice), or 30% salmon-fed mice (vs. 30% control diet). Data shown as p-values of the log-transformed, normalised peak intensities as per XCMS, with significance evaluated by ANOVA at each time-point independently. Interaction p-value (genotype × diet) given for the third time-point only. "n.s." indicates ions that are not significantly different between a given comparison. Data represent two to eight biological replicates per treatment group. P-values ≤ 0.001 were considered significant.

XCMS RT	*XCMS ions (m/z)*[1]	*Discriminant time-point*	*Il10*$^{-/-}$ *vs. C57BL/6J*				*30% salmon vs. 30% control*				*Interaction*[2]
			FC	*1st*	*2nd*	*3rd*	*FC*	*1st*	*2nd*	*3rd*	*3rd*
Negative											
181	246	2	↑	n.s.	7.8E-05	1.8E-04	n.s.				n.s.
232	269	3	↓	n.s.	1.4E-07	1.4E-06	n.s.				n.s.
253	304	1	↓	1.1E-07	n.s.	n.s.	↑	7.3E-18	1.7E-07	1.3E-07	n.s.
273	261	2	↑	n.s.	7.4E-06	n.s.	n.s.				n.s.
292	332.1	2	n.s.				↑	1.2E-12	1.2E-13	8.8E-10	n.s.
297	456.1	1	↑	1.6E-06	n.s.	n.s.	n.s.				n.s.
322	510.1	3	↓	1.1E-05	n.s.	4.9E-11	↑	8.1E-04	n.s.	n.s.	n.s.
325	324.1	2	n.s.				↑	1.5E-13	4.0E-15	2.6E-14	n.s.
328	388.1	2	↑	2.0E-04	n.s.	n.s.	↑	4.7E-13	8.1E-16	1.2E-16	n.s.
335	483.2	3	↓	1.2E-05	3.5E-04	2.6E-09	↓	7.1E-06	n.s.	4.7E-05	n.s.
368	602.2	1	↓	4.7E-06	5.5E-04	5.1E-07	n.s.				n.s.
373	302.1	1, 2, 3	↓	4.5E-08	n.s.	n.s.	↑	5.8E-19	6.2E-18	4.0E-16	n.s.
393	212.1	2	n.s.				↑	1.9E-09	3.9E-16	1.0E-10	n.s.
393	**316.1**, 318.1	1	↓	3.1E-08	n.s.	n.s.	↑	8.5E-18	4.8E-09	4.1E-16	n.s.
431	311.8	3	n.s.				↑	n.s.	1.4E-07	1.6E-16	n.s.
432	165.1, **266.1**, 267.1	1, 3	↓	2.7E-08	n.s.	n.s.	↑	5.0E-18	5.3E-13	1.8E-15	n.s.
Positive											
117	210	2	↑	n.s.	1.2E-04	n.s.	n.s.				n.s.
264	232	1	↓	n.s.	n.s.	4.5E-05	↑	2.8E-04	3.9E-09	5.0E-15	n.s.

269	157	3	↑	n.s.	7.2E-04	5.1E-07	↓	3.5E-04	n.s.	n.s.	n.s.
271	263	2	↑	n.s.	1.0E-04	6.7E-04	n.s.				n.s.
284	310.1	1	↓	n.s.	n.s.	2.7E-04	↑	1.5E-05	6.6E-04	4.5E-06	n.s.
297	286	1	↓	n.s.	2.6E-04	3.4E-04	↑	8.3E-04	1.0E-04	8.5E-06	n.s.
301	445.1	2	n.s.				↑	4.6E-11	1.8E-10	1.0E-14	n.s.
306	628.5	3	↑	n.s.	n.s.	3.0E-08	n.s.				n.s.
306	816.6	3	↑	n.s.	n.s.	9.9E-06	n.s.				n.s.
324	163	1	↓	5.6E-04	n.s.	n.s.	↑	4.7E-05	5.4E-04	5.3E-05	n.s.
326	452.2	1	↑	1.2E-04	n.s.	n.s.	↑	2.5E-08	3.3E-04	2.3E-09	n.s.
327	209	2	↑	3.5E-05	n.s.	n.s.	↑	4.8E-12	2.4E-11	2.1E-17	n.s.
330	195	2	n.s.				↑	2.4E-07	1.4E-10	7.5E-11	n.s.
333	105.9	2, 3	↓	n.s.	9.3E-05	3.6E-05	n.s.				n.s.
343	200.9	2	n.s.				↑	4.9E-08	1.7E-09	9.9E-17	n.s.
431	382.2	3	↑	n.s.	n.s.	3.9E-04	↓	8.2E-05	5.3E-04	4.3E-07	2.5E-04
432	151	2	↑	2.9E-04	n.s.	n.s.	↑	1.1E-12	1.2E-10	1.4E-04	n.s.

RT: Retention time in seconds as per XCMS.

m/z: Mass-per-charge ratio.

[1] Ions in bold were quantitated (only applicable if more than one ion is listed for a specific metabolite).

[2] As per permutation MANOVA, interaction of genotype × diet is only significant at 11.5 weeks of age.

Appendix XIII Proteins identified from previous experiments.

Spot-feature	*Accession number (NCBI)*	*Protein identified*	*Abbreviation*	*Reference gel ID*
17	13435747	Rho GDP dissociation inhibitor (GDI) alpha	ARHGDIA	262
29	42490888	Sulfotransferase family 1D, member 1	SULT1D1	110
77	2121248	Phosphatidylinositol transfer protein alpha	PITPN	322
84	31982861	Carbonic anhydrase 3	CA3	118
135	226958349	Triosephosphate isomerase 1	TPI1	312

REFERENCES

1. Molodecky, N.A., Soon, I.S., Rabi, D.M., Ghali, W.A., Ferris, M., Chernoff, G., Benchimol, E.I., Panaccione, R., Ghosh, S., Barkema, H.W., and Kaplan, G.G. (2012) *Increasing incidence and prevalence of the inflammatory bowel diseases with time, based on systematic review.* Gastroenterology 142(1): p. 46-54.
2. Baumgart, D.C. and Sandborn, W.J. (2007) *Inflammatory bowel disease: clinical aspects and established and evolving therapies.* The Lancet 369(9573): p. 1641-1657.
3. Bassaganya-Riera, J. and Hontecillas, R. (2006) *CLA and n-3 PUFA differentially modulate clinical activity and colonic PPAR-responsive gene expression in a pig model of experimental IBD.* Clinical Nutrition 25(3): p. 454-465.
4. Hassan, A., Ibrahim, A., Mbodji, K., Coeffier, M., Ziegler, F., Bounoure, F., Chardigny, J.M., Skiba, M., Savoye, G., Dechelotte, P., and Marion-Letellier, R. (2010) *An {alpha}-linolenic acid-rich formula reduces oxidative stress and inflammation by regulating NF-{kappa}B in rats with TNBS-induced colitis.* The Journal of Nutrition 140: p. 1714-1721.
5. Barros, K.V., Xavier, R.A.N., Abreu, G.G., Martinez, C.A.R., Ribeiro, M.L., Gambero, A., Carvalho, P.O., Nascimento, C.M.O., and Silveira, V.L.F. (2010) *Soybean and fish oil mixture increases IL-10, protects against DNA damage and decreases colonic inflammation in rats with dextran sulfate sodium (DSS) colitis.* Lipids in Health and Disease 9(68).
6. Knoch, B., Barnett, M.P.G., Zhu, S., Park, Z.A., Nones, K., Dommels, Y.E.M., Knowles, S.O., McNabb, W., and Roy, N.C. (2009) *Genome-wide analysis of dietary eiosapentaenoic acid- and oleic acid-induced modulation of colon inflammation in interleukin-10-deficient mice.* Journal of Nutrigenetics and Nutrigenomics 2: p. 9-28.
7. Camuesco, D., Galvez, J., Nieto, A., Comalada, M., Rodriguez-Cabezas, M.E., Concha, A., Xaus, J., and Zarzuelo, A. (2005) *Dietary olive oil supplemented with fish oil, rich in EPA and DHA (n-3) polyunsaturated fatty acids, attenuates colonic inflammation in rats with DSS-induced colitis.* The Journal of Nutrition 135(4): p. 687-694.
8. Sollid, L.M. and Khosla, C. (2005) *Future therapeutic options for celiac disease.* Nature Clinical Practice Gastroenterology & Hepatology 2(3): p. 140-147.
9. Triggs, C.M., Munday, K., Hu, R., Fraser, A.G., Gearry, R.B., Barclay, M.L., and Ferguson, L.R. (2010) *Dietary factors in chronic inflammation: food tolerances and intolerances of a New Zealand Caucasian Crohn's disease population.* Mutation Research 690(1-2): p. 123-138.
10. Strimbu, K. and Tavel, J.A. (2010) *What are biomarkers?* Current opinion in HIV and AIDS 5(6): p. 463-466.
11. Ministry of Health – Manatū Hauora. *Inflammatory bowel disease*. 2014 21 May 2013 [cited 2014 Feburary]; Available from: http://www.health.govt.nz/your-health/conditions-and-treatments/diseases-and-illnesses/inflammatory-bowel-disease.

12. Matsui, T., Yao, T., Sakurai, T., Yao, K., Hirai, F., Matake, H., Tsuda, S., Wada, Y., Iwashita, A., and Kamachi, S. (2003) *Clinical features and pattern of indeterminate colitis: Crohn's disease with ulcerative colitis-like clinical presentation.* The Journal of Gastroenterology 38(7): p. 647-655.

13. Ekbom, A., Helmick, C., Zack, M., and Adami, H.O. (1990) *Increased risk of large-bowel cancer in Crohn's disease with colonic involvement.* The Lancet 336(8711): p. 357-359.

14. O'Sullivan, M. and O'Morain, C. (2006) *Nutrition in inflammatory bowel disease.* Best Practice & Research in Clinical Gastroenterology 20(3): p. 561-573.

15. Duchmann, R., Kaiser, I., Hermann, E., Mayet, W., Ewe, K., and Meyer zum Buschenfelde, K.H. (1995) *Tolerance exists towards resident intestinal flora but is broken in active inflammatory bowel disease (IBD).* Clinical and Experimental Immunology 102(3): p. 448-455.

16. Halfvarson, J., Bodin, L., Tysk, C., Lindberg, E., and Järnerot, G. (2003) *Inflammatory bowel disease in a Swedish twin cohort: a long-term follow-up of concordance and clinical characteristics.* Gastroenterology 124(7): p. 1767-1773.

17. Orholm, M., Binder, V., Sorensen, T.I.A., Rasmussen, L.P., and Kyvik, K.O. (2000) *Concordance of inflammatory bowel disease among Danish twins: Results of a nationwide study.* Scandinavian Journal of Gastroenterology 35(10): p. 1075-1081.

18. Thompson, N.P., Driscoll, R., Pounder, R.E., and Wakefield, A.J. (1996) *Genetics versus environment in inflammatory bowel disease: results of a British twin study.* British Medical Journal 312(7023): p. 95-96.

19. Laharie, D., Debeugny, S., Peeters, M., Van Gossum, A., Gower-Rousseau, C., Bélache, J., Fiasse, R., Dupas, J.L., Lerebours, E., Piotte, S., Cortot, A., Vermeire, S., Grandbastien, B., and Colombel, J.F. (2001) *Inflammatory bowel disease in spouses and their offspring.* Gastroenterology 120(4): p. 816-819.

20. Kruglyak, L. and Nickerson, D.A. (2001) *Variation is the spice of life.* Nature Genetics 27(3): p. 234-235.

21. Stover, P.J. (2006) *Influence of human genetic variation on nutritional requirements.* The American Journal of Clinical Nutrition 83(2): p. 436S-442S.

22. Lee, G. and Buchman, A.L. (2009) *DNA-driven nutritional therapy of inflammatory bowel disease.* Nutrition 25: p. 885-891.

23. Hugot, J.P., Laurent-Puig, P., Gower-Rousseau, C., Olson, J.M., Lee, J.C., Beaugerie, L., Naom, I., Dupas, J.L., Van Gossum, A., Orholm, M., Bonaiti-Pellie, C., Weissenbach, J., Mathew, C.G., Lennard-Jones, J.E., Cortot, A., Colombel, J.F., and Thomas, G. (1996) *Mapping of a susceptibility locus for Crohn's disease on chromosome 16.* Nature 379(6568): p. 821-823.

24. Hugot, J.P., Chamaillard, M., Zouali, H., Lesage, S., Cezard, J.P., Belaiche, J., Almer, S., Tysk, C., O'Morain, C.A., Gassull, M., Binder, V., Finkel, Y., Cortot, A., Modigliani, R., Laurent-Puig, P., Gower-Rousseau, C., Macry, J., Colombel, J.F., Sahbatou, M., and Thomas, G. (2001) *Association of NOD2 leucine-rich repeat variants with susceptibility to Crohn's disease.* Nature 411(6837): p. 599-603.

25. Jostins, L., Ripke, S., Weersma, R.K., Duerr, R.H., McGovern, D.P., Hui, K.Y., Lee, J.C., Philip Schumm, L., Sharma, Y., Anderson, C.A., Essers, J., Mitrovic, M., Ning, K., Cleynen, I., Theatre, E., Spain, S.L., Raychaudhuri, S., Goyette, P., Wei, Z., Abraham, C., Achkar, J.-P., Ahmad, T., Amininejad, L., Ananthakrishnan, A.N., Andersen, V., Andrews, J.M., Baidoo, L., Balschun, T., Bampton, P.A., Bitton, A., Boucher, G., Brand, S., Buning, C., Cohain, A., Cichon, S., D'Amato, M., De Jong, D., Devaney, K.L., Dubinsky, M., Edwards, C., Ellinghaus, D., Ferguson, L.R., Franchimont, D., Fransen, K., Gearry, R., Georges, M., Gieger, C., Glas, J., Haritunians, T., Hart, A., Hawkey, C., Hedl, M., Hu, X., Karlsen, T.H., Kupcinskas, L., Kugathasan, S., Latiano, A., Laukens, D., Lawrance, I.C., Lees, C.W., Louis, E., Mahy, G., Mansfield, J., Morgan, A.R., Mowat, C., Newman, W., Palmieri, O., Ponsioen, C.Y., Potocnik, U., Prescott, N.J., Regueiro, M., Rotter, J.I., Russell, R.K., Sanderson, J.D., Sans, M., Satsangi, J., Schreiber, S., Simms, L.A., Sventoraityte, J., Targan, S.R., Taylor, K.D., Tremelling, M., Verspaget, H.W., De Vos, M., Wijmenga, C., Wilson, D.C., Winkelmann, J., Xavier, R.J., Zeissig, S., Zhang, B., Zhang, C.K., Zhao, H., Silverberg, M.S., Annese, V., Hakonarson, H., Brant, S.R., Radford-Smith, G., Mathew, C.G., Rioux, J.D., Schadt, E.E., Daly, M.J., Franke, A., Parkes, M., Vermeire, S., Barrett, J.C. and Cho, J.H. (2012) *Host-microbe interactions have shaped the genetic architecture of inflammatory bowel disease.* Nature 491(7422): p. 119-124.

26. Lees, C.W., Barrett, J.C., Parkes, M., and Satsangi, J. (2011) *New IBD genetics: common pathways with other diseases.* Gut 60(12): p. 1739-1753.

27. Anderson, R.C., Dalziel, J.E., Gopal, P.K., Bassett, S., Ellis, A., and Roy, N.C., *The role of intestinal barrier function in early life in the development of colitis*, in *Colitis*, M. Fukata, Editor. 2012.

28. Hollander, D., Vadheim, C.M., Brettholz, E., Petersen, G.M., Delahunty, T., and Rotter, J.I. (1986) *Increased intestinal permeability in patients with Crohn's Disease and their relatives: A possible etiologic factor.* Annals of Internal Medicine 105(6): p. 883-885.

29. van der Flier, L.G. and Clevers, H. (2009) *Stem cells, self-renewal, and differentiation in the intestinal epithelium.* Annual Review of Physiology 71(1): p. 241-260.

30. Johansson, M.E., Phillipson, M., Petersson, J., Velcich, A., Holm, L., and Hansson, G.C. (2008) *The inner of the two Muc2 mucin-dependent mucus layers in colon is devoid of bacteria.* Proceedings of the National Academy of Sciences 105(39): p. 15064-15069.

31. Van der Sluis, M., De Koning, B.A.E., De Bruijn, A., Velcich, A., Meijerink, J.P.P., Van Goudoever, J.B., Buller, H.A., Dekker, J., Van Seuningen, I., Renes, I.B., and Einerhand, A.W.C. (2006) *Muc2-deficient mice spontaneously develop colitis, indicating that Muc2 is critical for colonic protection.* Gastroenterology 131(1): p. 117-129.

32. Ayabe, T., Satchell, D.P., Wilson, C.L., Parks, W.C., Selsted, M.E., and Ouellette, A.J. (2000) *Secretion of microbicidal α-defensins by intestinal Paneth cells in response to bacteria.* Nature Immunology 1(2): p. 113.

33. Meyer-Hoffert, U., Hornef, M.W., Henriques-Normark, B., Axelsson, L.-G., Midtvedt, T., Pütsep, K., and Andersson, M. (2008) *Secreted enteric antimicrobial activity localises to the mucus surface layer.* Gut 57(6): p. 764-771.

34. Vaishnava, S., Behrendt, C.L., Ismail, A.S., Eckmann, L., and Hooper, L.V. (2008) *Paneth cells directly sense gut commensals and maintain homeostasis at the intestinal host-microbial interface.* Proceedings of the National Academy of Sciences 105(52): p. 20858-20863.

35. Loonen, L.M., Stolte, E.H., Jaklofsky, M.T., Meijerink, M., Dekker, J., van Baarlen, P., and Wells, J.M. (2014) *REG3gamma-deficient mice have altered mucus distribution and increased mucosal inflammatory responses to the microbiota and enteric pathogens in the ileum.* Mucosal Immunology 7(4): p. 939-947.

36. Suzuki, K., Meek, B., Doi, Y., Muramatsu, M., Chiba, T., Honjo, T., and Fagarasan, S. (2004) *Aberrant expansion of segmented filamentous bacteria in IgA-deficient gut.* Proceedings of the National Academy of Sciences 101(7): p. 1981-1986.

37. Rojas, R. and Apodaca, G. (2002) *Immunoglobulin transport across polarized epithelial cells.* Nature Reviews: Molecular Cell Biology 3(12): p. 944-956.

38. Mowat, A.M. and Agace, W.W. (2014) *Regional specialization within the intestinal immune system.* Nature Reviews. Immunology 14(10): p. 667-685.

39. Macpherson, A.J., Gatto, D., Sainsbury, E., Harriman, G.R., Hengartner, H., and Zinkernagel, R.M. (2000) *A primitive T cell-independent mechanism of intestinal mucosal IgA responses to commensal bacteria.* Science 288(5474): p. 2222-2226.

40. Balda, M.S., Fallon, M.B., Van Itallie, C.M., and Anderson, J.M. (1992) *Structure, regulation, and pathophysiology of tight junctions in the gastrointestinal tract.* The Yale Journal of Biology and Medicine 65(6): p. 725-735.

41. Arnott, I.D., Kingstone, K., and Ghosh, S. (2000) *Abnormal intestinal permeability predicts relapse in inactive Crohn disease.* Scandinavian Journal of Gastroenterology 35(11): p. 1163-1169.

42. Söderholm, J.D., Olaison, G., Peterson, K.H., Franzén, L.E., Lindmark, T., Wirén, M., Tagesson, C., and Sjödahl, R. (2002) *Augmented increase in tight junction permeability by luminal stimuli in the non-inflamed ileum of Crohn's disease.* Gut 50(3): p. 307-313.

43. Gassler, N., Rohr, C., Schneider, A., Kartenbeck, J., Bach, A., Obermüller, N., Otto, H.F., and Autschbach, F. (2001) *Inflammatory bowel disease is associated with changes of enterocytic junctions.* American Journal of Physiology - Gastrointestinal and Liver Physiology 281(1): p. G216-G228.

44. Kucharzik, T., Walsh, S.V., Chen, J., Parkos, C.A., and Nusrat, A. (2001) *Neutrophil transmigration in inflammatory bowel disease is associated with differential expression of epithelial intercellular junction proteins.* The American Journal of Pathology 159(6): p. 2001-2009.

45. Zeissig, S., Bürgel, N., Günzel, D., Richter, J., Mankertz, J., Wahnschaffe, U., Kroesen, A.J., Zeitz, M., Fromm, M., and Schulzke, J.D. (2007) *Changes in*

expression and distribution of claudin 2, 5 and 8 lead to discontinuous tight junctions and barrier dysfunction in active Crohn's disease. Gut 56(1): p. 61-72.

46. Farhadi, A., Banan, A., Fields, J., and Keshavarzian, A. (2003) *Intestinal barrier: an interface between health and disease.* Journal of Gastroenterology and Hepatology 18(5): p. 479-497.

47. Steed, E., Balda, M.S., and Matter, K. (2010) *Dynamics and functions of tight junctions.* Trends in Cell Biology 20(3): p. 142-149.

48. Sydora, B.C., MacFarlane, S.M., Walker, J.W., Dmytrash, A.L., Churchill, T.A., Doyle, J., and Fedorak, R.N. (2007) *Epithelial barrier disruption allows nondisease-causing bacteria to initiate and sustain IBD in the IL-10 gene-deficient mouse.* Inflammatory Bowel Disease 13(8): p. 947-954.

49. Ulluwishewa, D., Anderson, R.C., McNabb, W.C., Moughan, P.J., Wells, J.M., and Roy, N.C. (2011) *Regulation of tight junction permeability by intestinal bacteria and dietary components.* The Journal of Nutrition 141(5): p. 769-776.

50. Fuss, I.J., Heller, F., Boirivant, M., Leon, F., Yoshida, M., Fichtner-Feigl, S., Yang, Z., Exley, M., Kitani, A., Blumberg, R.S., Mannon, P., and Strober, W. (2004) *Nonclassical CD1d-restricted NK T cells that produce IL-13 characterize an atypical Th2 response in ulcerative colitis.* Journal of Clinical Investigation 113(10): p. 1490-1497.

51. Fuss, I.J., Neurath, M., Boirivant, M., Klein, J.S., de la Motte, C., Strong, S.A., Fiocchi, C., and Strober, W. (1996) *Disparate CD4+ lamina propria (LP) lymphokine secretion profiles in inflammatory bowel disease. Crohn's disease LP cells manifest increased secretion of IFN-gamma, whereas ulcerative colitis LP cells manifest increased secretion of IL-5.* The Journal of Immunology 157(3): p. 1261-1270.

52. Monteleone, G., Biancone, L., Marasco, R., Morrone, G., Marasco, O., Luzza, F., and Pallone, F. (1997) *Interleukin 12 is expressed and actively released by Crohn's disease intestinal lamina propria mononuclear cells.* Gastroenterology 112(4): p. 1169-1178.

53. Parronchi, P., Romagnani, P., Annunziato, F., Sampognaro, S., Becchio, A., Giannarini, L., Maggi, E., Pupilli, C., Tonelli, F., and Romagnani, S. (1997) *Type 1 T-helper cell predominance and interleukin-12 expression in the gut of patients with Crohn's disease.* The American Journal of Pathology 150(3): p. 823-832.

54. Yen, D., Cheung, J., Scheerens, H., Poulet, F., McClanahan, T., Mckenzie, B., Kleinschek, M.A., Owyang, A., Mattson, J., and Blumenschein, W. (2006) *IL-23 is essential for T cell–mediated colitis and promotes inflammation via IL-17 and IL-6.* Journal of Clinical Investigation 116(5): p. 1310-1316.

55. Kobayashi, T., Okamoto, S., Hisamatsu, T., Kamada, N., Chinen, H., Saito, R., Kitazume, M.T., Nakazawa, A., Sugita, A., Koganei, K., Isobe, K., and Hibi, T. (2008) *IL23 differentially regulates the Th1/Th17 balance in ulcerative colitis and Crohn's disease.* Gut 57(12): p. 1682-1689.

56. Neefjes, J., Jongsma, M.L., Paul, P., and Bakke, O. (2011) *Towards a systems understanding of MHC class I and MHC class II antigen presentation.* Nature Reviews Immunology 11(12): p. 823-836.

57. Sakuraba, A., Sato, T., Kamada, N., Kitazume, M., Sugita, A., and Hibi, T. (2009) *Th1/Th17 immune response is induced by mesenteric lymph node dendritic cells in Crohn's disease.* Gastroenterology 137(5): p. 1736-1745.

58. Luckey, T. (1972) *Introduction to intestinal microecology.* The American Journal of Clinical Nutrition 25(12): p. 1292-1294.

59. Whitman, W.B., Coleman, D.C., and Wiebe, W.J. (1998) *Prokaryotes: The unseen majority.* Proceedings of the National Academy of Sciences 95(12): p. 6578-6583.

60. Qin, J., Li, R., Raes, J., Arumugam, M., Burgdorf, K.S., Manichanh, C., Nielsen, T., Pons, N., Levenez, F., Yamada, T., Mende, D.R., Li, J., Xu, J., Li, S., Li, D., Cao, J., Wang, B., Liang, H., Zheng, H., Xie, Y., Tap, J., Lepage, P., Bertalan, M., Batto, J.M., Hansen, T., Le Paslier, D., Linneberg, A., Nielsen, H.B., Pelletier, E., Renault, P., Sicheritz-Ponten, T., Turner, K., Zhu, H., Yu, C., Li, S., Jian, M., Zhou, Y., Li, Y., Zhang, X., Li, S., Qin, N., Yang, H., Wang, J., Brunak, S., Dore, J., Guarner, F., Kristiansen, K., Pedersen, O., Parkhill, J., Weissenbach, J., Meta, H.I.T.C., Bork, P., Ehrlich, S.D., and Wang, J. (2010) *A human gut microbial gene catalogue established by metagenomic sequencing.* Nature 464(7285): p. 59-65.

61. Bäckhed, F., Ley, R.E., Sonnenburg, J.L., Peterson, D.A., and Gordon, J.I. (2005) *Host-bacterial mutualism in the human intestine.* Science 307(5717): p. 1915-1920.

62. Wu, G.D., Bushmanc, F.D., and Lewis, J.D. (2013) *Diet, the human gut microbiota, and IBD.* Anaerobe 24(0): p. 117-120.

63. Berry, D. and Reinisch, W. (2013) *Intestinal microbiota: a source of novel biomarkers in inflammatory bowel diseases?* Best Practice & Research Clinical Gastroenterology 27(1): p. 47-58.

64. Frank, D.N., Robertson, C.E., Hamm, C.M., Kpadeh, Z., Zhang, T., Chen, H., Zhu, W., Sartor, R.B., Boedeker, E.C., Harpaz, N., Pace, N.R., and Li, E. (2011) *Disease phenotype and genotype are associated with shifts in intestinal-associated microbiota in inflammatory bowel diseases.* Inflammatory Bowel Disease 17(1): p. 179-184.

65. Jansson, J., Willing, B., Lucio, M., Fekete, A., Dicksved, J., Halfvarson, J., Tysk, C., and Schmitt-Kopplin, P. (2009) *Metabolomics reveals metabolic biomarkers of Crohn's disease.* PLoS ONE 4(7): p. e6386.

66. Rigottier-Gois, L. (2013) *Dysbiosis in inflammatory bowel diseases: the oxygen hypothesis.* The Journal of the International Society for Microbial Ecology 7(7): p. 1256-1261.

67. Valatas, V., Vakas, M., and Kolios, G. (2013) *The value of experimental models of colitis in predicting efficacy of biological therapies for inflammatory bowel diseases.* American Journal of Physiology - Gastrointestinal and Liver Physiology 305(11): p. G763-G785.

68. Neurath, M.F. (2014) *Cytokines in inflammatory bowel disease.* Nature Reviews Immunology 14(5): p. 329-342.

69. Krishnan, A. and Korzenik, J.R. (2002) *Inflammatory bowel disease and environmental influences.* Gastroenterology Clinics of North America 31(1): p. 21-39.

70. Loftus, E.V. (2004) *Clinical epidemiology of inflammatory bowel disease: Incidence, prevalence, and environmental influences.* Gastroenterology 126(6): p. 1504-1517.

71. Ungaro, R., Bernstein, C.N., Gearry, R., Hviid, A., Kolho, K.-L., Kronman, M.P., Shaw, S., Van Kruiningen, H., Colombel, J.-F., and Atreja, A. (2014) *Antibiotics associated with increased risk of new-onset Crohn's disease but not ulcerative colitis: a meta-analysis.* The American Journal of Gastroenterology 109(11): p. 1728-1738.

72. Shaw, S.Y., Blanchard, J.F., and Bernstein, C.N. (2011) *Association between the use of antibiotics and new diagnoses of Crohn's disease and ulcerative colitis.* The American Journal of Gastroenterology 106(12): p. 2133-2142.

73. Jakobsson, H.E., Jernberg, C., Andersson, A.F., Sjölund-Karlsson, M., Jansson, J.K., and Engstrand, L. (2010) *Short-term antibiotic treatment has differing long-term impacts on the human throat and gut microbiome.* PLoS ONE 5(3): p. e9836.

74. Shaw, S.Y., Blanchard, J.F., and Bernstein, C.N. (2010) *Association between the use of antibiotics in the first year of life and pediatric inflammatory bowel disease.* The American Journal of Gastroenterology 105(12): p. 2687-2692.

75. Vanuytsel, T., van Wanrooy, S., Vanheel, H., Vanormelingen, C., Verschueren, S., Houben, E., Salim Rasoel, S., Tomicronth, J., Holvoet, L., Farre, R., Van Oudenhove, L., Boeckxstaens, G., Verbeke, K., and Tack, J. (2014) *Psychological stress and corticotropin-releasing hormone increase intestinal permeability in humans by a mast cell-dependent mechanism.* Gut 63(8): p. 1293-1299.

76. Cordain, L., Eaton, S.B., Sebastian, A., Mann, N., Lindeberg, S., Watkins, B.A., O'Keefe, J.H., and Brand-Miller, J. (2005) *Origins and evolution of the Western diet: health implications for the 21st century.* The American Journal of Clinical Nutrition 81(2): p. 341-354.

77. Simopoulos, A.P. (2008) *The importance of the omega-6/omega-3 fatty acid ratio in cardiovascular disease and other chronic diseases.* Experimental Biology and Medicine 233(6): p. 674-688.

78. Eaton, S.B., Eaton III, S.B., Sinclair, A.J., Cordain, L., and Mann, N.J. (1998) *Dietary intake of long-chain polyunsaturated fatty acids during the Paleolithic.* World review of nutrition and dietetics 83: p. 12-23.

79. James, M.J., Gibson, R.A., and Cleland, L.G. (2000) *Dietary polyunsaturated fatty acids and inflammatory mediator production.* The American Journal of Clinical Nutrition 71(1): p. 343s-348s.

80. Goyens, P.L., Spilker, M.E., Zock, P.L., Katan, M.B., and Mensink, R.P. (2006) *Conversion of alpha-linolenic acid in humans is influenced by the absolute amounts of alpha-linolenic acid and linoleic acid in the diet and not by their ratio.* The American Journal of Clinical Nutrition 84(1): p. 44-53.

81. Kohlmeier, L. (1995) *Future of dietary exposure assessment.* The American Journal of Clinical Nutrition 61(3): p. 702S-709S.

82. Hegazi, R.A.F., Mady, H.H., Melhem, M.F., Sepulveda, A.R., Mohi, M., and Kandil, H.M. (2003) *Celecoxib and rofecoxib potentiate chronic colitis and premalignant changes in interleukin 10 knockout mice.* Inflammatory Bowel Disease 9(4): p. 230-236.

83. Koboziev, I., Karlsson, F., Zhang, S., and Grisham, M.B. (2011) *Pharmacological intervention studies using mouse models of the inflammatory bowel diseases: translating preclinical data into new drug therapies.* Inflammatory Bowel Disease 17(5): p. 1229-1245.

84. Seok, J., Warren, H.S., Cuenca, A.G., Mindrinos, M.N., Baker, H.V., Xu, W., Richards, D.R., McDonald-Smith, G.P., Gao, H., Hennessy, L., Finnerty, C.C., López, C.M., Honari, S., Moore, E.E., Minei, J.P., Cuschieri, J., Bankey, P.E., Johnson, J.L., Sperry, J., Nathens, A.B., Billiar, T.R., West, M.A., Jeschke, M.G., Klein, M.B., Gamelli, R.L., Gibran, N.S., Brownstein, B.H., Miller-Graziano, C., Calvano, S.E., Mason, P.H., Cobb, J.P., Rahme, L.G., Lowry, S.F., Maier, R.V., Moldawer, L.L., Herndon, D.N., Davis, R.W., Xiao, W., Tompkins, R.G., Inflammation, t., and Host Response to Injury, L.S.C.R.P. (2013) *Genomic responses in mouse models poorly mimic human inflammatory diseases.* Proceedings of the National Academy of Sciences 110(9): p. 3507-3512.

85. Saraiva, M. and O'Garra, A. (2010) *The regulation of IL-10 production by immune cells.* Nature Reviews: Immunology 10(3): p. 170-181.

86. Paul, G., Khare, V., and Gasche, C. (2012) *Inflamed gut mucosa: downstream of interleukin-10.* European Journal of Clinical Investigation 42(1): p. 95-109.

87. Alex, P., Zachos, N.C., Nguyen, T., Gonzales, L., Chen, T.E., Conklin, L.S., Centola, M., and Li, X. (2009) *Distinct cytokine patterns identified from multiplex profiles of murine DSS and TNBS-induced colitis.* Inflammatory Bowel Disease 15(3): p. 341-352.

88. Dothel, G., Vasina, V., Barbara, G., and De Ponti, F. (2013) *Animal models of chemically induced intestinal inflammation: Predictivity and ethical issues.* Pharmacology & Therapeutics 139(1): p. 71-86.

89. Araki, Y., Mukaisyo, K., Sugihara, H., Fujiyama, Y., and Hattori, T. (2010) *Increased apoptosis and decreased proliferation of colonic epithelium in dextran sulfate sodium-induced colitis in mice.* Oncology Reports 24(4): p. 869.

90. Kim, C.J., Kovacs-Nolan, J.A., Yang, C., Archbold, T., Fan, M.Z., and Mine, Y. (2010) *L-Tryptophan exhibits therapeutic function in a porcine model of dextran sodium sulfate (DSS)-induced colitis.* The Journal of Nutritional Biochemistry 21(6): p. 468-475.

91. Powrie, F., Leach, M.W., Mauze, S., Menon, S., Caddle, L.B., and Coffman, R.L. (1994) *Inhibition of Th1 responses prevents inflammatory bowel disease in SCID mice reconstituted with CD45RB(HI) CD4(+) T-cells.* Immunity 1(7): p. 553-562.

92. Ostanin, D.V., Bao, J., Koboziev, I., Gray, L., Robinson-Jackson, S.A., Kosloski-Davidson, M., Price, V.H., and Grisham, M.B. (2009) *T cell transfer model of chronic colitis: concepts, considerations, and tricks of the trade.* American Journal of Physiology - Gastrointestinal and Liver Physiology 296(2): p. G135-146.

93. Banner, K.H., Cattaneo, C., Net, J.L.L., Popovic, A., Collins, D., and Gale, J.D. (2004) *Macroscopic, microscopic and biochemical characterisation of spontaneous colitis in a transgenic mouse, deficient in the multiple drug resistance 1a gene.* British Journal of Pharmacology 143(5): p. 590-598.

94. Panwala, C.M., Jones, J.C., and Viney, J.L. (1998) *A novel model of inflammatory bowel disease: mice deficient for the multiple drug resistance gene, mdr1a, spontaneously develop colitis.* The Journal of Immunology 161(10): p. 5733-5744.

95. Kühn, R., Lohler, J., Rennick, D., Rajewsky, K., and Muller, W. (1993) *Interleukin-10-deficient mice develop chronic enterocolitis.* Cell 75(2): p. 263-274.

96. Kim, Y.S., Lee, M.H., Ju, A.S., and Rhee, K.-J. (2011) *Th17 responses are not induced in Dextran Sodium Sulfate model of acute colitis.* Immune Network 11(6): p. 416-419.

97. Mariman, R., Kremer, B., van Erk, M., Lagerweij, T., Koning, F., and Nagelkerken, L. (2012) *Gene expression profiling identifies mechanisms of protection to recurrent trinitrobenzene sulfonic acid colitis mediated by probiotics.* Inflammatory Bowel Disease 18(8): p. 1424-1433.

98. Bosco, N., Brahmbhatt, V., Oliveira, M., Martin, F.P., Lichti, P., Raymond, F., Mansourian, R., Metairon, S., Pace-Asciak, C., Bastic Schmid, V., Rezzi, S., Haller, D., and Benyacoub, J. (2013) *Effects of increase in fish oil intake on intestinal eicosanoids and inflammation in a mouse model of colitis.* Lipids in Health and Disease 12(1): p. 81.

99. Gomes-Santos, A.C., Moreira, T.G., Castro-Junior, A.B., Horta, B.C., Lemos, L., Cruz, D.N., Guimarães, M.A.F., Cara, D.C., McCafferty, D.-M., and Faria, A.M.C. (2012) *New insights into the immunological changes in IL-10-deficient mice during the course of spontaneous inflammation in the gut mucosa.* Clinical and Developmental Immunology 2012: p. 13.

100. Hans, W., Schölmerich, J., Gross, V., and Falk, W. (2000) *The role of the resident intestinal flora in acute and chronic dextran sulfate sodium-induced colitis in mice.* European Journal of Gastroenterology & Hepatology 12(3): p. 267-273.

101. Bylund-Fellenius, A.C., Landström, E., Axelsson, L.G., and Midtvedt, T. (1994) *Experimental colitis induced by dextran sulphate in normal and germfree mice.* Microbial Ecology in Health and Disease 7(4): p. 207-215.

102. Wirtz, S. and Neurath, M.F. (2007) *Mouse models of inflammatory bowel disease.* Advanced Drug Delivery Reviews 59(11): p. 1073-1083.

103. Elson, C.O., Cong, Y., McCracken, V.J., Dimmitt, R.A., Lorenz, R.G., and Weaver, C.T. (2005) *Experimental models of inflammatory bowel disease reveal innate, adaptive, and regulatory mechanisms of host dialogue with the microbiota.* Immunological Reviews 206(1): p. 260-276.

104. Gabryšová, L., Howes, A., Saraiva, M., and O'Garra, A., *The regulation of IL-10 expression*, in *Interleukin-10 in Health and Disease*, S. Fillatreau and A. O'Garra, Editors. 2014, Springer: Heidelberg, Berlin. p. 157-190.

105. Li, X., Mai, J., Virtue, A., Yin, Y., Gong, R., Sha, X., Gutchigian, S., Frisch, A., Hodge, I., Jiang, X., Wang, H., and Yang, X.-F. (2012) *IL-35 is a novel responsive anti-inflammatory cytokine - a new system of categorizing anti-inflammatory cytokines.* PLoS ONE 7(3): p. e33628.

106. Barrat, F.J., Cua, D.J., Boonstra, A., Richards, D.F., Crain, C., Savelkoul, H.F., de Waal-Malefyt, R., Coffman, R.L., Hawrylowicz, C.M., and O'Garra, A. (2002)

In vitro generation of interleukin 10–producing regulatory CD4+ T cells is induced by immunosuppressive drugs and inhibited by T helper type 1 (Th1)–and Th2-inducing cytokines. The Journal of Experimental Medicine 195(5): p. 603-616.

107. Skeen, M.J., Miller, M.A., Shinnick, T.M., and Ziegler, H.K. (1996) *Regulation of murine macrophage IL-12 production. Activation of macrophages in vivo, restimulation in vitro, and modulation by other cytokines.* Journal of Immunology 156(3): p. 1196-1206.

108. Podolsky, D.K. (2002) *Inflammatory bowel disease.* The New England Journal of Medicine 347(6): p. 417-429.

109. Berg, D.J., Davidson, N., Kuhn, R., Muller, W., Menon, S., Holland, G., Thompson-Snipes, L., Leach, M.W., and Rennick, D. (1996) *Enterocolitis and colon cancer in interleukin-10-deficient mice are associated with aberrant cytokine production and CD4(+) TH1-like responses.* Journal of Clinical Investigation 98(4): p. 1010-1020.

110. Sellon, R.K., Tonkonogy, S., Schultz, M., Dieleman, L.A., Grenther, W., Balish, E., Rennick, D.M., and Sartor, R.B. (1998) *Resident enteric bacteria are necessary for development of spontaneous colitis and immune system activation in interleukin-10-deficient mice.* Infection and Immunity 66(11): p. 5224-5231.

111. Taurog, J.D., Richardson, J.A., Croft, J.T., Simmons, W.A., Zhou, M., Fernández-Sueiro, J.L., Balish, E., and Hammer, R.E. (1994) *The germfree state prevents development of gut and joint inflammatory disease in HLA-B27 transgenic rats.* The Journal of Experimental Medicine 180(6): p. 2359-2364.

112. Dianda, L., Hanby, A.M., Wright, N.A., Sebesteny, A., Hayday, A.C., and Owen, M.J. (1997) *T cell receptor-alpha beta-deficient mice fail to develop colitis in the absence of a microbial environment.* The American Journal of Pathology 150(1): p. 91-97.

113. Engle, S.J., Ormsby, I., Pawlowski, S., Boivin, G.P., Croft, J., Balish, E., and Doetschman, T. (2002) *Elimination of colon cancer in germ-free transforming growth factor beta 1-deficient mice.* Cancer Research 62(22): p. 6362-6366.

114. Onderdonk, A.B. and Bartlett, J.G. (1979) *Bacteriological studies of experimental ulcerative colitis.* The American Journal of Clinical Nutrition 32(1): p. 258-265.

115. Balish, E. and Warner, T. (2002) *Enterococcus faecalis induces inflammator bowel disease in Interleukin-10 knockout mice.* The American Journal of Pathology 160: p. 2253-2257.

116. Barnett, M.P., McNabb, W.C., Cookson, A.L., Zhu, S., Davy, M., Knoch, B., Nones, K., Hodgkinson, A.J., and Roy, N.C. (2010) *Changes in colon gene expression associated with increased colon inflammation in interleukin-10 gene-deficient mice inoculated with Enterococcus species.* BMC Immunology 11: p. 39.

117. Kang, J.X. (2012) *Nutrigenomics and systems biology.* Journal of Nutrigenetics and Nutrigenomics 5(6): p. I-II.

118. Zhang, W., Li, F., and Nie, L. (2010) *Integrating multiple 'omics' analysis for microbial biology: application and methodologies.* Microbiology 156(Pt 2): p. 287-301.

119. Ideker, T., Thorsson, V., Ranish, J.A., Christmas, R., Buhler, J., Eng, J.K., Bumgarner, R., Goodlett, D.R., Aebersold, R., and Hood, L. (2001) *Integrated genomic and proteomic analyses of a systematically perturbed metabolic network.* Science 292(5518): p. 929-934.

120. Rezzi, S., Ramadan, Z., Fay, L.B., and Kochhar, S. (2007) *Nutritional metabonomics: applications and perspectives.* Journal of Proteome Research 6(2): p. 513-525.

121. Nicholson, J.K. and Wilson, I.D. (2003) *Opinion: understanding 'global' systems biology: metabonomics and the continuum of metabolism.* Nature Reviews Drug Discovery 2(8): p. 668-676.

122. Benson, A.K., Kelly, S.A., Legge, R., Ma, F., Low, S.J., Kim, J., Zhang, M., Oh, P.L., Nehrenberg, D., Hua, K., Kachman, S.D., Moriyama, E.N., Walter, J., Peterson, D.A., and Pomp, D. (2010) *Individuality in gut microbiota composition is a complex polygenic trait shaped by multiple environmental and host genetic factors.* Proceedings of the National Academy of Sciences 107(44): p. 18933-18938.

123. Wu, G.D., Chen, J., Hoffmann, C., Bittinger, K., Chen, Y.-Y., Keilbaugh, S.A., Bewtra, M., Knights, D., Walters, W.A., and Knight, R. (2011) *Linking long-term dietary patterns with gut microbial enterotypes.* Science 334(6052): p. 105-108.

124. Cani, P.D., Amar, J., Iglesias, M.A., Poggi, M., Knauf, C., Bastelica, D., Neyrinck, A.M., Fava, F., Tuohy, K.M., Chabo, C., Waget, A., Delmée, E., Cousin, B., Sulpice, T., Chamontin, B., Ferrières, J., Tanti, J.-F., Gibson, G.R., Casteilla, L., Delzenne, N.M., Alessi, M.C., and Burcelin, R. (2007) *Metabolic endotoxemia initiates obesity and insulin resistance.* Diabetes 56(7): p. 1761-1772.

125. Walker, A., Sanderson, J., Churcher, C., Parkes, G., Hudspith, B., Rayment, N., Brostoff, J., Parkhill, J., Dougan, G., and Petrovska, L. (2011) *High-throughput clone library analysis of the mucosa-associated microbiota reveals dysbiosis and differences between inflamed and non-inflamed regions of the intestine in inflammatory bowel disease.* BMC Microbiology 11(1): p. 7.

126. dos Santos, M.V., Müller, M., and de Vos, W.M. (2010) *Systems biology of the gut: the interplay of food, microbiota and host at the mucosal interface.* Current Opinion in Biotechnology 21(4): p. 539-550.

127. Kaput, J. and Rodriguez, R.L. (2004) *Nutritional genomics: the next frontier in the postgenomic era.* Physiological Genomics 16(2): p. 166-177.

128. van Ommen, B. (2004) *Nutrigenomics: exploiting systems biology in the nutrition and health arenas.* Nutrition 20(1): p. 4-8.

129. Zhang, J.A., Wang, C.R., Li, L.X., Man, Q.Q., Song, P.K., Meng, L.P., Du, Z.Y., and Froyland, L. (2010) *Inclusion of Atlantic salmon in the Chinese diet reduces cardiovascular disease risk markers in dyslipidemic adult men.* Nutrition Research 30(7): p. 447-454.

130. Ideker, T., Galitski, T., and Hood, L. (2001) *A new approach to decoding life: Systems biology.* Annual Review of Genomics and Human Genetics 2: p. 343-372.

131. Tyers, M. and Mann, M. (2003) *From genomics to proteomics.* Nature 422(6928): p. 193-197.

132. Dettmer, K., Aronov, P.A., and Hammock, B.D. (2007) *Mass spectrometry-based metabolomics.* Mass Spectrometry Reviews 26(1): p. 51-78.

133. Roux, A., Lison, D., Junot, C., and Heilier, J.-F. (2011) *Applications of liquid chromatography coupled to mass spectrometry-based metabolomics in clinical chemistry and toxicology: A review.* Clinical Biochemistry 44(1): p. 119-135.

134. Sauer, U., Heinemann, M., and Zamboni, N. (2007) *Genetics. Getting closer to the whole picture.* Science 316(5824): p. 550-551.

135. Afman, L. and Mueller, M. (2006) *Nutrigenomics: From molecular nutrition to prevention of disease.* Journal of the American Dietetic Association 106: p. 569-576.

136. Müller, M. and Kersten, S. (2003) *Nutrigenomics: Goals and strategies.* Genetics 4: p. 315-322.

137. Subbiah, M.T.R. (2008) *Understanding the nutrigenomic definitions and concepts at the food-genome junction.* Omics - a Journal of Integrative Biology 12(4): p. 229-235.

138. Ferguson, L.R. (2010) *Nutrigenomics and inflammatory bowel diseases.* Expert Review of Clinical Immunology 6(4): p. 573-583.

139. Lloyd, A.J., Favé, G., Beckmann, M., Lin, W., Tailliart, K., Xie, L., Mathers, J.C., and Draper, J. (2011) *Use of mass spectrometry fingerprinting to identify urinary metabolites after consumption of specific foods.* The American Journal of Clinical Nutrition 94(4): p. 981-991.

140. Tulipani, S., Llorach, R., Jáuregui, O., López-Uriarte, P., Garcia-Aloy, M., Bullo, M., Salas-Salvadó, J., and Andrés-Lacueva, C. (2011) *Metabolomics unveils urinary changes in subjects with metabolic syndrome following 12-week nut consumption.* Journal of Proteome Research 10(11): p. 5047-5058.

141. Lin, H.M., Edmunds, S.J., Zhu, S., Helsby, N.A., Ferguson, L.R., and Rowan, D.D. (2011) *Metabolomic analysis reveals differences in urinary excretion of kiwifruit-derived metabolites in a mouse model of inflammatory bowel disease.* Molecular Nutrition & Food Research 55(12): p. 1900-1904.

142. Iskandar, H.N. and Ciorba, M.A. (2012) *Biomarkers in inflammatory bowel disease: current practices and recent advances.* Translational Research 159(4): p. 313-325.

143. Faubion, W.A., Jr., Fletcher, J.G., O'Byrne, S., Feagan, B.G., de Villiers, W.J., Salzberg, B., Plevy, S., Proctor, D.D., Valentine, J.F., Higgins, P.D., Harris, J.M., Diehl, L., Wright, L., Tew, G.W., Luca, D., Basu, K., and Keir, M.E. (2013) *EMerging BiomARKers in Inflammatory Bowel Disease (EMBARK) study identifies fecal calprotectin, serum MMP9, and serum IL-22 as a novel combination of biomarkers for Crohn's disease activity: role of cross-sectional imaging.* The American Journal of Gastroenterology 108(12): p. 1891-1900.

144. Røseth, A., Schmidt, P., and Fagerhol, M. (1999) *Correlation between faecal excretion of indium-111-labelled granulocytes and calprotectin, a granulocyte marker protein, in patients with inflammatory bowel disease.* Scandinavian Journal of Gastroenterology 34(1): p. 50-54.

145. Van Rheenen, P.F., Van de Vijver, E., and Fidler, V. (2010) *Faecal calprotectin for screening of patients with suspected inflammatory bowel disease: diagnostic meta-analysis.* British Medical Journal 341.

146. Pot, G.K., Geelen, A., Majsak-Newman, G., Harvey, L.J., Nagengast, F.M., Witteman, B.J.M., van de Meeberg, P.C., Hart, A.R., Schaafsma, G., Lund, E.K., Rijkers, G.I., and Kampman, E. (2010) *Increased consumption of fatty and lean fish reduces serum c-reactive protein concentrations but not inflammation markers in feces and in colonic biopsies.* The Journal of Nutrition 140(2): p. 371-376.

147. de Mello, V.D.F., Kolehmanien, M., Schwab, U., Pulkkinen, L., and Uusitupa, M. (2012) *Gene expression of peripheral blood mononuclear cells as a tool in dietary intervention studies: What do we know so far?* Molecular Nutrition & Food Research 56: p. 1160-1172.

148. Bonne-Année, S., Kerepesi, L.A., Hess, J.A., O'Connell, A.E., Lok, J.B., Nolan, T.J., and Abraham, D. (2013) *Human and mouse macrophages collaborate with neutrophils to kill larval Strongyloides stercoralis.* Infection and Immunity 81(9): p. 3346-3355.

149. Burczynski, M.E., Peterson, R.L., Twine, N.C., Zuberek, K.A., Brodeur, B.J., Casciotti, L., Maganti, V., Reddy, P.S., Strahs, A., and Immermann, F. (2006) *Molecular classification of Crohn's disease and ulcerative colitis patients using transcriptional profiles in peripheral blood mononuclear cells.* The Journal of Molecular Diagnostics 8(1): p. 51-61.

150. Maraskovsky, E., Daro, E., Roux, E., Teepe, M., Maliszewski, C.R., Hoek, J., Caron, D., Lebsack, M.E., and McKenna, H.J. (2000) *In vivo generation of human dendritic cell subsets by Flt3 ligand.* Blood 96(3): p. 878-884.

151. Bouwens, M., van de Rest, O., Dellschaft, N., Bromhaar, M.G., de Groot, L.C., Geleijnse, J.M., Muller, M., and Afman, L.A. (2009) *Fish-oil supplementation induces antiinflammatory gene expression profiles in human blood mononuclear cells.* The American Journal of Clinical Nutrition 90(2): p. 415-424.

152. de Mello, V.D.F., Erkkila, A.T., Schwab, U.S., Pulkkinen, L., Kolehmainen, M., Atalay, M., Mussalo, H., Lankinen, M., Oresic, M., Lehto, S., and Uusitupa, M. (2009) *The effect of fatty or lean fish intake on inflammatory gene expression in peripheral blood mononuclear cells of patients with coronary heart disease.* European Journal of Nutrition 48(8): p. 447-455.

153. Camargo, A., Rangel-Zúñiga, O.A., Peña-Orihuela, P., Marín, C., Pérez-Martínez, P., Delgado-Lista, J., Gutierrez-Mariscal, F.M., Malagón, M.M., Roche, H.M., Tinahones, F.J., Perez-Jimenez, F., and Lopez-Miranda, J. (2013) *Postprandial changes in the proteome are modulated by dietary fat in patients with metabolic syndrome.* The Journal of Nutritional Biochemistry 24(1): p. 318-324.

154. Fuchs, D., Piller, R., Linseisen, J., Daniel, H., and Wenzel, U. (2007) *The human peripheral blood mononuclear cell proteome responds to a dietary flaxseed-intervention and proteins identified suggest a protective effect in atherosclerosis.* Proteomics 7(18): p. 3278-3288.

155. Trebble, T.M., Arden, N.K., Wootton, S.A., Calder, P.C., Mullee, M.A., Fine, D.R., and Stroud, M.A. (2004) *Fish oil and antioxidants alter the composition and*

function of circulating mononuclear cells in Crohn disease. The American Journal of Clinical Nutrition 80(5): p. 1137-1144.

156. Stephens, N.S., Siffledeen, J., Su, X., Murdoch, T.B., Fedorak, R.N., and Slupsky, C.M. (2013) *Urinary NMR metabolomic profiles discriminate inflammatory bowel disease from healthy.* Journal of Crohn's and Colitis 7(2): p. e42-e48.

157. Dawiskiba, T., Deja, S., Mulak, A., Ząbek, A., Jawień, E., Pawełka, D., Banasik, M., Mastalerz-Migas, A., Balcerzak, W., Kaliszewski, K., Skóra, J., Barć, P., Korta, K., Pormańczuk, K., Szyber, P., Litarski, A., and Młynarz, P. (2014) *Serum and urine metabolomic fingerprinting in diagnostics of inflammatory bowel diseases.* World Journal of Gastroenterology 20(1): p. 163-174.

158. Yoshida, M., Hatano, N., Nishiumi, S., Irino, Y., Izumi, Y., Takenawa, T., and Azuma, T. (2012) *Diagnosis of gastroenterological diseases by metabolome analysis using gas chromatography–mass spectrometry.* Journal of Gastroenterology 47(1): p. 9-20.

159. Bang, H.O., Dyerberg, J., and Hjoorne, N. (1976) *The composition of food consumed by Greenland Eskimos.* Acta medica Scandinavica 200(1-2): p. 69-73.

160. Kris-Etherton, P., Taylor, D.S., Yu-Poth, S., Huth, P., Moriarty, K., Fishell, V., Hargrove, R.L., Zhao, G., and Etherton, T.D. (2000) *Polyunsaturated fatty acids in the food chain in the United States.* The American Journal of Clinical Nutrition 71(1): p. 179S-188S.

161. Grimstad, T., Berge, R.K., Bohov, P., Skorve, J., Goransson, L., Omdal, R., Aasprong, O.G., Haugen, M., Meltzer, H.M., and Hausken, T. (2011) *Salmon diet in patients with active ulcerative colitis reduced the simple clinical colitis activity index and increased the anti-inflammatory fatty acid index - a pilot study.* Scandinavian Journal of Clinical and Laboratory Investigation 71(1): p. 68-73.

162. Rigaud, D., Angel, L.A., Cerf, M., Carduner, M.J., Melchior, J.C., Sautier, C., René, E., Apfelbaum, M., and Mignon, M. (1994) *Mechanisms of decreased food intake during weight loss in adult Crohn's disease patients without obvious malabsorption.* The American Journal of Clinical Nutrition 60(5): p. 775-781.

163. Vaisman, N., Dotan, I., Halack, A., and Niv, E. (2006) *Malabsorption is a major contributor to underweight in Crohn's disease patients in remission.* Nutrition 22(9): p. 855-859.

164. Kuroki, F., Iida, M., Tominaga, M., Matsumoto, T., Kanamoto, K., and Fujishima, M. (1994) *Is vitamin E depleted in Crohn's disease at initial diagnosis?* Digestive Diseases 12(4): p. 248-254.

165. Saibeni, S., Cattaneo, M., Vecchi, M., Zighetti, M.L., Lecchi, A., Lombardi, R., Meucci, G., Spina, L., and Franchis, R. (2003) *Low vitamin B6 plasma levels, a risk factor for thrombosis, in Inflammatory Bowel Disease: Role of inflammation and correlation with acute phase reactants.* The American Journal of Gastroenterology 98(1): p. 112-117.

166. Zhu, Y., Mahon, B.D., Froicu, M., and Cantorna, M.T. (2005) *Calcium and 1α,25-dihydroxyvitamin D3 target the TNF-α pathway to suppress experimental inflammatory bowel disease.* European Journal of Immunology 35(1): p. 217-224.

167. Tirosh, O., Levy, E., and Reifen, R. (2007) *High selenium diet protects against TNBS-induced acute inflammation, mitochondrial dysfunction, and secondary necrosis in rat colon.* Nutrition 23(11-12): p. 878-886.

168. Syväoja, E.L., Salminen, K., Piironen, V., Varo, P., Kerojoki, O., and Koivistoinen, P. (1985) *Tocopherols and tocotrienols in finnish foods: Fish and fish products.* Journal of the American Oil Chemists' Society 62(8): p. 1245-1248.

169. Gladyshev, M.I., Sushchik, N.N., Gubanenko, G.A., Demirchieva, S.M., and Kalachova, G.S. (2006) *Effect of way of cooking on content of essential polyunsaturated fatty acids in muscle tissue of humpback salmon (Oncorhynchus gorbuscha).* Food Chemistry 96(3): p. 446-451.

170. González, R., Sanchez de Medina, F., Gálvez, J., Rodriguez-Cabezas, J., Duarte, J., and Zarzuelo, A. (2001) *Dietary vitamin E supplementation protects the rat large intestine from experimental inflammation.* International Journal for Vitamin and Nutrition Research 71(4): p. 243-250.

171. Klein, E.A., Thompson, I.M., Tangen, C.M., and et al. (2011) *Vitamin E and the risk of prostate cancer: The selenium and vitamin E cancer prevention trial (select).* Journal of the American Medical Association 306(14): p. 1549-1556.

172. Lippman, S.M., Klein, E.A., Goodman, P.J., and et al. (2009) *Effect of selenium and vitamin E on risk of prostate cancer and other cancers: The selenium and vitamin E cancer prevention trial (SELECT).* Journal of the American Medical Association 301(1): p. 39-51.

173. Yang, C.S., Suh, N., and Kong, A.-N.T. (2012) *Does vitamin E prevent or promote cancer?* Cancer Prevention Research 5(5): p. 701-705.

174. Yamamoto, Y., Maita, N., Fujisawa, A., Takashima, J., Ishii, Y., and Dunlap, W.C. (1999) *A new vitamin E (α-tocomonoenol) from eggs of the pacific salmon Oncorhynchus keta.* Journal of Natural Products 62(12): p. 1685-1687.

175. Yamamoto, Y., Fujisawa, A., Hara, A., and Dunlap, W.C. (2001) *An unusual vitamin E constituent (α-tocomonoenol) provides enhanced antioxidant protection in marine organisms adapted to cold-water environments.* Proceedings of the National Academy of Sciences 98(23): p. 13144-13148.

176. Dunlap, W.C., Fujisawa, A., Yamamoto, Y., Moylan, T.J., and Sidell, B.D. (2002) *Notothenioid fish, krill and phytoplankton from Antarctica contain a vitamin E constituent (α-tocomonoenol) functionally associated with cold-water adaptation.* Comparative Biochemistry and Physiology Part B: Biochemistry and Molecular Biology 133(3): p. 299-305.

177. Gotoh, N., Watanabe, H., Oka, T., Mashimo, D., Noguchi, N., Hata, K., and Wada, S. (2009) *Dietary marine-derived tocopherol has a higher biological availability in mice relative to alpha-tocopherol.* Lipids 44(2): p. 133-143.

178. The New Zealand King Salmon Company Ltd. *Health & Nutrition: Average nutritional values per 100g of fresh salmon.* 2011 [cited 2011, 29th September]; Available from: https://www.regalsalmon.co.nz/nutrition/.

179. Erdmann, K., Cheung, B.W., and Schroder, H. (2008) *The possible roles of food-derived bioactive peptides in reducing the risk of cardiovascular disease.* The Journal of Nutritional Biochemistry 19(10): p. 643-654.

180. Chalamaiah, M., Dinesh kumar, B., Hemalatha, R., and Jyothirmayi, T. (2012) *Fish protein hydrolysates: Proximate composition, amino acid composition, antioxidant activities and applications: A review.* Food Chemistry 135(4): p. 3020-3038.

181. Kim, S.-Y., Je, J.-Y., and Kim, S.-K. (2007) *Purification and characterization of antioxidant peptide from hoki (Johnius belengerii) frame protein by gastrointestinal digestion.* The Journal of Nutritional Biochemistry 18(1): p. 31-38.

182. Wu, H.-C., Chen, H.-M., and Shiau, C.-Y. (2003) *Free amino acids and peptides as related to antioxidant properties in protein hydrolysates of mackerel (Scomber austriasicus).* Food Research International 36(9–10): p. 949-957.

183. Je, J.-Y., Qian, Z.-J., Byun, H.-G., and Kim, S.-K. (2007) *Purification and characterization of an antioxidant peptide obtained from tuna backbone protein by enzymatic hydrolysis.* Process Biochemistry 42(5): p. 840-846.

184. Rudkowska, I., Marcotte, B., Pilon, G., Lavigne, C., Marette, A., and Vohl, M.C. (2010) *Fish nutrients decrease expression levels of tumor necrosis factor-alpha in cultured human macrophages.* Physiological Genomics 40(3): p. 189-194.

185. Grimstad, T., Bjørndal, B., Cacabelos, D., Aasprong, O.G., Omdal, R., Svardal, A., Bohov, P., Pamplona, R., Portero-Otin, M., Berge, R.K., and Hausken, T. (2013) *A salmon peptide diet alleviates experimental colitis as compared with fish oil.* Journal of Nutritional Science 2: p. e2.

186. The New Zealand King Salmon Company Ltd. *The virtues of our king*. 2010 [cited 2010, 18th June]; Available from: http://www.kingsalmon.co.nz/Virtues/.

187. Hamilton, M.C., Hites, R.A., Schwager, S.J., Foran, J.A., Knuth, B.A., and Carpenter, D.O. (2005) *Lipid composition and contaminants in farmed and wild salmon.* Environmental Science & Technology 39(22): p. 8622-8629.

188. Pawlosky, R.J., Hibbeln, J.R., Novotny, J.A., and Salem, N. (2001) *Physiological compartmental analysis of α-linolenic acid metabolism in adult humans.* Journal of Lipid Research 42(8): p. 1257-1265.

189. Emken, E.A., Adlof, R.O., and Gulley, R.M. (1994) *Dietary linoleic acid influences desaturation and acylation of deuterium-labeled linoleic and linolenic acids in young adult males.* Biochimica et Biophysica Acta: Protein Structure and Molecular Enzymology 1213(3): p. 277-288.

190. Burdge, G.C. and Wootton, S.A. (2002) *Conversion of α-linolenic acid to eicosapentaenoic, docosapentaenoic and docosahexaenoic acids in young women.* British Journal of Nutrition 88(04): p. 411-420.

191. Mozaffarian, D., Ascherio, A., Hu, F.B., Stampfer, M.J., Willett, W.C., Siscovick, D.S., and Rimm, E.B. (2005) *Interplay between different polyunsaturated fatty acids and risk of Coronary Heart Disease in men.* Circulation 111(2): p. 157-164.

192. Wang, Y., Botolin, D., Xu, J., Christian, B., Mitchell, E., Jayaprakasam, B., Nair, M., Peters, J.M., Busik, J., and Olson, L.K. (2006) *Regulation of hepatic fatty acid elongase and desaturase expression in diabetes and obesity.* Journal of Lipid Research 47(9): p. 2028-2041.

193. Hegazi, R.A.F., Saad, R.S., Mady, H., Matarese, L.E., O'Keefe, S., and Kandil, H.M. (2006) *Dietary fatty acids modulate chronic colitis, colitis-associated colon*

neoplasia and COX-2 expression in IL-10 knockout mice. Nutrition 22(3): p. 275-282.

194. Woodworth, H.L., McCaskey, S.J., Duriancik, D.M., Clinthorne, J.F., Langohr, I.M., Gardner, E.M., and Fenton, J.I. (2010) *Dietary fish oil alters T lymphocyte cell populations and exacerbates disease in a mouse model of inflammatory colitis.* Cancer Research 70(20): p. 7960-7969.

195. Nieto, N., Torres, M.I., Rios, A., and Gil, A. (2002) *Dietary polyunsaturated fatty acids improve histological and biochemical alterations in rats with experimental ulcerative colitis.* The Journal of Nutrition 132(1): p. 11-19.

196. Chapkin, R.S., Davidson, L.A., Ly, L., Weeks, B.R., Lupton, J.R., and McMurray, D.N. (2007) *Immunomodulatory effects of (n-3) fatty acids: putative link to inflammation and colon cancer.* The Journal of Nutrition 137(1 Suppl): p. 200S-204S.

197. Piazzi, G., D'Argenio, G., Prossomariti, A., Lembo, V., Mazzone, G., Candela, M., Biagi, E., Brigidi, P., Vitaglione, P., Fogliano, V., D'Angelo, L., Fazio, C., Munarini, A., Belluzzi, A., Ceccarelli, C., Chieco, P., Balbi, T., Loadman, P.M., Hull, M.A., Romano, M., Bazzoli, F., and Ricciardiello, L. (2014) *Eicosapentaenoic acid free fatty acid prevents and suppresses colonic neoplasia in colitis-associated colorectal cancer acting on Notch signaling and gut microbiota.* International Journal of Cancer 135(9): p. 2004-2013.

198. Trebble, T., Arden, N.K., Stroud, M.A., Wootton, S.A., Burdge, G.C., Miles, E.A., Ballinger, A.B., Thompson, R.L., and Calder, P.C. (2003) *Inhibition of tumour necrosis factor-alpha and interleukin 6 production by mononuclear cells following dietary fish-oil supplementation in healthy men and response to antioxidant co-supplementation.* British Journal of Nutrition 90(2): p. 405-412.

199. Ramakers, J.D., Mensink, R.P., Verstege, M.I., Velde, A.A.T., and Plat, J. (2008) *An arachidonic acid-enriched diet does not result in more colonic inflammation as compared with fish oil- or oleic acid-enriched diets in mice with experimental colitis.* British Journal of Nutrition 100(2): p. 347-354.

200. Wall, R., Ross, R.P., Fitzgerald, G.F., and Stanton, C. (2010) *Fatty acids from fish: The anti-inflammatory potential of long-chain omega-3 fatty acids.* Nutrition Reviews 68(5): p. 280-289.

201. Kris-Etherton, P.M. and Hill, A.M. (2008) *N-3 fatty acids: food or supplements?* Journal of the American Dietetic Association 108(7): p. 1125-1130.

202. Oxford Dictionaries. *Bioavailability*. Oxford Dictionaries 2010 [cited 2011, 22nd February]; Available from: http://oxforddictionaries.com/view/entry/m_en_gb0078450.

203. Galli, C. and Calder, P.C. (2009) *Effects of fat and fatty acid intake on inflammatory and immune responses: A critical review.* Annals of Nutrition and Metabolism 55: p. 123-139.

204. Elvevoll, E.O., Barstad, H., Breimo, E.S., Brox, J., Eilertsen, K.E., Lund, T., Olsen, J.O., and Osterud, B. (2006) *Enhanced incorporation of n-3 fatty acids from fish compared with fish oils.* Lipids 41(12): p. 1109-1114.

205. Visioli, F., Rise, P., Barassi, M.C., Marangoni, F., and Galli, C. (2003) *Dietary intake of fish vs. formulations leads to higher plasma concentrations of n-3 fatty acids.* Lipids 38(4): p. 415-418.

206. Aursand, M., Jorgensen, L., and Grasdalen, H. (1995) *Positional distribution of omega-3-fatty-acids in marine lipid triacylglycerols by high-resolution C-13 nuclear-magnetic-resonance spectroscopy.* Journal of the American Oil Chemists Society 72(3): p. 293-297.

207. Christensen, M.S., Høy, C.E., Becker, C.C., and Redgrave, T.G. (1995) *Intestinal absorption and lymphatic transport of eicosapentaenoic (EPA), docosahexaenoic (DHA), and decanoic acids: dependence on intramolecular triacylglycerol structure.* The American Journal of Clinical Nutrition 61(1): p. 56-61.

208. Lawson, L.D. and Hughes, B.G. (1988) *Absorption of eicosapentaenoic acid and docosahexaenoic acid from fish oil triacylglycerols or fish oil ethyl-esters co-ingested with a high-fat meal.* Biochemical and Biophysical Research Communications 156(2): p. 960-963.

209. Arterburn, L.M., Oken, H.A., Hall, E.B., Hamersley, J., Kuratko, C.N., and Hoffman, J.P. (2008) *Algal-oil capsules and cooked salmon: Nutritionally equivalent sources of docosahexaenoic acid.* Journal of the American Dietetic Association 108(7): p. 1204-1209.

210. Ferguson, L.R., Smith, B.G., and James, B.J. (2010) *Combining nutrition, food science and engineering in developing solutions to Inflammatory bowel diseases - omega-3 polyunsaturated fatty acids as an example.* Food & Function 1(1): p. 60-72.

211. Vander, A.J., Sherman, J., Luciano, D.S., Widmaier, E.P., Raff, H., and Strang, H., *The digestion and absorption of food*, in *Human Physiology: The Mechanisms of Body Function*. 2001, The McGraw−Hill Companies.

212. Pan, X. and Hussain, M.M. (2012) *Gut triglyceride production.* Biochimica et Biophysica Acta (BBA) - Molecular and Cell Biology of Lipids 1821(5): p. 727-735.

213. Stremmel, W. (1988) *Uptake of fatty acids by jejunal mucosal cells is mediated by a fatty acid binding membrane protein.* Journal of Clinical Investigation 82(6): p. 2001-2010.

214. Nassir, F., Wilson, B., Han, X., Gross, R.W., and Abumrad, N.A. (2007) *CD36 is important for fatty acid and cholesterol uptake by the proximal but not distal intestine.* Journal of Biological Chemistry 282(27): p. 19493-19501.

215. Stahl, A., Hirsch, D.J., Gimeno, R.E., Punreddy, S., Pei, G., Watson, N., Patel, S., Kotler, M., Raimondi, A., Tartaglia, L.A., and Lodish, H.F. (1999) *Identification of the major intestinal fatty acid transport protein.* Molecular Cell 4(3): p. 299-308.

216. Schwenk, R.W., Holloway, G.P., Luiken, J.J.F.P., Bonen, A., and Glatz, J.F.C. (2010) *Fatty acid transport across the cell membrane: Regulation by fatty acid transporters.* Prostaglandins, Leukotrienes and Essential Fatty Acids 82(4–6): p. 149-154.

217. Storch, J. and McDermott, L. (2009) *Structural and functional analysis of fatty acid-binding proteins.* Journal of Lipid Research 50(Supplement): p. S126-S131.

218. Carey, M.C., Small, D.M., and Bliss, C.M. (1983) *Lipid digestion and absorption.* Annual Review of Physiology 45(1): p. 651-677.

219. Shi, Y. and Burn, P. (2004) *Lipid metabolic enzymes: Emerging during targets for the treatment of obesity.* Nature Reviews Drug Discovery 3(8): p. 695-710.

220. Jump, D.B. and Clarke, S.D. (1999) *Regulation of gene expression by dietary fat.* Annual Review of Nutrition 19: p. 63-90.

221. Yaqoob, P., Pala, H.S., Cortina-Borja, M., Newsholme, E.A., and Calder, P.C. (2000) *Encapsulated fish oil enriched in α-tocopherol alters plasma phospholipid and mononuclear cell fatty acid compositions but not mononuclear cell functions.* European Journal of Clinical Investigation 30(3): p. 260-274.

222. Gibney, M.J. and Hunter, B. (1993) *The effects of short- and long-term supplementation with fish oil on the incorporation of n-3 polyunsaturated fatty acids into cells of the immune system in healthy volunteers.* European Journal of Clinical Nutrition 47(4): p. 255-259.

223. Fletcher, M.P. and Ziboh, V.A. (1990) *Effects of dietary supplementation with eicosapentaenoic acid or gamma-linolenic acid on neutrophil phospholipid fatty acid composition and activation responses.* Inflammation 14(5): p. 585-597.

224. Harris, W.S., Sands, S.A., Windsor, S.L., Ali, H.A., Stevens, T.L., Magalski, A., Porter, C.B., and Borkon, A.M. (2004) *Omega-3 fatty acids in cardiac biopsies from heart transplantation patients: correlation with erythrocytes and response to supplementation.* Circulation 110(12): p. 1645-1649.

225. Kuratko, C.N. and Becker, S.A. (1998) *Dietary lipids alter fatty acid composition and PGE2 production in colonic lymphocytes.* Nutrition and Cancer 31(1): p. 56-61.

226. Chapkin, R.S., Hong, M.Y., Fan, Y.-Y., Davidson, L.A., Sanders, L.M., Henderson, C.E., Barhoumi, R., Burghardt, R.C., Turner, N.D., and Lupton, J.R. (2002) *Dietary n-3 PUFA alter colonocyte mitochondrial membrane composition and function.* Lipids 37(2): p. 193-199.

227. Ringø, E., Bendiksen, H.R., Gausen, S.J., Sundsfjord, A., and Olsen, R.E. (1998) *The effect of dietary fatty acids on lactic acid bacteria associated with the epithelial mucosa and from faecalia of Arctic charr, Salvelinus alpinus (L.).* Journal of Applied Microbiology 85(5): p. 855-864.

228. Kankaanpää, P.E., Salminen, S.J., Isolauri, E., and Lee, Y.K. (2001) *The influence of polyunsaturated fatty acids on probiotic growth and adhesion.* FEMS Microbiology Letters 194(2): p. 149-153.

229. Janes, P.W., Ley, S.C., and Magee, A.I. (1999) *Aggregation of lipid rafts accompanies signaling via the T cell antigen receptor.* The Journal of cell biology 147(2): p. 447-461.

230. Moran, M. and Miceli, M.C. (1998) *Engagement of GPI-Linked CD48 Contributes to TCR Signals and Cytoskeletal Reorganization: A Role for Lipid Rafts in T Cell Activation.* Immunity 9(6): p. 787-796.

231. Khoshnan, A., Bae, D., Tindell, C.A., and Nel, A.E. (2000) *The physical association of protein kinase Cθ with a lipid raft-associated inhibitor of κB factor kinase (IKK) complex plays a role in the activation of the NF-κB cascade by TCR and CD28.* The Journal of Immunology 165(12): p. 6933-6940.

232. Triantafilou, M., Miyake, K., Golenbock, D.T., and Triantafilou, K. (2002) *Mediators of innate immune recognition of bacteria concentrate in lipid rafts and facilitate lipopolysaccharide-induced cell activation.* Journal of Cell Science 115(12): p. 2603-2611.

233. Xu, S., Huo, J., Gunawan, M., Su, I.-H., and Lam, K.-P. (2009) *Activated dectin-1 localizes to lipid raft microdomains for signaling and activation of phagocytosis and cytokine production in dendritic cells.* Journal of Biological Chemistry 284(33): p. 22005-22011.

234. Rockett, B.D., Franklin, A., Harris, M., Teague, H., Rockett, A., and Shaikh, S.R. (2011) *Membrane raft organization is more sensitive to disruption by (n-3) PUFA than nonraft organization in EL4 and B cells.* The Journal of Nutrition 141(6): p. 1041-1048.

235. Schley, P.D., Brindley, D.N., and Field, C.J. (2007) *(n-3) PUFA alter raft lipid composition and decrease epidermal growth factor receptor levels in lipid rafts of human breast cancer cells.* The Journal of Nutrition 137(3): p. 548-553.

236. Li, Q., Wang, M., Tan, L., Wang, C., Ma, J., Li, N., Li, Y., Xu, G., and Li, J. (2005) *Docosahexaenoic acid changes lipid composition and interleukin-2 receptor signaling in membrane rafts.* Journal of Lipid Research 46(9): p. 1904-1913.

237. Stulnig, T.M., Huber, J., Leitinger, N., Imre, E.-M., Angelisová, P., Nowotny, P., and Waldhäusl, W. (2001) *Polyunsaturated eicosapentaenoic acid displaces proteins from membrane rafts by altering raft lipid composition.* Journal of Biological Chemistry 276(40): p. 37335-37340.

238. Simopoulos, A.P. (1991) *Omega-3-fatty-acids in health and disease and in growth and development.* The American Journal of Clinical Nutrition 54(3): p. 438-463.

239. Shaikh, S.R., Rockett, B.D., Salameh, M., and Carraway, K. (2009) *Docosahexaenoic acid modifies the clustering and size of lipid rafts and the lateral organization and surface expression of MHC class I of EL4 cells.* The Journal of Nutrition 139(9): p. 1632-1639.

240. Chapkin, R.S., Kim, W., Lupton, J.R., and McMurray, D.N. (2009) *Dietary docosahexaenoic and eicosapentaenoic acid: Emerging mediators of inflammation.* Prostaglandins, Leukotrienes and Essential Fatty Acids 81: p. 187-191.

241. Godson, C., Mitchell, S., Harvey, K., Petasis, N.A., Hogg, N., and Brady, H.R. (2000) *Cutting edge: lipoxins rapidly stimulate nonphlogistic phagocytosis of apoptotic neutrophils by monocyte-derived macrophages.* The Journal of Immunology 164(4): p. 1663-1667.

242. Serhan, C.N. and Petasis, N.A. (2011) *Resolvins and protectins in inflammation resolution.* Chemical Reviews 111(10): p. 5922-5943.

243. Serhan, C.N., Clish, C.B., Brannon, J., Colgan, S.P., Chiang, N., and Gronert, K. (2000) *Novel functional sets of lipid-derived mediators with antiinflammatory actions generated from omega-3 fatty acids via Cyclooxygenase 2–nonsteroidal antiinflammatory drugs and transcellular processing.* The Journal of Experimental Medicine 192(8): p. 1197-1204.

244. Fischer, S., von Schacky, C., and Schweer, H. (1988) *Prostaglandins E3 and F3α are excreted in human urine after ingestion of n−3 polyunsaturated fatty acids.* Biochimica et Biophysica Acta (BBA) - Lipids and Lipid Metabolism 963(3): p. 501-508.

245. Serhan, C.N., Hong, S., Gronert, K., Colgan, S.P., Devchand, P.R., Mirick, G., and Moussignac, R.-L. (2002) *Resolvins: A family of bioactive products of omega-3 fatty acid transformation circuits initiated by aspirin treatment that counter proinflammation signals.* The Journal of Experimental Medicine 196(8): p. 1025-1037.

246. Mukherjee, P.K., Marcheselli, V.L., Serhan, C.N., and Bazan, N.G. (2004) *Neuroprotectin D1: a docosahexaenoic acid-derived docosatriene protects human retinal pigment epithelial cells from oxidative stress.* Proceedings of the National Academy of Sciences 101(22): p. 8491-8496.

247. Buczynski, M.W., Dumlao, D.S., and Dennis, E.A. (2009) *Thematic Review Series: Proteomics. An integrated omics analysis of eicosanoid biology.* Journal of Lipid Research 50(6): p. 1015-1038.

248. Deckelbaum, R.J., Worgall, T.S., and Seo, T. (2006) *N-3 fatty acids and gene expression.* The American Journal of Clinical Nutrition 83(6 Suppl): p. 1520S-1525S.

249. Bassaganya-Riera, J., Reynolds, K., Martino-Catt, S., Cui, Y., Hennighausen, L., Gonzalez, F., Rohrer, J., Benninghoff, A.U., and Hontecillas, R. (2004) *Activation of PPAR γ and δ by conjugated linoleic acid mediates protection from experimental inflammatory bowel disease.* Gastroenterology 127(3): p. 777-791.

250. Iwami, D., Zhang, Q., Aramaki, O., Nonomura, K., Shirasugi, N., and Niimi, M. (2009) *Purified eicosapentaenoic acid induces prolonged survival of cardiac allografts and generates regulatory T cells.* American Journal of Transplantation 9(6): p. 1294-1307.

251. Anderson, E.J., Thayne, K.A., Harris, M., Shaikh, S.R., Darden, T.M., Lark, D.S., Williams, J.M., Chitwood, W.R., Kypson, A.P., and Rodriguez, E. (2014) *Do fish oil omega-3 fatty acids enhance antioxidant capacity and mitochondrial fatty acid oxidation in human atrial myocardium via PPARgamma activation?* Antioxidants & Redox Signaling 21(8): p. 1156-1163.

252. Grimstad, T., Bjørndal, B., Cacabelos, D., Aasprong, O.G., Janssen, E.A.M., Omdal, R., Svardal, A., Hausken, T., Bohov, P., Portero-Otin, M., Pamplona, R., and Berge, R.K. (2012) *Dietary supplementation of krill oil attenuates inflammation and oxidative stress in experimental ulcerative colitis in rats.* Scandinavian Journal of Gastroenterology 47(1): p. 49-58.

253. Bookout, A.L., Jeong, Y., Downes, M., Yu, R.T., Evans, R.M., and Mangelsdorf, D.J. (2006) *Anatomical profiling of nuclear receptor expression reveals a hierarchical transcriptional network.* Cell 126(4): p. 789-799.

254. Braissant, O., Foufelle, F., Scotto, C., Dauça, M., and Wahli, W. (1996) *Differential expression of peroxisome proliferator-activated receptors (PPARs): tissue distribution of PPAR-alpha,-beta, and-gamma in the adult rat.* Endocrinology 137(1): p. 354-366.

255. Berger, J. and Moller, D.E. (2002) *The mechanisms of action of PPARs.* The Annual Review of Medicine 53: p. 409-435.

256. Buenger, M., van den Bosch, H.M., van der Meijde, J., Kersten, S., Hooiveld, G.J.E.J., and Mueller, M. (2007) *Genome-wide analysis of PPAR(alpha) activation in murine small intestine.* Physiological Genomics 30: p. 192-204.

257. Costet, P., Legendre, C., Moré, J., Edgar, A., Galtier, P., and Pineau, T. (1998) *Peroxisome proliferator-activated receptor α-isoform deficiency leads to progressive dyslipidemia with sexually dimorphic obesity and steatosis.* Journal of Biological Chemistry 273(45): p. 29577-29585.

258. Knoch, B., Barnett, M.P., McNabb, W.C., Zhu, S., Park, Z.A., Khan, A., and Roy, N.C. (2010) *Dietary arachidonic acid-mediated effects on colon inflammation using transcriptome analysis.* Molecular Nutrition & Food Research 54(1 Supplement): p. S62-74.

259. Turk, H.F., Monk, J.M., Fan, Y.-Y., Callaway, E.S., Weeks, B., and Chapkin, R.S. (2013) *Inhibitory effects of omega-3 fatty acids on injury-induced epidermal growth factor receptor transactivation contribute to delayed wound healing.* American Journal of Physiology - Cell Physiology 304(9): p. C905-C917.

260. Cho, J.Y., Chi, S.G., and Chun, H.S. (2011) *Oral administration of docosahexaenoic acid attenuates colitis induced by dextran sulfate sodium in mice.* Molecular Nutrition & Food Research 55(2): p. 239-246.

261. Li, K., Huang, T., Zheng, J., Wu, K., and Li, D. (2014) *Effect of marine-derived n-3 polyunsaturated fatty acids on C-reactive protein, interleukin 6 and tumor necrosis factor alpha: a meta-analysis.* PLoS ONE 9(2): p. e88103.

262. Langmann, T. and Schmitz, G. (2006) *Loss of detoxification in inflammatory bowel disease.* Nature Clinical Practice Gastroenterology & Hepatology 3(7): p. 358-359.

263. Sarkadi, B.H.L.S.G.V.A. (2006) *Human multidrug resistance ABCB and ABCG transporters: participation in a chemoimmunity defense system.* Physiological Reviews 86(4): p. 1179-1236.

264. Crotty, B. (1994) *Ulcerative colitis and xenobiotic metabolism.* The Lancet 343(8888): p. 35-38.

265. Martínez-Augustin, O., Merlos, M., Zarzuelo, A., Suárez, M.D., and de Medina, F.S. (2008) *Disturbances in metabolic, transport and structural genes in experimental colonic inflammation in the rat: a longitudinal genomic analysis.* BMC Genomics 9(1): p. 490.

266. Melgar, S., Bjursell, M., Gerdin, A.-K., Svensson, L., Michaëlsson, E., and Bohlooly-Y, M. (2007) *Mice with experimental colitis show an altered metabolism with decreased metabolic rate.* American Journal of Physiology - Gastrointestinal and Liver Physiology 292(1): p. G165-G172.

267. Heimerl, S., Moehle, C., Zahn, A., Boettcher, A., Stremmel, W., Langmann, T., and Schmitz, G. (2006) *Alterations in intestinal fatty acid metabolism in inflammatory bowel disease.* Biochimica Et Biophysica Acta-Molecular Basis of Disease 1762(3): p. 341-350.

268. Cooney, J.M., Barnett, M.P., Brewster, D., Knoch, B., McNabb, W.C., Laing, W.A., and Roy, N.C. (2012) *Proteomic analysis of colon tissue from interleukin-*

10 gene-deficient mice fed polyunsaturated fatty acids with comparison to transcriptomic analysis. Journal of Proteome Research 11(2): p. 1065-1077.

269. Ahmed, A.A., Balogun, K.A., Bykova, N.V., and Cheema, S.K. (2014) *Novel regulatory roles of omega-3 fatty acids in metabolic pathways: a proteomics approach.* Nutrition and Metabolism 11(1): p. 6.

270. Sumanasekera, W.K., Tien, E.S., Davis, J.W., Turpey, R., Perdew, G.H., and Vanden Heuvel, J.P. (2003) *Heat shock protein-90 (Hsp90) acts as a repressor of peroxisome proliferator-activated receptor-α (PPARα) and PPARβ activity.* Biochemistry 42(36): p. 10726-10735.

271. Larsson, E., Tremaroli, V., Lee, Y.S., Koren, O., Nookaew, I., Fricker, A., Nielsen, J., Ley, R.E., and Bäckhed, F. (2012) *Analysis of gut microbial regulation of host gene expression along the length of the gut and regulation of gut microbial ecology through MyD88.* Gut 61(8): p. 1124-1131.

272. Kelly, D., Campbell, J.I., King, T.P., Grant, G., Jansson, E.A., Coutts, A.G., Pettersson, S., and Conway, S. (2004) *Commensal anaerobic gut bacteria attenuate inflammation by regulating nuclear-cytoplasmic shuttling of PPAR-gamma and RelA.* Nature Immunology 5(1): p. 104-112.

273. Simon, G.M., Cheng, J., and Gordon, J.I. (2012) *Quantitative assessment of the impact of the gut microbiota on lysine ε-acetylation of host proteins using gnotobiotic mice.* Proceedings of the National Academy of Sciences 109(28): p. 11133-11138.

274. Ivanov, I.I., Atarashi, K., Manel, N., Brodie, E.L., Shima, T., Karaoz, U., Wei, D., Goldfarb, K.C., Santee, C.A., and Lynch, S.V. (2009) *Induction of intestinal Th17 cells by segmented filamentous bacteria.* Cell 139(3): p. 485-498.

275. Everard, A., Belzer, C., Geurts, L., Ouwerkerk, J.P., Druart, C., Bindels, L.B., Guiot, Y., Derrien, M., Muccioli, G.G., Delzenne, N.M., de Vos, W.M., and Cani, P.D. (2013) *Cross-talk between Akkermansia muciniphila and intestinal epithelium controls diet-induced obesity.* Proceedings of the National Academy of Sciences 110(22): p. 9066-9071.

276. Arumugam, M., Raes, J., Pelletier, E., Le Paslier, D., Yamada, T., Mende, D.R., Fernandes, G.R., Tap, J., Bruls, T., and Batto, J.-M. (2011) *Enterotypes of the human gut microbiome.* Nature 473(7346): p. 174-180.

277. Knoch, B., Nones, K., Barnett, M.P.G., McNabb, W.C., and Roy, N.C. (2010) *Diversity of caecal bacteria is altered in interleukin-10 gene-deficient mice before and after colitis onset and when fed polyunsaturated fatty acids.* Microbiology 156: p. 3306-3316.

278. Hudault, S., Guignot, J., and Servin, A.L. (2001) *Escherichia coli strains colonising the gastrointestinal tract protect germfree mice against Salmonella typhimurium infection.* Gut 49(1): p. 47-55.

279. Ghosh, S., DeCoffe, D., Brown, K., Rajendiran, E., Estaki, M., Dai, C., Yip, A., and Gibson, D.L. (2013) *Fish oil attenuates omega-6 polyunsaturated fatty acid-induced dysbiosis and infectious colitis but impairs LPS dephosphorylation activity causing sepsis.* PLoS ONE 8(2): p. e55468.

280. Knoch, B., Barnett, M.P.G., Cooney, J., McNabb, W.C., Barraclough, D., Laing, W., Zhu, S.T., Park, Z.A., MacLean, P., Knowles, S.O., and Roy, N.C. (2010)

Molecular characterization of the onset and progression of colitis in inoculated interleukin-10 gene-deficient mice: A role for PPAR alpha. PPAR Research 2010: p. 621069.

281. Lin, H.M., Barnett, M.P., Roy, N.C., Joyce, N.I., Zhu, S., Armstrong, K., Helsby, N.A., Ferguson, L.R., and Rowan, D.D. (2010) *Metabolomic analysis identifies inflammatory and noninflammatory metabolic effects of genetic modification in a mouse model of Crohn's disease.* Journal of Proteome Research 9(4): p. 1965-1975.

282. Jett, B.D., Huycke, M.M., and Gilmore, M.S. (1994) *Virulence of enterococci.* Clinical Microbiology Reviews 7(4): p. 462-478.

283. Sghir, A., Gramet, G., Suau, A., Rochet, V., Pochart, P., and Dore, J. (2000) *Quantification of bacterial groups within human fecal flora by oligonucleotide probe hybridization.* Applied and Environmental Microbiology 66(5): p. 2263-2266.

284. Kim, S.C., Tonkonogy, S.L., Karrasch, T., Jobin, C., and Sartor, R.B. (2007) *Dual-association of genotobiotic IL10-/- mice with 2 nonpathogenic commensal bacteria induces aggressive pancolitis.* Inflammatory Bowel Disease 13(12): p. 1457-1466.

285. Anonymous (1977) *Report of the American Institute of Nutrition ad hoc committee on standards for nutritional studies.* The Journal of Nutrition 107(7): p. 1340-1348.

286. Knoch, B., Barnett, M.P.G., Cooney, J., McNabb, W.C., Barraclough, D., Laing, W., and Roy, N.C. (2010) *Dietary oleic acid as a control fatty acid for polyunsaturated fatty acid intervention studies: A transcriptomics and proteomics investigation using interleukin-10 gene-deficient mice.* Biotechnology Journal 5(11): p. 1226-1240.

287. Petrik, M.B., McEntee, M.F., Chiu, C.H., and Whelan, J. (2000) *Antagonism of arachidonic acid is linked to the antitumorigenic effect of dietary eicosapentaenoic acid in Apc(Min/+) mice.* The Journal of Nutrition 130(5): p. 1153-1158.

288. Reeves, P.G., Nielsen, F.H., and Fahey JR, G.C. (1993) *AIN-93 purified diets for laboratory rodents: Final report of the American Institute of Nutrition Ad Hoc Writing Committee on the reformulation of the AIN-76A rodent diet.* The Journal of Nutrition 123: p. 1939-1951.

289. Park, E.I., Paisley, E.A., Mangian, H.J., Swartz, D.A., Wu, M., O'Morchoe, P.J., Behr, S.R., Visek, W.J., and Kaput, J. (1997) *Lipid level and type alter stearoyl CoA desaturase mRNA abundance differently in mice with distinct susceptibilities to diet-influenced diseases.* The Journal of Nutrition 127: p. 566-573.

290. Roy, N.C., Barnett, M.P.G., Knoch, B., Dommels, Y., and McNabb, W. (2007) *Nutrigenomics applied to an animal model of inflammatory bowel disease: Transciptomic analysis of the effects of eicosapentaenoic acid- and arachidonic acid-enriched diets.* Mutation Research 622: p. 103-116.

291. Somers, C.M., Valdes, E.V., and Quinn, J.S. (2006) *An approach to feeding high-percentage fish diets to mice for human and wildlife toxicology studies.* Ecotoxicology and Environmental Safety 63(3): p. 481-487.

292. Cleland, G.B., Leatherland, J.F., and Sonstegard, R.A. (1987) *Toxic effects in C57B1/6 and DBA/2 mice following consumption of halogenated aromatic hydrocarbon-contaminated Great Lakes coho salmon (Oncorhynchus kisutch Walbaum).* Environmental Health Perspectives 75: p. 153-158.

293. The New Zealand King Salmon Company Ltd. *Average nutritional values per 100g of fresh salmon*. 2009 [cited 2010, 8th June]; Available from: http://www.regalsalmon.co.nz/nutrition/.

294. Bannon, C.D., Craske, J.D., and Hilliker, A.E. (1985) *Analysis of fatty acid methyl esters with high accuracy and reliability. IV. Fats with fatty acids containing four or more carbon atoms.* JAOCS 62(10): p. 1501-1507.

295. Anderson, R.C., Bermingham, E.N., McNabb, W.C., Cookson, A.L., Tavendale, M.H., Armstrong, K.M., Knowles, S.O., and Roy, N.C. (2010) *Moderate levels of dietary sheep milk powder reduce experimentally induced colonic inflammation in rats.* Animal Production Science 50(7): p. 714-721.

296. Paturi, G., Mandimika, T., Butts, C.A., Zhu, S., Roy, N.C., McNabb, W.C., and Ansell, J. (2012) *Influence of dietary blueberry and broccoli on cecal microbiota activity and colon morphology in mdr1a−/− mice, a model of inflammatory bowel diseases.* Nutrition 28(3): p. 324-330.

297. Maglott, D., Ostell, J., Pruitt, K.D., and Tatusova, T. (2005) *Entrez Gene: gene-centered information at NCBI.* Nucleic Acids Research 33(suppl 1): p. D54-D58.

298. Schroeder, A., Mueller, O., Stocker, S., Salowsky, R., Leiber, M., Gassmann, M., Lightfoot, S., Menzel, W., Granzow, M., and Ragg, T. (2006) *The RIN: an RNA integrity number for assigning integrity values to RNA measurements.* BMC Molecular Biology 7: p. 3.

299. Smyth, G.K. (2004) *Linear models and empirical Bayes methods for assessing differential expression in microarray experiments.* Statistical Applications in Genetics and Molecular Biology 3: p. Article 3.

300. Smyth, G.K. and Speed, T.P. (2003) *Normalization of cDNA microarray data.* Methods 31(265-273).

301. Subramanian, A., Tamayo, P., Mootha, V.K., Mukherjee, S., Ebert, B.L., Gillette, M.A., Paulovich, A., Pomeroy, S.L., Golub, T.R., Lander, E.S., and Mesirov, J.P. (2005) *Gene set enrichment analysis: A knowledge-based approach for interpreting genome-wide expression profiles.* Proceedings of the National Academy of Sciences 102(43): p. 15545-15550.

302. O'Farrell, P.H. (1975) *High resolution two-dimensional electrophoresis of proteins.* Journal of Biological Chemistry 250(10): p. 4007-4021.

303. Unlu, M., Morgan, M.E., and Minden, J.S. (1997) *Difference gel electrophoresis: A single gel method for detecting changes in protein extracts.* Electrophoresis 18(11): p. 2071-2077.

304. Barraclough, D., Obenland, D., Laing, W., and Carroll, T. (2004) *A general method for two-dimensional protein electrophoresis of fruit samples.* Postharvest Biology and Technology 32(2): p. 175-181.

305. Edmunds, S.J., Roy, N.C., Davy, M., Cooney, J.M., Barnett, M.P., Zhu, S., Park, Z., Love, D.R., and Laing, W.A. (2011) *Effects of kiwifruit extracts on colonic*

gene and protein expression levels in IL-10 gene-deficient mice. British Journal of Nutrition: p. 1-17.

306. Bradford, M.M. (1976) *A rapid and sensitive method for the quantitation of microgram quantities of protein utilizing the principle of protein-dye binding.* Analytical Biochemistry 72(1-2): p. 248-254.

307. Neuhoff, V., Arold, N., Taube, D., and Ehrhardt, W. (1988) *Improved staining of proteins in polyacrylamide gels including isoelectric focusing gels with clear background at nanogram sensitivity using Coomassie Brilliant Blue G-250 and R-250.* Electrophoresis 9(6): p. 255-262.

308. Bowen, B.P. and Northen, T.R. (2010) *Dealing with the unknown: metabolomics and metabolite atlases.* Journal of the American Society for Mass Spectrometry 21(9): p. 1471-1476.

309. Otter, D., Cao, M., Lin, H.M., Fraser, K., Edmunds, S., Lane, G., and Rowan, D. (2011) *Identification of urinary biomarkers of colon inflammation in IL10$^{-/-}$ mice using short-column LCMS metabolomics.* Journal of Biomedicine and Biotechnology 2011: p. 974701.

310. Smith, C.A., Want, E.J., O'Maille, G., Abagyan, R., and Siuzdak, G. (2006) *XCMS: Processing mass spectrometry data for metabolite profiling using nonlinear peak alignment, matching and identification.* Analytical Chemistry 78: p. 779-787.

311. Smith, C.A., O'Maille, G., Want, E.J., Qin, C., Trauger, S.A., Brandon, T.R., Custodio, D.E., Abagyan, R., and Siuzdak, G. (2005) *METLIN: a metabolite mass spectral database.* Therapeutic Drug Monitoring 27(6): p. 747-751.

312. Wishart, D.S., Tzur, D., Knox, C., Eisner, R., Guo, A.C., Young, N., Cheng, D., Jewell, K., Arndt, D., Sawhney, S., Fung, C., Nikolai, L., Lewis, M., Coutouly, M.A., Forsythe, I., Tang, P., Shrivastava, S., Jeroncic, K., Stothard, P., Amegbey, G., Block, D., Hau, D.D., Wagner, J., Miniaci, J., Clements, M., Gebremedhin, M., Guo, N., Zhang, Y., Duggan, G.E., Macinnis, G.D., Weljie, A.M., Dowlatabadi, R., Bamforth, F., Clive, D., Greiner, R., Li, L., Marrie, T., Sykes, B.D., Vogel, H.J., and Querengesser, L. (2007) *HMDB: the Human Metabolome Database.* Nucleic Acids Research 35(Database issue): p. D521-526.

313. Sangster, T., Major, H., Plumb, R., Wilson, A.J., and Wilson, I.D. (2006) *A pragmatic and readily implemented quality control strategy for HPLC-MS and GC-MS-based metabonomic analysis.* Analyst 131(10): p. 1075-1078.

314. Kessner, D., Chambers, M., Burke, R., Agus, D., and Mallick, P. (2008) *ProteoWizard: Open source software for rapid proteomics tools development* Bioinformatics 24(21): p. 2534-2536.

315. Chambers, M.C., MacLean, B., Burke, R., Amode, D., Ruderman, D.L., Neumann, S., Gatto, L., Fischer, B., Pratt, B., Egertson, J., Hoff, K., Kessner, D., Tasman, N., Shulman, N., Frewen, B., Baker, T.A., Brusniak, M.-Y., Paulse, C., Creasy, D., Flashner, L., Kani, K., Moulding, C., Seymour, S.L., Nuwaysir, L.M., Lefebvre, B., Kuhlmann, F., Roark, J., Rainer, P., Detlev, S., Hemenway, T., Huhmer, A., Langridge, J., Connolly, B., Chadick, T., Holly, K., Eckels, J., Deutsch, E.W., Moritz, R.L., Katz, J.E., Agus, D.B., MacCoss, M., Tabb, D.L., and Mallick, P. (2012) *A cross-platform toolkit for mass spectrometry and proteomics.* Nature Biotechnology 30: p. 918-920.

316. Tautenhahn, R. and Boettcher, C.N., S. (2008) *Highly sensitive feature detection for high resolution LC/MS.* BMC Bioinformatics 9: p. 504.

317. Benjamini, Y. and Hochberg, Y. (1995) *Controlling the false discovery rate: a practical and powerful approach to multiple testing.* Journal of the Royal Statistical Society. Series B (Methodological): p. 289-300.

318. Lepage, P., Leclerc, M.C., Joossens, M., Mondot, S., Blottière, H.M., Raes, J., Ehrlich, D., and Doré, J. (2013) *A metagenomic insight into our gut's microbiome.* Gut 62(1): p. 146-158.

319. Weisburg, W.G., Barns, S.M., Pelletier, D.A., and Lane, D.J. (1991) *16S ribosomal DNA amplification for phylogenetic study.* Journal of Bacteriology 173(2): p. 697-703.

320. Thomas, T., Gilbert, J., and Meyer, F. (2012) *Metagenomics - a guide from sampling to data analysis.* Microbial Informatics and Experimentation 2(1): p. 3.

321. Luo, C., Tsementzi, D., Kyrpides, N., Read, T., and Konstantinidis, K.T. (2012) *Direct comparisons of Illumina vs. Roche 454 sequencing technologies on the same microbial community DNA sample.* PLoS ONE 7(2): p. e30087.

322. Wommack, K.E., Bhavsar, J., and Ravel, J. (2008) *Metagenomics: read length matters.* Applied and Environmental Microbiology 74(5): p. 1453-1463.

323. Ramette, A. (2007) *Multivariate analyses in microbial ecology.* FEMS Microbiology Ecology 62(2): p. 142-160.

324. Whittaker, R.H. (1972) *Evolution and measurement of species diversity.* Taxon 21(2/3): p. 213-251.

325. Chao, A. (1984) *Nonparametric estimation of the number of classes in a population.* Scandinavian Journal of Statistics 11(4): p. 265-270.

326. Welham, S., Cullis, B., Gogel, B., Gilmour, A., and Thompson, R. (2004) *Prediction in linear mixed models.* Australian & New Zealand Journal of Statistics 46(3): p. 325-347.

327. Lozupone, C. and Knight, R. (2005) *UniFrac: a new phylogenetic method for comparing microbial communities.* Applied and Environmental Microbiology 71(12): p. 8228-8235.

328. Kanehisa, M. and Goto, S. (2000) *KEGG: Kyoto Encyclopedia of Genes and Genomes.* Nucleic Acids Research 28(1): p. 27-30.

329. Rahmatallah, Y., Emmert-Streib, F., and Glazko, G. (2012) *Gene set analysis for self-contained tests: complex null and specific alternative hypotheses.* Bioinformatics 28(23): p. 3073-3080.

330. Dalman, M., Deeter, A., Nimishakavi, G., and Duan, Z.-H. (2012) *Fold change and p-value cutoffs significantly alter microarray interpretations.* BMC Bioinformatics 13(Suppl 2): p. S11.

331. Jiang, Z. and Gentleman, R. (2007) *Extensions to gene set enrichment.* Bioinformatics 23(3): p. 306-313.

332. Mootha, V.K., Lindgren, C.M., Eriksson, K.F., Subramanian, A., Sihag, S., Lehar, J., Puigserver, P., Carlsson, E., Ridderstrale, M., Laurila, E., Houstis, N., Daly, M.J., Patterson, N., Mesirov, J.P., Golub, T.R., Tamayo, P., Spiegelman, B.,

Lander, E.S., Hirschhorn, J.N., Altshuler, D., and Groop, L.C. (2003) *PGC-1alpha-responsive genes involved in oxidative phosphorylation are coordinately downregulated in human diabetes.* Nature Genetics 34(3): p. 267-273.

333. Wu, D., Lim, E., Vaillant, F., Asselin-Labat, M.-L., Visvader, J.E., and Smyth, G.K. (2010) *ROAST: rotation gene set tests for complex microarray experiments.* Bioinformatics 26(17): p. 2176-2182.

334. Goeman, J.J. and Buhlmann, P. (2007) *Analyzing gene expression data in terms of gene sets: methodological issues.* Bioinformatics 23: p. 980-987.

335. Langsrud, O. (2005) *Rotation tests.* Statistics and Computing 15: p. 53-60.

336. Kutmon, M., Lotia, S., Evelo, C.T., and Pico, A.R. (2014) *WikiPathways app for Cytoscape: Making biological pathways amenable to network analysis and visualization.* F1000Res 3: p. 152.

337. Shannon, P., Markiel, A., Ozier, O., Baliga, N.S., Wang, J.T., Ramage, D., Amin, N., Schwikowski, B., and Ideker, T. (2003) *Cytoscape: a software environment for integrated models of biomolecular interaction networks.* Genome Research 13(11): p. 2498-2504.

338. Delerive, P., Gervois, P., Fruchart, J.C., and Staels, B. (2000) *Induction of IkappaBalpha expression as a mechanism contributing to the anti-inflammatory activities of peroxisome proliferator-activated receptor-alpha activators.* Journal of Biological Chemistry 275(47): p. 36703-36707.

339. Remels, A.H., Langen, R.C., Gosker, H.R., Russell, A.P., Spaapen, F., Voncken, J.W., Schrauwen, P., and Schols, A.M. (2009) *PPARgamma inhibits NF-kappaB-dependent transcriptional activation in skeletal muscle.* American Journal of Physiology - Endocrinology and metabolism 297(1): p. E174-183.

340. Murdoch, T.B., Fu, H., MacFarlane, S., Sydora, B.C., Fedorak, R.N., and Slupsky, C.M. (2008) *Urinary metabolic profiles of inflammatory bowel disease in interleukin-10 gene-deficient mice.* Analytical Chemistry 80(14): p. 5524-5531.

341. Williams, H.R., Cox, I.J., Walker, D.G., North, B.V., Patel, V.M., Marshall, S.E., Jewell, D.P., Ghosh, S., Thomas, H.J., and Teare, J.P. (2009) *Characterization of inflammatory bowel disease with urinary metabolic profiling.* The American Journal of Gastroenterology 104(6): p. 1435-1444.

342. Hansen, J.J., Holt, L., and Sartor, R.B. (2009) *Gene expression patterns in experimental colitis in IL-10-deficient mice.* Inflammatory Bowel Disease 15(6): p. 890-899.

343. Reiff, C., Delday, M., Rucklidge, G., Reid, M., Duncan, G., Wohlgemuth, S., Hormannsperger, G., Loh, G., Blaut, M., Collie-Duguid, E., Haller, D., and Kelly, D. (2009) *Balancing inflammatory, lipid, and xenobiotic signaling pathways by VSL#3, a biotherapeutic agent, in the treatment of Inflammatory Bowel Disease.* Inflammatory Bowel Disease 15(11): p. 1721-1736.

344. Fallarino, F., Grohmann, U., Hwang, K.W., Orabona, C., Vacca, C., Bianchi, R., Belladonna, M.L., Fioretti, M.C., Alegre, M.L., and Puccetti, P. (2003) *Modulation of tryptophan catabolism by regulatory T cells.* Nature Immunology 4(12): p. 1206-1212.

345. Maes, M., Mihaylova, I., Ruyter, M.D., Kubera, M., and Bosmans, E. (2007) *The immune effects of TRYCATs (tryptophan catabolites along the IDO pathway):*

relevance for depression - and other conditions characterized by tryptophan depletion induced by inflammation. Neuro endocrinology letters 28(6): p. 826-831.

346. Miao, Y.-L., Xiao, Y.-L., Du, Y., and Duan, L.-P. (2013) *Gene expression profiles in peripheral blood mononuclear cells of ulcerative colitis patients.* World Journal of Gastroenterology 19(21): p. 3339-3346.

347. Rudkowska, I., Paradis, A.-M., Thifault, E., Julien, P., Tchernof, A., Couture, P., Lemieux, S., Barbier, O., and Vohl, M.-C. (2013) *Transcriptomic and metabolomic signatures of an n-3 polyunsaturated fatty acids supplementation in a normolipidemic/normocholesterolemic Caucasian population.* The Journal of Nutritional Biochemistry 24(1): p. 54-61.

348. Russ, A.E., Peters, J.S., McNabb, W.C., Barnett, M.P., Anderson, R.C., Park, Z., Zhu, S., Maclean, P., Young, W., Reynolds, G.W., and Roy, N.C. (2013) *Gene expression changes in the colon epithelium are similar to those of intact colon during late inflammation in interleukin-10 gene deficient mice.* PLoS ONE 8(5): p. e63251.

349. Draper, J., Enot, D., Parker, D., Beckmann, M., Snowdon, S., Lin, W., and Zubair, H. (2009) *Metabolite signal identification in accurate mass metabolomics data with MZedDB, an interactive m/z annotation tool utilising predicted ionisation behaviour 'rules'.* BMC Bioinformatics 10(1): p. 227.

350. Cho, J.Y., Kang, D.W., Ma, X., Ahn, S.H., Krausz, K.W., Luecke, H., Idle, J.R., and Gonzalez, F.J. (2009) *Metabolomics reveals a novel vitamin E metabolite and attenuated vitamin E metabolism upon PXR activation.* Journal of Lipid Research 50(5): p. 924-937.

351. Fuller, N. and Rand, R.P. (2001) *The influence of lysolipids on the spontaneous curvature and bending elasticity of phospholipid membranes.* Biophysical Journal 81(1): p. 243-254.

352. Quinn, M.T., Parthasarathy, S., and Steinberg, D. (1988) *Lysophosphatidylcholine: a chemotactic factor for human monocytes and its potential role in atherogenesis.* Proceedings of the National Academy of Sciences 85(8): p. 2805-2809.

353. Kawachi, S., Jennings, S., Panes, J., Cockrell, A., Laroux, F.S., Gray, L., Perry, M., van der Heyde, H., Balish, E., Granger, D.N., Specian, R.A., and Grisham, M.B. (2000) *Cytokine and endothelial cell adhesion molecule expression in interleukin-10-deficient mice.* American Journal of Physiology - Gastrointestinal and Liver Physiology 278(5): p. G734-G743.

354. Hall, J.A., Brockman, J.A., and Jewell, D.E. (2011) *Dietary fish oil alters the lysophospholipid metabolomic profile and decreases urinary 11-dehydro thromboxane B 2 concentration in healthy Beagles.* Veterinary Immunology and Immunopathology 144(3): p. 355-365.

355. Zhang, X., Yang, N., Ai, D., and Zhu, Y. (2015) *Systematic metabolomic analysis of eicosanoids after omega-3 polyunsaturated fatty acid supplementation by a highly specific liquid chromatography-tandem mass spectrometry-based method.* Journal of Proteome Research 14(4): p. 1843-1853.

356. Lefils, J., Géloën, A., Vidal, H., Lagarde, M., and Bernoud-Hubac, N. (2010) *Dietary DHA: time course of tissue uptake and effects on cytokine secretion in mice.* British Journal of Nutrition 104(09): p. 1304-1312.

357. Whiting, C.V., Bland, P.W., and Tarlton, J.E. (2005) *Dietary n-3 polyunsaturated fatty acids reduce disease and colonic proinflammatory cytokines in a mouse model of colitis.* Inflammatory Bowel Disease 11(4): p. 340-349.

358. Bouwens, M., Grootte Bromhaar, M., Jansen, J., Muller, M., and Afman, L.A. (2010) *Postprandial dietary lipid-specific effects on human peripheral blood mononuclear cell gene expression profiles.* The American Journal of Clinical Nutrition 91(1): p. 208-217.

359. Dieckgraefe, B., Stenson, W., Korzenik, J., Swanson, P., and Harrington, C. (2000) *Analysis of mucosal gene expression in inflammatory bowel disease by parallel oligonucleotide arrays.* Physiological Genomics 4: p. 1-11.

360. Yui, S., Nakatani, Y., and Mikami, M. (2003) *Calprotectin (S100A8/S100A9), an inflammatory protein complex from neutrophils with a broad apoptosis-inducing activity.* Biological & Pharmaceutical Bulletin 26(6): p. 753-760.

361. Sartor, R.B. (1995) *Current concepts of the etiology and pathogenesis of ulcerative colitis and Crohn's disease.* Gastroenterology Clinics of North America 24(3): p. 475-507.

362. Funderburg, N.T., Stubblefield Park, S.R., Sung, H.C., Hardy, G., Clagett, B., Ignatz-Hoover, J., Harding, C.V., Fu, P., Katz, J.A., Lederman, M.M., and Levine, A.D. (2013) *Circulating CD4+ and CD8+ T cells are activated in inflammatory bowel disease and are associated with plasma markers of inflammation.* Immunology 140(1): p. 87-97.

363. Cash, H.L., Whitham, C.V., Behrendt, C.L., and Hooper, L.V. (2006) *Symbiotic bacteria direct expression of an intestinal bactericidal lectin.* Science 313(5790): p. 1126-1130.

364. Vaishnava, S., Yamamoto, M., Severson, K.M., Ruhn, K.A., Yu, X., Koren, O., Ley, R., Wakeland, E.K., and Hooper, L.V. (2011) *The antibacterial lectin RegIIIgamma promotes the spatial segregation of microbiota and host in the intestine.* Science 334(6053): p. 255-258.

365. Wolf, A.M., Wolf, D., Rumpold, H., Moschen, A.R., Kaser, A., Obrist, P., Fuchs, D., Brandacher, G., Winkler, C., and Geboes, K. (2004) *Overexpression of indoleamine 2, 3-dioxygenase in human inflammatory bowel disease.* Clinical Immunology 113(1): p. 47-55.

366. Gupta, N.K., Thaker, A.I., Kanuri, N., Riehl, T.E., Rowley, C.W., Stenson, W.F., and Ciorba, M.A. (2012) *Serum analysis of tryptophan catabolism pathway: Correlation with Crohn's disease activity.* Inflammatory Bowel Disease 18(7): p. 1214-1220.

367. Nowak, E.C., de Vries, V.C., Wasiuk, A., Ahonen, C., Bennett, K.A., Le Mercier, I., Ha, D.-G., and Noelle, R.J. (2012) *Tryptophan hydroxylase-1 regulates immune tolerance and inflammation.* The Journal of Experimental Medicine 209(11): p. 2127-2135.

368. Sumi-Ichinose, C., Ichinose, H., Takahashi, E., Hori, T., and Nagatsu, T. (1992) *Molecular cloning of genomic DNA and chromosomal assignment of the gene for*

human aromatic L-amino acid decarboxylase, the enzyme for catecholamine and serotonin biosynthesis. Biochemistry 31(8): p. 2229-2238.

369. Børglum, A., Bruun, T., Kjeldsen, T., Ewald, H., Mors, O., Kirov, G., Russ, C., Freeman, B., Collier, D., and Kruse, T. (1999) *Two novel variants in the DOPA decarboxylase gene: association with bipolar affective disorder.* Molecular Psychiatry 4(6): p. 545-551.

370. Coates, M.D., Mahoney, C.R., Linden, D.R., Sampson, J.E., Chen, J., Blaszyk, H., Crowell, M.D., Sharkey, K.A., Gershon, M.D., Mawe, G.M., and Moses, P.L. (2004) *Molecular defects in mucosal serotonin content and decreased serotonin reuptake transporter in ulcerative colitis and irritable bowel syndrome 1.* Gastroenterology 126(7): p. 1657-1664.

371. Towne, J.E., Garka, K.E., Renshaw, B.R., Virca, G.D., and Sims, J.E. (2004) *Interleukin (IL)-1F6, IL-1F8, and IL-1F9 signal through IL-1Rrp2 and IL-1RAcP to activate the pathway leading to NF-kappaB and MAPKs.* Journal of Biological Chemistry 279(14): p. 13677-13688.

372. Suzawa, M., Takada, I., Yanagisawa, J., Ohtake, F., Ogawa, S., Yamauchi, T., Kadowaki, T., Takeuchi, Y., Shibuya, H., Gotoh, Y., Matsumoto, K., and Kato, S. (2003) *Cytokines suppress adipogenesis and PPARG function through the TAK1/TAB1/NIK cascade.* Nature Cell Biology 5(3): p. 224-230.

373. Subbaramaiah, K., Lin, D.T., Hart, J.C., and Dannenberg, A.J. (2001) *Peroxisome proliferator-activated receptor gamma ligands suppress the transcriptional activation of cyclooxygenase-2. Evidence for involvement of activator protein-1 and CREB-binding protein/p300.* Journal of Biological Chemistry 276(15): p. 12440-12448.

374. Leslie, C.C. (2004) *Regulation of arachidonic acid availability for eicosanoid production.* Biochemistry and Cell Biology 82(1): p. 1-17.

375. Franceschi, C., Bonafè, M., Valensin, S., Olivieri, F., de Luca, M., Ottaviani, E., and de Benedictis, G. (2000) *Inflamm-aging: an evolutionary perspective on immunosenescence.* Annals of the New York Academy of Sciences 908(1): p. 244-254.

376. Bassal, N.K., Hughes, B.P., and Costabile, M. (2012) *Arachidonic acid and its COX1/2 metabolites inhibit interferon-γ mediated induction of indoleamine-2,3 dioxygenase in THP-1 cells and Human monocytes.* Prostaglandins, Leukotrienes and Essential Fatty Acids 87(4–5): p. 119-126.

377. Berger, A., Roberts, M.A., and Hoff, B. (2006) *How dietary arachidonic- and docosahexaenoic- acid rich oils differentially affect the murine hepatic transcriptome.* Lipids Health Disease 5: p. 10.

378. Jia, Q., Ivanov, I., Zlatev, Z.Z., Alaniz, R.C., Weeks, B.R., Callaway, E.S., Goldsby, J.S., Davidson, L.A., Fan, Y.-Y., and Zhou, L. (2011) *Dietary fish oil and curcumin combine to modulate colonic cytokinetics and gene expression in dextran sodium sulphate-treated mice.* British Journal of Nutrition 106(04): p. 519-529.

379. Healy, D.A., Wallace, F.A., Miles, E.A., Calder, P.C., and Newsholme, P. (2000) *Effect of low-to-moderate amounts of dietary fish oil on neutrophil lipid composition and function.* Lipids 35(7): p. 763-768.

380. Browning, L.M., Walker, C.G., Mander, A.P., West, A.L., Madden, J., Gambell, J.M., Young, S., Wang, L., Jebb, S.A., and Calder, P.C. (2012) *Incorporation of eicosapentaenoic and docosahexaenoic acids into lipid pools when given as supplements providing doses equivalent to typical intakes of oily fish.* The American Journal of Clinical Nutrition 96(4): p. 748-758.

381. Kalha, I. and Sellin, J.H. (2004) *Common variable immunodeficiency and the gastrointestinal tract.* Current Gastroenterology Reports 6(5): p. 377-383.

382. Carsetti, R., Rosado, M.M., Donnanno, S., Guazzi, V., Soresina, A., Meini, A., Plebani, A., Aiuti, F., and Quinti, I. (2005) *The loss of IgM memory B cells correlates with clinical disease in common variable immunodeficiency.* Journal of Allergy and Clinical Immunology 115(2): p. 412-417.

383. Barnett, M., Bermingham, E., McNabb, W., Bassett, S., Armstrong, K., Rounce, J., and Roy, N. (2010) *Investigating micronutrients and epigenetic mechanisms in relation to inflammatory bowel disease.* Mutation Research-Fundamental and Molecular Mechanisms of Mutagenesis 690(1-2): p. 71-80.

384. Boasso, A., Herbeuval, J.-P., Hardy, A.W., Anderson, S.A., Dolan, M.J., Fuchs, D., and Shearer, G.M. (2007) *HIV inhibits CD4+ T-cell proliferation by inducing indoleamine 2,3-dioxygenase in plasmacytoid dendritic cells.* Immunobiology 109(8): p. 3351-3359.

385. Hosomi, S., Oshitani, N., Kamata, N., Sogawa, M., Okazaki, H., Tanigawa, T., Yamagami, H., Watanabe, K., Tominaga, K., Watanabe, T., Fujiwara, Y., Maeda, K., Hirakawa, K., and Arakawa, T. (2011) *Increased numbers of immature plasma cells in peripheral blood specifically overexpress chemokine receptor CXCR3 and CXCR4 in patients with ulcerative colitis.* Clinical & Experimental Immunology 163(2): p. 215-224.

386. Brinkman, C.C., Rouhani, S.J., Srinivasan, N., and Engelhard, V.H. (2013) *Peripheral tissue homing receptors enable T cell entry into lymph nodes and affect the anatomical distribution of memory cells.* Journal of Immunology 191(5): p. 2412-2425.

387. Zelman-Toister, E., Bakos, E., Cohen, S., Zigmond, E., Shezen, E., Grabovsky, V., Sagiv, A., Hart, G., Kaushansky, N., Ben-Nun, A., Maharshak, N., Sonnenberg, A., Alon, R., Becker-Herman, S., and Shachar, I. (2016) *CD151 regulates T-cell migration in health and inflammatory bowel disease.* Inflammatory Bowel Disease 22(2): p. 257-267.

388. Movahedi, K., Guilliams, M., Van den Bossche, J., Van den Bergh, R., Gysemans, C., Beschin, A., De Baetselier, P., and Van Ginderachter, J.A. (2008) *Identification of discrete tumor-induced myeloid-derived suppressor cell subpopulations with distinct T cell-suppressive activity.* Blood 111(8): p. 4233-4244.

389. Wang, Y., Liu, X.P., Zhao, Z.B., Chen, J.H., and Yu, C.G. (2011) *Expression of CD4+ forkhead box P3 (FOXP3)+ regulatory T cells in inflammatory bowel disease.* Journal of Digestive Diseases 12(4): p. 286-294.

390. Flörcken, A., Takvorian, A., Singh, A., Gerhardt, A., Ostendorf, B.N., Dörken, B., Pezzutto, A., and Westermann, J. (2015) *Myeloid-derived suppressor cells in human peripheral blood: Optimized quantification in healthy donors and patients with metastatic renal cell carcinoma.* Immunology Letters 168(2): p. 260-267.

391. Bouwens, M., Afman, L.A., and Muller, M. (2007) *Fasting induces changes in peripheral blood mononuclear cell gene expression profiles related to increases in fatty acid beta-oxidation: functional role of peroxisome proliferator activated receptor alpha in human peripheral blood mononuclear cells.* The American Journal of Clinical Nutrition 86(5): p. 1515-1523.

392. Cain, C.D., Schroeder, F.C., Shankel, S.W., Mitchnick, M., Schmertzler, M., and Bricker, N.S. (2007) *Identification of xanthurenic acid 8-O-β-d-glucoside and xanthurenic acid 8-O-sulfate as human natriuretic hormones.* Proceedings of the National Academy of Sciences 104(45): p. 17873-17878.

393. Lin, H.M., Edmunds, S.I., Helsby, N.A., Ferguson, L.R., and Rowan, D.D. (2009) *Nontargeted urinary metabolite profiling of a mouse model of Crohn's disease.* Journal of Proteome Research 8(4): p. 2045-2057.

394. Chojnacki, J., Wiśniewska-Jarosińska, M., Śliwiński, T., Błasiak, J., and Chojnacki, C. (2011) *Melatonin modulates DNA damage and repair in colonocytes of subjects with ulcerative colitis.* Gastroenterologia Polska/Gastroenterology 18(2).

395. Chen, M., Mei, Q., Xu, J., Lu, C., Fang, H., and Liu, X. (2012) *Detection of melatonin and homocysteine simultaneously in ulcerative colitis.* Clinica Chimica Acta 413(1–2): p. 30-33.

396. Huang, Y.H., Schafer-Elinder, L., Wu, R., Claesson, H.E., and Frostegard, J. (1999) *Lysophosphatidylcholine (LPC) induces proinflammatory cytokines by a platelet-activating factor (PAF) receptor-dependent mechanism.* Clinical and Experimental Immunology 116(2): p. 326-331.

397. Hye Kyeong, M., Sangsoo, L., Bong Chul, C., and Myeong Hee, M. (2011) *Shotgun lipidomics for candidate biomarkers of urinary phospholipids in prostate cancer.* Analytical & Bioanalytical Chemistry 399(2): p. 823-830.

398. Kim, H., Ahn, E., and Moon, M.H. (2008) *Profiling of human urinary phospholipids by nanoflow liquid chromatography/tandem mass spectrometry.* Analyst 133(12): p. 1656-1663.

399. Ottestad, I., Hassani, S., Borge, G.I., Kohler, A., Vogt, G., Hyötyläinen, T., Orešič, M., Brønner, K.W., Holven, K.B., Ulven, S.M., and Myhrstad, M.C.W. (2012) *Fish oil supplementation alters the plasma lipidomic profile and increases long-chain PUFAs of phospholipids and triglycerides in healthy subjects.* PLoS ONE 7(8): p. e42550.

400. Letts, L.G., Cirino, M., Yusko, P., Fitzsimonns, B., Ford-Hutchinson, A.W., and Rokach, J. (1985) *Actions of synthetic leukotrienes on platelets and blood vessels in the anesthetised pig: the release of a platelet derived vasodilator.* Prostaglandins 29(6): p. 1049-1062.

401. Pfefferkorn, E.R., Rebhun, S., and Eckel, M. (1986) *Characterization of an indoleamine 2,3-dioxygenase induced by gamma-interferon in cultured human fibroblasts.* Journal of Interferon Research 6(3): p. 267-279.

402. Smith, E.A. and Macfarlane, G.T. (1997) *Formation of phenolic and indolic compounds by anaerobic bacteria in the human large intestine.* Microbial Ecology 33(3): p. 180-188.

403. Arita, M., Yoshida, M., Hong, S., Tjonahen, E., Glickman, J.N., Petasis, N.A., Blumberg, R.S., and Serhan, C.N. (2005) *Resolvin E1, an endogenous lipid mediator derived from omega-3 eicosapentaenoic acid, protects against 2, 4, 6-trinitrobenzene sulfonic acid-induced colitis.* Proceedings of the National Academy of Sciences 102(21): p. 7671-7676.

404. Sierra, S., Lara-Villoslada, F., Comalada, M., Olivares, M., and Xaus, J. (2008) *Dietary eicosapentaenoic acid and docosahexaenoic acid equally incorporate as decosahexaenoic acid but differ in inflammatory effects.* Nutrition 24(3): p. 245-254.

405. European Food Safety Authority (2010) *Scientific opinion on fish oil for human consumption. Food hygiene, including rancidity.* European Food Safety Authority Journal 8(10): p. 1874.

406. Petrik, M.B.H., McEntee, M.F., Johnson, B.T., Obukowicz, M.G., and Whelan, J. (2000) *Highly unsaturated (n-3) fatty acids, but not α-linolenic, conjugated linoleic or γ-linolenic acids, reduce tumorigenesis in Apc$^{Min/+}$ mice.* The Journal of Nutrition 130(10): p. 2434-2443.

407. Fini, L., Piazzi, G., Ceccarelli, C., Daoud, Y., Belluzzi, A., Munarini, A., Graziani, G., Fogliano, V., Selgrad, M., Garcia, M., Gasbarrini, A., Genta, R.M., Boland, C.R., and Ricciardiello, L. (2010) *Highly purified eicosapentaenoic acid as free fatty acids strongly suppresses polyps in Apc$^{Min/+}$ Mice.* Clinical Cancer Research 16(23): p. 5703-5711.

408. Reagan-Shaw, S., Nihal, M., and Ahmad, N. (2008) *Dose translation from animal to human studies revisited.* The FASEB Journal 22(3): p. 659-661.

409. Kris-Etherton, P.M., Grieger, J.A., and Etherton, T.D. (2009) *Dietary reference intakes for DHA and EPA.* Prostaglandins, Leukotrienes and Essential Fatty Acids 81(2-3): p. 99-104.

410. Australia and New Zealand National Health and Medical Research Council, *Nutrient reference values for Australia and New Zealand including recommended dietary intakes*. 2006.

411. Calder, P.C. (2008) *Polyunsaturated fatty acids, inflammatory processes and inflammatory bowel disease.* Molecular Nutrition & Food Research 52: p. 885-897.

412. Kim, W., McMurray, D.N., and Chapkin, R.S. (2010) *N-3 polyunsaturated fatty acids - physiological relevance of dose.* Prostaglandins, Leukotrienes and Essential Fatty Acids 82(4-6): p. 155-158.

413. EFSA Panel on Dietetic Products Nutrition and Allergies (NDA) (2012) *Scientific opinion on the Tolerable Upper Intake Level of eicosapentaenoic acid (EPA), docosahexaenoic acid (DHA) and docosapentaenoic acid (DPA).* EFSA Journal 10(7): p. 2815.

414. Feskens, E.J.M. and Kromhout, D. (1993) *Epidemiologic studies on Eskimos and fish intake.* Annals of the New York Academy of Sciences 683(1): p. 9-15.

415. Miller, M., *Oxidation of food grade oils*. 2010, Plant & Food Research: Nelson.

416. Awada, M., Soulage, C.O., Meynier, A., Debard, C., Plaisancié, P., Benoit, B., Picard, G., Loizon, E., Chauvin, M.-A., Estienne, M., Peretti, N., Guichardant, M., Lagarde, M., Genot, C., and Michalski, M.-C. (2012) *Dietary oxidized n-3*

PUFA induce oxidative stress and inflammation: role of intestinal absorption of 4-HHE and reactivity in intestinal cells. Journal of Lipid Research 53(10): p. 2069-2080.

417. Rao, R.V., Peel, A., Logvinova, A., del Rio, G., Hermel, E., Yokota, T., Goldsmith, P.C., Ellerby, L.M., Ellerby, H.M., and Bredesen, D.E. (2002) *Coupling endoplasmic reticulum stress to the cell death program: role of the ER chaperone GRP78.* FEBS Letters 514(2–3): p. 122-128.

418. Van Kuijk, F.J.G.M., Holte, L.L., and Dratz, E.A. (1990) *4-Hydroxyhexenal: a lipid peroxidation product derived from oxidized docosahexaenoic acid.* Biochimica et Biophysica Acta - Lipids and Lipid Metabolism 1043(1): p. 116-118.

419. Marnett, L.J. (2002) *Oxy radicals, lipid peroxidation and DNA damage.* Toxicology 181-182: p. 219-222.

420. Kastan, M.B., Onyekwere, O., Sidransky, D., Vogelstein, B., and Craig, R.W. (1991) *Participation of p53 protein in the cellular response to DNA damage.* Cancer Research 51(23 Part 1): p. 6304-6311.

421. Sanchez, Y. and Elledge, S.J. (1995) *Stopped for repairs.* Bioessays 17(6): p. 545-548.

422. Yonish-Rouach, E., Resnitzky, D., Lotem, J., Sachs, L., Kimchi, A., and Oren, M. (1991) *Wild-type p53 induces apoptosis of myeloid leukemic cells that is inhibited by interleukin-6.* Nature 352(6333): p. 345-347.

423. Cenini, G., Sultana, R., Memo, M., and Butterfield, D.A. (2008) *Elevated levels of pro-apoptotic p53 and its oxidative modification by the lipid peroxidation product, HNE, in brain from subjects with amnestic mild cognitive impairment and Alzheimer's disease.* Journal of Cellular and Molecular Medicine 12(3): p. 987-994.

424. Cao, Z.-G., Xu, X., Xue, Y.-M., and Zhao, S.-L. (2014) *Comparison of 4-hydroxynonenal-induced p53-mediated apoptosis in prostate cancer cells LNCaP and DU145.* Contemporary Oncology 18(1): p. 22-28.

425. Baeuerle, P.A. and Henkel, T. (1994) *Function and Activation of NF-kappaB in the Immune System.* Annual Review of Immunology 12(1): p. 141-179.

426. Siebenlist, U., Franzoso, G., and Brown, K. (1994) *Structure, regulation and function of NF-kappaB.* Annual Review of Cell Biology 10(1): p. 405-455.

427. Kumar, J.S., Subramanian, V.S., Kapadia, R., Kashyap, M.L., and Said, H.M. (2013) *Mammalian colonocytes possess a carrier-mediated mechanism for uptake of vitamin B3 (niacin): studies utilizing human and mouse colonic preparations.* American Journal of Physiology - Gastrointestinal and Liver Physiology 305(3): p. G207-G213.

428. Kliewer, S.A., Sundseth, S.S., Jones, S.A., Brown, P.J., Wisely, G.B., Koble, C.S., Devchand, P., Wahli, W., Willson, T.M., Lenhard, J.M., and Lehmann, J.M. (1997) *Fatty acids and eicosanoids regulate gene expression through direct interactions with peroxisome proliferator-activated receptors α and γ.* Proceedings of the National Academy of Sciences 94(9): p. 4318-4323.

429. Roediger, W.E.W. (1980) *The colonic epithelium in ulcerative colitis: an energy-deficiency disease?* The Lancet 316(8197): p. 712-715.

430. Gervois, P., Kleemann, R., Pilon, A., Percevault, F., Koenig, W., Staels, B., and Kooistra, T. (2004) *Global suppression of IL-6-induced acute phase response gene expression after chronic in vivo treatment with the Peroxisome Proliferator-activated Receptor-α activator fenofibrate.* Journal of Biological Chemistry 279(16): p. 16154-16160.

431. Takata, Y., Kitami, Y., Yang, Z.-H., Nakamura, M., Okura, T., and Hiwada, K. (2002) *Vascular inflammation is negatively autoregulated by interaction between CCAAT/Enhancer-Binding Protein-δ and Peroxisome Proliferator-Activated Receptor-γ.* Circulation Research 91(5): p. 427-433.

432. Xiao, W., Wang, L., Yang, X., Chen, T., Hodge, D., Johnson, P.F., and Farrar, W. (2001) *CCAAT/Enhancer-binding Protein β mediates Interferon-γ-induced p48 (ISGF3-γ) gene transcription in human monocytic cells.* Journal of Biological Chemistry 276(26): p. 23275-23281.

433. Roy, S.K., Wachira, S.J., Weihua, X., Hu, J., and Kalvakolanu, D.V. (2000) *CCAAT/Enhancer-binding Protein-β regulates Interferon-induced transcription through a novel element.* Journal of Biological Chemistry 275(17): p. 12626-12632.

434. Kawashima, A., Harada, T., Imada, K., Yano, T., and Mizuguchi, K. (2008) *Eicosapentaenoic acid inhibits interleukin-6 production in interleukin-1β-stimulated C6 glioma cells through peroxisome proliferator-activated receptor-gamma.* Prostaglandins, Leukotrienes and Essential Fatty Acids 79(1–2): p. 59-65.

435. Hsiang, C.-Y., Lo, H.-Y., Huang, H.-C., Li, C.-C., Wu, S.-L., and Ho, T.-Y. (2013) *Ginger extract and zingerone ameliorated trinitrobenzene sulphonic acid-induced colitis in mice via modulation of nuclear factor-κB activity and interleukin-1β signalling pathway.* Food Chemistry 136(1): p. 170-177.

436. Jia, H., Aw, W., Hanate, M., Takahashi, S., Saito, K., Tanaka, H., Tomita, M., and Kato, H. (2014) *Multi-faceted integrated omics analysis revealed parsley (Petroselinum crispum) as a novel dietary intervention in dextran sodium sulphate induced colitic mice.* Journal of Functional Foods 11: p. 438-448.

437. Dyerberg, J., Madsen, P., Moller, J.M., Aardestrup, I., and Schmidt, E.B. (2010) *Bioavailability of marine n-3 fatty acid formulations.* Prostaglandins, Leukotrienes and Essential Fatty Acids 83(3): p. 137-141.

438. Babior, B.M., Kipnes, R.S., and Curnutte, J.T. (1973) *Biological defense mechanisms. The production by leukocytes of superoxide, a potential bactericidal agent.* Journal of Clinical Investigation 52(3): p. 741-744.

439. McKenzie, S.J., Baker, M.S., Buffinton, G.D., and Doe, W.F. (1996) *Evidence of oxidant-induced injury to epithelial cells during inflammatory bowel disease.* Journal of Clinical Investigation 98(1): p. 136-141.

440. Lih-Brody, L., Powell, S., Collier, K., Reddy, G., Cerchia, R., Kahn, E., Weissman, G., Katz, S., Floyd, R., McKinley, M., Fisher, S., and Mullin, G. (1996) *Increased oxidative stress and decreased antioxidant defenses in mucosa of inflammatory bowel disease.* Digestive Diseases and Sciences 41(10): p. 2078-2086.

441. Zhang, X., Dong, F., Ren, J., Driscoll, M.J., and Culver, B. (2005) *High dietary fat induces NADPH oxidase-associated oxidative stress and inflammation in rat cerebral cortex.* Experimental Neurology 191(2): p. 318-325.

442. Bamba, T., Shimoyama, T., Sasaki, M., Tsujikawa, T., Fukuda, Y., Koganei, K., Hibi, T., Iwao, Y., Munakata, A., Fukuda, S., Matsumoto, T., Oshitani, N., Hiwatashi, N., Oriuchi, T., Kitahora, T., Utsunomiya, T., Saitoh, Y., Suzuki, Y., and Nakajima, M. (2003) *Dietary fat attenuates the benefits of an elemental diet in active Crohn's disease: a randomized, controlled trial.* European Journal of Gastroenterology & Hepatology 15(2): p. 151-157.

443. Björkholm, B., Bok, C.M., Lundin, A., Rafter, J., Hibberd, M.L., and Pettersson, S. (2009) *Intestinal microbiota regulate xenobiotic metabolism in the liver.* PLoS ONE 4(9): p. e6958.

444. Kusunoki, Y., Ikarashi, N., Hayakawa, Y., Ishii, M., Kon, R., Ochiai, W., Machida, Y., and Sugiyama, K. (2014) *Hepatic early inflammation induces downregulation of hepatic cytochrome P450 expression and metabolic activity in the dextran sulfate sodium-induced murine colitis.* European Journal of Pharmaceutical Sciences 54: p. 17-27.

445. Pastor Rojo, O., Lopez San Roman, A., Albeniz Arbizu, E., de la Hera Martinez, A., Ripoll Sevillano, E., and Albillos Martinez, A. (2007) *Serum lipopolysaccharide-binding protein in endotoxemic patients with inflammatory bowel disease.* Inflammatory Bowel Disease 13(3): p. 269-277.

446. Håkansson, Å., Bränning, C., Molin, G., Adawi, D., Hagslätt, M.-L., Jeppsson, B., Nyman, M., and Ahrné, S. (2012) *Blueberry husks and probiotics attenuate colorectal inflammation and oncogenesis, and liver injuries in rats exposed to cycling DSS-treatment.* PLoS ONE 7(3): p. e33510.

447. Trivedi, P.P. and Jena, G.B. (2013) *Ulcerative colitis-induced hepatic damage in mice: Studies on inflammation, fibrosis, oxidative DNA damage and GST-P expression.* Chemico-Biological Interactions 201(1–3): p. 19-30.

448. Urwin, H.J., Miles, E.A., Noakes, P.S., Kremmyda, L.S., Vlachava, M., Diaper, N.D., Godfrey, K.M., Calder, P.C., Vulevic, J., and Yaqoob, P. (2014) *Effect of salmon consumption during pregnancy on maternal and infant faecal microbiota, secretory IgA and calprotectin.* British Journal of Nutrition 111(5): p. 773-784.

449. Sepehri, S., Kotlowski, R., Bernstein, C.N., and Krause, D.O. (2007) *Microbial diversity of inflamed and noninflamed gut biopsy tissues in inflammatory bowel disease.* Inflammatory Bowel Disease 13(6): p. 675-683.

450. Adriaens, M., Ahles, P., Jagers, F., and Evelo, C., *Fatty acid beta oxidation (Homo sapiens)*. 2015, WikiPathways.

451. Tamaki, H., Nakamura, H., Nishio, A., Nakase, H., Ueno, S., Uza, N., Kido, M., Inoue, S., Mikami, S., Asada, M., Kiriya, K., Kitamura, H., Ohashi, S., Fukui, T., Kawasaki, K., Matsuura, M., Ishii, Y., Okazaki, K., Yodoi, J., and Chiba, T. (2006) *Human thioredoxin-1 ameliorates experimental murine colitis in association with suppressed macrophage inhibitory factor production.* Gastroenterology 131(4): p. 1110-1121.

452. Nordberg, J. and Arnér, E.S.J. (2001) *Reactive oxygen species, antioxidants, and the mammalian thioredoxin system1.* Free Radical Biology and Medicine 31(11): p. 1287-1312.

453. Nakamura, H., Nakamura, K., and Yodoi, J. (1997) *Redox regulation of cellular activation.* Annual Review of Immunology 15(1): p. 351-369.

454. Bertini, R., Howard, O.M., Dong, H.F., Oppenheim, J.J., Bizzarri, C., Sergi, R., Caselli, G., Pagliei, S., Romines, B., Wilshire, J.A., Mengozzi, M., Nakamura, H., Yodoi, J., Pekkari, K., Gurunath, R., Holmgren, A., Herzenberg, L.A., and Ghezzi, P. (1999) *Thioredoxin, a redox enzyme released in infection and inflammation, is a unique chemoattractant for neutrophils, monocytes, and T cells.* Journal of Experimental Medicine 189(11): p. 1783-1789.

455. Hasnain, S.Z., Lourie, R., Das, I., Chen, A.C.-H., and McGuckin, M.A. (2012) *The interplay between endoplasmic reticulum stress and inflammation.* Immunology and Cell Biology 90(3): p. 260-270.

456. Shkoda, A., Ruiz, P.A., Daniel, H., Kim, S.C., Rogler, G., Sartor, R.B., and Haller, D. (2007) *Interleukin-10 blocked endoplasmic reticulum stress in intestinal epithelial cells: impact on chronic inflammation.* Gastroenterology 132(1): p. 190-207.

457. Hori, O., Ichinoda, F., Tamatani, T., Yamaguchi, A., Sato, N., Ozawa, K., Kitao, Y., Miyazaki, M., Harding, H.P., Ron, D., Tohyama, M., D, M.S., and Ogawa, S. (2002) *Transmission of cell stress from endoplasmic reticulum to mitochondria: enhanced expression of Lon protease.* Journal of Cell Biology 157(7): p. 1151-1160.

458. Sartor, R.B. (1997) *Pathogenesis and immune mechanisms of chronic inflammatory bowel diseases.* The American Journal of Gastroenterology 92(12 Suppl): p. 5S-11S.

459. Selhub, J., Byun, A., Liu, Z., Mason, J.B., Bronson, R.T., and Crott, J.W. (2013) *Dietary vitamin B6 intake modulates colonic inflammation in the IL10−/− model of inflammatory bowel disease.* The Journal of Nutritional Biochemistry 24(12): p. 2138-2143.

460. Chen, Y., Orlicky, D.J., Matsumoto, A., Singh, S., Thompson, D.C., and Vasiliou, V. (2011) *Aldehyde dehydrogenase 1B1 (ALDH1B1) is a potential biomarker for human colon cancer.* Biochemical and Biophysical Research Communications 405(2): p. 173-179.

461. Kyoto Encyclopedia of Genes and Genomes (KEGG), *Tryptophan metabolism*. 2014.

462. Toye, A.A., Dumas, M.E., Blancher, C., Rothwell, A.R., Fearnside, J.F., Wilder, S.P., Bihoreau, M.T., Cloarec, O., Azzouzi, I., Young, S., Barton, R.H., Holmes, E., McCarthy, M.I., Tatoud, R., Nicholson, J.K., Scott, J., and Gauguier, D. (2007) *Subtle metabolic and liver gene transcriptional changes underlie diet-induced fatty liver susceptibility in insulin-resistant mice.* Diabetologia 50(9): p. 1867-1879.

463. Kruidenier, L., Kuiper, I., Lamers, C.B.H.W., and Verspaget, H.W. (2003) *Intestinal oxidative damage in inflammatory bowel disease: semi-quantification,*

localization, and association with mucosal antioxidants. The Journal of Pathology 201(1): p. 28-36.

464. Miyamoto, S., Kawano, H., Takazoe, K., Soejima, H., Sakamoto, T., Hokamaki, J., Yoshimura, M., Nakamura, H., Yodoi, J., and Ogawa, H. (2004) *Vitamin E improves fibrinolytic activity in patients with coronary spastic angina.* Thrombosis Research 113(6): p. 345-351.

465. Mahmood, S., Yamada, G., Niiyama, G., Kawanaka, M., Togawa, K., Sho, M., Ito, T., Sasagawa, T., Okita, M., Nakamura, H., and Yodoi, J. (2003) *Effect of vitamin E on serum aminotransferase and thioredoxin levels in patients with viral Hepatitis C.* Free Radical Research 37(7): p. 781-785.

466. Dolan, B.P., Bennink, J.R., and Yewdell, J.W. (2011) *Translating DRiPs: progress in understanding viral and cellular sources of MHC class I peptide ligands.* Cellular and Molecular Life Sciences 68(9): p. 1481-1489.

467. Golovina, T.N., Morrison, S.E., and Eisenlohr, L.C. (2005) *The impact of misfolding versus targeted degradation on the efficiency of the MHC class I-restricted antigen processing.* The Journal of Immunology 174(5): p. 2763-2769.

468. Zhou, X., Xie, Y., Qi, Q., Cheng, X., Liu, F., Liao, K., Wang, G., and Hao, H. (2013) *Disturbance of hepatic and intestinal UDP-glucuronosyltransferase in rats with Trinitrobenzene Sulfonic Acid–induced colitis.* Drug metabolism and pharmacokinetics 28(4): p. 305-313.

469. Scott, J.R. and Fox-Robichaud, A.E. (2002) *Hepatic leukocyte recruitment in a model of acute colitis.* American Journal of Physiology - Gastrointestinal and Liver Physiology 283(3): p. G561-G566.

470. Maitra, U., Gan, L., Chang, S., and Li, L. (2011) *Low-dose endotoxin induces inflammation by selectively removing nuclear receptors and activating CCAAT/enhancer-binding protein δ.* The Journal of Immunology 186(7): p. 4467-4473.

471. Langrish, C.L., Chen, Y., Blumenschein, W.M., Mattson, J., Basham, B., Sedgwick, J.D., McClanahan, T., Kastelein, R.A., and Cua, D.J. (2005) *IL-23 drives a pathogenic T cell population that induces autoimmune inflammation.* The Journal of Experimental Medicine 201(2): p. 233-240.

472. Ruddy, M.J., Wong, G.C., Liu, X.K., Yamamoto, H., Kasayama, S., Kirkwood, K.L., and Gaffen, S.L. (2004) *Functional cooperation between Interleukin-17 and Tumor Necrosis Factor-α is mediated by CCAAT/Enhancer-binding protein family members.* Journal of Biological Chemistry 279(4): p. 2559-2567.

473. Huang, J.H. and Liao, W.S. (1994) *Induction of the mouse serum amyloid A3 gene by cytokines requires both C/EBP family proteins and a novel constitutive nuclear factor.* Molecular and Cellular Biology 14(7): p. 4475-4484.

474. Eckhardt, E.R., Witta, J., Zhong, J., Arsenescu, R., Arsenescu, V., Wang, Y., Ghoshal, S., de Beer, M.C., de Beer, F.C., and de Villiers, W.J. (2010) *Intestinal epithelial serum amyloid A modulates bacterial growth in vitro and pro-inflammatory responses in mouse experimental colitis.* BMC Gastroenterology 10: p. 133.

475. Martin, F.-P.J., Rezzi, S., Montoliu, I., Philippe, D., Tornier, L., Messlik, A., Hölzlwimmer, G., Baur, P., Quintanilla-Fend, L., Loh, G., Blaut, M., Blum, S.,

Kochhar, S., and Haller, D. (2009) *Metabolic assessment of gradual development of moderate experimental colitis in IL-10 deficient mice.* Journal of Proteome Research 8(5): p. 2376-2387.

476. Chambers, R.E., Stross, P., Barry, R.E., and Whicher, J.T. (1987) *Serum amyloid A protein compared with C-reactive protein, alpha 1-antichymotrypsin and alpha 1-acid glycoprotein as a monitor of inflammatory bowel disease.* European Journal of Clinical Investigation 17(5): p. 460-467.

477. Masubuchi, Y. and Horie, T. (2004) *Endotoxin-mediated disturbance of hepatic cytochrome P450 function and development of endotoxin tolerance in the rat model of dextran sulfate sodium-induced experimental colitis.* Drug Metabolism and Disposition 32(4): p. 437-441.

478. Abdulla, D., Goralski, K.B., Del Busto Cano, E.G., and Renton, K.W. (2005) *The signal transduction pathways involved in hepatic cytochrome P450 regulation in the rat during a lipopolysaccharide-induced model of central nervous system inflammation.* Drug Metabolism and Disposition 33(10): p. 1521-1531.

479. Maglich, J.M., Stoltz, C.M., Goodwin, B., Hawkins-Brown, D., Moore, J.T., and Kliewer, S.A. (2002) *Nuclear pregnane X receptor and constitutive androstane receptor regulate overlapping but distinct sets of genes involved in xenobiotic detoxification.* Molecular Pharmacology 62(3): p. 638-646.

480. Martin, P.G.P., Guillou, H., Lasserre, F., Déjean, S., Lan, A., Pascussi, J.-M., SanCristobal, M., Legrand, P., Besse, P., and Pineau, T. (2007) *Novel aspects of PPARα-mediated regulation of lipid and xenobiotic metabolism revealed through a nutrigenomic study.* Hepatology 45(3): p. 767-777.

481. Schwanhaeusser, B., Busse, D., Li, N., Dittmar, G., Schuchhardt, J., Wolf, J., Chen, W., and Selbach, M. (2011) *Global quantification of mammalian gene expression control.* Nature 473(7347): p. 337-342.

482. Mustacich, D.J., Gohil, K., Bruno, R.S., Yan, M., Leonard, S.W., Ho, E., Cross, C.E., and Traber, M.G. (2009) *Alpha-tocopherol modulates genes involved in hepatic xenobiotic pathways in mice.* The Journal of Nutritional Biochemistry 20(6): p. 469-476.

483. Thatcher, J.E., Zelter, A., and Isoherranen, N. (2010) *The relative importance of CYP26A1 in hepatic clearance of all-trans retinoic acid.* Biochemical Pharmacology 80(6): p. 903-912.

484. Blomhoff, R. and Blomhoff, H.K. (2006) *Overview of retinoid metabolism and function.* Journal of Neurobiology 66(7): p. 606-630.

485. Bjerkeng, B., *Carotenoids in aquaculture: fish and crustaceans*, in *Carotenoids*, G. Britton, S. Liaaen-Jensen, and H. Pfander, Editors. 2008, Birkhäuser Basel. p. 237-254.

486. Megdal, P.A., Craft, N.A., and Handelman, G.J. (2009) *A simplified method to distinguish farmed (Salmo salar) from wild salmon: fatty acid ratios versus astaxanthin chiral isomers.* Lipids 44(6): p. 569-576.

487. Garner, S.R., Neff, B.D., and Bernards, M.A. (2010) *Dietary carotenoid levels affect carotenoid and retinoid allocation in female Chinook salmon Oncorhynchus tshawytscha.* Journal of Fish Biology 76(6): p. 1474-1490.

488. Sangeetha, R.K. and Baskaran, V. (2010) *Retinol-deficient rats can convert a pharmacological dose of astaxanthin to retinol: antioxidant potential of astaxanthin, lutein, and β-carotene.* Canadian Journal of Physiology and Pharmacology 88(10): p. 977-985.

489. Birringer, M., Drogan, D., and Brigelius-Flohe, R. (2001) *Tocopherols are metabolized in HepG2 cells by side chain ω-oxidation and consecutive β-oxidation.* Free Radical Biology and Medicine 31(2): p. 226-232.

490. Horton, J.D., Shah, N.A., Warrington, J.A., Anderson, N.N., Park, S.W., Brown, M.S., and Goldstein, J.L. (2003) *Combined analysis of oligonucleotide microarray data from transgenic and knockout mice identifies direct SREBP target genes.* Proceedings of the National Academy of Sciences 100(21): p. 12027-12032.

491. Dobrzyn, P., Dobrzyn, A., Miyazaki, M., Cohen, P., Asilmaz, E., Hardie, D.G., Friedman, J.M., and Ntambi, J.M. (2004) *Stearoyl-CoA desaturase 1 deficiency increases fatty acid oxidation by activating AMP-activated protein kinase in liver.* Proceedings of the National Academy of Sciences 101(17): p. 6409-6414.

492. Ntambi, J.M., Miyazaki, M., Stoehr, J.P., Lan, H., Kendziorski, C.M., Yandell, B.S., Song, Y., Cohen, P., Friedman, J.M., and Attie, A.D. (2002) *Loss of stearoyl–CoA desaturase-1 function protects mice against adiposity.* Proceedings of the National Academy of Sciences 99(17): p. 11482-11486.

493. Hunt, M.C., Rautanen, A., Westin, M.A., Svensson, L.T., and Alexson, S.E. (2006) *Analysis of the mouse and human acyl-CoA thioesterase (ACOT) gene clusters shows that convergent, functional evolution results in a reduced number of human peroxisomal ACOTs.* FASEB Journal 20(11): p. 1855-1864.

494. Tillander, V., Bjorndal, B., Burri, L., Bohov, P., Skorve, J., Berge, R., and Alexson, S. (2014) *Fish oil and krill oil supplementations differentially regulate lipid catabolic and synthetic pathways in mice.* Nutrition & Metabolism 11(1): p. 20.

495. Evans, M., Lai, K., Shaw, L., Harnish, D., and Chadwick, C. (2002) *Estrogen receptor alpha inhibits IL-1beta induction of gene expression in the mouse liver.* Endocrinology 143(7): p. 2559-2570.

496. Ray, A. and Ray, B.K. (1994) *Serum amyloid A gene expression under acute-phase conditions involves participation of inducible C/EBP-beta and C/EBP-delta and their activation by phosphorylation.* Molecular and Cellular Biology 14(6): p. 4324-4332.

497. Wechter, W.J., Kantoci, D., Murray, E.D., D'Amico, D.C., Jung, M.E., and Wang, W.-H. (1996) *A new endogenous natriuretic factor: LLU-alpha.* Proceedings of the National Academy of Sciences 93(12): p. 6002-6007.

498. Leonard, S.W., Gumpricht, E., Devereaux, M.W., Sokol, R.J., and Traber, M.G. (2005) *Quantitation of rat liver vitamin E metabolites by LC-MS during high-dose vitamin E administration.* Journal of Lipid Research 46(5): p. 1068-1075.

499. Imai, E., Tsuji, T., Sano, M., Fukuwatari, T., and Shibata, K. (2011) *Association between 24 hour urinary alpha-tocopherol catabolite, 2,5,7,8-tetramethyl-2(2'-carboxyethyl)-6-hydroxychroman (alpha-CEHC) and alpha-tocopherol intake in*

intervention and cross-sectional studies. Asia Pacific Journal of Clinical Nutrition 20(4): p. 507-513.

500. Kiyose, C., Saito, H., Kaneko, K., Hamamura, K., Tomioka, M., Ueda, T., and Igarashi, O. (2001) *Alpha-tocopherol affects the urinary and biliary excretion of 2,7,8-trimethyl-2 (2'-carboxyethyl)-6-hydroxychroman, gamma-tocopherol metabolite, in rats.* Lipids 36(5): p. 467-472.

501. Behrens, W.A. and Madere, R. (1987) *Mechanisms of absorption, transport and tissue uptake of RRR-alpha-tocopherol and d-gamma-tocopherol in the white rat.* The Journal of Nutrition 117(9): p. 1562-1569.

502. Zingg, J.-M., Han, S.N., Pang, E., Meydani, M., Meydani, S.N., and Azzi, A. (2013) *In vivo regulation of gene transcription by alpha- and gamma-tocopherol in murine T lymphocytes.* Archives of Biochemistry and Biophysics 538(2): p. 111-119.

503. Jiang, Q., Elson-Schwab, I., Courtemanche, C., and Ames, B.N. (2000) *γ-Tocopherol and its major metabolite, in contrast to α-tocopherol, inhibit cyclooxygenase activity in macrophages and epithelial cells.* Proceedings of the National Academy of Sciences 97(21): p. 11494-11499.

504. Devaraj, S., Leonard, S., Traber, M.G., and Jialal, I. (2008) *Gamma-tocopherol supplementation alone and in combination with alpha-tocopherol alters biomarkers of oxidative stress and inflammation in subjects with metabolic syndrome.* Free Radical Biology and Medicine 44(6): p. 1203-1208.

505. Sokol, H., Seksik, P., Furet, J.P., Firmesse, O., Nion-Larmurier, I., Beaugerie, L., Cosnes, J., Corthier, G., Marteau, P., and Doré, J. (2009) *Low counts of Faecalibacterium prausnitzii in colitis microbiota.* Inflammatory Bowel Disease 15(8): p. 1183-1189.

506. Swidsinski, A., Weber, J., Loening-Baucke, V., Hale, L.P., and Lochs, H. (2005) *Spatial organization and composition of the mucosal flora in patients with inflammatory bowel disease.* Journal of Clinical Microbiology 43(7): p. 3380-3389.

507. Swidsinski, A., Ladhoff, A., Pernthaler, A., Swidsinski, S., Loening–Baucke, V., Ortner, M., Weber, J., Hoffmann, U., Schreiber, S., Dietel, M., and Lochs, H. (2002) *Mucosal flora in inflammatory bowel disease.* Gastroenterology 122(1): p. 44-54.

508. Bassett, S.A., Young, W., Barnett, M.P., Cookson, A.L., McNabb, W.C., and Roy, N.C. (2015) *Changes in composition of caecal microbiota associated with increased colon inflammation in interleukin-10 gene-deficient mice inoculated with Enterococcus species.* Nutrients 7(3): p. 1798-1816.

509. Zhang, X., Zhao, Y., Zhang, M., Pang, X., Xu, J., Kang, C., Li, M., Zhang, C., Zhang, Z., Zhang, Y., Li, X., Ning, G., and Zhao, L. (2012) *Structural changes of gut microbiota during berberine-mediated prevention of obesity and insulin resistance in high-fat diet-fed rats.* PLoS ONE 7(8): p. e42529.

510. Tedelind, S., Westberg, F., Kjerrulf, M., and Vidal, A. (2007) *Anti-inflammatory properties of the short-chain fatty acids acetate and propionate: a study with relevance to inflammatory bowel disease.* World Journal of Gastroenterology 13(20): p. 2826-2832.

511. Roediger, W. (1980) *Role of anaerobic bacteria in the metabolic welfare of the colonic mucosa in man.* Gut 21(9): p. 793-798.

512. Derrien, M., Vaughan, E.E., Plugge, C.M., and de Vos, W.M. (2004) *Akkermansia muciniphila gen. nov., sp. nov., a human intestinal mucin-degrading bacterium.* International Journal of Systematic and Evolutionary Microbiology 54(5): p. 1469-1476.

513. Vigsnæs, L.K., Brynskov, J., Steenholdt, C., Wilcks, A., and Licht, T.R. (2012) *Gram-negative bacteria account for main differences between faecal microbiota from patients with ulcerative colitis and healthy controls.* Beneficial Microbes 3(4): p. 287-297.

514. Png, C.W., Linden, S.K., Gilshenan, K.S., Zoetendal, E.G., McSweeney, C.S., Sly, L.I., McGuckin, M.A., and Florin, T.H. (2010) *Mucolytic bacteria with increased prevalence in IBD mucosa augment in vitro utilization of mucin by other bacteria.* The American Journal of Gastroenterology 105(11): p. 2420-2428.

515. Everard, A., Lazarevic, V., Derrien, M., Girard, M., Muccioli, G.G., Neyrinck, A.M., Possemiers, S., Van Holle, A., François, P., de Vos, W.M., Delzenne, N.M., Schrenzel, J., and Cani, P.D. (2011) *Responses of gut microbiota and glucose and lipid metabolism to prebiotics in genetic obese and diet-induced leptin-resistant mice.* Diabetes 60(11): p. 2775-2786.

516. Ganesh, B.P., Klopfleisch, R., Loh, G., and Blaut, M. (2013) *Commensal Akkermansia muciniphila exacerbates gut inflammation in salmonella typhimurium-infected gnotobiotic mice.* PLoS ONE 8(9): p. e74963.

517. Turnbaugh, P.J., Bäckhed, F., Fulton, L., and Gordon, J.I. (2008) *Diet-induced obesity is linked to marked but reversible alterations in the mouse distal gut microbiome.* Cell Host & Microbe 3(4): p. 213-223.

518. Bakker, G.C., van Erk, M.J., Pellis, L., Wopereis, S., Rubingh, C.M., Cnubben, N.H., Kooistra, T., van Ommen, B., and Hendriks, H.F. (2010) *An antiinflammatory dietary mix modulates inflammation and oxidative and metabolic stress in overweight men: a nutrigenomics approach.* The American Journal of Clinical Nutrition 91(4): p. 1044-1059.

519. Ferrante, L.M., Willighagen, E., Hanspers, K., and Digles, D., *Tryptophan metabolism (Mus musculus)*. 2015.

520. Dai, X. and Zhu, B.T. (2010) *Indoleamine 2,3-Dioxygenase tissue distribution and cellular localization in mice: implications for its biological functions.* Journal of Histochemistry and Cytochemistry 58(1): p. 17-28.

521. Matteoli, G., Mazzini, E., Iliev, I.D., Mileti, E., Fallarino, F., Puccetti, P., Chieppa, M., and Rescigno, M. (2010) *Gut CD103+ dendritic cells express indoleamine 2,3-dioxygenase which influences T regulatory/T effector cell balance and oral tolerance induction.* Gut 59(5): p. 595-604.

522. Gurtner, G.J., Newberry, R.D., Schloemann, S.R., McDonald, K.G., and Stenson, W.F. (2003) *Inhibition of indoleamine 2,3-dioxygenase augments trinitrobenzene sulfonic acid colitis in mice.* Gastroenterology 125(6): p. 1762-1773.

523. Niño-Castro, A., Abdullah, Z., Popov, A., Thabet, Y., Beyer, M., Knolle, P., Domann, E., Chakraborty, T., Schmidt, S.V., and Schultze, J.L. (2014) *The IDO1-*

induced kynurenines play a major role in the antimicrobial effect of human myeloid cells against Listeria monocytogenes. Innate Immunity 20(4): p. 401-411.

524. DeMoss, R.D. and Moser, K. (1969) *Tryptophanase in diverse bacterial species.* Journal of Bacteriology 98(1): p. 167-171.

525. Chung, K.T., Fulk, G.E., and Slein, M.W. (1975) *Tryptophanase of fecal flora as a possible factor in the etiology of colon cancer.* Journal of the National Cancer Institute 54(5): p. 1073-1078.

526. Bloom, S.M., Bijanki, V.N., Nava, G.M., Sun, L., Malvin, N.P., Donermeyer, D.L., Dunne, W.M., Jr., Allen, P.M., and Stappenbeck, T.S. (2011) *Commensal Bacteroides species induce colitis in host-genotype-specific fashion in a mouse model of inflammatory bowel disease.* Cell Host Microbe 9(5): p. 390-403.

527. Rabizadeh, S., Rhee, K.J., Wu, S., Huso, D., Gan, C.M., Golub, J.E., Wu, X., Zhang, M., and Sears, C.L. (2007) *Enterotoxigenic bacteroides fragilis: a potential instigator of colitis.* Inflammatory Bowel Disease 13(12): p. 1475-1483.

528. Reboul, E., Klein, A., Bietrix, F., Gleize, B., Malezet-Desmoulins, C., Schneider, M., Margotat, A., Lagrost, L., Collet, X., and Borel, P. (2006) *Scavenger receptor class B type I (SR-BI) is involved in vitamin E transport across the enterocyte.* Journal of Biological Chemistry 281(8): p. 4739-4745.

529. Reboul, E., Soayfane, Z., Goncalves, A., Cantiello, M., Bott, R., Nauze, M., Terce, F., Collet, X., and Comera, C. (2012) *Respective contributions of intestinal Niemann-Pick C1-like 1 and scavenger receptor class B type I to cholesterol and tocopherol uptake: in vivo v. in vitro studies.* British Journal of Nutrition 107(9): p. 1296-1304.

530. Traber, M.G., Labut, E.M., Leonard, S.W., and Lebold, K.M. (2011) *α-Tocopherol injections in rats up-regulate hepatic ABC transporters, but not cytochrome P450 enzymes.* Free Radical Biology and Medicine 51(11): p. 2031-2040.

531. Traber, M.G. (2010) *Regulation of xenobiotic metabolism, the only signaling function of α-tocopherol?* Molecular Nutrition & Food Research 54(5): p. 661-668.

532. Landes, N., Pfluger, P., Kluth, D., Birringer, M., Rühl, R., Böl, G.-F., Glatt, H., and Brigelius-Flohé, R. (2003) *Vitamin E activates gene expression via the pregnane X receptor.* Biochemical Pharmacology 65(2): p. 269-273.

533. Johnson, C.H., Slanar, O., Krausz, K.W., Kang, D.W., Patterson, A.D., Kim, J.H., Luecke, H., Gonzalez, F.J., and Idle, J.R. (2012) *Novel metabolites and roles for alpha-tocopherol in humans and mice discovered by mass spectrometry-based metabolomics.* The American Journal of Clinical Nutrition 96(4): p. 818-830.

534. Mustacich, D.J., Leonard, S.W., Devereaux, M.W., Sokol, R.J., and Traber, M.G. (2006) *α-Tocopherol regulation of hepatic cytochrome P450s and ABC transporters in rats.* Free Radical Biology and Medicine 41(7): p. 1069-1078.

535. Wagner, M., Halilbasic, E., Marschall, H.-U., Zollner, G., Fickert, P., Langner, C., Zatloukal, K., Denk, H., and Trauner, M. (2005) *CAR and PXR agonists stimulate hepatic bile acid and bilirubin detoxification and elimination pathways in mice.* Hepatology 42(2): p. 420-430.

536. Miyazaki, M., Kim, Y.-C., Gray-Keller, M.P., Attie, A.D., and Ntambi, J.M. (2000) *The biosynthesis of hepatic cholesterol esters and triglycerides is impaired in mice with a disruption of the gene for Stearoyl-CoA Desaturase 1.* Journal of Biological Chemistry 275(39): p. 30132-30138.

537. Schultz, M., Leist, M., Petrzika, M., Gassmann, B., and Brigelius-Flohé, R. (1995) *Novel urinary metabolite of alpha-tocopherol, 2,5,7,8-tetramethyl-2(2'-carboxyethyl)-6-hydroxychroman, as an indicator of an adequate vitamin E supply?* The American Journal of Clinical Nutrition 62(6): p. 1527S-1534S.

538. Traber, M.G., Siddens, L.K., Leonard, S.W., Schock, B., Gohil, K., Krueger, S.K., Cross, C.E., and Williams, D.E. (2005) *α-tocopherol modulates Cyp3a expression, increases γ-CEHC production, and limits tissue γ-tocopherol accumulation in mice fed high γ-tocopherol diets.* Free Radical Biology and Medicine 38(6): p. 773-785.

539. Swanson, J., Ben, R., Burton, G., and Parker, R. (1999) *Urinary excretion of 2, 7, 8-trimethyl-2-(β-carboxyethyl)-6-hydroxychroman is a major route of elimination of γ-tocopherol in humans.* Journal of Lipid Research 40(4): p. 665-671.

540. Fernandez-Peralbo, M.A. and Luque de Castro, M.D. (2012) *Preparation of urine samples prior to targeted or untargeted metabolomics mass-spectrometry analysis.* Trends in Analytical Chemistry 41: p. 75–85.

541. Powell, E.E. and Kroon, P.A. (1994) *Low density lipoprotein receptor and 3-hydroxy-3-methylglutaryl coenzyme A reductase gene expression in human mononuclear leukocytes is regulated coordinately and parallels gene expression in human liver.* Journal of Clinical Investigation 93(5): p. 2168-2174.

542. Puigserver, P., Wu, Z., Park, C.W., Graves, R., Wright, M., and Spiegelman, B.M. (1998) *A cold-inducible coactivator of nuclear receptors linked to adaptive thermogenesis.* Cell 92(6): p. 829-839.

543. Frank, D.N., St. Amand, A.L., Feldman, R.A., Boedeker, E.C., Harpaz, N., and Pace, N.R. (2007) *Molecular-phylogenetic characterization of microbial community imbalances in human inflammatory bowel diseases.* Proceedings of the National Academy of Sciences 104(34): p. 13780-13785.

544. Maharshak, N., Packey, C.D., Ellermann, M., Manick, S., Siddle, J.P., Huh, E.Y., Plevy, S., Sartor, R.B., and Carroll, I.M. (2013) *Altered enteric microbiota ecology in interleukin 10-deficient mice during development and progression of intestinal inflammation.* Gut Microbes 4(4): p. 316-324.

545. Belzer, C. and de Vos, W.M. (2012) *Microbes inside - from diversity to function: the case of Akkermansia.* The Journal of the International Society for Microbial Ecology 6(8): p. 1449-1458.

546. Madsen, K.L., Malfair, D., Gray, D., Doyle, J.S., Jewell, L.D., and Fedorak, R.N. (1999) *Interleukin-10 gene-deficient mice develop a primary intestinal permeability defect in response to enteric microflora.* Inflammatory Bowel Disease 5(4): p. 262-270.

547. Arrieta, M.C., Madsen, K., Doyle, J., and Meddings, J. (2009) *Reducing small intestinal permeability attenuates colitis in the IL10 gene-deficient mouse.* Gut 58(1): p. 41-48.

548. Kennedy, R.J., Hoper, M., Deodhar, K., Erwin, P.J., Kirk, S.J., and Gardiner, K.R. (2000) *Interleukin 10-deficient colitis: new similarities to human inflammatory bowel disease.* The British Journal of Surgery 87(10): p. 1346-1351.

549. Schaedler, R.W., Dubos, R., and Costello, R. (1965) *The development of the bacterial flora in the gastrointestinal tract of mice.* The Journal of Experimental Medicine 122(1): p. 59-66.

550. Gygi, S.P., Rochon, Y., Franza, B.R., and Aebersold, R. (1999) *Correlation between protein and mRNA abundance in yeast.* Molecular and Cellular Biology 19(3): p. 1720-1730.

551. Chen, G., Gharib, T.G., Huang, C.C., Taylor, J.M., Misek, D.E., Kardia, S.L., Giordano, T.J., Iannettoni, M.D., Orringer, M.B., Hanash, S.M., and Beer, D.G. (2002) *Discordant protein and mRNA expression in lung adenocarcinomas.* Molecular and Cellular Proteomics 1(4): p. 304-313.

552. Washburn, M.P., Wolters, D., and Yates, J.R., 3rd (2001) *Large-scale analysis of the yeast proteome by multidimensional protein identification technology.* Nature Biotechnology 19(3): p. 242-247.

553. Nandal, U.K., Vlietstra, W.J., Byrman, C., Jeeninga, R.E., Ringrose, J.H., van Kampen, A.H., Speijer, D., and Moerland, P.D. (2015) *Candidate prioritization for low-abundant differentially expressed proteins in 2D-DIGE datasets.* BMC Bioinformatics 16: p. 25.

554. Meissner, F. and Mann, M. (2014) *Quantitative shotgun proteomics: considerations for a high-quality workflow in immunology.* Nature Immunology 15(2): p. 112-117.

555. Veselkov, K.A., Vingara, L.K., Masson, P., Robinette, S.L., Want, E., Li, J.V., Barton, R.H., Boursier-Neyret, C., Walther, B., Ebbels, T.M., Pelczer, I.n., Holmes, E., Lindon, J.C., and Nicholson, J.K. (2011) *Optimized preprocessing of ultra-performance liquid chromatography/mass spectrometry urinary metabolic profiles for improved information recovery.* Analytical Chemistry 83(15): p. 5864-5872.

556. Martin, J.-C., Maillot, M., Mazerolles, G., Verdu, A., Lyan, B., Migné, C., Defoort, C., Canlet, C., Junot, C., Guillou, C., Manach, C., Jabob, D., Bouveresse, D.-R., Paris, E., Pujos-Guillot, E., Jourdan, F., Giacomoni, F., Courant, F., Favé, G., Le Gall, G., Chassaigne, H., Tabet, J.-C., Martin, J.-F., Antignac, J.-P., Shintu, L., Defernez, M., Philo, M., Alexandre-Gouaubau, M.-C., Amiot-Carlin, M.-J., Bossis, M., Triba, M., Stojilkovic, N., Banzet, N., Molinié, R., Bott, R., Goulitquer, S., Caldarelli, S., and Rutledge, D. (2015) *Can we trust untargeted metabolomics? Results of the metabo-ring initiative, a large-scale, multi-instrument inter-laboratory study.* Metabolomics 11(4): p. 807-821.

557. Martin, J.-C., Berton, A., Ginies, C., Bott, R., Scheercousse, P., Saddi, A., Gripois, D., Landrier, J.-F., Dalemans, D., Alessi, M.-C., and Delplanque, B. (2015) *Multi-level systems biology modeling characterized the atheroprotective efficiencies of modified dairy fats in a hamster model.* American Journal of Physiology - Heart and Circulatory Physiology.

558. Hill, D.A., Hoffmann, C., Abt, M.C., Du, Y., Kobuley, D., Kirn, T.J., Bushman, F.D., and Artis, D. (2010) *Metagenomic analyses reveal antibiotic-induced*

temporal and spatial changes in intestinal microbiota with associated alterations in immune cell homeostasis. Mucosal Immunology 3(2): p. 148-158.

559. Nava, G.M., Friedrichsen, H.J., and Stappenbeck, T.S. (2011) *Spatial organization of intestinal microbiota in the mouse ascending colon.* The Journal of the International Society for Microbial Ecology 5(4): p. 627-638.

560. Eckburg, P.B., Bik, E.M., Bernstein, C.N., Purdom, E., Dethlefsen, L., Sargent, M., Gill, S.R., Nelson, K.E., and Relman, D.A. (2005) *Diversity of the human intestinal microbial flora.* Science 308(5728): p. 1635-1638.

561. Cario, E. and Podolsky, D.K. (2000) *Differential alteration in intestinal epithelial cell expression of toll-like receptor 3 (TLR3) and TLR4 in inflammatory bowel disease.* Infection and Immunity 68(12): p. 7010-7017.

562. Laukoetter, M.G., Nava, P., Lee, W.Y., Severson, E.A., Capaldo, C.T., Babbin, B.A., Williams, I.R., Koval, M., Peatman, E., Campbell, J.A., Dermody, T.S., Nusrat, A., and Parkos, C.A. (2007) *JAM-A regulates permeability and inflammation in the intestine in vivo.* Journal of Experimental Medicine 204(13): p. 3067-3076.

563. Brahmbhatt, V., Oliveira, M., Briand, M., Perrisseau, G., Bastic Schmid, V., Destaillats, F., Pace-Asciak, C., Benyacoub, J., and Bosco, N. (2013) *Protective effects of dietary EPA and DHA on ischemia–reperfusion-induced intestinal stress.* The Journal of Nutritional Biochemistry 24(1): p. 104-111.

564. Masoodi, M., Pearl, D.S., Eiden, M., Shute, J.K., Brown, J.F., Calder, P.C., and Trebble, T.M. (2013) *Altered colonic mucosal polyunsaturated fatty acid (PUFA) derived lipid mediators in ulcerative colitis: new insight into relationship with disease activity and pathophysiology.* PLoS ONE 8(10): p. e76532.

565. Sterz, K., Scherer, G., and Ecker, J. (2012) *A simple and robust UPLC-SRM/MS method to quantify urinary eicosanoids.* Journal of Lipid Research 53(5): p. 1026-1036.

566. Minihane, A.M., Vinoy, S., Russell, W.R., Baka, A., Roche, H.M., Tuohy, K.M., Teeling, J.L., Blaak, E.E., Fenech, M., and Vauzour, D. (2015) *Low-grade inflammation, diet composition and health: current research evidence and its translation.* British Journal of Nutrition 114(07): p. 999-1012.

567. Dommels, Y.E., Butts, C.A., Zhu, S., Davy, M., Martell, S., Hedderley, D., Barnett, M.P., McNabb, W.C., and Roy, N.C. (2007) *Characterization of intestinal inflammation and identification of related gene expression changes in mdr1a$^{-/-}$ mice.* Genes and Nutrition 2(2): p. 209-223.

568. Pfaffl, M.W., Horgan, G.W., and Dempfle, L. (2002) *Relative expression software tool (REST) for group-wise comparison and statistical analysis of relative expression results in real-time PCR.* Nucleic Acids Research 30(9): p. 36.

569. Gaj, S., Eijssen, L., Mensink, R.P., and Evelo, C.T. (2008) *Validating nutrient-related gene expression changes from microarrays using RT(2) PCR-arrays.* Genes and Nutrition 3(3-4): p. 153-157.